Demodulator techniques in satellite communication systems for direct broadcast systems

Thesis

UNRESTRICTED

DEMODULATOR TECHNIQUES

IN

SATELLITE COMMUNICATIONS SYSTEMS

FOR

DIRECT BROADCAST SYSTEMS

A Thesis submitted in fulfilment of the
requirements for the degree of Doctor of Philosophy

by

Remo G. A. Marzolini, B.A. (Hons), C.Eng., M.I.E.E.

The Open University

Discipline - Electronics

Date of Submission - 28th February, 1996

EX12

HIGHER DEGREES OFFICE

LIBRARY AUTHORISATION FORM

Please return this form to the Higher Degrees Office with the bound library copies of your thesis. All students should complete Part 1. Part 2 applies only to PhD students.

Student: R.G.A. MARZOLINI PI: A0236478

Degree: Ph.D.

Thesis title: DEMODULATOR TECHNIQUES IN SATELLITE COMMUNICATIONS SYSTEMS FOR DIRECT BROADCAST SYSTEMS

Part 1 Open University Library Authorisation (to be completed by all students)

I confirm that I am willing for my thesis to be made available to readers by the Open University Library, and that it may be photocopied, subject to the discretion of the Librarian.

Signed: R.G.A. Marzolini Date: April 24th 1996

Part 2 British Library Authorisation (to be completed by PhD students only)

If you want a copy of your PhD thesis to be held by the British Library, you must sign a British Doctoral Thesis Agreement Form. You should return it to the Higher Degrees Office with this form and your bound thesis. *You are also required to supply a third, unbound copy of your thesis.* The British Library will use this to make their microfilm copy; it will not be returned. Information on the presentation of the thesis is given in the Agreement Form.

If your thesis is part of a collaborative group project, you will need to obtain the signatures of others involved for the Agreement Form.

The University has agreed that the lodging of your thesis with the British Library should be voluntary. Please tick either (a) or (b) below to indicate your intentions.

(a) ☑ I am willing for the Open University to supply the British Library with a copy of my thesis. A signed Agreement Form and 3 copies of my thesis are attached (two bound as specified in Section 9.4 of the Research Degree Handbook and the third unbound).

(b) ☐ I do not wish the Open University to supply a copy of my thesis to the British Library.

Signed: R.G.A. Marzolini Date: April 24th 1996

EX12/January 1993/dg/akb

ABSTRACT

This thesis is concerned with the FM demodulator techniques used in terrestrial TV receiver designs for Direct Broadcast Systems (DBS) from satellites. The various MAC/Packet schemes intended for DBS applications are described and the international standards that apply to them considered, with particular emphasis on the D2-MAC system. Noise in FM systems is discussed and a suitable threshold noise model is chosen for use in DBS TV demodulator systems. The characteristics of the various types of noise effects are considered in terms of their effect upon the TV picture. The threshold performance of a conventional FM demodulator for differing types of modulation is reviewed and it is shown how the threshold characteristic depends upon the nature of the modulation. The literature review carried out represents a significant component of the thesis and combines material from patent literature with more conventional source materials from professional journals, conferences, textbooks, etc.

Some ten existing demodulator concepts that exhibit threshold extension characteristics are examined, and where relevant their potential performance in D2-MAC format systems is assessed. The demodulator characteristics that limit their performance in TV systems are identified. It is concluded that designing a threshold extension demodulator, with reliable operation, for all picture contents and for a wide range of input carrier-to-noise ratios, is a formidable task using existing design techniques. On the basis of this examination an adaptive threshold extension demodulator concept is proposed, that utilises information contained within the signal structure to achieve an improved performance over a wide range of input carrier-to-noise ratios and picture content. It is shown how the relevant signal structures may be derived from conventional (PAL, SECAM and NTSC), MAC format and all-digital television systems. Illustrations are given that show how the adaptive demodulator concept can be applied to certain existing threshold extension demodulators, enhancing their performance for television picture reception. Future trends in all-digital DBS TV systems intended ultimately for DBS applications are briefly discussed together with their demodulation requirements.

CONTENTS

1. INTRODUCTION

2. PROBLEM DEFINITION

2.1 General

2.2 Approaches to problem

2.3 Summary of previous work

2.4 References

3. DIRECT BROADCAST SATELLITE TV SYSTEMS

3.1 General

3.2 Direct broadcast satellite TV systems

3.3 DBS standards

3.3.1 Sources

3.3.2 MAC/Packet systems

3.3.3 D2-MAC/Packet parameters relevant to threshold extension demodulators

3.3.4 Digital TV parameters relevant to threshold extension demodulators

3.4 Typical satellite television transmitter

3.5 Typical DBS receiver

3.6 DBS link performance

3.6.1 Introduction

3.6.2 Signal-to-noise ratio at terrestrial TV receiver input

3.6.3 Figure of merit for terrestrial TV receiving equipment

3.7 Satellite to ground link analysis

3.7.1 General

3.7.2 Analysis

3.7.3 Effects of threshold extension on a typical satellite to ground link

3.8 References

4. NOISE IN FM SYSTEMS

4.1 Introduction

4.2 Noise characteristics at FM threshold

4.3 Click analysis

4.4 Click rates

4.5 Threshold noise in television systems

4.6 Noise spectra convention

4.7 References

5. DBS QUALITY CRITERIA

5.1 General

5.2 Direct broadcast FM systems

5.3 Definition of threshold extension

5.4 Pre-emphasis and de-emphasis characteristics

5.5 Carrier-to-noise ratio and signal-to-noise ratio criteria

5.6 References

6. IDEAL AND CONVENTIONAL DEMODULATOR THRESHOLD

6.1 General

6.2 Ideal demodulator threshold characteristics

6.3 Conventional demodulator threshold characteristics

6.3.1 General

6.3.2 Limiter-discriminator analysis

6.3.3 Output signal and noise powers

6.3.4 Conventional discriminator threshold

6.4 Discussion

6.5 References

7. THRESHOLD EXTENSION DEMODULATORS

7.1 General

7.2 References

8. TRACKING FILTER DEMODULATOR

8.1 Introduction

8.2 Previous design approaches

8.3 Analysis of tracking filter

8.4 Application of the tracking filter analysis to the D2/MAC system

8.5 Summary

8.6 References

9. FREQUENCY DEMODULATION WITH FEEDBACK

9.1 Introduction

9.2 Basic FMFB demodulator mode of operation

9.3 Output signal-to-noise ratio at threshold

9.4 Discussion

9.5 References

10. PHASE LOCK LOOP DEMODULATORS

10.1 Introduction

10.2 Basic PLL demodulator approaches

10.3 Circuit operation

10.4 First order phase lock loop demodulator

10.5 Second order phase lock loop demodulator

10.6 Third order phase lock loop demodulator

10.7 Discussion

10.8 References

11. FREQUENCY LOCK LOOP DEMODULATORS

11.1 Introduction

11.2 Basic operation of frequency lock loop demodulator

11.3 Analysis of the frequency lock loop FM demodulator (RF version)

11.4 Analysis of the frequency lock loop FM demodulator (baseband version)

11.5 Discussion

11.6 References

12. AUTOCORRELATION DEMODULATOR

12.1 Introduction

12.2 Basic operation

12.3 Brief analysis

12.4 Discussion

12.5 References

13. PHASE FILTER DEMODULATOR

13.1 Introduction

13.2 Analysis

13.3 Mathematical model

13.4 Discussion

13.5 References

14. SWITCHED CAPACITOR DEMODULATOR

14.1 Introduction

14.2 Principle of operation

14.3 Discussion

14.4 References

15. SPIKE CANCELLATION TECHNIQUES

15.1 Introduction

15.2 Loch-Conrad scheme

15.3 Discussion

15.4 References

16 MISCELLANEOUS THRESHOLD EXTENSION DEMODULATOR TECHNIQUES

16.1 Introduction

16.2 Envelope multiplication

16.2.1 General

16.2.2 Analysis

16.3 Optimum demodulation

16.3.1 General

16.3.2 Brief analysis

16.4 Discussion

16.5 References

17. EQUALITY OF THRESHOLD EXTENSION DEMODULATORS

17.1 General

17.2 Equivalence of PLL, FLL and FMFB Demodulators

17.2.1 Introduction

17.2.2 Frequency-locked loop equation

17.2.3 Phase-locked loop equation

17.2.4 FMFB demodulator defining equation

17.3 Discussion

17.4 References

18. AN ADAPTIVE THRESHOLD EXTENSION DEMODULATOR

18.1 Introduction

18.2 Adaptive threshold extension demodulator concepts

18.2.1 General

18.2.2 Error rate as a function of carrier-to-noise ratio

18.2.3 Estimation of probability of bit error rate from sync word error rate

18.2.4 Error rate as a function of modulation index

18.2.5 Error rate as a function of receiver bandwidth

18.2.6 Error rate as a function of offset frequency effects

18.2.7 Error rate as a function of interference

18.2.8 Summary of parameter variation on bit error rate

18.3 Error controlled adaptive threshold extension demodulator concepts

18.3.1 Error controlled adaptive threshold extension demodulator utilising a tracking filter

18.3.2 Error controlled adaptive threshold extension demodulator concepts applied to conventional TV systems

18.3.3 Error controlled adaptive threshold extension demodulator concepts applied to MAC/Packet TV systems

18.3.4 Error controlled adaptive threshold extension demodulator concepts

applied to Digital TV systems

18.4 Error controlled adaptive threshold extension demodulator design aspects

18.4.1 Centre frequency and bandwidth control

18.5 Alternative error controlled adaptive threshold extension demodulator concepts

18.5.1 General

18.5.2 FMFB error controlled adaptive threshold extension demodulator

18.5.3 Frequency lock loop error controlled adaptive threshold extension demodulator

18.5.4 Phase lock loop error controlled adaptive threshold extension demodulator

18.5.5 Envelope multiplication error controlled adaptive threshold extension demodulator

18.5.6 Other threshold extension demodulators

18.6 Discussion

18.7 References

19. DIGITAL TELEVISION SYSTEMS

19.1 Introduction

19.2 Digital TV systems

19.3 Digital demodulation

19.4 Discussion

19.5 References

20. SUMMARY AND CONCLUSIONS

20.1 Summary

20.2 Conclusion

20.3 Suggestions for future research

APPENDICES

A. Proposed U.S. Digital Television Standards

A.1 Introduction

A.2 Proposed standard

A.3 References

B. Television Standards for the Broadcasting Service

B.1 Introduction

B.2 Vision/Data multiplex structure

B.3 Vision coding

B.4 Data multiplex structure

B.5 Modulation parameters

C. DBS Link Calculations

C.1 Introduction

C.2 Analysis

C.3 Typical characteristics (clear sky)

C.4 Typical characteristics (rain)

C.5 Summary

C.6 References

D. Gaussian Angle Modulated Signal Bandwidth Relationships

D.1 Introduction

D.2 References

GLOSSARY

The following gives the list of principal symbols and abbreviations used in this thesis.

Abbreviations

AGC	-	Automatic Gain control
CCIR	-	Comité Consultatif International de Radiocommunication
CMOS	-	Complementary Metal Oxide Silicon
CNR	-	Carrier-to-noise ratio
DBS	-	Direct Broadcasting Satellite
EIRP	-	Effective radiated power above isotropic
erfc	-	Complimentary Error Function
ERP	-	Effective radiated power
FLL	-	Frequency lock loop
FMFB	-	Frequency modulation feed back
HDTV	-	High Definition Television
IF	-	Intermediate frequency
MPA	-	Microwave Power Amplifier
MPEG	-	Moving Picture Experts Group
NTSC	-	National television systems committee
PAL	-	Phase alternation by line
PDF	-	Probability density function
PLL	-	Phase lock loop
PSD	-	Power spectral density
PSK	-	Phase Shift Keying
RF	-	Radio Frequency
RGB	-	Red, Green and Blue
RLC	-	Resistor, inductor, capacitor
r.m.s.	-	Root mean square
SCO	-	Switched capacitor oscillator
SECAM	-	Séquentiel Couleur à Mémoire

SIS	-	Sound in Sync
SNR	-	Signal-to-noise ratio
TED	-	Threshold Extension Demodulation
TV	-	Television
TWT	-	Travelling wave tube
VCO	-	Voltage controlled oscillator

Symbols Used

A	FM propagating wave amplitude
A_c	Envelope of the signal
A_R	Attenuation due to rain and cloud formations
A_{eff}	Terrestrial TV receiver aerial effective aperture (square meters)
A_G	Gain of the feedback loop amplifier, which also provides a phase inversion
A_L	Limited amplitude of carrier
$a(t)$	Instantaneous signal amplitude
B	VCO sinusoidal output amplitude
B	A single-sided bandwidth
B_C	RF filter (rectangular) bandwidth, or Carson's occupied bandwidth rule (Hz)
B_i	Input noise bandwidth (Hz)
B_{IF}	Receiver (I.F.) bandwidth (Hz)
B_M	Baseband or modulating signal bandwidth (Hz)
B_N	Equivalent noise bandwidth of receiver (Hz)
B_{PD}	Post discriminator bandwidth (Hz)
b_0	3 dB bandwidth of single resonant circuit
b_1	Input I.F. bandwidth
C	Average (d.c.) values of the respective coefficient of the $\cos\omega_2 t$ and $\sin\omega_2 t$ terms
c	Velocity of light in a vacuum, $(2.998\times10^8\ m/s)$

$C(t)$	Signal output of RF filter
$c_1(t)$	Inphase component of signal
$c_2(t)$	Quadrature component of signal
C_i	Channel capacity (bits/second)
C_I	Input carrier power to demodulator
C_{IP}	Input carrier power
C/N	Pre-detection carrier-to-noise ratio in bandwidth, B_C , (dB)
C/N_0	System carrier power-to-noise spectral density ratio (dB/Hz)
C/T	System carrier power-to-noise temperature ratio (watts/K)
C_T	Input carrier power at threshold
$c(t)$	Respective values of the coefficient C less it's average value
$c(t)$	Signal vector
D	Average (d.c.) values of the respective coefficient of the $\cos\omega_2 t$ and $\sin\omega_2 t$ terms
D	Compression factor
D_{p-p}	Peak-to-peak deviation (Hz)
D_R	Terrestrial TV aerial effective diameter (metres)
D_T	Satellite transmitting aerial effective diameter (metres)
$d(t)$	Respective values of the coefficient D less it's average value
f	Frequency (Hz)
f_C	Centre frequency (Hz)
f_{CH}	Change in the instantaneous angular frequency produced by a change in control voltage (Hz)
F	Power ratio
f_M	Maximum baseband modulation (video) frequency (Hz)
F_{NF}	Terrestrial TV receiver noise figure (dB)
f_O	Carrier frequency (Hz)
f_{pd}	Peak deviation of the TV signal (Hz)
$F[R(t)]$	Function of $R(t)$ used for multiplication

f_v	Maximum modulation frequency (Hz)
$G(j\omega)$	Single-sided spectral density (watts/Hz)
G_0	Frequency sensitivity of VCO (rad / (s) (volt)), a constant
G_p	Phase comparator constant of proportionality
G_R	Terrestrial receiver aerial gain with respect to isotropic
$G_{R_{MAX}}$	G_R modified by losses
$G_S(f)$	Power spectral density of spike noise (watts/Hz)
G_T	Satellite transmitter aerial gain with respect to isotropic
G/T	Ratio of receiver gain to system noise temperature
H	Number of clicks per second at threshold
$H(f)$	Discriminator network transfer characteristic
$H_B(f)$	Baseband filter transfer characteristic
$H_{BP}(f)$	Limiter output bandpass filter transfer characteristic
$H_C(f)$	IF filter transfer characteristic
$H(s)$	Closed loop transfer function, or the transfer characteristic of a linear filter H
$H_+(t)$	Average number of positive clicks
$H_-(t)$	Average number of negative clicks
$h(t)$	Impulse response of a low pass filter
$h_L(t)$	Impulse response of low pass equivalent filter of the narrow band I.F. filter
$h_0(t)$	Impulse response of PLL loop filter
$I_1(x)$	Modified Bessel function of the first kind, of order n
$J_i(m_f)$	Bessel function of the first kind, of order n
k	Boltzmann's constant (1.38×10^{-23} J/K)
k_1	A constant
K	Temperature Degrees Kelvin
K_f	Loop scale factor
k_L	Conversion factor (6 dB) from r.m.s. to peak-to-peak deviation
K_T	Third order filter scale factor

k_W	Combined de-emphasis and weighting improvement factor specific to FM TV system
K_1	An arbitrary demodulator constant
K_ϕ	Third order filter scale factor
L	Laplace transform operator
L_A	Atmospheric attenuation (dB)
L_{FS}	Free space path loss (dB)
L_P	Total path loss, $(L_{FS} + L_A)$ (dB)
L_T	Edge of coverage footprint, -n dB contour, 3 dB
L_0	Polarisation loss (dB)
L_1	Loss between satellite transmitter and satellite aerial (dB)
L_2	Loss between terrestrial TV aerial and receiver (dB)
L_α	Receiving aerial pointing loss (dB)
$m(t)$	Frequency modulated baseband signal
N	System thermal noise (watts)
$N_a(t)$	Limiter discriminator output noise
N_C	Total number of spikes at discriminator output for unmodulated carrier
N_{DISC}	Total average number of spikes at discriminator output
N_F	Noise power of reference filter
N_G	Band limited Gaussian noise with respect to rectangular RF filter
N_{IF}	Mean squared I.F. noise for a rectangular I.F. noise spectrum of spectral density η
N_M	Input noise power in baseband bandwidth, B_m
N_s	Total spike noise spectral density (watts/Hz)
$N(t)$	Noise envelope referred to unit signal amplitude
N_0	Output noise power
N_T	Output noise power of adaptive filter
$N_1(s)$	Fourier transform of $N_1(t)$
$N_1(t)$	An independent Gaussian process

$N_2(s)$	Fourier transform of $N_2(t)$
$N_2(t)$	An independent Gaussian process
$n(t)$	Zero mean Gaussian noise at limiter - discriminator input
$n_c(t)$	Envelope of the noise component
$n_c(t)$	In phase component of noise that is a statistically independent zero-mean Gaussian process
$n_s(t)$	Quadrature component of noise that is a statistically independent zero-mean Gaussian process
$n_0(t)$	A noise waveform at the output of the demodulator
$n_1(t)$	A quadrature component of the relatively narrow band noise. It is an independent Gaussian variable having zero mean and variance σ^2
$n_2(t)$	A quadrature component of the relatively narrow band noise. It is an independent Gaussian variable having zero mean and variance σ^2
P_e	Probability of error
P_F	Output noise power of reference filter
P_I	Signal power at input of reference filter
$P(j\omega)$	Fourier transform of the spike waveform
P_R	Signal power at receiving aerial terminal (watts)
P_{RX}	Signal power at receiver input (watts)
P_S	Signal power
P_T	Isotropic radiated power of satellite transmitter (watts)
P_T	Output signal power of adaptive filter
P_{TW}	Power in an FM waveform of amplitude A
P_{TX}	Satellite transmitter power output (watts)
P_χ	Probability of observing χ errors in a digital (sync) word
R	Range of terrestrial receiver from satellite (metres)
$R_C(t)$	Envelope of waveform consisting of the superposition of a carrier of amplitude A_C and the noise $n_C(t)$
R_E	Information rate

$R(t)$	Envelope of waveform plus noise
r	Radius of gyration, in Hz
r_c	r.m.s. bandwidth of input noise spectral density
r_f	Radius of gyration of the single tuned filter (approximated by a Gaussian type filter with the same 3 dB bandwidth)
s	$\frac{d}{dt}$
s	$j\omega$
S_i	Signal input power (watts)
$S(j\omega)$	Double-sided spectral density (watts/Hz)
S/N	Ratio of peak-to-peak luminance amplitude in weighted r.m.s. noise
S_0/N_0	Output signal-to-noise ratio
$s_0(t)$	Signal at the output of the demodulator
S_o	Signal output power (watts)
T_A	Antenna noise temperature (K)
T_C	Mean time interval between demodulator spikes or clicks (sec)
T_E	Receiver noise temperature (K)
T_F	Thermodynamic temperature of terrestrial connection (K)
$T(f)$	Transfer function of adaptive filter
T_G	Ground noise temperature (K)
T_M	Mean thermodynamic temperature of rain and cloud formations (K)
T_R	Receiver noise temperature (K)
T_S	System temperature (K)
T_{Sky}	Noise contribution of clear sky (K)
T_0	Reference temperature, 290 K
t_n	Instant at which negative pulse (clicks) occur
t_p	Instant at which positive pulse (clicks) occur
$V_i(t)$	Signal input voltage
v	Frequency controlling voltage
v_{in}	Signal voltage input

v_{osc}	Voltage controlled oscillator output
$v_0(t)$	A voltage controlled oscillator output providing a carrier having a phase proportional to the integral of its input voltage
v_p	Multiplier or phase detector output
W_H	A double-sided bandwidth
W_L	Number of bits in a digital word
$w(f)$	Power spectrum
$X_c(t)$	Noise component inphase with signal
$x(t)$	In-phase component of $N(t)$
$Y_c(t)$	Noise component in quadrature with signal
$y(t)$	Quadrature-phase component of $N(t)$
$\lvert Y'(j\omega)\rvert^2$	Power spectral density of $Y'(t)$
α	Distance of the poles of $H_{IF}(s)$ from the imaginary axis in the complex s plane
α	Half power angular bandwidth of single tuned filter
α	A discriminator constant dependent upon limited signal amplitude
α_R	Maximum (receiving) antenna misalignment (degrees)
α_T	Angle formed from antenna boresight axis to edge of -N dB contour (degrees)
β	Modulation index
β_{rms}	r.m.s. modulation index
γ	Carrier-to-noise ratio for the single tuned filter output
Δf	Deviation
$\Delta(f)$	Signal modulation
Δf_{rms}	r.m.s. frequency change of the modulation signal; alternatively, variance of Gaussian spectral density
δf	Carrier frequency offset
δN	Increase in the number of spikes
ζ	Threshold level improvement factor

η	Noise spectral density of rectangle IF filter input (watts/Hz)
η_B	Ratio of bandwidths
η_i	Noise input power spectral density (watts/Hz)
η_O	Noise output power spectral density (watts/Hz)
η_1	Half power spectral density of $x(t)$ and $y(t)$
η_1	Satellite transmitting aerial efficiency
η_2	Terrestrial TV receiving aerial efficiency
θ	Satellite transmitting aerial beamwidth (degrees)
θ_c	Phase angle between signal envelope and resultant noise and signal vectors
$\dot{\theta}_c(t)$	Demodulated noise term
θ_M	PLL phase modulation error
$\theta(t)$	Noise phase
$\dot{\theta}(t)$	Instantaneous frequency
$\theta_1(t)$	Time varying phase of sinusoidal signals, with amplitude A and frequency ω
$\theta_2(t)$	Time varying phase of sinusoidal signals, with amplitude B and frequency ω
λ	Wavelength (metres)
$\lambda_c(t)$	Phase of the noise component
ξ_p	Damping ratio of the transfer function $H(s)$
ξ_z	Damping ratio of the transfer function $H(s)$
ρ	Carrier-to-noise ratio for twice baseband bandwidth
σ	A constant
τ	Differential group delay
ϕ_c	Phase of the signal
$\dot{\phi}_c(t)$	Demodulated signal
$\phi(t)$	Signal input whose Laplace transform is $\Phi(s)$
$\phi(t)$	Instantaneous signal phase
$\dot{\phi}(t)$	Output of the frequency locked loop
$\lvert\phi_e(j\omega)\rvert^2$	Power spectral density of $\phi_e(t)$
$\phi_e(s)$	Fourier transform of $\phi_e(t)$

$\phi_e(t)$	Phase error at the centre frequency of the I.F. filter
ϕ_r	Feedback phase
$\phi_i(s)$	Fourier transform of $\phi_i(t)$
$\phi_i(t)$	An independent Gaussian process
$\phi_i(t)$	Modulated signal phase
$\phi_n(t)$	Angular modulation due to the noise
$\phi_{osc}(t)$	VCO output phase
$\phi_s(t)$	Angular modulation due to the signal
χ	Number of errors in a digital (sync) word
$\psi(t)$	Modulated phase
$\psi(t)$	Phase angle difference of phase comparator input whose Laplace transform is $\Psi(s)$
$\psi_c(t)$	Phase of resultant signal and noise vector with respect to inphase signal vector
ω_c	An angular frequency (radians)
ω_1	Voltage controlled oscillator output frequency (radians)
$\omega_i(t)$	Instantaneous angular frequency (radians)
ω_2	Difference between the VCO output frequency ω_1 and the input frequency ω_o, (radians)
ω_i	Centre frequency of RF filter (radians)
ω_{IF}	Angular I.F. frequency
ω_{IP}	Input frequency (radians)
ω_M	Angular modulation frequency
ω_o	Centre frequency of the I.F. filter for a symmetrical passband (radians)
ω_o	Carrier frequency (radians)
ω_p	Zero resonant frequency in the complex plane (radians)
ω_r	VCO free running frequency (radians)
ω_S	Angular signal frequency
ω_z	Zero resonant frequency in the complex plane (radians)

ω_α	FLL attenuator characteristic
ω_β	Integrator constant

DEMODULATOR TECHNIQUES IN SATELLITE COMMUNICATION SYSTEMS FOR DIRECT BROADCAST SYSTEMS

1. INTRODUCTION

1.1 This thesis is concerned with the demodulator techniques used in satellite communication systems for direct broadcast systems (DBS) and with the improvements that may be made to them. DBS systems allow domestic TV receivers to receive broadcast signals direct from a satellite thus revolutionising domestic television reception. Potentially they allow the domestic user to receive a number of transmissions from one or more satellites. The problem investigated in this thesis is the threshold effect that occurs in angle modulated (e.g. FM) systems and in particular those FM demodulator techniques used in the receiver that reduce the threshold and allow an improved performance to be obtained with poor signal-to-noise levels. These FM demodulator techniques are generally called threshold extension demodulators (TED).

Increasing the sensitivity of the receiving system by means of threshold extension techniques offers a number of advantages. Firstly, they can be used to extend the footprint of the satellite. That is, they can be used to receive the TV signal over a wider area than that which can be received with conventional receivers. Alternatively they can be used to reduce the size of the receiving antenna. Currently this is a major and desirable objective with existing DBS systems. Thirdly, these threshold extension techniques can be used to reduce the satellite's RF transmitter power output. Some of these implementations allow significant cost reductions to be achieved in the TV receiver.

Although impressive results with experimental threshold extension demodulators have been reported, there is evidence in the published literature [1] that commercially manufactured

versions do not offer consistent 'extension' for all possible picture and sound material. The possible reason why is discussed elsewhere in this thesis and solutions offered to overcome this limitation.

1.2 The use of satellite transmission results in a different approach to system design compared to terrestrial systems. In the latter the objective is to reduce the cost of the domestic receiver; systems that achieve this objective use expensive, high power, transmitters. Thus in a terrestrial TV system the cost is contained in the (single) transmitter, resulting in the (many) receivers being low cost. In a satellite system however physical restrictions prevent the same approach being followed. The cost of putting a satellite into space is high. This results in the satellite payload being limited, which in turn restricts the amount of RF power that a satellite can radiate. Since the satellite is in synchronous orbit, some 19,300 miles above earth, the distance between the satellite and domestic receiver is much greater than in terrestrial systems, which are limited by line-of-sight considerations. This greater distance results in a much increased signal attenuation. This greater transmission range and low transmitter power characteristics of satellite TV systems result in a much lower signal level at the receiver antenna. To satisfy the communication link budget requirements, the receiver and antenna performance must therefore be enhanced. To ease the demands upon the link budget, satellite direct broadcast systems use FM techniques, since for the same transmitter power, these offer a greater sensitivity than other modulation systems.

A further significant difference between satellite and terrestrial television systems is the spectral occupancy (or bandwidth) used. Early terrestrial systems, which operated in the lower VHF bands (30 - 50 MHz), were required to utilise systems that minimised the bandwidth occupied. This led to the use of vestigial sideband modulation techniques. Satellite DBS systems however operate in the 11 to 12.5 GHz band and bandwidth, or spectral occupancy minimisation, is not a prime requirement. This allows a much higher data rate, or information content, and frequency modulation techniques to be used in DBS

satellite systems.

Domestic DBS TV receivers are thus faced with the problem of receiving a weak signal and of providing a TV picture with an acceptable performance. To achieve these objectives current DBS receiving systems contains a directional high gain antenna, which normally consists of a parabolic antenna, requiring a reasonable margin of pointing accuracy; a low noise head amplifier which for optimum performance is required to be placed near the feed of the high gain antenna system, and a down-converter for use with a conventional (terrestrial) TV receiver. The use of these sub-systems allows an acceptable carrier-to-noise ratio signal to be received within the satellite footprint. Threshold extension demodulators enhance the performance of the system in allowing a weaker carrier-to-noise signal to be received.

1.3 Section 2 of this thesis deals with the problem definition in terms of the need for threshold extension demodulator techniques. A summary of previous work is given that reviews noise in FM systems, threshold extension demodulators and those extension techniques that have been applied to television systems. The literature review carried out represents a significant component of the thesis and combines material from US patent literature with more conventional source materials from professional journals, conferences, textbooks, etc. Finally the approach to the problem followed in this study is described.

A description of direct broadcast satellite television systems is given in section 3. The relevant TV standards that are proposed for future applications are briefly described, namely the MAC format systems, and the design of a typical DBS satellite receiver and ground receiver is discussed. The latter is used as the baseline system for this study. As part of this reference baseline the performance of an overall DBS television link is calculated, and the link margins established.

Noise in FM is discussed in section 4, particularly as it affects the demodulator process. The

noise model developed by Rice is considered, which defines the model in terms of clicks and Gaussian noise, and its closeness to physical reality discussed.

Section 5 discusses the quality criteria used to assess the performance of the threshold extension techniques considered. A definition of threshold extension demodulation is given, together with the criteria used for carrier-to-noise and signal-to-noise ratio.

Using Rice's noise model the threshold characteristics of a conventional demodulator and an ideal demodulator are derived in section 6. These are used as baseline references in the comparisons made with the various threshold extension demodulator techniques.

Section 7 considers the general threshold extension demodulator problem, particularly in terms of DBS television systems. An important concept that illustrates how threshold extension is obtained, namely the tracking filter demodulator, is considered in section 8. In section 9 the characteristics of the FMFB demodulator are examined and in section 10 the Phase Lock Loop demodulator is analysed. Section 11 discusses the Frequency Lock Loop demodulator. Section 12 discusses the autocorrelation demodulator and section 13 considers a theoretical concept, that of the phase filter demodulator. A unique approach to demodulators that uses a switched capacitor approach, is discussed in section 14.

Section 15 describes the spike cancellation, or click elimination, technique. This is the only technique considered which does not rely on an effective reduction in bandwidth or carrier deviation to achieve an improvement in threshold. Miscellaneous threshold extension demodulator techniques are considered in section 16, consisting of the envelope multiplication method of threshold extension demodulation, and optimum demodulation.

On the basis of the studies carried out, the equality of various threshold extension demodulators is considered in section 17. It is shown that certain demodulators are derived from a basic type, except that the bandwidth varies with each version.

Section 18 discusses the limitations that have been encountered with the previous approaches to threshold extension techniques and an adaptive threshold extension demodulator is proposed which is intended to solve in part a number of deficiencies that occur with these previous types of demodulators. This adaptive approach utilises information contained within the signal structure to achieve an improved performance over a wide range of input carrier-to-noise ratios and picture content. It is shown how the relevant signal structures may be derived from conventional (PAL, SECAM and NTSC), MAC format and all-digital television systems. Illustrations are given that show how the adaptive demodulator concept can be applied to some of the existing threshold extension demodulators considered in this thesis, enhancing their performance for television picture reception.

Recent developments in all-digital television systems for future DBS applications are discussed in section 19, together with the impact that threshold extension demodulation techniques will have upon them.

Section 20 summarises the thesis together with the conclusions derived. Recommendations are given for future studies. Various appendices are included which discuss specific aspects in greater detail.

Finally a brief comment on the convention adopted for noise spectra. There are two conventions used in the literature, namely single-sided and double-sided noise spectra. Both concepts are used in this thesis, the notation used and the text makes clear which convention is being used in any particular application. Further discussion of this noise spectra convention is given in chapter 4.

1.4 References

[1] Gandy, G. "Satellite Links for Television Contribution", B.B.C. Research Department Report - BBC RD 1991/5.

Blank Page

2. PROBLEM DEFINITION

2.1 General

As satellite direct broadcast systems are power limited, frequency modulation (FM) is generally used. This allows a power-bandwidth trade-off to be made to satisfy the communication link margins.

FM systems like all angle modulated systems exhibit what is called a threshold in the relationship between the receiver input carrier-to-noise ratio and the demodulator output signal-to-noise ratio. The threshold point occurs when the input carrier-to-noise ratio is reduced to a point where the output noise (which is Gaussian in form) increases. A further reduction in the input carrier-to-noise ratio results in a change to the demodulator output noise statistics in that spikes or clicks appear at the output. These have a Poisson type distribution. The onset of these clicks or spikes is termed the threshold.

The point at which threshold occurs tends to be a function of the FM carrier deviation. For a conventional DBS demodulator this occurs at about an input carrier-to-noise ratio of 12 dB. This thesis is concerned with those demodulator techniques that offer a reduction in signal threshold, typically to a carrier-to-noise ratio of 7 or 8 dB.

Such a successful implementation of threshold extension techniques offers the following advantages:

(i) For a given performance implementing threshold extension demodulation techniques results in the lowest overall earth terminal cost. For example smaller receiving antennas can be used.

(ii) Satellites with a lower RF transmitter output can be used. This in current

satellite designs means that additional lower power TV channels could be provided from a high power satellite.

(iii) A larger coverage area (footprint) could be obtained from an existing satellite. Alternatively reception could be obtained from an adjacent satellite that is not intended to serve the area in which the specific TV receiver is sited.

(iv) Threshold extension demodulators can be used to provide an improved receiver signal quality for maximum transmission time regardless of the atmospheric conditions, i.e. the outage time is reduced. For a typical DBS system [35] the percentage time that the carrier-to-noise ratio of a signal exceeds a value of 12 dB is 99.9 %. If the threshold of the system was reduced to 8 dB the percentage time this latter value was exceeded would improve to 99.98 %.

(v) The improvement in system threshold performance that is obtained can be used to offset system losses such as antenna pointing errors, etc.

(vi) The improvement in system threshold performance may be sufficient to allow the antenna to be sited indoors, allowing the losses experienced with windows (some 4 dB) and some types of roof tiles to be overcome.

Thus in any angled modulated system, including those satellite TV receivers, threshold phenomenon is encountered which in areas of low signal strength can cause difficulties. The onset of threshold phenomena cannot be eliminated but it can be delayed by the use of a threshold extension demodulator. As FM is used exclusively for satellite direct broadcast systems and as FM demodulators exhibit a threshold effect, then at low carrier-to-noise ratios the link can be impaired severely by the threshold noise spikes appearing in the received picture. This is exacerbated when sound-in-sync (SIS) systems are used to carry

the companion sound channels. SIS being digital is prone to abrupt failure when threshold noise starts to appear. Currently the only practical approach to dealing with weak satellite signals is to increase the size of the terrestrial receiving station antenna.

2.2 Approaches to Problem

The approaches taken in this research programme to study the improvement in threshold characteristics of FM demodulators in direct broadcast satellite TV system is as follows:

(i) The definition of direct broadcast satellite TV systems in terms of the CCIR standards for existing and proposed systems, within which threshold extension demodulation techniques would be expected to operate.

(ii) The definition of a model that would best represent the noise characteristics of the FM demodulator at threshold and which would allow the effects of threshold extension techniques to be examined.

(iii) The investigation and definition of a suitable quality criterion which allows the improvements in performance to be determined and compared when examining the threshold extension characteristics of FM demodulator techniques.

(iv) The investigation of the theoretical characteristics of an ideal FM demodulator together with that of a conventional FM demodulator. The difference in threshold characteristics allowing the maximum performance in threshold extension that can be obtained to be determined.

(v) Examine the previously published work on FM demodulation techniques that have exhibited threshold extension characteristics and ascertain their performance in direct broadcast TV systems. The approaches that offer the

best performance can thus be identified.

(vi) Examine the commonalty of the various types of threshold extension demodulators to determine those approaches that are a variation of a common design approach. The aim is to achieve a common design approach that allows the performance advantage of each demodulator technique to be obtained under differing reception conditions.

(vii) From the results of the investigation into the various FM demodulator techniques, ascertain if an improved design can be postulated which offers advantages over existing approaches

2.3 Summary of Previous Work

The published literature on noise statistics and the performance of FM demodulators at threshold is considerable and reflects the difficult nature of the subject and the many unsolved problems remaining. An exhaustive and concise review of this literature would itself form a significant volume. The references discussed here have been selected predominately because of their relevance to the subject matter of this thesis. Each chapter lists the references to the major developments in threshold extension, relevant to that chapter, from when it was first proposed in 1939. Included in these are the relevant references to noise statistics and noise in FM systems, together with the use of threshold extension receivers. The literature review carried out represents a significant component of the thesis and combines material from US patent literature with more conventional source materials from professional journals, conferences, textbooks, etc.

Although there are references in the early literature to phase and frequency locked systems (Klapper and Frankle [1] is a detailed and excellent source) the starting point for threshold extension demodulators is that of Chaffee [2] in 1939, whose paper concerned the FMFB demodulator. The next significant development of this particular approach was reported by

Enloe [3], [4] in 1962 followed by Chaffee [5] in 1963.

Similarly for the phase lock loop (PLL) demodulator. Although the earliest reference to its use is in 1932 [1], the first significant publication was the paper by Jaffe and Rectin [6] in 1955. Most subsequent PLL work tends to take this paper as the starting point.

The frequency lock loop FM demodulator was described by Clarke and Hess [7] in 1967. There has been little subsequent work published on this technique. The concept is discussed in this thesis.

In 1968 Hess [8] published his note on equivalence of FM threshold extension receivers. This showed that the frequency lock loop (FLL) and the phase lock loop (PLL) were limiting forms of the frequency modulated with feedback demodulator (FMFB). This work is also discussed in this thesis.

Other threshold extension approaches are due to Park [9], Hamer [10], Mikael and Tu [11], Hummels [12], Murakami [13], Roberts [14], Guida and Schilling [15] and Galdos [16].

The threshold models used to analyse FM threshold receptions have been derived from the work of Rice [17] and Cohn [18].

The digital representation of the phase lock loop and its threshold is discussed by Garodnick, et. al. [19]. The interesting observations made in this paper do not appear to have attracted wide attention.

Non-demodulator (i.e. signal processing) techniques for improving the threshold are discussed by Brofferio [20].

A patent survey has disclosed several interesting approaches to threshold extension demodulation. Some of these are novel and others are just minor improvements to existing

techniques.

The basic threshold extension demodulator patents for the FMFB approach were obtained by Chaffee in 1937 [21] and 1942 [22].

The click elimination threshold extension demodulator was described by Loch and Conrad in their notable 1971 patent [23]. In this scheme they placed a click elimination device at the output of a conventional demodulator. Its object is to detect and eliminate the click that occurs in the discriminated signal at the onset of threshold.

Haggai in his 1971 patent [24] described a phase lock loop threshold extension demodulator. The scheme described is a basic phase lock loop but with a third order loop RLC filter.

Hess and Clarke described their frequency locked loop approach in their 1971 patent [25]. Like their article referred to above this gave few details of any practical results.

Bush et. al. in their 1976 patent [26] proposed an interesting variation of the phase lock loop approach. The scheme uses a click elimination system in conjunction with the PLL. Bush claims it differs from previous approaches in that the scheme detects the cause rather than the actual occurrence of the click impulse.

Rogers in his 1978 patent [27] described a further development of the FMFB approach. The scheme uses two pole crystal filters in the predetection filter in an attempt to achieve a more stable design. The approach does not appear to offer any great advantage.

Clayton and Livaditis in their 1978 patent [28] proposed a threshold extension demodulator for use with colour television signal reception. This elegant scheme uses an oscillating limiter proceeding the demodulator. This scheme is claimed to handle wideband colour signals. It is a development of Clayton's 1977 patent [29].

Jarger in his 1981 patent [30] described a technique based upon a FMFB approach, but with frequency drift correction. The scheme contains two feedback loops. One uses a phase detector that responds to the slight lack of alignment between the phase of the I.F. signal and the phase of the local oscillator. The other is the frequency compression loop. The invention is aimed at the reception of satellite signals. It is one of those rare patents that quotes a realistic improvement of performance of some 4 dB.

Mobley and Womble in their 1987 patent [31] described an interesting threshold extension technique. The approach is unusual and utilises a conventional limiter demodulator. It claims to achieve threshold extension by frequency selective phase modulation of the input FM signal in a bandpass filter to reduce phase error between the input and output of the filter. The design is intended to be used for FM satellite television signals. Broadly the technique consists of a means of utilising a filter ahead of the demodulator that has a narrower bandwidth than that required by the signal and uses phase modulation of the signal to reduce the resulting signal distortion.

O'Conner in his 1988 patent [32] described a threshold extension demodulator for satellite TV systems using a carrier tracking FM demodulator. The approach is unusual and has some similarity to the FMFB demodulator except that frequency compression does not occur at the input of the frequency detector. It also has some similarity to the tracking filter approach.

Naumann in his 1989 patent [33] for satellite multichannel telephone communications again based his approach upon a phase lock loop demodulator. He claimed an improvement in performance of some 7 dB. This value is interesting as all this technique appears to do is to match the bandwidth of the signal to the PLL. The bandwidth of the signal varies as the baseband telephone loading varies.

Mita and Koboyashi in their 1992 patent [34] disclosed a threshold extension receiver for DBS satellite television signals. The approach is basic and consists of a phase lock loop

system proceeded by an inverse limiting circuit. The system basically functions by rapidly reducing the input to a phase lock loop system when a weak signal is received. It relies on the basic characteristics of the PLL of its bandwidth being reduced when its input is reduced thus providing a threshold extension effect but with a reduced resolution. The inverse AGC circuit functions with a control signal that is a measure of the carrier to noise ratio. The viewer is intended to act as the assessor of the carrier to noise ratio and manually adjust the control signal.

2.4 References

[1] Klapper, J., Frankle, J. T. "*Phase-Locked and Frequency-Feedback Systems*", Academic Press, (1972).

[2] Chaffee, J. G. "Application of negative feedback to frequency modulated systems", B.S.T.J., Vol. 18, (July 1939), pp. 404-437.

[3] Enloe, L. H. "Decreasing the threshold in FM by frequency feedback." Proc., No. 1, Vol. 50, (Jan. 1962), pp. 18-30.

[4] Enloe. L. H. "The synthesis of frequency feedback demodulators." Proc. Nat. Elect. Conf., Vol. 18, (1962), pp. 477-497.

[5] Ginger, A. J., Chaffee, J. G. "The FM demodulator with negative feedback." B.S.T.J., Vol. 42, (1963), pp. 1109-1135.

[6] Jaffe, R., Rechtin, E. "Design and performance of phase - lock circuits capable of near optimum performance over a wide range of input signals and noise levels." IRE Trans. Inform. Theory. Vol. IT-1, 66, (1955).

[7] Clarke, K. K., Hess, D. T. "Frequency locked loop FM demodulator" IEEE Trans.

Com. Tech., Vol. COM-15, No. 4, (August 1967) pp. 502-506.

[8] Hess, D. T. "Equivalence of FM threshold extension receivers." IEEE Trans. Comms. Tech. (October 1968) pp. 746-748.

[9] Park, J. H. "An FM Detector for Low S/N," IEEE Trans. on Communication Technology, Vol. COM - 18, No. 2, April 970, pp. 110 - 118.

[10] Hamer, R. "Autocorrelation Threshold - Extension Demodulator," Proc. IEE, Vol. 117, No. 6, June 1970, pp. 1073 - 1081.

[11] Mikhael, W. B., Tu, S. "Frequency Compression Employing Switched Capacitor Oscillators (SCO's) and its application to FM Detection," IEEE Int. Symp. Circuits and Systems 1981. pp. 58 - 61.

[12] Hummels, D. R. "Phase Filter. An Untested Demodulator", Electronic Letters. Vol. 5. No. 26., 27th December 1969, pp. 720-721.

[13] Murakami, T. "Analysis of multiple signal FM Detection System", RCA Review, 1966, **27**, p. 425.

[14] Roberts, J. H. "*Angle Modulation*," England, Peter Pereginus, 1977.

[15] Guida, A., Schilling, D. L. "Optimum frequency modulation receivers." Proc. Int. Comms. Conf., 1967, p.58.

[16] Galdos, J. I. "A lower bound on filtering error with application to phase demodulation." IEEE Trans. Inform. Theory. Vol. IT-25, (July 1979), pp. 452-462.

[17] Rice, S. O. "Statistical Properties of a Sinewave plus Random Noise." B.S.T.J.,

Vol. 27, (Jan. 1948), pp. 109-157.

[18] Cohn, J. "A new approach to the analysis of FM threshold reception." Proc. Nat. Elect. Conf., Vol. 12, (1956), pp. 221-236.

[19] Garodnick, J., Greco, J. and Schilling, D. L. "Response of an all digital phase lock loop." IEEE Trans. Comms., Vol. COM-22, No. 6, (June 1974), pp. 751-763.

[20] Brofferio, S., Rocca, F. "Threshold extended FM demodulator for black and white video signal." IEEE Trans. Comms., (April 1972), pp. 235-242).

[21] Chaffee, J. G., US Patent 2,075,503 (March 1937)

[22] Chaffee, J. G., US Patent 2,272,401 (February 1942)

[23] Loch, F. J., Conrad, W. M. "Frequency - Modulation Demodulator Threshold Extension Device", U.S. Patent 3,588,705, June 28th, 1971.

[24] Haggai, T. F. "Threshold extension phase lock demodulator." US Patent 3,611,168 (Oct.5, 1971).

[25] Hess, D. T., Clarke, K. K. "Frequency demodulator for noise threshold extension" US Patent 3,611,169 (October 5th, 1971).

[26] Bush, J. A., Lance, D. R. and Alstatt, J. E. "Frequency modulation demodulator threshold extension device." US Patent 3,983,488 (Sept. 28, 1976).

[27] Rogers Jr., W. D. "FM feedback demodulator having threshold extension circuit with two pole crystal filter." US Patent 4,087,756 (May 2, 1978).

[28] Clayton Jr., L., Livaditis, E. "Threshold extension FM demodulator apparatus for wide bandwidth FM signals." US Patent 4,101,837 (July 18, 1978).

[29] Clayton, L. "FM noise threshold extension demodulator apparatus." US Patent 4,035,730 (July 12, 1977).

[30] Jarger, H. F. "Frequency modulation threshold extension demodulator utilising frequency compression feedback with frequency drift correction." US Patent 4,293,818 (Oct. 6, 1981).

[31] Mobley, J. G., Womble, D. P. "FM demodulator system with threshold extension", US Patent 4,698,598 (Oct. 6, 1987).

[32] O'Connor, E., "Threshold Extension FM Demodulator Apparatus and Method," US Patent 4,777,449. October 11th, 1988.

[33] Naumann, G. R. "Adaptive FM threshold extension demodulator", US Patent 4,816,770 (Mar. 28, 1989).

[34] Mitra, H., Kobayashi, K. "FM signal detection apparatus with automatic gain control circuit connected to phase detector input terminal". US Patent 5,175,881 (Dec. 29, 1992).

[35] CCIR, "Systems for the broadcasting service (sound and television)", Report No. 215-7, 1990.

Blank Page

3. DIRECT BROADCAST SATELLITE TELEVISION SYSTEMS

3.1 General

This chapter discusses the characteristics of the main satellite broadcast systems that have been developed for television transmission with sound and data services. In particular those parameters that influence the design of threshold extension demodulators are identified.

At the time of writing (1994) many systems are being considered or have been proposed for future domestic TV applications, including digital television systems. In this study only those direct broadcast TV systems that have been adopted, or are seriously being considered for adoption by at least one national administration, are listed. The DBS standards proposed for these systems are discussed below. Where relevant the characteristics of the D2-MAC/Packet system have been used in various threshold extension techniques considered in this thesis.

One significant recent development was the vetoing in 1993, by the UK Government, of the D2-MAC system for the future UK high definition TV system (HDTV). The UK proposes to support in its place the use of digital TV for future HDTV direct broadcast systems. Parameters postulated for these proposed digital systems are discussed below.

Based upon these analogue direct broadcast TV standards the design of a typical satellite television transmitter and terrestrial TV receiver is discussed. The various threshold extension demodulators analysed herein will be considered in relation to these typical systems.

Finally the performance of this typical DBS satellite link will be considered in terms of the various system standards. The performance will define the baseline against which the various threshold extension demodulator techniques will be judged.

3.2 Direct broadcast satellite television systems

3.2.1 The terrestrial colour television systems (PAL, SECAM and NTSC) currently in national use were designed several decades ago with the prime requirement to be compatible with reception on the monochrome TV receivers in use at time. The extra colour information had to fit within the existing channels of limited bandwidth. This led to a compromise in the way that these conventional colour systems carried information, having to share part of the bandwidth already occupied by the luminance signal. Adding this colour information in the form of a colour subcarrier introduces spurious patterning effects where the receiver mistakes the high frequency luminance details for colour information.

The development of geostationary satellites in an orbit some 22,300 miles above the earth's surface allows television systems to be used which broadcast directly into the home. Figure 3/1 illustrates the basic scheme used and the major subsystems used in the domestic receiving installation.

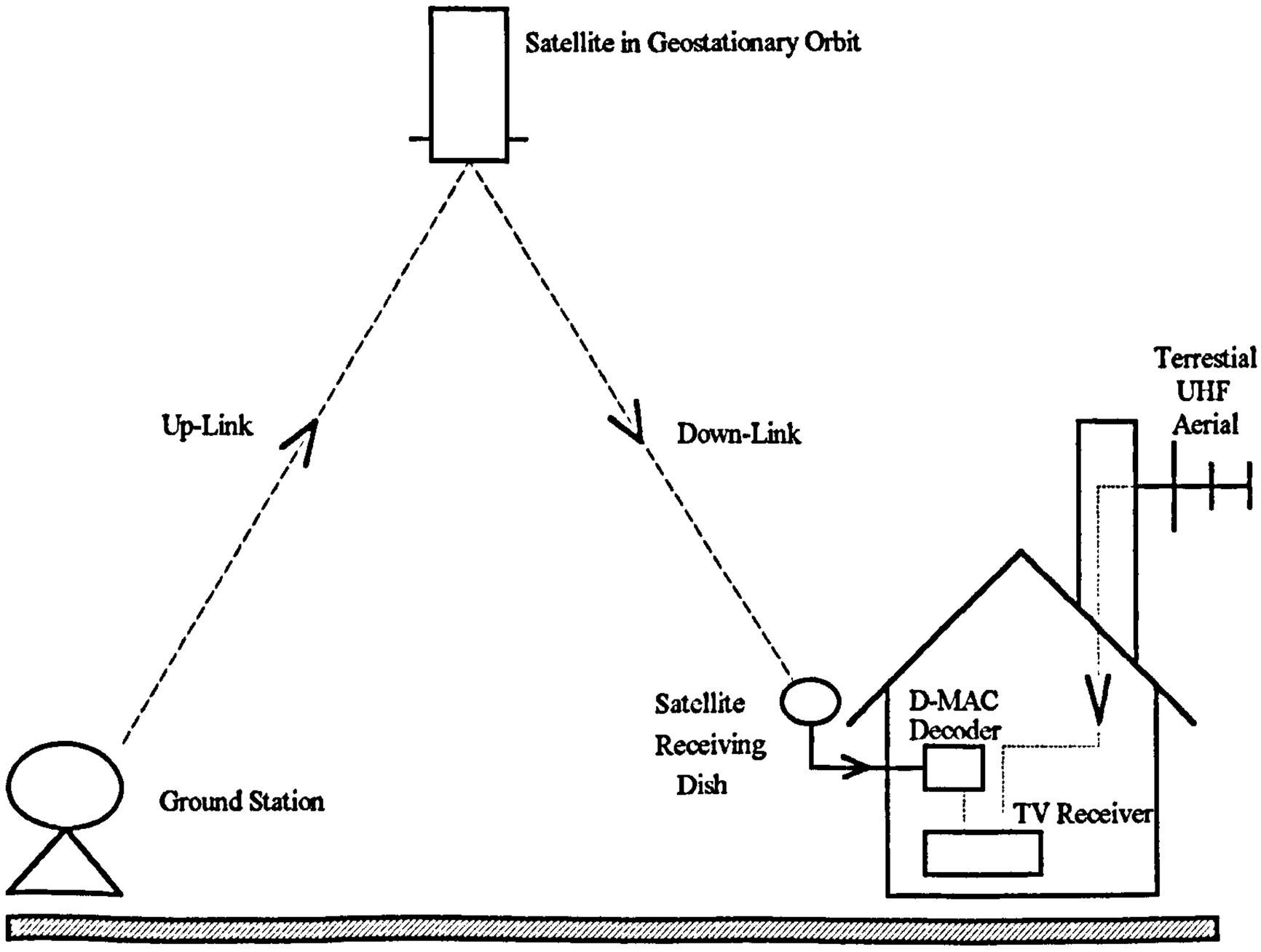

Figure 3/1 - DBS Domestic Link

In Europe these satellite television systems operate directly in the band 11.7 to 12.5 GHz.

Unlike terrestrial television systems that use amplitude modulation (AM), satellite television systems use frequency modulation (FM). This is done to minimise the power required to be transmitted by the satellite. A feature of FM systems is that the received noise increases with the baseband frequency, unlike AM systems where the noise is constant. This means that for those satellite television systems, which have adopted the terrestrial television systems of PAL, SECAM or NTSC, the colour subcarrier is subjected to a disproportionate amount of noise. The result is increased susceptibility to noise in the coloured areas of the picture. Figure 3/2 illustrates the baseband spectrum for the PAL system.

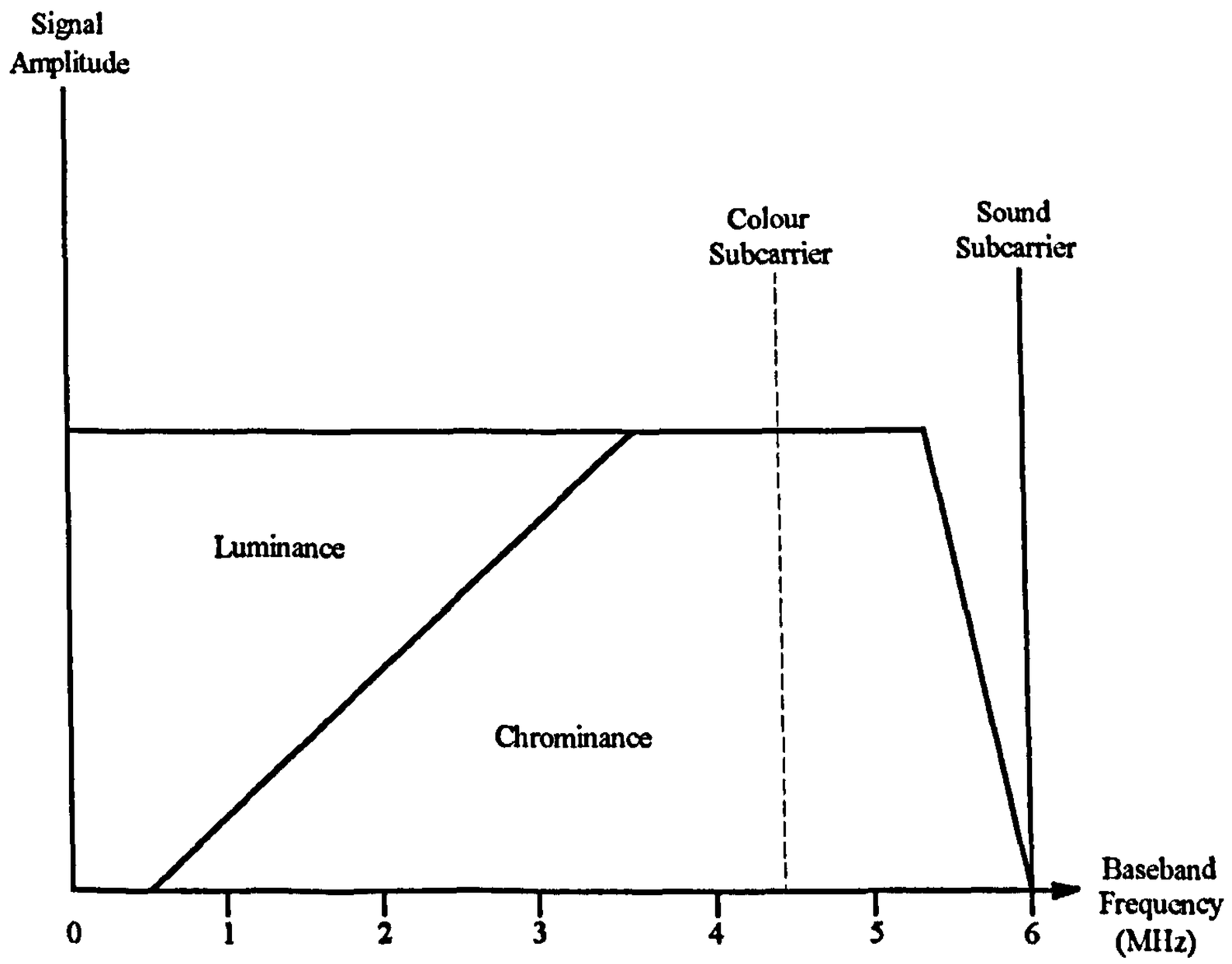

Figure 3/2 - PAL System 1 Baseband Spectrum

With a new transmission band and wider channels, direct broadcasting from satellites has created the opportunity for newer television systems that overcome the deficiencies of the traditional systems. The D-MAC/Packet system has been designed to meet both the needs of satellite broadcasting and cable distribution well into the next century. The luminance and colour components of the picture are kept completely separate eliminating the cross-colour patterning effects of PAL, figure 3/2, and giving clearer, sharper pictures. Sound quality is also improved making use of digital techniques. D-MAC offers up to eight high quality sound channels allowing the use of (say) multi-language broadcasts. This digital data

stream, that carries the sound can also contain other services such as teletext. D-MAC has also considerable inbuilt development potential allowing the introduction of wide-screen and higher-definition television pictures without making existing receivers obsolete.

Whatever system is used for DBS, viewers will need to obtain new equipment (receiving dish, down-converter and set-top adapter); it is therefore better for a system to be adopted which offers improvements and is better matched to FM transmission, than continue to use the terrestrial systems from the past (PAL, SECAM and NTSC). Such a system is D-MAC/Packet.

3.2.2 The basic principle behind the MAC range of TV systems is the use, in time-sequence, of separate signals for luminance and colour difference. There are no subcarriers; instead the luminance and colour-difference video signals are time-compressed before transmission, as shown in figure 3/3.

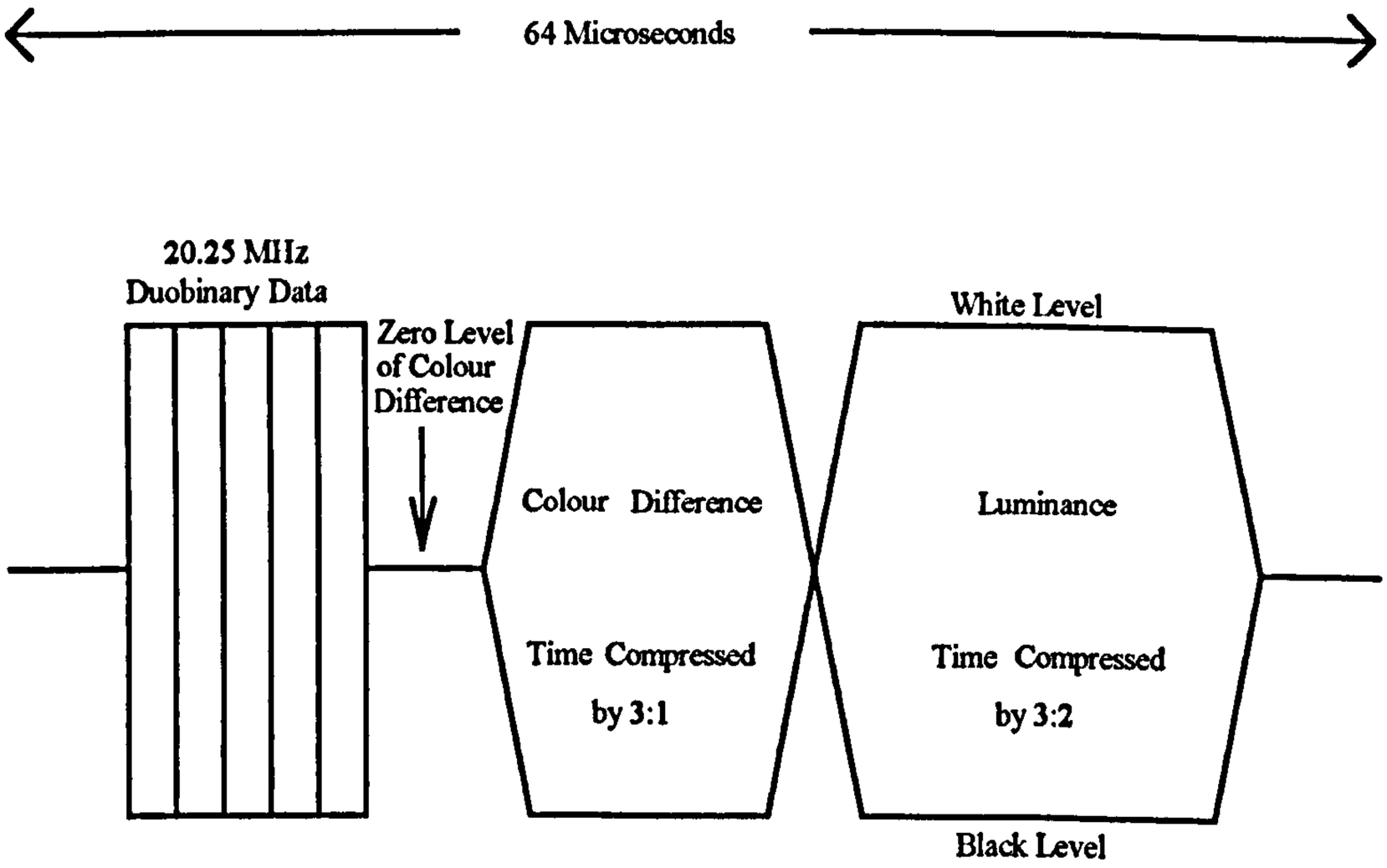

Figure 3/3 - D-MAC Baseband Video Waveform

Within the time occupied by one conventional line period, 64 microseconds for 625 line systems, it is possible to include one of the colour-difference components followed by the luminance. For the colour difference components, alternate lines contain U and V, the blue

and red difference signals.

Each line of luminance is compressed by a factor of 3:2, and this reduces the time occupied from 52 microseconds to approximately 35 microseconds. Similarly each line of colour-difference is compressed by a factor of 3:1 reducing the time to about 17.5 microseconds.

The process of time compression results in an increase in baseband bandwidth. For luminance the maximum uncompressed video bandwidth is about 5.7 MHz. Following compression, prior to modulation, the picture signal occupies a bandwidth of about 8.5 MHz.

3.2.3 In the D-MAC system unused portions of the video signal before the start of each picture line carry a high capacity digital data signal in place of the inefficient synchronising pulses of conventional television signals.

This data signal occupies a nominal 10 microseconds of each line period and consists of a 20.25 MBit/s duobinary data burst inserted in the line at baseband frequencies. Each line carries 206 bits of data resulting in a mean data capacity of some 3 MB/s. Line 625 is occupied entirely by the data signal and conveys 1296 bits.

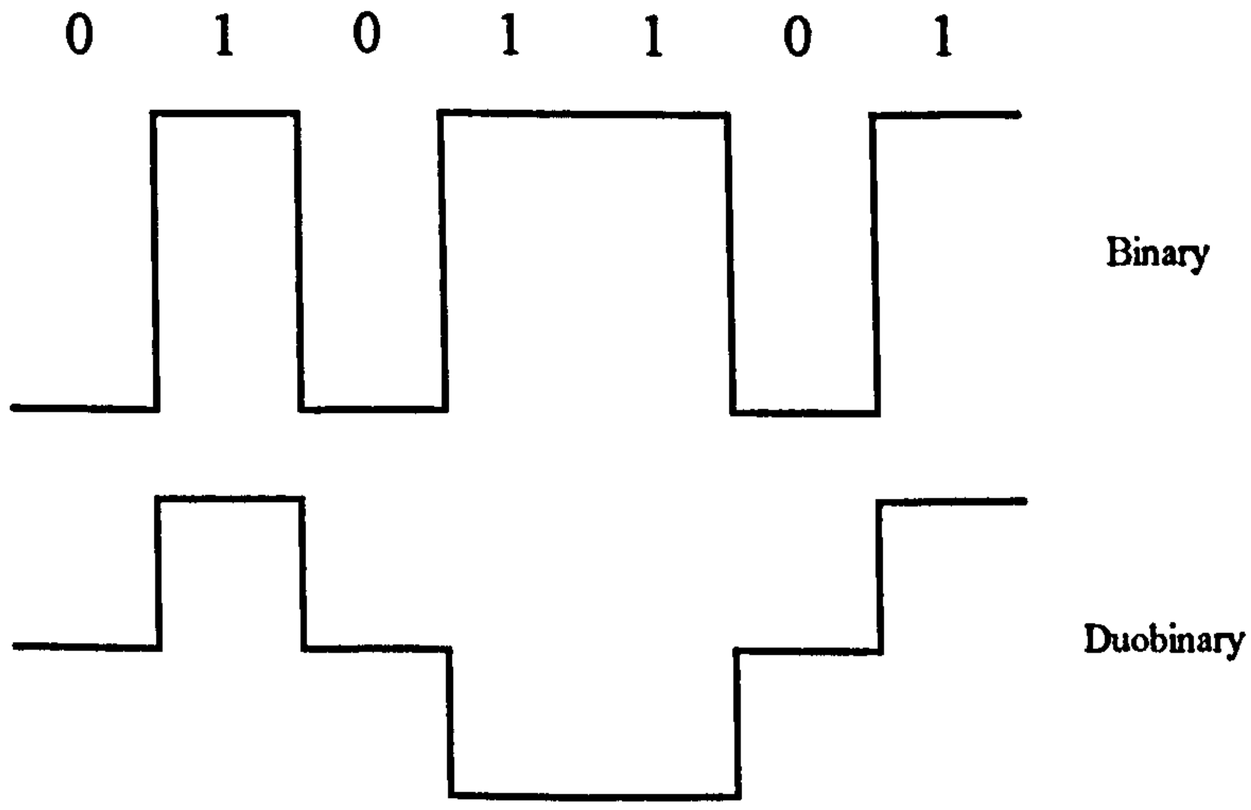

Figure 3/4 - Comparison of Duobinary and Binary

Duobinary (three-level) coding, figure (3/4), allows a data signal to be carried in a narrower bandwidth than would be required for a binary (two-level) coding system. The data signal can be one of three levels, the extremes representing a '1' and the intermediate level '0'. This arrangement allows a 20.25 MBit/s data rate to be occupied by the MAC vision signal. After low-pass filtering, the duobinary data signal is time-division multiplexed with the time compressed vision signal.

3.2.4 The digital data is organised into packets, each containing 751 bits. Each television frame of 625 lines carries 164 packets, with a total capacity of 4,100 packets/sec, figure 3/5.

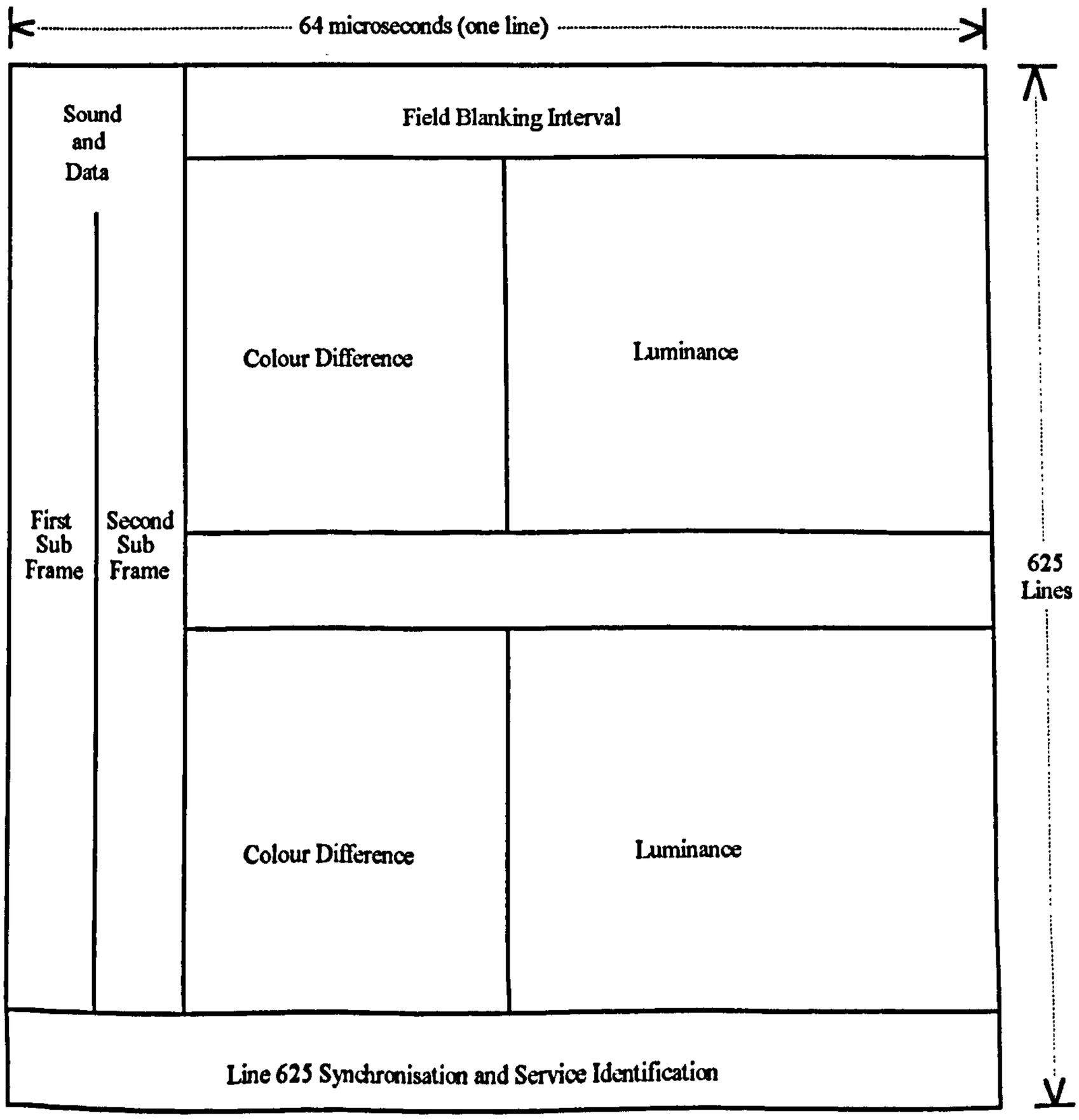

Figure 3/5 - D-MAC/Packet Frame (Simplified Structure)

Each packet contains data relating to a particular service, such as a sound channel. A sound or data channel is made up from data from many such packets, for high quality sound some

500 to 900 packets/sec. would be used.

Each individual data packet incorporates an address to identify which service it belongs to. Packets with address '0' serves a particular function in forming the service identification channel. This channel informs the receiver as to the number and type of services available. This (say) would allow a list of options to be displayed on the screen, allowing the viewer to select which to receive, e.g. a sound channel in a particular language or a teletext service.

In the absence of vision the entire signal could be used to carry data. This would give a vast increase in capacity, by a factor of more than six.

3.2.5 The digital sound system offers high quality stereo, with the possibility of additional multi-language sound channels. High quality sound with an audio bandwidth of 15 kHz, using a digital sampling rate of 32 kHz, is offered by either linear coding of 14 bit/sample or near instantaneous companding (NICAM) of 14 bits/sample. The latter option is the coding method that has been adopted for digital stereo for the UK terrestrial networks. It is the preferred option for UK DBS.

Medium quality sound channels for commentary purposes can be provided by using a digital sampling rate of 16 kHz giving an audio bandwidth of 7 kHz. As many as 16 sound channels could be provided if the data multiplex was devoted exclusively to this level of sound quality.

Within the overall data capacity of the system, approximately 3 MBits, the numbers and type of sound channels can be varied at any time to suit the particular needs of the programme, thus providing a very flexible system.

3.2.6 The introduction of the D-MAC system allows a more efficient synchronisation system to be used. It allows the inefficient conventional synchronisation pulses to be dispensed with. Instead data at the beginning of each line includes six synchronisation bits.

The pattern of these bits varies from line to line, whilst towards the end of each frame the pattern changes, signalling the start of the next frame. An alternative method of synchronisation is available from a fixed pattern of bits in line 625 that signals the start of each frame.

The original intention was that all UK DBS vision signals would be scrambled whether intended for free access, subscription or pay-per-view. A vision scrambling system known as 'double cut' component rotation has been proposed. This renders the picture unwatchable unless the receiver is equipped with the 'key' to unlock the signal. Given the correct key, it is no more difficult for the receiver to recreate a picture whether the signal is scrambled or not. Part of the digital data capacity will be used for an over-air addressing system to transmit the key. In the case of subscription or pay-per-view services the correct key will be provided, by the programme controller, to individual receivers or groups of receivers as appropriate.

3.2.7 In the D-MAC system one or more teletext services can be carried in the form of packet data. The satellite receiver indoor unit would either include its own teletext decoder or would recode the data into the vertical interval for use with an existing teletext receiver.

Using the packet multiplexer to carry teletext can give a much higher data capacity than is possible with conventional terrestrial teletext transmission. It will allow advanced forms of teletext to be introduced.

D-MAC vision decoders will be equipped with two sets of expansion ratios. This will allow pictures with an aspect ratio of 16 to 9 to be transmitted for wide screen display. Conventional receivers will automatically display the appropriate portion of the wide-screen image. This is achieved in the vision decoder by expanding the luminance by a factor of 2:1, instead of 3:2, and the colour difference by 4:1, instead of 2:1. It is proposed that the portion of the wide screen image to be displayed on a conventional receiver could be varied from scene to scene.

D-MAC has the capacity for further development leading to higher definition television (HDTV). One technique proposed is where the control data is carried in the vertical blanking interval, enabling a special receiver to reconstruct a 1250 display. It is intended that the introduction of HDTV would not be at the expense of compatibility with conventional D-MAC receiving equipment.

DBS reception of D-MAC is rugged offering better pictures than PAL or SECAM when the signal is weak. Combined with the general improvements in the performance of the overall system, the viewer will be offered superior performance and facilities with these future systems. The use of threshold extension demodulator techniques will enhance this performance even further.

The design of the DBS uplink television transmitter and downlink terrestrial receiver is discussed in section 3.4 and 3.5 below.

3.3 DBS Standards

3.3.1 Sources

Television standards for the broadcasting satellite service are currently defined by two CCIR reports, [7] and [8]. For the purpose of this thesis the former report tends to be more useful in the way the parameters are defined, presented and compared.

The basic characteristics of the systems adopted for satellite television broadcasting systems are discussed below and summarised in Appendix B of this thesis. Certain of these systems have adopted the general principle of time division multiplexing since it permits an improvement in the quality of the signals by eliminating in particular the problems of intermodulation and cross colour. A time division multiplex structure also permits future expansion of the system, e.g. wide screen aspect ratio pictures can be transmitted.

All the systems described below use digital techniques for sound and data in order to utilise to the greatest extent channel capacity. Possibilities of scrambling the signal for secure transmission and controlled reception is increasingly viewed as an important feature of such systems.

3.3.2 MAC/Packet systems

The MAC/Packet system standards contain four members, three of which are preferred for satellite broadcasting. These are C-MAC/Packet, D-MAC/Packet and D2-MAC/Packet; the fourth non-preferred member is B-MAC/Packet. These meet the various broadcasting-satellite service requirements in the 12 GHz band where the 625 line standard is used with a 27 MHz bandwidth. These three systems contain the following common features:

(i) Time Division Multiplexing.

(ii) MAC picture coding, with capacity for extended aspect ratio.

(iii) Packet multiplexing for sound and data.

(iv) Digital high and medium sound coding and error protection.

(v) Full channel digital mode, when the area of the television frame normally reserved for the MAC vision signal, and its blanking interval, is replaced by a data burst.

The close relationship between these systems allows for the development and introduction of receivers capable of functioning with all the standards. For completeness details of the fourth system (B-MAC/Packet) are also given.

(a) C-MAC/Packet

The C-MAC/Packet system was in part, developed to provide a high data channel capacity. The particular features of the C-MAC/Packet system are:

(i) The use of an RF time division multiplex wherein the carrier is frequency modulated by analogue picture signals during a certain fraction of line duration and 2-4-PSK modulated during the remainder of the line duration by a multiplex conveying several sound channels, synchronisation and data signals. Appendix B, section B.1 shows that nominal vision bandwidth (8.4 MHz) with this technique, is greater than for the other MAC systems.

(ii) The capacity of the sound/data multiplex is about 3 MBit/s, equivalent to eight high quality sound channels of 15 kHz bandwidth with near instantaneous 14/10 companding (protected by one parity bit per sample). The spare data capacity can be used for other services.

(b) <u>D-MAC/Packet</u>

One of the objectives in developing the D-MAC/Packet system was to provide a high data channel capacity and a single baseband interface to other transmissions and distribution media. The principle features of the D-MAC/Packet system are:

(i) A baseband time division multiplex in which the analogue picture signals are combined with duobinary encoded digital sound, synchronisation and data signals.

(ii) The capacity of the sound/data multiplex is approximately 3 MBit/s, equivalent to eight high quality sound channels of 15 kHz bandwidth with near instantaneous 14/10 bit companding (protected by one parity bit per sample). The spare data capacity can be used for other services.

(iii) The single baseband representation of the time division multiplex signal is frequency modulated for satellite broadcasting. Appendix B, section B.5 gives the modulation parameters.

(c) D2-MAC/Packet

The D2-MAC/Packet system developed to provide a single broadband interface to other transmission and interface media. The particular features of the D2-MAC/packet system are:

(i) A baseband time division multiplex in which an analogue picture signal is combined with duobinary encoded digital sound, synchronisation and data signals.

(ii) The capacity of the sound/data multiplex is about 1.5 MBit/s, equivalent to four high quality 15 kHz sound channels with near instantaneous 14/10 bit companding (protected by one parity bit per sample). The spare data capacity can be used for other services.

(iii) The single baseband representation of the time division multiplex signal is frequency modulated for satellite broadcasting. Appendix B, section B.1 shows that the nominal transmitted vision bandwidth (6.3 MHz) is less than the D-MAC system at 7.5 MHz. The occupied data spectrum is halved at 5 MHz.

(d) B-MAC Systems

Implementations of the B-MAC system have been developed for the 525 and 625 line applications. Both systems are well suited for use in DBS service applications in the 12 GHz band using either 24 MHz and 27 MHz channelling. The particular features of the B-MAC system are:

(i) The B-MAC signal is a baseband time division multiplex comprising analogue picture signals combined with four (or two) level data burst containing digital sound, synchronisation and data information.

(ii) Vision signal coding is performed using the time compression factors used in the C-MAC/Packet and D2-MAC/Packet systems. The clock frequencies of 625/50 and 525/60 are the same multiples of the relevant line scan frequencies. In the 525 line version the clock frequencies are simply related to the NTSC subcarrier frequency, facilitating simple transcoding to NTSC. Both B-MAC systems can be configured to permit transmission of pictures with 16:9 aspect ratios. The nominal transmitted vision bandwidth is the lowest of all the MAC systems at 4.5 MHz (Appendix B, section B.1).

(iii) The B-MAC system provides a total data capacity of approximately 1.6 MBs. This can be used to provide six high quality 15 kHz audio channels using adaptive delta modulation that features error concealment and parity protection. Alternatively these channels may be configured as 204 kBit/s data channels. A utility data channel makes use of spare capacity in the data multiplex.

(iv) Included in the B-MAC structure is a conditional access system based on line translational scrambling for video and data encryption for digital audio. The B-MAC system provides a single baseband interface to other transmission and distribution media.

3.3.3 D2-MAC/Packet parameters relevant to threshold extension demodulators

The basic characteristics of the D2-MAC/Packet system relevant to the threshold extension demodulator calculations carried out in this thesis are given below. The parameters are derived from the tables given in Appendix B.

Nominal transmitted vision bandwidth - 6.3 MHz

Frequency Deviation sensitivity - 13.5 MHz/volt

Nominal vision amplitude - 1 volt peak-to-peak

Nominal channel bandwidth - 27 MHz

Although the CCIR MAC standards do not give the value of the modulation index and the maximum baseband frequency (vision plus sound and data), an estimate may be made of these parameters using the modulation values given above. Firstly the transmitted signal must be contained within the occupied bandwidth, B_C , specified at 27 MHz. The nominal transmitted vision bandwidth is 6.3 MHz. To allow for the additional bandwidth incurred by the sound and data channels, the CCIR suggest that this figure is increased by 10 %, to say 7 MHz. Thus $f_M = 7$ MHz.

Now from Carson's Rule (section 5 below):

$$B_C = D_{p-p} + 2 f_M \qquad \text{..... (3-1)}$$

$$27 = D_{P-P} + (2*7)$$

$$\therefore \quad D_{P-P} = 27 - 14 = 13 \text{ MHz}$$

Using the alternative form of Carson's Rule gives:

$$B_C = 2 (\beta + 1) f_M \qquad \text{..... (3-2)}$$

$$\therefore \quad \beta = \frac{27}{2*7} - 1 = 0.93$$

From the above the peak-to-peak deviation appears to tend to the specified deviation sensitivity and nominal peak-to-peak vision amplitude, and the modulation index tends to unity.

Therefore the modulation parameters that will be used for the D2-MAC/packet applications considered in this thesis are:

Modulation index $\beta = 0.93$

Occupied channel bandwidth $B_C = 27$ MHz

Maximum component baseband signal bandwidth $f_M = 7$ MHz

Peak-to-peak deviation $D_{P-P} = 13$ MHz

A point to note is that this value of maximum baseband bandwidth is contradicted by

another CCIR report [9, page 255] which states that the D2-MAC/Packet baseband signal is transmitted with a bandwidth of at least 8.4 MHz. For the occupied channel bandwidth specified this gives a modulation index of the order of 0.6, which is rather low for a system of this nature. This thesis will use the lower figure of 7 MHz derived from the standards.

3.3.4 Digital TV parameters relevant to threshold extension demodulators

At the time of writing (1994) little information is available about the parameters of the proposed future DBS digital television system(s). Thus for the purpose of this thesis a hypothetical digital system will be postulated using the following assumptions. Firstly any future digital DBS system will be expected to conform to the maximum channel allocation, namely 27 MHz, that has been assigned to current analogue DBS systems. From this allocation the maximum bit rate can be determined if the baseband signalling code is assumed. Here the simplest will be assumed, namely NRZ-L. For such a baseband code, optimum performance is approached when the maximum bit rate is assumed to be equal to the occupied bandwidth, viz. 27 Megabits. This typically is the order of bit rate expected to be transmitted as some form of data compression will be used, see section 19 below. Therefore the modulation parameters that will be used for the D2-MAC/packet applications considered in this thesis are:

Occupied channel bandwidth $B_c = 27$ MHz

Baseband signalling code = NRZ-L

Maximum bit rate = 27 Megabits

3.4 Typical satellite television transmitter

A typical satellite transmitter intended for the MAC DBS television service was described by Neuman and Vargas [1] in 1988. This satellite was intended to provide shaped beam coverage of the UK. To meet the specified high power requirements each spacecraft was to broadcast three 110 watt channels in MAC format. For a reliable design the required 110 watts per channel is provided by operating two 55 watts travelling wave tubes (TWT) in parallel. A block diagram of the proposed transmitter is shown in figure 3/6 and the

characteristics of the proposed satellite communications subsystem are given in table 3-1.

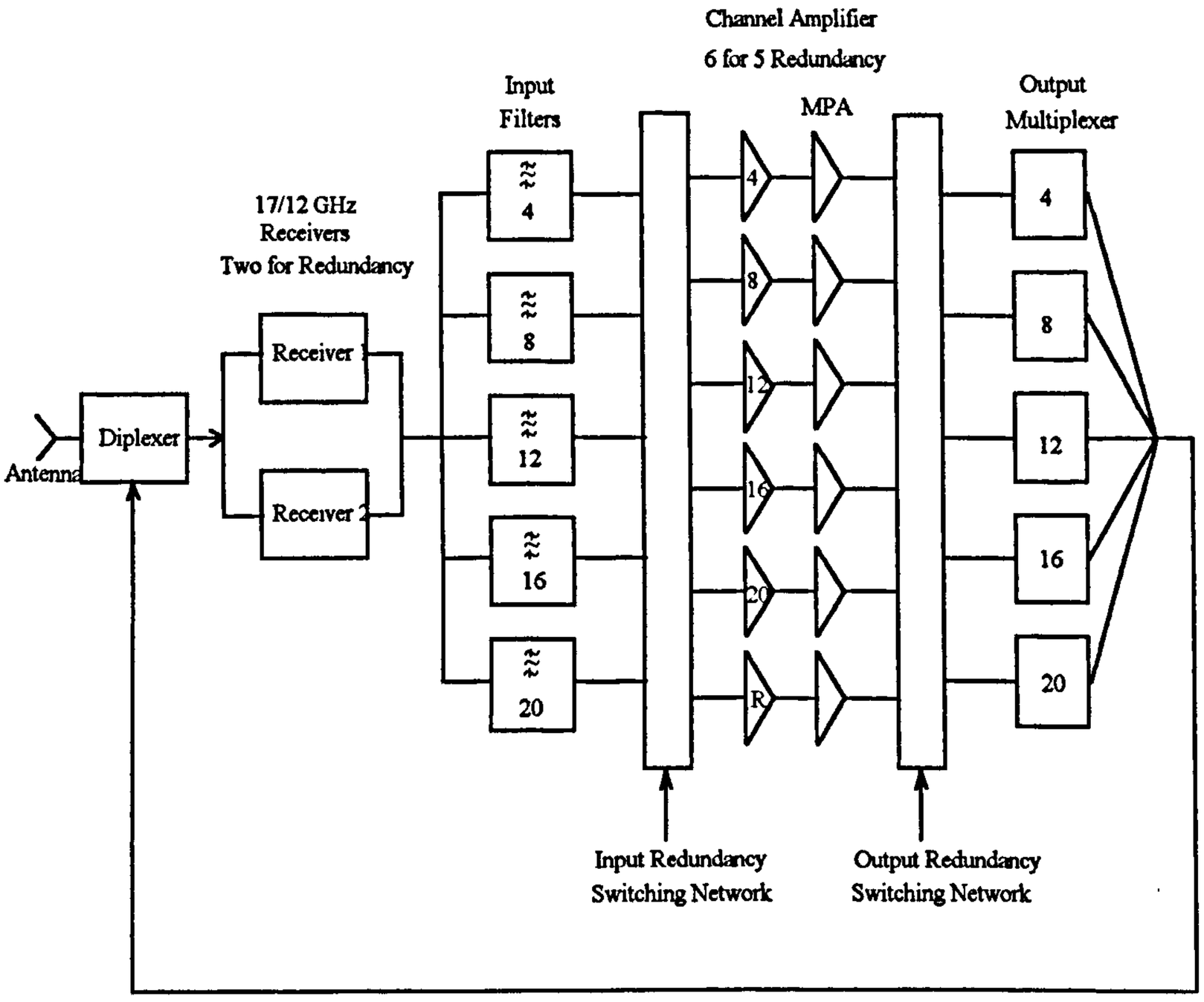

Figure 3/6 Satellite TV Transmitter Simplified Block Diagram

The satellite communication system consists of three operational channels at 110 watts selectable from any of the five channels allocated to the UK. Consider the simplified block diagram of the repeater (figure 3/6). The 17 GHz signal is received by the offset fed parabolic antenna and converted to 12 GHz in one of the two redundant broadband receivers.

The received signals are then channelled in the input multiplexer and fed to the individual channel amplifiers, which has a six for five redundancy. Each channel amplifier has an automatic level control and an attenuator that can be commanded. These are used to maintain a constant drive level to the microwave power amplifier (MPA). The MPA consists of two 55 watts TWT's and the associated microwave components required to power combine them. Each MPA can be configured independently to operate either in the high power mode (110 watts) or in the low power mode (55 watts), which is achieved by

selecting either of the two TWT's in the channel amplifier to operate alone.

FUNCTION	PARAMETER
Uplink Frequency Band	17371.52 to 17705.4 MHz
Uplink Coverage Area	Southern UK
Uplink SFD (nominal)	-80dBW/m
Receive G/T	11dB/K
Receiver Redundancy	2 for 1
Transponders	5
Transponder Bandwidth	27MHz
Total Payload Saturated Gain	120dB
Downlink Frequency Band	11771.52 to 12105.4 MHz
Downlink Coverage Area	UK
High Power Amplifier Redundancy	6 for 5
Transmit ERP (UK)	59 dBW
Antenna	2.54 by 1.73 m offset fed paraboloid.

Table 3-1 Satellite Communications System Characteristics

A maximum of six TWT's can be operated simultaneously to provide either of three channel configurations, i.e. three high power channels, two high power and two low power, or one high power and four low power. The outputs of the MPA's are fed to the output multiplexer, which combines the five channels and routes them to the transmit port on the antenna.

The receiver provides low noise broadband reception of the uplink and performs frequency conversion from the 17 GHz receive band to the 12 GHz transmit band. The input multiplexer is composed of five filters that correspond to the frequency channels allocated to the UK. Its purpose is to isolate the signals from each other and to limit the noise bandwidth at the input of the channel amplifiers. The filters have a pseudo-elliptic function characteristic. The automatic level control and commandable step attenuator function within each amplifier provide a 15 dB dynamic range to the MPA's and gain control. The

automatic level control detects fluctuations in uplink power, such as that due to rain fades, and provides a constant drive to the MPA's. The step attenuator provides gain control over the mission life and is commandable from the ground.

Parallel addition of the two 55 watts TWT's in each MPA require that the phase of their signals be properly aligned. Variable phase shifters and selectable coaxial attenuators are used to match the phase paths. The MPA can also be operated in a single TWT mode. The output multiplexer recombines the signal after their amplification for transmission to the ground. The six contiguous channel (five broadcast and one telemetry channel) multiplexer uses a four pole elliptic function characteristic for each filter. The multiplexer also contains filters to reduce the harmonic frequency components generated by the TWT's.

The antenna system consists of a parabolic reflector system and two omnidirectional radiating antennas. The reflector system is used for the reception and transmission of the broadcast signals and for on-station telemetry, tracking and command. The omnidirectional antennas are used for telemetry and command during the transfer orbit phase and for on-station backup. The antenna feed system consists of circular polarised horns. Broadcast signals are transmitted (12 GHz) using right circular polarisation. They are received (17 GHz) using left circular polarisation. Tracking and command functions use linear horizontal polarisation.

3.5 Typical DBS television receiver

A basic illustration of the terrestrial receiving system is shown in figure 3/1 and the associated block diagram in figure 3/7. Currently all terrestrial DBS television receivers require a high gain aerial together with associated head amplifier and downconverter. The aerial is normally located outdoors and must have an unobstructed view towards the satellite. The 12 GHz satellite signals are converted to a lower intermediate frequency in the down-converter and are fed by cable to the D-MAC television receiver or set top converter unit. An interesting future development may be the use of fibre optic technology for this

cable connection [5].

The satellite receiver unit tunes to the wanted channel that is amplified and demodulated. D-MAC signal structures have the advantage that a single demodulator is suitable for both the vision and data parts of the signal. The compressed vision signal is descrambled and decoded into separate red, green and blue vision signals. These would be fed to an existing television receiver using its RGB video inputs. For those receivers without such inputs the signal is converted to a PAL format at UHF.

Terrestrial domestic receiving antennas tend to be parabolic in nature with an offset feed. Due to the intrinsic insensitivity to frequency of both the feed horn and the parabolic dish a satisfactory flat response can be obtained over the desired frequency band. The low noise head amplifier/ down-converter at the aerial end of the ground installation coverts the signal frequency from 12 GHz to typically 1 GHz. Currently, block conversion techniques are used. Low noise transistors (such as HEMT's) are used in the low noise amplifier and the frequency conversion circuit normally uses a bandpass filter, mixer and local oscillator. Dielectric resonator techniques are used in the local oscillator. Finally the basic functions of the set top unit are tuning, demodulation, video and audio. A brief review of satellite receiver technologies was given by Konoshi, et al. [4].

3.6 DBS link performance

3.6.1 Introduction

This section considers the basic characteristics of a DBS downlink, that is the propagation path, including end terminal characteristics, between the satellite transmitter and the terrestrial television receiver. The basic satellite link system is described in the previous sections and is illustrated in figure 3/7. It consists of an uplink (the transmitting terrestrial TV station, and the satellite TV receiver that is part of the transponder) and a downlink (the satellite TV transmitter part of the transponder, and the terrestrial domestic TV receiver).

Although both paths influence the characteristics of the received signal on the ground, in general the overall system limitations are determined by the downlink characteristics and it is this part of the overall system that this section considers.

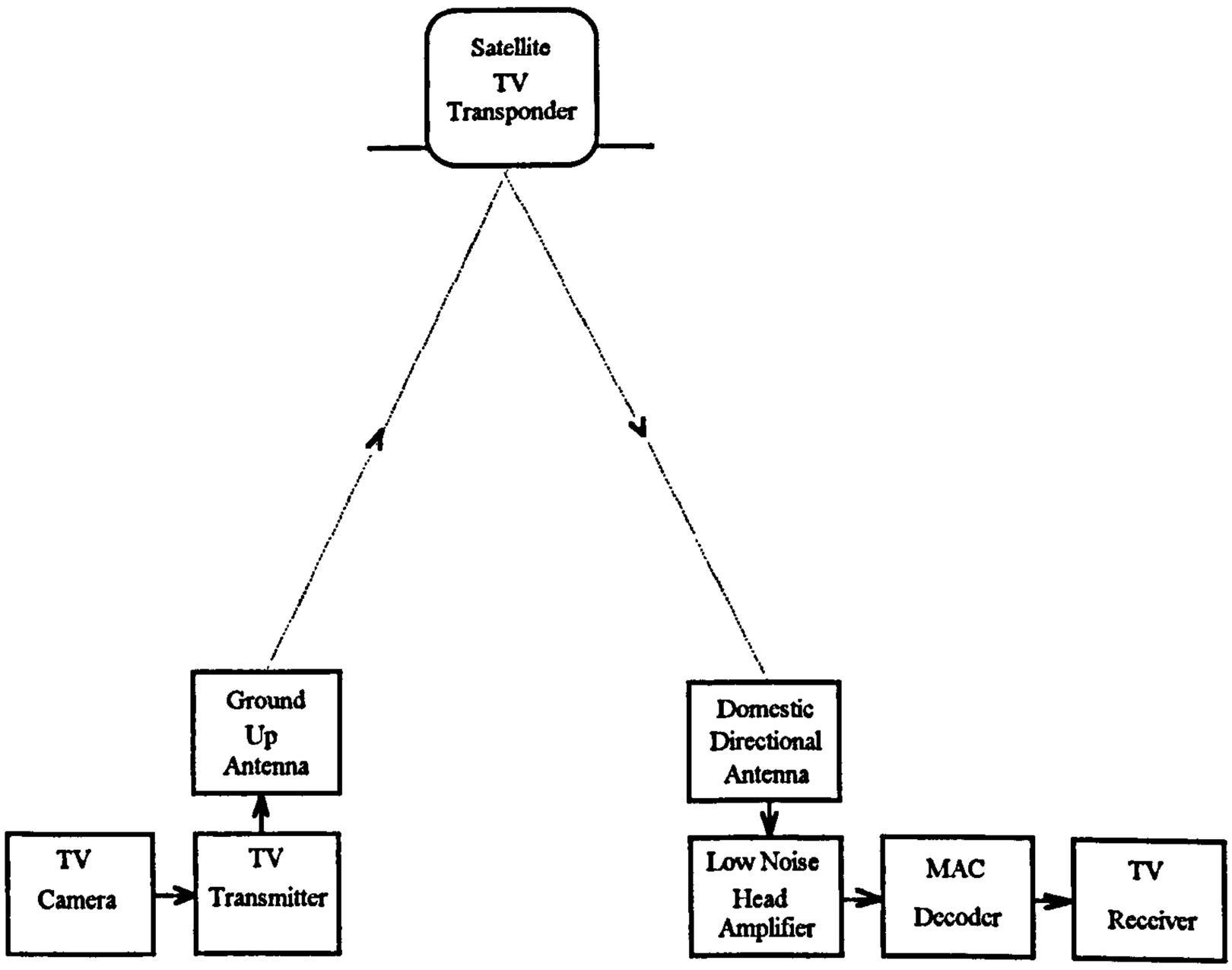

Figure 3/7 DBS Transmission and Receiving System

3.6.2 Signal-to-noise ratio at terrestrial TV receiver input

The signal-to-noise ratio is a measure that allows the relative magnitude of the received signal to be specified with respect to the noise present at the receiver input. There are a number of ratios that can be specified for this relative magnitude. Some of the more popular are defined as follows:

(a) The ratio of signal power-to-noise power. This approach would appear to be the most natural since magnitudes of the same kind are being compared. The power of the modulated carrier is usually designated by C. As the noise power is N, the ratio is written C/N.

(b) The ratio of signal power-to-spectral density of the noise. This is written C/N_o and is expressed in Hz. It has the advantage, compared to the ratio C/N, of not in any way presupposing the bandwidth used. In fact the latter implies knowledge of the equivalent noise bandwidth B_N of the receiver that is matched to the bandwidth B_C occupied by the modulated carrier. In the course of the system design one needs to evaluate the link quality before the nature of the transmitted signal is specified. The bandwidth occupied by the carrier is then unknown and prevents further insight into the C/N value. It is for this reason that the C/N_o metric is preferred.

(c) The ratio of signal power-to-the noise temperature. This ratio is derived from the ratio C/N_o by the multiplication by Boltzmann's constant, k. It is written C/T and is expressed in watts/degrees K.

The definition given in (b) above, that of C/N_o corresponds to the most widespread practice and is adopted in the following calculations. Elsewhere in this thesis it is necessary to use the other two definitions when appropriate, frequently when they have been specified in source documents.

3.6.3 Figure of merit for terrestrial TV receiving equipment

A figure of merit that is used for the receiving system is the ratio of the receiver gain to system noise temperature, or G/T. The aerial gain is proportional to the square of the aerial diameter and is dependent on the efficiency of the feed reflector system. The system noise temperature is composed of three components: the noise of the receiver, the noise due to losses between the antenna feed system and the receiver, and finally, the antenna noise.

3.7 Satellite to ground link analysis

3.7.1 General

To illustrate the impact of threshold extension demodulation upon a DBS down link, an analysis of a DBS down link is given in Appendix C. In the latter the parameters of a typical D2-MAC/Packet system are given based on the characteristics system given earlier in this section.

3.7.2 Analysis

In Appendix C the equation giving the carrier-to-noise spectral density ratios $\left(\frac{C}{N_0}\right)$ in terms of four factors are derived. These factors are the equivalent isotropic radiated power, the path loss of the transmission medium, the receiver gain/noise temperature and the factor due to Boltzmann's constant.

Using these relationships and for clear sky conditions, the carrier-to-noise spectral density ratio $\left(\frac{C}{N_0}\right)$ is calculated. Two further conditions are also calculated namely that for 3 and 7 dB rain attenuation. The results obtained are summarised below. Also included in Appendix C are power level diagrams for the clear air and 7 dB rain attenuation conditions that illustrate where the losses in the system occur.

3.7.3 Effects of threshold extension on a typical satellite to ground TV link

(a) In Appendix C the value of the carrier power-to-noise spectral density ratio $\left(\frac{C}{N_0}\right)$ has been calculated for various conditions. These were:

(i) For clear air, $\left(\frac{C}{N_0}\right) = 90.11$ dB(Hz)

(ii) For 3 dB rain attenuation, $\left(\frac{C}{N_0}\right) = 86.28$ dB(Hz)

(iii) For 7 dB rain attenuation, $\left(\frac{C}{N_0}\right) = 80.97$ dB(Hz)

To determine the carrier-to-noise ratio $\left(\frac{C}{N}\right)$ in the receiver bandwidth B_{IF} these values should be modified as follows (from Appendix C, equations C-5 and C-6):

$$\left(\frac{C}{N}\right)_{dB} = \left(\frac{C}{N_O}\right)_{dB} - (B_{IF})_{dB} \qquad \text{..... (3-3)}$$

Now for D2-MAC/Packet, the occupied transmission bandwidth is 27 MHz (section 3.3.3 above). Assume that the I.F. bandwidth B_{IF}, of the receiver is 27 MHz.

Then: $$\left(\frac{C}{N}\right)_{Clear\ Air} = 90.11 - 74.3 = 15.8 \text{ dB}$$

and $$\left(\frac{C}{N}\right)_{3\ dB\ Rain} = 86.28 - 74.3 = 11.98 \text{ dB}$$

and $$\left(\frac{C}{N}\right)_{7\ dB\ Rain} = 80.97 - 74.3 = 6.67 \text{ dB}$$

If it is assumed that for a conventional D2-MAC/Packet system, the demodulator threshold point would typically be of the order of $\left(\frac{C}{N}\right) = 12$ dB. It can be seen that for the system considered the clear air figure of 15.8 dB exceeds the threshold figure and would provide continuous reception in clear air.

The 3 dB rain condition, with an outage of 0.1%, just satisfies the threshold point. Any rain attenuation more than 3 dB would increase the outage figure, as is clearly shown by the 7 dB rain condition.

Now if a threshold extension demodulator was introduced with a threshold improvement factor of some 4 dB, then the performance of the whole system would be improved. In this case the 3 dB rain condition now has a margin above the new threshold figure thus reducing the 0.1 % outage. The 7 dB rain condition now is at or just below the new threshold figure thus reducing the outage significantly.

The importance of a successful threshold extension demodulator is that it offers a relatively economic improvement to performance. To achieve a similar improvement in performance elsewhere in the system would require an increase in EIRP or receiving antenna gain, solutions that are relatively costly.

3.8 References

[1] Neuman, M. E. and Vargas, T. F. "Direct Broadcast Satellite Service for the United Kingdom," Direct Broadcast by Satellite Conference held at IBA, 16/17 June 1988, Pub. Consert, London.

[2] Stott, J. H. "Satellite Broadcasting: Requirements for the Receiving Antenna," BBC Research Report BBC RD1989/5.

[3] Gandy, C. "Satellite Links for Television Contribution," BBC Research Report BBC RD 1991/5

[4] Konishi, Y. and Fukuoka, Y. "Satellite Receiver Technologies," IEEE Trans. Broadcasting, Vol. 34, No. 4, December 1988, pp 449 - 456.

[5] Ikeda, H. et al. "New Type of DBS Receiver utilising Optical Fibre as I.F. Transmission Line," IEEE Trans. on Consumer Electronics, Vol. 34, No. 4, Nov. 1992, pp. 790 - 794.

[6] CCIR "*Broadcasting Satellite Systems*", Geneva, 1983, (ISBN 92.61.01751.7)

[7] CCIR "Television standards for the broadcasting satellite service". Report No. 1073-1.

[8] CCIR "Systems for the broadcasting satellite service (sound and television)". Report No. 215-7.

[9] CCIR "Broadcast satellite service (sound and television)". Report No. 632-4, 1990.

Blank Page

4. NOISE IN FM SYSTEMS

4.1 Introduction

4.1.1. A detailed examination of any threshold extension demodulation technique requires a detailed knowledge of the noise characteristics of the system at threshold, and in particular, the nature of the noise model that will be used to characterise the various threshold extension demodulator systems. A summary analysis of signals and noise in FM receivers is given below. This section considers the effect of noise in FM receivers and in particular in the demodulation process. Rice's concept [1] of the noise at the output of an FM discriminator is discussed, particularly in terms of the carrier demodulation process in the RF receiver. In Rice's milestone paper [1], the concept of clicks to explain the noise observed near threshold was introduced. In this model Rice assumed the occurrence of clicks was governed by a Gaussian process. His model separates the noise at the output of the ideal limiter-discriminator into two components when the input noise is Gaussian and additive. One component is small and nearly Gaussian whilst the other consists of randomly occurring impulses called spikes or clicks governed by a Poisson process. Since this pioneering work the click and Gaussian noise model for the output of a limiter-demodulator in FM receivers has dominated studies in the field. It has all the attributes of a good model, namely conceptual simplicity coupled with amenability to analysis, as well as a remarkable closeness to reality. The model not only accurately predicts the noise threshold in wide-band FM reception, but it has also prompted several avenues of theoretical investigation into the statistics of the clicks and their influence on digital FM systems, as well as creative innovation for the extension of noise threshold by click elimination. Two recent publications, [2], [3], contain excellent surveys of the work in this field. Much of the analysis carried out in this report has been based upon the use of Rice's click and Gaussian noise model. The treatment of threshold noise given below follows that of Rice [1] and Bar-David [3].

4.1.2 Frequency modulation has long been known to possess substantial signal-to-noise improvement properties above the threshold phenomena. Schwartz in his 1962 paper [4] discussed the existence of two FM thresholds. The first, or conventional threshold, is at about 10 dB, and the second, lesser known threshold, is at about 0 dB. The signal-to-noise characteristics of FM systems [4] may be summarised as follows:

(a) For a FM carrier-to-noise ratio C/N greater than about 10 dB, the output signal-to-noise ratio S_0/N_0 is given by :

$$\frac{S_0}{N_0} = 3\beta^2 \frac{C}{2\,\eta f_M} = 3\beta^2 \left(\frac{B_{IF}}{f_M}\right)\frac{C}{N} \qquad \text{..... (4-1)}$$

where $N = 2\,\eta B_{IF}$ is the mean squared I.F. noise if a rectangular I.F. noise spectrum of spectral density η is assumed and C is the carrier power. The output signal-to-noise ratio (S_0/N_0) thus increases as the square of the bandwidth if the noise spectral density η is held fixed. Equation (4-1) indicates both the (S_0/N_0) improvement possible and the corresponding bandwidth increase necessary for FM. That is in an FM system, bandwidth can be traded for an increase in output signal-to-noise ratio.

(b) For FM carrier-to-noise ratios of less than 10 dB, the noise at the output of an FM receiver increases very sharply, changing in the order of 30 dB for a 10 dB decrease in (C/N). This represents the first carrier-to-noise threshold.

(c) For still further decreases in carrier-to-noise ratios, the output signal itself begins to be suppressed by the noise. This is equivalent to 'capture' of the system by noise. This represents the second threshold effect.

This study will only be concerned with the first threshold effect described in (b) above; for it is in this region that any improvement obtained with threshold extension demodulator

techniques occurs.

4.2 Noise Characteristics at the FM threshold

4.2.1 Consider an ideal FM receiver as shown in figure 4/1. The receiver input additive noise term is assumed to be a Gaussian process that will then add to the internally generated receiver noise, also a normal process, yielding a resultant Gaussian process. The power spectrum of the total additive noise is assumed wide enough so that the filter in the receiver determines its net spectral shape. The additive noise will thus be treated as a Gaussian stationary random process of zero mean.

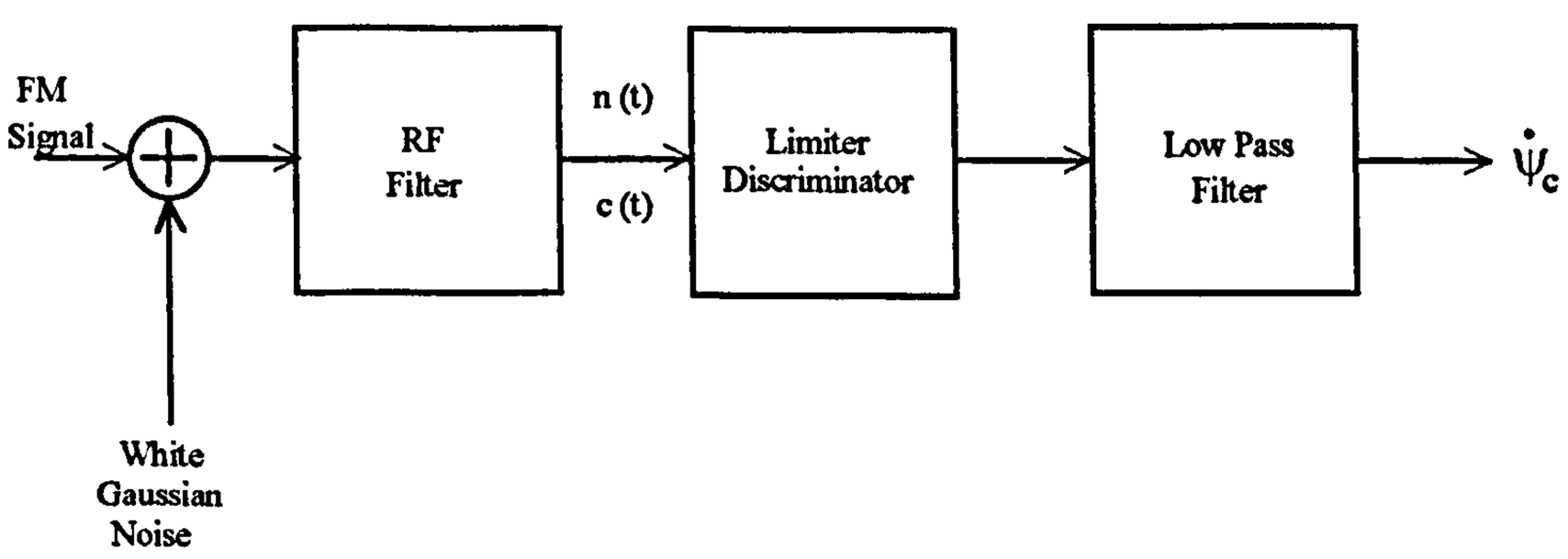

Figure 4/1 Ideal FM Receiver

A white Gaussian noise is added to the FM signal and the sum is processed by the receiver. The noise $n(t)$ at the output of the RF filter is shown in vector form in figure 4/2 and can be written as:

$$n(t) = n_1(t)\cos(2\pi f_0 t) - n_2(t)\sin(2\pi f_0 t) \qquad \text{..... (4-2)}$$

$$\therefore \quad n(t) = \mathrm{Re}\left\{n_c(t)\exp j\left[2\pi f_0 t + \lambda_c(t)\right]\right\} \qquad \text{..... (4-3)}$$

Where $n_1(t)$ and $n_2(t)$ are the quadrature components of the relatively narrow band noise. They are independent Gaussian variables having zero mean and variance σ^2.

The functions $n_c(t)$ and $\lambda_c(t)$ are the envelope and phase of the noise. The envelope is

Rayleigh distributed and the phase is uniformly distributed over 2π radians and is independent of the envelope.

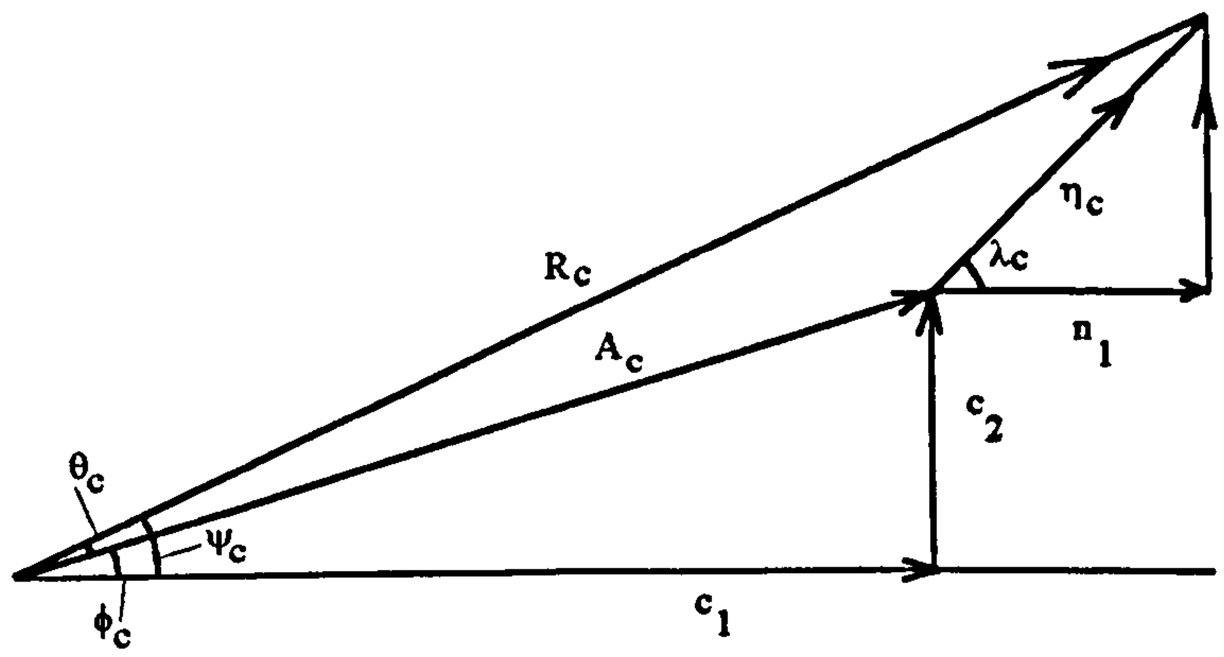

Figure 4/2 Signal and noise phase diagrams

The variables are related by the following equations:

$$n_c(t) = \sqrt{n_1^2 + n_2^2} \qquad \text{..... (4-4)}$$

$$\lambda_c(t) = \tan^{-1}\left[\frac{n_2}{n_1}\right] \qquad \text{..... (4-5)}$$

Similarly, the signal output $c(t)$ of the filter may be written in terms of quadrature components:

$$c(t) = c_1(t)\cos(2\pi f_0 t) - c_2(t)\sin(2\pi f_0 t) \qquad \text{.....(4-6)}$$

$$\therefore \quad c(t) = \mathrm{Re}\left\{A_c \exp j\left[\,2\pi f_0 t + \phi_c(t)\,\right]\right\} \qquad \text{.....(4-7)}$$

Where A_c and ϕ_c are the envelope and phase of the signal. The output of the RF filter due to the signal and noise is then:

$$c(t) + n(t) = \mathrm{Re}\left\{\,R_c(t)\exp j\left[2\pi f_0 t + \psi_c(t)\right]\right\} \qquad \text{..... (4-8)}$$

where from figure 4/2:

$$R_c(t) = \sqrt{[c_1 + n_1]^2 + [c_2 + n_2]^2} \qquad \text{..... (4-9)}$$

and

$$\psi_c(t) = \tan^{-1}\left[\frac{c_2 + n_2}{c_1 + n_1}\right] \qquad \text{..... (4-10)}$$

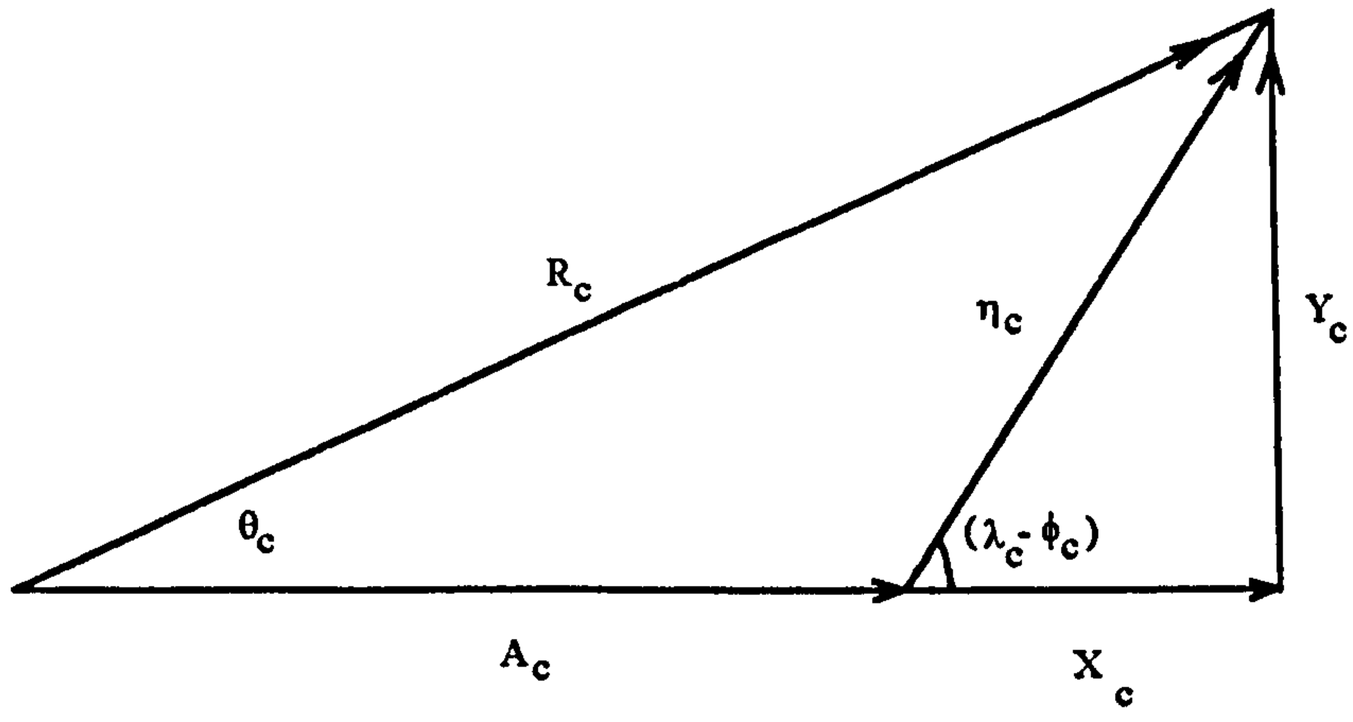

Figure 4/3 Signal/noise diagrams with reference to the signal phasor

4.2.2 A more convenient vector diagram is shown in figure 4/3 where the signal is taken as the reference vector. The noise can thus be resolved into two quadrature components, one in phase and the other in quadrature with the signal. From inspection these components can be seen to be:

$$X_c(t) = n_c \cos(\lambda_c - \phi_c) = n_1 \cos\phi_c + n_2 \sin\phi_c \qquad \text{.....(4-11)}$$

$$Y_c(t) = n_c \sin(\lambda_c - \phi_c) = n_2 \cos\phi_c - n_1 \sin\phi_c \qquad \text{.....(4-12)}$$

Where from figure 4/2: $n_1 = n_c \cos\lambda_c$ ..... (4-13)

and $n_2 = n_c \sin\lambda_c$ ..... (4-14)

Since $n_1(t)$ and $n_2(t)$ are Gaussian, so are $X_c(t)$ and $Y_c(t)$. The phase $\psi_c(t)$ of the resultant vector can be obtained directly from figure 4/2 as:

$$\psi_c(t) = \phi_c(t) + \theta_c(t) \qquad \text{..... (4-15)}$$

$$\therefore \quad \psi_c = \phi_c(t) + \tan^{-1}\frac{Y_c}{A_c + X_c} \qquad \text{..... (4-16)}$$

This is in a convenient form to use since the signal term $\phi_c(t)$ is separated from the noise term $\theta_c(t)$. However the latter noise term is a function of the signal through X_c and Y_c. Assuming the limiter-discriminator to be ideal, the output of the discriminator is:

$$\dot{\psi}_c(t) = \dot{\phi}_c(t) + \dot{\theta}_c(t) \qquad \text{..... (4-17)}$$

The wanted demodulated signal is $\dot{\phi}_c(t)$. The behaviour of the noise term $\dot{\theta}_c(t)$ is discussed below.

4.3 Click analysis

4.3.1 The noise [1] at the output of a discriminator is observed experimentally to be composed of small nearly Gaussian noise plus randomly occurring impulses. This observation can be explained by referring to the vector diagram of figure 4/3.

As the noise components $X_c(t)$ and $Y_c(t)$ fluctuate randomly, the angle $\theta_c(t)$ will fluctuate correspondingly. When the input carrier-to-noise ratio, (C/N) is large,

$$\text{i.e.} \qquad A_c >> n_c(t) \qquad \text{..... (4-18)}$$

the fluctuation of $\theta_c(t)$ will be small. The latter may be approximated by:

$$\theta_c(t) \cong \tan^{-1}\frac{Y_c}{A_c} \cong \frac{Y_c}{A_c} \qquad \text{..... (4-19)}$$

Since $Y_c(t)$ is a Gaussian random variable, $\theta_c(t)$ is very nearly Gaussian also. The noise at the output of the discriminator is then :

$$\dot{\theta}_c(t) \cong \frac{\dot{Y}_c}{A_c} \qquad \text{..... (4-20)}$$

and $\dot{\theta}_c(t)$ is also essentially Gaussian.

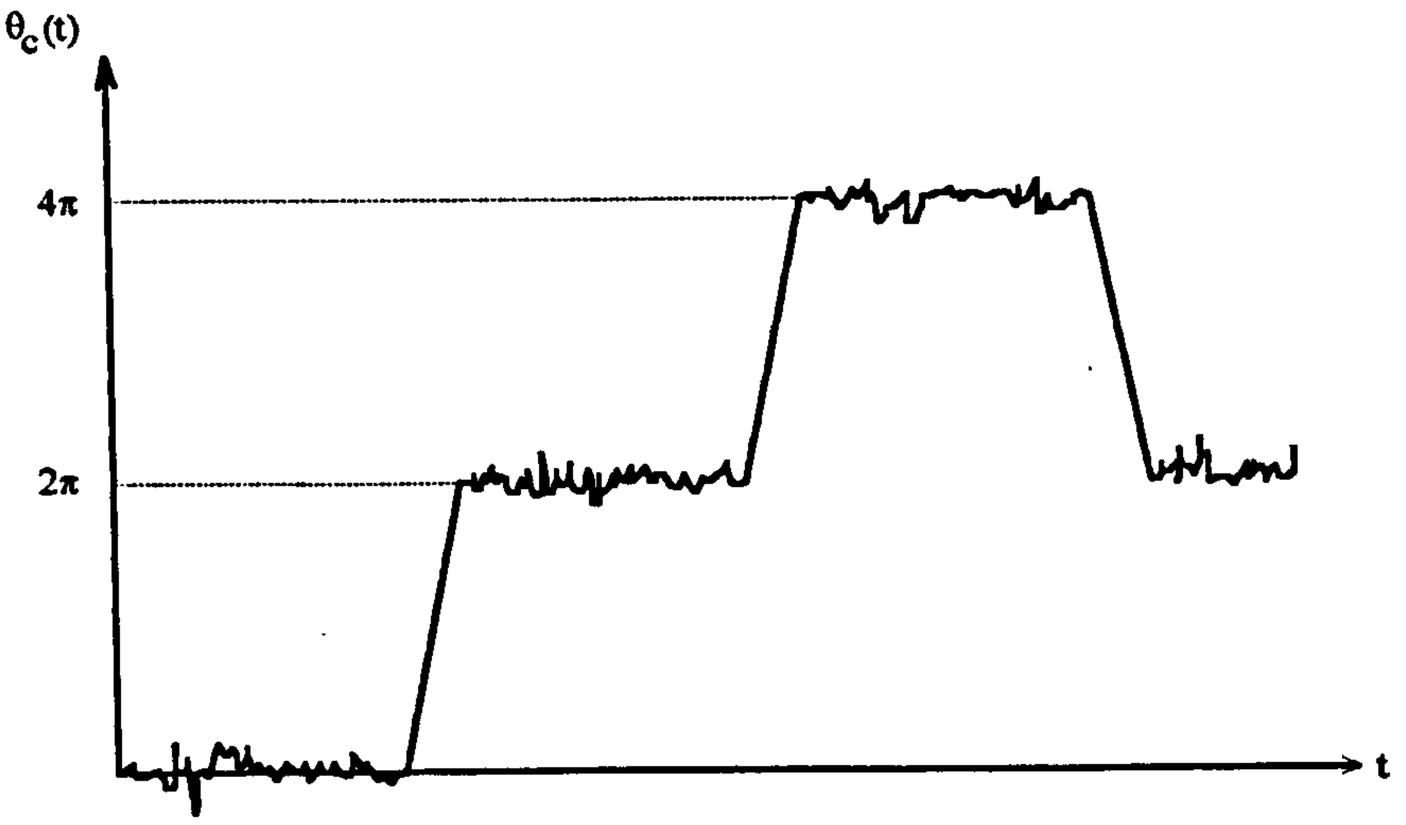

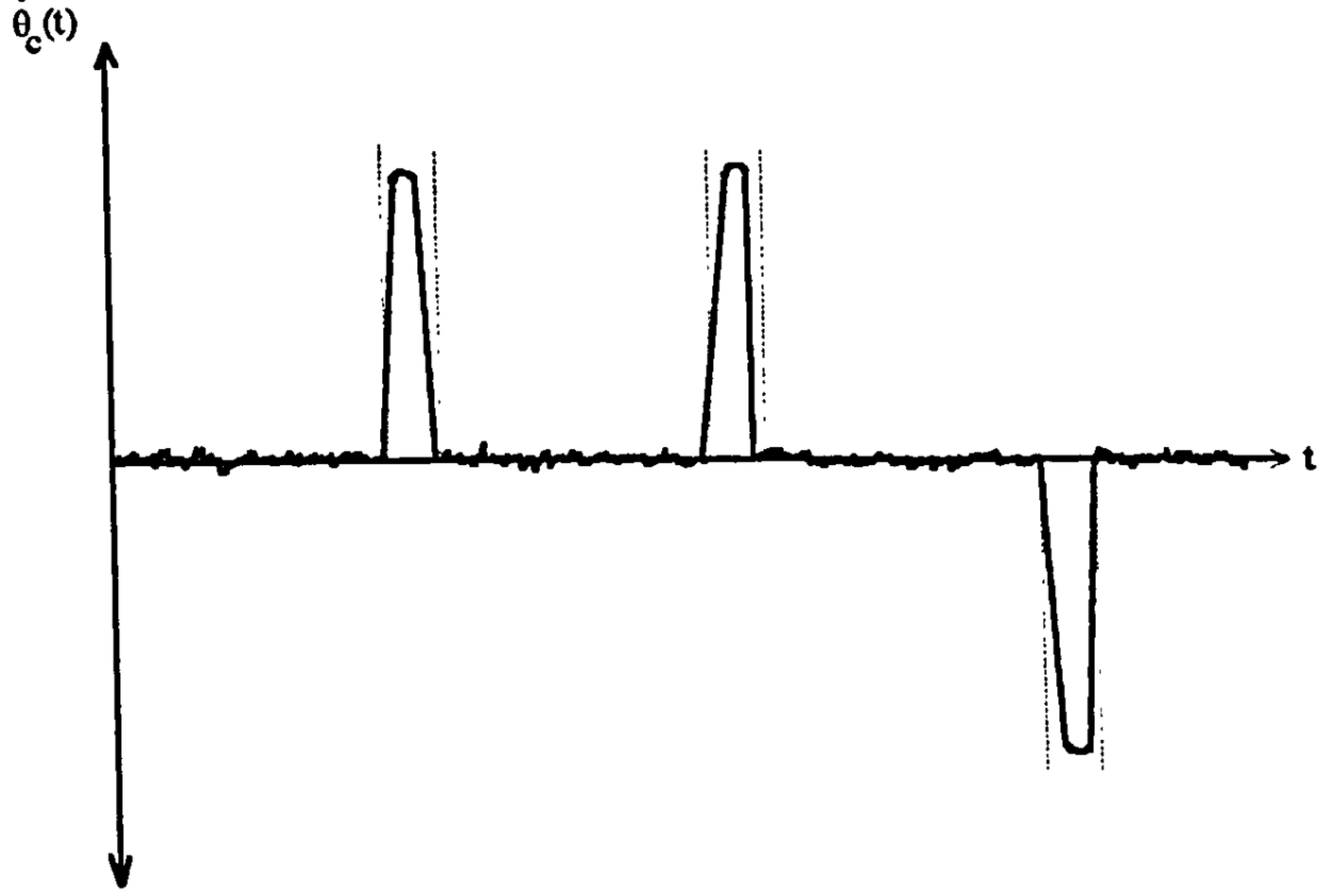

Figure 4/4 Typical variation of $\theta_c(t)$ and $\dot{\theta}_c(t)$

Occasionally, as $X_c(t)$ and $Y_c(t)$ fluctuate randomly, $Y_c(t)$ may go through zero whilst $X_c(t) \rangle -A_c$ causing the resultant vector R_c to encircle the origin rapidly. In this case, $\theta_c(t)$ rapidly changes by $+2\pi$ or -2π depending on the direction of encirclement. The discriminator response to this phase change is a sharp pulse with an area of $\pm 2\pi$. For

receivers with an audio output, this pulse is heard as a distinct *click* and hence the name.

The noise at the output of the discriminator, $\dot{\theta}_c(t)$, will then have pulses of area of $\pm 2\pi$ superimposed on a lower level background of approximately Gaussian noise. A typical variation of $\theta_c(t)$ and $\dot{\theta}_c(t)$ is shown in figure 4/4.

4.3.2 Rice's model thus relates the generation of clicks to the random encirclement of the origin by the received signal plus noise vector. Physically these clicks may be described as the gain or loss of an additional cycle of the received signal. A stylised diagram is shown in figure 4/5. From this figure it can be seen that for a click to be generated the tip of the noise vector appears in the left hand plane. This means the envelope of the signal plus noise is likely to be small.

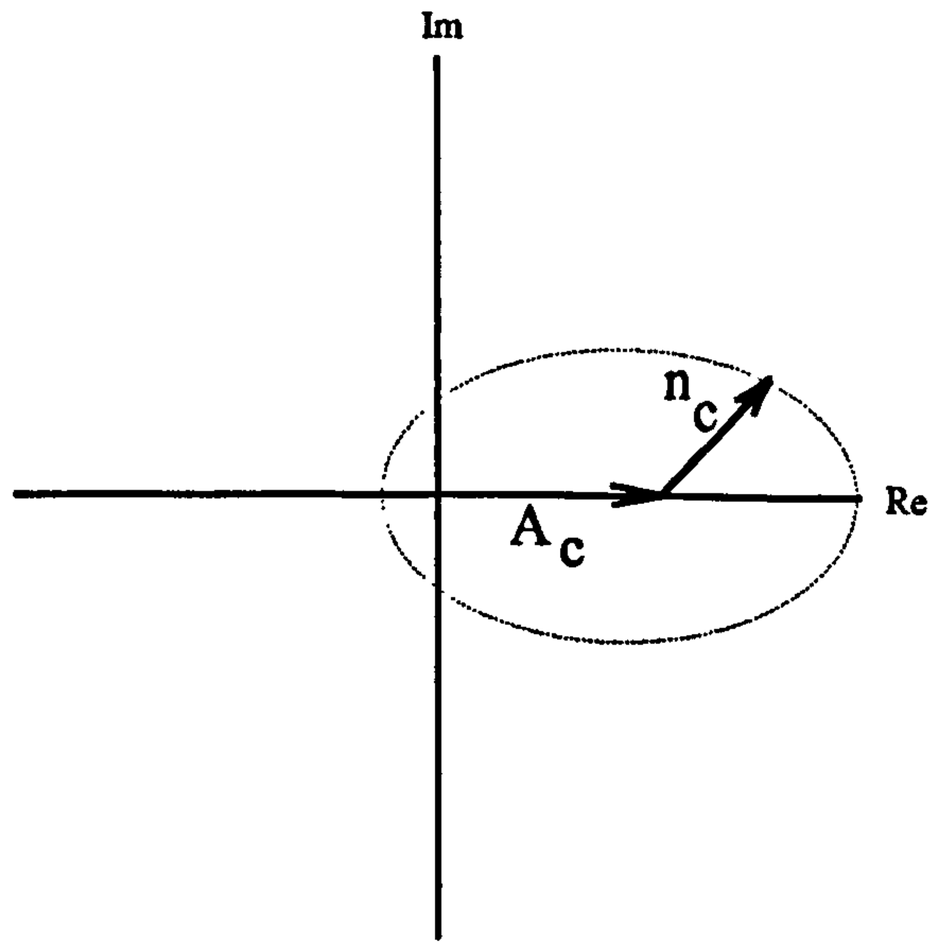

Figure 4/5 Stylised path of received phase for Clicks

It has been shown [9] that the duration of the pulse noise is less than, $(1/2\ B_{PD})$, since the bandwidth of the post discriminator video filter B_{PD} would be narrower than that required to pass the pulse. When a pulse occurs, it can be represented by an impulse of area 2π at the discriminator output.

If the discriminator output $\dot{\theta}_c(t)$ is regarded as consisting of two components [1, p.401] one a small Gaussian component and the other a succession of randomly occurring impulses, or clicks. This latter impulse noise can then approximated by a series of delta

functions of weight $\pm 2\pi$, viz. :

$$2\pi \sum_{p=-\infty}^{\infty} \delta(t-t_p) + (-2\pi) \sum_{n=-\infty}^{\infty} \delta(t-t_n) \qquad \text{..... (4-21)}$$

where t_p and t_n represent respectively, the instants at which positive and negative pulses occur.

When the carrier-to-noise ratio (C/N) is large, the individual impulses of equation (4-21) tend to occur randomly and independently of each other. Each of the sets of times were regarded by Rice as being Poisson events. Furthermore they are assumed to be independent of the Gaussian noise component [16]. A stylised diagram is shown in figure 4/6.

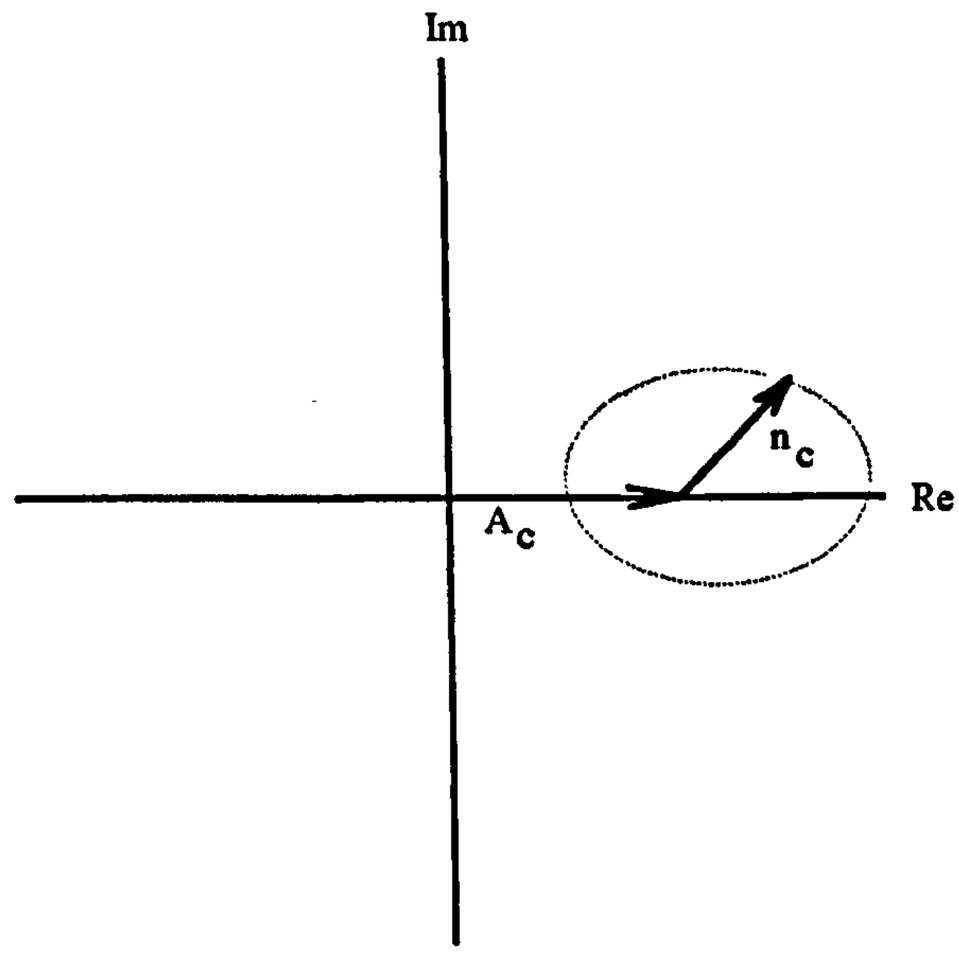

Figure 4/6 Stylised path of received phase for Gaussian-like signals

When the clicks form a Poisson process the rate of occurrence of these clicks is required in order to determine their statistical properties; this is derived below.

When the vector motion results in an unfulfilled encirclement, *false clicks* are generated. False clicks are more rarer than real clicks and the net gain in phase θ for false clicks is zero and so if only the mean value is considered the false clicks blend into the nearly Gaussian noise component of the Rice model. A stylised diagram is shown in figure 4/7. False clicks are categorised into three types, namely 1,2 and 3. Each category depending upon in which quadrant the vector reverses.

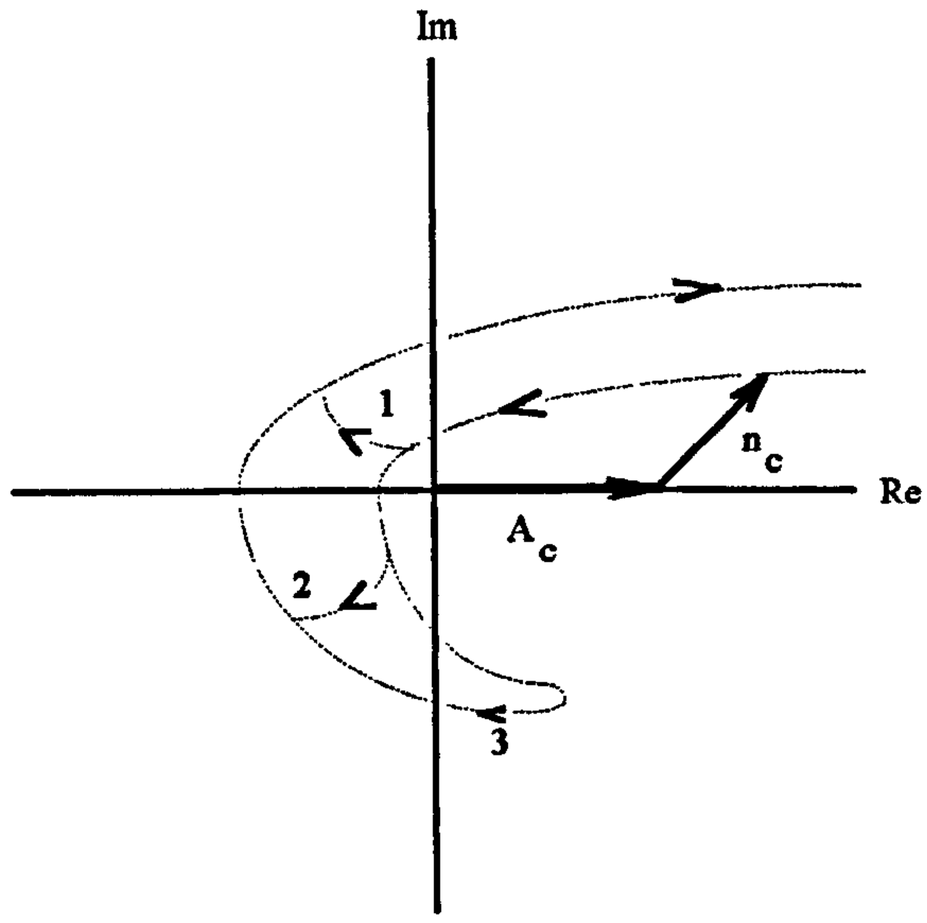

Figure 4/7 Stylised path of received phase for false clicks type 1, 2 and 3

If the vector traces a path that comes close to the origin the result is an occurrence of a *doublet* that has zero area. A stylised diagram is shown in figure 4/8. To a first approximation the false click and doublet can be classified as events that are smoothed out by a post-discriminator filter at high carrier-to-noise ratios, their effect on the signal-to-noise output is negligible.

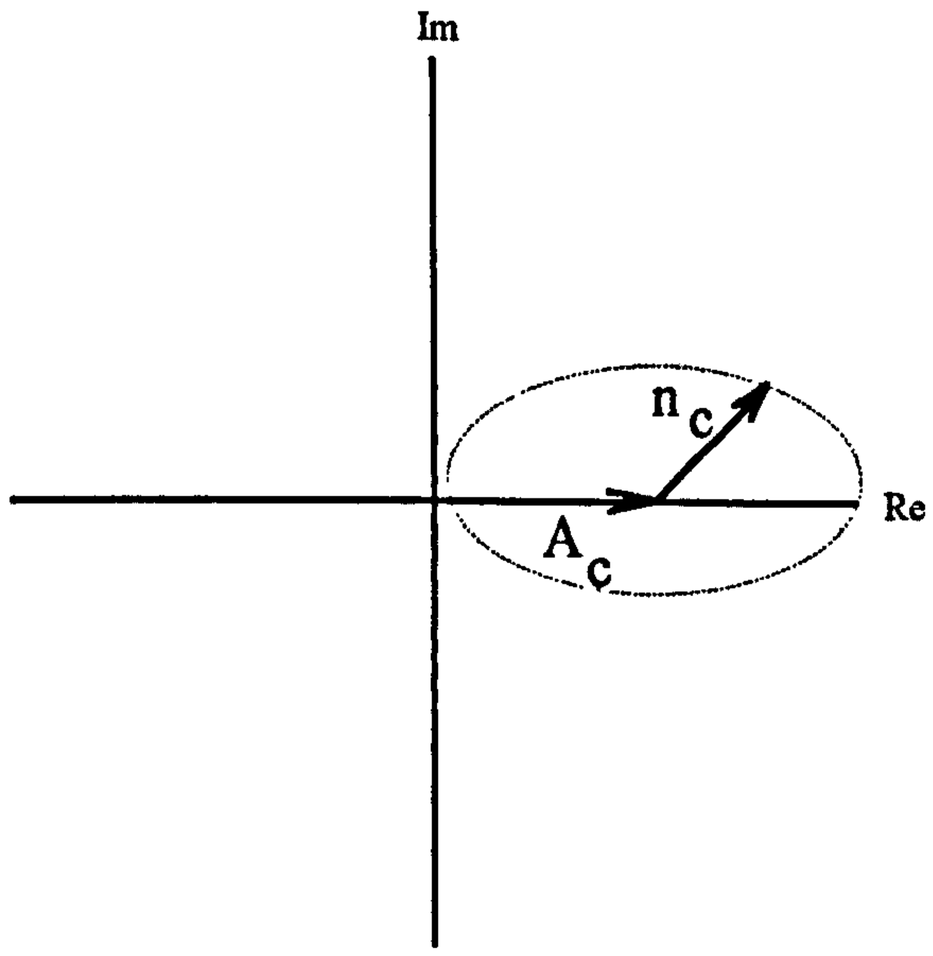

Figure 4/8 Stylised path of received phase for doublets

Only the clicks that have an area of $\pm 2\pi$ strongly excite the low pass filter and are therefore responsible for the noise threshold. This occurrence is more frequent than that of

false clicks.

One difficulty in any click elimination scheme is that large clicks appearing at the demodulator output can also be caused by the carrier modulation, making discrimination between them difficult. One of the characteristics of clicks is that they occur when the instantaneous envelope $R(t)$ is likely to be small. This information helps to discriminate between clicks and modulating signals but not between clicks and doublets.

The difference between spectral properties of clicks, false clicks, doublets and modulating signals has been exploited in some types of threshold extension demodulators [3]. Doublets contain more high frequency components than the clicks. High frequency components in the modulation $\phi(t)$ are less than those present in clicks and the Gaussian component of the discriminator noise has an approximate parabolic spectrum. This has lead to click detection schemes being attempted that have been based upon observing the output of an appropriately designed baseband filter. These schemes have not been totally successful [3].

4.4 Click rates

Expressions for the rates of positive and negative clicks, $H_+(t)$ and $H_-(t)$ have been obtained by Rice [1]. In his observations he assumes the spectral density of the input noise is symmetrical with respect to the carrier frequency of the FM signal, f_0

In Rice's result the click rate is determined by the input carrier-to-noise ratio (C/N), the modulating signal $\dot{\phi}_c(t)$, and the r.m.s. bandwidth (standard deviation) of the input noise spectral density, r_c..

The average number of positive clicks is given by:

$$H_+(t)=\frac{1}{2}r_c\left\{\sqrt{1+\mu_c^2}\,erfc\sqrt{(C/N)-(C/N)\mu_c^2}-\mu_c e^{-(C/N)}\,erfc\,\mu_c\sqrt{(C/N)}\right\}\text{.....} \quad (4\text{-}22)$$

The average number of negative clicks are:

$$H_{-}(t) = H_{+}(t) + r_c \mu_c e^{-(C/N)} \qquad \text{..... (4-23)}$$

where:

$$r_c = \frac{1}{2\pi}\sqrt{\frac{b_2}{b_0}} \qquad \text{..... (4-24)}$$

$$b_0 = \sigma^2 = \int_0^\infty G(f)\, df \qquad \text{..... (4-25)}$$

$$b_2 = (2\pi)^2 \int_0^\infty (f - f_0)^2\, G(f)\, df \qquad \text{..... (4-26)}$$

$$\mu_c = \frac{\dot{\phi}_c(t)}{2\pi r_c} \qquad \text{..... (4-27)}$$

$$(C/N) = \frac{A_c^2}{2\delta^2} \qquad \text{..... (4-28)}$$

$G(f)$ is the single-sided power spectral density of the input noise. $erfc(x)$ is the complementary error function defined by:

$$erfc(x) = 1 - erf(x) = \frac{2}{\sqrt{\pi}} \int_x^\pi e^{-y^2}\, dy \qquad \text{..... (4-29)}$$

There are a number of excellent references concerning the stochastic properties of clicks and their importance to the performance of conventional limiter discriminator receivers. A simple alternative derivation of the click rates is given in [7]. The click duration and amplitude are discussed in [8] - [11] and the first investigation of the click shape is given in [12]. Lindgren in [2], [3], presents an analytical treatment of these properties in both the unmodulated and modulated cases at large carrier-to-noise ratios. Rice [1] and Rainal [13]

have investigated the approximate spectral properties of clicks. The Poisson nature of the click instants, when considered as a point process, can be established at large carrier-to-noise ratios by using Kac and Slepian's [14] results. The statistical dependence between the Gaussian and the click components is discussed in [15]. This reference also discusses the Poisson nature of the click instants and the statistical independence between the justification of the Gaussian and the click components at large carrier-to-noise ratios.

4.5 Threshold noise in television systems

4.5.1 In DBS systems, frequency modulation techniques are used that give a noise voltage that is proportional to frequency. Noise power is thus proportional to the square of the video frequency. Figure 4/9 illustrates the variation of power spectral density with frequency at the output of a FM discriminator. The characteristic shown varies about the I.F. centre frequency.

Figure 4/9 - FM Discriminator Output Power Spectral Density vs. Baseband Frequency

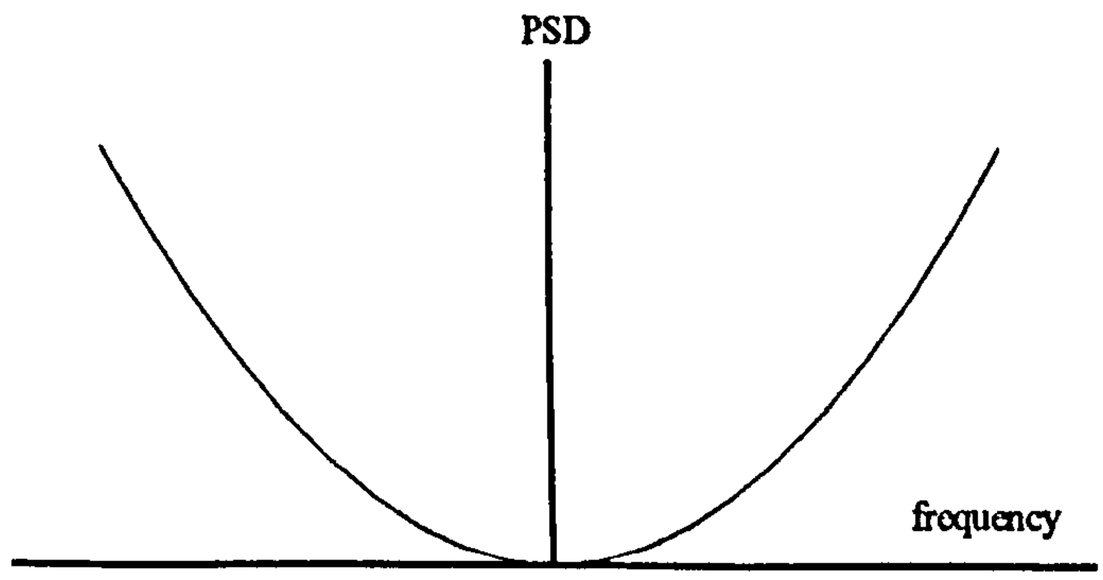

Rhodes [17] and Lowry [18] discussed the effects of noise on the satellite transmission of both the NTSC and MAC systems. Rhodes [17] highlighted the mismatch that existed when the NTSC system was transmitted over a satellite link. In this case most of the noise is within the chrominance band, that is within ± 0.6 MHz of the 3.58 MHz subcarrier. High frequency noise, in a monochrome system, appears as a fine grained random 'snow' noise at 3 MHz and can be said to be 10.7 dB less noticeable than the same noise power at a much lower frequency. This effect is called the 'noise weighting factor' that has been determined

by subjective means. Noise at 4.2 MHz is said to be weighted by 13.3 dB as it is even finer in its structure and hence even less perceptible. For this reason and above threshold, FM transmission of monochrome television can be said to be virtually noise free where a 54 dB weighted signal-to-noise ratio corresponds to a 44 dB unweighted signal-to-noise ratio. Figure 4/10 illustrates that the human eye perceives a noise characteristic that is basically the opposite and which is complementary to the triangular FM noise, with noise visibility maximised at lower frequencies.

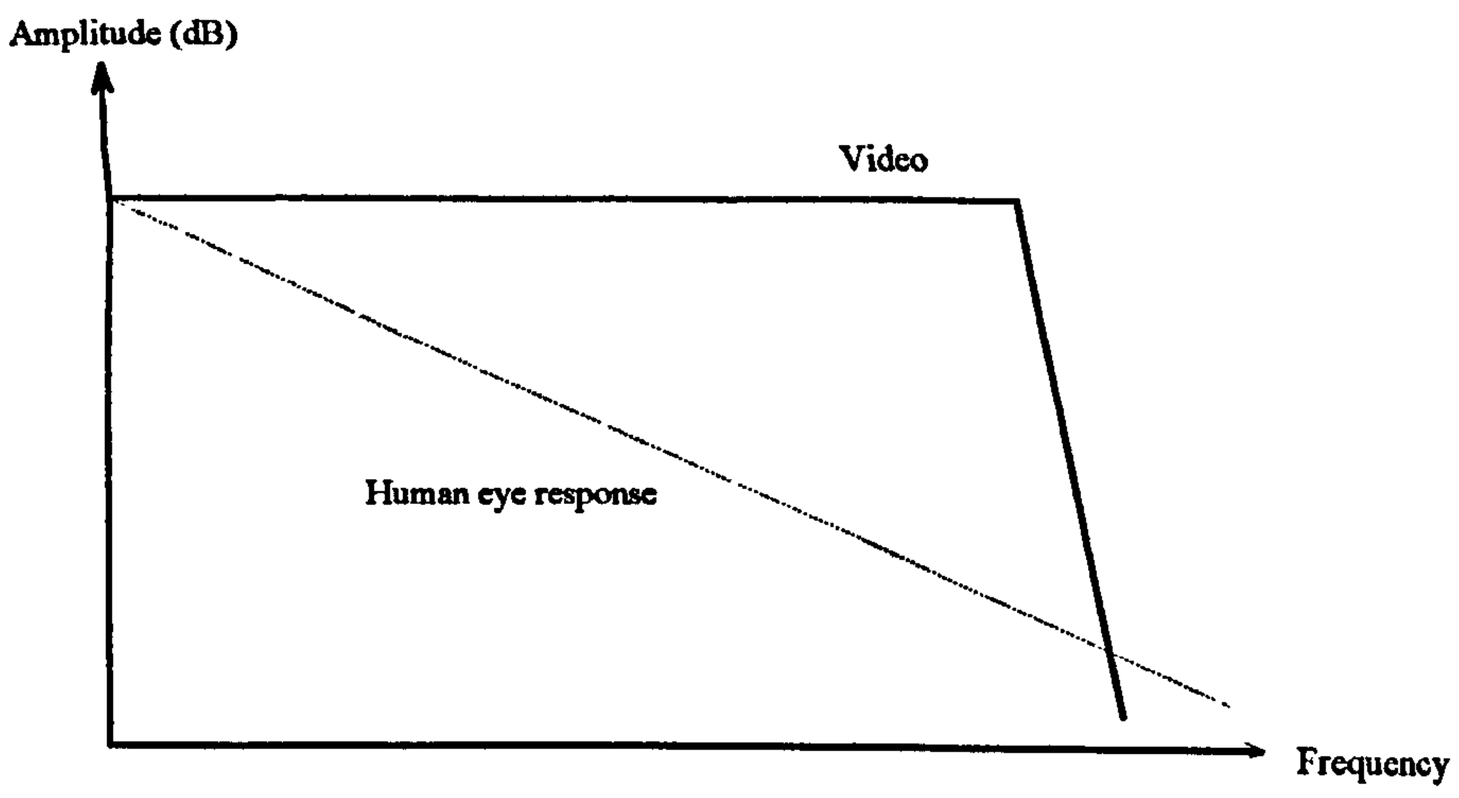

Figure 4/10 Human eye perception of noise is essentially triangular, decreasing with frequency

Demodulating the chrominance information in a NTSC system results in the noise being heterodyned to low video frequencies from the upper portion of the video band. The noise near the colour subcarrier is down converted to noise at such low frequencies that the weighting is negligible. Thus noise in the chrominance channel is perceived as being the dominant source of interference. This effect is illustrated in figure 4/11.

Noise immunity of modern NTSC receivers is also reduced by the high brightness phosphors. These differ from the original phosphors that were used for the basis of NTSC encoding that exploited the constant luminance principle, resulting in an increase in the visibility of chrominance noise. This results in the colour red being a particular problem with regard to noise when a NTSC picture has a satellite channel in part of its transmission path.

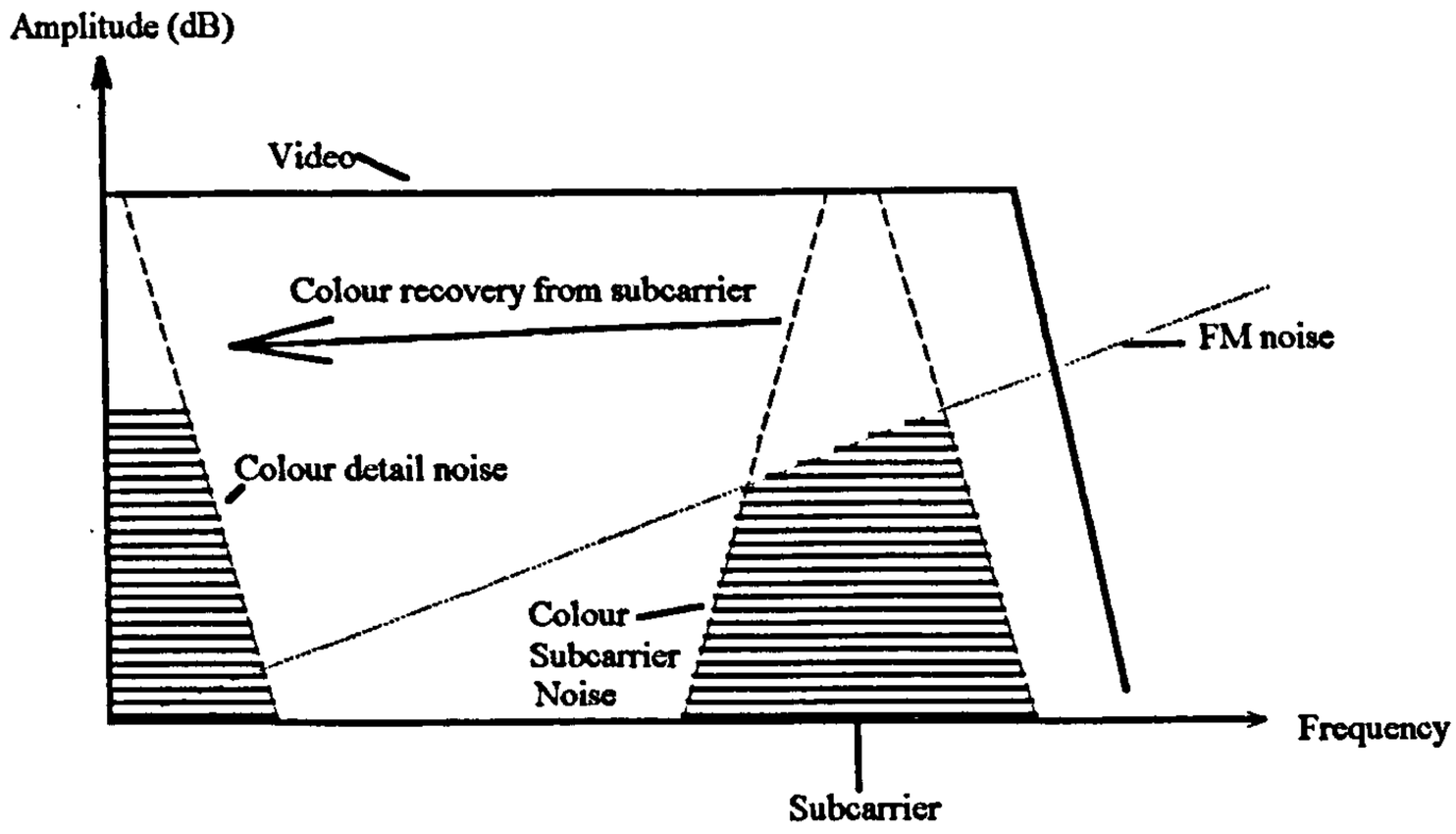

Figure 4/11 Chrominance demodulation converts high frequency, high amplitude noise into more visible low-frequency, high amplitude noise

4.5.2 These noise problems with frequency domain multiplex (NTSC) systems resulted in the development of time division multiplex of analogue components (MAC) systems. The latter use timing compression of the luminance and chrominance components. Above the frequency modulation threshold, the spectrum of the noise voltage is said to be triangular. Noise power at any frequency f is proportional to f^2 and the total noise power in a frequency range from zero to the bandwidth limit B_C is proportional to B_C^3. Now the occupied channel bandwidth B_C is greater than the video bandwidth B_M by the time compression factor. Time compression degrades the video signal-to-noise ratio by increasing the transmission (occupied) bandwidth B_C with respect to the video bandwidth B_M. This is because the same amount of information is transmitted in less time. The decrease in signal-to-noise ratio is given by the relationship:

$$S/N = 30 \log \frac{B_C}{B_M} \qquad \text{..... (4-30)}$$

The relationship given in equation 4-30 can be applied to the luminance signal. From Appendix B, table B.3, the uncompressed time luminance signal bandwidth for D2-MAC is 5.2 MHz and the compression factor is 3:2. These give a compressed time luminance

bandwidth of 7.2 MHz, resulting in decrease in signal-to-noise ratio of 5.28 dB. However care should be taken if the decrease in chrominance signal-to-noise ratio is based solely on equation 4-30. This is because the effects of noise weighting are not being taken into account. The signal-to-noise ratio using equation 4-30, for a chrominance signal of 2.4 MHz uncompressed bandwidth and a time compression ratio of 3:1, is 14.3 dB. However because time compression does not increase noise power but translates it to a lower frequency where at which the weighting is less, a lower FM improvement factor is obtained.

4.5.3 Below threshold, thermal (or Gaussian) noise largely is masked by impulse (or click) noise. The appearance of these clicks in a conventional television display is sometimes described as 'comet tails' and they are due to the effect of the video de-emphasis filter in the receiver. The impulses or clicks coming from the FM demodulator are extremely narrow. The de-emphasis filter stretches these out in time according to its own impulse characteristics. The long time constant and high low frequency gain of the de-emphasis filter required to equalise the video response, stretch the clicks so that they appear in the picture as 'comet tails'. With a time division multiplex system (MAC) the de-emphasis filter can have a shorter time constant and a lower low frequency gain. The effect of this change is to shorten the horizontal dimension of the noise and remove its bright 'comet' head. Much of the improvement in picture quality in the MAC systems at carrier-to-noise ratios in the region of threshold results from the way that click noise is filtered in the receiver de-emphasis network. Rhodes [17] claims that bright coloured noise just does not occur with the MAC systems because bright colours are combinations of the primary colours. It requires two impulses a precise time apart to generate bright coloured noise, an event that has a low statistical probability. Rhodes does not claim that the number of impulses is less with component (MAC) transmission compared to composite (NTSC) systems. It is the subjective appearance of the impulse noise that makes it more tolerable with the MAC systems.

4.6 Noise spectra convention

4.6.1 There is two conventions used in the literature [19], [20] for noise spectra that are termed single-sided and double-sided spectral density functions. This section discusses both and shows that, for any particular application, the noise output derived for each concept is the same.

Consider what happens when a white noise input with a spectral density N_0, that is uniform in the frequency domain $-\infty < \omega < +\infty$, is applied to a linear filter H, whose transfer characteristic is $H(s)$. N_0 can be considered to be the uniform height of the spectral density of the noise. The double-sided output spectral density [19] at the filter output is:

$$S_{yy}(j\omega) = N_0 \left| H(j\omega) \right|^2 \qquad \text{..... (14-31)}$$

The output noise power N of the filter is given by:

$$N = N_0 \left[\frac{1}{2\pi} \int_{-\infty}^{+\infty} \left| H(j\omega) \right|^2 d\omega \right] \qquad \text{..... (14-32)}$$

The effective, or equivalent (figure 4/12), noise bandwidth W_H, of the linear filter H is defined by:

$$W_H = \frac{\frac{1}{2\pi} \int_{-\infty}^{+\infty} \left| H(j\omega) \right|^2 d\omega}{\left| H(j\omega) \right|^2_{\max}} \qquad \text{..... (14-33)}$$

Using the relationship in equation (14-33), the filter output noise power N, given in equation (14-32) can be written as:

$$N = N_0 W_H \left| H(j\omega) \right|^2_{\max} \qquad \text{..... (14-34)}$$

W_H is the spectral width of an ideal bandpass filter, as shown in figure 4/12, whose maximum response is the same as that of $H(s)$ and whose output power (in the presence of white noise) is the same as that of $H(s)$. Also defined in figure 4/12 is the maximum value of $H(s)$, which is given as $|H(j\omega)|^2_{max}$.

Some references prefer to consider single-sided behaviour of filters. They argue that negative frequencies are not really observable, and hence that all the concepts involving frequency should be defined accordingly to involve only positive frequency. This is not efficient mathematically, for it immediately rules out such powerful analysis tools as the ordinary Fourier transform. Hence these references are led to a double-sided analysis and a single-sided interpretation. For example the filter response in figure 4/13 has a noise bandwidth $W = 2B$ Hz, whereas most of these references would agree that the band of frequencies passed is only B Hz wide.

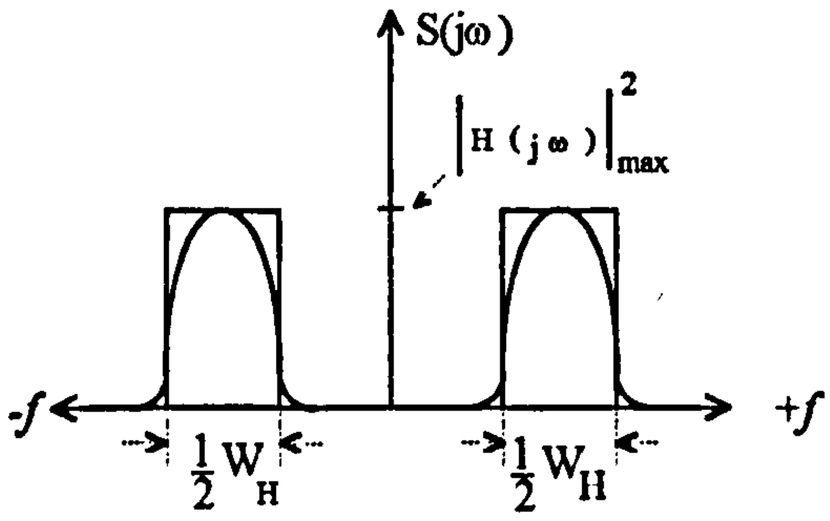

Figure 4/12 Equivalent noise bandwidth

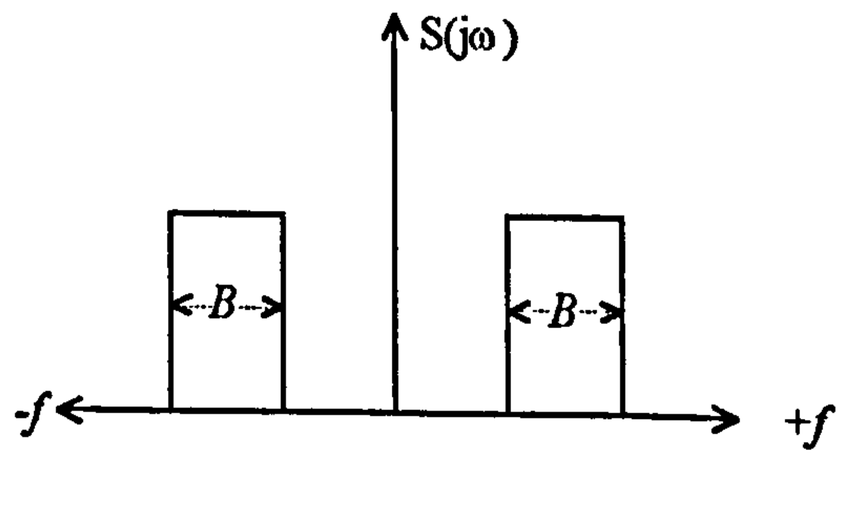

Figure 4/13 Double-sided frequency response

Working with a single-sided spectral system, as in figures 4/14 and 4/15, one folds the negative frequency response on to the positive. The result is the single-sided spectrum, which is written:

$$G_{ss}(j\omega) = \begin{cases} 2S_{ss}(j\omega) & \omega \geq 0 \\ 0 & \omega < 0 \end{cases} \qquad \text{..... (14-35)}$$

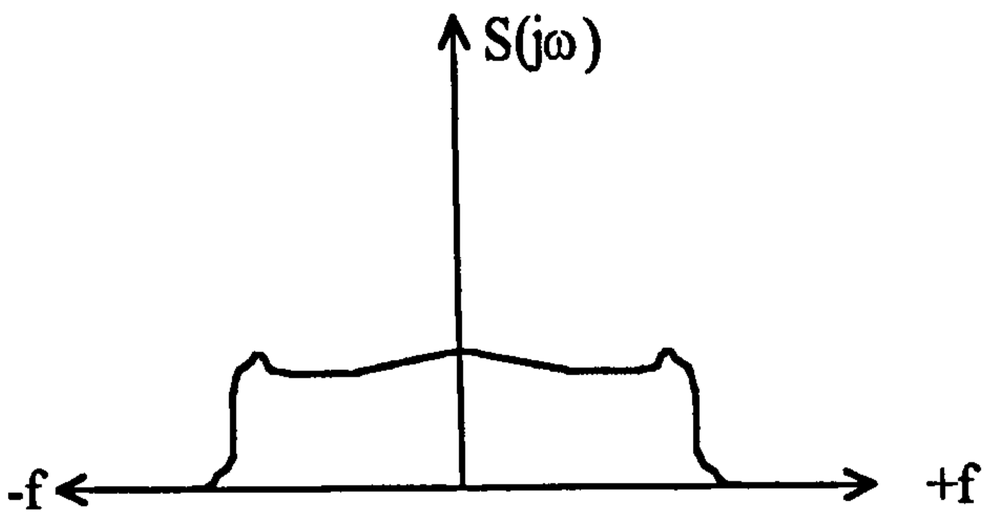

Figure 4/14 Double-sided spectra

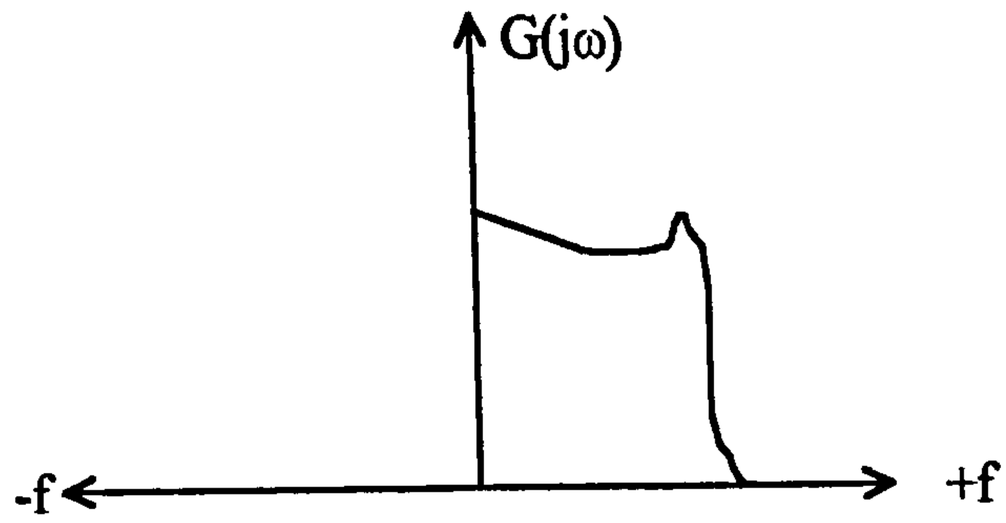

Figure 4/15 Single-sided spectra

The equivalent single-sided bandwidth can be written:

$$B_H = \frac{\frac{1}{2\pi}\int_0^{+\infty} |H(j\omega)|^2 \, d\omega}{|H(j\omega)|^2_{max}} = \frac{1}{2} W_H \qquad \text{..... (14-36)}$$

Using this single-sided notation the noise power spectral density can be written:

$$G_{nn}(j\omega) = \begin{cases} N_{SS} \\ 0 \end{cases} = \begin{cases} 2N_0 & for \quad \omega \geq 0 \\ 0 & \omega < 0 \end{cases} \qquad \text{..... (14-37)}$$

The resulting noise output is the same as equation (14-34) but appears written in single-sided parameters as:

$$N = N_{SS} \, B_H \, |H(j\omega)|^2_{max} \qquad \text{..... (14-38)}$$

There is little practical advantage [19] to be gained from a single-sided treatment once it is realised that since physical filters have both a positive and negative frequency response, it is not possible to measure only the positive side or the negative side of a spectrum by using linear filters, it is only possible to measure the composite effect of both positive and negative frequencies with a filter. However some references, e.g. [20], state that it is desirable to use the double-sided spectral density function for analytical studies, but for

practical applications it is more convenient to use single-sided spectral density functions. Both double-sided and single-sided concepts are used in this thesis, the notation used and the text makes clear which convention is being used in any particular case. $S(j\omega)$ is a double-sided spectral density, W_H is a double-sided bandwidth, $G(j\omega)$ refers to a single-sided spectral density and B is a single-sided bandwidth.

4.7 References

[1] Rice, S. O. "Noise in FM Receivers," Ch. 25, *Time Series Analysis*, Rosenblatt, Ed., New York : Wiley, 1963, pp 395 - 422.

[2] Forestieri, E., Prati, G. "FM Click Statistics in the Presence of Phase Noise", IEEE Trans. Communications, Volume 42, Number 2/3/4, Part 1 of three parts, February/March/April 1994, pp. 549 - 561.

[3] Bar-David, I., Sham, S. "On the Rice Model of Noise in FM Receivers", IEEE Trans. Information Theory, Vol. 34, No. 6, November 1988, pp. 1406 - 1419.

[4] Schwartz, M. "Signal-to-Noise Effects and Threshold Effects in FM", Proceedings of the N.E.C., 1962, Vol. 18, pp. 59 - 71.

[5] Lindgren, G. "On the shape and duration of FM clicks", IEEE Trans. Information Theory, Vol. IT-29, No. 4, pp. 536 - 543, July 1983.

[6] Lindgren, G. "Shape and duration of clicks in FM transmission", IEEE Trans. Information Theory, Vol. IT-30, No. 5, pp. 728 - 735, Sept. 1984.

[7] Blachman, N. M., Roberts, J. H. "FM Click Rates: A simple derivation," Electron. Letters., Vol. 10, No. 15, pp. 305 - 307, July 1974.

[8] Rainal, A. J. " Theoretical duration and amplitude of an FM click", IEEE Trans. Information Theory, Vol. IT-26, pp. 369 - 372, May 1980.

[9] Lob, W. H. " The distribution of FM discriminator click widths", Proc. IEEE, Vol. 57, pp. 732 - 733, April 1969.

[10] Glazer, A. " Distribution of click amplitudes", IEEE Trans. Communications Technology, Volume COM - 19, pp. 539 - 543. August 1971.

[11] Bozzoni, E., Marchetti, G., Russo, F. " Probability density of the click duration in an ideal FM discriminator", IEEE Trans. Aerosp. Electron. Systems, Vol. AES - 6, pp. 249 - 252, March 1970.

[12] Yavuz, D. "FM Click Shapes", IEEE Trans. Communications Technology, Volume COM - 19, No. 6, pp. 1271 - 1273, December 1971.

[13] Rainal, A. J. "Power Spectra of FM clicks", IEEE Trans. Information Theory, Vol. IT-30, No. 1, pp. 122 - 124, Jan. 1984.

[14] Kac, M., Slepian, D. "Large Excursions of Gaussian Processes", Ann. Math. Statist., Vol. 30, pp. 1215 - 1228, 1959.

[15] Yavuz, D., Hess, D. T. " FM Noise and Clicks", IEEE Trans. Communications Technology, Volume COM - 17, No. 6, pp. 648 - 653, December 1969.

[16] Schilling, D. L., Ringdald, I. "On the Distribution of Spikes seen at the output of an FM Discriminator below Threshold", Proc. IEEE, Vol. 52, December 1964, p. 1756.

[17] Rhodes, C. W. "A tutorial on improved systems for color television transmission by satellite". IEEE Trans. Broadcasting, Vol. BC -31, No. 1, March 1985, pp. 1 - 9.

[18] Lowry. J. D. "B-MAC: An optimum format for satellite television transmission". SMPTE Journal, November 1984, pp. 1034 - 1043.

[19] Tausworth, R. C. "Theory and practical design of phase-locked receivers", Vol. 1. National Aeronautics and Space Administration, Technical Report No. 32-819, February 15th, 1966, (N66-17323).

[20] Bendat, J. S., Piersol, A. G. "*Engineering Applications of Correlation and Spectral Analysis*", 2nd. Ed., John Wiley, New York, 1993, ISBN 0-471-57055-9.

5. DBS QUALITY CRITERIA

5.1 General

5.1.1 In the design of direct broadcast television systems, the designer's aim is that a satisfactory picture quality shall be obtained at the receiver for a wide variety of conditions. The field strength of the signal at the receiver location is thus regarded as being basic to receiver quality. As the signal power applied to a receiver is decreased, the level of noise displayed on the picture increases. Threshold extension techniques aim to alter the relationship between the vision carrier-to-noise ratio (C/N) and the picture signal-to-noise ratio (S/N) from that which exists with conventional receiving techniques.

This section discusses the advantages of implementing threshold extension techniques together with giving a definition of threshold extension. The criteria used for vision carrier-to-noise ratio and picture signal-to-noise ratio is given together with the relationship between them.

5.2 Direct broadcast FM bandwidth

5.2.1 The necessary bandwidth for FM television channels in satellite direct broadcast systems are interrelated with some important parameters [4], namely signal quality and availability, radiated power for a given earth terminal figure of merit and the number of audio and data signals carried in addition to the picture signal.

Signal quality is affected by bandwidth since it is not possible to transmit the complete spectrum of a frequency modulated signal that is theoretically infinite. The resulting inevitable spectrum truncation, which occurs at both the transmitter and the receiver I.F. filter, results in impairments to both the luminance and chrominance of a composite video signal. A further parameter that is important to obtaining a good signal-to-noise ratio is the

FM deviation, this is also limited by the available bandwidth.

The percentage of time that a signal of minimum allowable video signal-to-noise ratio is available is determined by the RF, or vision, carrier-to-noise ratio at the demodulator input. These ratios are a function of channel bandwidth, thus for any designed signal quality in terms of video signal-to-noise ratio, the signal availability must be greater than the minimum level required for a defined percentage of the transmission time. Since it is economical to carry the audio that accompanies the picture, as well as other audio and data signals, within the DBS channel that transmits the video signal, the quality and quantity of these additional paths are also a function of the channel bandwidth.

5.2.2 Throughout this thesis Carson's rule will be used to establish the RF bandwidth in terms of the carrier deviation and maximum sinusoidal modulation frequency. For noise-like modulation signals modifications to this rule will be used, see chapter 6, equation (6-5), and Appendix D. Carson's rule may be stated as:

$$B_C = D_{p-p} + 2 f_M \qquad \text{..... (5-1)}$$

where: B_C = Bandwidth (Hz)

D_{p-p} = Peak-to-Peak Deviation (Hz)

f_M = Maximum video modulation frequency (Hz)

The bandwidth established by Carson's rule allows 98% of the power transmitted to be received. Reference [4] discusses the bandwidth requirements for conventional composite TV systems, i.e. PAL, SECAM and NTSC, and concludes that Carson's rule gives a larger bandwidth than is required. When pre-emphasis is used care should be exercised in selecting the bandwidth in relation to other system parameters in order to avoid truncation noise when operating near threshold. Rhodes [7] confirms that Carson's rule applies well for

composite systems, but questions its validity for component (MAC) systems. He suggests that care should be taken in specifying the deviation for the latter.

5.3 Definition of threshold extension

5.3.1 In comparing the various approaches to threshold extension demodulation, it is necessary to have a definition of the effect so as to establish the improvement that can be obtained with each approach. Two definitions, or methods, have been used in the literature. The click count approach and the 'one dB' extension point. The former is widely used in the early literature, the latter is the current popular definition and will be used in this study. Both approaches are defined below.

5.3.2 The click count approach was proposed by Rice in his fundamental paper on noise in FM receivers, [6]. Here he proposed the break point in the linear carrier-to-noise ratio and signal-to-noise ratio characteristic could be determined by the click rate. That is the relationship between the break point and the expected number of clicks per second in the demodulator output could be used to define the threshold. For an unmodulated carrier he gave an exact result, namely that the expected number of clicks per second, H , is:

$$H = r\left(1 - erf\sqrt{C/N}\right) \qquad \text{..... (5-2)}$$

C/N is the input carrier-to-noise ratio. Rice [6] defines r as the radius of gyration, in Hz, of $w(f)$ the power spectrum about its axis of symmetry at the carrier frequency, or as the 'representative frequency' of the in-phase and quadrature components of the narrow band Gaussian noise current whose power spectrum is $w(f)$. The radius of gyration is analogous to the r.m.s. value of a random process; it is defined [8] as the positive square root of the second moment of a stationary random process. Rice in his paper [6] gives values for r for two conditions, namely a rectangular I.F. filter characteristic and a normal law I.F. filter characteristic. The difficulty of using the clicks per second definition is that the TV carrier is modulated by a complex waveform and that it is difficult to count the number of clicks

when they appear as flashes of interference on the picture.

5.3.3 In an FM system the relationship between the carrier-to-noise ratio (C/N) and the signal-to-noise ratio (S/N) at the demodulator output is of the form shown in figure 5/1. In the linear region the output signal-to-noise ratio is related directly to the input carrier-to-noise ratio. At very high input carrier-to-noise ratios, the output signal-to-noise ratio reaches a limiting value determined by the inherent noise of the demodulator. At low carrier-to-noise ratios the linear relationship breaks down and a reduction in carrier-to-noise ratio produces a disproportionate reduction in signal-to-noise ratio. This is termed the threshold point.

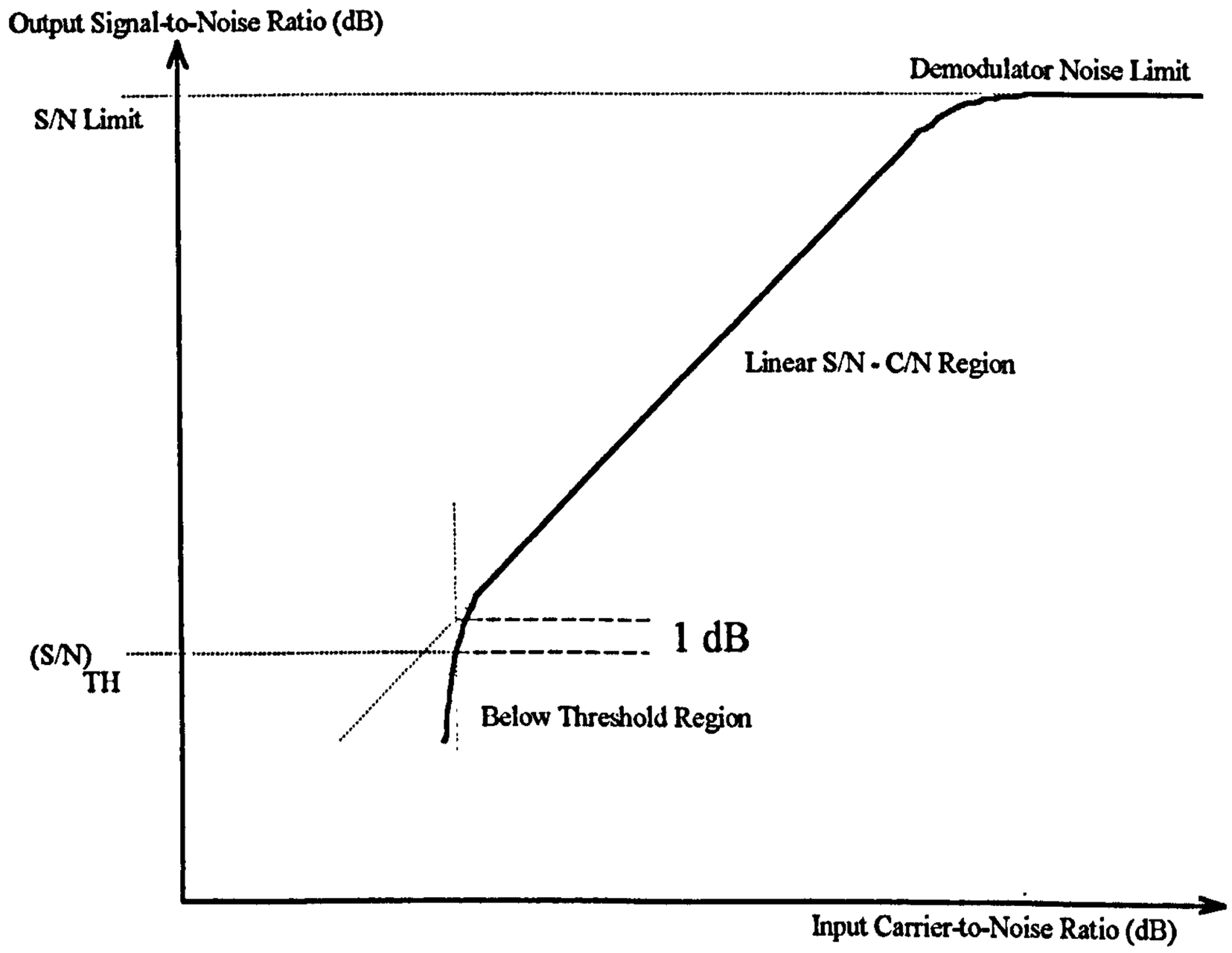

Figure 5/1 - Typical Noise Characteristics of an FM System

(Second threshold is not shown)

The traditional definition of threshold point is the value of the carrier-to-noise ratio at which the signal-to-noise ratio is 1 dB less than it would have been as defined by the linear relationship.

The 1 dB threshold point can be measured objectively and normally this corresponds to a carrier-to-noise ratio that is somewhat lower than the subjective (just visible) threshold in TV pictures. In the latter the onset of threshold shows as the sudden appearance of spike noise (comet tails) on the picture.

5.4 Pre-emphasis and de-emphasis characteristics

5.4.1 In various television systems it is usual to utilise both weighting and pre-emphasis/de-emphasis networks in the system. Pre-emphasis networks are used in the transmitter and de-emphasis networks in the receiver. The subjective effect of noise upon the TV picture, depends upon the spectral distribution of the noise energy within the video frequency band. When measuring noise power, it is the practice to use weighting networks that take account of this fact, with the result that the weighted noise power at video frequencies is lower than the total noise power by a factor depending upon the spectral distribution. For most television systems the weighting networks are designed so that for various spectral distributions of the noise the measurements represent the subjective impression on the picture than do unweighted noise measurements. Care should be taken when using the weighting factors specified by the CCIR ([1], chapter 1) as they are not valid when an FM system is working near threshold and where the noise loses its Gaussian characteristics and becomes impulsive. However for the purposes of this thesis the weighting factors are used for comparison purposes only and thus the distortion in the results is considered acceptable.

5.4.2 The effect of threshold noise should also be taken into account when considering the effects of emphasis, see sect 4.5 above. The use of de-emphasis causes the threshold spikes to appear as streaks (comet tails) on the screen. The resulting impairment depends on the number and amplitude of the spikes, together with the length of the disturbance. The use of time compression causes the streaks to be stretched by the compression factor. The use of pre-emphasis is beneficial in reducing the amplitude and the number of the spikes but it has the effect of increasing the length of the spikes. Subjective

tests indicate that with a suitable choice of the pre-emphasis characteristic, the beneficial effects more than compensate for the negative effects. At low carrier-to-noise ratios the performance of MAC systems are better than the conventional systems such as PAL, SECAM or NTSC. The picture is more acceptable, as the threshold streaks are much shorter, due to the smaller amount of de-emphasis and the shorter time constants. Details of analogue and digital non-linear pre/de-emphasis networks for the MAC systems are given in [2]. The effect of their application is a subjective improvement in picture quality equivalent to a 3 dB increase in carrier-to-noise ratio of the received signal. Reference [2] also gives the reasons for the choice of the parameters specified for the MAC systems in [3]. An excellent description of optimising the pre-emphasis characteristic for satellite TV signals near threshold is given in [5].

5.5 Carrier-to-noise and signal-to-noise ratio criteria

5.5.1 In determining the amount of threshold extension improvement obtained with the various design improvements considered in this thesis a criterion is required to allow a comparison to be made with a baseline system. This section discusses a suitable criterion that is used in TV system design [1]. The picture quality is determined by the quality of the video signal that is defined in terms of the peak-to-peak signal-to-weighted noise ratio. The CCIR [1] has determined picture quality ratings in terms of the (video) signal-to-noise ratio. In the design of a TV system the signal quality parameter is important as it directly affects the satellite transmitter power and the ground terminal (G/T) characteristic.

The quality of the television image on the receiving screen depends on the picture signal-to-noise ratio and on the various distortions occurring in the transmission chain. Various methods of making subjective assessments of the quality of television pictures and the parameters involved may be found in the references given in [1], together with references to the scales for assessing the quality of television pictures. The signal-to-noise ratio is a very important parameter in designing television systems and in selecting its value account must

be taken of other television signal distortions.

In television therefore, the signal-to-noise ratio at video frequencies is defined as '*the ratio, expressed in decibels, of the nominal peak-to-peak amplitude of the picture-luminance signal to the r.m.s. value of the noise in the working video frequency band.*'

It is this definition of picture signal-to-noise ratio that will be used in this thesis.

5.5.2 A method [1] of calculating the signal-to-noise ratio for FM television systems is as follows.

$$(S/N) = (C/N)\ 3\left(\frac{D_{p-p}}{f_M}\right)^2\left(\frac{B_C}{2f_M}\right)\ k_W \qquad \ldots\ldots\ (5\text{-}3)$$

which when expressed in decibels becomes:

$$(S/N)_{dB} = (C/N)_{dB} + F_{dB} + (k_W)_{dB} \qquad \ldots\ldots\ (5\text{-}4)$$

Now
$$(C/N) = (C/N_0)\frac{1}{B} \qquad \ldots\ldots\ (5\text{-}5)$$

Equation (5-4) when put into (5-3) and (5-4) gives the form of the equation in terms of the carrier power to noise spectral density ratio.

$$\therefore \quad (S/N) = (C/N_0)\ \frac{1}{B_C}\ 3\left(\frac{D_{p-p}}{f_M}\right)^2\left(\frac{B_C}{2f_M}\right)\ k_W \qquad \ldots\ldots\ (5\text{-}6a)$$

$$(S/N) = (C/N_0)\frac{3}{2}\frac{D_{p-p}^2}{f_V^3}k_W \qquad \ldots\ldots\ (5\text{-}6b)$$

In the decibel form equation (5-6) becomes:

$$(S/N)_{dB} = (C/N_0)_{dB} + \left(\frac{3}{2}\frac{D_{p-p}^2}{f_M^3}\right)_{dB} + (k_W)_{dB} \qquad \text{..... (5-7)}$$

where:

(S/N) = Ratio of peak-to-peak luminance amplitude in weighted r.m.s. noise.

(C/N) = Pre-detection carrier-to-noise ratio in bandwidth, B_C

(C/N_0) = System carrier power to noise spectral density ratio (dB/Hz)

$F = 3\left(\frac{D_{p-p}}{f_M}\right)^2 \left(\frac{B_C}{2f_M}\right)$, a power ratio

D_{p-p} = peak-to-peak deviation by video signal (in composite systems includes synchronisation pulses where appropriate)

f_M = Highest modulating (video) frequency.

B_C = RF bandwidth, usually taken as $D_{p-p} + 2f_M$ (Hz)

k_W = Combined de-emphasis and weighting improvement factor in FM systems. A value which depends upon the TV system used.

In a conventional demodulator system note that the carrier-to-noise ratio (C/N_0) must be greater than the FM threshold that is of the order of 9-10 dB, where $(C/N) = (C/N_0)\left(\frac{1}{B}\right)$.

Note that in the literature two forms of equation (5-3) appear, one using the peak-to-peak deviation and the other using the peak deviation. Although this difference appears trivial, it is important because in the latter version a parameter k_L is included which is a conversion

factor from r.m.s. to peak-to-peak deviation (6 dB).

5.5.3 Consider each of the parameters in equation 5-4 above and determine practical values for them when the equation is applied to the D2-MAC format system. A review of the CCIR recommendations has failed to establish values of k_W for the MAC television systems. Values for the C, D, and D2-MAC format TV systems however can be derived from the pre-emphasis characteristics given in Table 1 of reference [2], page 53. Here the weighted luminance signal-to-noise ratio $(S/N) = 42.23$ dB that corresponds to $(C/N) = 14$ dB for a bandwidth of 6 MHz. From the tables given in Appendix B the value of peak-to-peak deviation (D_{p-p}) can be obtained, i.e. 13.5 MHz. Note that for these tables a maximum vision bandwidth of 8.4 MHz is specified, but since the values of signal and carrier-to-noise ratios are given for a 6 MHz bandwidth, this is the figure that will be used. The parameters for equation 5-4 can thus be determined.

$$(S/N)_{dB} = (C/N)_{dB} + 10 \log\left\{ 3 \left(\frac{D_{p-p}}{F_v}\right)^2 \left(\frac{D_{p-p} + 2F_V}{2F_v}\right)\right\} + (k_W)_{dB} \quad \text{..... (5-8)}$$

$$42.23 = 14 + 10\log 3\left(\frac{13.5\times10^6}{6\times10^6}\right)^2 \left(\frac{(13.5\times10^6)+(2\times6\times10^6)}{2\times6\times10^6}\right) + (k_W)_{dB}$$

$$42.23 = 14 + 15.1 + (k_W)_{dB}$$

$$\therefore \ (k_W)_{dB} = 13.13 \text{ dB}$$

Compared to the values specified for the monochrome television systems [1], page 20, this value is at the low end of the range for k_W. Note that if the vision bandwidth of 8.4 MHz

was used then a value of $k_W = 16.78$ dB would be obtained, which would be towards the higher end of the range. The lower value will be used in the following example. For the C, D and D2 - MAC format television systems the general relationship between the signal-to-noise and carrier-to-noise ratios is therefore given by:

$$(S/N)_{dB} = (C/N)_{dB} + 15.1 \text{ dB} + 13.13 \text{ dB}$$

$$(S/N)_{dB} = (C/N)_{dB} + 28.23 \text{ dB} \quad \ldots\ldots\ldots \quad (5\text{-}9)$$

Thus at threshold, say $(C/N)_{dB} = 9$ dB, would give a value of $(S/N)_{dB} = 37.23$ dB. The relationship shown in equation (5-9) is plotted below in figure 5/2.

Figure 5/2 - C, D and D2 TV Systems

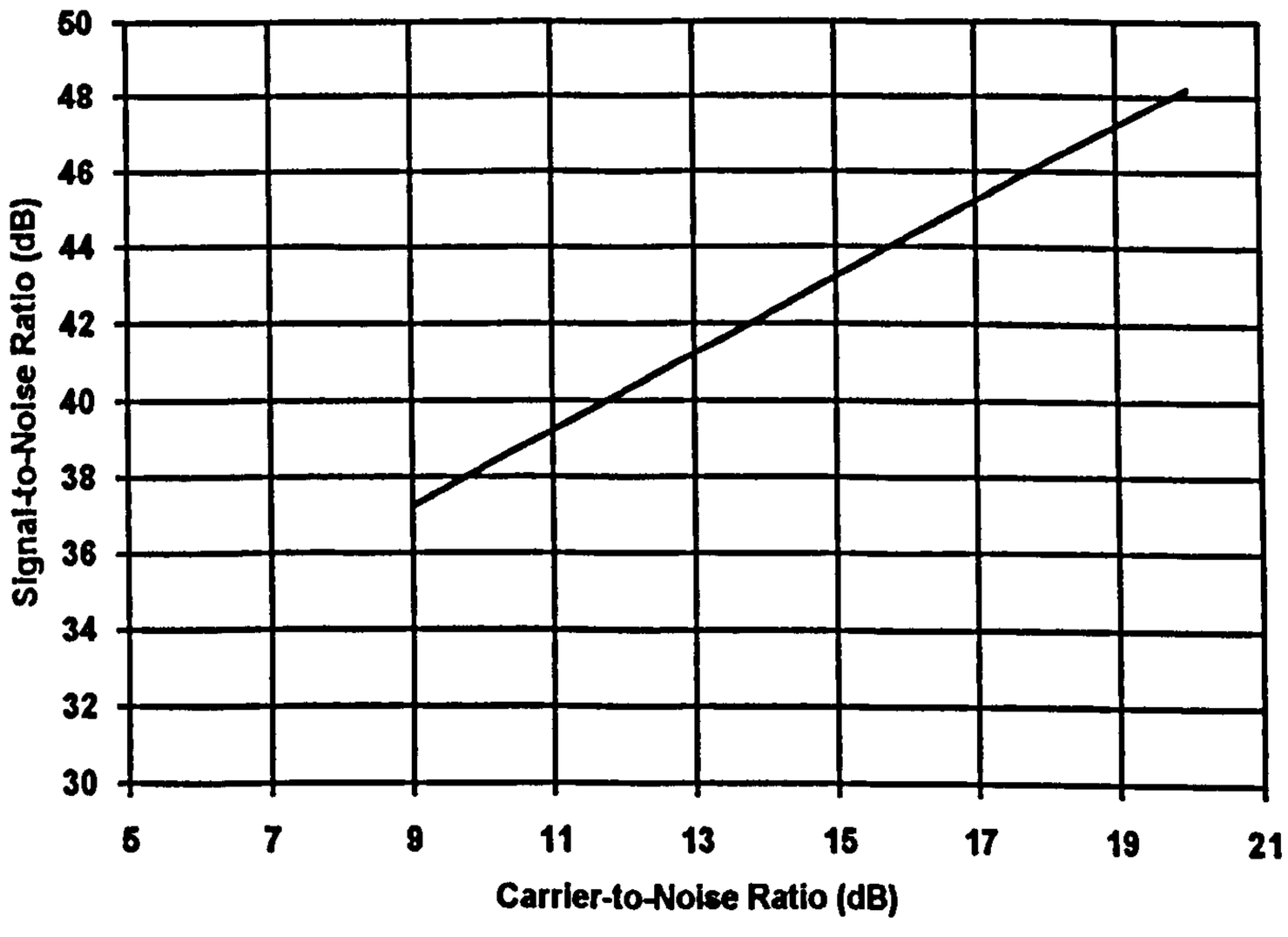

5.6 References

[1] CCIR "*Broadcasting Satellite Systems*", Geneva, 1983, (ISBN 92.6.01751.7)

[2] CCIR "Satellite Transmission of Multiplexed Analogue Component (MAC) Vision Signals". Report No. 1074-1.

[3] CCIR "Television Standards for the Broadcasting - Satellite Service", Report 1073-1, (1986 - 1990).

[4] Siocos, C. A. "Satellite FM Television Bandwidth", Space Communication and Broadcasting, 2, (1984), pp 363-369.

[5] Loo, Chun. "Optimum Pre-Emphasis Network for Satellite Transmission of an FM TV Signal near or at Threshold", IEEE Transactions on Broadcasting, Vol. BC-28, No. 2, June 1982, pp 37 - 43.

[6] Rice, S. O., Chapter 25 (Noise in FM Receivers) of *"Time Series Analysis"*, M. Rosenblatt, Ed., New York, 1963, pp. 395 - 422.

[7] Rhodes, C. W. "A tutorial on improved systems for color television transmission by satellite". IEEE Trans. Broadcasting, Vol. BC -31, No. 1, March 1985, pp. 1 - 9.

[8] Bendat, J. S., Piersol, A. G. "*Engineering Applications of Correlation and Spectral Analysis*", 2nd. Ed., John Wiley, New York, 1993, ISBN 0-471-57055-9.

Blank Page

6. IDEAL AND CONVENTIONAL DEMODULATOR THRESHOLD

6.1 General

A question that immediately arises in any examination of FM threshold extension techniques, is the magnitude of the improvement in demodulation performance that can be obtained. In the literature various claims to improvements in performance have been made for DBS applications. In general these tend to be of the order of 2 to 3 dB, [1-2], although some patents [3] claim high values of the order of 7 dB; values that tend to raise questions about the method of measurement used.

To determine the theoretical maximum improvement in performance that is possible for DBS applications, the method adopted here is to determine the performance of an ideal demodulator using basic information theory considerations. This will give the maximum threshold improvement possible when compared to the threshold characteristics of a conventional demodulator. The improvement possible for any particular threshold extension demodulator technique will lie between these two characteristics. The detailed analysis of the conventional modulator is given to show how the threshold characteristic is dependent upon the nature of the modulation. A dependence which assumes some importance when considering threshold extension demodulators.

6.2 Ideal demodulator threshold characteristics

Previous studies on threshold extension demodulators have shown that by increasing the complexity of the demodulator in FM systems, an improvement in system threshold can be obtained. However the question that then arises is can the threshold performance of the FM demodulator be improved ad infinitum by increasing its complexity? The answer is no as Shannon's limit for errorless transmission results in a linear demodulator boundary as is shown below. While the ideal demodulator boundary derived from Shannon's theory is not

based upon the 1 dB criteria it does indicate from the information-theoretic viewpoint a limit on linear demodulation. In comparing various demodulator techniques particularly in terms of their efficiency, an ideal demodulator [4-5], [10], can be formulated to serve as a reference. Goblick [4] provides a useful treatment of the ideal demodulator based upon Shannon's original theorem on information theory [11]. A necessary condition for transmitting a waveform with an information rate R_E to a receiver over a noise channel with capacity C_i, with mean-squared error ε or less is $R_E \leq C_i$. This condition was stated by Shannon [11].

The information channel capacity at the input of an ideal demodulator is:

$$C_i = B_i \log_2 \left(1 + \frac{S_i}{\eta_i B_i}\right) \qquad \text{..... (6-1)}$$

where C_i = Channel capacity (bits/second)

S_i = Average signal power (watts)

η_i = Noise power spectral density (watts)

B_i = Noise bandwidth (Hz)

The subscript '*i*' denotes an input quantity.

At the output, for a given output signal to noise ratio, the information rate R_E must not exceed:

$$R_E \geq B_M \log_2 \left(\frac{S_o}{\eta_o B_M}\right) \qquad \text{..... (6-2)}$$

where S_o = Average signal power (watts)

η_o = Noise power spectral density (watts)

B_M = Base bandwidth (Hz)

The subscript 'o' denotes an output quantity.

Whilst the channel capacity is the boundary of errorless transmission, it is a very sharp boundary, with error increasing very rapidly if violated. Therefore the channel capacity must equal or exceed the minimum rate given in equation (6-2). Thus:

$$B_i \log_2\left(1+\frac{S_i}{\eta_i B_i}\right) \geq B_M \log_2\left(\frac{S_o}{\eta_o B_M}\right) \qquad \text{.....} \quad (6\text{-}3)$$

which results in

$$\frac{S_o}{\eta_o B_M} \leq \left(1+\frac{S_i}{\eta_i B_i}\right)^{\frac{B_i}{B_M}} \qquad \text{.....} \quad (6\text{-}4)$$

In order to interpret these results [7] in terms of FM, the r.m.s. modulation index β_{rms} for noise like signals, is related to the bandwidth B_i by :

$$B_i = 2\,B_M\left(1+\sqrt{10}\,\beta_{rms}\right) \qquad \text{.....} \quad (6\text{-}5)$$

Inserting equation (6-5) into (6-4) gives:

$$\frac{S_o}{\eta_o B_M} \leq \left(1+\frac{S_i}{\eta_i B_M}\frac{1}{2\left(1+\sqrt{10}\,\beta_{rms}\right)}\right)^{2\left(1+\sqrt{10}\,\beta_{rms}\right)} \qquad \text{.....} \quad (6\text{-}6)$$

This equation now relates the carrier-to-noise ratio and signal-to-noise ratio, for a constant baseband bandwidth, and the modulation index. A plot of it is shown in figure 6/1 for a value of $\beta_{rms} = 1$.

Figure 6/1 - Ideal Demodulator

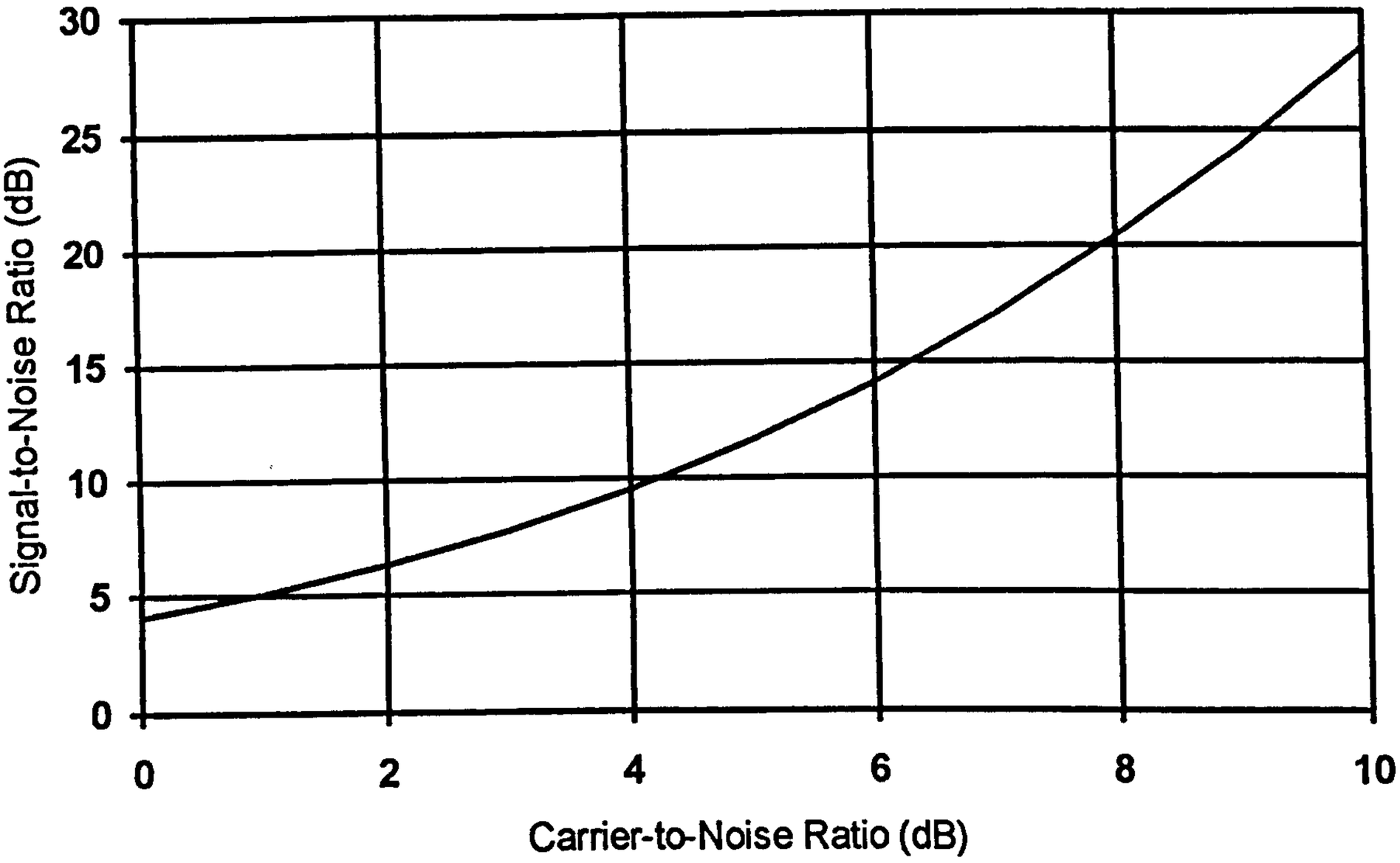

6.3 Threshold Characteristics of a Conventional Demodulator

6.3.1 General

The threshold performance of a conventional limiter-demodulator has been treated by a number of authors; among the more important approaches are those due to Rice [6], Frankle [7], Camp [8], Taub and Schilling [9] and Klapper [10]. The following analysis is quite conventional and may be found in several of these sources. This section will be based upon the Taub and Schilling approach as modified by Camp's treatment. A functional block diagram of a conventional limiter-discriminator (or demodulator) is illustrated in figure 6/2.

A conventional FM demodulator contains two basic circuit functions: a limiter and a discriminator. In normal applications the demodulator is preceded by a pre-detection, or I.F. bandpass, filter with a transfer characteristic $H_c(f)$ and is followed by a post detection, or

baseband, filter with a transfer characteristic $H_B(f)$. In an FM system the baseband signal causes the carrier frequency to vary. Any amplitude variation of the carrier at the receiver will be due to noise and propagation variations. Because a discriminator will respond to carrier disturbances as well as frequency variations, a limiter circuit is used to remove any such amplitude variation. In this section the limiter characteristic assumed is that of an ideal hard limiter, i.e. the limiter output is assumed to be a constant amplitude square wave no matter how the input signal $V_1(t)$ varies. The bandpass filter at the output of the limiter, with a transfer characteristic $H_{BP}(f)$ selects the fundamental component of the square wave such that the output V_2 is a modulated sinewave of constant amplitude.

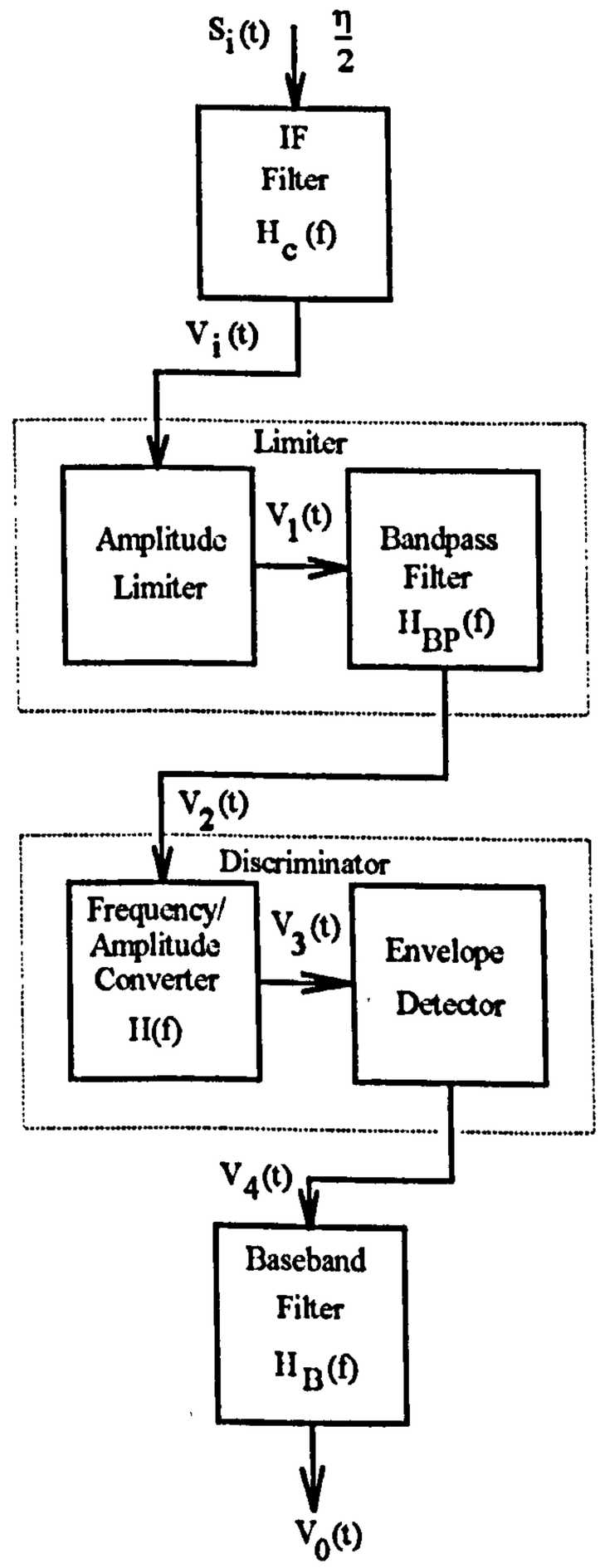

Figure 6/2 - FM Limiter Discriminator

The discriminator contains two component parts, a frequency to amplitude converter (or differentiator) and an envelope detector. The former consists of a network which over the operating range exhibits a transfer characteristic $H(f)$ such that $|H(f)|$ varies linearly with frequency. When the limited frequency modulated signal, $V_2(t)$, is applied to this network, it appears at the output, $V_3(t)$, with an envelope (amplitude) variation that varies with time precisely as does the instantaneous frequency of the carrier. Note that this signal is both frequency and amplitude modulated. This signal is now applied to the envelope detector to recover the baseband signal, $V_4(t)$, which is then filtered by the baseband filter, whose output is the wanted demodulated signal $V_o(t)$.

6.3.2 Limiter-Discriminator Analysis

Assume that in the frequency-to-amplitude converter, $|H(j\omega)|$ varies linearly with ω over a limited range and that its slope is either positive or negative and that the phase variation of $H(j\omega)$ is unimportant. Also assume that:

$$H(j\omega) = j\,K_1\,\omega \qquad \text{..... (6-6)}$$

where K_1 is a constant.

Thus the input-output relationship for the frequency-to-amplitude converter becomes:

$$V_3(t) = K_1 \frac{d}{dt} V_2(t) \qquad \text{..... (6-7)}$$

Now let the frequency-to-amplitude converter input be:

$$V_2(t) = A_L \cos\left[\omega_c\, t + \phi(t)\right] \qquad \text{..... (6-8)}$$

where A_L = limited (constant) amplitude of carrier.

and $\left(\omega_c t + \phi(t)\right)$ = instantaneous phase.

Inserting equation (6-8) into (6-7) and differentiating:

$$V_3(t) = K_1 \frac{d}{dt}\left(A_L \cos\left[\omega_c t + \phi(t)\right]\right) \qquad \text{..... (6-9)}$$

$$\therefore \quad V_3(t) = -K_1 A_L \left(\omega_c + \frac{d}{dt}\phi(t)\right) \sin\left[\omega_c t + \phi(t)\right] \qquad \text{..... (6-10)}$$

Thus the output of the envelope detector is:

$$V_4(t) = K_1 A_L \left[\omega_c + \frac{d}{dt}\phi(t)\right] \qquad \text{..... (6-11a)}$$

Let $\alpha \equiv K_1 A_L$,then:

$$V_4(t) = \alpha\,\omega_c + \alpha \frac{d}{dt}\phi(t) \qquad \text{..... (6-11b)}$$

Note that equation (6-11b) shows that at the output of the discriminator contains two components, one a dc level $(\alpha\,\omega_c)$ and the other the wanted component that is proportional to the input, $\left(\alpha \frac{d}{dt}\phi(t)\right)$.

6.3.3 Output Signal and Noise Powers

Consider figure (6/2), and let the input signal to the I.F. filter be:

$$S_i(t) = A \cos\left[\omega_c t + k \int_{-\infty}^{t} m(t)\, d\, t\right] \qquad \text{..... (6-12)}$$

where $m(t)$ is the frequency modulated baseband waveform and k is a constant.

Assume: (i) That the signal is embedded in white Gausssian noise of a double-sided power spectral density $\frac{\eta}{2}$ (see [9], sections 7.9 and 14.5).

(ii) The bandwidth of the I.F. filter is determined by Carson's Rule, $B_C = 2\,\Delta f + 2\,f_M$ or alternatively $B_C = D_{P\text{-}P} + 2\,f_M$.

The signal at the output of the demodulator appears as a signal $s_0(t)$ and a noise waveform $n_0(t)$. At high signal-to-noise levels the noise value can be neglected in determining the output signal power, thus the signal at the output of the limiter, $V_2(t)$, can be written as:

$$V_2(t) = A_L \cos\left[\omega_c\, t + k \int_{-\infty}^{t} m(t)\, dt\right] \qquad \text{..... (6-13)}$$

Now let $$\phi(t) = k \int_{-\infty}^{t} m(t)\, dt \qquad \text{..... (6-14)}$$

from which $$\frac{d}{dt}\phi(t) = k\, m(t) \qquad \text{..... (6-15)}$$

Thus from equation (6-11b) the demodulator output is:

$$V_4(t) = \alpha\, \omega_c + \alpha\, k\, m(t) \qquad \text{..... (6-16)}$$

The baseband filter rejects the dc component $\alpha\, \omega_c$ and selects the wanted output signal that is:

$$V_0(t) = \alpha\, k\, m(t) \qquad \text{..... (6-17)}$$

The output signal power is therefore:

$$S_0(t) = \alpha^2\, k^2\, \overline{m^2(t)} \qquad \text{..... (6-18)}$$

The output noise power may be derived as follows. Assume that in addition to the signal, a white noise input is applied to the demodulator having a double-sided power spectral density of $\frac{\eta}{2}$. Now as the noise output is approximately independent [9] of the modulation $m(t)$, the latter will be set equal to zero, thus $m(t)=0$. After the signal and noise pass through the I.F. filter assume that the input $V_i(t)$ to the limiter is:

$$V_i(t) = A\cos\omega_c t + n_c(t)\cos\omega_c t - n_s(t)\sin\omega_c t$$

$$\therefore \quad V_i(t) = \left[A + n_c(t)\right]\cos\omega_c t - n_s(t)\sin\omega_c t \qquad \text{..... (6-19)}$$

From (6-19) the envelope $R(t)$, and the phase $\theta(t)$ may be derived:

$$R(t) = \sqrt{\left[A + n_c(t)\right]^2 + \left[n_s(t)\right]^2} \qquad \text{..... (6-20)}$$

and

$$\theta(t) = \tan^{-1}\frac{n_s(t)}{A + n_c(t)} \qquad \text{..... (6-21)}$$

Thus $V_i(t)$ can be written as:

$$V_i(t) = R(t)\cos\left[\omega_c t + \theta(t)\right] \qquad \text{..... (6-22)}$$

and the output, $V_2(t)$, of the limiter's filter becomes:

$$V_2(t) = A_L\cos\left[\omega_c t + \theta(t)\right] \qquad \text{..... (6-23)}$$

where the time varying envelope amplitude, $R(t)$, is replaced by the constant value, A_L, determined by the limiter.

For a high input signal-to-noise ratio, the signal power is much greater than the noise power, thus:

$$|n_c(t)| << A \quad \text{and} \quad |n_s(t)| << A$$

Thus equation (6-21) can be approximated to $\theta(t) \approx \tan^{-1} \frac{n_s(t)}{A}$ but since for small values of angle $\tan\theta \approx \theta$, then:

$$\theta(t) \approx \frac{n_s(t)}{A} \qquad \text{..... (6-24)}$$

Thus equation (6-23) can be approximated to:

$$V_2(t) \approx A_L \cos\left[\omega_c t + \frac{n_s(t)}{A}\right] \qquad \text{..... (6-25)}$$

Comparing this equation with that of equation (6-8) above shows that:

$$\phi(t) \equiv \frac{n_s(t)}{A} \qquad \text{..... (6-26)}$$

Thus from equation (6-11b), the discriminator output may be written as:

$$V_4(t) = \alpha\,\omega_c + \frac{\alpha}{A}\frac{d}{dt} n_s(t) \qquad \text{..... (6-27)}$$

Ignoring $\alpha\,\omega_c$, the d.c. component, the noise input to the baseband filter consists of the second term, viz.

$$V_4(t) = \frac{\alpha}{A}\frac{d}{dt} n_s(t) \qquad \text{..... (6-28)}$$

Let the single-sided spectral density of $n_s(t)$, for the frequency range $|f| \le \frac{B_C}{2}$, be η. In equation (6-28) the differentiation of $n_s(t)$ is equivalent to it being passed through a network whose transfer characteristic is:

$$H(j\omega)=\frac{j\alpha\omega}{A} \qquad \text{..... (6-29a)}$$

From which $$|H(f)|^2=\frac{\alpha^2\,4\,\pi^2\,f^2}{A^2} \qquad \text{..... (6-29b)}$$

Therefore let the spectral density of $V_4(t)$ be $G_4(f)$. Hence:

$$G_4(f)=|H(f)|^2\,\eta \qquad \text{..... (6-29c)}$$

Substituting equation (6-29b) gives:

$$G_4(f)=\frac{\alpha^2\,4\,\pi^2\,f^2}{A^2}\,\eta \qquad for \quad |f|\le\frac{B}{2} \qquad \text{..... (6-30)}$$

The output (Gaussian) noise power, N_0 , is thus:

$$N_0=\int_{-f_M}^{f_M} G_4(f)\,df$$

$$=\frac{\alpha^2\,\eta}{A^2}\int_{-f_M}^{f_M} 4\,\pi^2 f^2\,df$$

$$=\frac{\alpha^2\,\eta}{A^2}\left[4\,\pi^2\frac{f^3}{3}\right]_{-f_M}^{f_M}$$

$$\therefore \quad N_0=\frac{8\,\pi^2}{3}\,\frac{\alpha^2\,\eta}{A^2}\,{f_M}^3 \qquad \text{..... (6-31)}$$

Equation (6-31) is used for calculating the Gaussian noise power N_o in the threshold cases below. The output signal-to-noise ratio can now be computed using equations (6-18) and (6-31):

$$\frac{S_0}{N_0} = \frac{\alpha^2 k^2 \overline{m^2(t)}}{\frac{8\pi^2}{3}\frac{\alpha^2 \eta}{A^2} f_M{}^3}$$

$$\frac{S_0}{N_0} = \frac{3}{4\pi^2}\frac{k^2 \overline{m^2(t)}}{f_M{}^2}\frac{\frac{A^2}{2}}{\eta f_M} \qquad \text{.....(6-32)}$$

To determine $k^2 \overline{m^2(t)}$ assume that the modulating input signal $m(t)$ is a sinusoid with a deviation Δf . Equation (6-12) may be written as:

$$S_i(t) = A\cos\left(\omega_c t + \frac{\Delta f}{f_M}\sin(2\pi f_M t)\right) \qquad \text{..... (6-33)}$$

Comparing this equation with (6-18) shows that:

$$k\int_{-\infty}^{t} m(t)\,dt = \frac{\Delta f}{f_M}\sin(2\pi f_M t)$$

Differentiating gives:

$$k\,m(t) = 2\pi\Delta f\cos(2\pi f_M t) \qquad \text{..... (6-34)}$$

Therefore using the identity $\cos^2 A = \frac{1}{2}(1+\cos 2A)$ and ignoring higher order terms:

$$k^2\overline{m^2(t)} = \frac{4\pi^2(\Delta f)^2}{2}$$

$$\therefore \quad k^2\overline{m^2(t)} = 2\pi^2(\Delta f)^2 \qquad \text{..... (6-35)}$$

Inserting this result into equation (6-32) gives:

$$\frac{S_0}{N_0} = \frac{3}{2}\left(\frac{\Delta f}{f_M}\right)^2 \frac{\frac{A^2}{2}}{\eta f_M} \qquad \text{..... (6-36a)}$$

where $\beta = \dfrac{\Delta f}{f_M}$ (modulation index).

$S_i = \dfrac{A^2}{2}$ (input signal power).

$N_M = \eta f_M$ (input noise power in baseband bandwidth f_M).

Hence: $$\frac{S_0}{N_0} = \frac{3}{2}\beta^2 \frac{S_i}{N_M} \qquad \text{..... (6-36b)}$$

Or in the other notation used in this report:

$$S/N = \frac{3}{2}\beta^2\, C/N \qquad \text{..... (6-37)}$$

6.3.4 Conventional Discriminator Threshold

(a) Unmodulated Carrier

The onset of threshold in an FM discriminator is signified by the occurrence of spike or click noise. This spike output is much greater for a modulated carrier than for an unmodulated carrier. In this and the following section the signal-to-noise ratio at the discriminator output is calculated for both the unmodulated and modulated carrier conditions.

Now the double-sided power spectral density (psd) of the spike noise is given by [see 9, Chapters 2 and 10]:

$$G_s(f) = \frac{1}{T_c} \overline{|P(j\omega)|^2} \qquad \text{..... (6-38)}$$

Where: $P(j\omega)$ = Fourier transform of the spike waveform

T_c = Mean time interval between spikes

Now $|P(j\omega)|$ is approximately constant and equal to $|P(0)|$, in the range $-f_M$ to $+f_M$ for $\frac{B}{2} \rangle\rangle f_M$.

Let the signal phase $\theta(t)$ rotate by 2π so that a spike is generated. Thus the waveform of the output noise voltage spike from the discriminator is :

$$[n(t)]_{spike} = \alpha \frac{d\theta}{dt} \qquad \text{..... (6-39)}$$

where α is the discriminator constant.

Now [9, Chap. 10] shows that $|P(0)|$ is equal to the area of $[n(t)]_{spike}$, and when α is constant the area under the waveform $\frac{d\theta}{dt}$ is 2π, thus:

$$|P(0)| = 2\pi\alpha \qquad \text{..... (6-40)}$$

This equation also gives the average value of $|P(0)|$ since each spike has the same area 2π. Thus from equation (6-38):

$$G_s(f) = \frac{4\pi^2\alpha^2}{T_c} \qquad \text{..... (6-41)}$$

The total noise output due to the spikes is thus:

$$N_s = \frac{4\,\pi^2\,\alpha^2}{T_C} 2\,f_M \qquad \text{..... (6-42)}$$

Now [9, Chap. 10] for an unmodulated carrier:

$$\frac{1}{T_C} = \frac{B_C}{2\sqrt{3}}\, erfc \sqrt{\frac{f_M}{B_C}\frac{S_i}{N_m}} \qquad \text{..... (6-43)}$$

where *erfc* is the complimentary error function, viz.

$$erfc\,x = \frac{2}{\sqrt{\pi}}\int_x^\infty e^{-\lambda^2}\,d\lambda = 1 - \frac{2}{\sqrt{\pi}}\int_0^x e^{-\lambda^2}\,d\lambda \qquad \text{..... (6-44)}$$

From equations (6-42) and (6-43) thus:

$$N_s = \frac{4\,\pi^2\,\alpha^2\,B_C\,f_M}{\sqrt{3}}\; erfc \sqrt{\frac{f_M}{B_C}\frac{S_i}{N_m}} \qquad \text{..... (6-45)}$$

The total output noise power is:

$$N_0 = N_G + N_s \qquad \text{..... (6-46)}$$

where N_G = Gaussian noise given by equation (6-31).

N_s = Spike noise given by equation (6-45)

S_0 = Output signal power given by equation (6-18)

Let $S_i = \frac{A^2}{2}$ ..... (6-47a)

and $N_M = \eta\, f_M$ ..... (6-47b)

Combining these equations gives:

$$\frac{S_0}{N_0} = \frac{\alpha^2 k^2 \overline{m^2(t)}}{\frac{8}{3}\pi^2 \frac{\alpha^2 \eta}{A^2} f_M^3 + \frac{4\pi^2 \alpha^2 B_C f_M}{\sqrt{3}} erfc \sqrt{\frac{f_M}{B_C}\frac{S_i}{N_M}}} \qquad \text{..... (6-47c)}$$

from which, after substituting (6-47a) and (6-47b), gives:

$$\frac{S_0}{N_0} = \frac{\left[\frac{3}{4\pi^2}\frac{k^2 \overline{m^2(t)}}{f_M^{\,2}}\right]\left(\frac{S_i}{N_M}\right)}{1+\left(\frac{\sqrt{3}B_C}{f_M}\right)\left(\frac{S_i}{N_M}\right) erfc \sqrt{\left(\frac{f_M}{B_C}\right)\left(\frac{S_i}{N_M}\right)}} \qquad \text{..... (6-47d)}$$

This equation only applies when an unmodulated carrier is used, or if the modulated signal bandwidth is very small compared to the I.F. bandwidth B_C.

(b) <u>Sinusoidal Modulated Carrier</u>

When the frequency of the carrier is offset by an amount δf from the carrier frequency f_c, the number of spikes increases by δN. The relationship [9] is:

$$\delta N = |\delta f| \exp\left(-\left(\frac{f_M}{B_C}\right)\left(\frac{S_i}{N_M}\right)\right) \qquad \text{..... [6-48]}$$

For a sinusoidal modulated input at frequency f_M with a frequency deviation of Δf, then the input is:

$$v(t) = A\cos\left(\omega_c t + \frac{\Delta f}{f_M}\sin(2\pi f_M t)\right) \qquad \text{..... [6-49]}$$

Then
$$\delta f = \Delta f \cos(2\pi f_M t) \qquad \text{..... [6-50]}$$

and the average $$\overline{|\delta f|} = \left(\frac{2}{\pi}\right)\Delta f \qquad \text{..... [6-51]}$$

The average value of δN is:

$$\overline{\delta N} = \frac{2\,\Delta f}{\pi}\,\exp\left[-\left(\frac{f_M}{B_C}\right)\left(\frac{S_i}{N_M}\right)\right] \qquad \text{..... [6-52]}$$

The total number of spikes per second is $N = N_c + \overline{\delta N}$, the latter two terms being given by $N_c = \dfrac{B_C\, erfc\sqrt{\left(\frac{f_M}{B_C}\right)\left(\frac{S_i}{N_M}\right)}}{2\sqrt{3}}$ and equation [6-52].

Now, from [9], at or near threshold, $\delta N \rangle\rangle N_c$ thus the total average number of spikes is $N \cong \delta N$.

Thus the average time between spikes is :

$$T_c = \frac{1}{N} \approx \frac{1}{\overline{\delta N}} \qquad \text{..... [6-53]}$$

The FM discriminator output signal-to-noise ratio may now be calculated for a sinusoidal modulated carrier where:

$$\delta f = \frac{k\ \overline{m(t)}}{2\,\pi} = \Delta f\,\cos\omega_m t \qquad \text{..... [6-54]}$$

Inserting equation (6-52) into (6-53) and the result into equation (6-42) gives:

$$N_s = 16\,\pi\alpha^2\, f_M\,\Delta f\,\exp\left[-\left(\frac{f_M}{B_C}\right)\left(\frac{S_i}{N_M}\right)\right] \qquad \text{..... (6-55a)}$$

Now letting N_0 equal the sum of equation (6-31a) and (6-55a) gives:

$$N_0 = \frac{8}{3}\pi^2 \alpha \frac{\eta}{A^2} f_M^3 + 16\pi\alpha^2 f_M \Delta f \exp\left[-\left(\frac{f_M}{B_C}\right)\left(\frac{S_i}{N_M}\right)\right] \qquad \text{.....(6-55b)}$$

Letting S_0 equal equation (6-36b) and dividing by equation (6-55b) gives:

$$\frac{S_0}{N_0} = \frac{\frac{3}{2}\beta^2\left(\frac{S_i}{N_M}\right)}{\frac{8}{3}\pi^2 \alpha \frac{\eta}{A^2} f_M^3 + 16\pi\alpha^2 f_M \Delta f \exp\left[-\left(\frac{f_M}{B_C}\right)\left(\frac{S_i}{N_M}\right)\right]} \qquad \text{..... (6-55c)}$$

which after simplifying gives:

$$\frac{S_0}{N_0} = \frac{\frac{3}{2}\beta^2\left(\frac{S_i}{N_M}\right)}{1 + \frac{6\alpha}{\pi}\frac{\Delta f}{f_M}\frac{A^2}{\eta f_M}\exp\left[-\left(\frac{f_M}{B_C}\right)\left(\frac{S_i}{N_M}\right)\right]} \qquad \text{..... (6-55d)}$$

Letting $\beta = \frac{\Delta f}{f_M}$ and $\frac{A^2}{2\eta f_M} = \frac{S_i}{N_M}$ together with substituting Carson's rule $B_C = 2\Delta f + 2 f_M$ in the exponent gives the following:

$$\frac{S_0}{N_0} = \frac{\left(\frac{3}{2}\right)\beta^2\left(\frac{S_i}{N_M}\right)}{1 + \left(\frac{12\beta}{\pi}\right)\left(\frac{S_i}{N_M}\right)\exp\left[-\frac{1}{2}\left[\frac{1}{(\beta+1)}\right]\left(\frac{S_i}{N_M}\right)\right]} \qquad \text{..... [6-55e]}$$

A graph of equation 6-55e is shown in figure 6/3 below for a modulation index of $\beta = 1$. An examination of equation 6-55e shows that above threshold, for large values of carrier-to-noise ratios $\left(\frac{S_i}{N_M}\right)$, the exponential term tends to zero, resulting in the denominator equalling unity and the equation reducing to the numerator term only. Below threshold, for small values of carrier-to-noise ratios $\left(\frac{S_i}{N_M}\right)$, the exponential term becomes increasingly significant, causing the denominator of equation 6-55e to become larger and reducing the value of the numerator accordingly. It is this exponential term that models the effect of the

increasing click rate, at and below threshold.

(c) Gaussian Modulated Carrier

Assume the input signal was modulated by a Gaussian random process, then:

$$v(t) = A\cos\left[\omega_c t + k\int_{-\infty}^{t} m(t)\,dt\right] + n(t) \qquad \text{..... [6-56]}$$

where $k\,m(t)$ is the instantaneous frequency deviation. Thus the r.m.s. frequency deviation produced is:

$$\Delta f_{rms} = \frac{\sqrt{k^2\,\overline{m^2(t)}}}{2\,\pi} \qquad \text{..... [6-57]}$$

Calculating the output signal power from equations [6-18] and [6-57] gives:

$$S_0 = \alpha^2\,k^2\,\overline{m^2(t)} \quad = \alpha^2\,4\,\pi^2(\Delta f_{rms})^2 \qquad \text{..... [6-58]}$$

Neglecting spikes, the FM noise is given by equation [6-31]:

$$N_G = \alpha^2\frac{8\,\pi^2}{3}\frac{\eta\,f_M{}^3}{A^2} \qquad \text{..... [6-59]}$$

Combining equations [6-42], [6-48] and [6-53] gives the spike noise:

$$N_s = \alpha^2(8\,\pi^2\,f_M)\overline{|\delta f|}\,\exp\left[-\left(\frac{f_M}{B_C}\right)\left(\frac{S_i}{\eta f_M}\right)\right] \qquad \text{..... [6-60]}$$

Where $\delta f = \dfrac{k\ \overline{m(t)}}{2\,\pi}$ is the instantaneous frequency deviation and $\overline{|\delta f|}$ is its average value.

To evaluate the latter the Gaussian probability function is used, viz:

$$\overline{X} = \int_{-\infty}^{\infty} \frac{x \exp \dfrac{-(x-m)^2}{2\sigma^2}}{2\pi\sigma^2} dx = m \qquad \text{..... [6-61a]}$$

Where m is the average value and σ^2 the variance associated with $f(x)$. Now $m(t)$ is Gaussian and thus δf is Gaussian with an average value of zero and a standard deviation Δf_{rms}. Thus substituting these values, and letting $x = \delta f$, in equation (6-61a) gives:

$$\overline{|\delta f|} = \int_{-\infty}^{\infty} \frac{|\delta f| \exp\left[-\dfrac{(\delta f)^2}{2(\Delta f_{rms})^2}\right]}{\sqrt{2\pi}(\Delta f_{rms})} d(\delta f) \qquad \text{..... [6-61b]}$$

To evaluate multiply by 2, and multiply the numerator and denominator by Δf_{rms}, and integrating from zero to infinity, gives:

$$\overline{|\delta f|} = \sqrt{\frac{2}{\pi}} (\Delta f_{rms}) \int_0^{\infty} \frac{\delta f}{(\Delta f_{rms})^2} \exp\left[-\frac{(\delta f)^2}{2(\Delta f_{rms})^2}\right] d(\delta f) \qquad \text{..... [6-62]}$$

Directly integrating by changing the variables to $x = \dfrac{(\delta f)^2}{2(\Delta f_{rms})^2}$ as follows:

Now
$$x = \frac{(\delta f)^2}{2(\Delta f_{rms})^2} \qquad \text{..... [6-63a]}$$

differentiating x with respect to δf gives:

$$\therefore \quad \frac{dx}{d(\delta f)} = \frac{\delta f}{\Delta f_{rms}}$$

Hence
$$d(\delta f) = \frac{\Delta f_{rms}^2}{\delta f} dx \qquad \text{..... [6.63b]}$$

Substituting [6-63a] and [6.63b] into (6.62) gives:

$$\overline{|\delta f|} = \sqrt{\frac{2}{\pi}}(\Delta f_{rms}) \int_0^{\infty} \frac{\delta f}{(\Delta f_{rms})^2} \exp(-x) \frac{(\Delta f_{rms})^2}{\delta f} dx \qquad \text{..... [6.63c]}$$

$$\overline{|\delta f|} = \sqrt{\frac{2}{\pi}}(\Delta f_{rms}) \int_0^{\infty} \exp(-x) \quad dx$$

$$\overline{|\delta f|} = \sqrt{\frac{2}{\pi}}(\Delta f_{rms}) [-\exp(-x)]_0^{\infty}$$

$$\overline{|\delta f|} = \sqrt{\frac{2}{\pi}}(\Delta f_{rms}) \qquad \text{..... [6-63d]}$$

Substituting equation [6-63d] into equation [6-60] gives:

$$N_s = \alpha^2 (8\pi^2 f_M) \left(\sqrt{\frac{2}{\pi}}(\Delta f_{rms}) \right) \exp\left[-\left(\frac{f_M}{B_C}\right)\left(\frac{S_i}{\eta f_M}\right) \right] \qquad \text{..... [6-64]}$$

Combining equations [6-58], [6-59] and [6-64] gives:

$$\frac{S_0}{N_0} = \frac{S_0}{N_G + N_S}$$

$$\frac{S_0}{N_0} = \frac{\alpha^2 4\pi^2 \Delta f_{rms}^2}{\alpha^2 \frac{8\pi^2}{3} \frac{\eta f_M^3}{A^2} + \alpha^2 (8\pi^2 f_M) \sqrt{\frac{2}{\pi}} \Delta f_{rms} \exp\left[-\left(\frac{f_M}{B_C}\right)\left(\frac{S_i}{\eta f_M}\right) \right]} \qquad \text{..... [6-65a]}$$

$$\frac{S_0}{N_0} = \frac{3\frac{A^2}{2}\frac{\Delta f_{rms}^2}{\eta f_M^2}}{1 + \frac{6\sqrt{\frac{2}{\pi}} \Delta f_{rms} \frac{A^2}{2}}{\eta f_M^2} \exp\left[-\left(\frac{f_M}{B_C}\right)\left(\frac{S_i}{\eta f_M}\right) \right]} \qquad \text{..... [6-65b]}$$

where $S_i = \frac{A^2}{2}$ gives:

$$\frac{S_0}{N_0} = \frac{3\left(\frac{\Delta f_{rms}}{f_M}\right)^2\left(\frac{S_i}{\eta f_M}\right)}{1+6\sqrt{\frac{2}{\pi}}\left(\frac{\Delta f_{rms}}{f_M}\right)\left(\frac{S_i}{\eta f_M}\right)\exp\left[-\left(\frac{f_M}{B_C}\right)\left(\frac{S_i}{\eta f_M}\right)\right]} \quad \text{..... [6-65c]}$$

and when $N_i = \eta f_M$ gives:

$$\frac{S_0}{N_0} = \frac{3\left(\frac{\Delta f_{rms}}{f_M}\right)^2\left(\frac{S_i}{N_i}\right)}{1+6\sqrt{\frac{2}{\pi}}\left(\frac{\Delta f_{rms}}{f_M}\right)\left(\frac{S_i}{N_i}\right)\exp\left[-\left(\frac{f_M}{B_C}\right)\left(\frac{S_i}{N_i}\right)\right]} \quad \text{..... [6-66]}$$

Now the relationship between the Carson bandwidth B_C (i.e. that bandwidth required to transmit 98% of the signal power without distortion) and a Gaussian modulated signal is given in Appendix D, namely:

$$B_C = 4.6\,\Delta f_{rms} \quad \text{..... [6-67]}$$

Dividing each side by f_M and inverting gives:

$$\frac{f_M}{B_C} = \frac{f_M}{4.6\,\Delta f_{rms}} \quad \text{..... [6-68]}$$

Substituting into equation 6-66 gives:

$$\frac{S_0}{N_0} = \frac{3\left(\frac{\Delta f_{rms}}{f_M}\right)^2\left(\frac{S_i}{N_i}\right)}{1+6\sqrt{\frac{2}{\pi}}\left(\frac{\Delta f_{rms}}{f_M}\right)\left(\frac{S_i}{N_i}\right)\exp\left[-\left(\frac{1}{4.6}\right)\left(\frac{f_M}{\Delta f_{rms}}\right)\left(\frac{S_i}{N_i}\right)\right]} \quad \text{..... [6-69]}$$

Equation 6-55e for sinusoidal modulation, for a modulation index of $\beta = 1$, is plotted in figure 6/3. Also plotted in the same figure is equation 6-69 for Gaussian modulation, for a modulation index $\frac{\Delta f_{rms}}{f_M} = 1$. Below a carrier-to-noise ratio of some 3 to 5 dB the curves should not be considered to be reliable. The effects of the nature of the modulation upon the threshold break point and the actual input-output relationship can clearly be seen.

Following the discussion given for equation 6-55e, an examination of equation 6-69 shows

that above threshold, for large values of carrier-to-noise ratios $\left(\frac{S_i}{N_M}\right)$, the exponential term tends to zero, resulting in the denominator equalling unity and the equation reducing to the numerator term only. The numerator term of equation 6-69 is similar to that of equation 6-55e, except that an r.m.s. value of modulation index is used. Below threshold, for small values of carrier-to-noise ratios $\left(\frac{S_i}{N_M}\right)$, the exponential term becomes increasingly significant, causing the denominator of equation 6-69 to become larger and reducing the value of the numerator accordingly. As for equation 6-55e, it is this exponential term that models the effect of the increasing click rate, at and below threshold.

Figure 6/3 Demodulator Threshold Characteristics for Sinusoidal and Gaussian Modulation

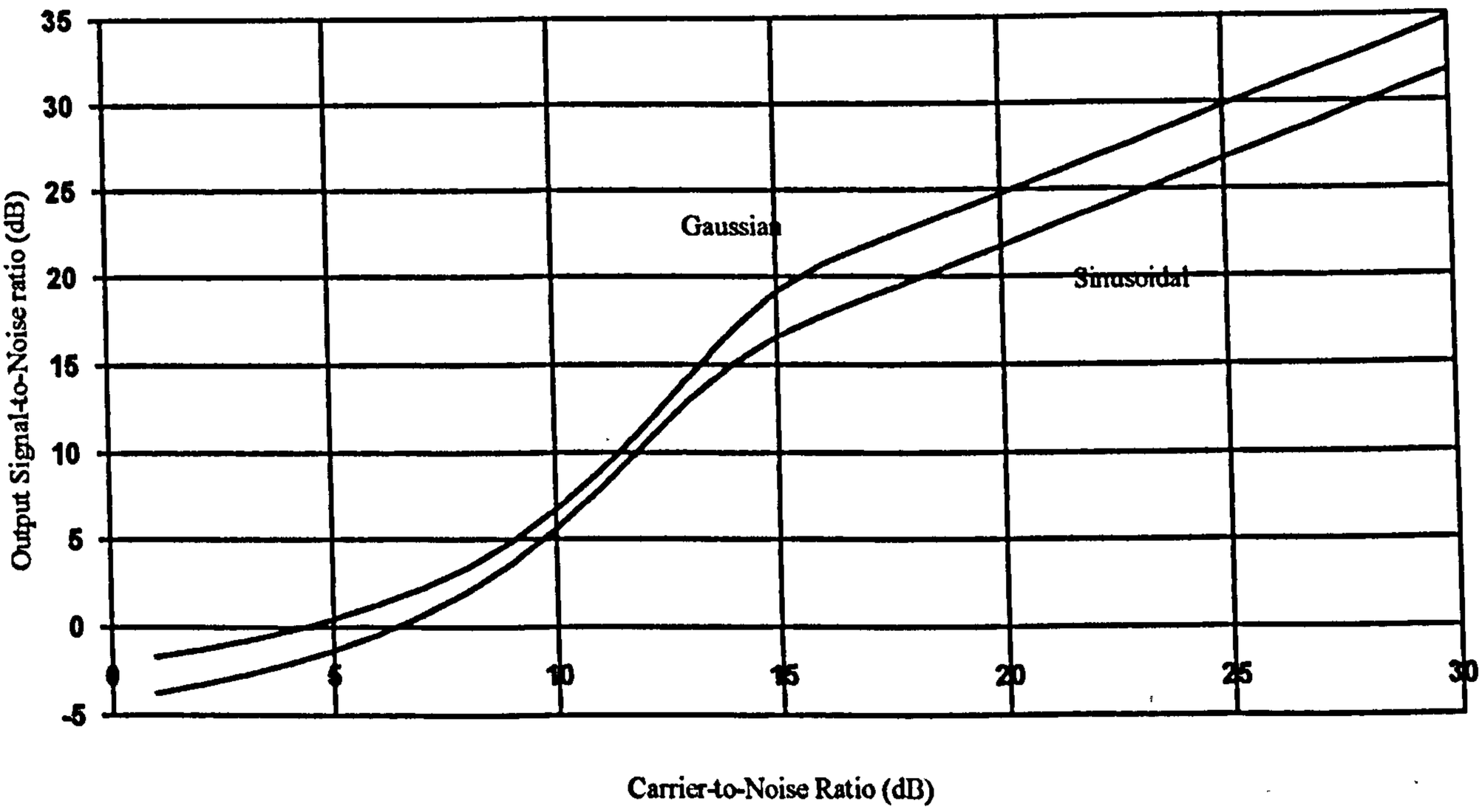

6.4 Discussion

Equation (6-47d), the expression for an unmodulated carrier, equation (6-55e), the expression for sinusoidal modulation, and equation (6-66), the expression for Gaussian modulation, clearly shows the effect of the nature of the modulation upon the threshold of the demodulator. The sinusoidal and Gaussian characteristics are plotted in figure 6/3.

These show how the characteristic and the threshold break point of the demodulator changes as the modulation becomes more complex. In addition these characteristics also vary as a result of the modulation index changing as a result of the maximum frequency content of the signal. Thus when a complex signal is in the threshold region the spike or click phenomena that occurs will be influenced by the increase in complexity of the modulation. For a TV signal in the vicinity of the threshold region, and for a constant input carrier-to-noise level, the noise that appears in the picture will depend upon the picture content. This non-linear dependence of the demodulation process upon the signal structure is one of the major difficulties that occurs in designing a threshold extension demodulator with a satisfactory performance. It is this non linearity that is considered to be the source of variable performance reported in the literature.

6.5 References

[1] US. Patent 5,161,004. "Television receiver including a frequency demodulator for lowering the threshold". Egger, J., November 3rd, 1992.

[2] US. Patent 4,563,651. "FM demodulator with variable bandpass filter". Ohta, T., et al., January 7th, 1986.

[3] US. Patent 4,816,770. "Adaptive FM threshold extension demodulator". Naumann, G. R., March 28th, 1989.

[4] Goblick, T. J. "Theoretical limitations on the transmission of data from analog sources", IEEE Trans. Information Theory, Vol. IT-11, No. 4, October 1965, pp. 558 - 567.

[5] Slepian, D. " Bounds on communication", Bell System Technical Journal, May 1963, pp 687 - 707.

[6] Rice, S. O. "Noise in FM receivers," Ch. 25, *Time Series Analysis*, Rosenblatt, Ed. New York : Wiley, 1963, pp 395 - 422.

[7] Frankle, J. "Threshold performance of analog FM demodulators", RCA Review, December 1966, pp. 521 - 562.

[8] Camp, J. A. "A comparison of the threshold capabilities of FMFB and Phase-Lock Loop demodulators employed in FDM-FM communication systems", IEEE Trans. on Communications Technology, Vol. COM-18, No. 3, June 1970, pp. 191 - 200.

[9] Taub, H., Schilling, D. "*Principles of Communication Systems*" McGraw-Hill, 1986, New York, ISBN 0-07-062955-2

[10] Klapper, J., Frankle, J. T. "*Phase-Locked and Frequency-Feedback Systems*", Academic Press, (1972).

[11] Shannon, C. E. "A mathematical theory of communication", Bell System Technical Journal, Vol. 27, pp. 379 and 623, 1948.

Blank Page

7. THREshold EXTENSION DEMODULATION

7.1 General

7.1.1 The review of previous work published that was carried out during this study has shown that although threshold extension demodulator techniques have been known for many years, since Chaffee's first patent in 1937 [1], they have rarely been used. Only when there has been a problem in reception with low signal levels has there been a resurgence in interest such as at the commencement of the space programme in the 1960's and the commencement of DBS service in the 1980's, [2-3]. The reason for this lack of interest in threshold extension techniques is the difficulty in obtaining a consistent performance with these demodulators, both in operation and production, where the optimum performance is dependent both upon the signal level and content, and the stability of the design. In the previous section it was shown that there is a non-linear dependence of the demodulation process upon the frequency content of the carrier modulation in the threshold region. A change in picture content from a predominately single frequency component to a Gaussian type frequency content alters the threshold point at which clicks occur to a higher input signal level. This non-linear action is one the major source of difficulties experienced with a threshold extension demodulator. These aspects are considered in further depth for certain of the demodulators discussed below.

In the following sections some eleven techniques for achieving threshold extension demodulation are discussed in depth. A close examination of these techniques shows that the majority of these approaches fall into two broad categories. Firstly the demodulator exhibits an improvement in performance because there is a reduction in the system bandwidth in some way or other. The second approach uses a processing circuit, normally at the output of the demodulator, to eliminate the spikes, or clicks, that occur on the demodulated signal at threshold.

7.1.2 For those threshold extension demodulators that operate on a reduced bandwidth principle to obtain an improved performance, a simple illustration shows how this is achieved. The signal level at which threshold occurs can be derived as follows:

Let the single-sided noise spectral density at the receiver input be given by:

$$N_0 = k\,T_s \qquad \text{..... (7-1)}$$

where k = Boltzmann's constant (1.38×10^{-23} joules K^{-1})

T_S = System noise temperature obtained by summing the noise generated prior to the receiver input (T_A) and the noise generated within the receiver (T_E).

Thus
$$N_0 = k\,(T_A + T_E) \qquad \text{..... (7-2)}$$

where T_A = Antenna noise temperature (K)

T_E = Receiver noise temperature (K)

The noise power will be determined by the receiver I.F. bandwidth, thus:

$$N = k\,(T_A + T_E)\,B_C \qquad \text{..... (7-3)}$$

where B_C = Receiver (I.F.) bandwidth (Hz)

N = Receiver noise power (watts)

The signal level at which threshold occurs is thus obtained by multiplying equation (7-3) by the minimum carrier-to-noise level (C/N) acceptable, thus:

$$P_R = k\,(T_A + T_E)\,B_C\,(C/N) \qquad \text{..... (7-4)}$$

where: P_R = Signal power at receiver input (watts)

C/N = Carrier to noise ratio

If this equation (7-4) is rearranged in terms of the carrier-to-noise ratio, then the effects of

bandwidth can be clearly seen, viz.:

$$C/N = \frac{P_R}{k\left(T_A + T_E\right) B_C} \qquad \text{..... (7-5)}$$

The importance of this relationship given in equation (7-5) is that if the bandwidth is reduced the carrier-to-noise ratio improves. Thus for those threshold extension demodulators that operate on a reduced bandwidth principle this relationship shows the mechanism of operation. The tracking filter demodulator (section 8 below) is the most clear example of this approach. This demodulator consists of a narrow band filter ahead of the conventional demodulator. Generally two of the filter characteristics are varied. Firstly, the filter centre frequency is made to track the carrier frequency, thus eliminating the need for an increase in system bandwidth to accommodate system frequency drifts. Secondly, the filter bandwidth is varied depending upon the carrier-to-noise ratio, resulting in the filter being narrower than that dictated by signal bandwidth considerations. The narrow filter is made to follow the input signal whilst enhancing the carrier-to-noise ratio at the input to the conventional demodulator. This gives an improvement in threshold (for a possible loss of picture resolution) over a conventional I.F. and discriminator system. In this approach the design of the demodulator tends to revolve around how the reduction in bandwidth is achieved and how the signal is tracked.

7.2 References

[1] Chaffee, J. G., US Patent 2,075,503 (March 1937)

[2] Maurice, R. D. A. "Threshold extension in FM reception: an elementary treatment", EBU Review (Technical Part), No. 168, April 1978, pp. 56 - 63.

[3] Beech, B., Moor, S. "Threshold Extension Techniques", IBA Experimental and Development Report 130/84, July 1985.

Blank Page

8. TRACKING FILTER DEMODULATOR

8.1 General

8.1.1 The tracking filter demodulator, also known as the dynamic tracking filter, aroused interest in the early days of satellite transmission because of its simple implementation compared to other forms of threshold extension demodulators [1-2], [13]. Over the years it has continued to attract interest and there has been a steady flow of patents, [3] - [12], suggesting improvements to the technique; the current application being satellite DBS television transmission [3], [10]. Indeed it appears to be the most utilised approach for this application. The basic tracking filter demodulator circuit configuration is shown in figure 8/1 and in a slightly different form in figure 8/2.

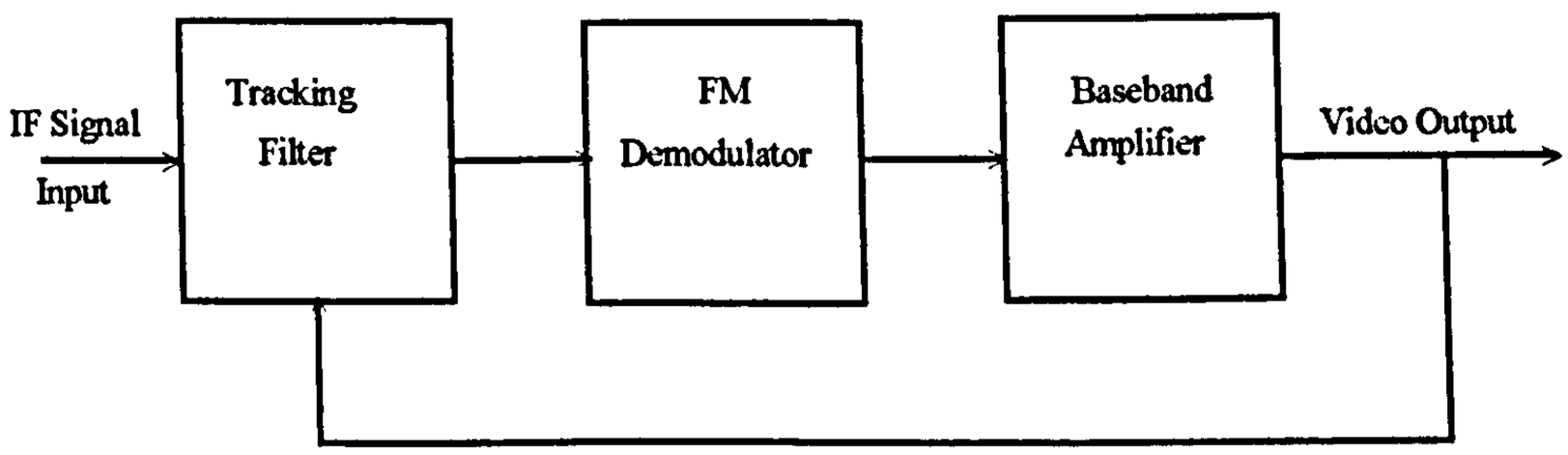

Figure 8/1 Basic Tracking Filter Demodulator

Although the instantaneous frequency of a frequency modulated carrier may operate over a wide frequency range, this demodulator takes advantage of the fact that if these variations in frequency can be followed by a tuned circuit, satisfactory demodulation may be achieved with a consequent saving in bandwidth and giving a considerable improvement in threshold.

In most implementations of this demodulator approach the centre frequency of the I.F. filter is made to follow the input frequency; by reducing the bandwidth of this I.F. (tracking) filter, threshold extension is obtained. However if the bandwidth of the tracking filter is made too narrow the signal delay increases, leading to degradation of the signal and circuit instabilities. Analytically the tracking filter demodulator shows some resemblance to the FMFB demodulator and as with the latter it is a difficult circuit to analyse in detail due to

the nonlinearities encountered by the circuit.

The evolution of the designs in the patent area is of some interest as it shows how some of the formidable problems encountered with threshold extension have been tackled. Clayton's work [7-8], is of importance in the application of the tracking filter to television demodulation as this design was amongst the earliest to attempt to deal with DBS colour TV reception.

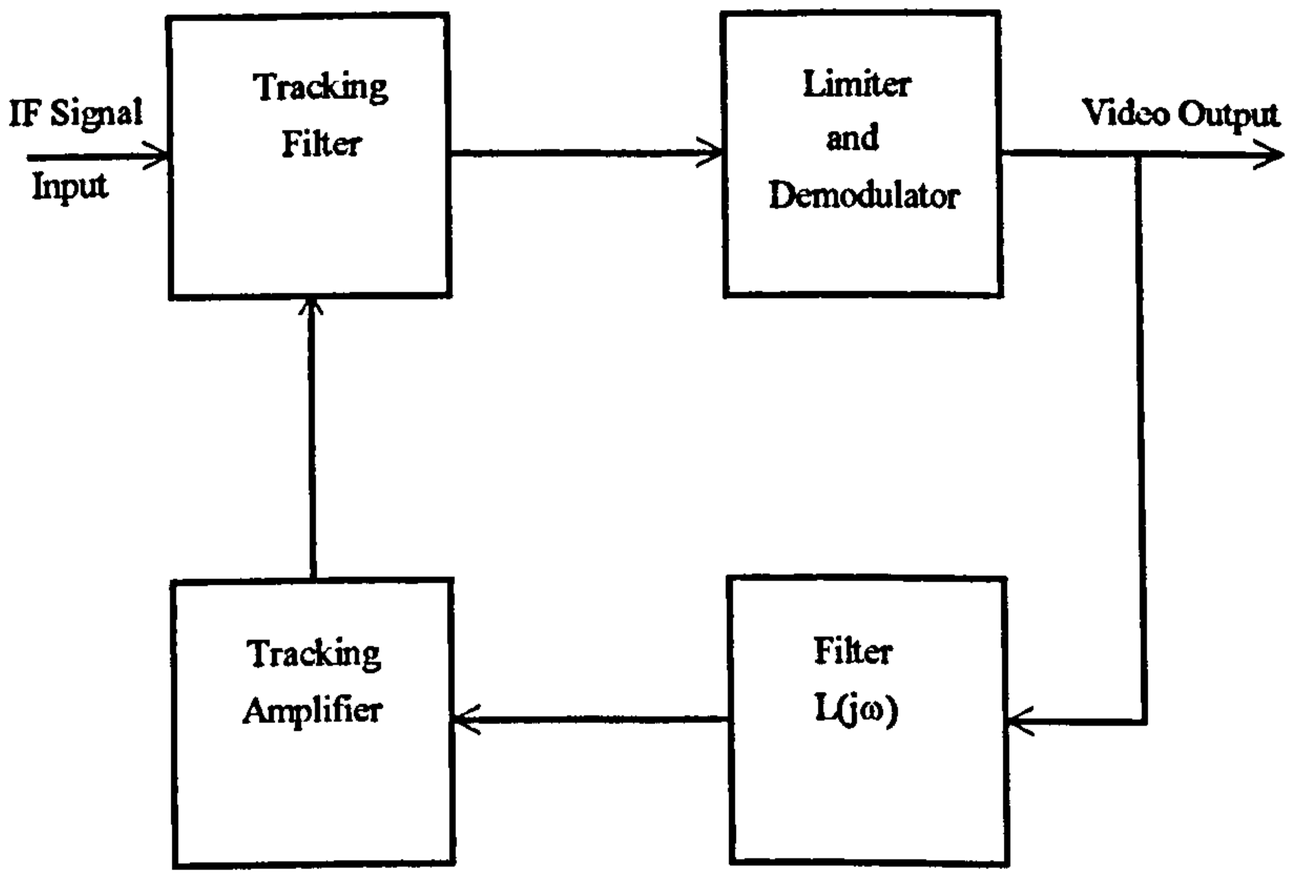

Figure 8/2 Tracking Filter Demodulator

All subsequent tracking filter patents quote these references as the source for their work. The majority of the tracking filter demodulators discussed below have been designed for satellite TV reception and, in particular, colour TV reception.

8.2 Previous design approaches

8.2.1 Clayton's first patent [8] is illustrated in figure 8/3. It was designed for those systems that used low modulation index (< 4) narrow bandwidth FM signals. This demodulator uses an old concept, namely the oscillating limiter [14], [19]-[21]. In this design the demodulator is preceded by an oscillating limiter, formed by a limiter and bandpass filter in a regenerative circuit connection. In operation the tuneable bandpass filter

is tuned to the centre frequency of the I.F. input signal. In the presence of a strong input signal, whose amplitude is greater than the oscillator knee, the oscillating limiter functions as a conventional amplitude limiter whose output is a squarewave of constant amplitude. When the envelope of the input composite waveform (signal plus noise plus feedback) has an amplitude less than the knee of the limiter, the oscillating limiter output waveform is a replica of the composite input waveform. For input signals near the threshold carrier-to-noise ratio the oscillating limiter functions as a bandpass filter whose bandwidth is an adaptive function related to the amplitude of the input signal. When there is no input signal the limiter oscillates at a value, determined by the feedback loop, limiter and filter, near the I.F. nominal centre frequency.

A steering signal is generated in response to the demodulated signal from an FM demodulator and in a positive feedback arrangement tunes the tuneable filter. The centre frequency of the latter tracks the best available estimate of the input signal from the I.F. amplifier. The steering signal is generated by filtering the demodulated signal with a low pass filter, to remove the high frequency or noise signals above the baseband frequencies. Other smoothing circuits that are used include a nonlinear rate of change limiter that passes the demodulated signal without modification, except when the derivative of the latter with respect to time exceeds a pre-determined value, such as is encountered with noise or spikes. In the latter event the demodulated signal is modified and transmitted as the steering signal.

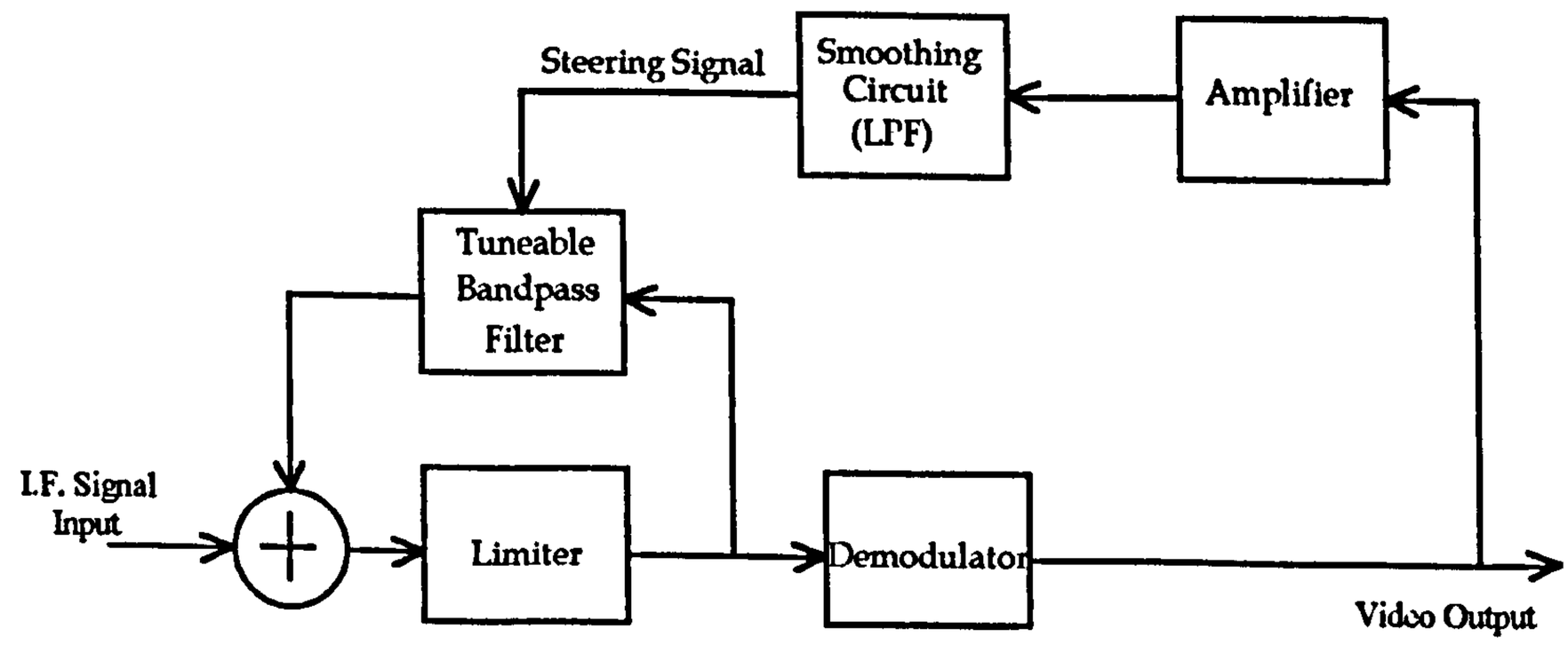

Figure 8/3 Clayton-1 Tracking Filter Demodulator

The amplitude of the steering or feedback signal is adjusted so that the centre frequency of the tuneable filter matches the centre frequency of the input FM signal.

Clayton approach is an elegant and original attempt to solve the threshold demodulator problem. However he does not give any performance figures in his patent and his solution does not overcome the basic click problem. Namely how is the demodulated output processed to eliminate the click low frequency content that is contained in the baseband? Although this approach will eliminate the spikes and noise that occurs outside the baseband it does not provide an accurate estimate of the input signal centre frequency, under click conditions, to allow the tuneable filter to be accurately controlled. Any improvement in threshold that occurs is probably is due to the adaptive bandwidth of the oscillating limiter when operating below its knee characteristic. A further disadvantage of the approach is a practical one. Namely the difficulties of designing a stable regenerative system, particularly when its operation is so dependent upon both the input and feedback amplitudes.

8.2.2 Clayton's second patent [7] was developed for receiving DBS TV colour signals. It basically operated on the same principles as his first approach [8] and is shown in figure 8/4. To receive baseband, or video, signals with an upper limit of some 5 MHz, difficulties are experienced with the basic design due to the delays encountered in the FM discriminator.

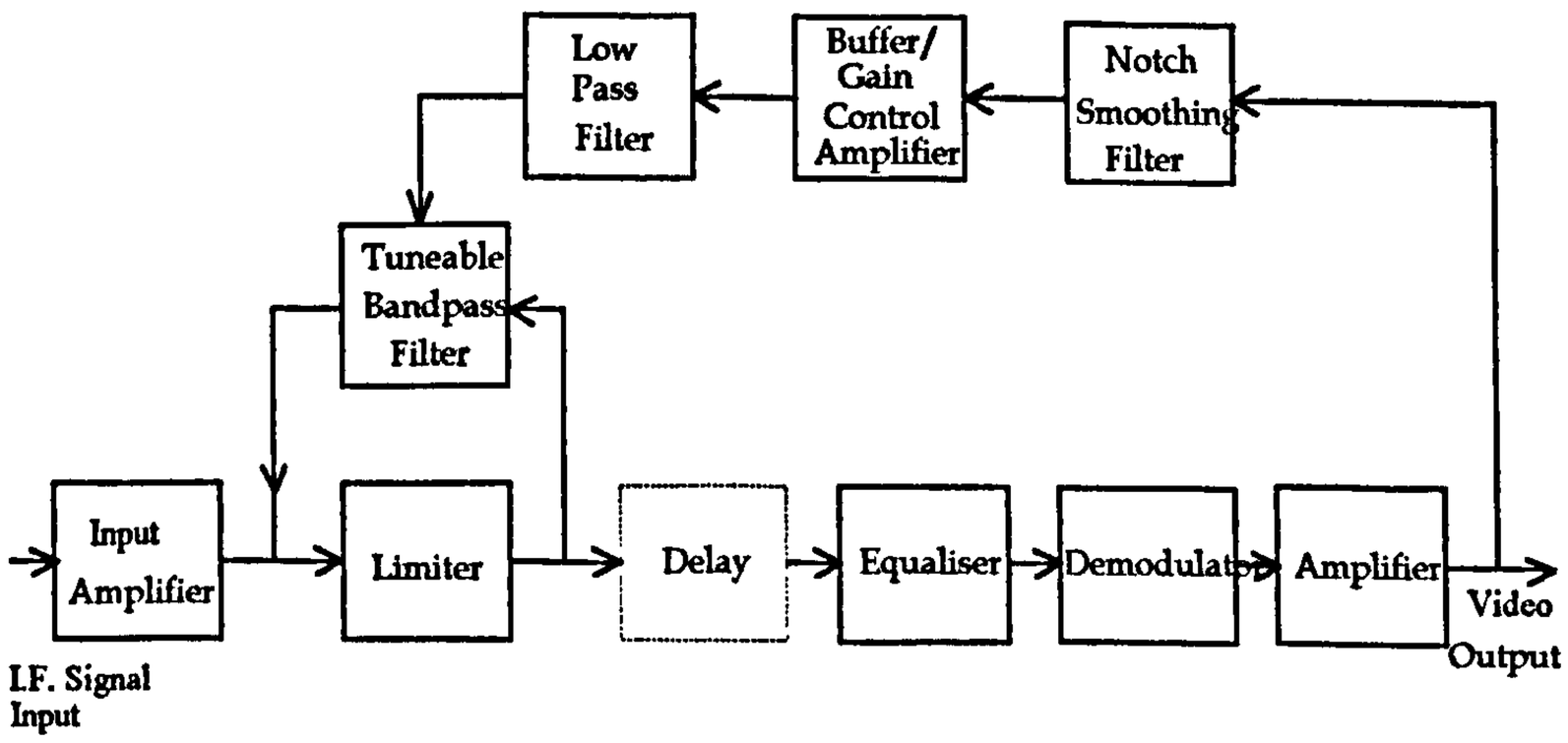

Figure 8/4 Clayton-2 Tracking Filter Demodulator

At the higher baseband frequencies these delays affect the steering signal such that it causes the tuning of the limiter to be away from the signal rather than to be towards its instantaneous frequency. The delay is represented by the dashed box in the diagram. To overcome these difficulties Clayton proposed some modifications to his basic approach.

Referring to figure 8/4, the overall feedback loop around the oscillating limiter consists of the unavoidable delay, equaliser, demodulator, amplifier, notch smoothing filter, buffer and gain control amplifier and a low pass filter. The notch smoothing filter provides a notch or region of increased attenuation at frequencies where the loop phase delay causes unsatisfactory tracking of the instantaneous signal frequency. The steering signal is thus attenuated sufficiently to prevent the oscillating limiter degrading the FM threshold performance. The phase response of the notch smoothing filter is such that the total phase delay where sync is located is minimal. At the colour subcarrier frequency the total phase delay is 2π radians.

Although the key difference with this design is the introduction of the notch filter, the disadvantages are the same as for the previous scheme described in section 8.2.1. Again no performance figures are given in this reference.

8.2.3 The Favreau-Marguimaud design is described in [11]. Their scheme is similar to the Clayton-2 scheme [7], except that the implementation is somewhat different and more complex. In this approach both the centre frequency and the bandwidth of the tracking filter are controlled. The scheme is illustrated in figure 8/5. The aim of the design is to achieve an improvement in carrier-to-noise ratio of conventional demodulators by taking into account at each moment, the instantaneous frequency and the instantaneous bandwidth occupied by the FM input signal.

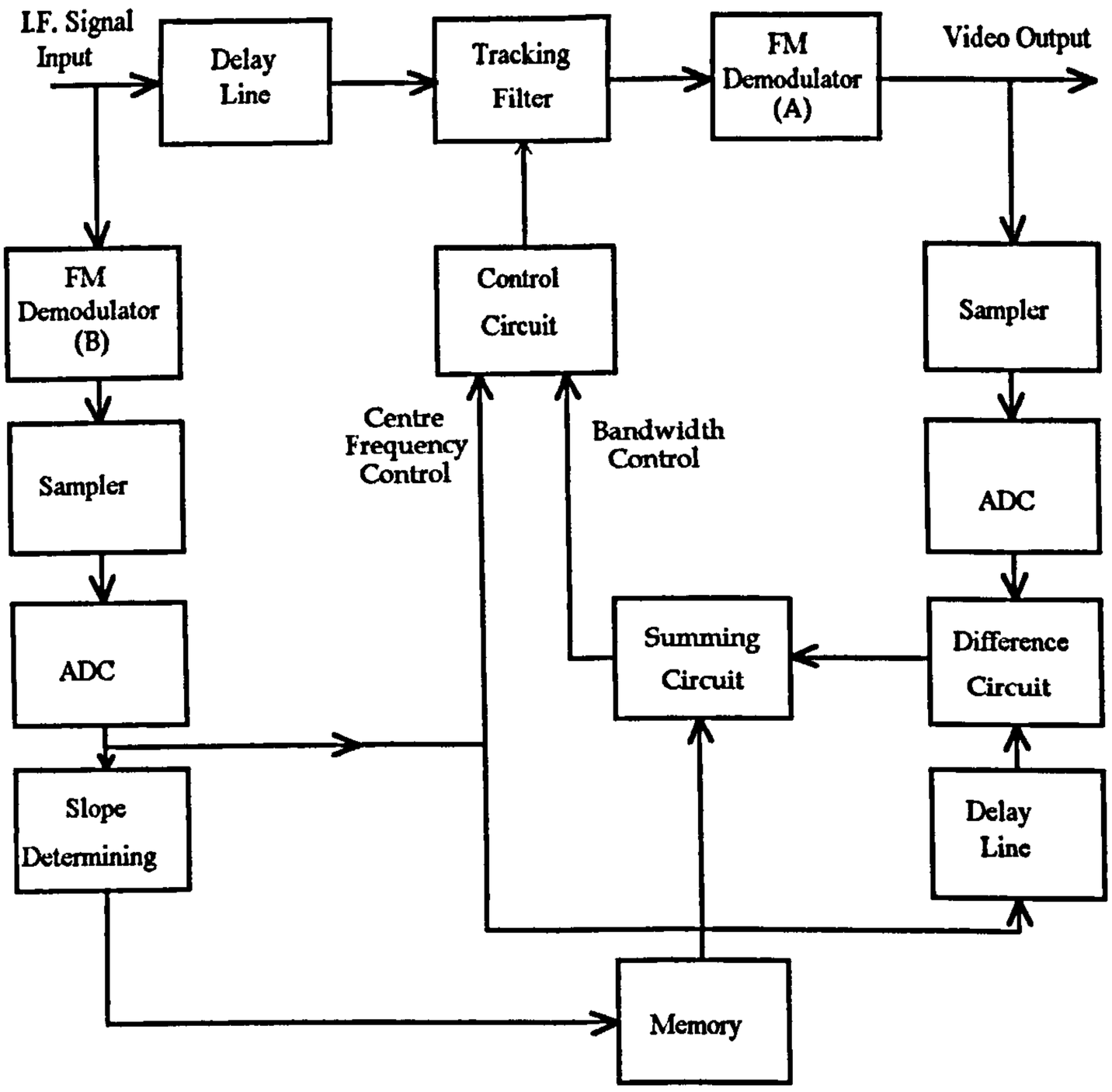

Figure 8/5 Favreau-Marguimaud Tracking Filter Demodulator

The forward, or signal, path of the design consists of a delay circuit, tracking filter and an FM demodulator (A). The delay circuit provides time delay to compensate for the delay experienced by the various control loops. The forward loop from the input, consisting of FM demodulator (B), sampler, ADC, slope determining circuit and memory, determines the instantaneous frequency and frequency band of the signal. The feedback loop from the output, consisting of the sampler, ADC, difference circuit and delay line, compares the demodulated signal from the output with that received from the input. The output of the difference circuit denotes the error in the instantaneous bandwidth determination. The control circuit provides the centre frequency and bandwidth controls for the active filters.

No performance figures are given in the reference and it is difficult to see what improvement such a complex design provides, as the clicks generated by demodulator (B) will affect the metric that controls the tracking filter.

8.2.4 Ohta in his first patent [6] described a threshold extension demodulator for DBS TV (NTSC) colour reception and for which he gave a sound theoretical treatment. This design approach also controls the instantaneous centre frequency and the bandwidth of the tracking filter. In this design the main signal path consists of the reference bandpass filter, variable bandpass filter, limiter and demodulator.

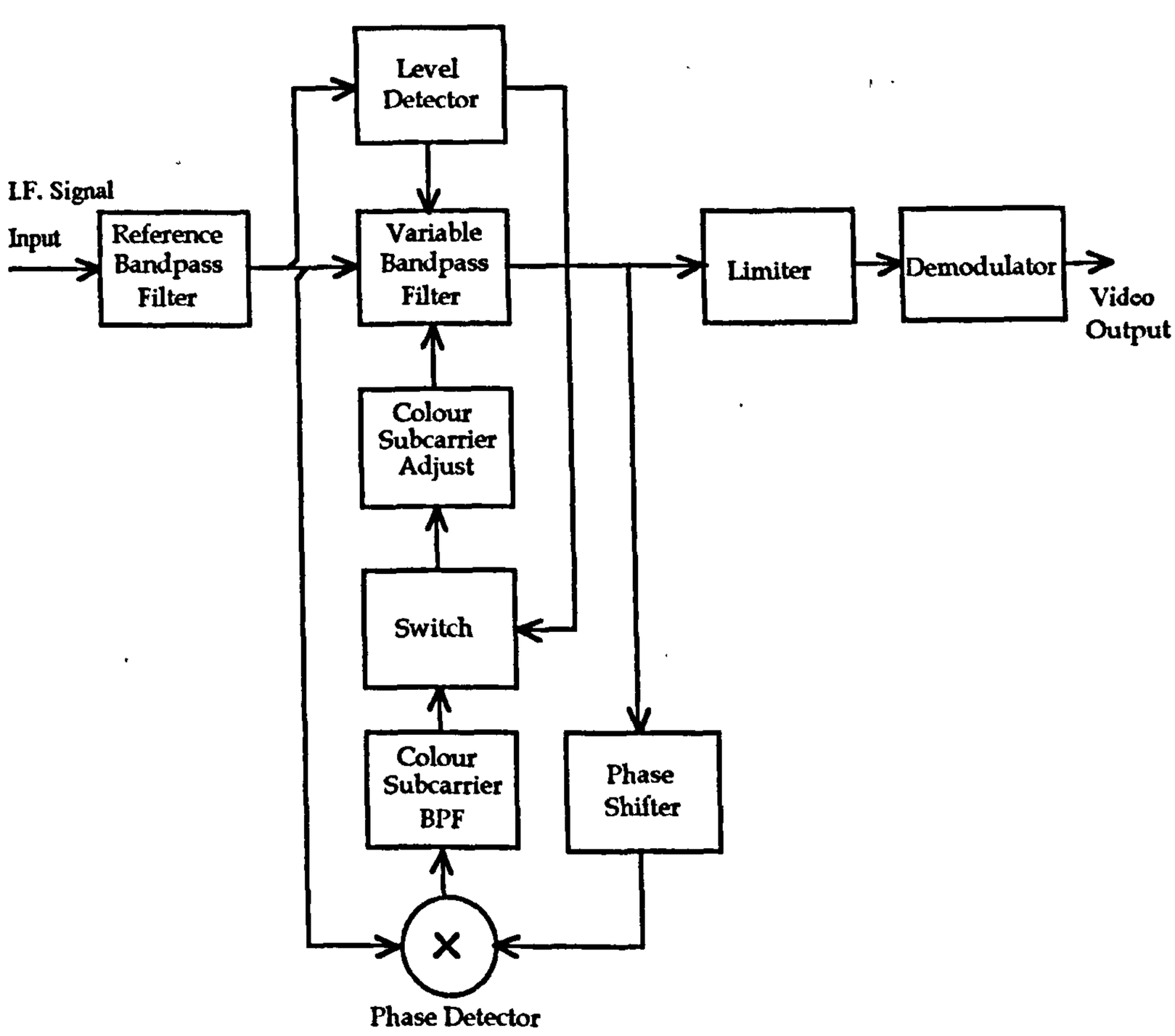

Figure 8/6 Ohta-1 Tracking Filter Demodulator

The phase detector compares the phase of the input signal to the variable band pass filter, and the phase of the output signal from the latter, to determine highest frequency component in the signal, namely the colour subcarrier component. This has the spectrum of almost a single frequency and as it is the highest modulation component (and pre-emphasised) it has a predominant effect on the carrier-to-noise ratio of the signal. This colour subcarrier is derived by the bandpass filter at the output of the phase detector. This colour subcarrier signal, after adjustment of its amplitude by the colour adjust circuit, is used to control the centre frequency of the variable bandpass filter. The switch in this part of the circuit is used to disconnect the control signal under high carrier-to-noise signals. The

level detector monitors the input carrier-to-noise signal and the detected level is used to adjust the bandwidth of the variable bandpass filter. When the carrier-to-noise level is above the threshold level (10-12 dB) the switch in the subcarrier loop is operated and the control signal is disconnected from the variable bandpass filter. Under this condition the latter bandwidth is set to be wider than the reference bandpass filter at the input. The performance of the circuit is then determined by this reference filter. This action implies that the performance of this demodulator is degraded under high carrier-to-noise signal conditions when compared to a conventional demodulator. This is confirmed in Ohta's second patent.

Broadly the circuit appears to operate by locking on to the colour subcarrier frequency and following its small frequency variations. The input signal level adjusts the bandwidth of the signal in either steps or continuously. What is not clear from this patent is the algorithm that is followed to adjust the bandwidth of the variable filter, although the effects of an incorrect algorithm are clearly discussed.. The effects of threshold upon the phase detector also do not appear to have been considered. However it is an intriguing approach which has potential.

8.2.5 Ohta's second patent [5] is illustrated in figure 8/7. Here some of the problems encountered in his first patent were addressed.

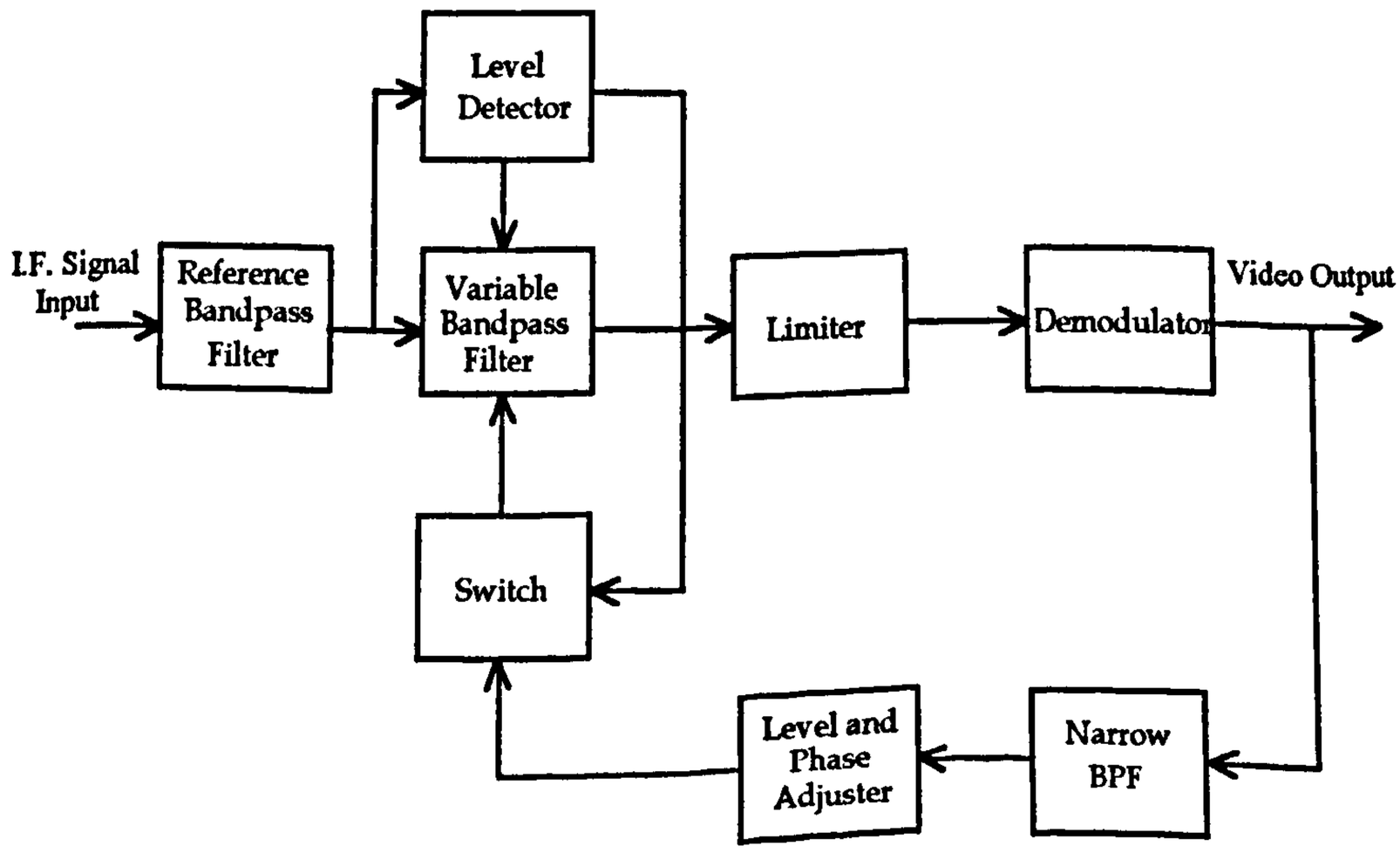

Figure 8/7 Ohta-2 Tracking Filter Demodulator

This design operates in a similar fashion to Ohta's first approach except this time the colour subcarrier is taken from the output of the main demodulator thus benefiting from any improvement that occurs in threshold performance. Because the level of the colour subcarrier component can vary to a low level and thus severely degrade the performance of the system, it is necessary to ensure that the feedback level has a nonlinear characteristic to compensate for this level variation. For this design a 2 to 4.5 dB improvement in performance is claimed, however the degradation in picture quality (resolution) is not specified.

8.2.6 Ohta's third patent [4] is illustrated in figure 8/8. For this simplier design a threshold improvement of 2 dB is claimed. Here only the bandwidth of the of the adaptive bandpass filter is changed. The centre frequency remains fixed. In figure 8/8 the bandpass filter at the input of the design has a fixed bandwidth which would normally be designed in accordance with Carson's rule.

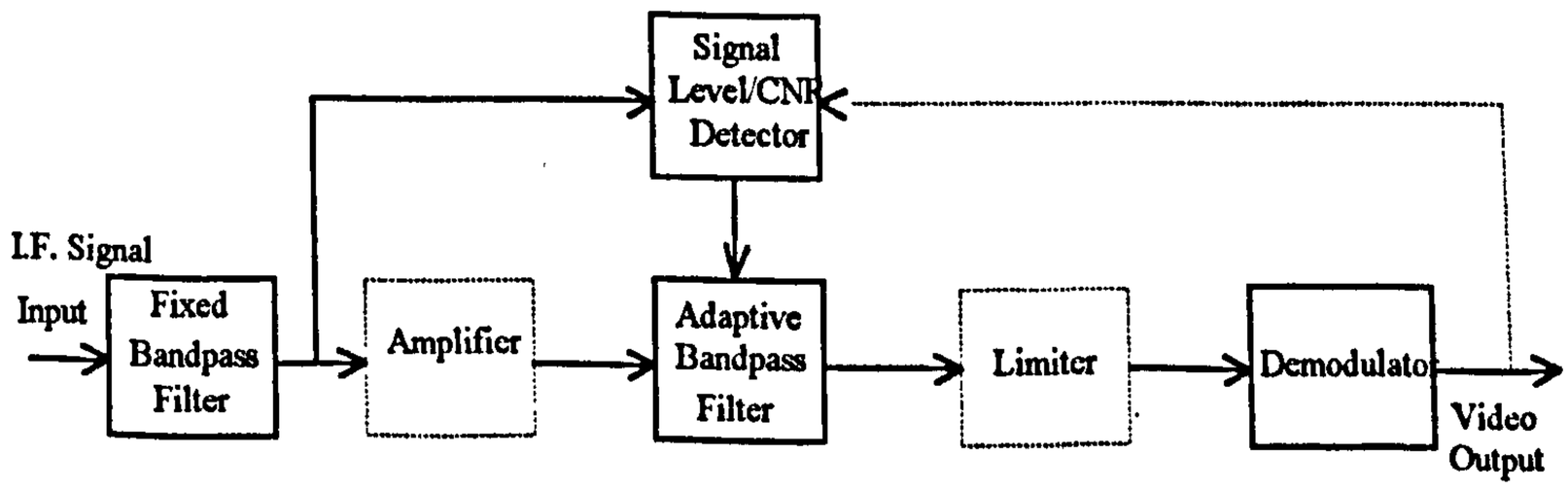

Figure 8/8 Ohta-3 Tracking Filter Demodulator

This is followed by an optional amplifier, and then by an adaptive bandpass filter that has a variable bandwidth. The bandwidth of the latter is far wider than the fixed bandwidth filter when the signal is a high level above threshold. When the signal strength is near or below threshold the adaptive bandpass filter has a narrower bandwidth than the input fixed bandpass filter. The bandwidth of the latter is adjusted according to the level of the total signal power itself or according to some noise component at the output. Because the bandwidth of the adaptive filter is controlled by the input signal level, it is stated that AGC cannot be used with this approach. These require that the limiter shown in figure 8/8 is used

and combined by some form of AGC action. This approach has some merit compared to the previous designs because of its simplicity, however the AGC limitation could be restrictive in its application.

8.2.7 Mobley's approach [3] to a DBS colour TV threshold extension demodulator is illustrated in figure 8/9. Although the design shown is intended for the NTSC system, Mobley claims that modifications to receive MAC signals are readily achieved. A key aspect of this design's approach is the development of a metric to control the tracking filter centre frequency.

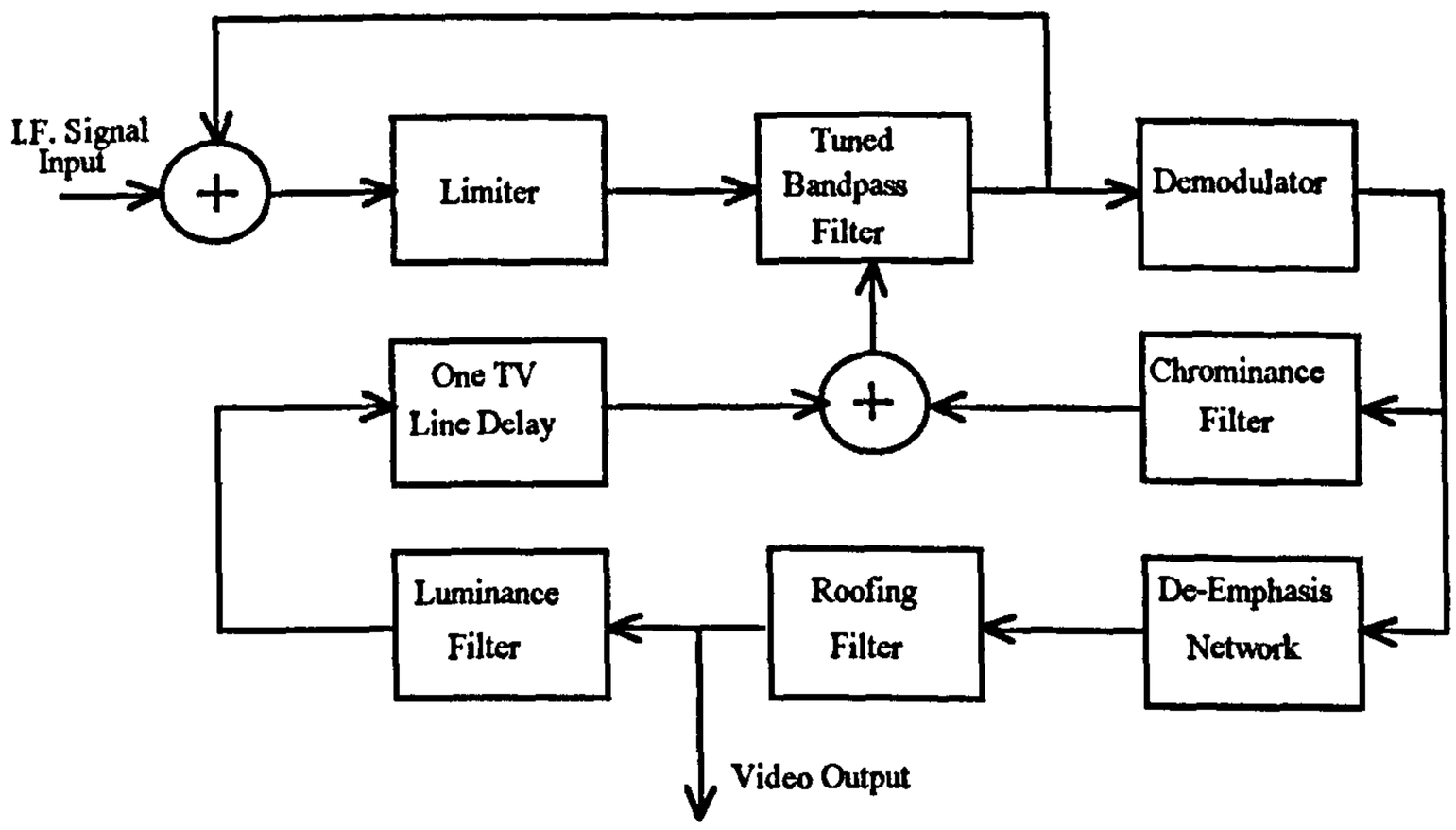

Figure 8/9 Mobley Tracking Filter Demodulator

Mobley observes that in general both luminance and chrominance do not occupy the entire bandwidth allocated to the television signal and in practice have varying instantaneous frequencies within the band, whatever the format is that they are transmitted in, viz. NTSC or MAC. For this reason it is possible to obtain additional noise reduction by using a tuneable bandpass filter ahead of the demodulator. The tuning signal for the filter is derived from the demodulator output and is fed back to the filter to tune it to the centre frequency of the input signal, allowing the design to capture the maximum amount of signal with the minimum amount of noise. The input signal from the I.F. amplifier is applied to a summing junction where it is added to a feedback signal from the limiter feedback loop. The

combined signal is applied to the limiter input. The limiter in conjunction with the tuneable bandpass filter and the overall feedback loop around them, form an oscillating limiter similar to the design described above in the Clayton approaches, [7-8]. When the composite level is above the knee of the limiter characteristic, the output is a constant amplitude square wave. When the composite input is below the knee of the limiter characteristic then the bandwidth of the oscillating limiter reduces to enhance its output carrier-to-noise level. The constant amplitude output of the limiter is then demodulated. The demodulator output is applied to two functions. The first is the chrominance filter that selects out the chrominance part of the video signal. This filter provides a one half cycle delay so that this chrominance signal is in phase with the chrominance information in the I.F. signal input. The demodulated signal is also applied to the second function, the de-emphasis network. After de-emphasis the demodulated signal is applied to a roofing filter whose output is the NTSC video signal. This signal is also applied to a luminance filter whose output is the luminance portion of the signal and which is delayed by one line period. The one line delayed luminance signal and the one half cycle delayed chrominance signal are combined in the summing network and the composite output forms the tuning signal for the voltage controlled filter. This provides an accurate measure of the instantaneous frequency component of the I.F. input signal.

Although the approach is an interesting one, it suffers from the same disadvantages as the Clayton [7-8] approaches. No performance figures are given in the patent and there is very little discussion of the click effect at threshold.

8.2.8 O'Connor's demodulator patent is described in [12] and illustrated in figure 8/10. It is an unusual approach and although treated here as a tracking filter, it does share some of the FMFB demodulator characteristics. This approach is a carrier tracking demodulator for TV signals. It effectively tracks the instantaneous frequency of the FM signal without frequency compression. To track the instantaneous carrier frequency a number of cascaded mixers are used with various local oscillators. A control loop is utilised to provide feedback from the demodulator and a local oscillator that enables the FM signal to be tracked with a narrow bandwidth.

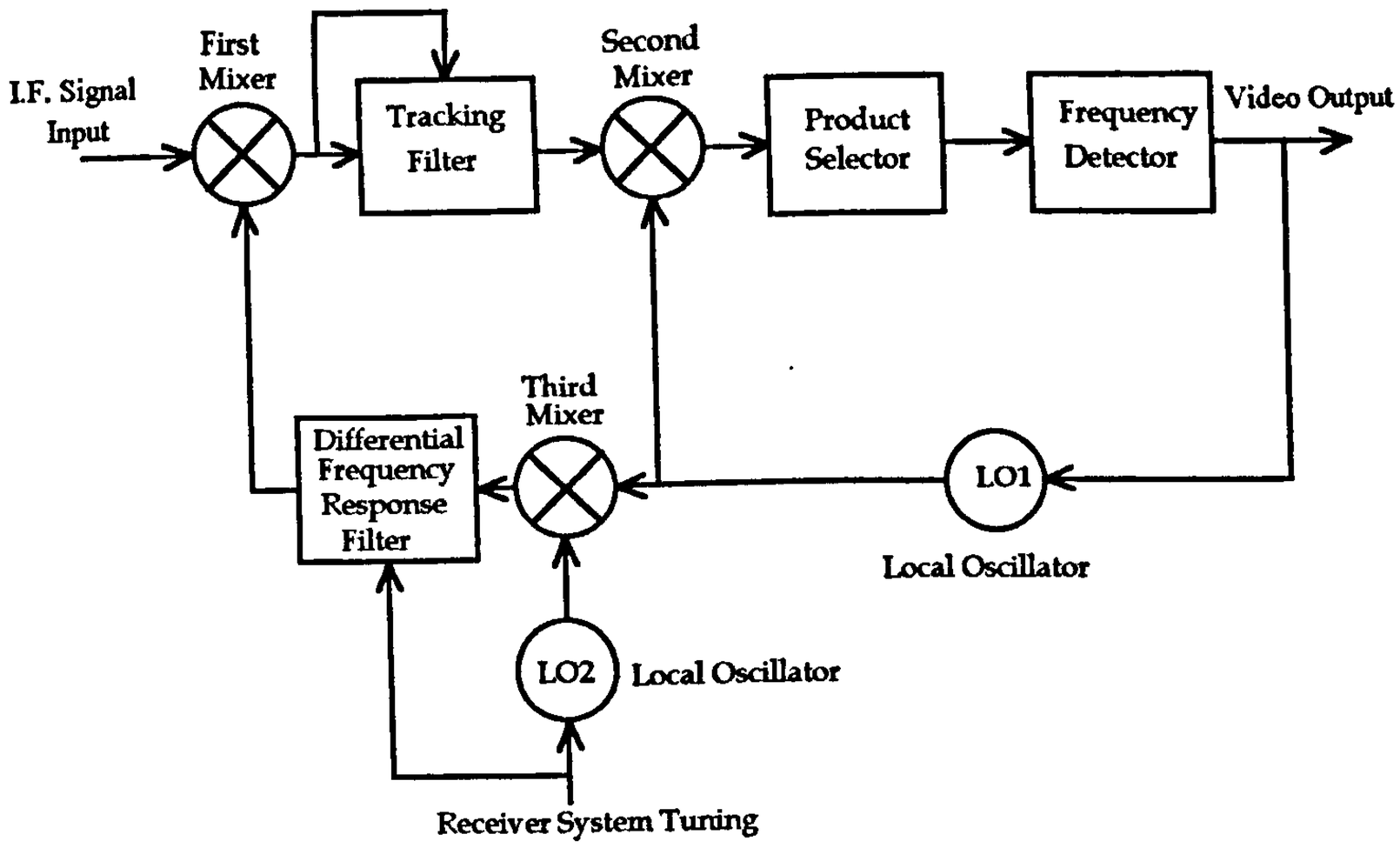

Receiver System Tuning

Figure 8/10 O'Connor Tracking Filter Demodulator

This design is very complex and it is difficult to see the magnitude of any threshold extension that may be achieved with wide band TV video signals. The stability of the approach is probably a particular problem.

8.2.9 Idogawa-Amazawa describe their tracking filter demodulator approach in [9]. Again this attempts to improve performance by following the instantaneous frequency more precisely. The design is illustrated in figure 8/11. The I.F. input signal is applied to the narrow band tracking filter whose central frequency follows the instantaneous frequency of the input signal.

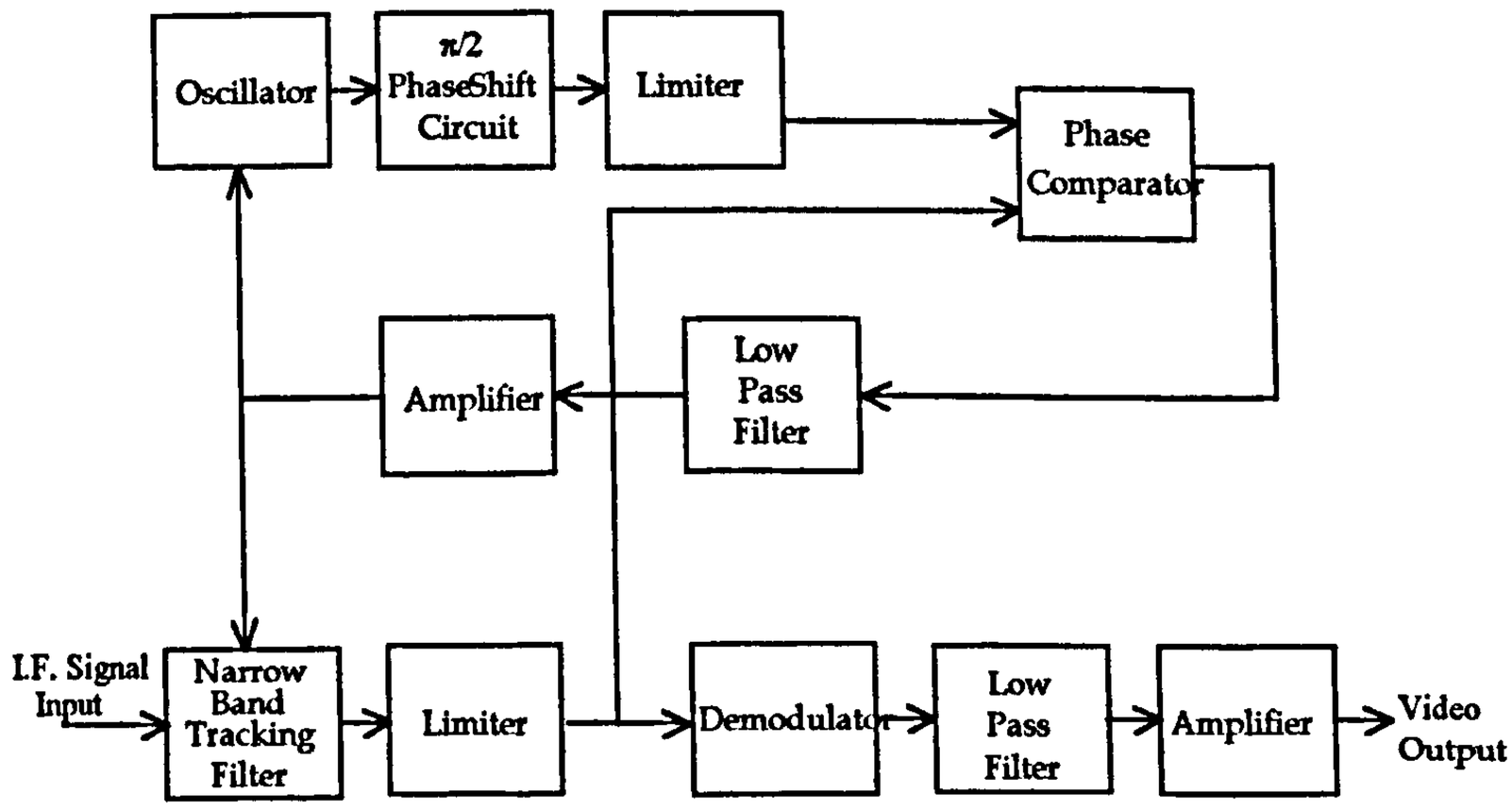

Figure 8/11 Idogawa-Amazawa Tracking Filter Demodulator

The output of the narrow band tracking filter is limited and then applied to the demodulator. The post demodulator filter has a low pass characteristic and its output is applied to an amplifier, the output of which provides the demodulated video output signal. The limiter output is also applied to one input of the phase comparator. The other input to the phase comparator is derived, via a phase shifter and limiter, from the oscillator that is generating the same frequency as the instantaneous frequency. The phase shifter provides a 90 degree phase shift at the appropriate frequency. The phase comparator provides an output dependent upon the phase difference between the two input signals. This output after being filtered and amplified is used to control both the tracking filter centre frequency and the local oscillator frequency.

The design is somewhat similar to the synchronous detector technique used in the early communication systems. Although no performance figures are given the claim is made that the 'improvement in signal-to-noise ratio is remarkable'. It is anticipated that stability will be a problem with such a system and that difficulties will be encountered in making it operate over a wide frequency baseband. However in view of the claims made the approach would merit a more detailed analysis.

8.2.10 Egger's tracking filter patent [10] is illustrated in figure 8/12. It also is intended to provide an improvement in threshold performance for PAL, NTSC or MAC TV signals and in particular those used in DBS satellite applications. The design is intended to be used with a multi-standard receiver.

Considering figure 8/12 the input signal from the I.F. is applied to a fixed bandpass filter and then to a tuned bandpass filter. The output of the latter is then applied to a demodulator whose video output, via various feedback loops, is used to control the tuned filter. For NTSC and PAL signals two feedback loops are used. The first consisting of an amplifier and low pass filter, and the second consisting of a bandpass filter. The outputs from the two loops are summed before being used to control the tuneable filter. For MAC signals the second loop is rendered inoperative by means of a switch. The bandpass filter used in the

second loop is tuned to the chrominance frequency. The high pass filter in series is used to control the overall phase shift. To improve the tracking characteristic the low pass filter in the first loop is chosen to be a compromise between signal and noise characteristics.

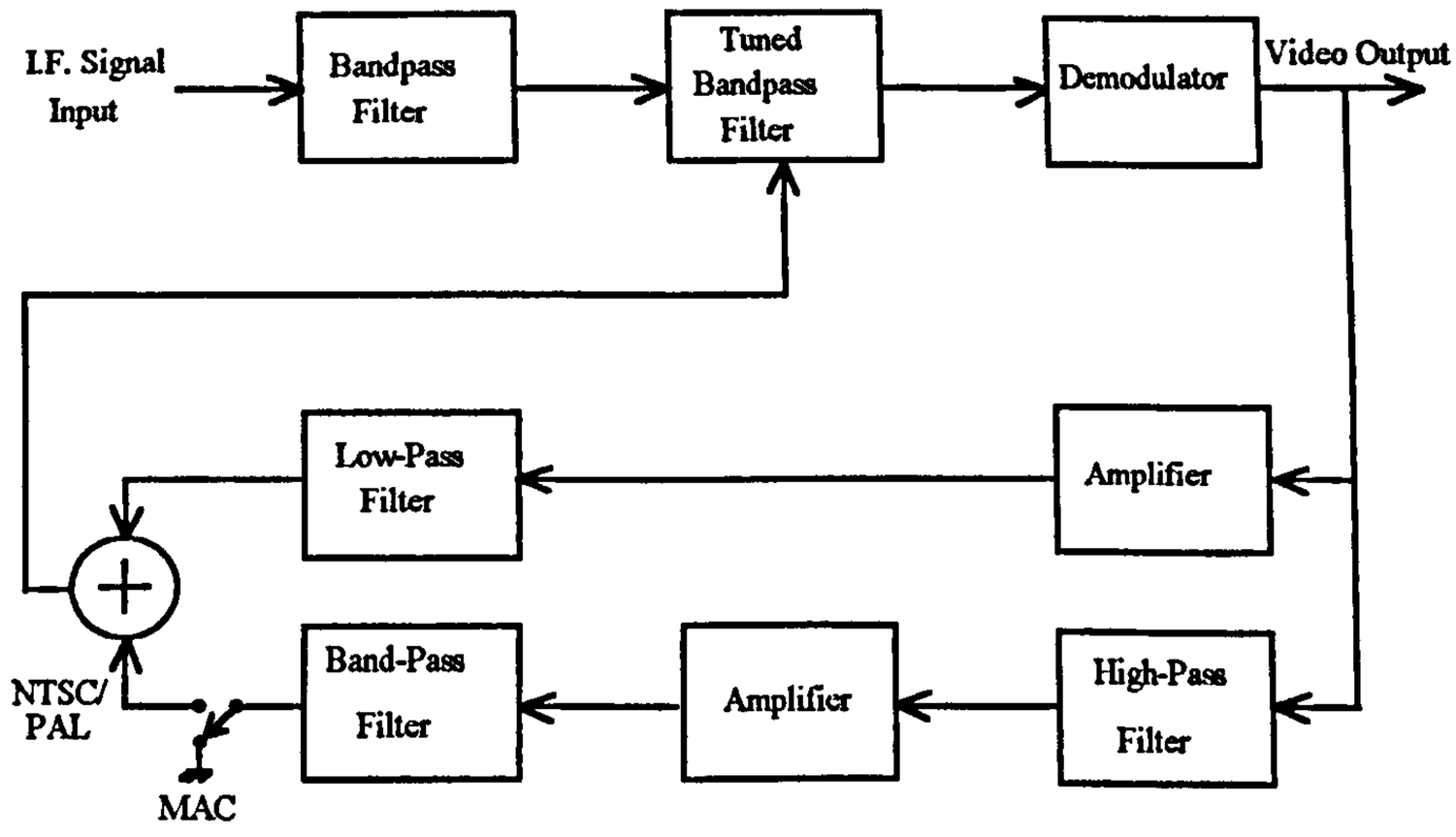

Figure 8/12 Egger Tracking Filter Demodulator

This is one of those rare patents that provides not only performance details but actual characteristics of the various filters used so that the performance can be theoretically verified. A 3 dB improvement in threshold is claimed for the PAL 25 MHz system. In view of the surprising simplicity of the approach and the performance figures claimed the design merits further study.

8.3 Analysis of the tracking filter

8.3.1 The following analysis of the tracking filter, although simplified, gives a measure of the threshold improvement gain achieved. Assume the circuit being analysed is the circuit described in 8.2.4 above, or one of its variants that uses a reference (fixed bandwidth) filter at the input. A simplified diagram of the demodulator is shown in figure 8/13a.

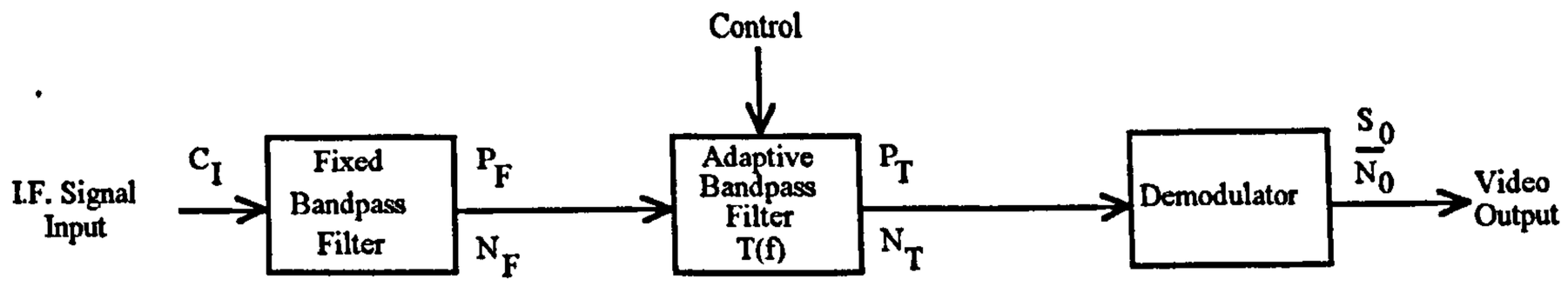

Figure 8/13a - Simplified Tracking Filter Demodulator

For the purpose of the following analysis assume that C_T = input carrier power at threshold. Now when the input power $C_I \rangle\rangle C_T$ also assume that the adaptive bandpass filter is cut out and the performance of the demodulator is defined by the input (fixed bandpass) reference filter. In this condition the noise power of the reference filter is defined by N_F . When $C_I \langle\langle C_T$ the performance of the demodulator is defined by the tracking (adaptive bandpass) filter. Let the modulation index be $\beta = \frac{\Delta f}{f_M}$ and assume that the reference bandpass filter characteristic is flat in the pass band and has infinite attenuation in the stop band, and that its bandwidth is given by Carson's rule, viz:

$$B_C = 2(\Delta f + f_M) \qquad \text{..... (8-1)}$$

8.3.2 The approach that will be adopted to demonstrate the effectiveness of the tracking filter demodulator, is to determine the effect of the reference and variable adaptive bandpass filters upon the individual frequency components of the signal. The frequency spectrum of a FM carrier modulated by a single sinusoid, can be determined by an expansion of the basic equation for the latter [15], [16], [17]:

$$v(t) = V_c \sin(\omega_c t + \beta \sin \omega_m t) \qquad \text{.....(8-2a)}$$

$$\therefore \quad v(t) = V_c [\sin \omega_c t \cos(\beta \sin \omega_m t) + \cos \omega_c t \sin(\beta \sin \omega_m t)] \qquad \text{..... (8-2b)}$$

Where ω_c is the angular carrier frequency and ω_m is the angular modulation frequency. The $\cos(\beta \sin \omega_m t)$ term in equation 8-2b is equal to the following Bessel function series [16]:

$$\cos(\beta \sin \omega_m t) = \sum_{n=-\infty}^{\infty} J_{2n}\, \beta \cos 2n\omega_m t \qquad \text{..... (8-2c)}$$

The $\sin(\beta \sin \omega_m t)$ term in equation 8-2b is equal to the following Bessel function series [16]:

$$\sin(\beta \sin \omega_m t) = \sum_{n=-\infty}^{\infty} J_{(2n-1)}\, \beta \sin(2n-1)\omega_m t \qquad \text{..... (8-2d)}$$

where the Bessel function are of the first kind and zero order, first order, second order, etc. of argument β. By substituting the Bessel function series into equation 8-2b and making the trigonometric substitution $2 \sin A \cos B = \sin(A+B) + \sin(A-B)$ gives:

$$\begin{aligned} v(t) = V_c [& J_0\, \beta \sin \omega_c t \\ & + J_1\, \beta \sin(\omega_c + \omega_m) t - J_1\, \beta \sin(\omega_c - \omega_m) t \\ & + J_2\, \beta \sin(\omega_c + 2\,\omega_m) t + J_2\, \beta \sin(\omega_c - 2\,\omega_m) t \\ & + J_3\, \beta \sin(\omega_c + 3\,\omega_m) t - J_3\, \beta \sin(\omega_c - 3\,\omega_m) t \\ & \qquad \text{------}] \end{aligned} \qquad \text{..... (8-2e)}$$

$$\therefore \quad v(t) = V_c \sum_{n=-\infty}^{\infty} J_n\, \beta\, \sin(\omega_c + n\,\omega_m) t \qquad \text{..... (8-2f)}$$

The summation form follows from the result $J_{-n}(x) = (-1)^n J_n(x)$. The frequency components of a frequency modulated waveform are given by equation 8-2f. Frequency modulation of a carrier by a single sinusoid results in the creation of an infinite number of sideband signals spaced by an amount ω_m from another and having amplitudes determined by the Bessel coefficients in equation 8-2f. The Bessel coefficients are functions of the modulation index β, so that as the amplitude of the modulating sinusoid varies, causing the deviation to vary, the amplitudes of the various sideband signals are changed.. The amplitude of the carrier is reduced by the frequency modulation in accordance with the Bessel coefficient $J_0(\beta)$. Frequency modulation removes power from the carrier and puts it into the sidebands. Since the amplitude of the envelope of a FM carrier remains

unchanged by the modulation, the total power in the carrier and the sidebands is equal to the unmodulated carrier power. That is the total power in the waveform is constant and is independent of the modulation index β. This characteristic is also shown by the following Bessel function identity:

$$[J_0(\beta)]^2 + 2[J_1(\beta)]^2 + 2[J_2(\beta)]^2 + 2[J_3(\beta)]^2 + \cdots = \sum_{n=-\infty}^{\infty} J_n^2(\beta) = 1 \quad \text{..... (8-2g)}$$

From equation 8-2g assume that the signal power at the input to the reference filter of an FM signal modulated by a frequency f_M , is given by:

$$P_I = \sum_{n=-\infty}^{\infty} J_n^2(\beta) = J_0^2(\beta) + 2J_1^2(\beta) + 2J_2^2(\beta) + \cdots = 1 \quad \text{..... (8-2h)}$$

where $J_n(\beta)$ is the Bessel function of the first kind and of order n and argument β.

The reference bandpass filter restricts the bandwidth to B_C and therefore the component satisfying $nf_M < \frac{B_C}{2}$ is transmitted and appears at the output of the reference bandpass filter. The output power of the bandpass filter is designated P_F. The noise power N_F of the reference bandpass filter is proportional to the bandwidth and is expressed as $N_F = \eta B_C$ where η is a constant.

The carrier-to-noise ratio at the output of the reference bandpass filter is :

$$\frac{C}{N} = \frac{P_F}{N_F} \quad \text{..... (8-3)}$$

8.3.3 Now let the transfer function of the variable or tuned (adaptive) bandpass filter be $H(f)$. The transfer function is used here in its conventional sense to denote the same quantity as the frequency response function [18]. Note that the value of frequency that will be used in the following analysis is the line frequency f of the specific sideband that is

measured from the carrier centre frequency, f_c . The carrier centre frequency is treated as a reference frequency with a value of zero. Thus at $f = 0$, let the transfer function satisfies the relationship $H(f) = 1$. Also let the output signal power of the variable or tuned (adaptive) bandpass filter be P_T . The output signal power is then:

$$P_T = \sum_{n=-\infty}^{\infty} J_n^2(\beta)\ H^2(n f_M) \qquad \text{..... (8-4)}$$

Expanding the Bessel series gives:

$$P_T = J_0^2(\beta) + 2\,J_1^2(\beta)\ H^2(f_M) + 2\,J_2^2(\beta)\ H^2(2 f_M) + \cdots + 2\,J_n^2(\beta)\ H^2(n f_M)$$

.....(8-5)

where $n f_M \ \langle\ \frac{B_C}{2}$ is satisfied.

For a single-sided bandwidth, the noise power at the output of the adaptive bandpass filter is given by :

$$N_T = 2\int_0^{\frac{B_C}{2}} H^2(f)\,df \qquad \text{..... (8-6)}$$

The carrier-to-noise ratio at the output of the adaptive bandpass filter is:

$$\frac{C}{N} = \frac{P_T}{N_T} \qquad \text{..... (8-7)}$$

When the input signal level decreases below the threshold level C_T, the adaptive bandpass filter is controlled to satisfy the inequality:

$$\frac{P_T}{N_T} \ \rangle\ \frac{P_F}{N_F} \qquad \text{..... (8-8)}$$

In this case the threshold level is improved by ζ, viz.:

$$\zeta = \frac{P_T}{N_T} \cdot \frac{N_F}{P_F} \qquad \text{..... (8-9)}$$

8.4 Application of the tracking filter analysis to the D2/MAC System

8.4.1 This section gives an example of the application of the tracking filter analysis derived in 8.3 above to the D2/MAC system. The basic characteristics of the D2/MAC system are given in Appendix B and the parameters relevant to threshold extension demodulators are derived and summarised in section 3.3.3. Those that will be used here are:

Modulation index $\beta = 0.93$

Occupied channel bandwidth $B_C = 27\ MHz$

Maximum component baseband signal bandwidth $f_M = 7\ MHz$

Peak-to-peak deviation $D_{P-P} = 13\ MHz$

Let the bandwidth of the reference bandpass filter be 27 MHz. (Note that using Carson's rule to determine the bandwidth results in the second harmonic of the highest video frequency, 28 MHz, being attenuated slightly).

Now from equation (8-2h) :

$$P_F = \sum_{n=-\infty}^{\infty} J_n^2(\beta) = J_0^2(\beta) + 2\,J_1^2(\beta) + 2\,J_2^2(\beta) + \cdots +$$

Therefore $$P_F = (0.795)^2 + 2(0.417)^2 + 2(0.101)^2$$

$$P_F = 0.632 + 0.348 + 0.020 = 1 \qquad \text{..... (8-10)}$$

The resolution of the Bessel function values and the value of modulation index used (0.93) gives a result where all the transmitted power is contained in the first three sidebands. In

practice this would not be the case as part of the transmitted power would be contained in the higher order sidebands. However the value obtained does not affect the illustration being given of the effectiveness of the tracking filter. The first term shows the carrier (centre frequency) component, the second term shows the first sideband component, which is separated from the centre frequency by 7.0 MHz, and the third term shows the second sideband, which is separated by 14 MHz from the centre frequency. Normalising the noise power density by $\frac{1}{MHz}$ gives the noise power at the of the reference bandpass filter, thus:

$$N_F = B_C = 27 \qquad \text{..... (8-11)}$$

This is a valid assumption as although the noise bandwidth is greater than the actual bandwidth, the ratio of the noise bandwidths taken below cancels any factors used in obtaining the noise bandwidth from the actual bandwidth.

Accordingly $$\frac{P_F}{N_F} = \frac{1}{27} \qquad \text{..... (8-12)}$$

8.4.2 Ideal filter

Assume that the tuned or adaptive bandpass filter has a narrow passband B_T and infinite attenuation outside the passband. Now with the adaptive filter, the ratio of signal power (P_T) to noise power (N_T) and the improvement ζ of the carrier-to-noise ratio at the output of the bandpass filter is as follows.

Now $\frac{P_F}{N_F} = \frac{1}{27}$ and $\frac{P_T}{N_T} = \frac{1}{B_T}$

$$\therefore \quad \zeta = \frac{P_T}{N_T}\frac{N_F}{P_F} = \frac{1}{B_T}\frac{27}{1}$$

$$\therefore \quad \zeta = \text{ratio of bandwidths} = \frac{27}{B_T} \qquad \text{..... (8-13)}$$

When $B_T = 27$ MHz, then $\zeta = \frac{27}{27} = 1$ or 0 dB.

When $b' = 13.5$ MHz, then $\eta = \frac{27}{14} = 1.928$ or 2.85 dB.

Thus by attenuating the second sideband of the signal an improvement in threshold of some 2.85 dB would be obtained at some loss of picture resolution.

8.4.3 Practical filter

(a) Consider the same example as 8.4.2 above but using a practical adaptive filter. In this case a parallel tuned circuit is used, which is implemented by a fixed inductor L in parallel with a fixed capacitor C, and their loss components being represented by a parallel resistor r. This parallel $r\,LC$ network is in series with a variable resistor R (normally a PIN or Schottky diode). The transfer function of this adaptive network, shown in figure 8/13b, is denoted by $H(f)$.

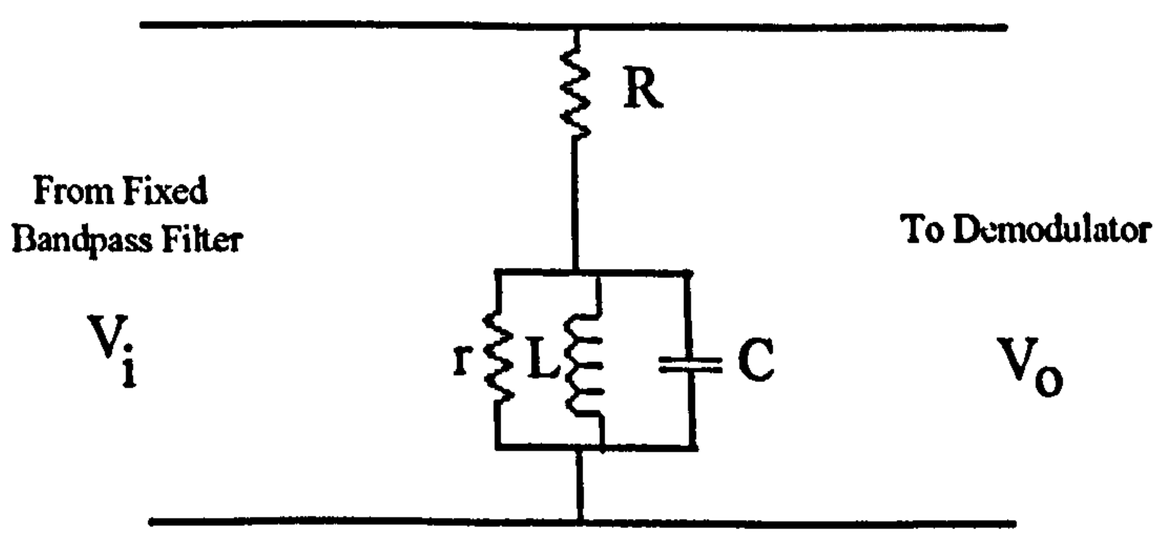

Figure 8/13b - Adaptive bandpass filter

When the input signal is high, above the threshold value, the resistor R is controlled to be high, preventing this tuned filter from operating on the input signal. The bandwidth of the signal is thus determined by the reference input bandpass filter. When the input signal drops to, or below, the threshold level, the resistor R is controlled to a low value so that the tuned or adaptive filter begins to act upon the input signal and determines its frequency

characteristics. When the value of R is in the low region, the transfer function $H(f)$ of the single resonant circuit can be approximated by:

$$H(f) = \frac{1}{\left(1+\left(\frac{2f}{b_0}\right)^2\right)^{\frac{1}{2}}} \qquad \text{..... (8-14)}$$

where b_0 is the 3 dB bandwidth and f is the centre frequency.

(b) The signal power P_T at the output of the adaptive bandpass filter is derived as follows:

$$P_T = \sum_{n=-\infty}^{\infty} J_n^2(\beta)\, H^2(nf) = \sum_{n=-\infty}^{\infty} J_n^2(\beta) \frac{1}{\left(1+\left(\frac{2nf}{b_0}\right)^2\right)} \qquad \text{..... (8-15a)}$$

$$= J_0^2(\beta) + 2J_1^2(\beta)H^2(f) + 2J_2^2(\beta)H^2(2f) + \cdots + 2J_n^2(\beta)H^2(nf)$$

$$= J_0^2(\beta) + 2J_1^2(\beta)\frac{1}{\left(1+\left(\frac{2f}{b_0}\right)^2\right)} + 2J_2^2(\beta)\frac{1}{\left(1+\left(\frac{4f}{b_0}\right)^2\right)} + \cdots + \qquad \text{..... (8-15b)}$$

Using the Bessel values derived in equation (8-10) above gives:

$$P_T = (0.795)^2 + 2(0.417)^2 \frac{1}{\left(1+\left(\frac{2(7.00)}{b_0}\right)^2\right)} + 2(0.101)^2 \frac{1}{\left(1+\left(\frac{4(7.00)}{b_0}\right)^2\right)}$$

where f and b_0 are in MHz.

$$\therefore P_T = 0.632 + \frac{0.348}{\left(1+\left(\frac{14}{b_0}\right)^2\right)} + \frac{0.020}{\left(1+\left(\frac{28}{b_0}\right)^2\right)}$$

$$P_T = 0.632 + \frac{0.348}{\left(1+\frac{196}{b_0^2}\right)} + \frac{0.020}{\left(1+\frac{784}{b_0^2}\right)} \qquad \text{..... (8-16)}$$

(c) The noise power ratio at the output of the bandpass filter is derived as follows:

$$N_T = 2\int_0^{\frac{B_C}{2}} \frac{1}{\left(1+\left(\frac{2f}{b_0}\right)^2\right)} df \qquad \text{..... (8-17)}$$

$$\therefore \quad N_T = b_0 \tan^{-1}\left(\frac{B_C}{b_0}\right) \qquad \text{..... (8-18)}$$

(d) The signal power-noise power ratio is obtained from equations (8-15a) and (8-18):

$$\frac{P_T}{N_T} = \frac{\sum_{n=-\infty}^{\infty} J_n^2(\beta) \frac{1}{\left(1+\left(\frac{2nf}{b_0}\right)^2\right)}}{2\int_0^{\frac{B_C}{2}} \frac{1}{\left(1+\left(\frac{2f}{b_0}\right)^2\right)} df} \qquad \text{.....(8-19)}$$

$$\frac{P_T}{N_T} = \frac{J_0^2(\beta) + 2J_1^2(\beta)\dfrac{1}{\left(1+\left(\dfrac{2f}{b_0}\right)^2\right)} + 2J_2^2(\beta)\dfrac{1}{\left(1+\left(\dfrac{4f}{b_0}\right)^2\right)}}{b_0 \tan^{-1}\left(\dfrac{B_C}{b_0}\right)}$$

$$\frac{P_T}{N_T} = \frac{0.632 + \dfrac{0.348}{\left(1+\dfrac{196}{b_0^2}\right)} + \dfrac{0.020}{\left(1+\dfrac{784}{b_0^2}\right)}}{b_0 \tan^{-1}\left(\dfrac{27}{b_0}\right)} \quad \text{..... (8-20)}$$

Thus from equation (18-9) $\zeta = \dfrac{P_T}{N_T} \cdot \dfrac{N_F}{P_F}$ where $\dfrac{N_F}{P_F} = \dfrac{27}{1}$

Therefore: $$\zeta = \frac{27\left[0.632 + \dfrac{0.348}{\left(1+\dfrac{196}{b_0^2}\right)} + \dfrac{0.020}{\left(1+\dfrac{784}{b_0^2}\right)}\right]}{b_0 \tan^{-1}\left(\dfrac{27}{b_0}\right)} \quad \text{..... (8-21)}$$

A graph of equation (8-21) is plotted in figure 8/14. Here the adaptive filter bandwidth b_0 is varied from 5 to 30 MHz, showing that at 5 MHz bandwidth a threshold gain improvement of some 4.2 dB is obtained. Although the value of 5 MHz may appear to be too low compared to the maximum value of 7 MHz assumed for the video signal bandwidth, note that the latter is a maximum, and the maximum frequency content would frequently be lower than this.

Figure 8/14 - Threshold Improvement vs. Adaptive Filter Bandwidth

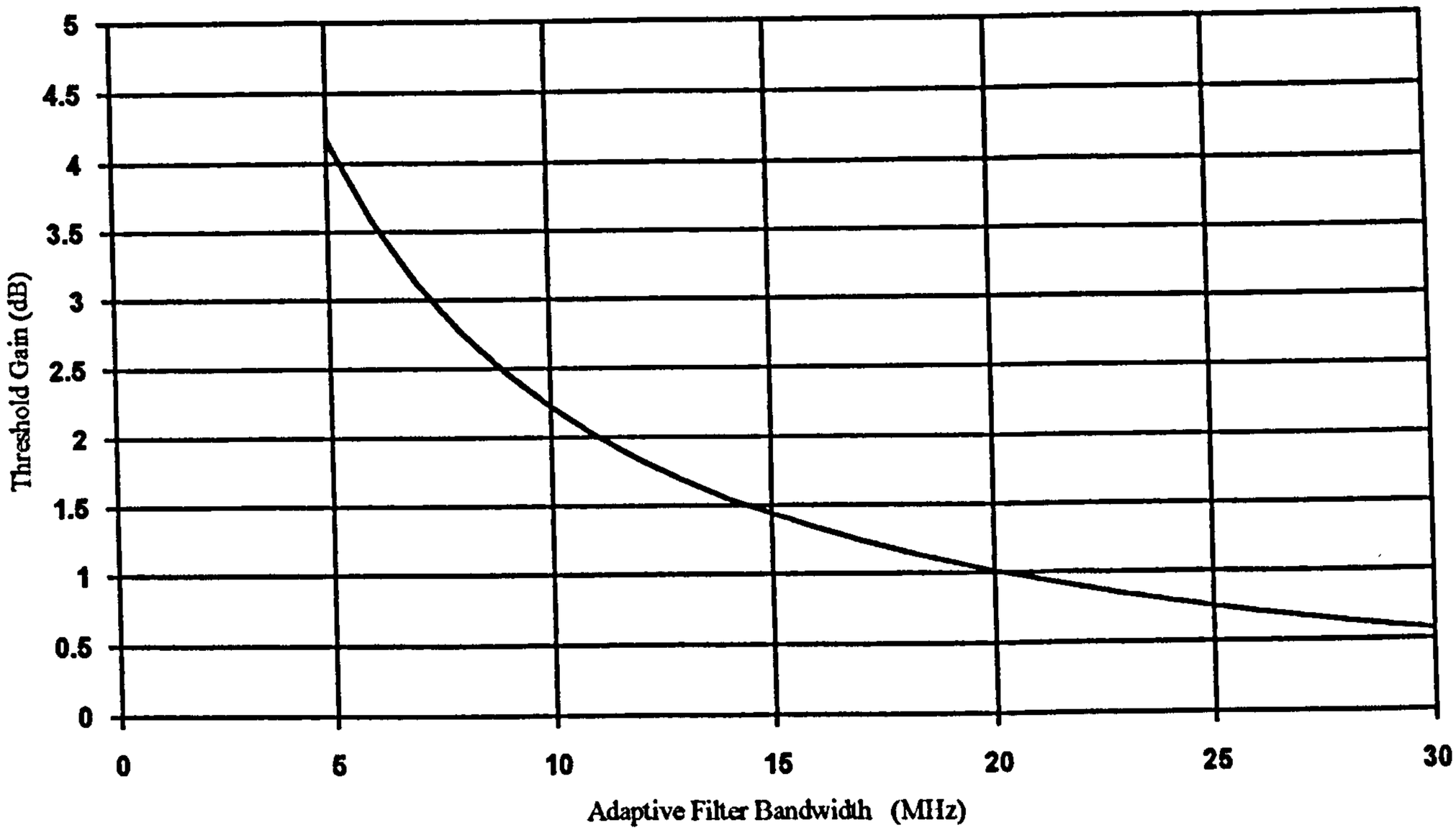

8.5 Summary

8.5.1 The simplified analysis of the tracking filter carried out above shows clearly how an improvement in threshold extension is achieved by reducing the bandwidth of the system. However the disadvantages incurred are a lack of picture resolution and distortion by reducing the higher order sidebands in the signal.

The survey of various design approaches published illustrate the basic problem with the tracking filter, namely the two metrics used for adjusting the centre frequency of the filter and its bandwidth adjustment. The adjustment of the centre frequency does not pose a major problem as there are several references in the signal structure that can be used, viz. the chrominance frequency in conventional TV systems. However the metric for detecting the occurrence of threshold has not really been solved. How the metric detects the click, rather than the doublet or false click, and controls the filter is a problem that the references cited herein had not addressed. A proposed solution resulting from this study is given in chapter 18 below.

8.6 References

[1] Lockyer, K. S. "Threshold extension of an FM demodulator using a dynamic tracking filter," Proc. IEE, 1968, **115**, (11), pp. 1102 - 1108.

[2] Roberts, J. H. "Dynamic tracking filter as a low threshold demodulator in FM/FDM satellite systems," Proc. IEE, 1968, **115**, (11), pp. 1597 - 1606.

[3] Mobley, J. G. "Signal to noise ratio enhancement using baseband signals in an FM television system", US Patent 4,584,599, April 22, 1986.

[4] Ohta, T., Tsutsumi, Y., Konishi, Y. "FM demodulator with variable bandpass filter", US Patent 4,563,651, January 6th, 1986.

[5] Ohta, T., Tsutsumi, Y., Sugano, M.,. "High sensitivity FM signal demodulation system", US Patent 4,531,148, July 23, 1985.

[6] Ohta, T., "High sensitivity FM signal demodulation system", US Patent 4,527,187. July 2nd, 1985.

[7] Clayton, L., Livaditis, E. J. "Threshold extension FM demodulator apparatus for wide bandwidth FM signals", US Patent 4,101,837. July 18th, 1978.

[8] Clayton, L., "FM noise threshold extension demodulator apparatus", US Patent 4,035,730. July 12th, 1977.

[9] Idogawa, K. and Amazawa, K., "FM demodulator with tracking filter", US Patent 5,051,703. September 24th, 1991.

[10] Egger, J., "Television receiver including a frequency demodulator for lowering the

threshold", US Patent 5,161,004. November 3rd, 1992.

[11] Favreau, M., Marguimaud, A., "FM demodulator with variable bandpass filter", US Patent 4,458,207. July 3rd, 1984.

[12] O'Connor, E., "Threshold extension FM demodulator apparatus and method," US Patent 4,777,449. October 11th, 1988.

[13] Roberts, J. H. "*Angle Modulation*," England, Peter Pereginus, 1977.

[14] Baghdady, E. J., IRE Trans. Communications Systems, September 1964, page 194.

[15] Haykin, S. "*Communication Systems*", 3rd. Ed., John Wiley & Sons, New York, 1994, ISBN 0-471-57176-8.

[16] Giacoletto, L. J. "*Electronic Designers' Handbook*", 2nd. Ed., New York, McGraw-Hill, 1977, ISBN 0-07-023149-4 .

[17] Taub, H., Schilling, D. "*Principles of Communication Systems*" McGraw-Hill, 1986, New York, ISBN 0-07-062955-2.

[18] Bendat, J. S. & Piersol, A. G. "*Engineering Applications of Correlation and Spectral Analysis*", 2nd. Ed., John Wiley & Sons, New York, 1993, ISBN 0-471-57055-9.

[19] Baghdady, E. J., "Theory of feedback around the limiter". 1957 IRE National Convention Record, Vol. 5, Part 8, pp. 176-202.

[20] Bozzoni, E. and Mengali, U. "A general analysis of the performance of the oscillating limiter with noiseless signals". IEEE Trans. Communications Technology,

Vol. COM-14, pp. 578-588, October 1966.

[21] Bozzoni, E. and Mengali, U. "Experimental verification of a model of the oscillating limiter". IEEE Trans. Communications Technology, Vol. COM-15, No. 6, pp. 865-867, December 1967.

9. FREQUENCY DEMODULATOR WITH FEEDBACK

9.1 Introduction

9.1.1 The FM demodulator with negative feedback (FMFB), sometimes called the FM feedback receiver or frequency compression demodulator, is a further design that exhibits threshold extension capabilities. The threshold improvement is achieved by virtue of the feedback action reducing deviation of the signal, that permits transmission of the resulting compressed signal through a narrow bandpass filter prior to detection. In implementation the approach bears some similarity to the phase lock loop demodulator in that both designs use a Voltage Controlled Oscillator (VCO) that is frequency modulated by the output, and where the signal input is multiplied by the output of the VCO. However in the FMFB the frequency of the VCO is offset.

Of all the threshold extension demodulator techniques the FMFB demodulator is probably the most elegant. As will be shown later in this thesis (section 17) the FMFB demodulator defining equation without a limiter, degenerates into the defining equations for the phase lock loop (PLL) and frequency lock loop (FLL), as the loop I.F. filter bandwidth approach zero and infinity respectively. This shows there is only one basic threshold extension device (FMFB) from which the other two threshold extension devices (PLL) and (FLL) are derivable.

The FMFB technique appears to offer a useful threshold extension improvement, but has several problems that make it difficult to obtain a consistent performance in use. One difficulty is that the probability density function (pdf) of the modulation signal affects the threshold extension characteristics significantly. Other problems concern the stability of the FMFB demodulator, the solution of which has received much attention in recent years.

This chapter considers the basic operation of the FMFB, gives a brief review of FMFB

operation and gives a summary of its operating equations. The basic problems with the design are discussed and past solutions described. The problems identified may be overcome in the solution offered in chapter 18 below, where an error controlled adaptive threshold extension demodulator is proposed and a version of which is based upon the FMFB demodulator.

9.2 Basic FMFB demodulator mode of operation

9.2.1 General

A block schematic of the FMFB demodulator is shown in figure 9/1. The carrier frequency input, after filtering in the RF or predetection filter, is applied to the multiplier, where it is multiplied by the output of the VCO. This VCO is frequency modulated by the demodulated output baseband signal. The nominal frequency of the VCO is offset from the carrier centre frequency by an amount equal to the centre frequency of the I.F. stage.

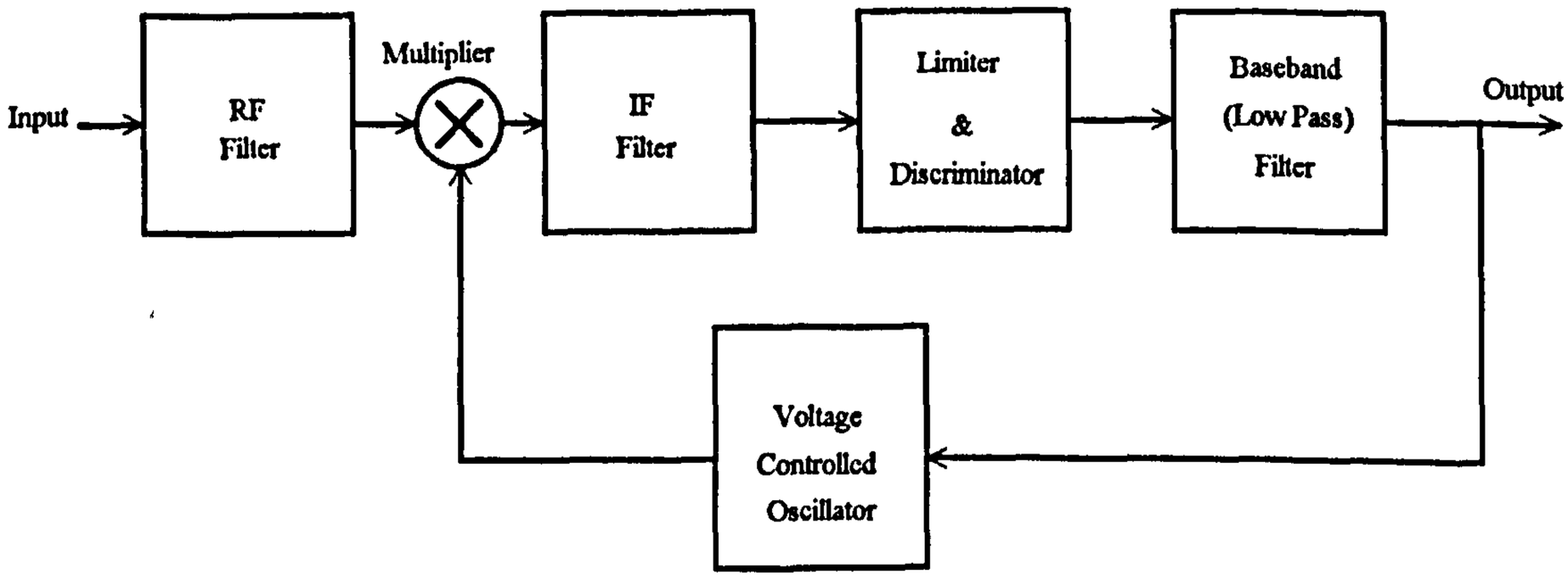

Figure 9/1 Frequency Demodulator with Feedback

At the multiplier or mixer output, the forward loop selects the difference frequency component. The FMFB includes in its forward path an I.F. bandpass filter, centred at the offset frequency, and a conventional limiter-discriminator. The recovered baseband signal at the output of the discriminator is filtered by the baseband filter. The output of this filter

provides both the output of the FMFB and the input to the VCO. For the latter the demodulated signal is fed back in such a way as to reduce significantly the instantaneous frequency difference between the two signals being applied to the mixer. The modulation index of the I.F. signal is thus reduced. If this reduction is substantial, the resultant multiplier output FM signal will occupy a much narrower band at the I.F. frequency than the input RF signal applied to the multiplier, resulting in the bandwidth of the I.F. amplifier being reduced. The operation of the FMFB demodulator therefore results in a compression of the input signal, i.e. the deviation is reduced; allowing a significant reduction in the bandwidth of the I.F. bandpass filter without distortion of the signal. The FMFB is one of those demodulator types that achieves threshold extension by deviation reduction. In practice the RF, or predetection, filter should be regarded as an integral part of the demodulator because it band-limits noise components falling within the closed loop response of the FMFB. In addition the FMFB should be proceeded by an AGC system to control the input level to the multiplier, or mixer, so as to prevent clipping on the signal noise peaks during the mixing process.

Deviation in the FM demodulator is compressed in proportion to the feedback factor, defined as the open loop gain plus one. The bandwidth of the I.F. bandpass filter in the forward path of the loop is important since it determines the noise power presented to the limiter. It is related to the baseband signal bandwidth and to the compressed modulation index. The exact relationship between these parameters depends on the various performance criteria used to determine the bandwidth of the I.F. filter. That used below is based upon Carson's rule modified for a r.m.s. modulation index. These parameters control what has been termed the open-loop threshold.

The second threshold mechanism present in the FMFB demodulator is due to the application of feedback. Additive input noise is transferred to the baseband by the loop discriminator and modulates the VCO. The resulting VCO phase jitter mixes with the input carrier and noise to produce noise modulation in the loop I.F. There is an uncorrelated

component of VCO jitter that is not suppressed by feedback action. As the input carrier-to-noise ratio is lowered, a point is reached where the loop fails to track the input signal, and impulses appear in the baseband signal signifying the approach of the feedback threshold. Enloe's work [2], [6], showed that the two thresholds are nearly independent and an optimum is realised when the two thresholds occur at the same value of input carrier-to-noise ratio.

Despite the many works published on the FMFB demodulator, practical design methods seem to have been greatly dependent upon experimental results. This may be due to the difficulty in understanding the correct operation of the FMFB demodulator, because of the existence of so many non-linear elements, resulting in any analysis of the operation being conducted using an approximation approach. Iwanami, et al., [14] made the understanding of the FMFB design a little more complete by analysing the threshold characteristic using a quasi-linear approximation in the vicinity of threshold. Their analysis takes into account the open loop threshold due to non-linear limiter-discriminator operation, and the feedback threshold due to I.F. filter band limited distortion. Taub's [10] simplified analysis of the FMFB is the approach followed below, together with a brief description of Iwanami's [14] approach.

9.3 FMFB Literature Review

9.3.1 The frequency demodulator with feedback (FMFB), or frequency compression demodulator, originated with Chaffee in his patent of 1937 [1]. It was devised as a device that would reduce distortion in the detected output of an FM discriminator not proceeded by a limiter. There was little interest in the concept until the early 1960's when it was recognised as having threshold extension capabilities, particularly when used in space applications. This early interest resulted in Enloe's paper [2] on the FMFB. However since that time its operation as a threshold extension device has led to much controversy. Numerous approaches have been proposed to explain its operation. None of these seem

theoretically justifiable and none seem to comply with experimental fact, especially under modulation conditions. The most useful approaches appear to be due to Cassera [3] and Iwanami [14].

Interest in the FMFB technique was revived with the development of satellite television systems for DBS and TVRO applications in the late 1980's. For these applications there has been an increase in interest resulting in a steady flow of patents, viz. [4], [5], [15].

Since the threshold extension characteristic of the FMFB demodulator was first appreciated in the 1960s a number of investigations has been published into the various methods of design. However despite these many works practical design methods of the FMFB demodulator have been greatly dependent upon experimental results. Among the investigations into the FMFB threshold characteristics, three main effects have been studied by several investigators. These are:

(i) Non-linear operation of the limiter discriminator due to noise. These characteristic have been investigated by Enloe [2,6], Schilling [7], Kobayashi [8], Frutiger [9], Roberts [10], Taub [11] and Klapper [12].

(ii) Band limited distortion of the I.F. filter due to increased feedback noise. This effect has been investigated by Develet [13] and Roberts [10]. Develet's work is of considerable importance in the development of FMFB theoretical analysis. The analysis of distortion by the I.F. filter in the FMFB demodulator for the case of no noise has been considered by Hoffman [17], Nelan [18], Stojanovie [19], and Takanashi [20].

(iii) Occurrence of excess noise due to product of feedback noise and input noise. This characteristic has been investigated by Enloe [2], [6], and Klapper [12].

In general the threshold caused by the first effect is termed the open loop threshold, and that by second and third effects is called the feedback threshold. To have an FM demodulator with threshold extension optimised requires a consideration of these important effects.

Enloe's [2], [6], is an experimental design method that takes into account the open threshold and feedback threshold.

The design methods of Kobayashi [8], Fruitiger [9] and Schilling [7], gives a bandwidth in which the FM signal propagates without distortion accompanied by the open loop threshold and feedback noise. However this approach requires the distortion to be identified experimentally.

Develet [13] and Schilling [7] approach has been called the wide band design method [16], [12]. It is not a practical design method when the feedback coefficients become extremely large.

The method of Gerber [16] and Cassera [3] differ from the above in theory and they demonstrate experimentally that the approach is a practical design method for the FMFB demodulator.

Iwanami [14] developed a quasi-linear approximation model in which both the open-loop and feedback thresholds were considered. Together with Taub's [10] simplified analysis that provides an overall view of the FMFB, they are the approaches discussed below.

Patents that disclose modifications to the FMFB demodulator have been filed by Owen [15], Rogers [4] and Jarger [5]. Owen's patent concentrates on improving the stability of the FMFB by utilising a drift cancelling discriminator technique. Jarger patent is complex and is also aimed at reducing the effects of drift by using two feedback loops. Rogers patent uses crystal controlled filters also in an attempt to improve the stability of the demodulator.

All these techniques confirm that one of the major practical problems with the FMFB is the effect of instability.

9.4 Analysis of FMFB Operation

9.4.1 Simplified Analysis

(a) In the following two approaches will be used for the analysis of the FMFB. Firstly a simplified global FMFB analysis will be given of which Taub's [10] approach is a typical example. This will be followed, in section 9.4.2, by a brief summary of the analysis proposed by Iwanami [14]. The basic FMFB circuit given in figure 9/2 will be used for both approaches.

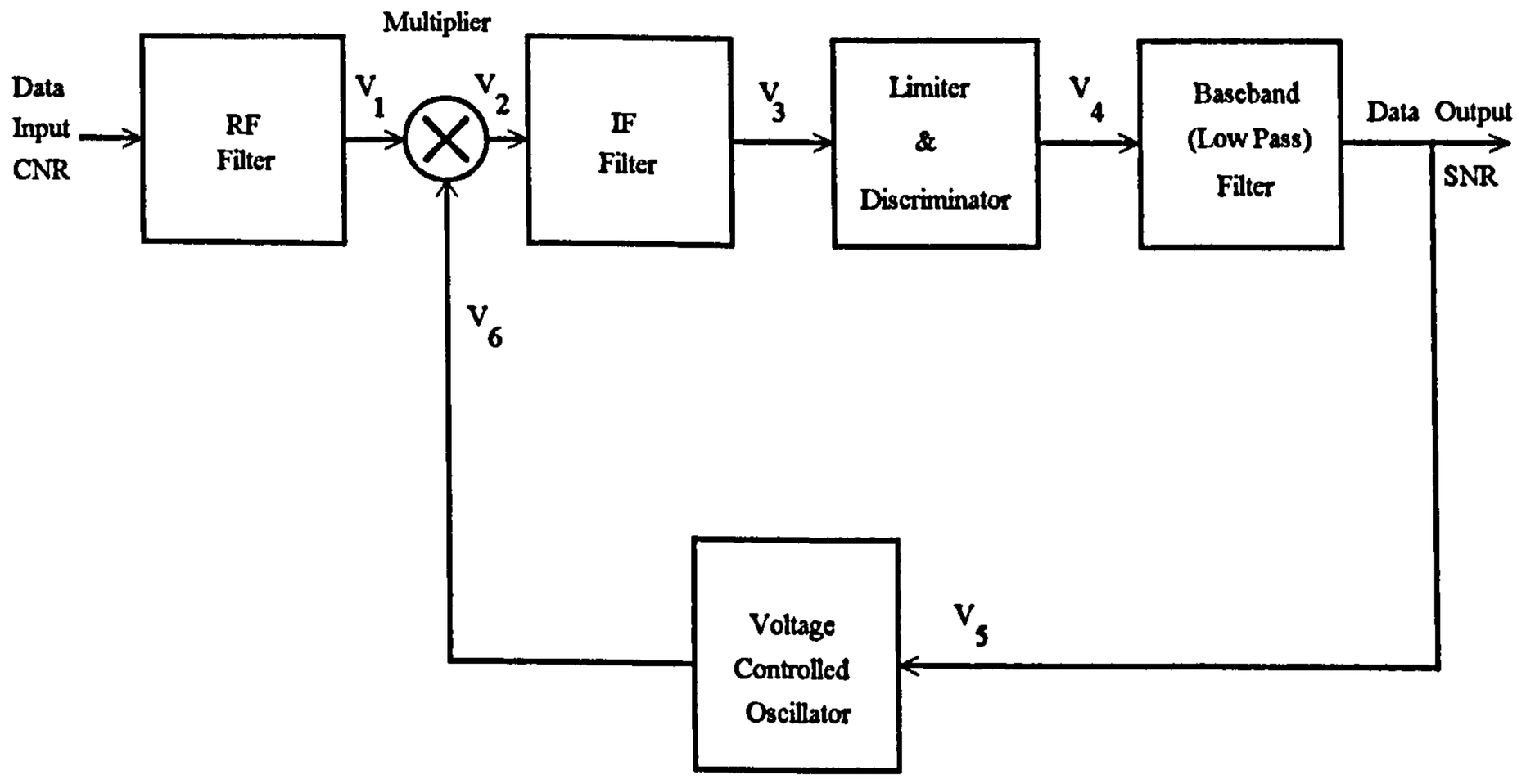

Figure 9/2 Frequency Demodulator with Feedback

Let the signal and noise input to the multiplier be:

$$V_1(t) = R(t)\sin\left[\omega_c t + \phi_s(t) + \phi_n(t)\right] \qquad \text{..... (9-1)}$$

where $R(t)$ = envelope of the signal plus noise

$\phi_s(t)$ = angular modulation due to signal

$\phi_n(t)$ = angular modulation due to noise

If the input V_1 is applied to a conventional limiter-discriminator whose output is α times the rate of change of the carrier frequency, the output voltage of the discriminator can be written:

$$V_5(t) = \alpha \frac{d}{dt}[\ \phi_s(t) + \phi_n(t)] \qquad \text{.....(9-2)}$$

This equation will be used later in the analysis as a basis for comparison with the FMFB.

Let the output of the voltage controlled oscillator, VCO, be given by:

$$V_6 = B\cos\left[(\omega_s - \omega_{IF})t + G_0 \int_{-\alpha}^{t} V_5(\lambda)\, d\lambda\right] \qquad \text{..... (9-3)}$$

where ω_S = angular signal frequency

ω_{IF} = angular I.F. frequency

B = VCO amplitude

G_0 = Sensitivity of VCO, i.e. change in VCO angular frequency per unit change in output.

Ignoring the characteristics of the I.F. filter, apart from it selecting the wanted difference frequency, $V_3(t)$, the output of the I.F. filter is given by:

$$V_3(t) = \frac{A\,B}{2}\cos\left[\omega_{IF}\, t + \phi_s(t) + \phi_n(t) - G_0 \int_{-\alpha}^{t} V_5(\lambda)\, d\lambda\right] \qquad \text{..... (9-4)}$$

where A represents the effects of the I.F. filter upon amplitude.

The output, $V_5(t)$, of the discriminator is given by:

$$V_5(t) = \alpha\left[\frac{d\,\phi_s(t)}{dt} + \frac{d\,\phi_n(t)}{dt} - G_0\,V_5(t)\right] \qquad \text{..... (9-5)}$$

Solving equation (9-5) for $V_5(t)$ gives:

$$V_5(t) = \left[\frac{\alpha}{1+\alpha G_0}\right]\frac{d}{dt}(\phi_s + \phi_n) \qquad \text{..... (9-6)}$$

Comparing the equation for the output of the FMFB in equation (9-6) with that for a conventional limiter-discriminator is given by equation (9-2). It can be seen that both equations are identical, except the output of the FMFB is reduced by $\left[\frac{1}{1+\alpha G_0}\right]$.

The performance of the FMFB is determined by the bandwidth of the I.F. filter in the forward path. To determine the minimum I.F. bandwidth that can be used without distorting the demodulated signal, for a given modulation index, inserting equation (9-6) into equation (9-4), gives:

$$V_3(t) = \frac{A\,B}{2}\cos\left[\omega_{IF}\,t + \left[\frac{\alpha}{1+\alpha G_0}\right](\phi_s + \phi_n)\right] \qquad \text{..... (9-7)}$$

Equation (9-7) shows that the frequency deviation of the signal ϕ_s has been reduced by the factor $\left[\frac{\alpha}{1+\alpha G_0}\right]$ by the overall feedback of the FMFB.

If the modulation is sinusoidal then: $\phi_s(t) = \beta \sin\,\omega_m t$ ..... (9-8)

and the phase of the compressed signal has been reduced to:

$$\frac{\phi_s(t)}{1+\alpha G_0} = \frac{\beta}{(1+\alpha G_0)}\sin\,\omega_m t \qquad \text{..... (9-9)}$$

Hence using Carson's rule, the bandwidth, B_{IF} , of the I.F. filter is given by:

$$B_{IF} = 2\left(\frac{\beta}{1+\alpha G_0}+1\right)f_M \qquad \text{..... (9-10)}$$

and the bandwidth, B_C , of the RF filter is given by:

$$B_C = 2(\beta+1)f_M \qquad \text{..... (9-11)}$$

Solving equations (9-10) and (9-11), to provide the relationship between B_{IF} and B_C gives:

$$B_{IF} = 2\left(\frac{\left[\frac{\beta}{1+\alpha G_0}\right]+1}{\beta+1}\right)B_C \qquad \text{..... (9-12)}$$

(b) To assess the threshold conditions of the FMFB, consider the values of G_0 for two extremes, namely zero and infinity. Firstly let the value of $G_0 = 0$. As can be seen from figure (9-2), this condition results from the feedback loop being effectively open circuited. With $G_0 = 0$, equation (9-12) reduces to:

$$B_{IF} = B_C \qquad \text{..... (9-13)}$$

showing that the FMFB is reduced to a conventional limiter-discriminator and that no deviation compression, and hence no threshold improvement, occurs. The action of the VCO is purely that of a fixed frequency local oscillator, causing the carrier frequency to be translated to the I.F. frequency.

With $G_0 = \infty$, the VCO output voltage can be written as:

$$V_6(t) = B\cos\left[(\omega_s - \omega_{IF})t + \phi_{OSC}(t)\right] \qquad \text{..... (9-14)}$$

Comparing equation (9-14) with equation (9-3), it can be seen that:

$$\phi_{OSC}(t) = G_0 \int_{-\alpha}^{t} V_5(\lambda)\, d\lambda \qquad \text{..... (9-15)}$$

For $\phi_{OSC}(t)$ to remain finite when $G_0 = \infty$, $V_5(t)$ must infinitesimally small.

Replacing $G_0 V_5(t)$ by $\phi_{OSC}(t)$ in equation (9-5) gives:

$$V_5(t) = \frac{1}{G_0}\frac{d\phi_{OSC}(t)}{dt} \qquad \text{..... (9-16)}$$

$$= \alpha\left(\frac{d\,\phi_s}{dt} + \frac{d\,\phi_n}{dt} - \frac{d\,\phi_{OSC}}{dt}\right)$$

For $G_0 = \infty$, $V_5(t) = 0$ and hence equation (9-16) becomes:

$$\frac{d\,\phi_{OSC}}{dt} \approx \frac{d\,\phi_s}{dt} + \frac{d\,\phi_n}{dt} \qquad \text{..... (9-17)}$$

Equation (9-17) shows that as the amount of feedback becomes very large, the VCO frequency approaches the sum of the input signal frequency and the frequency of the input noise. The difference frequency becomes a very narrow band FM signal.

Equation (9-17) can also be used to determine what happens at threshold under click conditions. If ϕ_n rotates by 2π, resulting in a click at the discriminator output then ϕ_{OSC} will rotate by 2π causing a click in the FMFB. Hence no threshold extension occurs when $G_0 = \infty$.

Now in [9, chap. 10] it is shown that:

$$N_{DISC} = N_C + \overline{\delta N} \qquad \text{..... (9-18)}$$

where: $\delta N =$ the increase in the number of spikes at the output of a conventional discriminator that occurs at threshold when the discriminator input frequency is changed by an amount δf.

$N_C =$ Total number of spikes at the output of a conventional discriminator that occurs at threshold for an unmodulated carrier.

$N_{DISC} =$ Total average number of spikes at the output of a conventional discriminator that occurs at threshold.

The average value of δN is given [9, chap. 10] by:

$$\overline{\delta N} = \frac{2\Delta f}{\pi} \exp -\left[\left(\frac{f_M}{B_C}\right)\left(\frac{S_i}{N_M}\right)\right] \qquad \text{..... (9-19)}$$

where $B_C =$ I.F. bandwidth

$\Delta f =$ frequency deviation of sinusoidally modulated carrier

and the number of spikes at the output of a conventional modulator that occurs at threshold for an unmodulated carrier is given by:

$$N_C = \frac{B_C}{2\sqrt{3}} erfc \sqrt{\left(\frac{f_M}{B_C}\right)\left(\frac{S_i}{N_M}\right)} \qquad \text{..... (9-20)}$$

Inserting both equations (9-19) and (9-20) into equation (9-18) gives:

$$N_{DISC} = \frac{B_C}{2\sqrt{3}} erfc \sqrt{\frac{f_M}{B_C}\frac{S_i}{N_M}} + \frac{2\Delta f}{\pi} \exp -\left[\left(\frac{f_M}{B_C}\right)\left(\frac{S_i}{N_M}\right)\right] \qquad \text{..... (9-21)}$$

Taub [9, chap. 10] shows that equation (9-21) can be used for the FMFB demodulator if B_C is replaced by B_{IF} and Δf is replaced by $\frac{\Delta f}{(1+\alpha G_0)}$, which gives:

$$N_{FMFB} = \frac{B_{IF}}{2\sqrt{3}} erfc \sqrt{\frac{f_M}{B_{IF}}\frac{S_i}{N_M}} + \frac{2\Delta f}{\pi(1+\alpha G_0)} \exp\left[-\left(\frac{f_M}{B_{IF}}\right)\left(\frac{S_i}{N_M}\right)\right] \qquad \text{..... (9-22)}$$

Assume that at the output of B_C or of B_{IF}, $\frac{S_i}{N_M}$ is the same [10]. If in the first major term $B_{IF} < B_C$, and if in the second major term $\frac{1}{(1+\alpha G_0)} > 1$, then comparing equation (9-22) with (9-21), it can be seen that N_{FMFB} is less than N_{DISC} and hence threshold extension is obtained.

9.4.2 Iwanami's FMFB Demodulator Approach

Iwanami, et al. [10], utilised quasi-linear approximation techniques for the threshold analysis and design of the FMFB demodulator. This approach was proposed because the existence of so many non-linear elements in the FMFB demodulator made it difficult to understand its operation and to obtain a practical design. The following is a brief summary of Iwanami's paper that mainly uses the original notation, showing the derivation of the quasi-linear model and the design procedure that is followed. To design an FMFB demodulator using their model, Iwanami, et al. utilised numerical computational techniques to obtain an optimised design.

For the following summary the block diagram of the FMFB demodulator given in figure (9/2) will be used. The expressions for V_1, V_2 and V_6 are conventional and are given below:

From figure 9/2 assume that the output V_1 of the RF filter is given by:

$$V_1(t) = A\cos[\omega_i t + \phi_i(t)] + N(t) \qquad \text{..... (9-23)}$$

and:

$$N(t) = x(t)\cos\omega_i t - y(t)\sin\omega_i t \qquad \text{..... (9-24)}$$

where: A = FM propagating wave amplitude

ω_i = Centre frequency of RF filter

$\phi_i(t)$ = Modulated signal phase

$N(t)$ = Band limited Gaussian noise with respect to rectangular RF filter

$x(t)$ = In-phase component of $N(t)$

$y(t)$ = Quadrature-phase component of $N(t)$

The output V_6 of the VCO shown in figure 9/2 is given by:

$$V_6(t) = B\cos[\omega_r t + \phi_r(t)] \qquad \text{..... (9-25)}$$

where: B = VCO output amplitude

ω_r = VCO free running frequency

ϕ_r = feedback phase

The mixer output frequency difference $V_2(t)$, in figure 9/2, can be shown to be:

$$V_2(t) = \frac{AB}{2}\cos\left[(\omega_i - \omega_r)t + (\phi_i(t) - \phi_r(t))\right] +$$
$$\frac{B}{2}\left[\left[x(t)\cos(\phi_r(t)) + y(t)\sin(\phi_r(t))\right]\cos(\omega_i t - \omega_r t) +\right.$$
$$\left.\left[x(t)\sin(\phi_r(t)) - y(t)\cos(\phi_r(t))\right]\sin(\omega_i t - \omega_r t)\right]$$

..... (9-26)

Let: $$C = \frac{AB}{2} \qquad \text{..... (9-27)}$$

$$\omega_o = \omega_i - \omega_r \qquad \text{..... (9-28)}$$

$$\phi_e(t) = \phi_i(t) - \phi_r(t) \qquad \text{..... (9-29)}$$

Substituting equations (9-27), (9-28) and (9-29) into equation (9-26) allows the mixer output frequency component to be written as:

$$V_2(t) = C\cos[\omega_o t + \phi_e(t)] + \frac{B}{2}[x(t)\cos\phi_r(t) + y(t)\sin\phi_r(t)]\cos\omega_o t - \frac{B}{2}[-x\sin\phi_r(t) + y\cos\phi_r(t)]\sin\omega_o t$$

..... (9-30)

Let $$X(t) = \frac{B}{2}(x\cos\phi_r + y\sin\phi_r) \qquad \text{..... (9-31)}$$

and $$Y(t) = \frac{B}{2}(-x\sin\phi_r + y\cos\phi_r) \qquad \text{..... (9-32)}$$

Substituting equations (9-31) and (9-32) into equation (9-30) allows the wanted mixer

output frequency component to be written as:

$$V_2(t) = C\cos\left[\omega_o t + \phi_e(t)\right] + X(t)\cos\omega_o t - Y(t)\sin\omega_o t \quad \ldots\ldots\ldots \quad (9\text{-}33)$$

Where ω_o is the centre frequency of the I.F. filter, and $\phi_e(t)$ is the phase error.

In equation (9-33), $V_2(t)$ is the input to the I.F. filter shown in figure 9/2. Because of stability considerations, the I.F. filter in a FMFB demodulator normally consists of a single tuned circuit. As the FMFB demodulator is a feedback system, a more complex I.F. filter will generally result in instability.

The distortion in the vicinity of the threshold is calculated from the single-tuned filter using the quasi-linear approximation given in figure 9/3, and whose derivation is given in reference [14]. A useful approximation treatment is also given in reference [17]. In this Iwanami treatment of the FMFB demodulator, the band-limited distortion in the I.F. filter with increased feedback noise will be considered as causing the feedback threshold.

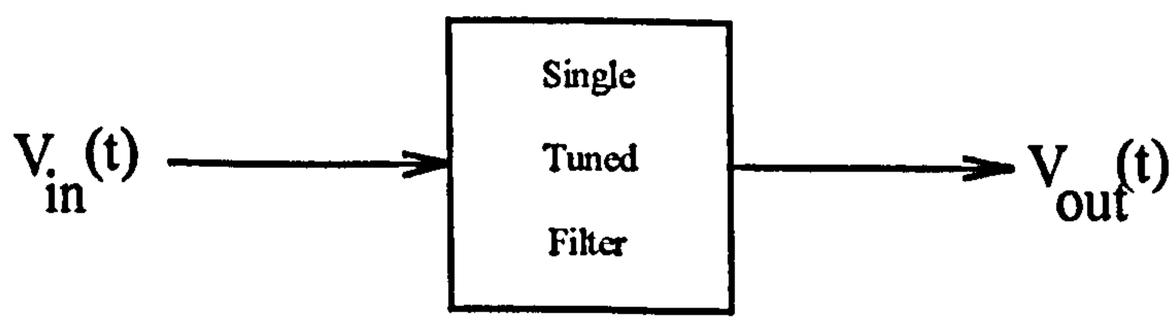

$$V_{in}(t) = A\cos(\omega_o t + \phi_{in}(t))$$

$$V_{out}(t) = A\exp\left(\frac{-\sigma^2}{2}\right)\cos(\omega_o t + \phi_{out}(t))$$

$$\phi_{out}(s) = \left(\frac{\alpha}{s+\alpha}\right)\phi_{in}(s)$$

$$\varepsilon(t) = \phi_{in}(t) - \phi_{out}(t) \qquad \text{where} \quad \sigma^2 = \langle \varepsilon^2 \rangle$$

Figure 9/3 - Approximation of single tuned filter

Allowing the expression for $V_{in}(t)$ in figure 9/3 to be equal to equation (9-33) and using the expressions for $V_{out}(t)$ given in figure 9/3, the expression for $V_3(t)$ can be obtained. Specifically, $\phi_e(t)$ of equation (9-33) in the region of threshold can be considered to have an approximate Gaussian distribution, so that the I.F. filter output, $V_3(t)$, can be approximated by:

$$V_3(t) = C\exp\left(-\frac{\sigma^2}{2}\right)\cos\left[\omega_o t + \dot{\phi}_e(t)\right] + \dot{X}(t)\cos\omega_o t - \dot{Y}(t)\sin\omega_o t \qquad \text{..... (9-34)}$$

Where:

$$\dot{\phi}_e(s) = \left[\frac{\alpha}{s+\alpha}\right]\phi_e(s) \qquad \text{..... (9-35a)}$$

$$\dot{X}(s) = \left[\frac{\alpha}{s+\alpha}\right]X(s) \qquad \text{..... (9-35b)}$$

$$\dot{Y}(s) = \left[\frac{\alpha}{s+\alpha}\right]Y(s) \qquad \text{..... (9-35c)}$$

Letting

$$\sigma^2 = \int_{-\infty}^{+\infty}\left|\frac{s}{s+\alpha}\right|_{s=j\omega}^2 |\phi_e(j\omega)|^2\, df \qquad \text{..... (9-35d)}$$

We can evaluate the amplitude distortion term $D = C\exp\left(-\frac{\sigma^2}{2}\right)$ ..... (9-35e)

Inserting equation (9-35e) into equation (9-34) gives:

$$V_3(t) = D\cos\left[\omega_o t + \dot{\phi}_e(t)\right] + \dot{X}(t)\cos\omega_o t - \dot{Y}(t)\sin\omega_o t \qquad \text{..... (9-36)}$$

$V_3(t)$ given in equation (9-36) above is the input to the limiter-discriminator in figure 9/2. From these relationships derived in equation (9-35) together with equation (9-36), Rice's click model of the limiter-discriminator operation in the non-linear threshold region can be derived.

The limiter-discriminator operation in the vicinity of the threshold region can be derived below using a quasi-linear approximation model of the limiter-discriminator (figure 9/4) together with Rice's click model. This model shows the demodulated signal $\ddot{\phi}_e(t)$ being summed with the output noise $N_a(t)$. In figure 9/4 a Gaussian process approximates the limiter-discriminator output noise $N_a(t)$. Its power spectral density $N_a(f)$ is given by the sum of the spike noise power spectral density $N_s(f)$, using Rice's click model in the given bandwidth, and the Gaussian noise spectral density $N_G(f)$. The output noise $N_a(t)$ is a function of an input dependent linear filter whose input is defined as $\frac{\dot{Y}(t)}{D}$.

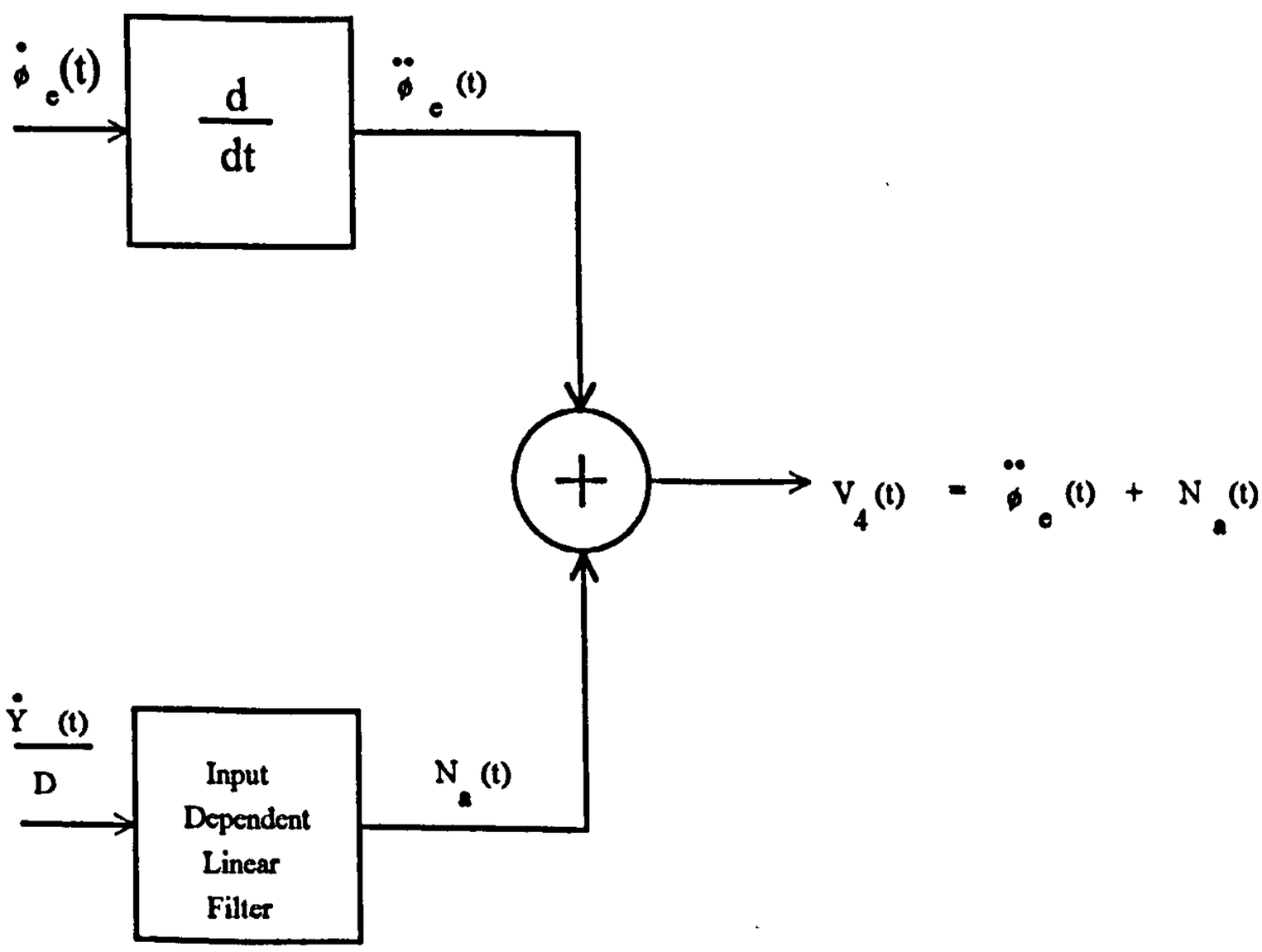

Figure 9/4 Quasi - Linear Approximation Limiter-Discriminator

The general expression for V_4 in figure 9/4, the output of the limiter-discriminator, can be written as:

$$V_4(t) = \ddot{\phi}_e(t) + N_a(t) \qquad \text{..... (9-37a)}$$

$$\therefore \qquad V_4(t) = \ddot{\phi}_e(t) + N_G(f) + N_S(f) \qquad \text{..... (9-37b)}$$

where • denotes the time derivative, and where:

$$N_a(t) = N_G(f) + N_S(f) \qquad \text{for} \quad |f| \le \frac{B_c}{2} \qquad \text{..... (9-38)}$$

$N_G(f)$ and $N_S(f)$ are derived below.

Iwanami determines the Gaussian noise power spectral density $N_G(f)$ as follows, let:

$$N_G(f) = \frac{\omega^2 \left| \dot{Y}(j\omega) \right|^2}{D^2} \qquad \text{for} \quad |f| \le \frac{B_c}{2} \qquad \text{..... (9-39a)}$$

Thus

$$N_G(f) = \left(\frac{\exp(\sigma^2)}{4 f_2 \rho} \right) \left(\frac{\alpha^2 \omega^2}{\alpha^2 + \omega^2} \right) \qquad \text{..... (9-39b)}$$

and where

$$\rho = \frac{\left(\frac{A^2}{2} \right)}{(2\eta 2 f_2)} \qquad \text{..... (9-39c)}$$

according to the triangle noise theorem [10], and where:

$\left| \dot{Y}(j\omega) \right|^2$ = double-sided power spectral density of $\dot{Y}(t)$

2η = double-sided power spectral density of $x(t)$ and $y(t)$

ρ = carrier-to-noise ratio for $2 f_2$ bandwidth

f_2 = maximum modulation frequency

Iwanami determines the click noise power spectral density $N_s(f)$, using Rice's click model, as follows, let: $N_s(f) = (2\pi)^2 2r\exp(-\gamma)\left[\frac{(1+2d\gamma)}{(4\pi\gamma)}\right]^{\frac{1}{2}}$ *for* $|f| \le \frac{B_c}{2}$ .....

(9-40a)

where $r = \frac{\alpha}{2\pi\sqrt{2\ln 2}}$ ..... (9-40b)

and $d = \frac{\left\langle \left(\ddot{\phi}_e\right)^2 \right\rangle}{(2\pi r)^2} = \frac{1}{(2\pi r)^2} \int_{-\infty}^{+\infty} \left[\left| \frac{\alpha s}{\alpha + s} \right|_{s=j\omega}^2 |\phi_e(j\omega)|^2 \right] df$

$\therefore \quad d = [2\ln 2]\sigma^2$ ..... (9-40c)

and $\gamma = \frac{\frac{c^2 \exp(-\sigma^2)}{2}}{2\left(\frac{B_C}{2}\right)^2 \eta \int_{\frac{-B_c}{2}}^{\frac{B_c}{2}} \left| \frac{\alpha}{s+\alpha} \right|_{s=j\omega}^2 df}$

hence $\gamma = \frac{f_2}{\exp(\sigma^2)} \frac{\rho}{\left[\frac{\alpha}{2\pi}\right] \arctan\left[\left(\frac{2\pi}{\alpha}\right)\left(\frac{B_c}{2}\right)\right]}$ ..... (9-40d)

where $r =$ radius of gyration of the single tuned filter (approximated by a Gaussian type filter with the same 3 dB bandwidth).

$\gamma =$ carrier-to-noise for the single tuned filter output

From equations (9-37) and (9-40), Iwanami obtained the desired FMFB demodulator model that is used for design and analysis. This is shown in figure 9/5.

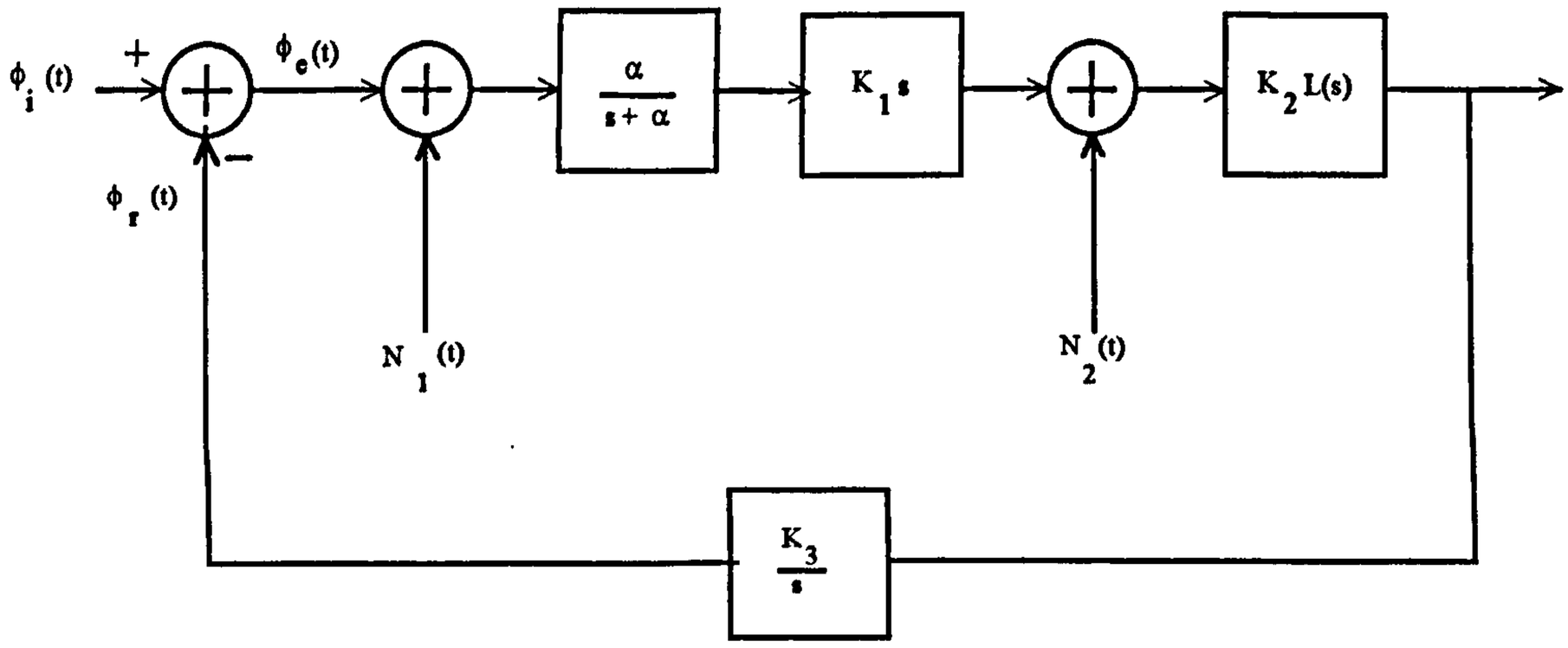

Figure 9/5 Quasi Linear Approximation FMFB Model

$N_1(t)$ and $N_2(t)$ in figure 9/5 are the Gaussian processes corresponding to the noise components of equations (9-39) and (9-40) and $N_1(f)$ and $N_2(f)$ are the respective double-sided power spectral densities, then:

$$N_1(f) = \left[\frac{\omega^2 + \alpha^2}{K_1^2\ \alpha^2\ \omega^2}\right]\ N_G(f) \qquad \text{..... (9-41a)}$$

$$N_2(f) = N_s(f) \qquad \text{..... (9-41b)}$$

Iwanami points out that in figure 9/5, as $\alpha \to 0$ the limit becomes Develet [13] FMFB model, and as $\sigma^2 \to 0$ and $\rho \rangle\rangle 1$ then the linear FMFB model can be recovered (see equation 9-46 below).

From figure 9/5 the output signal-to-noise ratio at threshold can be derived as follows:

$$\phi_e(s) = T(s)\,\phi_i(s) - H(s)\,N_1(s) - Q(s)\,N_2(s) \qquad \text{..... (9-42a)}$$

where $$T(s) = [1 - H(s)] \qquad \text{..... (9-42b)}$$

and $$Q(s) = \left[\frac{s+\alpha}{\alpha\, s}\right] H(s) \qquad \text{..... (9-42c)}$$

where $s = j\omega$, and $H(s)$ is the closed loop transfer function that is defined as:

$$H(s) = \frac{\phi_r(s)}{\phi_i(s)} \qquad \text{..... (9-42d)}$$

$$H(s) = \frac{(F-1)}{(F)} \frac{\left(\frac{\omega_n}{\alpha_0}\right)s + \omega_n^2}{s^2 + 2\zeta\omega_n s + \omega_n^2} \qquad \text{..... (9-42e)}$$

where

$$F = 1 + K$$

$$K = K_1 K_2 K_3$$

$$\alpha_0 = \frac{\alpha}{\sqrt{F}}$$

$$\omega_n = \omega_2 \sqrt{F}$$

$$\zeta = \frac{\left[2\,\eta + \frac{(F-1)}{\alpha}\right]}{2\sqrt{F}}$$

σ^2 , the variance of $\varepsilon(t)$ (figure 9/3), can be determined from equations (9-35) and (9-42) and is given by:

$$\sigma^2 = \int_{-\infty}^{\infty} \left| \frac{s}{s+\alpha} T(s) \right|_{s=j\omega}^2 |\phi_i(j\omega)|^2 \, df + \int_{-\infty}^{\infty} \left| \frac{s}{s+\alpha} H(s) \right|_{s=j\omega}^2 N_1(f) \, df + \int_{-\infty}^{\infty} \left| \frac{H(s)}{\alpha} \right|_{s=j\omega}^2 N_2(f) \, df \qquad \text{.....(9-43)}$$

Rearranging equation (9-43) allows it to be simplified as is shown in the version given in equation (9-44a) below:

$$\sigma^2 = U + \frac{\exp(\sigma^2)}{\rho} V + \nu W \qquad \text{..... (9-44a)}$$

where:

$$U = \int_{-\infty}^{\infty} \left| \frac{s}{s+\alpha} T(s) \right|_{s=j\omega}^{2} \left| \phi_i(j\omega) \right|^2 df \qquad \text{..... (9-44b)}$$

and

$$V = \frac{1}{4 f_2} \int_{\frac{-B_c}{2}}^{\frac{B_c}{2}} \left| \frac{s}{s+\alpha} H(s) \right|_{s=j\omega}^{2} df \qquad \text{..... (9-44c)}$$

and

$$W = \frac{1}{\alpha^2} \int_{\frac{-B_c}{2}}^{\frac{B_c}{2}} \left| H(j\omega) \right|^2 df \qquad \text{..... (9-44d)}$$

and

$$\nu = (2\pi)^2 \, 2r \exp(-\gamma) \left[\frac{(1+2d\gamma)}{4\pi\gamma} \right]^{\frac{1}{2}} \qquad \text{..... (9-44e)}$$

The expression given in equation (9-44a) represents the model shown in figure 9/5. The signal-to-noise ratio of this threshold extension frequency modulation feedback demodulator is given by:

$$\left(\frac{S_0}{N_0} \right) = \frac{2 \int_{f_1}^{f_2} \omega^2 \left| \phi_i(j\omega) \right|^2 df}{\frac{\exp(\sigma^2)}{4\pi f_2} 2 \int_{f_1}^{f_2} \omega^2 \, df + \nu \cdot 2 \int_{f_1}^{f_2} \frac{\omega^2 + \alpha^2}{\alpha^2} df} \qquad \text{..... (9-45)}$$

where $f_1 \sim f_2$ = baseband bandwidth, and υ is defined in equation (9-44e) above. Note that Iwanami's definition of threshold is the point where the output signal-to-noise ratio of the FMFB shown in figure 9/5 is 3 dB lower that the output signal-to-noise ratio of the linear FMFB model.

The baseband signal-to-noise ratio of the linear FMFB model can be obtained by letting $\nu \rightarrow 0$ and $\sigma^2 \rightarrow 0$ giving:

$$\left(\frac{S_0}{N_0} \right)_{Linear} = \frac{4\pi f_2 \int_{f_1}^{f_2} \omega^2 \left| \phi_i(j\omega) \right|^2 df}{\int_{f_1}^{f_2} \omega^2 \, df} \qquad \text{..... (9-46)}$$

Iwanami [14] derives a reference equation from equation (9-45) that is:

$$\exp(\sigma^2) + \frac{4 f_2 \sigma v \int_{f_1}^{f_2} \frac{\omega^2 + \alpha^2}{\alpha^2} d f}{\int_{f_1}^{f_2} \omega^2 \, d f} = 10^{0.1} \qquad \text{..... (9-47)}$$

The first term in this equation, $\exp(\sigma^2)$, represents the increase in noise due to I.F. filter band limited distortion. The second (quotient) term represents the increase in noise due to the non-linear operation of the limiter-discriminator. As $\sigma^2 \to 0$ the sole contribution to the threshold is due to the limiter-discriminator. When $\sigma^2 \to [0.1 \ln 10]$ the contribution is due to the IF filter alone and not to the limiter-discriminator. This equation (9-47) readily allows the contribution to be determined of the limiter-discriminator and the I.F. filter band limited distortion.

Iwanami's design methodology revolves around equations [9-44] and [9-47] that give the threshold characteristic of the FMFB demodulator shown in figure 9/5. The threshold can be obtained by solving these simultaneous equations. The design procedure that Iwanami proposes is briefly as follows:

(i) The initial step would consist of specifying a suitable loop filter *L(s)* such as that proposed by Enloe [12]. This then allows the closed loop transfer function $H(s)$ to be obtained from equation (9-42e). For a given σ^2, the variance of $\varepsilon(t)$, the noise bandwidth W in equation (9-44d) is minimised with respect to α. Equations (9-44) for *U*, *V* and *W* then become functions of α and ω_N.

(ii) The next step is to determine that value of ω_N that gives minimum ρ with respect to α.

(iii) The equation (9-44) that results from (b) is solved with equation (9-47) and the initial threshold value for the given variance of $\varepsilon(t)$ is obtained.

Iwanami [14] points out that the design parameters obtained with this CAD approach are almost the same as those obtained by experimentally optimising the Enloe filter. However his method does give a larger feedback factor and I.F. bandwidth compared to the earlier experimental approaches.

9.5 Discussion

In the above two approaches for the analysis of the FMFB are discussed. Firstly a simplified global FMFB analysis has been given and secondly a brief summary of the analysis proposed by Iwanami [14]. The simplified global analysis has shown how the noise characteristic is modified by the FMFB action. The summary of the Iwanami approach followed in this treatment of the FMFB demodulator gives a deeper insight into the operation of this circuit and of the close control it gives to the various parameters. It allows the relationships between the demodulation signal, feedback factor and I.F. bandwidth with respect to the threshold value to become clearer. However like all other threshold extension demodulators it can only be designed for a specific set of signal conditions and hence threshold level. Since the signal structure is dependent upon the picture content, the threshold point of the demodulator will vary, thus altering the performance of the demodulator. For the successful application of the FMFB demodulator to DBS reception, an adaptive design is required which optimises its parameters to the signal structure. This approach is discussed below in chapter 18, where an error controlled adaptive threshold extension demodulator is proposed and a version of which is based upon the FMFB demodulator.

9.6 References

[1] Chaffee, J. G., US Patent 2,075,503 (March 1937)

[2] Enloe, L. H. "Decreasing the threshold in FM by frequency feedback." Proc. IRE, No. 1, Vol. 50, (Jan. 1962), pp. 18-30.

[3] Cassara, F. A., Hess, D. T. " FM threshold performance of the frequency demodulator with feedback", IEEE Trans. Aerospace and Electron., AES-8, 5, pp. 596 - 601, 1972.

[4] Rogers Jr., W. D. "FM feedback demodulator having threshold extension circuit with two pole crystal filter." US Patent 4,087,756 (May 2, 1978).

[5] Jarger, H. F. "Frequency modulation threshold extension demodulator utilising frequency compression feedback with frequency drift correction." US Patent 4,293,818 (Oct. 6, 1981).

[6] Enloe. L. H. "The synthesis of frequency feedback demodulators." Proc. Nat. Elect. Conf., Vol. 18, (1962), pp. 477-497.

[7] Schilling, D. L., Billing, J. "A comparison of the threshold performance of the frequency demodulator using feedback and phase lock loop", Int. Space Electronics Symp. Record, p.3-E1, 1965.

[8] Kobayashi, et. al. "Optimised design of FM negative feedback", Journ. IEE, Japan, 49, .pp. 249 - 256, February 1966.

[9] Frutiger, P. "Noise in FM receivers with negative feedback", Proc. IEEE. 54,

No. 11, pp. 1506 - 1520, 1966.

[10] Taub, H., Schilling, D. "*Principles of Communication Systems*" McGraw-Hill, 1986, New York, ISBN 0-07-062955-2.

[11] Roberts, J. H. "Frequency - feedback receiver as a low threshold demodulator in FM/FDM satellite systems", Proc. IEE, 115, pp. 1607 -1618, 1968.

[12] Klapper, J., Frankle, J. T. "*Phase-Locked and Frequency-Feedback Systems*", Academic Press, (1972).

[13] Develet, A. J. "Statistical design and performance of high - sensitivity, frequency - feedback receivers", IEEE Military Electronics, MIL-7, 4, pp. 281 - 284, October 1963.

[14] Iwanami, Y., Nemoto, Y., Sato, R. "Threshold analysis and design of an FMFB demodulator through quasi-linear approximation", Electronics and Communications in Japan, Vol. 63-B, No. 12, (1980), pp. 38-47.

[15] Owen, J. C. "Full threshold FM demodulator". US Patent No. 5.034,695 (Jul. 23, 1991).

[16] Gerber, M. M. "A universal thresholding frequency modulated feedback demodulator." IEEE. Trans. Commun., COM-18, Vol. 4, (Aug. 1970), pp. 176-180.

[17] Hoffman, E., Schilling, D. L. " Distortion in the frequency demodulator using feedback." IEEE Trans. Comms. Vol. COM-20, 2, (April 1972), pp. 157-165.

[18] Nelin, B. "Baseband modelling and distortion equalization of the feedback FM

demodulator by functional methods." IEEE Trans. Aero. and Elect. Syst., Vol. AES-10, 1 (1974), pp. 149-152.

[19] Stojanovie, Z. D. "Nonlinear distortion analysis in the frequency demodulator using feedback." IEEE Trans. Comms., Vol. COM-23, No. 9, (Sept. 1975), pp. 884-891.

[20] Takashashi, et. al. "High frequency distortion of the frequency feedback type FM demodulator." IEEE Trans. Inform. Theory, Vol. IT-25, No. 4, (July 1979), pp. 452-462.

Blank Page

10. PHASE LOCKED LOOP (PLL) DEMODULATOR

10.1 Introduction

10.1.1 The phase lock loop (PLL) is a circuit that has found, and continues to find, many applications in the communication and allied fields. As well as threshold extension demodulation, these include acquisition, synchronisation and frequency synthesis. Both analogue and digital forms of the loop are used. In the analogue version a phase detector compares the phase of a received signal with that of a voltage controlled oscillator (VCO) and the circuit corrects, or attempts to correct, for the difference. By feeding back to the VCO a portion of the phase detector output that has been filtered by a suitable filter, the instantaneous frequency of the VCO can be made to follow frequency changes in the input signal. It is this feature that leads to threshold extension, the characteristics of the filter being the key to the performance and magnitude of the threshold extension. A typical analogue phase lock loop circuit is illustrated in figure 10/1.

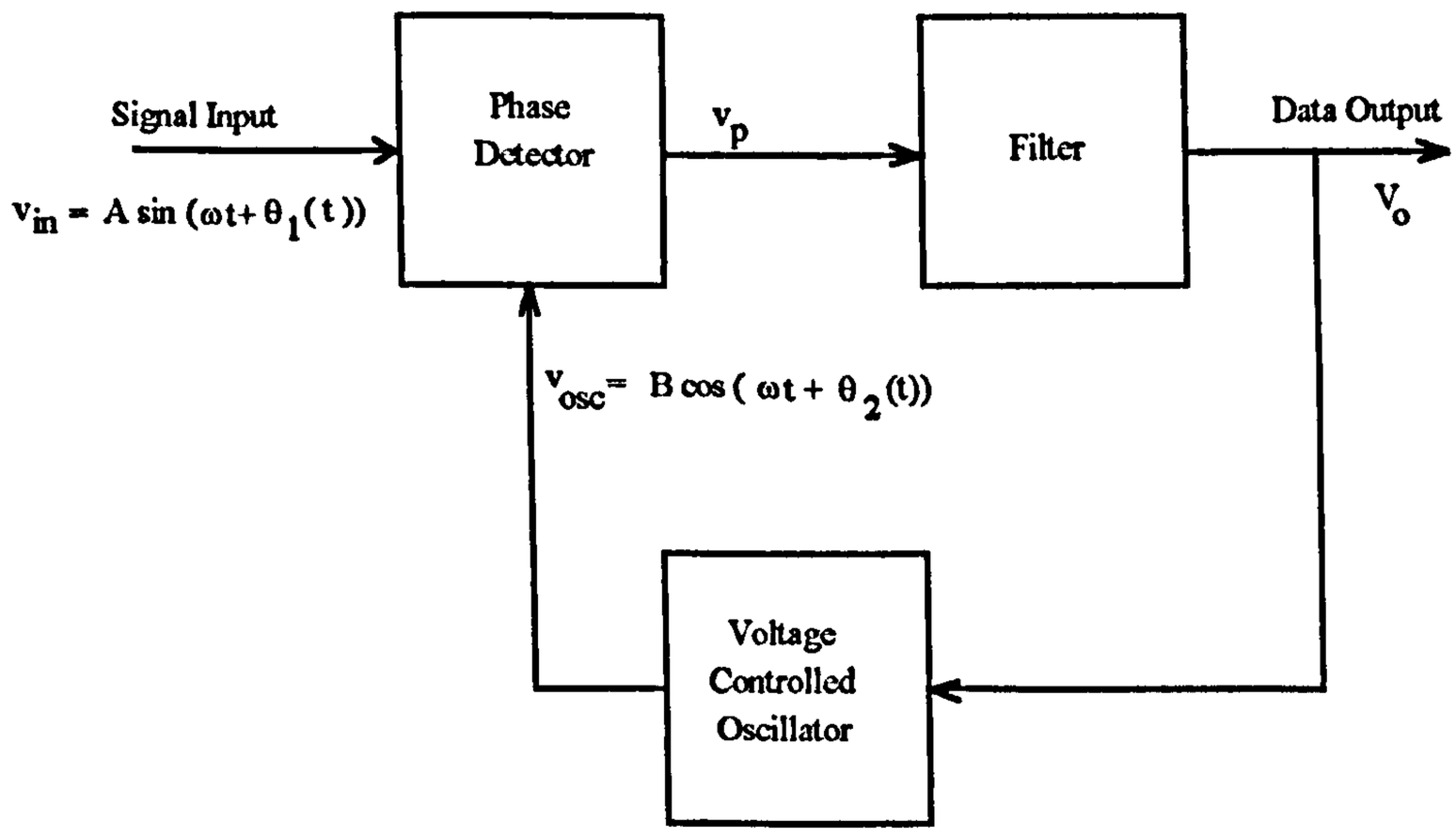

Figure 10/1 Phase Lock Loop Demodulator

10.1.2 In the digital version of the phase lock loop, the phase detector is replaced by a sampler, and the VCO by a digital clock running at the nominal carrier frequency of the input. The phase of the input is tracked by taking samples at or near the zero crossings of

the received carrier wave, and in both analogue and digital forms of the loop a locked condition is aimed for which means a pseudo coherent detection facility is obtained. The term pseudo is used because in practice, noise prevents a perfect phase match being achieved at all times and a phase error $\phi(t)$ is present.

This section will consider solely the analogue phase lock loop. This has been extensively studied in the literature, commencing with Jaffe and Rectin's notable paper [1]. Other useful analyses are given in references [2-4] and [6]. In passing it will be mentioned that the digital phase lock loop may offer some advantages [5], [10] in threshold extension demodulator applications. Also considered in this section are the characteristics of various order loop filters and the effects they may have on the threshold performance of the phase lock loop demodulator. This is done to show how the difficulties encountered may be overcome by the error controlled adaptive threshold extension demodulator solution proposed in chapter 18.

10.2 Circuit operation

10.2.1 The Phase Lock Loop (PLL) demodulator is a feedback circuit that may be used to extract a baseband signal from an FM carrier. From figure 10/1 it may be seen that the basic circuit functions consist of a phase detector (or comparator), a voltage controlled oscillator (VCO) and a filter that determines the overall performance of the PLL. The analytical treatment given in this section is quite conventional and follows that given in such references as [8], [12] and [23].

10.2.2 Phase detector

The function of the phase detector is to take two inputs of identical frequencies but with a phase (or timing) difference and produce an output that is dependent upon this phase or timing difference. From figure 10/1, if the input signals are assumed to sinusoidal, with amplitudes A and B, frequency ω, and with time varying phases $\theta_1(t)$ and $\theta_2(t)$,

then Signal input $v_{in} = A \sin(\omega t + \theta_1(t))$ ..... (10-1)

and VCO output $v_{osc} = B \cos(\omega t + \theta_2(t))$ ..... (10-2)

Assuming a multiplier-detector, the phase detector output v_p is therefore:

$$v_p = A \sin(\omega t + \theta_1(t))\, B \cos(\omega t + \theta_2(t)) \quad \text{..... (10-3)}$$

Expanding equation (10-3) gives:

$$v_p = AB\left[(\sin \omega t \cos\theta_1(t) + \cos \omega t \sin \theta_1(t))\right]\left[(\cos \omega t \cos\theta_2(t) - \sin \omega t \sin \theta_2(t))\right]$$

..... (10-4)

Rearranging the terms in equation (10-4) gives:

$$v_p = AB\left[\sin \omega t \cos \omega t\left[\cos \theta_1(t)\cos \theta_2(t) - \sin \theta_1(t)\sin \theta_2(t)\right] - \sin^2 \omega t \cos \theta_1(t)\sin \theta_2(t) + \cos^2 \omega t \sin \theta_1(t)\cos \theta_2(t)\right]$$

..... (10-5)

Simplifying the first term in equation (10-5) gives:

$$v_p = AB\left[\sin \omega t \cos \omega t\left[\cos\left(\theta_1(t) + \theta_2(t)\right)\right] - \sin^2 \omega t \cos \theta_1(t)\sin \theta_2(t) + \cos^2 \omega t \sin \theta_1(t)\cos \theta_2(t)\right]$$

..... (10-6)

Expanding the terms in equation (10-6) gives:

$$v_p = AB\left[\frac{1}{2}\sin 2\omega t\left[\cos\left(\theta_1(t) + \theta_2(t)\right)\right] - \frac{1}{2}(1 - \cos 2\omega t)\cos \theta_1(t)\sin \theta_2(t) + \frac{1}{2}(1 + \cos 2\omega t)\sin \theta_1(t)\cos \theta_2(t)\right]$$

..... (10-7)

Rearranging equation (10-7) gives:

$$v_p = \frac{AB}{2}\left[\sin 2\omega t\left[\cos\left(\theta_1(t)+\theta_2(t)\right)\right]+\left[\sin\theta_1(t)\cos\theta_2(t)-\cos\theta_1(t)\sin\theta_2(t)\right]+\left[\cos 2\omega t\left[\sin\theta_1(t)\cos\theta_2(t)+\cos\theta_1(t)\sin\theta_2(t)\right]\right]\right]$$

..... (10-8)

Expanding the second term and the third term in equation (10-8) gives:

$$v_p = \frac{AB}{2}\left[\sin\left(\theta_1(t)-\theta_2(t)\right)+\sin 2\omega t\left[\cos\left(\theta_1(t)+\theta_2(t)\right)\right]+\cos 2\omega t\left[\sin\left(\theta_1(t)+\theta_2(t)\right)\right]\right]$$

..... (10-9)

Then as can be seen from equation (10-9) the following phase difference term is contained in the output:

$$v_p = \frac{AB}{2}\sin\left[\theta_1(t)-\theta_2(t)\right] \qquad \text{..... (10-10)}$$

Letting the phase angle difference $\psi(t) = \theta_1(t)-\theta_2(t)$ ..... (10-11)

gives $v_p = \frac{AB}{2}\sin\psi(t)$ ..... (10-12)

The output given in equation (10-9) contains terms at twice the carrier frequency as well as the wanted phase difference, but the former can be rejected by means of the use of a suitable low pass filter, giving the latter in equation (10-12).

If the gain of the comparator is set at $2G_p$ the wanted output component in equation (10-12) can be written as:

$$v_p = ABG_p\sin\psi(t) \qquad \text{..... (10-12a)}$$

If the input sinusoids are made square waves with peak amplitudes A and B, by hard limiting before application to the multiplier, the comparator output instead of varying sinusoidally, varies with the phase difference ψ in a triangular fashion as shown in figure

10/2.

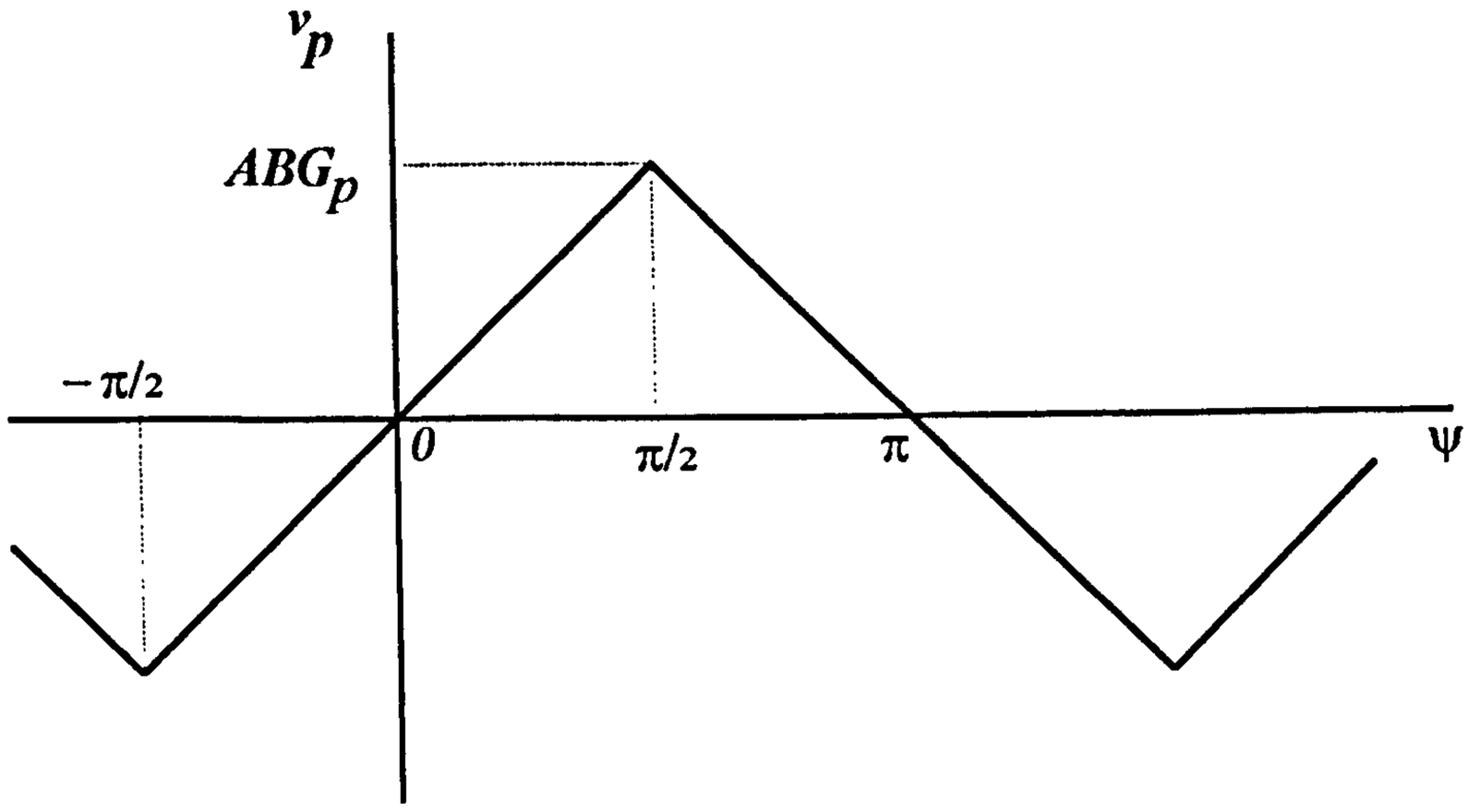

Figure 10/2 Phase characteristics of comparator with square wave inputs

The sinusoidal variation in output has been replaced by a piecewise-linear variation as follows:

For $|\psi| \leq \frac{\pi}{2}$ $\qquad v_p = A\,B\,G_p \frac{\psi}{\pi/2}$ ..... (10-12b)

For $\frac{\pi}{2} \leq \psi \leq \frac{3\,\pi}{2}$ $\qquad v_p = -\,A\,B\,G_p \frac{\psi - \pi}{\pi/2}$ ..... (10-12c)

and can be continued for increasing angles. These relationships form the piecewise-linear model for the comparator used in section 10.3.1 below.

10.2.3 Voltage controlled oscillator

The voltage controlled oscillator generates a periodic signal whose frequency is determined by a voltage applied to its input. Assume that there is no voltage input applied to the VCO. The latter then generates a sinusoidal output of amplitude B and at an angular frequency ω_c.

Assume: G_0 = Frequency sensitivity of VCO, a constant. (rad / (s) (volt))

ω_c = frequency with zero control voltage (volts)

$\omega_i(t)$ = Instantaneous angular frequency (Hz)

v = Frequency controlling voltage (volts)

v_{osc} = Voltage controlled oscillator output

G_0 , the frequency sensitivity, is the change in the instantaneous angular frequency produced by a change in the frequency controlling voltage v .

That is: $$G_0 = \frac{d\omega_i}{dv} \qquad \text{..... (10-13)}$$

Thus the voltage controlled output defining equation is:

$$v_{osc} = B\cos\left(\omega_c t + G_0 \int_{-\infty}^{t} v(\lambda)\, d\lambda \right) \qquad \text{..... (10-14)}$$

where the instantaneous angular frequency is:

$$\omega_i(t) = \omega_c + G_0\, v(t) \qquad \text{..... (10-15)}$$

10.3 First order phase lock loop demodulator

10.3.1 Figure 10/3 illustrates a first order phase lock loop system. This basically means that there is no filter in the loop. In this figure the parameters are defined as follows:

ω_c = Carrier frequency (Hz)

$m(t)$ = Modulating baseband signal

k = A constant

Let a frequency modulated input $A\sin\left(\omega_c t + \phi(t) \right)$ ..... (10-16a)

be applied to the input of the phase lock loop, where:

$$\phi(t) = k \int_{-\infty}^{t} m(\lambda)\, d\lambda. \qquad \text{..... (10-16b)}$$

Now assume a condition where $\phi(t) = 0$ and $v_0 = 0$. Then for this latter condition the VCO output differs in phase by 90^0 with respect to the input signal.

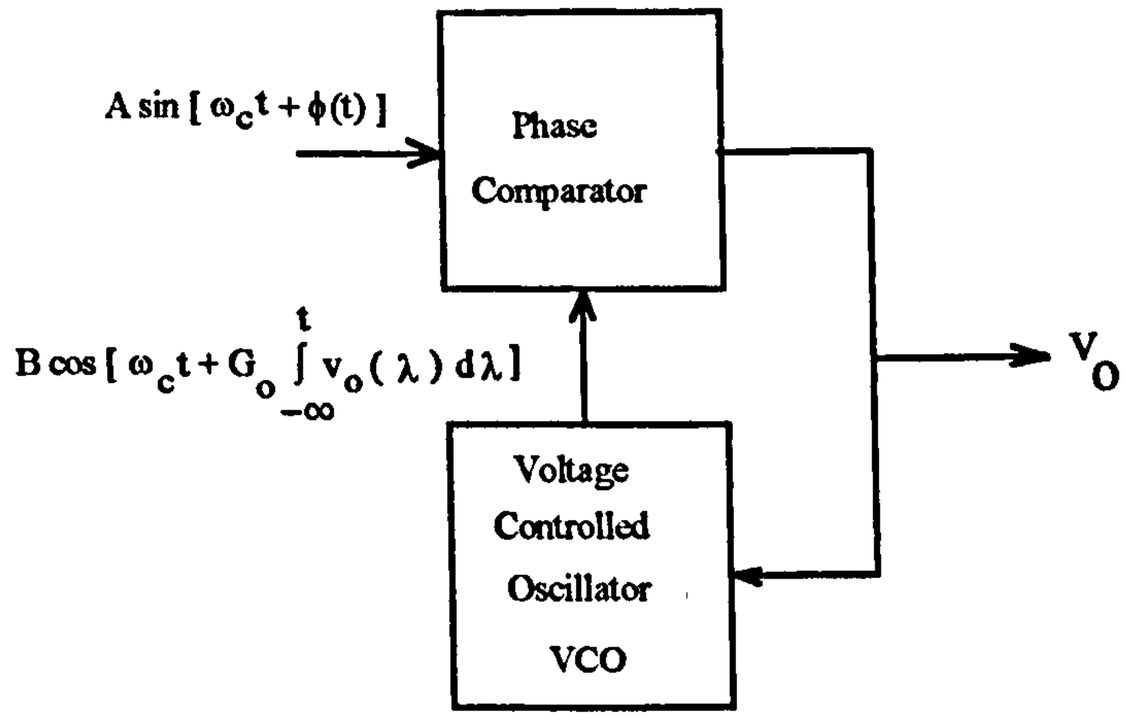

Figure 10/3 - First Order Phase Lock Loop

Now assume at time $t = 0$ the frequency of the input makes an abrupt change ω. Then at this instant, since $\frac{d\phi}{dt} = \omega$, then $\phi(t) = \omega$. The phase difference that will then exist at the input to the phase comparator will then produce an output v_0 that will change the frequency of the VCO until an equilibrium is established. Note that at this point although that the input frequency and the VCO frequency are equal, their phase difference is no longer 90^0 . The output voltage is thus proportional to the change in input frequency. The phase lock loop thus provides a demodulating action.

10.3.2 Analysing the first order phase lock loop circuit of figure 10/3, it can be seen that the phase angle difference $\psi(t)$ can be derived as follows. If the frequency modulated input is as given in equation (10-16) above, and the VCO output is as given in equation (10-14), then using equation (10-11):

Phase angle difference $$\psi(t)=\phi(t)-G_0\int_{-\infty}^{t}v_0(\lambda)d(\lambda)$$ ..... (10-17)

Differentiating and rearranging gives: $$\frac{d\psi}{dt}+G_0 v_0=\frac{d\phi}{dt}$$ ..... (10-18)

Using a piecewise-linear variation model for the phase comparator [23] developed in section 10.2.2 above, allows v_0 to be replaced by equation (10-12b), viz:

$$\frac{d\psi}{dt}+\frac{\psi}{\tau}=\frac{d\phi}{dt} \quad for \quad |\psi|\le\frac{\pi}{2}$$ ..... (10-19)

where $$\tau=\frac{\pi}{2\,A\,B\,G_p\,G_0}$$ ..... (10-20)

where:

A = Peak magnitude of the signal applied to signal input (figure 10/3)

B = Peak magnitude of the VCO output signal (figure 10/3)

G_p = A comparator constant

G_0 = Frequency sensitivity of the VCO [rad/(s)(volt)]

Using the piecewise-linear model for the comparator, equation (10-19) can be written as:

$$\frac{dv_0}{dt}+\frac{v_0}{\tau}=\frac{1}{G_0\,\tau}\frac{d\phi}{dt} \quad \text{for} \quad |\psi|\le\frac{\pi}{2}$$ ..... (10-21)

This equation gives the relationship between the frequency offset and the output voltage.

Note that equation (10-20) contains within it the amplitude A of the input signal. This relationship is of particular importance when discussing the effects of limiting, which is not used when the PLL is operating in the threshold region. As the input signal amplitude reduces, equation (10-20) shows that the time constant τ increases and its bandwidth decreases. It is this equation that is the basis of Mitra and Horvat's threshold extension patents discussed above. It is also why the use of a limiter in the threshold region results in an inferior performance.

10.4 Second order phase lock loop demodulator

10.4.1 Figure 10/4 illustrates a second order phase lock loop demodulator. For the purpose of this analysis the phases of the waveforms will be used.

$\phi(t)$ = signal input whose Laplace transform is $\Phi(s)$

G_p = Phase comparator constant of proportionality

$\psi(t)$ = Phase angle difference of phase comparator inputs whose Laplace transform is $\Psi(s)$

The VCO provides a carrier having a phase proportional to the integral of its input voltage $v_0(t)$. The VCO thus has a transform $\frac{G_0}{s}$.

With $H(s)=1$, figures 10/3 and 10/4 become identical, thus the loop transfer function may be written as:

$$\Psi(s) = \Phi(s) - \frac{G_p G_0 \Psi(s)}{s} \qquad \text{..... (10-22a)}$$

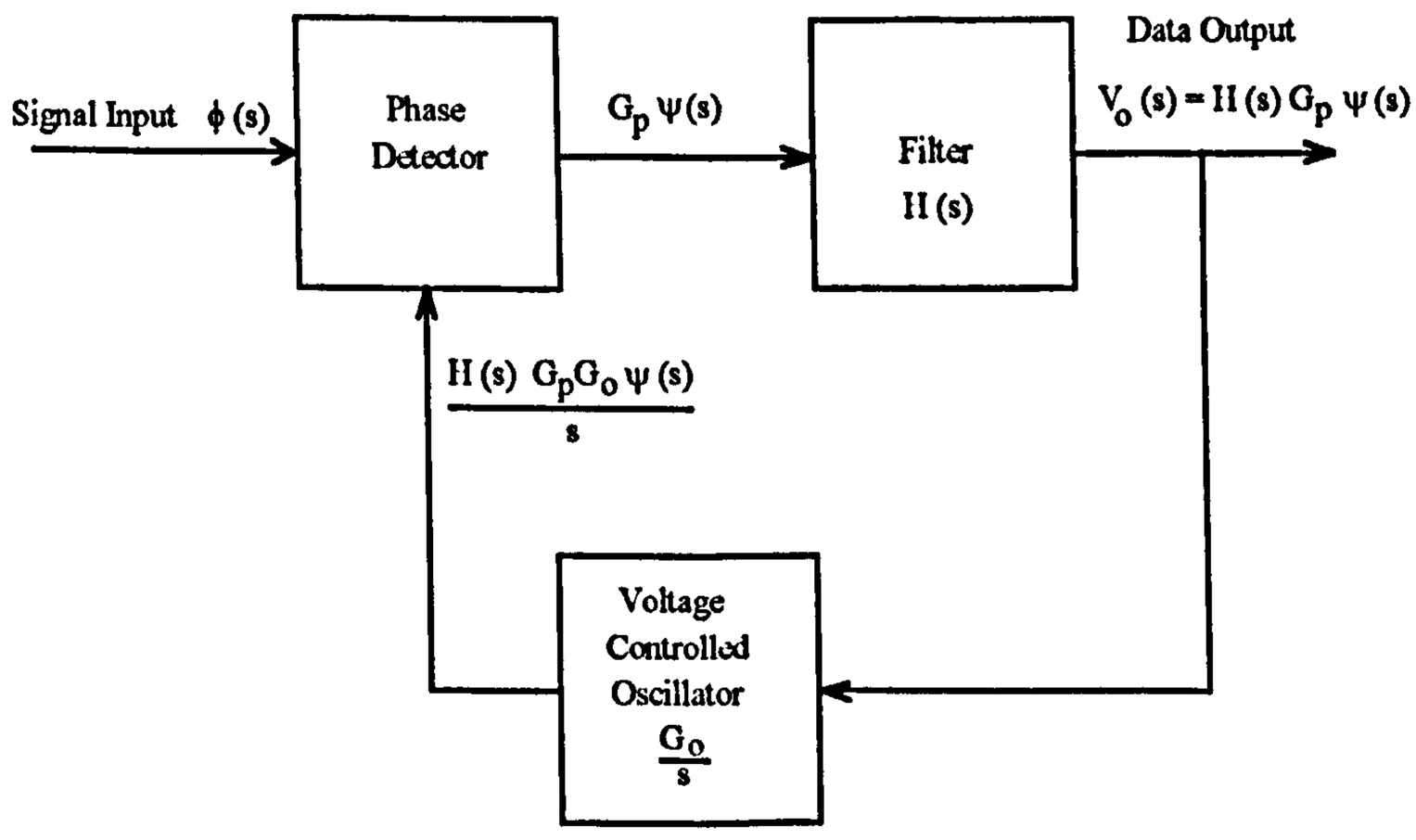

Figure 10/4 Second Order Phase Lock Loop Demodulator

Let $$\Omega(s) = s\Phi(s) = L\left(\frac{d\phi(t)}{dt}\right) \qquad \text{..... (10-22b)}$$

and $$\frac{1}{\tau} = G_0 G_p \qquad \text{..... (10-22c)}$$

where L is the Laplace transform. Inserting in equation (10-22a) gives:

$$\Psi(s) = \frac{s\Phi(s)}{s + G_0 G_p}$$

$$\therefore \quad \Psi(s) = \frac{\Omega(s)}{s + G_0 G_p}$$

$$\therefore \quad \Psi(s) = \frac{\Omega(s)}{s + \frac{1}{\tau}} \qquad |\psi(t)| \leq \frac{\pi}{2} \qquad \text{..... (10-23)}$$

From which the transfer function of the first order phase lock loop, and the second order phase lock loop when $H(s) = 1$, can be obtained, viz:

$$\frac{\Psi(s)}{\Omega(s)} = \frac{1}{s + \frac{1}{\tau}} \qquad \text{..... (10-24)}$$

Now let the loop filter be a proportional-plus-integral filter with a transfer function:

$$H(s) = 1 + \frac{K}{s} \qquad \text{..... (10-25)}$$

where K is a constant.

For this loop filter, the transform of the phase angle difference $\psi(t)$ can be derived from figure 10/5 and is:

$$\Psi(s) = \Phi(s) - \frac{G_p G_0 \Psi(s)}{s} - \frac{K G_p G_0 \Psi(s)}{s^2}$$

thus:
$$\Phi(s) = \Psi(s)\left(\frac{s^2 + sG_pG_0 + KG_pG_0}{s^2}\right)$$

giving:
$$\Psi(s) = \frac{s^2\,\Phi(s)}{s^2 + G_pG_0 + KG_pG_0}$$

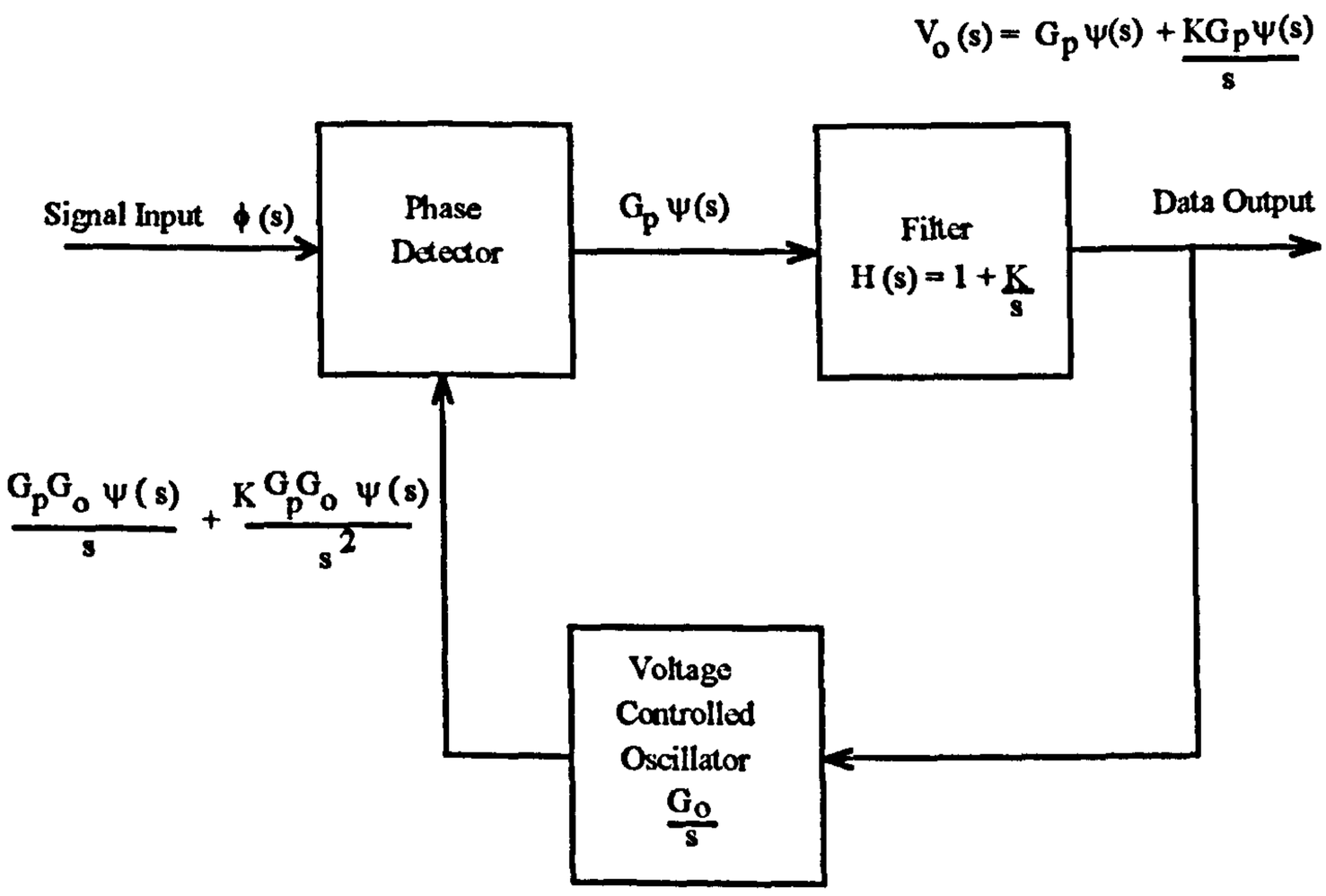

Figure 10/5 Second Order Phase Lock Loop Demodulator with Proportional-Plus-Integral Filter

but $G_pG_0 = \frac{1}{\tau}$, thus:

$$\Psi(s) = \frac{s^2\,\Phi(s)}{s^2 + \frac{s}{\tau} + \frac{K}{\tau}} \qquad \text{..... (10-26a)}$$

but $\Omega(s) = s\Phi(s)$, thus:

$$\Psi(s) = \frac{s\Omega(s)}{s^2 + \frac{s}{\tau} + \frac{K}{\tau}} \qquad |\psi(t)| \leq \frac{\pi}{2} \qquad \text{..... (10-26b)}$$

The output voltage $v_0(t)$ has, from figure 10/5, the transform:

$$v_0(s) = G_p \Psi(s) + \frac{K G_p \Psi(s)}{s}$$

from which

$$v_0(t) = \Psi(s)\left[G_p\left(1+\frac{K}{s}\right)\right]$$

inserting equation (10-26b) gives:

$$v_0(t) = \left(\frac{s^2 \Phi(s)}{s^2 + \frac{s}{\tau} + \frac{K}{\tau}}\right)\left[G_p\left(1+\frac{K}{s}\right)\right]$$

from which

$$v_0(t) = \frac{s\,\Phi(s) G_p (s+K)}{\left(s^2 + \frac{s}{\tau} + \frac{K}{\tau}\right)} \qquad \text{..... (10-27a)}$$

or alternately as $\Omega(s) \equiv s\Phi(s)$, then:

$$v_0(t) = \frac{\Omega(s) G_p (s+K)}{\left(s^2 + \frac{s}{\tau} + \frac{K}{\tau}\right)} \qquad \text{..... (10-27b)}$$

10.4.2 To calculate the output signal-to-noise ratio of the second order phase lock loop, assume the input signal to the FM demodulator is:

$$v_i(t) = R(t)\cos\left(\omega_c t + \phi(t)\right)$$

where $R(t)$= Envelope of waveform consisting of the superposition of a carrier of amplitude A and the noise $n(t)$.

and $\phi(t) = \phi_s(t) + \phi_n(t)$, where $\phi_s(t)$ is the angular modulation due to the

signal, and $\phi_n(t)$ is the angular modulation due to the noise.

Assume that $R(t) = A$, that is only the carrier amplitude is affecting the envelope, not the noise. From equation (10-21) and neglecting the effect of the time constant τ, that would be chosen to have little effect on the highest modulation frequency, then above threshold the following relationship applies:

$$v_0(t) = \frac{d\,\phi(t)}{dt} \qquad \text{..... (10-28)}$$

To calculate the signal to noise ratio, the output noise power due to the spikes, N_S, present at the phase lock loop output has to be determined (the input conditions for which are when a noise vector is added to a carrier vector; the locus of the end point of the resultant vector gives rise to a spike or click, see chapter 4). This spike output noise power can be derived from equation (6-42) in section 6, viz.

$$N_s = \frac{4\,\pi^2\,\alpha^2}{T_s} 2\,f_m$$

which can be rewritten as:

$$N_s = \frac{8\,\pi^2\,\alpha^2 f_m}{T_s}$$

Now let $\alpha = \frac{1}{G_0}$ and $\frac{1}{T_s}$ is replaced by $N = N_c + \delta N$, then:

$$N_s = \frac{8\,\pi^2 f_m N}{G_0^2} \qquad \text{..... (10-29)}$$

From equations (6-18) and (6-32) in section 6, and letting $\alpha = \frac{1}{G_0}$ and using (10-29) above, gives:

$$\frac{S_0}{N_0} = \frac{\overline{k^2 m^2(t)}}{\left(\frac{8\pi^2}{3}\right)\eta\frac{f_M^3}{A^2} + 8\pi^2 f_M N} \qquad \text{..... (10-30a)}$$

Computer simulations showing the effects of N are given in [27].

Equation (10-30) may be simplified as follows. Assume sinusoidal modulation of the form $k\,m(t) = \Delta\omega \cos\omega_m t$, or alternatively $k\,m(t) = 2\pi\Delta f \cos(2\pi f_M t)$, from (see equation 6-35 in chapter 6) which:

$$\overline{k^2 m^2(t)} = 2\pi^2 (\Delta f)^2 \qquad \text{..... (10-30b)}$$

Let $\beta = \frac{\Delta f}{f_M}$ (modulation index) ..... (10-30c)

$S_i = \frac{A^2}{2}$ (input signal power) ..... (10-30d)

$N_M = \eta f_M$ (input noise power in baseband bandwidth f_M)

..... (10-30e)

Then:
$$\frac{S_0}{N_0} = \frac{2\pi^2 (\Delta f)^2}{\left(\frac{8\pi^2}{3}\right)\eta\frac{f_M^3}{A^2} + 8\pi^2 f_M N} \qquad \text{..... (10-30f)}$$

Rearranging:
$$\frac{S_0}{N_0} = \frac{\frac{3}{2}\left(\frac{\Delta f}{f_M}\right)^2 \frac{A^2}{2}}{\eta f_M + 6\frac{N}{f_M}\frac{A^2}{2}} \qquad \text{..... (10-30g)}$$

Simplifying further:
$$\frac{S_0}{N_0} = \frac{\frac{3}{2}\left(\frac{\Delta f}{f_M}\right)^2 \frac{A^2}{2}\frac{1}{\eta f_M}}{1 + 6\frac{N}{f_M}\frac{A^2}{2}\frac{1}{\eta f_M}} \qquad \text{..... (10-30h)}$$

Substituting equations (10-30c), (10-30d) and (10-30e) into equation (10-30h) gives:

$$\frac{S_0}{N_0} = \frac{\frac{3}{2}\beta^2 \frac{S_i}{N_m}}{1+6\left(\frac{N}{f_M}\right)\left(\frac{S_i}{N_m}\right)} \qquad \text{..... (10-31)}$$

10.5 Third order phase lock loop demodulator

10.5.1 Attempts have been made in the past to improve the threshold extension performance by increasing the order of the filter to create a third order phase lock loop. Although such applications provide a more desirable open loop gain versus modulation frequency characteristics, little improvement is obtained in the loop signal-to-noise capabilities. Such third order loop approaches are more complex, require more components and are more difficult to stabilise than a second order loop.

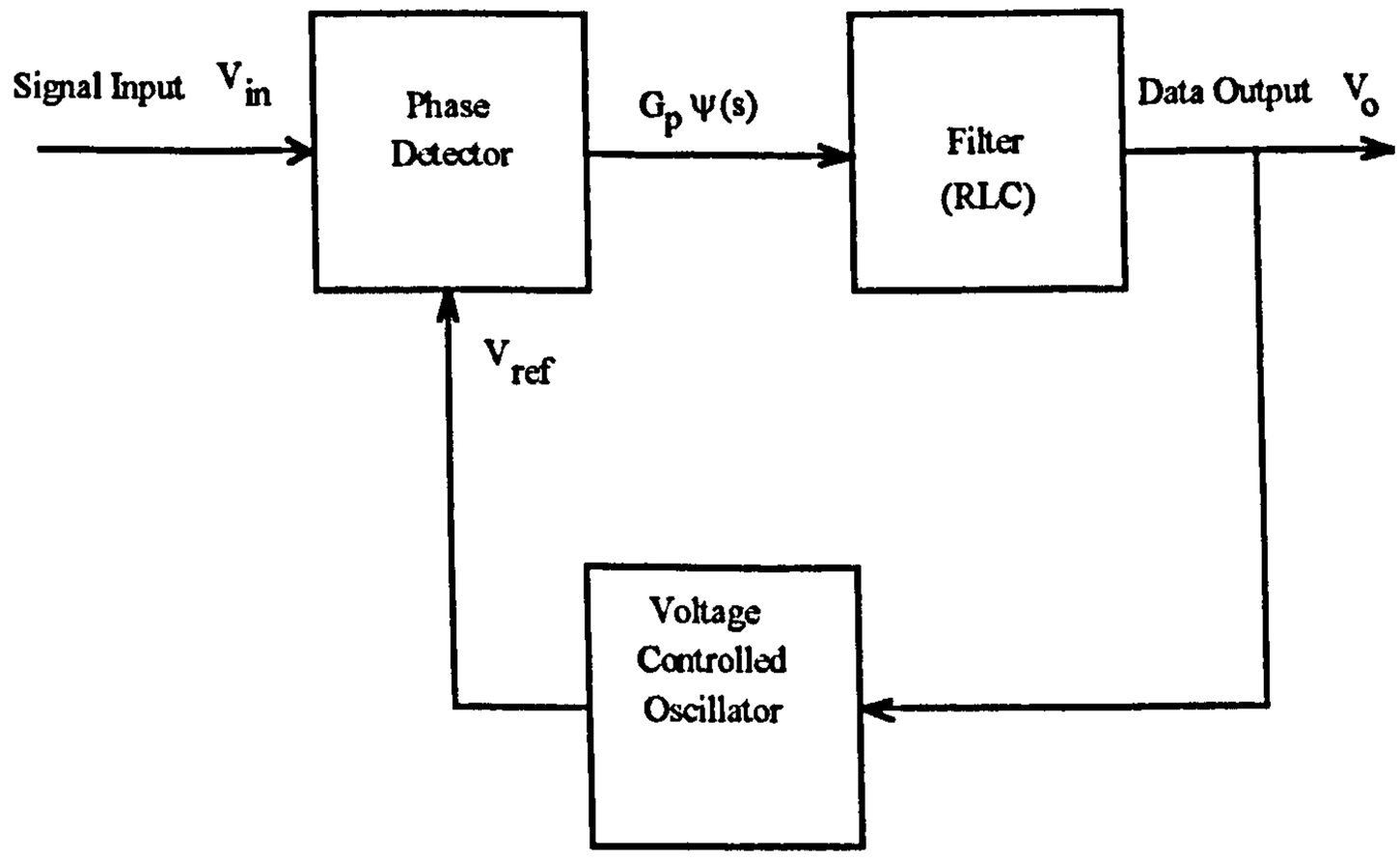

Figure 10/6 Third Order Phase Lock Loop Demodulator

A possible exception to these limitations of the third order phase lock loop is the approach proposed by Haggai [7]. In this interesting patent, a performance improvement of some 1.5 dB is claimed over the traditional third order phase lock loop demodulator, which in turn offers a 2 to 3 dB improvement over the conventional demodulator approach. Little interest appears to have been shown in this approach for DBS applications and further study may be

merited to establish if the gains in performance offered can be obtained. The scheme proposed by Haggai is illustrated in figure 10/6. The conventional third order phase lock loop demodulator has a pair of poles at the origin of the complex frequency (s) plane. Haggai's approach uses a more complex filter that has two poles and two zeros in the complex frequency plane. The latter are selected on the basis that the magnitude of the zero resonant frequency (i.e. the distance of the zero from the origin) is greater than the magnitude of the pole resonant frequency (i.e. distance of the pole from the origin). In addition the zero and pole damping ratios are selected such that they are less than unity. The damping ratios are equal to the magnitude of the sine of the angle between the jω axis and a vector drawn from the origin to the pole or zero. The analytical model of the scheme is shown in figure 10/7.

The RLC loop filter of figure 10/8 is designed to have a complex frequency transfer function of:

$$H(s) = K_f \frac{1 + 2\xi_z \frac{s}{\omega_z} + \frac{s^2}{\omega_z^2}}{1 + 2\xi_p \frac{s}{\omega_p} + \frac{s}{\omega_p^2}} \qquad \text{.....(10-32)}$$

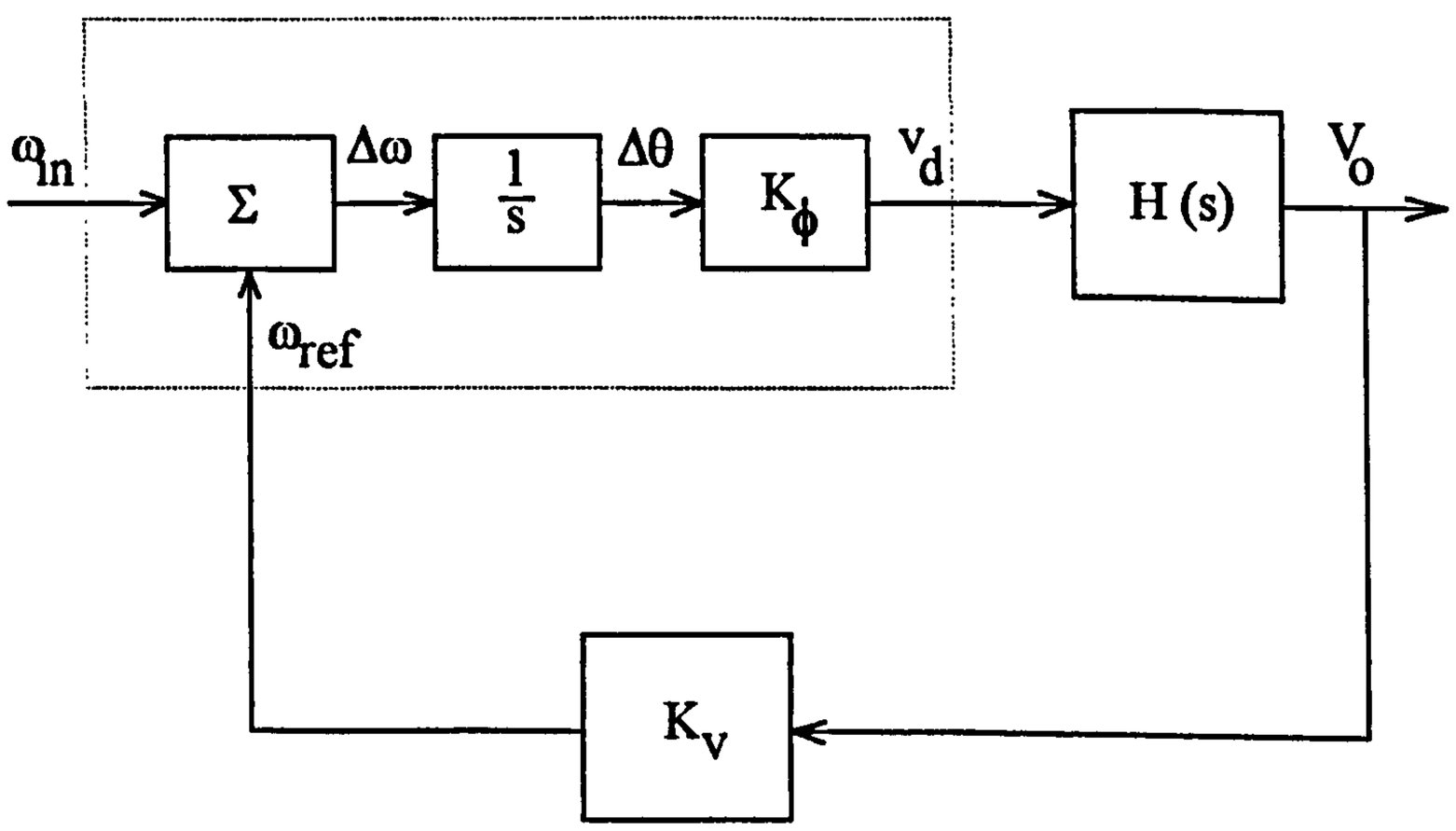

Figure 10/7 Third Order Phase Lock Loop Demodulator

The relationship [7] between the zero and the pole resonant frequencies ω_z and ω_p respectively and the damping ratios ξ_z and ξ_p of the transfer function $H(s)$ are as follows:

$$\omega_z = \frac{1}{\sqrt{LC}} \qquad \text{..... (10-33)}$$

$$\omega_p = \frac{\omega_z}{\sqrt{1+\alpha}} \qquad \text{.....(10-34)}$$

$$\xi_z = \frac{1}{2R}\sqrt{\frac{L}{C}} \qquad \text{..... (10-35)}$$

$$\xi_p = \frac{\xi_z}{\sqrt{1+\alpha}} \qquad \text{.....(10-36)}$$

K_f is the scale factor and for the passive filter shown would be unity.

The open loop gain of the demodulator is given by:

$$G_{OL}(s) = \frac{K_\phi K_r H(s)}{s} \qquad \text{..... (10-37)}$$

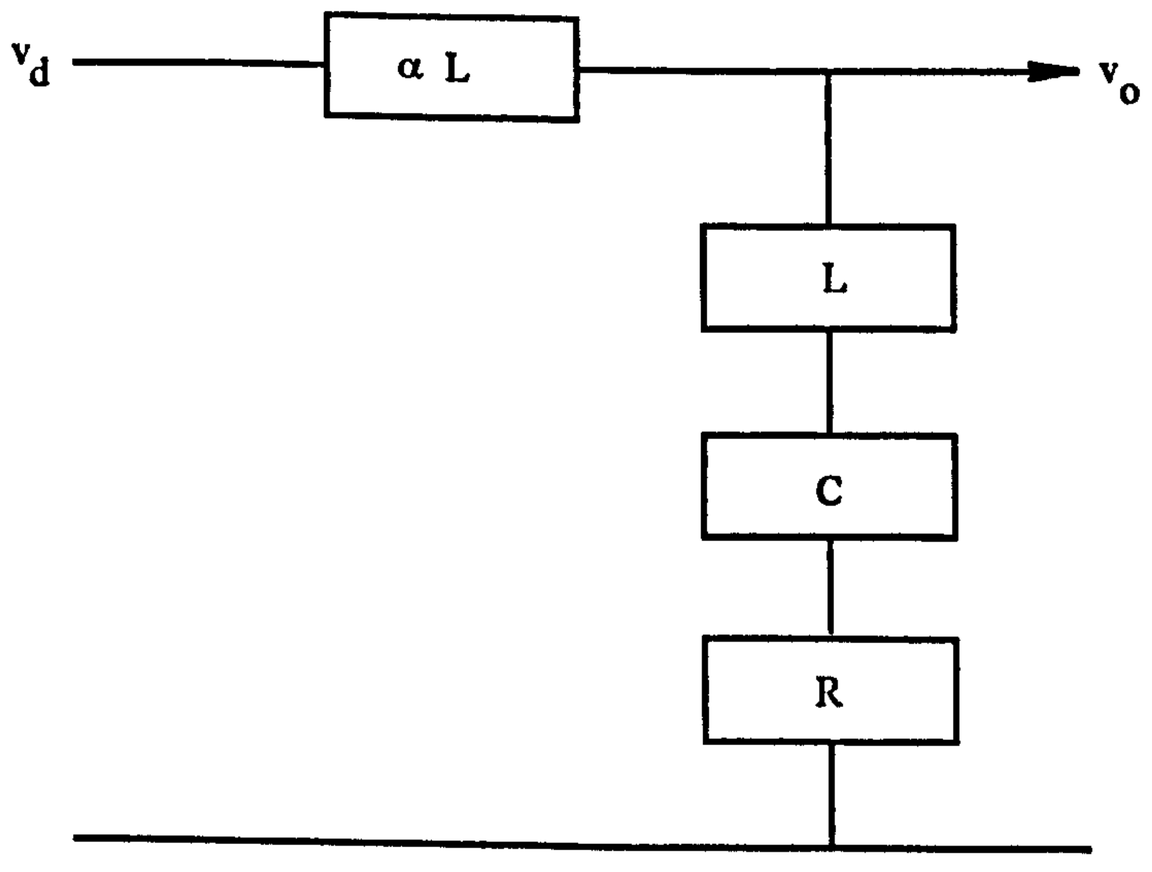

Figure 10/8 Third Order Phase Lock Loop Filter

Substituting equation (10-32) into (10-37) gives:

$$G_{OL}(s) = \frac{1+2\xi_z\frac{s}{\omega_z}+\frac{s^2}{\omega_z^2}}{\frac{s}{K}\left[1+2\xi_p\frac{s}{\omega_p}+\frac{s^2}{\omega_p^2}\right]} \qquad \text{..... (10-38)}$$

Where K is a loop scale factor given by

$$K = K_\phi K_r K_f \qquad \text{..... (10-39)}$$

The closed loop gain for the demodulator is given by:

$$G_{CL} = \frac{G_{OL}}{1+G_{OL}} \qquad \text{..... (10-40)}$$

Substituting equation (10-38) into (10-40) gives:

$$G_{CL}(s) = \frac{1+2\xi_z \frac{s}{\omega_z}+\frac{s^2}{\omega_z^2}}{1+\frac{s}{\omega_z}\left(2\xi_z+\frac{\omega_z}{K}\right)+\frac{s^2}{\omega_z^2}\left(\frac{2\xi\omega_z^2}{K\omega_p}+1\right)+\frac{s^3}{\omega_p^2 K}} \qquad \text{..... (10-41)}$$

10.5.2 The design procedure that would be followed in using this third order phase lock loop demodulator has been given by Haggai [7] and would be as follows. Normally the maximum modulation frequency f_b and the r.m.s. modulation index M of the signal that is required to be demodulated would be specified. In addition the maximum allowable noise power ratio (NPR) would also be specified. For the design of the loop filter the pole resonant frequency $f_p = \frac{\omega_p}{2\pi}$ is first selected by making it equal to the maximum modulation frequency f_b . This maximises the open loop gain G_{OL} throughout the baseband. Values for the filter attenuation constant α and the zero damping ratio ξ_z are selected as follows. The maximum phase modulation error θ_m is calculated from the specified maximum allowable noise power ratio:

$$NPR \cong 3 + 40\log\frac{1}{\theta_m} \quad dB \qquad \text{..... (10-42)}$$

The ratio of the r.m.s. modulation index M to the maximum allowable phase modulation error θ_m is calculated. A graph giving the plot of this ratio against filter attenuation

constant α for various values of the zero damping ratio ξ_z may be found in figure 6 of Haggai's patent, [7]. The values of α and ξ_z which minimise the noise bandwidth can also be selected from figure 7 of the same patent. This figure gives a plot of the ratio of one sided noise bandwidth to maximum modulating frequency as a function of the filter attenuation constant for various values of zero damping ratio. Once α and ξ_z have been determined then the zero resonant frequency ω_z may be determined from equation (10-34) above and the pole damping ratio ξ_p from equation (10-36).

10.5.3 A third order phase lock loop filter patent subsequent to that of Haggai was due to Crow and Tausworthe [24]. This approach is only mentioned here for completeness. This scheme was intended for receiving satellite signals that were subject to high Doppler rate changes in frequency. To achieve this the phase lock loop demodulator used a filter with an open loop transfer function as given in equation (10-43) and for a given set of loop constants setting the damping factor equal to unity.

$$H(s) = \frac{(1+\tau_2 s)}{(1+\tau_1 s)} + \frac{1}{(1+\tau_1 s)(\delta+\tau_3 s)} \qquad \text{..... (10-43)}$$

The scheme is shown in figure 10/9.

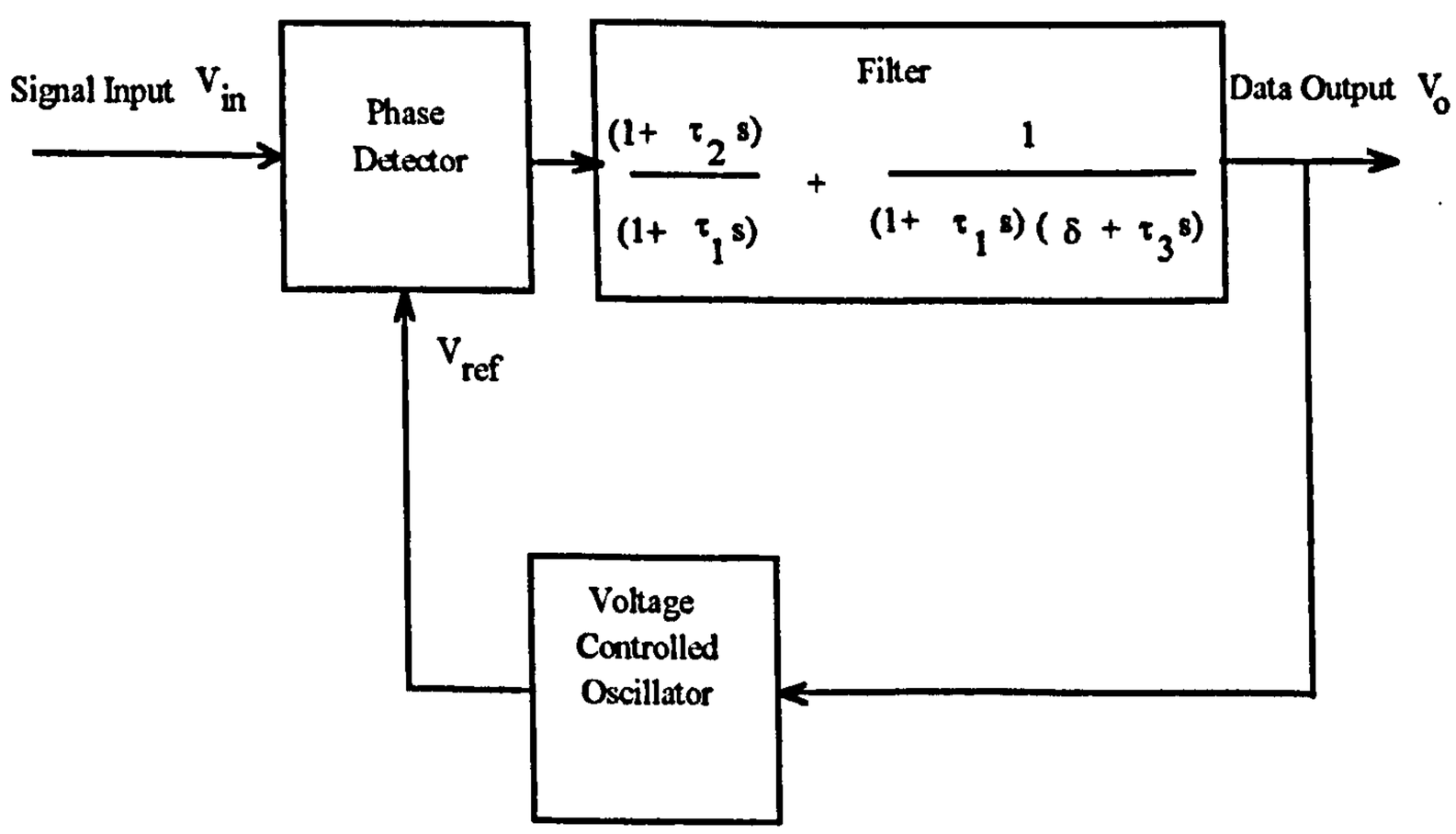

Figure 10/9 Third Order Phase Lock Loop Demodulator (Crow and Tausworthe)

10.6 Phase lock loop demodulator approaches

10.6.1 The phase lock loop demodulator is one of the most popular approaches for achieving threshold extension in DBS TV systems and has been extensively studied, [13-15] and [17]. Various schemes have appeared in the literature but none appear to have completely solved the various problems associated with satellite reception. This section will briefly describe those schemes that have been proposed, together with some others that are relevant, and which appear to offer some advantages.

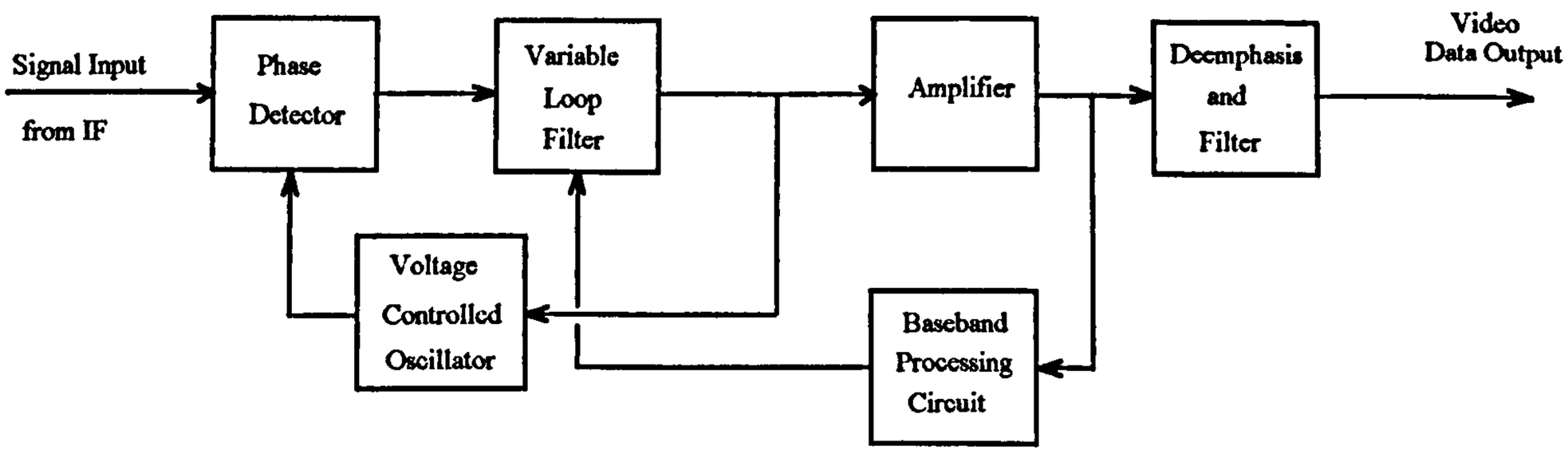

Figure 10/10 Yoshisato Threshold Extension Demodulator

Yoshisato in his first patent [16] shown in figure 10/10, proposed a phase lock loop FM demodulator with a variable bandwidth loop filter. The control for the latter is obtained by processing the demodulator output. The measure of noise is obtained by sampling it above the baseband bandwidth in the baseband processing circuit. With this design it is claimed that a demodulator is obtained with good tracking characteristics and which suppresses the noise in poor carrier-to-noise conditions. No performance figures are given and there is no mention of the threshold effect. The effect of click energy within the video baseband is not addressed. This circuit attempts to solve the threshold problem but is unlikely to produce satisfactory results.

Yoshisato in his second patent [19], describes a DBS receiver unit where a phase lock loop demodulator is used to control the AFC loop. The problem he seeks to circumvent is the erroneous operation of the AFC loop, in poor carrier-to-noise ratio conditions, when using

a conventional demodulator. In his solution he incorporates a phase lock loop demodulator and derives the AFC signal from the output of the phase lock loop VCO. Although performance figures are not quoted, very stable operation is claimed even when the input carrier-to-noise ratio is poor. Any performance advantage obtained with this approach is thus obtained by not having to provide the additional I.F. bandwidth required to allow for the instabilities in the system. However the problem of how to reduce the bandwidth of the system in the threshold region to enhance the output signal-to-noise ratio remains.

10.6.2 Mitra and Kobayashi's patent [22] introduces a technique called delayed threshold extension for the reception of DBS television signals. The approach broadly consists of a PLL demodulator proceeded by an elaborate AGC system that has a manual control input. It suffers from the possible disadvantage that the viewer is required to take manual action to initiate an increase in threshold extension. A basic diagram of the scheme is illustrated in figure 10/11. The circuit action relies on the characteristic of the PLL that results in a faster response characteristic when the loop gain is made larger and vice versa. If the loop gain is made smaller the response becomes slower and the bandwidth of the PLL demodulator becomes narrower.

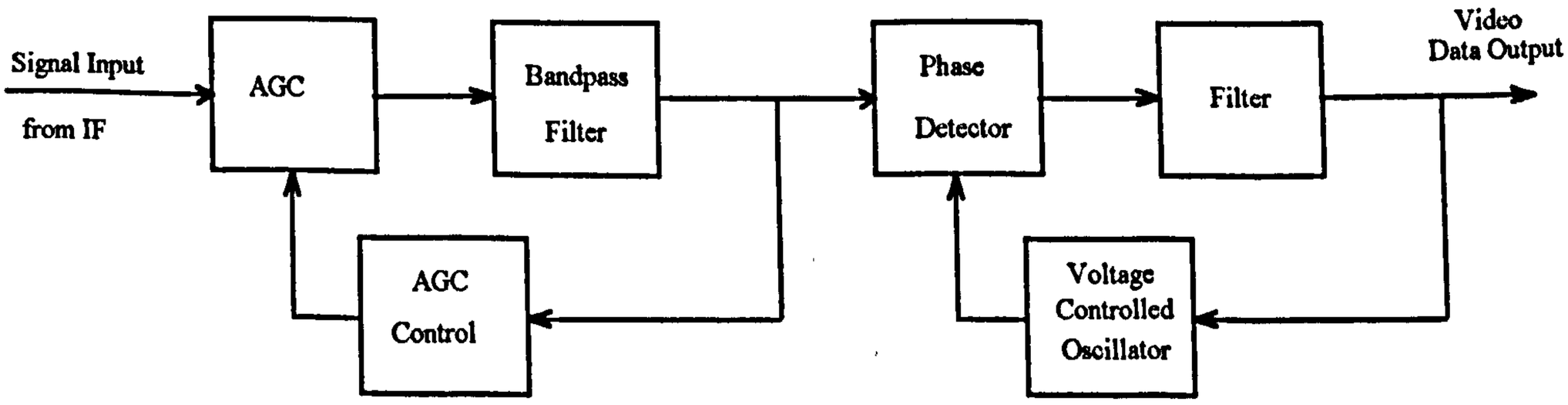

Figure 10/11 Mitra-Kobayashi Threshold Extension Demodulator

To describe the operation assume that the input carrier-to-noise ratio drops below the threshold level causing a picture degradation. The viewer then manually controls (AGC control) the AGC level reducing the input to the PLL demodulator. As the input signal level to the demodulator is reduced the loop gain of the PLL becomes reduced and the bandwidth

of the PLL becomes narrower improving the threshold extension. The noise on the image screen is then reduced and the image is improved, but at the expense of resolution. This approach goes to the heart of the threshold extension problem. Mitra and Kobayashi are one of the very few authorities who have recognised what the problem is in implementing threshold extension demodulators. That is the problem is not the means of controlling the threshold extension, but of finding a metric that determines when threshold extension should be applied. In Mitra and Kobayashi case, they used the viewer as the metric.

10.6.3 Naumann's patent [20] does not apply to TV systems but to satellite telephone communications. It is only mentioned here because of the adaptive nature of the approach. This method adjusts the threshold depending upon the loading of the baseband. Three methods are proposed for doing this, all of which in effect sense the highest frequency being used in the baseband and adjust the characteristics of the feedback loop to optimise the threshold. The problem with this approach is the metric used for determining the baseband signal bandwidth. This patent is a very broad one and proposes a number of concepts. One of the more interesting is the use of the modulated carrier spectral shape as a metric for determining the baseband loading. This approach may well form the basis of future threshold extension demodulators that use signal processing techniques.

10.6.4 Bush, et al. have also proposed a delayed approach in their patent [11] for achieving threshold extension. Although their technique is designed around a phase lock loop demodulator it could be applied to any demodulator. As the technique is basically a click suppression technique it is more fully discussed in Chapter 15.

10.6.5 Noguera's patent [21] was also intended to solve the problems encountered in satellite communications. His phase lock loop demodulator contained a primary feedback loop, for acquisition, and a secondary feedback loop that, after acquisition, is activated and increases the d.c. gain of the primary loop. This technique maintains threshold performance during temperature variation, ageing, radiation, etc. This approach is claimed to provide a threshold extension of some 2.2 dB over a conventional demodulator. However a

cautionary note should be made on this approach. The input signal for which it was designed has essentially a fixed structure. The approach is unlikely to offer much improvement with a variable signal structure such as those contained within a colour TV signal.

10.6.6 Horvat's patent [18] was also intended for satellite TV applications. His patent contained an automatic noise control circuit that modifies the gain of the AGC system. Broadly this circuit operates in the same manner as that described by Mitra [22] above, in that as the input signal level to the demodulator is reduced the loop gain of the PLL becomes reduced and the bandwidth of the PLL becomes narrower improving the threshold extension. The difference is in the metric used to detect the onset of the click phenomena where the positive and negative spikes generated at the onset of threshold are detected in the automatic noise control circuit. This metric is similar to those used in the click elimination schemes described in Chapter 15 and suffers from the same problem, namely how does one discriminate between clicks, false clicks, doublets and modulation transients? Brofferio proposed a similar approach in [9].

10.6.7 A patent of some interest is that due to Wason [25]. This patent is devoted to the detailed design of a threshold extension receiver that can receive both phase and frequency modulated signals. It introduces a number of concepts covering acquisition, dynamic range and threshold extension. The phase lock loop demodulator is of the so-called long-loop type that includes the I.F. amplifier within the loop. The performance improvement implied in this patent is a threshold extension of some 6 dB. However little specific performance data is given.

10.7 Discussion

This examination of the phase lock loop demodulator and its traditional analysis has shown that there are many unsolved problems remaining when it is operating in the threshold region and when the input signal is complex. When the input signal structure is fixed, such

as in deep space satellite transmission, successful operation of the PLL is possible and a 2 to 3 dB improvement is obtained. In general it may be concluded that any improvement in the phase lock loop demodulator that is obtained is due to its unusual threshold characteristic. That is when the input amplitude is reduced, the PLL bandwidth is reduced. This characteristic bears some similarity to that of the oscillating limiter discussed in section 8. The investigation of this similarity may be a possible area of future investigation.

When the input signal contains no modulation, and when operating in the threshold region, the number of spikes in the output of the PLL demodulator reduce as the gain of the PLL is reduced. When modulation is present there is a minimum loop bandwidth below which distortion results. In this region the spikes present are large. Increasing the PLL bandwidth results in a decrease in the number of spikes. If the bandwidth is made very large then the operation tends to that of a conventional discriminator [27]. Thus when modulation is present there is an optimum bandwidth which in turn depends upon the nature of the modulation. A PLL solution that may reduce these effects and may overcome them is suggested in chapter 18. This solution, termed the error controlled adaptive threshold extension demodulator, can be implemented utilising a phase lock loop demodulator with switchable loop filters, allowing the order of the loop to be varied depending upon the quality of the received signal.

10.8 References

[1] Jaffe, R., Rechtin, E. "Design and performance of phase-lock circuits capable of near optimum performance over a wide range of input signals and noise levels." IRE Trans. Inform. Theory. Vol. IT-1, 66 (1955).

[2] Acampora, A., Newton, A. "Use of phase subtraction to extend the range of a phase locked demodulator." RCA Review, (December 1966), pp 582-599.

[3] Frankle, J. "Threshold performance of analog FM demodulators." RCA review,

(December 1966), pp. 521-562.

[4] Tauseworthe, R. C. "A method for calculating phase-locked loop performance near threshold." IEEE Trans. Com. Tech., Vol. COM-15, No. 4, (August 1967), pp. 507-517.

[5] Schilling, D. L., Hoffman, E ., Nelson, E. A. "Error rate for digital signals demodulated by an FM discriminator." IEEE Trans. Com. Tech., Vol. COM-15, No. 4, (August 1967), pp. 502-506.

[6] Camp, J. A. "A comparison of the threshold extension capabilities of FMFB and Phase Lock Loop demodulators employed in FDM-FM communication systems." IEEE Trans. Comms., Vol. COM-18, No. 3, (June 1970), pp. 191-200.

[7] Haggai, T. F. "Threshold extension phase lock demodulator." US Patent 3,611,168 (Oct. 5th, 1971).

[8] Klapper, J., Frankle, J. T. "*Phase-Locked and Frequency-Feedback Systems*", Academic Press, (1972).

[9] Brofferio, S., Rocca, F. "Threshold extended FM demodulator for black and white video signal." IEEE Trans. Comms., (April 1972), pp. 235-242).

[10] Garodnick, J., Greco, J., Schilling, D. L. "Response of an all digital phase lock loop." IEEE Trans. Comms., Vol. COM-22, No. 6, (June 1974), pp. 751-763.

[11] Bush, J. A., Lance, D. R., Alstatt, J. E. "Frequency modulation demodulator threshold extension device." US Patent 3,983,488 (September 28, 1976).

[12] Roberts, J. H. "*Angle Modulation*". Pub. Peter Peregrinus, 1977.

[13] Maurice, R. D. A. "Threshold Extension in FM reception. An elementary treatment." E.B.U. Review. No. 168, (April 1978), pp 56-65.

[14] Beech, B., Moor, S. "Threshold Extension Techniques", IBA Report No. 130/84.

[15] Hajj, M. M., France, P. "Threshold extension demodulator", IEEE Consum. Elect., Vol. CE-30, No 3, (August 1984), pp. 272-277.

[16] Yoshisato, A. "Phase locked loop FM demodulator with variable bandwidth loop filter", US Patent 4,479,091 (Oct. 23, 1981).

[17] Beech, B., Moor, S. "Threshold Extension Techniques", IBA Experimental and Development Report 130/84, (July 1985).

[18] Horvat, P. "Demodulator comprising a phase locked loop", US Patent 4,600,890 (July 15,1986).

[19] Yoshisato, A. "Indoor unit of receiver for broadcasting satellite", US Patent 4,556,988 (Dec. 3 1985)

[20] Naumann, G. R. "Adaptive FM threshold extension demodulator", US Patent 4,816,770 (Mar. 28, 1989).

[21] Noguera, C., Triaud, P., Foucher, J. L. "Phase loop demodulator". US Patent 5,072,192 (Dec. 10, 1991).

[22] Mitra, H., Kobayashi, K. "FM signal detection apparatus with automatic gain control circuit connected to phase detector input terminal". US Patent 5,175,881 (Dec. 29, 1992).

[23] Taub, H., Schilling, D. "*Principles of Communication Systems*" McGraw-Hill, 1986, New York, ISBN 0-07-062955-2

[24] Crow, R. B. and Tausworthe, R. C. "Filter for Third-Order Phase-Locked Loops", US Patent 3,740,671 (June 19, 1973).

[25] Wason, C. B. "Threshold Extension Phase Modulated Feedback Receiver", US Patent 3,742,361 (June 26, 1973).

[26] Osborne, P., Schilling, D. L. "Threshold performance of phase locked loop demodulators", Proc. Int. Conf. Communications, 1968, pp. 466 - 470.

Blank Page

11. FREQUENCY LOCKED LOOP (FLL)

11.1 Introduction

The Frequency Locked Loop (FLL) FM Demodulator was first proposed by Clarke and Hess [1] in 1967 as a method of extending the noise threshold exhibited by the conventional FM limiter demodulator. Although a very interesting and elegant concept with some useful characteristics, the only other mention that can be found in the published literature is Clarke and Hess's 1971 US patent, [2] and Hess's note on equivalence of demodulators [3]. The FLL threshold extension characteristic is claimed to be due to its ability to greatly suppress the noise clicks which occur at low input signal-to-noise ratios in the conventional FM demodulator. In addition because the FLL does not include a VCO, it does not introduce additional loss of lock clicks as the phase locked loop (PLL) or FM with Feedback (FMFB) demodulators may. Clarke and Hess described two embodiments of the FLL in their original paper, one at RF and the other at baseband. These are stated to be mathematically equivalent. In this thesis both versions are considered with the baseband version being preferred as it is a stand alone device whose operation is more amenable to satellite DBS applications. This is the approach discussed in chapter 18 below, where an error controlled adaptive threshold extension demodulator is proposed. A version of which is based upon the FLL demodulator.

11.2 Basic operation of the frequency lock loop demodulator

11.2.1 Figure 11/1 illustrates the basic version of the baseband frequency lock loop (FLL) demodulator. Figure 11/2 illustrates the fuller concept that shows the development potential of the device. The FLL is an FM demodulation device which utilises the amplitude information inherent in a noise corrupted FM carrier to control the parameters of a feedback loop through which the demodulated FM information is passed, during the occurrence of large noise induced pulse like disturbances (spikes or clicks) in the demodulated baseband

signal.

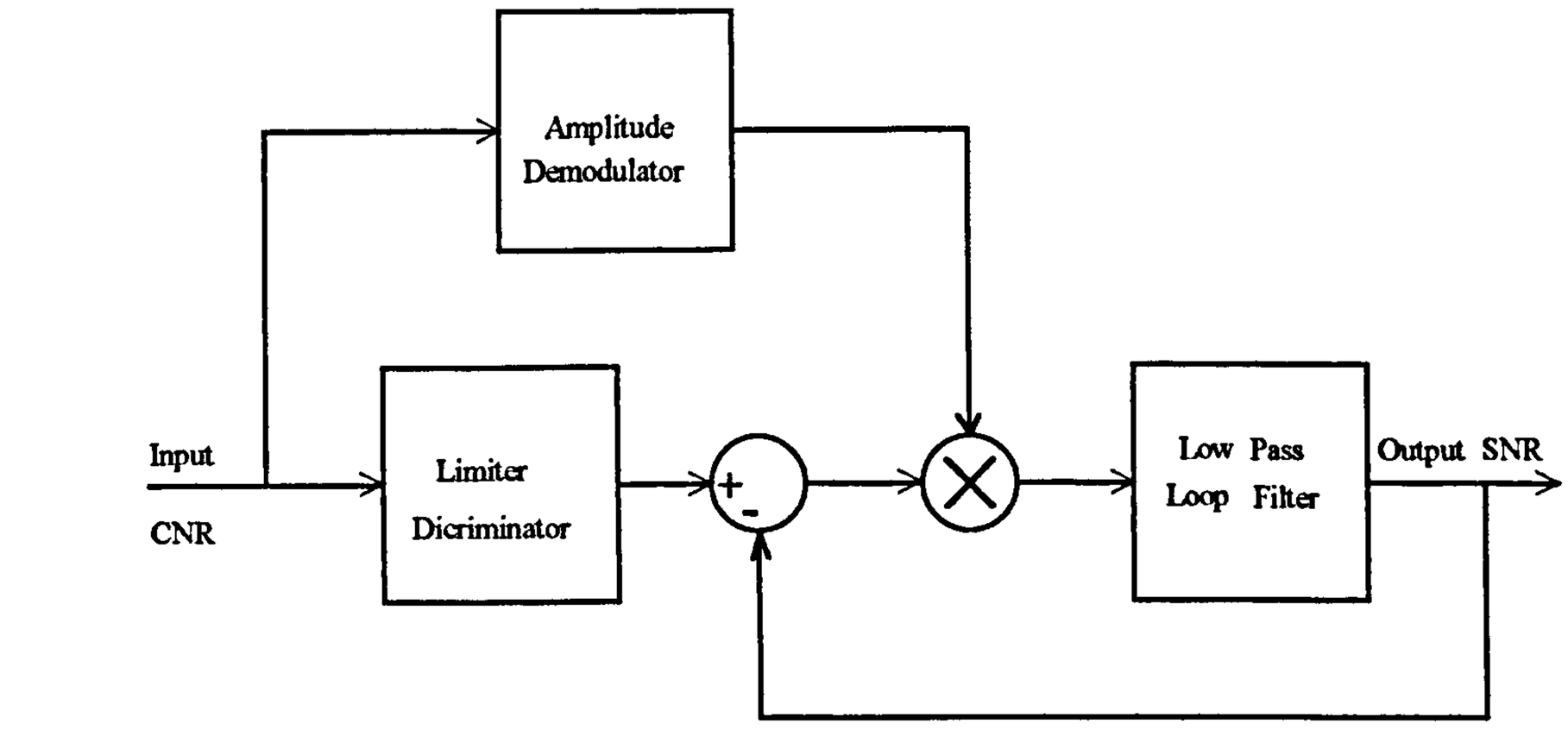

Figure 11/1 Frequency Lock Loop Demodulator (Baseband Version)

Figure 11/2 illustrates a circuit configuration where an amplitude demodulator and a frequency demodulator are supplied in parallel from the input to the system. These demodulators derive information signals that are respectively functions of the instantaneous envelope information and instantaneous frequency modulation information. The control of the parameters of the feedback loop may be accomplished by the instantaneous envelope information directly or by the envelope information that has been processed by some linear or non-linear function. The final output signal is taken from the output of the feedback loop through a low pass filter. If desired, an equalising filter may be interposed between the output of the feedback loop and the final low pass filter.

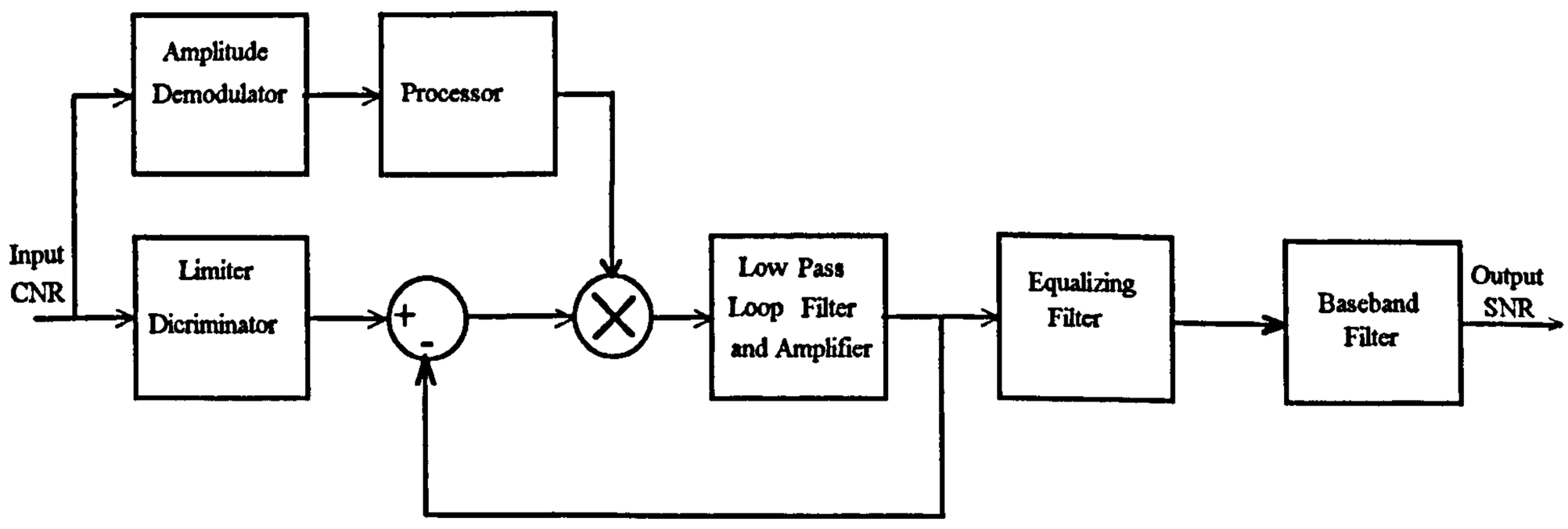

Figure 11/2 Frequency Lock Loop Demodulator Concept (Baseband Version)

11.2.2 The FLL demodulator takes advantage of a correlation that exists between the instantaneous envelope and instantaneous frequency. Specifically the instantaneous envelope almost always drops to a low level (compared with the average carrier level) when a frequency click occurs. The FLL makes use of this drop in the amplitude to control the parameters of a feedback loop through which the demodulated instantaneous frequency information of the carrier is passed. The feedback loop in figure 11/2 consists of an error junction followed by a multiplier. The error junction is driven by the output of the FM demodulator that produces a signal in proportional to the instantaneous frequency. The following multiplier takes the output of the error junction and multiplies it by a processed form of the instantaneous envelope. The multiplier in turn is followed by a low pass filter whose output is taken back to the error junction and also used as the system output of the device.

This use of the processed envelope information to control the loop gain of the feedback loop effectively controls the bandwidth of the feedback loop through which the FM signal is passed. Thus if the amplitude of the envelope decreases to a low level relative to its average amplitude, and this decrease is used to reduce the loop gain significantly, the FM signal passes through a very narrow bandwidth channel that effectively holds the output level to the value existing prior to the decrease in the envelope level. Since the FM noise threshold is characterised by the occurrences of clicks in the instantaneous frequency, and since near threshold these clicks are almost always accompanied by low amplitude levels on the incoming FM signal, the holding property of the feedback loop eliminates the majority of the clicks from its output and thus extends the noise threshold. The control of the loop gain of the feedback loop by the envelope information is achieved by multiplying the signal within the feedback loop by a processed form of the instantaneous envelope. The processed envelope is generally a signal that approaches zero quite closely each time the instantaneous envelope decreases towards zero. The ability of the feedback loop to hold its output when the processed envelope information decreases towards zero is directly related to the choice of low pass filter inserted at the multiplier output within the feedback loop. Depending on the choice of the loop filter, an equalising filter may be required at the output of the

feedback loop to ensure overall undistorted signal transmission when the loop is not being held. The equalising filter effectively compensates for any undesired filtering of the instantaneous frequency by the feedback loop.

11.2.3 Figure 11/3 illustrates the RF version of the frequency lock loop demodulator. It is built around the balanced demodulator concept described by Clarke and Hess in [4]. This balanced demodulator does not contain a separate limiter, but its operation is such as to make it insensitive to amplitude variations at the centre frequency of the input that it tracks. The balanced demodulator is modified into a FLL by means of the external multiplier.

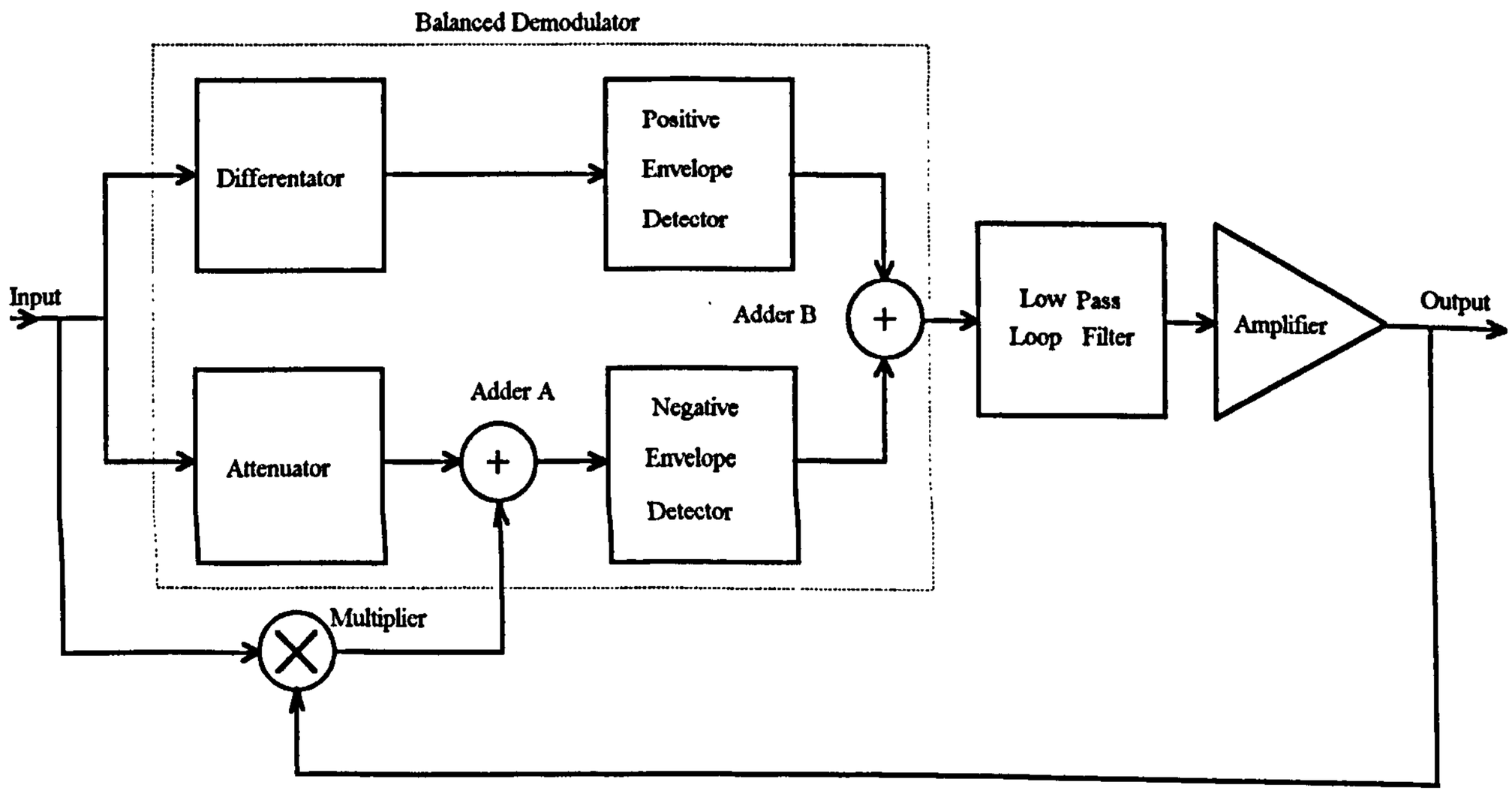

Figure 11/3 Frequency Lock Loop Demodulator (RF Version)

11.3 Analysis of the frequency lock loop FM demodulator (RF version)

11.3.1 Consider figure 11/4. This shows the RF version of the FLL demodulator with its signal flows.

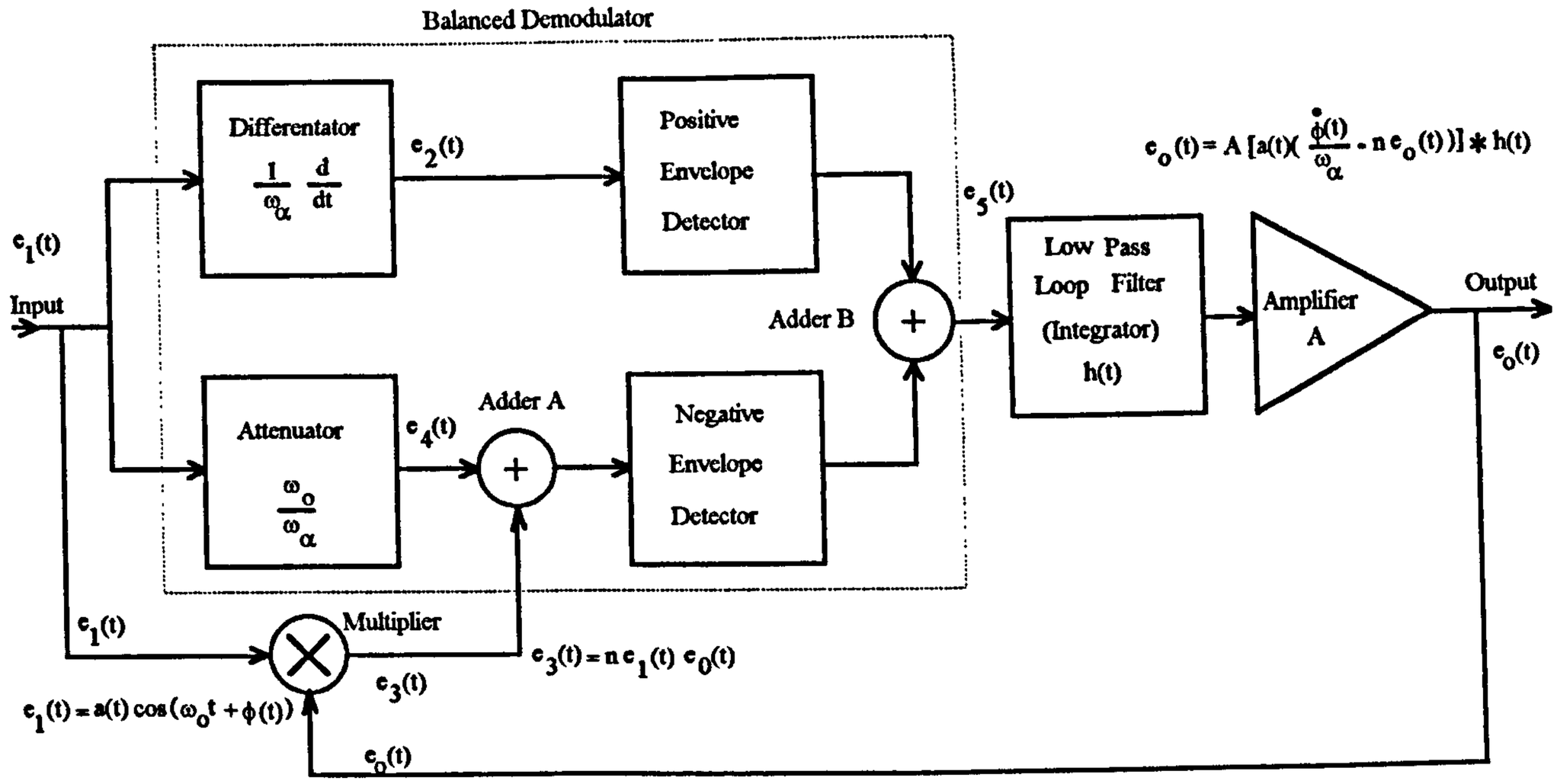

Figure 11/4 Frequency Lock Loop Demodulator (RF Version)

Assume that the following FM signal is applied to the input:

$$e_1(t) = a(t)\cos\left[\omega_o t + \phi(t)\right] \qquad \text{..... (11-1a)}$$

where $a(t)$ = Instantaneous signal amplitude

$\phi(t)$ = Instantaneous signal phase

ω_o = Carrier frequency

The method of analysis given below is an amplified version of that given by Clarke and Hess, but as applied to the RF version of the FLL. Note that the demodulators shown in figures 11/1 to 11/3 are not preceded by a limiter. Now in fig 11/4, the output of the demodulator (differentiator), or frequency to amplitude converter, is the differential of the input. For equation (11-1a) above, the output of the differentiator can be obtained by the use of the $\frac{d(uv)}{dx} = u\frac{dv}{dx} + v\frac{du}{dx}$ expression, where:

$$u = a(t) \qquad \text{..... (11-1b)}$$

Therefore

$$\frac{du}{dt} = \dot{a}(t) \qquad \text{..... (11-1c)}$$

and $$v = \cos\left(\omega_o t + \phi(t)\right) \quad \text{..... (11-1d)}$$

Therefore $$\frac{dv}{dt} = -(\omega_o + \dot{\phi}(t)) \sin(\omega_o t + \phi(t)) \quad \text{..... (11-1e)}$$

Thus:

$$e_2(t) = \frac{de_1}{dt} = -a(t)K_1(\omega_o + \dot{\phi}(t)) \sin(\omega_o t + \phi(t)) + \dot{a}(t)K_1 \cos(\omega_o t + \phi(t)) \quad \text{..... (11-2)}$$

where K_1 has an arbitrary value chosen for the demodulator constant.

Now for the condition where: $$a(t)\left(\omega_o + \dot{\phi}(t)\right) \gg \dot{a}(t)$$

the second term in equation (11-2) can be neglected. This condition is satisfied when the demodulator is preceded by an I.F. amplifier that would have a (Carson) bandwidth that was the minimum required to transmit the signal with an acceptable distortion, thus resulting in the second term in equation (11-2) being negligible.

Thus: $$e_2(t) = -a(t)K_1\left[\omega_o + \dot{\phi}(t)\right] \sin(\omega_o t + \phi(t)) \quad \text{..... (11-3)}$$

11.3.2 From figure 11/4, the output of Adder A is given by $e_3(t) + e_4(t)$.

The output of Adder B is given by:

$$e_5(t) = \hat{e}_2(t) + \hat{e}_3(t) + \hat{e}_4(t) \quad \text{..... (11-4)}$$

where $\hat{e}_2(t), \hat{e}_3(t)$ and $\hat{e}_4(t)$ denote the respective instantaneous amplitudes of $e_2(t), e_3(t)$ and $e_4(t)$.

The output of the multiplier is given by:

$$e_3(t) = n\, e_1(t)\, e_0(t) \qquad \text{..... (11-5)}$$

The attenuator output that forms the input to Adder A is given by:

$$e_4(t) = \frac{\omega_0}{\omega_\alpha} e_1(t) \qquad \text{..... (11-6)}$$

Putting equations (11-5) and (11-6) into (11-4) gives:

$$e_5(t) = \hat{e}_2(t) + n\, \hat{e}_1(t)\, e_0(t) + \frac{\omega_0}{\omega_\alpha} \hat{e}_1(t) \qquad \text{..... (11-7)}$$

Putting the envelope detected component of equation (11-3) into (11-7) gives:

$$e_5(t) = -a(t) K_1 \left[\omega_o + \dot{\phi}(t) \right] + n\, \hat{e}_1(t)\, e_0(t) + \frac{\omega_0}{\omega_\alpha} \hat{e}_1(t) \qquad \text{..... (11-8)}$$

The instantaneous signal amplitude of the input $\hat{e}_1(t) = a(t)$; inserting into equation (11-8) gives:

$$e_5(t) = -a(t) K_1 \left[\omega_o + \dot{\phi}(t) \right] + n\, a(t)\, e_0(t) + \frac{\omega_0}{\omega_\alpha} a(t) \qquad \text{..... (11-9)}$$

Simplifying gives:

$$e_5(t) = a(t) \left[-K_1 \omega_o - K_1 \dot{\phi}(t) + n\, e_0(t) + \frac{\omega_0}{\omega_\alpha} \right] \qquad \text{..... (11-10)}$$

Letting the demodulator constant $K_1 = \frac{1}{\omega_\alpha}$ gives:

$$e_5(t) = a(t) \left[-\frac{\omega_0}{\omega_\alpha} - \frac{\dot{\phi}(t)}{\omega_\alpha} + n\, e_0(t) + \frac{\omega_0}{\omega_\alpha} \right] \qquad \text{..... (11-11)}$$

Therefore: $$e_5(t) = a(t)\left[-\frac{\dot{\phi}(t)}{\omega_\alpha} + n\,e_0(t)\right] \qquad \text{..... (11-12)}$$

Now $$e_0(t) = A\,e_5(t) * h(t) \qquad \text{..... (11-13)}$$

Where A is the gain of the loop amplifier, and $h(t)$ is the impulse response of the low pass filter, which in this case is an integrator with an input-output relationship given by:

$$e_{out} = \omega_\beta \int^t e_{in}(\tau)\,d\tau \qquad \text{..... (11-14)}$$

where ω_β is the integrator constant.

Inserting equation (11-12) into (11-13) gives:

$$e_0(t) = A\,a(t)\left[-\frac{\dot{\phi}(t)}{\omega_\alpha} + n\,e_0(t)\right] * h(t) \qquad \text{..... (11-15)}$$

Therefore $$\frac{\dot{e_0}(t)}{\omega_\beta} = -A\,a(t)\frac{\dot{\phi}(t)}{\omega_\alpha} + n\,A\,a(t)e_0(t) \qquad \text{..... (11-16)}$$

Rearranging gives: $$\frac{\dot{e_0}(t)}{\omega_\beta} - n\,A\,a(t)e_0(t) = -A\,a(t)\frac{\dot{\phi}(t)}{\omega_\alpha} \qquad \text{..... (11-17)}$$

But if the loop gain is increased such that:

$$n\,A\,a(t)e_0(t) \;>>\; \frac{\dot{e_0}(t)}{\omega_\beta} \qquad \text{for} \quad a(t) \neq 0 \text{..... (11-18)}$$

Then $$n\,A\,a(t)e_0(t) = A\,a(t)\frac{\dot{\phi}(t)}{\omega_\alpha} \qquad \text{..... (11-19)}$$

Therefore: $$e_0(t) = \frac{\dot{\phi}(t)}{\omega_\alpha} \qquad \text{..... (11-20)}$$

Equation (11-20) shows that the demodulated output is independent of input amplitude variation for the conditions specified. Therefore for high carrier-to-noise ratios the FLL acts as a conventional limiter discriminator. It is indicated in [1] that the loop gain must be sufficiently high such that the wanted (demodulated) signal, $\dot{\phi}(t)$, passes through the closed loop bandwidth. In practice this means that the closed loop bandwidth, must occupy a bandwidth equal or greater than the I.F. bandwidth. However to minimise clicks, the closed loop bandwidth is required to be as small as possible. The optimum approach specified in [1] is to adjust the closed loop bandwidth such that it is just larger than the I.F. bandwidth.

The click suppression mechanism suggested in [1], is when a click occurs in $\dot{\phi}(t)$ due to noise, $a(t)$ usually becomes low. The reduction in $a(t)$ reduces the closed loop bandwidth that causes the loop output to remain virtually constant until $a(t)$ again increases thereby suppressing clicks from the demodulated output.

11.4 Analysis of the frequency lock loop FM demodulator (baseband version)

11.4.1 Figure 11/5 illustrates the baseband version of the frequency lock loop demodulator. The following brief analysis will follow that given above for the RF version. Note that the various circuit (signal) references given in figure 11/5 have differing definitions from those used in figure 11/4. The baseband version consists of a conventional limiter discriminator, whose output drives a feedback loop whose loop gain is directly proportional to the amplitude of the envelope of the input I.F. signal. This amplitude dependence is achieved by envelope detecting the input signal and multiplying the closed loop signal by the envelope $a(t)$.

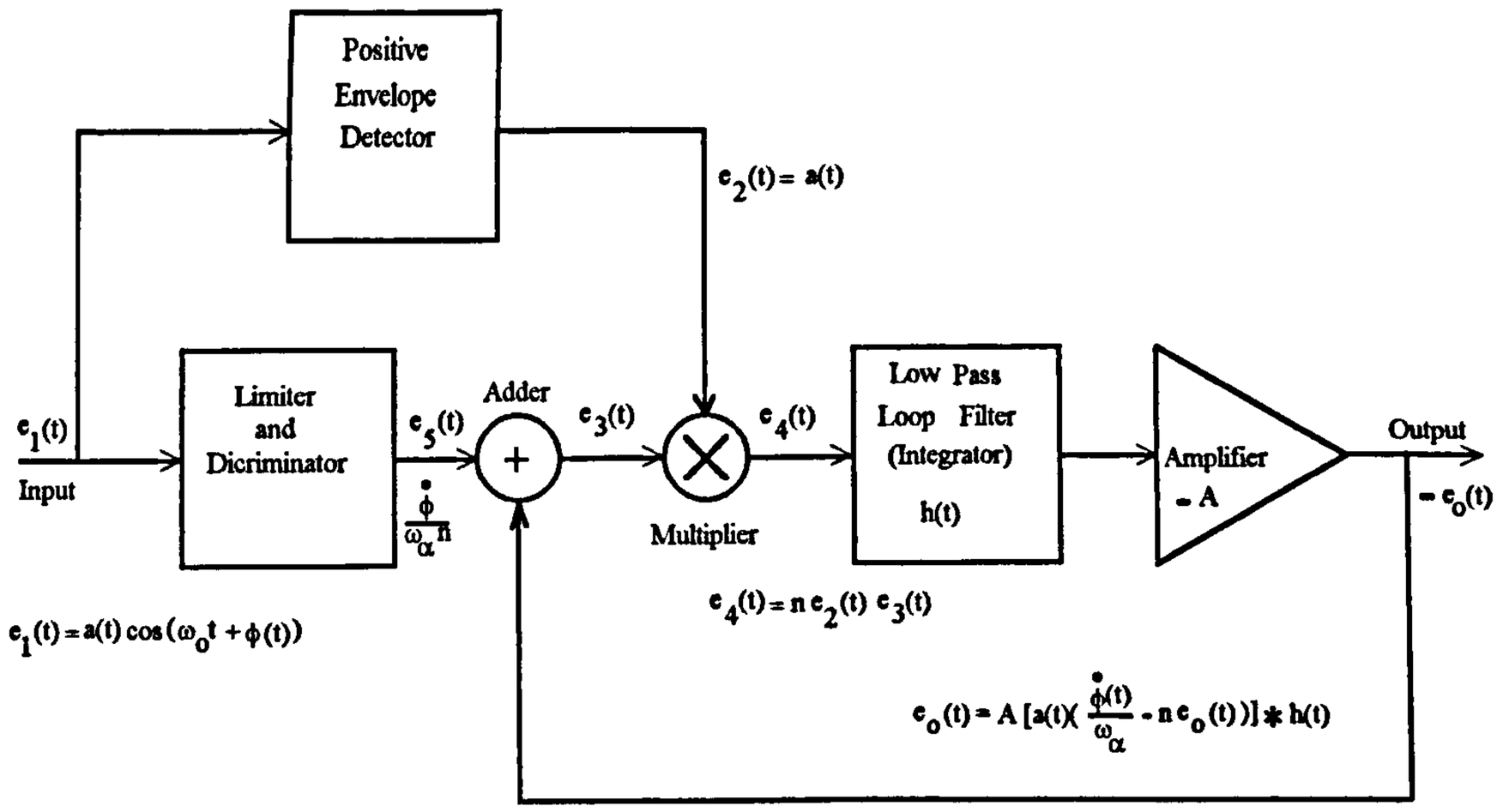

Figure 11/5 Frequency Lock Loop Signal Flows

The derivation of the output $e_5(t)$ of the discriminator in figure 11/5, differs from that given above for equation (11-3) because of the limiter contained within the discriminator. The derivation of $e_5(t)$ is as follows:

Now the signal input is given by equation (11-1a) above but with a constant (or limited envelope), viz.

$$e_1(t) = A_L \cos\left[\omega_o t + \phi(t)\right] \qquad \text{..... (11-21)}$$

Where A_L = Constant (or limited) envelope

$\phi(t)$ = Instantaneous signal phase

ω_o = Carrier frequency

Differentiating gives the output to the discriminator:

$$-A_L K_1\left[\omega_o + \dot{\phi}(t)\right]\sin\left(\omega_o t + \phi(t)\right) \qquad \text{..... (11-21)}$$

Letting the discriminator constant $K_1 = \dfrac{1}{n\omega_\alpha}$, the envelope output $e_5(t)$ is:

$$e_5(t) = A_L \frac{1}{n\omega_\alpha}\left[\omega_o + \dot{\phi}(t)\right]$$

Ignoring the d.c. component gives:

$$e_5(t) = A_L \frac{\dot{\phi}(t)}{n\omega_\alpha} \qquad \text{..... (11-22)}$$

From figure (11/5), the output of the adder is given by:

$$e_3(t) = -e_o(t) + e_5(t) \qquad \text{..... (11-23)}$$

and the output of the multiplier is given by:

$$e_4(t) = n\, e_2(t)\, e_3(t) \qquad \text{..... (11-24)}$$

Where n is the multiplier constant. Combining equations (11-22) and (11-23) gives:

$$e_4(t) = n\, e_2(t)\left[-e_o(t) + e_5(t)\right] \qquad \text{..... (11-25)}$$

The output of the low pass filter is given by:

$$e_o(t) = -A\, e_4(t) * h(t) \qquad \text{..... (11-26)}$$

Where A is the gain of the loop amplifier, which also provides a phase inversion, and $h(t)$ is the impulse response of a low pass filter. In this analysis the low pass filter consists of an integrator with an input-output relationship given by:

$$e_{out} = \omega_\beta \int^t e_{in}(\tau)\, d\tau \qquad \text{..... (11-27)}$$

Substituting equation (11-25) into (11-26) gives:

$$e_o(t) = -A\left[n\, e_2(t)\left(-e_o(t) + e_s(t)\right)\right] * h(t) \qquad \text{..... (11-28)}$$

Substituting equation (11-22) into (11-28) and letting $e_2(t) = a(t)$ gives:

$$e_o(t) = -A\left[n\, a(t)\left(-e_o(t) + A_L \frac{\dot{\phi}(t)}{n\omega_\alpha}\right)\right] * h(t) \qquad \text{..... (11-29)}$$

$$\frac{\dot{e_0}(t)}{\omega_\beta} = n\, a(t)\, A\, e_o(t) - n\, a(t)\, A\, A_L \frac{\dot{\phi}(t)}{n\omega_\alpha} \qquad \text{..... (11-30)}$$

Rearranging gives $\dfrac{\dot{e_0}(t)}{\omega_\beta} - n\, a(t)\, A\, e_o(t) = -n\, a(t)\, A\, A_L \dfrac{\dot{\phi}(t)}{n\omega_\alpha}$

Now if the loop gain is increased such that:

$$na(t)Ae_0(t) \;>>\; \frac{\dot{e_0}(t)}{\omega_\beta} \qquad for \quad a(t) \neq 0 \qquad \text{..... (11-31)}$$

Then $$e_o(t) = A_L \frac{\dot{\phi}(t)}{n\omega_\alpha} \qquad \text{..... (11-32)}$$

Equation (11-32) shows that for the baseband version, the demodulated output is multiplied by the limited input envelope and independent of the input envelope variations.

11.5 Discussion

11.5.1 At an initial glance the FLL looks a very attractive threshold extension demodulator concept with its lack of VCO. It is one of those rare concepts that makes use of the additional (amplitude) information in the signal that is normally discarded when the

limiter is used. However the above analysis reveals the following difficulties.

The assumption that the value of the envelope goes low when a click occurs is not a reliable metric for signifying the occurrence of a click. Frequently this change in amplitude does not occur. When it does, it can occur for both clicks and doublets, thus preventing essential discrimination taking place between them.

The reduction in loop bandwidth that occur as a result of the envelope going low and minimises the effects of clicks, is very similar to the effects described previously in other demodulators such as the PLL and oscillating limiter.

The difficulty in determining the bandwidth of the demodulator as a compromise between a low bandwidth for click elimination and a wide bandwidth for minimises distortion of the signal is a severe limitation. The design of the loop filter in this demodulator is rather critical, and for a DBS system probably impractical given the changing picture content. It may well be for this reason that the approach does not appear to have found wide application. However the adaptive technique described in chapter 18 below, termed the error controlled adaptive threshold extension demodulator, may lend itself to this type of circuit as it is a design that optimises its parameters to the signal structure. It is discussed further therein.

11.6 References

[1] Clarke, K. K., Hess, D. T. "Frequency Locked Loop FM Demodulator", IEEE Transactions on Communication Technology. Vol. COM-15, No. 4, August 1967, pp. 518 - 524.

[2] Hess, D. T., Clarke, K. K. "Frequency Demodulator for Noise Threshold Extension", US Patent 3,611,169. October 5th, 1971.

[3] Hess, D. T. "Equivalence of FM threshold extension receivers." IEEE Trans. Comms. Tech., October 1968, pp. 746 - 748.

[4] Clarke, K. K., Hess, D. T., "Demodulator for frequency modulation signal." US Patent 3,292,093. December 13th, 1966.

12. AUTOCORRELATION DEMODULATOR

12.1 Introduction

12.1.1 Hamer in his 1970 paper [1] introduced a new type of threshold extension FM demodulator that he termed an autocorrelation deviation-compression FM demodulator. Apart from this reference and the associated correspondence, it does not appear to have been discussed in the literature further. The technique (figure 12/1) although apparently an original approach, was subsequently shown [2-3] to be equivalent to the Park (inverse limiting) frequency discriminator [4], shown in figure 12/2. Both demodulator approaches were shown [2] to be identical to the linear balanced discriminator, using square law envelope detectors, without any form of amplitude limiting [5]. Although Hamer's demodulator has the grave disadvantage that as the FM deviation is increased, the performance deteriorates, the approach is of interest in that the effective deviation at any particular modulation frequency can either be increased by approximately two, or it can be reduced indefinitely. However Imboldi and Schemel [2] postulated that the autocorrelation demodulator could not be truly classed as a threshold extension device as it did not preserve the FM improvement at higher carrier-to-noise ratios as in conventional threshold extension demodulators. Hamer [3] however challenged this assertion and proposed that the above threshold degradation in performance of the autocorrelation demodulator could be circumvented by switching to a conventional demodulator for above threshold signal levels.

The limited analysis given below will not follow that of Hamer, but will be an amplified version of that given by Imboldi, et al. [2]. The latter tends to show the limitations of the scheme more fully as it considers the modulation dependent terms in the analysis which Hamer does not.

12.2 Basic operation

12.2.1 Figure 12/1 shows the basic circuit of the autocorrelation FM demodulator. The approach does not contain any amplitude limiters. The input signal V, which has an angular frequency ω, is derived from the preceding I.F. amplifier and is split into two paths. In the upper path the signal is delayed by a delay τ, and the applied to a mixer $M1$, which changes the angular frequency to $\omega - \omega_0$. The latter is then filtered in the band pass filter stage $F1$ and then to a second mixer $M2$. The lower path is applied directly to the mixer $M2$. A differential group delay τ, is inserted in the upper path. Hamer states that it is immaterial in which path the delay is inserted, and it may be provided entirely by circuit delays.

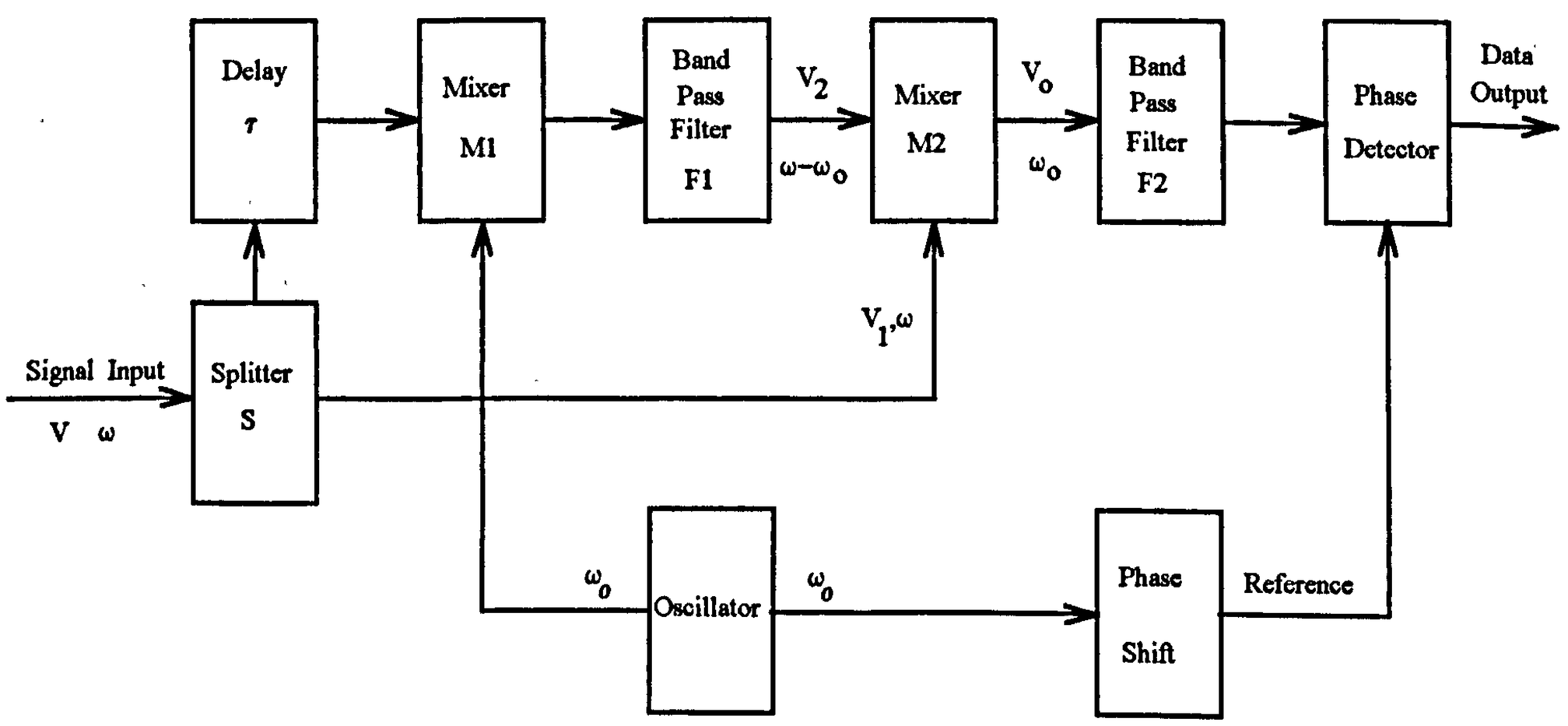

Figure 12/1 Autocorrelation FM Demodulator

The two signals V_1 and V_2, which can have unequal amplitudes, are multiplied in the mixer $M2$, to provide a difference output V_0. The basic operation of the circuit shows that with a fixed input frequency, the angular frequency of V_0 must be ω_0, whatever the value of ω, within the limits of the bandpass filters. When the input frequency is frequency modulated,

the angular frequency of V_2 lags behind that of V_1, owing to the delay τ, and the output then departs from ω_0 . However, the mean angular frequency output of $M2$ remains ω_0 and any residual carrier component is phase coherent with the oscillator frequency, ω_0. The bandpass filter $F2$ selects the difference output of $M2$, which is then applied to the phase sensitive demodulator; whose reference frequency is the oscillator output at ω_0 suitably adjusted in phase. The desired demodulated data output appears at the output of the phase detector.

The operation of this circuit is to convert the input frequency modulation to phase modulation, and the effective deviation at any particular modulation frequency can be increased (by a factor of two) or reduced indefinitely. Hamer shows [1, equation 13] that the peak deviation has been changed by a factor D, where $D = 2 \sin \omega_M \tau$ where τ is the time delay and ω_M is the modulation signal. It is the reduction in deviation that is of interest since if the phase deviation at the output of the mixer $M2$ is relatively small then it is possible to obtain linear coherent detection in the phase detector that leads to a threshold extension capability. The circuit makes the deviation a function of the modulation frequency so that in a spectrum of modulation frequencies, the shape of the spectrum is changed, the deviation compression being greater at the lower modulation frequency. Thus the input frequency modulation is converted to phase modulation.

12.2.2 The Park demodulator [4], to which Hamer's demodulator is identical, is shown in figure 12/2. This approach can be termed a zero intermediate frequency conjugate receiver. This demodulator effectively converts FM to AM and then synchronously detects the AM. Again no limiter is involved. The phase of the local oscillator is relatively unimportant as long as it is reasonably stable. Park point out that detuning of the local oscillator causes no distortion, except that due to the I.F. amplifiers. However being off - tune does degrade the signal-to-noise ratio.

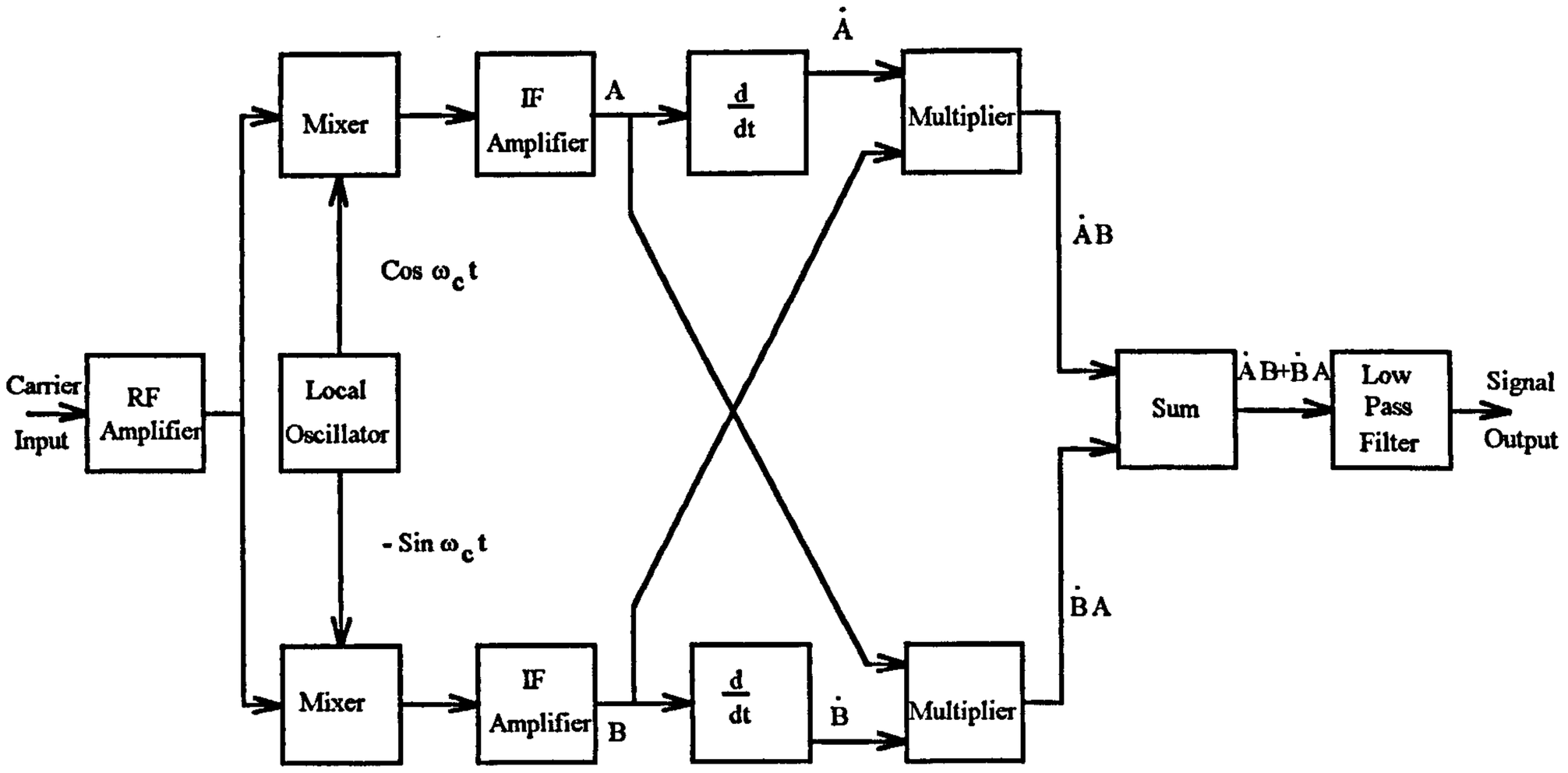

Figure 12/2 Park Demodulator

12.3 Brief analysis

12.3.1 Consider the received signal at the input of the autocorrelation demodulator as being:

$$v_i(t) = \sin[\omega t + \phi(t)] + N(t)\sin[\omega t + \theta(t)] \qquad \text{..... (12-1)}$$

where: $$\phi(t) = \int_{-\infty}^{t} \Delta(t)\, dt$$

and $\Delta(t) =$ Signal modulation $= \dot{\phi}(t)$

$N(t) =$ Noise envelope referred to unit signal amplitude

$\theta(t) =$ Noise phase

Equation (12-2) can be rewritten as:

$$v_i(t) = V(t)\sin(\omega t + \psi(t)) \qquad \text{..... (12-2)}$$

$$V^2(t) = 1 + 2N\cos(\theta - \phi) + N^2 \qquad \text{..... (12-3)}$$

$$\psi(t)=\phi+\tan^{-1}\frac{N\sin(\theta-\phi)}{1+N\cos(\theta-\phi)} \qquad \text{..... (12-4)}$$

where θ, ϕ and N are functions of time. As can be seen from figure 12/1, v_i is multiplied by a time delayed version of itself shifted in frequency. The filtered output is:

$$v_o=V(t)V(t-\tau)\sin\left(\omega_i\tau+\omega_o\tau+\psi(t)-\psi(t-\tau)\right) \qquad \text{..... (12-5)}$$

Both $\psi(t)$ and $V(t)$ may be expanded in a Taylor series about t.

Therefore:

$$\psi(t-\tau)=\psi(t)-\dot{\psi}(t)\tau+\ddot{\psi}(t)\frac{\tau^2}{2!}-\cdots\cdots \qquad \text{..... (12-6)}$$

Given small relative values of τ, the only significant terms of the series are the first two. This means that the modulation is recovered without linear frequency distortion.

Substituting equation (12-6) into (12-5) gives:

$$v_o=V(t)V(t-\tau)\sin\left(\omega_i\tau+\omega_o\tau+\dot{\psi}\tau\right) \qquad \text{..... (12-7)}$$

The term $V(t)V(t-\tau)$ is now expanded in a similar manner, resulting in:

$$V(t)V(t-\tau)=V^2(t)-\frac{\tau}{2}\frac{d}{dt}V^2(t)+\frac{\tau^2}{2!}V(t)\ddot{\psi}(t)- \qquad \text{..... (12-8)}$$

Imboldi [2] has pointed out that the inclusion of the second term can only give a reduction in detected signal-to-noise ratio. He also points out that neglect of the second term in equation (12-8) provides an upper bound for the Hamer demodulator.

Thus $$V(t)V(t-\tau)\cong V^2(t) \qquad \text{..... (12-9)}$$

Inserting equation (12-9) into equation (12-8) gives

$$v_o = V^2(t)\sin\left(\omega_i\,\tau+\omega_o\,\tau+\dot{\psi}\,\tau\right) \qquad \text{..... (12-10)}$$

Demodulating equation (12-10) by a quadrature reference carrier and assuming that $\psi'\,\tau$ is small or that the phase detection process is linear gives an output that is:

$$v_o = \tau V^2(t)\,\dot{\psi}(t) \qquad \text{..... (12-11)}$$

Substituting equations (12- 3) and (12-4) into equation (12-11) and rearranging, results in:

$$\frac{v_o}{\tau} = \dot{\phi} + N^2\,\dot{\theta} + N\sin(\theta-\phi) + N\left(\dot{\theta}+\dot{\phi}\right)\cos(\theta-\phi) \qquad \text{..... (12-12)}$$

This equation may be rearranged in the form:

$$\frac{v_o}{\tau} = \Delta + \frac{d}{dt}\left(N\sin(\theta-\phi)\right) + 2N\Delta\cos(\theta-\phi) + N^2\,\dot{\theta} \qquad \text{..... (12-13)}$$

Considering equation (12-13):

(i) The first term in this expression is the required modulation.

(ii) The second term represents the characteristic triangular noise spectrum present at the output of the ideal FM detector.

(iii) The third term is a noise component that is a function of the modulation, which would be suppressed by a limiter in an ideal FM demodulator.

(iv) This is a (noise times noise) process. This can be shown be shown by inserting $x(t) = N(t)\cos\theta(t)$ and $y(t) = N(t)\sin\theta(t)$ into the fourth term and obtaining: $N^2\ \dot{\theta} = y(t)\dot{x}(t) - \dot{y}(t)x(t)$ ..... (12-14).

It is the fourth term that is responsible for the square law behaviour of the demodulator.

Hamer in a letter [3] following his article gave an expression for the output signal-to-noise ratio in terms of the input carrier-to-noise ratio, for a modulated signal, but did not give its derivation. This relationship is as follows:

$$\left(\frac{C}{N}\right) = \frac{\left(\frac{S}{N}\right)_C}{\left[\frac{4\sin^2\left(\frac{1}{2}\omega_M\,\tau + \psi(\tau)\right)}{D^2} + \frac{\left(1-\frac{f_M}{b_1}\right)\left(1-\frac{\sin\theta}{\theta}\right)}{\gamma D^2}\right]}$$

..... (12-15)

where $\left(\frac{S}{N}\right)_C$ = Output signal-to-noise in a conventional demodulator above threshold.

b_1 = Input I.F. bandwidth.

γ = Carrier-to-noise ratio.

τ = Differential delay.

$\psi(\tau)$ = Average change of carrier phase due to modulation, within an interval τ.

D = Compression factor = $2\sin\frac{1}{2}\omega_M\,\tau$

$\theta = \pi\tau(b_1 - f_M)$

ω_M = Angular modulation frequency.

12.4 Discussion

12.4.1 Hamer's autocorrelation demodulator is an interesting approach. It appears to obtain any threshold improvement that it has by changing the carrier modulation from FM to PM and takes advantage of the inherent 3 dB advantage that coherent (PM) demodulation offers. The problem with the autocorrelation demodulator is that it is drastically affected by the signal modulation and that the FM improvement factor at high modulation indices is lost. Although equivalent to the Park [4] and Murakami [5] approaches, its characteristics are very similar to the Roberts envelope multiplication approach discussed in section 16 below. Because these approaches give an improvement below threshold and not above, they may offer some advantages in DBS applications. This aspect is discussed further below.

12.5 References

[1] Hamer, R. "Autocorrrelation Threshold - Extension Demodulator," Proc. IEE, Vol. 117, No. 6, June 1970, pp. 1073 - 1081.

[2] Imboldi, E. and Schemel, R. E. "Autocorrrelation Threshold - Extension Demodulator," (Letter) Proc. IEE, Vol. 118, No. 6, June 1971, pp. 757 - 758.

[3] Hamer, R. "Autocorrrelation Threshold - Extension Demodulator," (Letter Reply) Proc. IEE, Vol. 118, No. 6, June 1971, p. 758.

[4] Park, J. H. "An FM Detector for Low S/N," IEEE Trans. on Communication Technology, Vol. COM - 18, No. 2, April 1970, pp. 110 - 118.

[5] Murakami, T. "Analysis of multiple signal FM Detection System", RCA Review, 1966, **27**, p. 425.

13. PHASE FILTER DEMODULATOR

13.1 Introduction

13.1.1 An interesting approach to a threshold extension demodulator was reported by Hummels [1]. This approach, which he termed the phase filter, is shown in figure 13/1 and involves the marriage of the ideal discriminator and the phase lock loop demodulator. Although a theoretical concept, it is included here because of its mode of operation gives a deeper insight into some of the other concepts discussed. In addition certain patents, e.g. [2], have proposed a similar (phase filter) approach in their versions of threshold extension demodulators, but the practical implementation has been different.

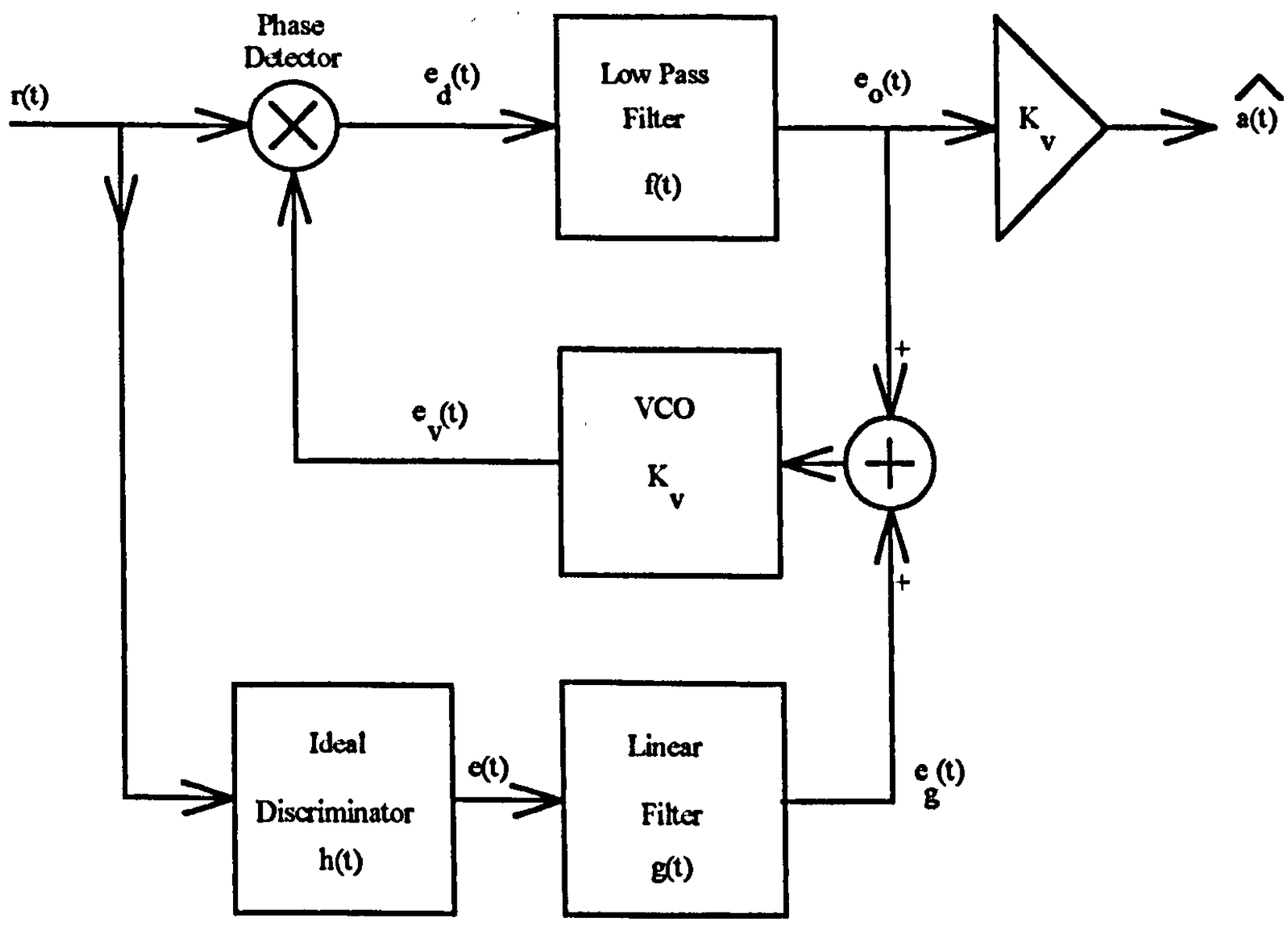

Figure 13/1 Phase Filter Demodulator

In the mathematical model, which is derived below, the structure is shown to be equivalent to a conventional phase-lock loop preceded by a linear filter operating on the phase of the received signal. The following will follow the analysis given by Hummels, but amplified and with a number of the minor errors corrected.

13.2 Analysis

13.2.1 Input signal

Let the input be a frequency modulated signal plus noise, thus:

$$r(t) = \sqrt{(2P_s)} \sin[\omega_c t + \theta(t)] + n(t) \quad \ldots\ldots\ldots \quad (13\text{-}1)$$

Where $$\theta(t) = \int_0^t a(\alpha) d\alpha \quad \ldots\ldots\ldots \quad (13\text{-}2)$$

and $$n(t) = N_s(t)\sqrt{2} \sin \omega_c t + N_c(t)\sqrt{2} \cos \omega_c(t) \quad \ldots\ldots\ldots \quad (13\text{-}3)$$

and P_S = Signal power

$a(t)$ = Modulation or message process,

$N_s(t)$ = In-phase component of noise that is a statistically independent zero-mean Gaussian process

$N_c(t)$ = Quadrature component of noise that is a statistically independent zero-mean Gaussian process

Following the method shown in Chapter 4, and from figure 13/1, it can be shown that:

$$r(t) = A_r(t) \sin(\omega_c t + \theta_r(t)) \quad \ldots\ldots\ldots \quad (13\text{-}4)$$

Where $$A_r(t) = \left[\left[\sqrt{(2P_s)} + \sqrt{2} N_s(t) \right]^2 + 2N_c^2(t) \right]^{\frac{1}{2}} \quad \ldots\ldots\ldots \quad (13\text{-}5)$$

$$\theta_r(t) = \tan^{-1} \left[\frac{N_c(t)}{\sqrt{P_s} + N_s(t)} \right] \quad \ldots\ldots\ldots \quad (13\text{-}6)$$

These relationships are illustrated in the vector diagram of figure 13/2.

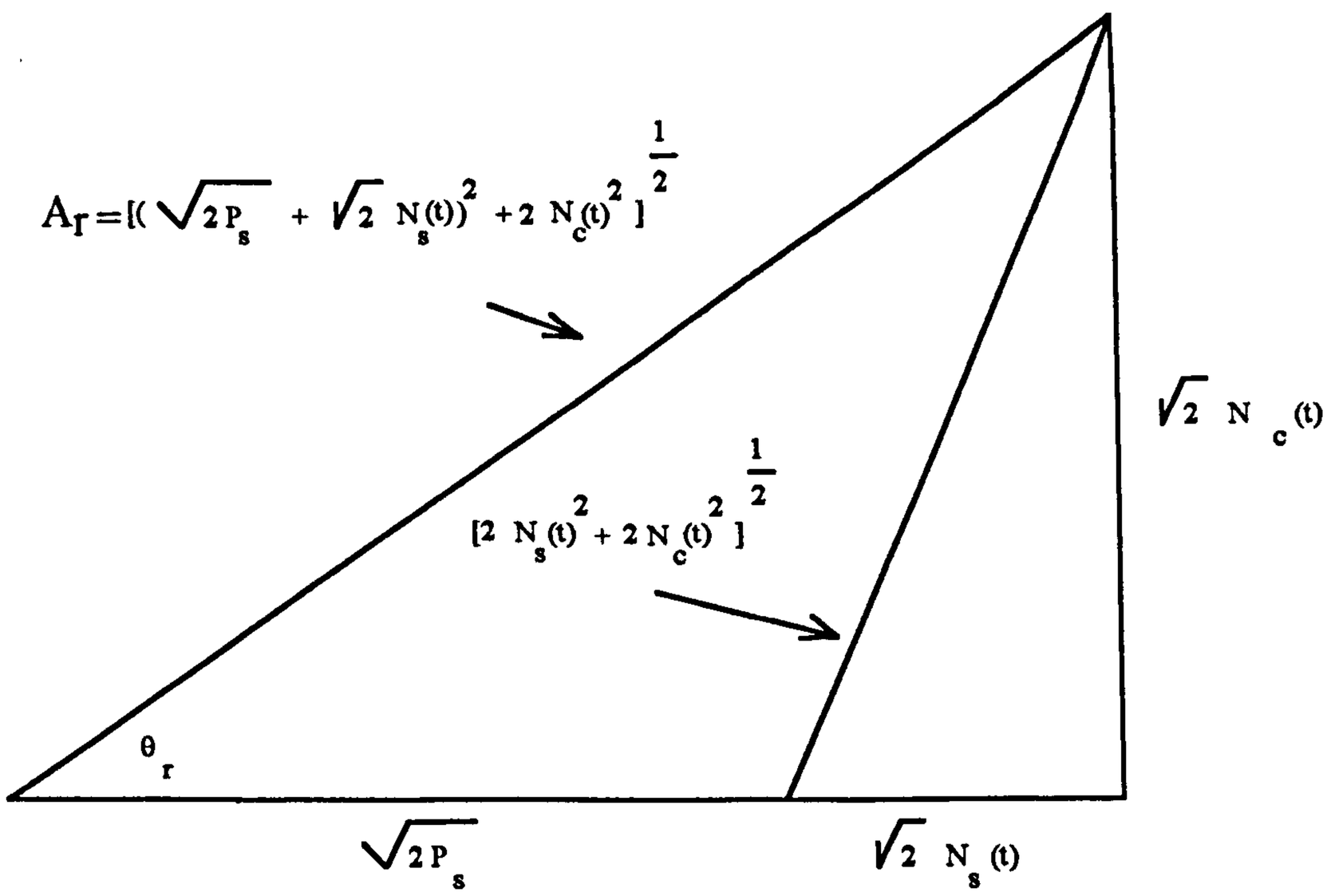

Figure 13/2 Phase Filter Signal Noise Vector Diagram

13.2.2 Determination of discriminator output $e(t)$

With the input defined by equation (13-4), the output of the ideal discriminator (figure 13/1) becomes:

$$e(t) = K\frac{d}{dt}\theta_r(t) \qquad \text{..... (13-7)}$$

Where K is the discriminator constant.

13.2.3 Determination of VCO output $e_v(t)$

The VCO output signal is: $e_v = E_v \cos(\omega_c t + P(t))$ ..... (13-8)

where $P(t)$ is: $P(t) = K_v \int_0^t [\, e_g(\alpha) + e_o(\alpha)\,]\, d\alpha$ ..... (13-9)

Where K_v is the VCO constant

Insert equation (13-9) into (13-8) gives the VCO output signal:

$$e_v(t) = E_v \cos(\omega_c t + K_v \int_0^t [e_g(\alpha) + e_o(\alpha)]\, d\alpha) \qquad \text{.....} \quad (13\text{-}10)$$

13.2.4 Determination of discriminator linear filter output $e_g(\alpha)$

Now $e_g(\alpha)$, the output of the ideal discriminator filter, can be written in terms of the ideal discriminator output, $e(t)$, as:

$$e_g(\alpha) = e(t) * g(t)$$

Thus
$$e_g(\alpha) = \int_0^\infty e(\alpha - u)\, g(u)\, du \qquad \text{.....} \quad (13\text{-}11)$$

Where $g(u)$ is the impulse response of the linear filter, at the discriminator output.

Inserting equation (13-11) into (13-10) gives:

$$e_v(t) = E_v \cos(\omega_c t + K_v \int_0^t [\int_0^\infty e(\alpha - u)\, g(u)\, du + e_o(\alpha)]\, d\alpha) \qquad \text{.....} \quad (13\text{-}12)$$

13.2.5 Determination of phase detector output $e_d(t)$

Forming the product of $r(t)$ and $e_v(t)$ to determine the phase detector output, $e_d(t)$:

$$e_d(t) = r(t)\, e_v(t)$$

$$\therefore \qquad e_d(t) = A_r(t) \sin(\omega_c t + \theta_r(t))\, E_v \cos(\omega_c t + \phi) \qquad \text{.....} \quad (13\text{-}13a)$$

Where from equation (13-12):

$$\phi = K_v \int_0^t [\int_0^\infty e(\alpha - u)\, g(u)\, du + e_o(\alpha)]\, d\alpha \qquad \text{.....} \quad (13\text{-}14)$$

Using the standard trigonometric identities, expand equation (13-14) to give:

$$e_d(t) = A_r(t)\, E_v \left[(\sin \omega_c t \cos\theta_r(t) + \sin\theta_r(t) \cos\omega_c t)\,(\cos\omega_c t \cos\phi - \sin\omega_c t \sin\phi)\right]$$

..... (13-15)

$$e_d(t) = A_r(t)\, E_v \left[\sin\omega_c t \cos\theta_r(t) \cos\omega_c t \cos\phi - \sin^2\omega_c t \cos\theta_r(t) \sin\phi \right.$$
$$\left. + \sin\theta_r(t) \cos^2\omega_c t \cos\phi - \sin\theta_r(t) \cos\omega_c t \sin\omega_c t \sin\phi\right]$$

..... (13-16)

Rearranging the first and fourth terms in the brackets, together with the second and third terms gives:

$$e_d(t) = A_r(t)\, E_v \left[\sin\omega_c t \cos\omega_c t\,(\cos\theta_r(t)\cos\phi - \sin\theta_r(t)\sin\phi)\right.$$
$$\left. + \cos^2\omega_c t \sin\theta_r(t)\cos\phi - \sin^2\omega_c t \cos\theta_r(t)\sin\phi\right]$$

$$= A_r(t)\, E_v \left[\sin\omega_c t \cos\omega_c t \cos(\theta_r(t)+\phi) + (1-\sin^2\omega_c t)\sin\theta_r(t)\cos\phi\right.$$
$$\left. - \sin^2\omega_c t \cos\theta_r(t)\sin\phi\right]$$

$$= A_r(t)\, E_v \left[\frac{1}{2}\sin 2\omega_c t \cos(\theta_r(t)+\phi) + \sin\theta_r(t)\cos\phi - \sin^2\omega_c t \sin\theta_r(t)\cos\phi\right.$$
$$\left. - \sin^2\omega_c t \cos\theta_r(t)\sin\phi\right]$$

$$= A_r(t)\, E_v \left[\frac{1}{2}\sin 2\omega_c t \cos(\theta_r(t)+\phi) + \sin\theta_r(t)\cos\phi\right.$$
$$\left. - \sin^2\omega_c t\,(\sin\theta_r(t)\cos\phi + \cos\theta_r(t)\sin\phi)\right]$$

$$= A_r(t)\, E_v \left[\frac{1}{2}\sin 2\omega_c t \cos(\theta_r(t)+\phi) + \sin\theta_r(t)\cos\phi\right.$$
$$\left. - (\frac{1}{2} - \frac{1}{2}\cos 2\omega_c t)(\sin\theta_r(t)\cos\phi + \cos\theta_r(t)\sin\phi)\right]$$

$$= A_r(t)\, E_v \left[\frac{1}{2}\sin 2\omega_c t \cos(\theta_r(t)+\phi) + \sin\theta_r(t)\cos\phi\right.$$
$$- \frac{1}{2}(\sin\theta_r(t)\cos\phi + \cos\theta_r(t)\sin\phi)$$
$$\left. + \frac{1}{2}\cos 2\omega_c t\,(\sin\theta_r(t)\cos\phi + \cos\theta_r(t)\sin\phi)\right]$$

$$= A_r(t)\,E_v\left[\frac{1}{2}\sin 2\omega_c t\cos(\theta_r(t)+\phi)+\frac{1}{2}\sin\theta_r(t)\cos\phi-\frac{1}{2}\cos\theta_r(t)\sin\phi\right.$$
$$\left.+\frac{1}{2}\cos 2\omega_c t\,(\sin\theta_r(t)\cos\phi+\cos\theta_r(t)\sin\phi)\right]$$

$$= A_r(t)\,E_v\left[\frac{1}{2}\sin 2\omega_c t\cos(\theta_r(t)+\phi)-\frac{1}{2}\sin(\theta_r(t)-\phi)+\frac{1}{2}\cos 2\omega_c t\sin(\theta_r(t)+\phi)\right]$$

$$\therefore \qquad e_d(t)=\frac{A_r(t)\,E_v}{2}\left[\sin 2\omega_c t\cos(\theta_r(t)+\phi)\ +\sin(\theta_r(t)-\phi)+\cos 2\omega_c t\sin(\theta_r(t)+\phi)\right]$$

The wanted product is obtained from the second term, with the second harmonic frequencies being neglected, as they would be filtered out.

Thus:
$$e_d(t)=\frac{A_r(t)\,E_v}{2}\sin(\theta_r(t)-\phi) \qquad \text{.....} \quad (13\text{-}17)$$

Inserting equation (13-14) into (13-17) gives:

$$e_d(t)=\frac{A_r(t)\,E_v}{2}\sin\left[\theta_r(t)-K_v\int_0^t\left[\int_0^\infty e(\alpha-u)\,g(u)\,du+e_o(\alpha)\right]d\alpha\right]$$

$$e_d(t)=\frac{A_r(t)\,E_v}{2}\sin\left[\theta_r(t)-K_v\int_0^t\int_0^\infty e(\alpha-u)\,g(u)\,du\,d\alpha+K_v\int_0^t e_o(\alpha)\,d\alpha\right] \qquad \text{.....} \quad (13\text{-}18)$$

Now from equation (13-7) it can be seen that $\theta_r(t)=\frac{1}{K}\int_0^t e(\alpha)\,d\alpha$ ..... (13-19)

Which in terms of $e(g)$ can be written as:

$$\theta_r(t)=\frac{1}{K}\int_0^t\int_0^\alpha e(\alpha-u)\,\delta u\,du\,d\alpha \qquad \text{.....} \quad (13\text{-}20)$$

Using equation (13-20) allows equation (13-18) to be rearranged in the form:

$$e_d(t) = \frac{A_r(t)\,E_v}{2} \sin\left[\frac{1}{K} \int_0^t \int_0^q e(\alpha - u)\,\delta(u)\,du\,d\alpha - K_v \int_0^t \int_0^q e(\alpha - u)\,g(u)\,du\;d\alpha - K_v \int_0^t e_o(\alpha)\,d\alpha \right]$$

Thus $$e_d(t) = \frac{A_r\,E_v}{2} \sin\left[\int_0^t \int_0^q e(\alpha - u)\left(\frac{\delta(u)}{K} - K_v\,g(u)\right) du\,d\alpha - K_v \int_0^t e_o(\alpha)\,d\alpha \right]$$

$$e_d(t) = \frac{A_r(t)\,E_v}{2} \sin\left[\int_0^t \int_0^q \frac{e(\alpha - u)}{K} \left(\delta(u) - K\,K_v\,g(u)\right) du\,d\alpha - K_v \int_0^t e(\alpha)\,d\alpha \right]$$

..... (13-21)

Substituting $\theta_r(t-u)$ for $\int_0^q \frac{e(\alpha-u)}{K} d\alpha$ and letting $K_d(t) = \left[\frac{A_r(t)\,E_v}{2}\right]$, thus:

$$e_d(t) = K_d(t) \sin\left[\int_0^t \theta_r(t-u)\left(\delta(u) - K\,K_v\,g(u)\right) du - K \int_0^t e_0(\alpha)\,d\alpha \right] \quad \text{..... (13-22)}$$

Now since: $$e_o(\alpha) = \int_0^q e_d(u)\,f(\alpha - u)\,du$$

The loop error, $e_d(t)$, or the equation of operation for the phase filter can be expressed as:

$$e_d(t) = K_d(t) \sin\left[\int_0^t \theta_r(t-u)\left(\delta(u) - K\,K_v\,g(u)\right) du - K_v \int_0^t \int_0^q e_d(u)\,f(\alpha - u)\,du\,d\alpha \right]$$

..... (13-23)

13.3 Mathematical Model

13.3.1 This equation (13-23) allows a mathematical model to be formulated which is shown in figure 13/3. Certain of the functions are equivalent to those in figure (13/1). This diagram shows that the input signal $A_r(t)$ is passed through a linear filter to a conventional phase lock loop demodulator. The impulse response of the linear filter is:

$$h(t) = \delta(t) - K K_v g(t) \qquad \text{..... (13-24)}$$

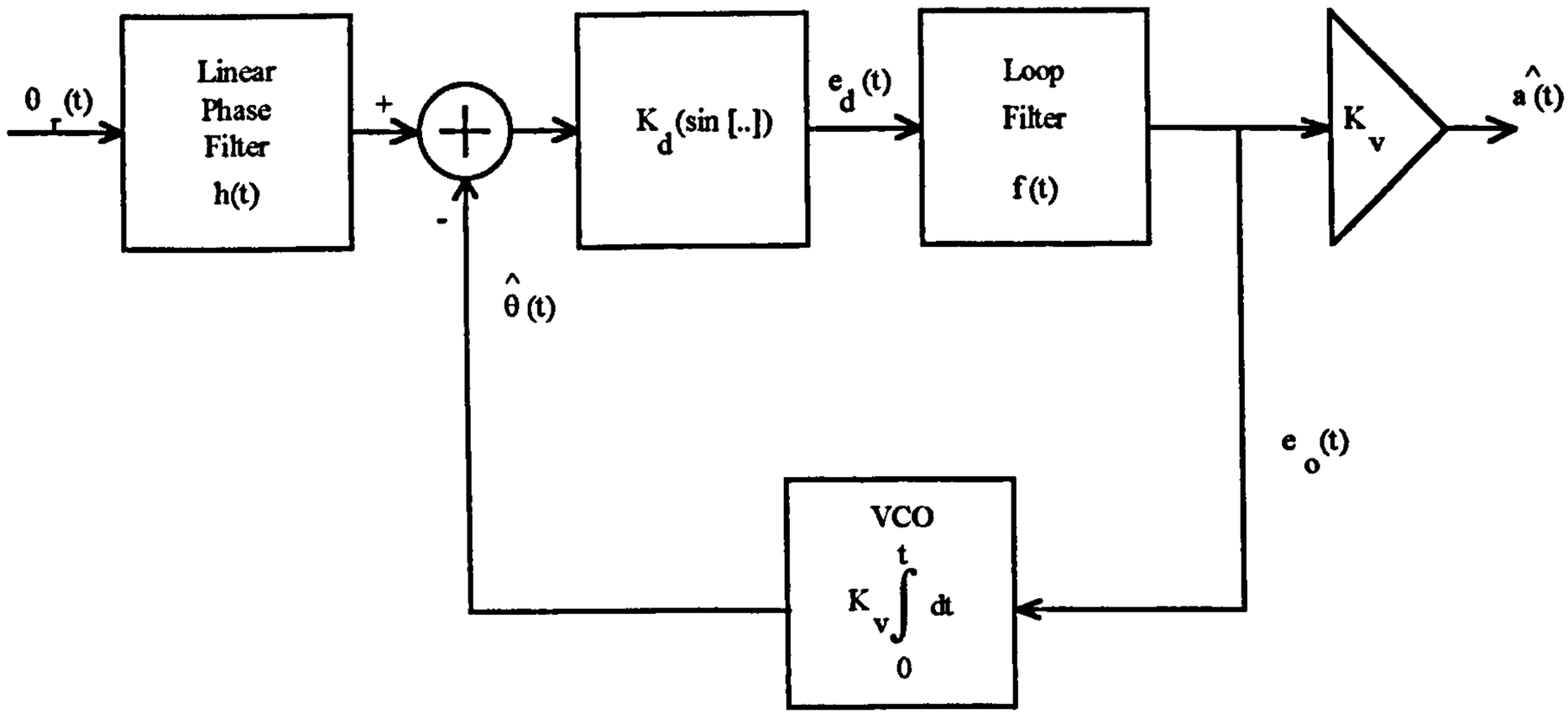

Figure 13/3 Phase filter Mathematical Model

Hummels in his original paper pointed out that since the power spectrum of the message is usually known in advance it should be possible by proper choice of $g(t)$ to design $h(t)$ such as to pass variations in $\theta_r(t)$ whilst rejecting a large portion of the noise. However this would not apply to TV systems such as DBS where one of the sources of threshold extension demodulator difficulties is that the power spectrum is not known.

Hummels gave two interesting examples of this concept; both involve equation (13-24) and how it is treated. The following illustrates the two examples:

13.3.2 Suppose the linear filter at the output of the ideal discriminator in figure 13/1 is a high pass filter g(t) with the transform:

$$G(s) = \frac{s}{s+\lambda} \qquad \text{..... (13-25)}$$

If the gain of the ideal discriminator is adjusted such that $KK_v = 1$, then from equation (13-24), the phase filter $h(t)$ has the transform:

$$H(s) \quad = 1 - G(s) \quad = 1 - \frac{s}{s+\lambda}$$

Which is:

$$H(s) = \frac{\lambda}{s+\lambda} \qquad \ldots\ldots\ldots \quad (13\text{-}26)$$

The equation (13-26) is of a single pole low pass network that appears at the input of the mathematical model shown in figure 13/2.

The value of λ would be set such that the 3 dB cut off frequency of the low pass filter would pass the wanted component of the signal, whilst rejecting the rapid variations due to noise. Hummels indicates that this can be used to minimise the threshold effect due to the noise impulses produced at the output of the demodulator by the anomalous variations in phase $\theta_r(t)$ of the received signal. These result in the noise impulses produced at the output of the demodulator.

If the input contained this anomalous variation then in the scheme proposed by Hummels an impulse would be produced at the output of the ideal demodulator. This would be passed by the high pass filter $g(t)$ even though the data signal was not.

The input to the VCO then consists of the discriminator impulse as well as the data signal component in $e_o(t)$. At the VCO output the phase of the phase detector reference $e_v(t)$ will then increase or decrease in accordance with the impulse from the discriminator.

Therefore when this reference signal is compared with $\theta_r(t)$ there is no error signal produced by the anomalous input. The result is that $e_o(t)$ which is derived from the error signal contains the data signal but not the impulse due to the anomaly. However this does not take into account the energy that is introduced within the wanted modulation bandwidth by threshold clicks.

13.3.3 The second example shows a rather interesting effect. This occurs when:

$$K K_{v} = 1 \qquad \text{..... (13-27)}$$

and $g(t)$ consists of a linear amplifier with gain G such that $0 \leq G \leq 1$. Under these circumstances, the transfer function of the phase filter $H(s)$ is:

$$H(s) = 1 - G(s) \qquad \text{..... (13-28)}$$

Hence $H(s) \triangleq H$ for $0 < H \leq 1$ ..... (13-29)

The phase lock loop of the equivalent mathematical model shown in figure 13/2 thus has an input $H\,\theta(t)$ where H is a number less than unity.

This in effect is a reduction in the effective deviation of the modulated signal as seen by the phase lock loop, thus allowing it to be designed for a narrower bandwidth that would result in an improved threshold.

13.4 Discussion

13.4.1 The above analysis has followed that given by Hummels. The approach is interesting as a theoretical concept but the approach would not be suitable for DBS applications because of the very wide band nature of the latter. The concept illustrates several interesting features. Firstly the mathematical representation of the concept shows the approach consists of a linear phase filter followed by a conventional phase lock loop demodulator. This is again an illustration of how many of the threshold extension demodulator approaches are basically similar.

Secondly system has the potential to reduce the effective deviation of the message (modulation). This characteristic is similar to the concept discussed in other sections (e.g. 9 and 14) of this thesis. Thirdly the impulse cancellation technique inherent in the concept is similar to the spike cancellation technique discussed in section 15 below.

13.4.2 The practical limitations that prevent this concept being put into practice are several. Among these are that an ideal demodulator cannot be realised and a VCO that has its output phase the exact integral of the input is not feasible. Inherently a wide band discriminator is required and the time delay of the discriminator and of the linear filter $g(t)$ must be compensated for. A problem that is not uncommon in threshold extension demodulators as is illustrated in section 12 above.

13.4.3 A limitation of the above analysis is that it treats threshold effects as appearing outside the wanted modulation bandwidth. This is a limitation that is common to many approaches. The fundamental problem being that threshold effects contain clicks, false clicks, doublets and modulation amplitude transients. The basic click that does all the harm contains low frequency energy in the modulation passband. This remains a problem common to all approaches.

13.5 References

[1] Hummels, D. R. "Phase Filter. An Untested Demodulator", Electronic Letters. Vol. 5. No. 26., 27th December 1969, pp. 720-721.

[2] Mobley, J. G. "FM Demodulator System With Threshold Extension", US Patent 4,698,598. October 6th, 1987.

Blank Page

14. SWITCHED CAPACITOR DEMODULATION

14.1 Introduction

14.1.1 The demodulation concept proposed by Mikael and Tu [1] is based upon a frequency compression technique employing switched capacitor oscillators (SCO's). It is a unique and original approach that has attracted little further attention in the literature. The technique is basically to convert the FM signal into a pulse train with a time-varying period. This pulse train is used as the clock controlling the switches of a switched capacitor oscillator. The action of the latter is such that its output contains a component that is a down translated compressed version of the input FM signal. This component allows the following demodulator to operate at a lower centre frequency and to have a narrower bandwidth, thus providing a measure of threshold extension. Since the proposed technique does not require a feedback loop, its realisation and analysis are much simpler compared with the existing methods of threshold extension.

The new class of oscillators utilising switched capacitor techniques was described by Mikael and Tu in reference [2]. The input to the oscillator is a clock and the output is a sinusoidal wave of a frequency that is related to the clock repetition rate by an arbitrary chosen (capacitor) ratio. None of the oscillator components need to be varied to change the oscillator frequency. The oscillation frequency of the switched capacitor oscillator is controlled by the clock repetition rate, and by the number of samples K in each sinusoid oscillation output cycle at the oscillator output. The constant K is independent of the clock. When an FM signal is used as the clock [1], the centre frequency of the output FM signal, as well as the modulation index, is reduced, or scaled down, by a factor of K.

The switched capacitor oscillator proposed for this application is illustrated in figure 14/1, and was briefly analysed in [2]. The version used here is the state variable oscillator whose basic principle of operation is to implement a loop that solves the differential equation

$\ddot{x} + \omega_0^2 x = 0$. The version used here has been realised using the Lossless Discrete Integration (LDI) transform [5]. Two integrators are used in this type of oscillator, the output of each being 90^0 out of phase. Mikael's derivation of the maintaining equation is followed below.

14.2 Principle of operation

14.2.1 The switched capacitor oscillator is a sampled and held sinusoidal wave for a clock of equal periods. Figure 14/1 shows one type of switched capacitor oscillator (LDI realisation) that has a fundamental frequency of oscillation given by equation (14-1).

$$f_0 = \frac{f_c}{\pi} \sin^{-1} \frac{C1}{2C} = \frac{f_c}{K} \qquad \text{..... (14-1)}$$

For an FM input signal, the clock does not have equal repetition periods. The response in this condition is as shown in [1] where the output of the switched capacitor oscillator changes its amplitude in a discrete manner from:

$$A \cos\left(\frac{2n\pi}{K}\right) \qquad \text{..... (14-2)}$$

to

$$A \cos\left[\frac{2(n+1)\pi}{K}\right] \qquad \text{..... (14-3)}$$

This change occurs at the instant of clock state transition and is independent of the clock periods. The analogue FM signal is thus hard limited. The pulse train with a time varying period is used as the clock controlling the switches in the switched capacitor oscillator shown in figure (14-1).

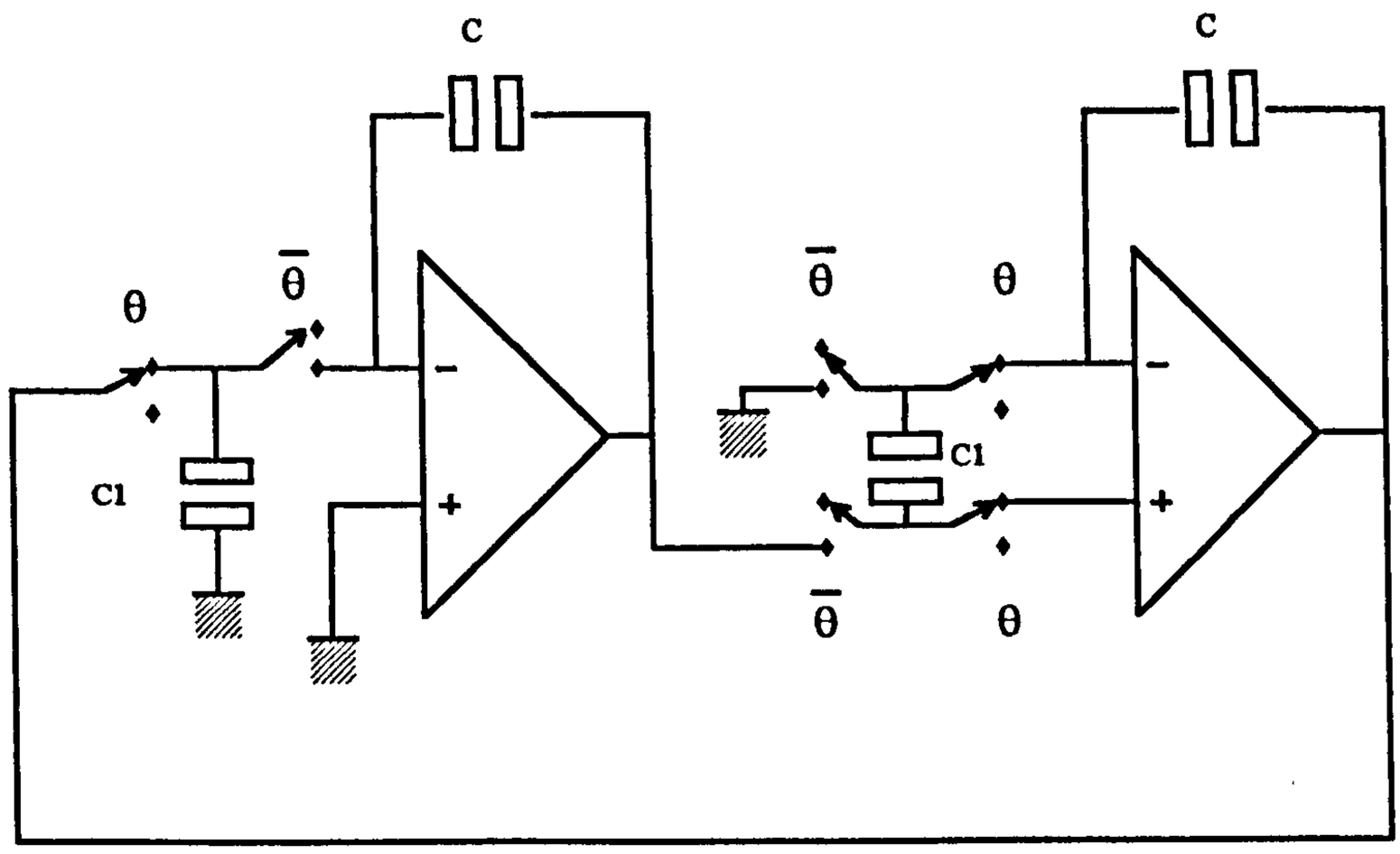

Figure 14/1 State Variable Switched Capacitor Oscillator

Using Lossless Discrete Integrators

Here the output $V_s(t)$ of the switched capacitor oscillator can be written as, [1]:

$$V_s(t) = A \sum_{-\infty}^{+\infty} P(\theta - 2n\pi) \cos \frac{2n\pi}{K} \qquad \text{.....(14-4)}$$

Where the original FM signal is: $V_{IF} = \cos\left[\omega_{cen} t + \psi(t)\right]$ .....(14-5)

In the above let: $\theta(t) = \omega_{cen} t + \psi(t)$ ..... (14-6)

and let $P(\theta)$ be the rectangular function defined as:

$$P(\theta) = +1, \quad for \quad 0 \le \theta < \pi \qquad \text{and} \qquad P(\theta) = -1, \quad for \quad \pi \le \theta < 2\pi$$

and: $P(\theta + 2\pi) = P(\theta)$

Equation (14-4) can be rewritten as:

$$V_s(t) = \left[A\, P(\theta)\right] * \left[\sum_{-\infty}^{+\infty} \delta(\theta - 2n\pi) \cos \frac{2n\pi}{K}\right] \qquad \text{..... (14-7)}$$

$$V_s(t) = A[P(\theta)] * \left(\cos\frac{1}{K}[\omega_{cen} t + \psi(t)] \cdot \sum_{-\infty}^{+\infty} \delta[\omega_{cen} t + \psi(t) - 2n\pi] \right) \qquad \text{.....(14-8)}$$

$$V_s(t) = A[P(\theta)] * \left(\cos\frac{1}{K}[\omega_{cen} t + \psi(t)] \cdot \frac{1}{2\pi}\left[1 + \sum_{n=1}^{+\infty} 2\cos(2n\,\omega_{cen} t + n\,\psi(t)) \right] \right)$$

..... (14-9)

Equation (14-9) contains a frequency component that is the original FM component but compressed in frequency by the factor K . This frequency component is:

$$\cos\left[\frac{\omega_{cen}}{K} t + \frac{1}{K}\psi(t) \right] \qquad \text{..... (14-10)}$$

14.2.2 Mikael and Tu in their paper [1] make several observations concerning the choice of K and particularly the constraints that must be imposed upon it. Firstly the lower limit of K should be chosen so that the unwanted spectra can be removed easily. This implies that K must be greater than 1.

As the centre frequency f_{cen} is divided by the same factor K as the modulation index β then the upper limit of K should be small enough so that $\frac{f_{cen}}{K} >> B_M$ where B_M is the baseband or modulating signal bandwidth. Since the centre frequency of the FM signal can change up or down by heterodyning, then the condition $\frac{f_{cen}}{K} >> B_M$ can always be met whilst satisfying $K >> 1$.

14.2.3 Figure 14/2 illustrates a block diagram of an FM receiver using a switched capacitor oscillator. Apart from the latter it is a conventional FM receiver, where the demodulator operates at a lower frequency. In this circuit an FM signal is heterodyned up or down to the chosen I.F. frequency and applied to the I.F. amplifier. The I.F. output signal is then hard limited and applied to the switched capacitor oscillator. Here the signal is frequency compressed and the centre frequency reduced by the factor K . The output of this compression circuit is then passed through the pre-detection filter and then to the

demodulator where the compressed signal is discriminator. The demodulated signal is finally passed through a post-discriminator filter.

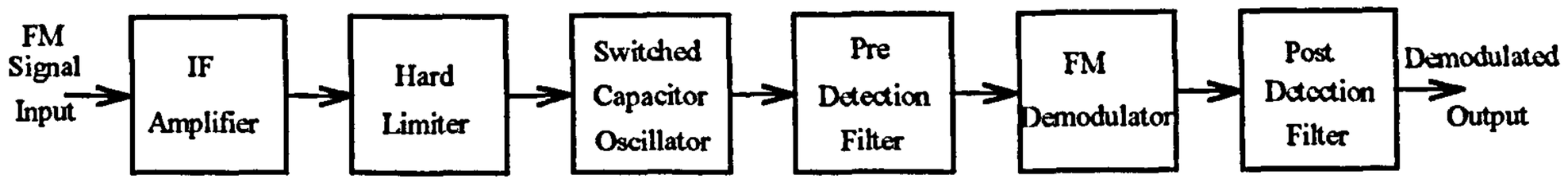

Figure 14/2 Proposed FM receiver using switched capacitor oscillator

14.3 Discussion

14.3.1 The switched capacitor demodulator concept appears very attractive as it is an open loop system without many of the stability problems associated with the more common FMFB and PLL demodulators. To prove the concept reference [1] only gives limited experimental data. Any threshold improvement that occurs is not be due to the frequency compression action itself, but to the reduction in bandwidth of the pre-detection filter that results.

As an illustration of such a technique, consider a D2/MAC system with a switched capacitor oscillator inserted between the I.F. and the pre-detection filter as shown in figure 14/2. Assume also that the I.F. frequency is 140 MHz. The basic characteristics of the D2/MAC system are given in Appendix B and the parameters relevant to threshold extension demodulators are derived and summarised in section 3.3.3. Those that will be used here are:

$$\textit{Modulation index } \beta = 0.93$$

$$\textit{Occupied channel bandwidth } B_c = 27\ MHz$$

$$\textit{Maximum component baseband signal bandwidth } f_M = 7\ MHz$$

$$\textit{Peak-to-peak deviation } D_{P-P} = 13\ MHz$$

The discussion on the restrictions on K given in 14.2.2 above specifies that $\frac{f_{cen}}{K} >> B_M$ or $\frac{f_{cen}}{B_M} << K$. Assume a value of $K = 3$. This gives a centre frequency of 46.6 MHz at

the input to the demodulator and a peak-to-peak deviation of 4.3 MHz. Now using Carson's rule, this is a reduction in occupied bandwidth to some 18.3 MHz giving a threshold improvement in the ratio of bandwidths of $\left(\frac{27}{18.3}=1.47\right)$ or 1.6 dB. On the surface, using typical system characteristics, this is an improvement in performance. However what is not revealed is the effect on the modulation index β and consequently on system performance.

14.3.2 At the output of the I.F. amplifier the modulation index is unity, but at the input to the demodulator it has been reduced to $\frac{B_M}{K}=\frac{1}{3}$. Now this value of β results in the transmission system being classed narrow-band FM, which results in the modulation characteristics being very similar to AM; hence the FM improvement factor is lost. Note that in an FM system it is in the demodulator where the FM improvement occurs. As it does not know that the SCO has been introduced, it considers that the characteristics of the modulation appearing at its input to have originated at the transmitter. This results in the question, what is the point of the SCO? The modulation originating at the transmitter may as well have had these narrow-band FM characteristics to start with. It is this limitation - the effect on the modulation index - which may be why this approach does not appear to have found application.

14.3.3 The SCO concept is mentioned in this report for its originality and for completeness. The approach is unlikely to be suitable for DBS television applications, because of the effect on the modulation index, and because of the difficulty of making a switched capacitor oscillator at the I.F. frequencies involved (c.70 - 140 MHz); although given the current state of the technology it may be just feasible [3-4] at the lower frequency. Although not addressed in reference [1], the effects of edge jitter and clock skew would have a significant effect on the performance of the switched capacitor oscillator and should be closely examined in any future application of this design, together with the effects of low value carrier-to-noise ratio's upon the clock operation.

14.4 References

[1] Mikhael, W. B. and Tu, S. "Frequency Compression Employing Switched Capacitor Oscillators (SCO's) and its application to FM Detection," IEEE Int. Symp. Circuits and Systems 1981. pp. 58 - 61.

[2] Mikhael, W. B. and Tu, S. "Switched Capacitor Oscillators with Linear Frequency Control," IEEE Int. Symp. Circuits and Systems. 1981. pp. 188 - 191.

[3] Ribner, D. B. and Copeland, M. A. "Biquad Alternatives for High Frequency Switched - Capacitor Filters," IEEE Journal of Solid State Circuits, Vol. SC - 20, No. 6, December 1985, pp. 1085 - 1095.

[4] Matsui, K., Matsuura, T., Fukasawa, S., Izawa, Y., Toba, Y., Miyake, N. and Nagasawa, K. "CMOS Video Filters Using Switched Capacitor 14 - MHz Circuits," IEEE Journal of Solid State Circuits, Vol. SC - 20, No. 6, December 1985, pp. 1097 - 1101

[5] Allen, P. E. and Sánchez - Sinencio, E. "*Switched Capacitor Circuits*," Van Nostrand Reinhold Company, New York, 1984, ISBN 0- 442 - 20873 - 1

Blank Page

15. SPIKE CANCELLATION TECHNIQUES

15.1 Introduction

15.1.1 Spike cancellation techniques, otherwise known as click elimination schemes, are the only approaches to threshold extension demodulator design that do not depend upon either an effective reduction in bandwidth somewhere in the demodulator, or on an effective reduction in deviation of the signal, either prior to being applied to, or within the demodulator. This simple and robust approach is thus unique among the various threshold extension demodulators considered in this report. The successful explanation of the noise threshold effect by the model proposed by Rice and the realisation that the clicks are responsible for the effect, resulted in the search for threshold extension by click detection and elimination.

When the input signal is reduced in level, the occurrences of spikes or clicks herald the arrival of the FM threshold. Between the point where they are distinct (first threshold) and the point where they are so numerous that they merge into a continuously distributed interference (second threshold), some form of impulse cancellation may improve demodulator performance. Such an approach usually involves the setting of a threshold to

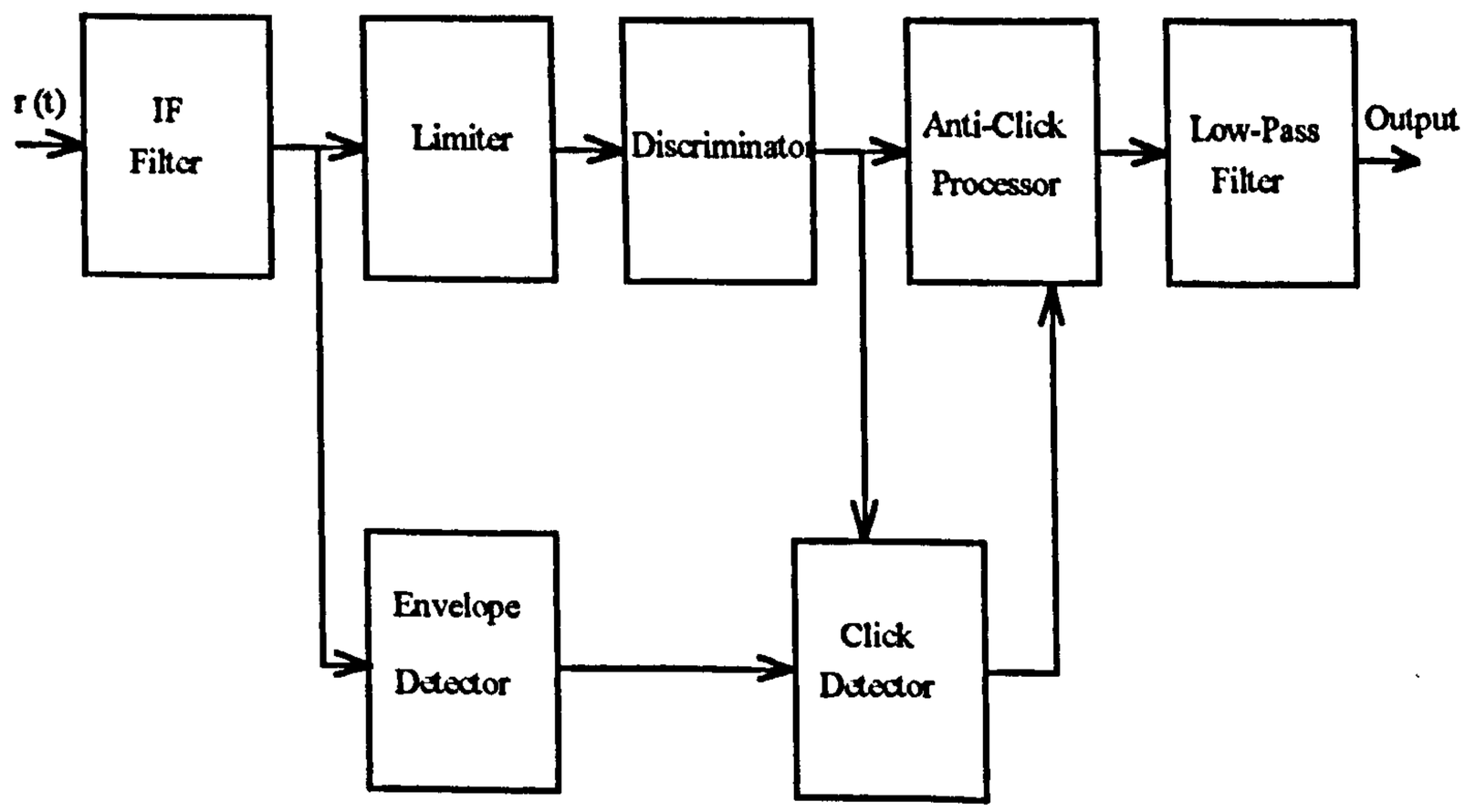

Figure 15/1 FM Demodulator with Click Elimination

indicate the presence of a click and a linear interpolator circuit that operates over the period occupied by the click.

An excellent overall review of this technique is given in the paper by Bar-David and Shamai [1]. Figure 15/1 shows a typical threshold extension FM receiver using click detection and elimination. Inputs to the click detector consist of both the discriminator output (phase derivative) and the envelope detector output of the noisy signal. When a click presence is detected, the anti click processor performs one of the following alternative operations:

(i) It clips the signal during the estimated period of click duration and substitutes an interpolated signal over the clipped interval. This approach is known as the clipping - and - interpolating technique.

(ii) It adds a narrow pulse of area 2π and of opposite polarity to that of the estimated polarity of the click. Hence if the click alert and estimated polarity are correct, the time average of the composite is zero and the residual effects of the click are concentrated at the higher frequencies and thus attenuated by the final low pass filter. This approach is known as the opposite-polarity-compensation technique.

15.1.2 Early work on spike elimination, or click detection was based solely on the presence of the large spike at the discriminator output, [4]-[7]. One immediate apparent difficulty was found to be that large peaks are also frequently due to the modulation. More elaborate detection schemes were thus used to provide additional indications from the instantaneous envelope $R(t)$, [8]-[11]. These relied on the instantaneous envelope characteristic that when a click occurs, $R(t)$ is likely to be small, [12]. This additional information helped to discriminate between clicks and modulation signals, but not between clicks and doublets. Such discrimination is very important in the opposite-polarity-compensation technique for the results are excellent when the detection is successful. However the incorrect detection of a doublet as a click causes as much damage as a missed click. Poor results in extending

the threshold in the early literature led to the suspicion that the Rice model was not valid at carrier-to-noise ratios below the unextended threshold [3], [13]-[14]. However further work showed that the model was indeed a good approximation down to a CNR of some 3 dB, [2]. The difference between the spectral properties of clicks, doublets and modulating signals were examined by Malone, [3], who attempted click detection by observing the output of an appropriately designed filter. This has been extended to improve the threshold further by using information from the instantaneous envelope, $R(t)$, and from a modified Malone type filter, [2]-[3]. Currently the optimum click detection problem remains to be solved.

15.1.3 There is a number of publications, including patents issued, in the field of click elimination demodulation. These can be divided into several categories; the two most important being those that process the clicks on the demodulated signal waveform, [15]-[16], [22], and those that process the actual video or picture signal, [17] - [21].

The Loch-Conrad scheme [15] is the classic click elimination processor that is part of the demodulator. Because of its importance it is described further in section 15.2 below.

Sato and Sugai, [16], in their patent described a noise suppressing circuit in which the signal, from which the noise is detected, is taken from the front end of the receiver and a correction to the noise is made prior to demodulation. It is only mentioned here as the technique does not deal with threshold induced noise, but with external impulsive noise. It is of interest as the problems encountered in threshold circuits occur in this design and the methods used to circumvent them, are similar.

Ardito and Barbieri [21] in their 1972 paper describe a technique for use with PAL coded TV colour signals where the impulse noise at the output of a phase lock loop demodulator is processed to remove unwanted information. In this approach the video signal has the threshold spikes detected and deleted and the wanted information is reconstructed by a prediction method termed 'contiguous lines acknowledgement'. In this approach the

performance improvement claimed with the noise suppression circuit is some 2 dB. This is in addition to the unquantified improvement obtained with the phase lock loop demodulator. However it is hinted that the system efficiency is less noticeable with certain critical pictures. The technique does not appear to deal with false clicks and doublets, or with multiple clicks occurring on the same line. Nevertheless the approach is of interest for several reasons. Firstly it is one of the earliest approaches where two threshold extension devices are operated in tandem; secondly, the performance measurements are very carefully made and based upon CCIR defined techniques. They are thus well documented. Finally it is one of the earliest approaches where TV lines are processed. However the technique has not found subsequent popularity, since apart from [22] the approach does not appear to have been used again.

Brofferio and Rocca [22] in their 1972 letter also described a threshold noise suppression circuit, at the output of a phase lock loop demodulator, for use with monochrome TV signals. The system described operated on the same principle as the Ardito and Barbieri [21] circuit, but in this case a performance improvement of some 3 dB is claimed.

Drewery [17] describes a technique for processing PAL colour TV signals. The technique although complex is an elegant method of reducing the effects of noise in the TV signal. It basically functions by comparing the luminance and chrominance signals with those that occurred 624 lines earlier. By subtracting these signals from their respective earlier signals, difference signals are obtained which contain components of any noise that has occurred. Low amplitude portions of this signal are assumed to represent noise and are attenuated, and high amplitude portions are assumed to represent a change in picture detail. The difference signal is modified and is added to the signal for the proceeding scan to provide a signal for the current scan in which the effects of noise have been subjectively reduced. Drewery's patent concentrates on the predictor for this scheme.

Maeyama and Naga [18] describe a comb filter circuit for the suppression of unwanted noise. The design deals with an undesired chrominance signal superimposed on the

luminance signal that results in 'dot' interference during the occurrence of decorrelation in the colour information of a line period and the next line period, can be easily removed in any type of comb filter circuit that separates a high frequency luminance signal component and a chrominance signal component by the provision of multipliers in the detection circuit. No information is contained in the publication of its performance, particularly under threshold conditions.

Sato [19] describes a further embodiment of the comb filter approach. Here the video processing circuit uses a comb filter that includes a delay circuit having a delay time of one or two horizontal scan intervals. The comb filter contains two mixers to split the chrominance and luminance signals. The first mixer is provided with input and output signals of the delay circuit in opposite polarity to each other. The second mixer is provided with an inverted output of the first mixer and the non delayed input to the first mixer. The separated signals from the first and second mixers are processed through processing circuits such as noise cancellers and emphasis circuits. The two processed signals are mixed in a third mixer to synthesise a composite colour video signal without distortion, false signals or delays at the edge of the input signal.

Raven [20] describes a technique that is a further development of Drewery's [17] approach. Raven claims that Drewery's approach results in travelling noise patterns and proposes a solution to these effects. The video signal noise suppression circuit he describes separates the video signal into its high and low frequency components. The signal at the output of a delay circuit is combined with the separated low frequency signal in a combining circuit whose output is applied to the input to the delay circuit. The time delay of the delay circuit is switched from field to field so that this time delay change from field to field, to a field period minus, and a field period plus, half a line period. The noise suppressed low frequency output from the combining circuit is added to the separated high frequency component in an adder circuit. In use, Raven claims that the circuit does not produce travelling noise patterns in a TV display.

Bush, et al. have also proposed a delayed approach in their patent [23] for achieving threshold extension. Although their technique, shown within the dotted outline in figure 15/2, is designed around a phase lock loop demodulator, it is basically a click suppression technique and could be applied to any demodulator. This approach is also a tandem threshold extension system with a phase lock loop demodulator followed by a click suppression circuit. The design claims to detect the conditions that cause the click impulses, rather than the presence of such impulses, and then effectively eliminate that portion of the demodulated signal that contains the click impulse. The detector in figure 15/2, compares the I.F. signal with the demodulated output, and if there is any missing or additional pulse activates the control signal generator to delete that portion of the contaminated signal, The latter is delayed to allow this action to occur.

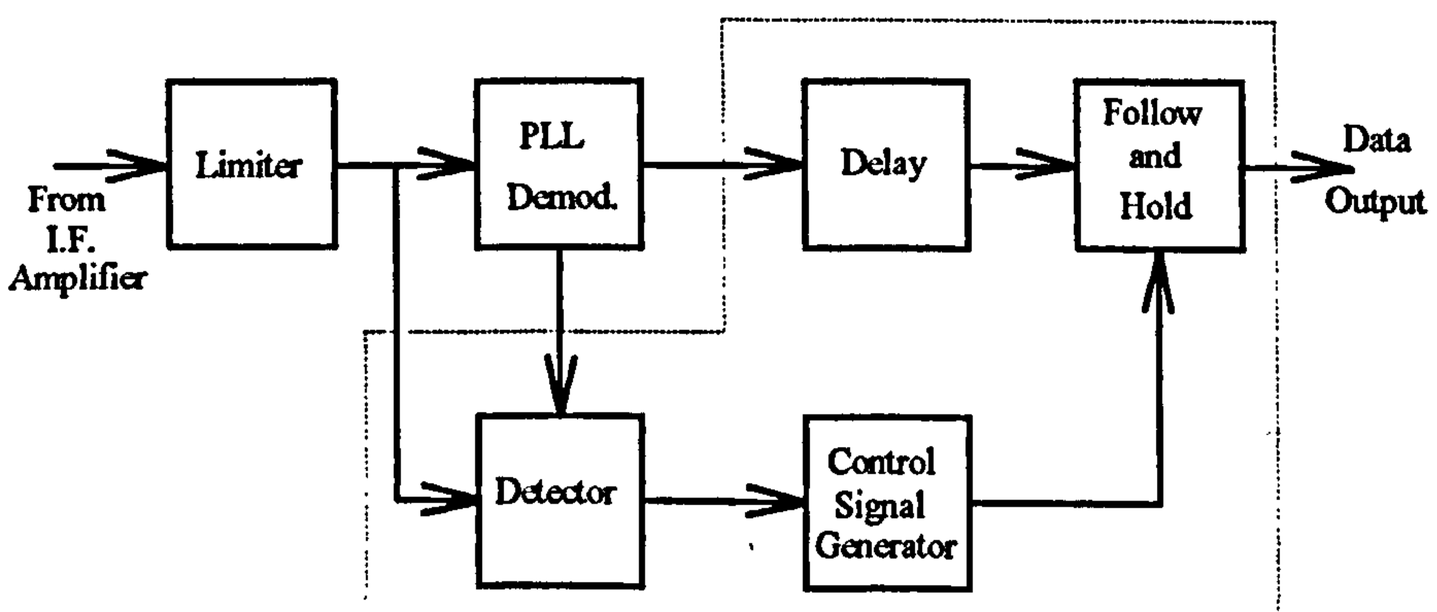

Figure 15/2 Bush FM Demodulator

The problem that with this approach is that the detector will have a threshold characteristic. In addition the approach does not appear to discriminate between clicks, false clicks and doublets. Little performance data is given in the reference.

15.2 Loch-Conrad scheme

15.2.1 Of those designs that process the clicks on the demodulated signal waveform, one of the most important is an early scheme due to Loch and Conrad, [6], [15]. The Loch-Conrad scheme [15] is illustrated in figure 15/3. Note that this scheme operates on the output of the demodulator.

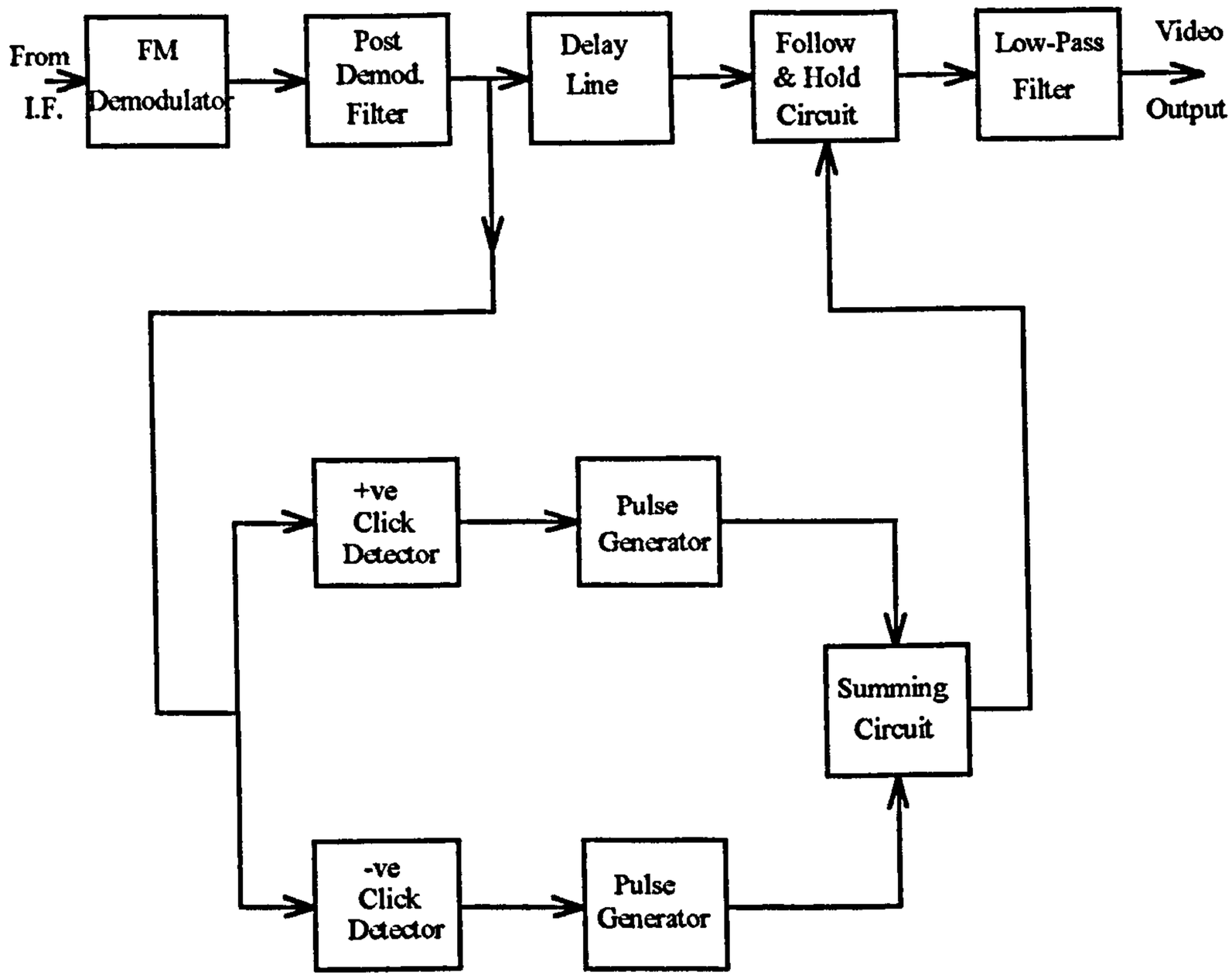

Figure 15/3 Loch-Conrad Click Elimination Scheme

It effectively processes the demodulated output by inserting a click elimination circuit between the output of the demodulator and the input of a low pass filter. At the output of the demodulator there is a post-demodulation filter, which is a matched filter, and whose function is to minimise the effects of Gaussian noise spikes contained at the output, whilst allowing the clicks that have a strong low frequency component to attain their full amplitude.

The circuit has two operating modes. The first or normal mode is when the signal is above threshold and not corrupted by clicks or spikes. In the first or normal operating mode the demodulated video signal is transferred directly from the post demodulation (matched) filter output to the low pass filter input.

In the second mode when a noisy signal is received, which is below threshold and clicks

occur, the actual signal is disconnected and an estimated signal value is connected to the low pass filter that has been based on a previous value of the actual signal. Any positive or negative going click is detected by the respective click detector. This detection is achieved by the clicks exceeding a predetermined signal level. When the relevant click detector detects the positive or negative going click, it produces an output that triggers the respective pulse generator. The pulse generator produces a narrow output pulse whose width duration is equal to the duration of the click impulse plus the delay line period. The pulses from each pulse generator are combined in the summing circuit to produce a single pulse chain. This pulse operates the follow-and-hold circuit that switches the latter to the hold condition for the duration of the click. At the termination of the control pulse the follow-and-hold circuit resumes transfer of the actual signal.

The holding action of the follow-and-hold circuit performs two actions. The first is to prevent passage of the clicks to the low pass filter, and secondly, it fills in the holes and gaps that would otherwise be produced in the signal supplied to the filter. These holes are filled in with signal values corresponding to estimates of what the signal value would have been in the absence of click impulses.

The delay line compensates for the time lag between the instant of time that the click impulse appears at the output of the matched filter and the instant of time that the clock impulse reaches full amplitude so that it can be detected by the appropriate click detector.

Bar-David and Shami's in their paper [1] indicate that the technique is not very successful because it does not discriminate between clicks, false clicks and doublets. It is however still an important design approach as it clearly shows how click eliminate circuits function.

15.3 Discussion

15.3.1 This limited review of click and elimination techniques have shown that many attempts have been made to use this technique to achieve threshold extension, but with

limited success. Using the click elimination technique in tandem with a threshold extension demodulator does not offer much advantage as the performance figures quoted are of the same order as the threshold extension demodulator. Where in carefully controlled conditions the click technique has been made to work the results achieved are good. As has been shown with previous demodulators the basic problem is in discriminating between clicks, false clicks, doublets and modulation spikes and in correctly activating the click elimination circuitry. Current trends are to use an appropriately designed filter to do this discrimination. But with complex signal (picture) structures this is unlikely to prove a satisfactory permanent solution.

Brief mention has been made of those click elimination techniques, which do not form part of the demodulator but operate upon the video signal. These are strictly signal processing approaches, and are mentioned here to shown the number of approaches that have been made to try to solve the threshold extension problem.

15.4 References

[1] Bar-David, I. and Shami, S. "On the Rice Model of Noise in FM Receivers". IEEE Transactions on Information Theory, Vol. 34, No. 6, November 1988, pp 1406 - 1419.

[2] Polacek, M., Shami, S. and Bar-David, I. "On Threshold Extending FM Receivers," IEEE Transactions on Communications, Vol. 36, No. 3, pp 375 - 380, March 1988.

[3] Malone, M.. "FM Threshold without Feedback," Proc. IEEE, No. 56, pp 200 - 201, 1968.

[4] Schilling, D. L., Hoffman, E., and Nelson, E. A. "Error Rates for Digital Signals Demodulated by an FM Discriminator," IEEE Transactions on Communications Technology, Vol. COM-15, pp 507 - 517, August 1967.

[5] Rainal, A. J. "Optimal Detection of FM Clicks," IEEE Transactions on Information Theory, Vol. IT-28, No. 6, November 1982, pp 971 - 973.

[6] Loch, F. J. "Threshold Extension Techniques using Impulse Noise Elimination," Proc. Nat. Telecommunications Conf., 1969, pp 545 - 549.

[7] Arndt, G. D. and Loch, F. J. "Correlation Detection of Impulse Noise for FM Threshold Detection," Proc. IEEE, No. 58, pp. 1141 - 1143, 1970.

[8] Guida, A. and Schilling, D. L. "Optimum FM Discriminator Type Demodulation," Proc. Int. Communications Conference, 1967, p.58.

[9] Calandrino, L. and Immovilli, G. "Coincidence of pulses in amplitude and frequency deviations produced by a random noise perturbing an FM wave: An amplitude - phase correlation FM demodulator," Alta Frequenza, Vol. 36, pp. 170E - 175E, August 1967.

[10] Calandrino, L. and Immovilli, G. "On the performance of amplitude phase correlation FM demodulators," Alta Frequenza, Vol. 37, pp. 19E - 25E, February 1968.

[11] Calandrino, L., Graffi, S. and Immovilli, G. "Correlation and statistical dependence between envelope and frequency deviation of a sine wave plus random noise," Alta Frequenza, Vol. 36, pp. 15E - 19E, 1967.

[12] Blachman, N. M. and Roberts, J. H. "FM click rates: A simple derivation," Electronic Letters, Vol. 10, No. 15, pp. 305 - 307, July 1974.

[13] Yavuz, D. and Hess, D. T. "False clicks in FM detection," IEEE Transactions on Communications Technology, Vol. COM-18, pp 751 - 756, December 1970.

[14] Roberts, J. H. "*Angle Modulation*," England, Peter Pereginus, 1977.

[15] Loch, F. J., Conrad, W. M. "Frequency - Modulation Demodulator Threshold Extension Device", U.S. Patent 3,588,705, June 28th, 1971

[16] Sato, R., Sagai, Y., "Noise Suppressing Device in FM Receivers", U.S. Patent 4,326,297, April 20th, 1982.

[17] Drewery, J. D. "Circuitry Providing A Delayed Colour Television Signal Having Luminance and Chrominance Components Derived from Adjacent Lines", U.S. Patent 4,223,341, September 16th,1980.

[18] Maeyama, T., Nakata, H., "Comb Filter Circuit", U.S. Patent 4,241,363, December 23rd, 1980.

[19] Sato, I., "Video Signal Processing Circuit with Comb Filter", U.S. Patent 4,355,333, October 9th, 1982.

[20] Raven, J. G., "Noise Suppression Circuit for a Video Signal", U.S. Patent 4,390,894, January 28th, 1983.

[21] Ardito, M., Barbieri, G. F., "Threshold Noise Suppressor in FM Demodulators for TV Signals", International Broadcasting Convention, September 25 29th, 1978, IEEE Conference Publication, No. 166, pp. 46 - 49.

[22] Brofferio, S., Rocca, F. "Threshold - Extended FM Demodulator for Black and White Video Signal", IEEE Trans. on Communications, April 1972, pp. 235 - 242.

[23] Bush, J. A., Lance, D. R., Alstatt, J. E. "Frequency modulation demodulator threshold extension device." US Patent 3,983,488 (Sept. 28, 1976).

Blank Page

16 MISCELLANEOUS THRESHOLD EXTENSION DEMODULATOR TECHNIQUES

16.1 Introduction

This section discusses those threshold extension demodulator techniques that have been discussed in the technical literature, mainly as theoretical concepts. Little subsequent interest appears to have been shown in some of them. They are mentioned here for completeness. Two techniques are briefly discussed, namely Envelope Multiplication and Optimum Demodulation. A further method has been mentioned in the literature [5], that of Optimal Non-linear Filtering, but it is not discussed here.

16.2 Envelope Multiplication

16.2.1 General

Envelope multiplication is a technique investigated by Roberts [1], [2], as a means of improving performance below threshold. Figure 16/1 illustrates the concept. It is an approach that has not attracted any significant subsequent interest, possibly because the technique has the disadvantage that the performance suffers severe degradation at high deviations and signal-to-noise ratios. This characteristic is similar to that of the Hamer and Park demodulators discussed in section 12. A limited discussion is given below, based upon references [1] and [2].

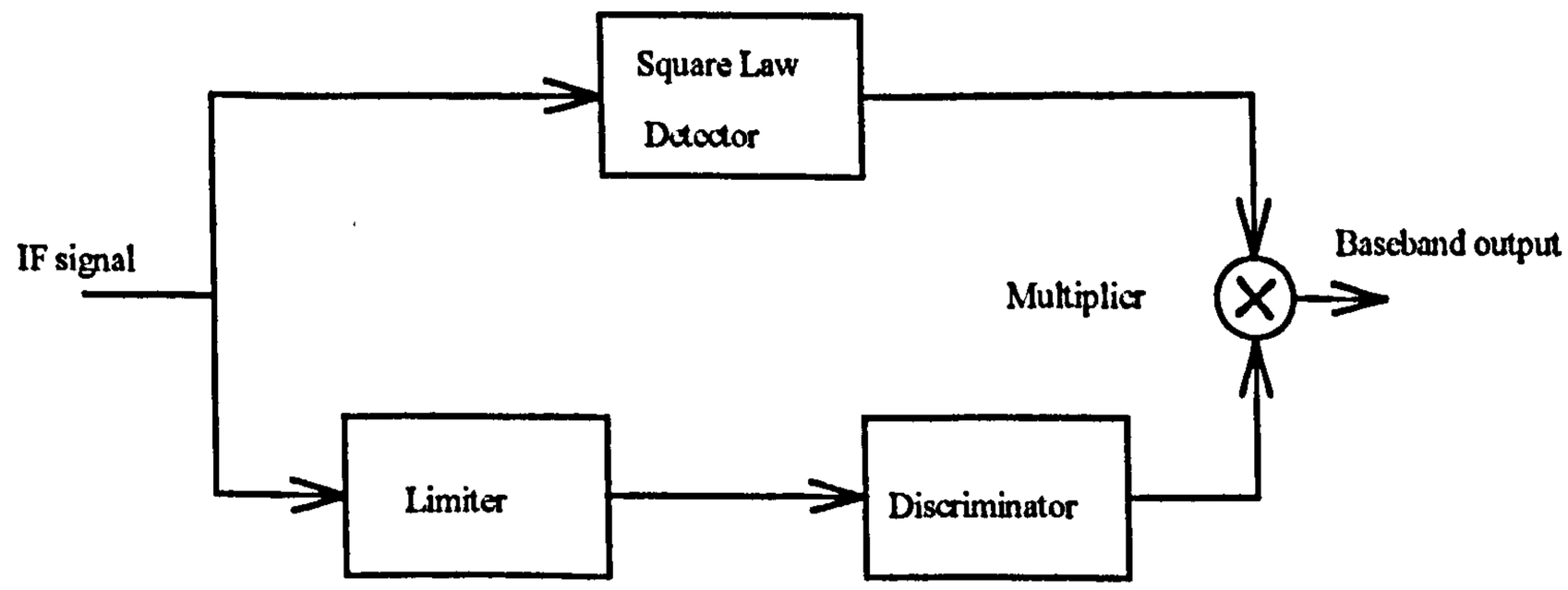

Figure 16/1 FM Demodulator incorporating multiplication by square of envelope

16.2.2 Discussion

The envelope multiplication technique offers an improvement over the demodulation capability of a conventional FM limiter-discriminator in the region well below threshold. In reference [2], Roberts' points out that although a limiter is specifically included in a conventional limiter-discriminator arrangement to remove amplitude fluctuations, it would initially appear that the envelope can play no part in the demodulation process once limiting has been effected. Roberts' shows however a close examination of the conventional FM limiter-discriminator reveals that the square of the envelope appears as the denominator in the expression for the discriminator output, viz.

$$\dot{\theta}(t) = \frac{P(t)\,\dot{Q}(t) - Q(t)\,\dot{P}(t)}{R^2(t)} \qquad \text{..... (16-1)}$$

where: $P(t)$ = In-phase component of general narrow-band transmission

$Q(t)$ = Quadrature component of general narrow-band transmission

$R(t)$ = Envelope of input waveform.

$\dot{\theta}(t)$ = Demodulated output

Roberts' argument is that as the envelope squared factor appears in the denominator of the output expression of a conventional limiter-discriminator output, then when the output becomes small it is likely that a click will appear in the demodulated output (see chapter 4 above). This click will be significantly reduced in level if the demodulated output is multiplied by the square of the envelope. It is this argument that leads to the demodulator scheme shown in figure 16/1. In this diagram it can be seen that the incoming signal from the I.F. amplifier is split into two paths, one is fed to a conventional limiter-discriminator and the other to a square law detector. the outputs of both parts is combined in a multiplier stage, the output of which forms the output of the demodulator.

The procedure of multiplying by the square of the envelope means that when a click is about to occur in the normal manner the envelope level is dropping and the result of the

multiplication is presumed to be that the output signal no longer contains sharp individual peaks (clicks). However in exchange for this apparent immunity from click noise, the demodulated output contains additional 'noise' and 'noise times modulation' components that are not present in a conventional demodulator. However as has been discussed in chapter 4 a reduction in the envelope level does not necessarily imply the occurrence of a click, thus the multiplication process is introducing some undesirable modification of the demodulated signal at such times. Roberts [1] points out that because of the uncorrelated terms that contribute to the demodulated output, multiplication by a function of $R(t)$ that is of a degree higher than two, cannot be expected to lead to an improvement in the balance of signal and distortion or noise. Therefore for multiplication by a function of the envelope to be effective, the degree of the function of $R(t)$ should not exceed two. The simplest cases are multiplication by the envelope, multiplication by the square of the envelope, or some combination of the two.

16.3 Optimum Demodulation

16.3.1 General

Among other techniques [3] for the demodulation of FM signals are two statistically optimum methods that offer a possible improvement in threshold performance. Although for DBS TV applications these techniques cannot be used in real time, they are briefly discussed here for completeness. Kobos [4] has given an excellent summary of both approaches.

16.3.2 Brief analysis

Detection theory is based upon deciding whether or not a specific signal waveform is present in a given interval. Continuous estimation is the process of deriving from the received signal an estimate of the desired signal waveform.

Optimal demodulation of angle modulated signals consists of applying continuous

estimation techniques through the use of estimators based upon two statistical criteria of optimisation, namely:

(i) Maximisation of the a posteriori (MAP) probability of the modulating signal.

(ii) Minimisation of the mean - squared error (MMSE) between the modulation and estimated signal.

Both techniques are briefly discussed below.

The maximum a posteriori (MAP) receiver is one that produces as its output the most probable estimate of the modulating signal, utilising all the pertinent statistics of the modulation signal and noise as well as the received signal. The system being considered is shown in figure 16/2. Here the modulating signal, $a(\tau)$, frequency modulates a sine wave to produce $e_2[\tau, a(\tau)]$. The noise, $n(\tau)$, is added to the modulated signal producing $e_1 = e_2[\tau, a(\tau)] + n(\tau)$ upon which the demodulator operates to produce the estimate $a^*(\tau, t)$ that is the most probable $a(\tau)$.

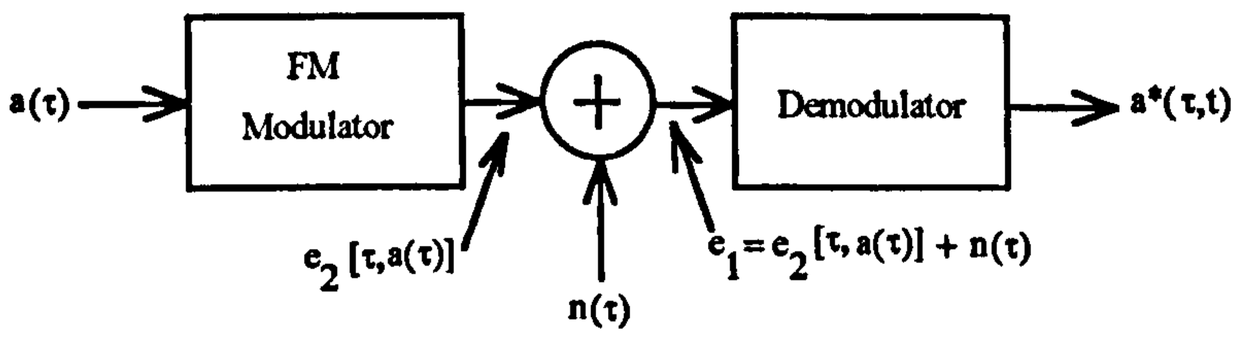

Figure 16/2 Demodulator Model

For frequency modulation the expression shown in equation (16-2) gives e_2 where ϕ represents the unknown phase at the start of the observation period.

$$e_2[\tau, a(\tau)] = E_0 \sin\left[\omega_o \tau + \beta \int_{t-T}^{t} a(u)\, du + \phi\right] \quad for \quad t - T \le \tau \le t \qquad \text{..... (16-2)}$$

The modulating signal and the noise are assumed to be independent Gaussian processes

with zero mean and continuous covariance functions $R_a(s,\tau)$ and $R_n(s,\tau)$. Kobos in his paper [4] gave two non-linear integral equations for the frequency modulation case, given here as (16-3) and (16-4), whose simultaneous solution gives a^*, the maximum a posteriori estimate of the modulating signal.

$$a^*(\tau,t) = E_0 \beta \int_{t-T}^{t} \cos\left(\omega_0 x + \beta \int_{t-T}^{x} a^*(u,t)\,du + \phi \right) \left(\int_{t-T}^{x} R_a(z,\tau)\,dz \right) g(x)\,dx \quad \text{..... (16-3)}$$

$$e_1(x) = E_0 \sin\left(\omega_0 x + \beta \int_{t-T}^{x} a^*(u,t)\,du + \phi \right) = \int_{t-\tau}^{t} g(z)\, R_n(x,z)\,dz \quad \text{..... (16-4)}$$

Kobos [4] states that for the infinite delay case, where T goes to infinity and for angle modulation, a solution to these equations can be obtained by using a phase lock loop demodulator with a non realisable filter. For high input signal-to-noise ratios the equations can be linearised allowing a realisable filter to be used within the loop, followed by a compensating filter outside the loop.

Instead of maximising the a posteriori probability, it is possible to minimise the average value of the square of the difference between the estimated signal and the desired signal. Since the value of the modulation waveform at any given time is, in effect, a random variable, the task of an MMSE receiver is to find the conditional expectation of the message that was sent given the received signal waveform. Under defined conditions the MMSE receiver performance can be shown to be equivalent to the MAP receiver performance.

16.4 Discussion

16.4.1 Roberts's concept [1], [2], for multiplying the demodulated signal by the square of the envelope although a sound theoretical concept does not appear to have been exploited. Roberts points out that a conventional demodulator cannot be improved upon at high carrier-to-noise ratios, but when the carrier-to-noise ratio is low and at or below threshold,

then signal suppression occurs. By multiplying by the square of the envelope the effect of signal suppression is reduced. This means that with this technique a (low) carrier-to-noise ratio exists below which the performance is superior to a conventional demodulator. A possible application of the technique is discussed in chapter 18 below.

16.4.2 Kobos's optimal demodulation results [4] indicates that all properly designed demodulators for angle-modulated signals can achieve the same performance above threshold with the major difference being the location of the threshold. For specific simulations there is no significant difference in the threshold location for MAP and MMSE receivers. Kobos indicates that a significant improvement in the demodulation of angle modulated signals may be possible if the application does not require real time processing. For DBS TV applications this approach is currently not feasible.

16.5 References

[1] Roberts, J. H. "*Angle Modulation*", Peter Peregrinus Ltd., England, 1977.

[2] Roberts, J. H. "Multiplication by Square of Envelope as a means of improving detection below the FM Threshold", IEEE Trans. Communication, COM - 18, 1971, pp. 349 - 353.

[3] Blachman, N. M. "*Noise and its effects on Communication*", McGraw - Hill, 1966.

[4] Kobos, A. "Optimum Detection of FM Signals", Proc. Int. Comms. Conf., 1968, pp. 476 - 481.

[5] Galdos, J. "A lower bound on filtering error with application to phase demodulation", IEEE Trans. Information Theory, Vol. IT-25, No. 4, pp. 452-462, July 1979.

17. EQUALITY OF THRESHOLD EXTENSION DEMODULATORS

17.1. General

Among the most interesting area of threshold extension demodulators, the work of Hess [1] in the equivalence of demodulators was notable. This work was concerned with showing that the frequency lock loop (FLL) and the phase lock loop (PLL) demodulators were limiting forms of the FMFB demodulator without a limiter in the loop. Cassara [2] developed the theory further and showed that the limiting forms of the FMFB demodulator, with a limiter in the loop, were the PLL and the conventional limiter discriminator. An interesting result is that the PLL was the common limiting form of both approaches.

These demonstrations of equivalence allow a deeper understanding of the FMFB and offer approaches of improved demodulator design. Chapter 18 below examines the possibility of using this work to develop an error controlled adaptive threshold extension demodulator that, depending upon the input carrier-to-noise value, changes its configuration from a FLL, through a FMFB, to a PLL. This section concentrates on the FMFB without a limiter and is an amplified version of Hess's approach.

17.2 Equivalence of PLL, FLL and FMFB demodulators

17.2.1 Introduction

The previous chapters in this thesis have shown how similar many of the approaches are in attaining threshold extension, either in reducing the bandwidth or the effective deviation. This section follows and develops Hess's method of equivalence [1] in deriving the frequency defining equations for the three most popular threshold extension demodulator approaches and considering the limiting conditions for a large and small I.F. bandwidth on the defining equation for the FMFB.

17.2.2 Frequency locked loop defining equation

Figure 17/1 shows a block diagram of the frequency locked loop operating at baseband. Assume that the general form of the input is:

$$e_1(t) = a(t)\cos\left[\omega_o t + \psi(t)\right] \qquad \text{..... (17-1)}$$

The expression given in (17-1) represents a carrier with frequency ω_o modulated by an amplitude $a(t)$ and a phase $\psi(t)$. The amplitude $a(t)$ arises when the FM carrier is added to narrow band noise centred about ω_o. The phase $\psi(t)$ consists of the desired FM modulation plus perturbations from the narrow band noise.

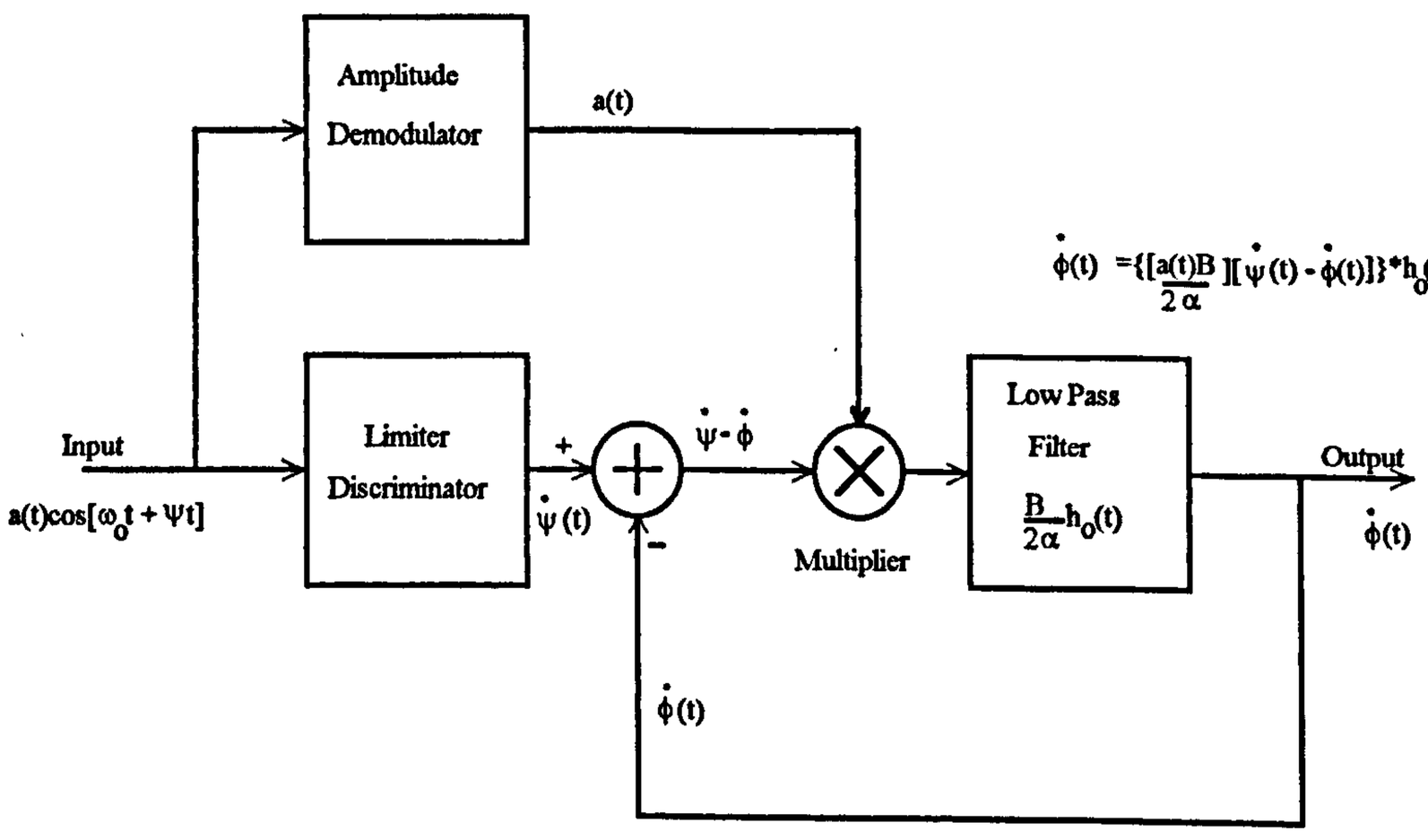

Figure 17/1 Block Diagram frequency Lock Loop

The limiter discriminator constant and the amplitude demodulator constant are taken as unity. From figure 19/1 the output of the limiter-discriminator is thus $\dot{\psi}(t)$ and the output of the summing network is $\left[\dot{\psi}(t) - \dot{\phi}(t)\right]$. The output of the multiplier then becomes $a(t)\left[\dot{\psi}(t) - \dot{\phi}(t)\right]$. This output is then applied to the loop filter with which the entire loop constant $\left(\frac{\beta}{2\alpha}\right)$ is associated. The impulse response of the loop filter is $h_o(t)$. The loop

constant $\left(\frac{\beta}{2\alpha}\right)$ was chosen by Hess so that the following equivalencies are more evident.

If the output of the frequency locked loop is defined as $\dot{\phi}(t)$, then from figure 19/1 the defining equation can be seen as being:

$$\dot{\phi}(t) = \left\{\frac{a(t)\,\beta}{2\alpha}\left[\dot{\psi}(t) - \dot{\phi}(t)\right]\right\} * h_o(t) \qquad \text{..... (17-2)}$$

Where * denotes convolution.

17.2.3 Phase locked loop defining equation

Figure 17/2 shows a block diagram of the phase locked loop operating at baseband. The same input and output signals are assumed as given above for the frequency locked loop, namely $e_1(t) = a(t)\cos\left[\omega_o t + \psi(t)\right]$ and $\dot{\phi}(t)$. The constant of the voltage controlled oscillator (VCO) is taken as unity and the entire loop constant β is associated with the output amplitude of the VCO.

From figure 17/2, the multiplier action, $e_m(t)$, is:

$$e_m(t) = a(t)\cos\left[\omega_o t + \psi(t)\right].\beta\left[\omega_o t + \phi(t)\right] \qquad \text{..... (17-3)}$$

Using standard trignometrical expansions:

$$e_m(t) = a(t)\beta\left[\cos\omega_o t\cos\psi(t) - \sin\omega_o t\sin\psi(t)\right]\left[\sin\omega_o t\cos\phi(t) + \cos\omega_o t\sin\phi(t)\right]$$

..... (17-4)

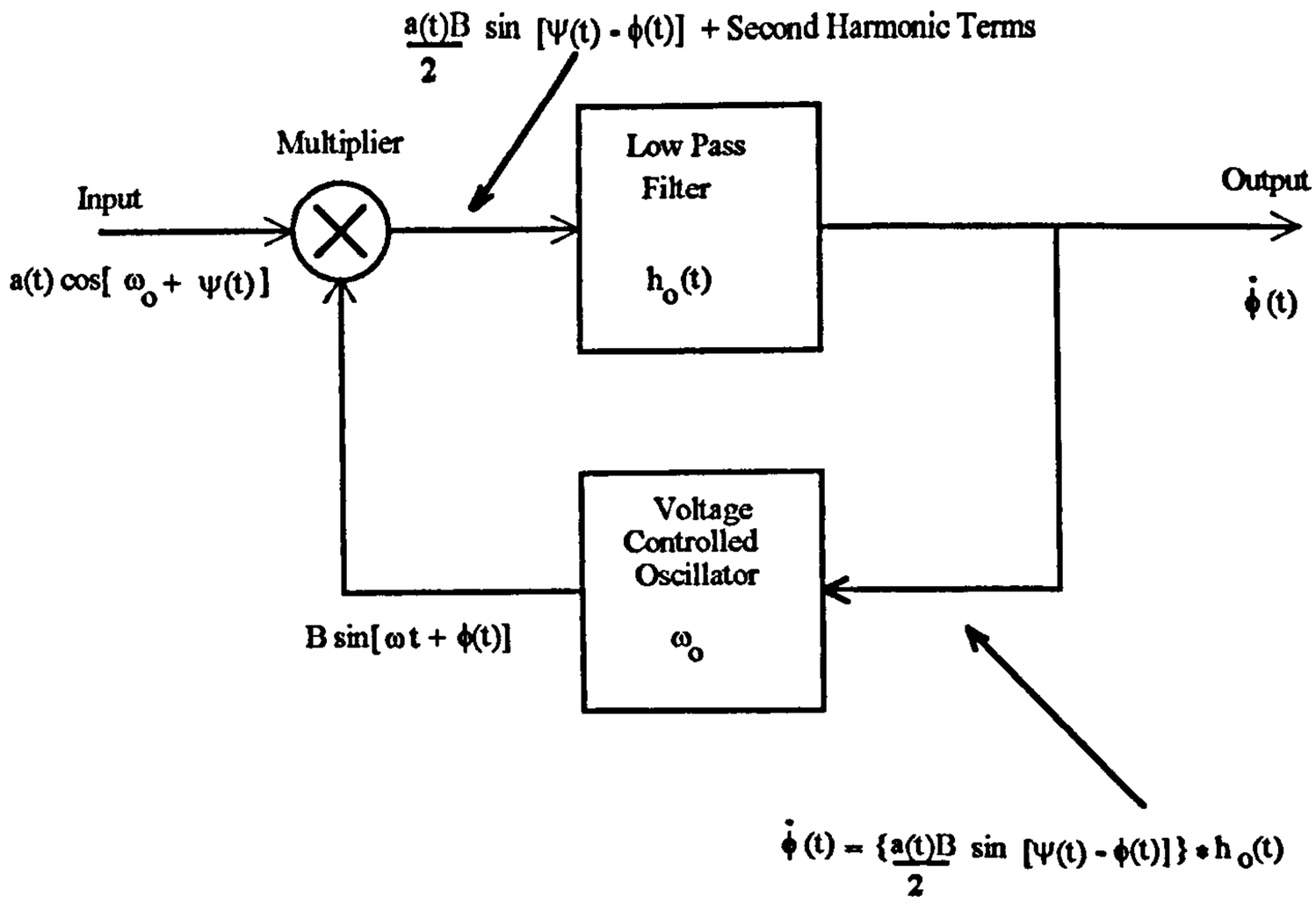

Figure 17/2 Block diagram Phase Lock Loop

Multiplying the contents of the brackets gives:

$$\therefore e_m(t) = a(t)\,\beta\big[\cos\omega_o t\cos\psi(t)\sin\omega_o t\cos\phi(t) + \cos\omega_o t\cos\psi(t)\cos\omega_o(t)\sin\phi(t) - \sin\omega_o t\sin\psi(t)\sin\omega_o t\cos\phi(t) - \sin\omega_o t\sin\psi(t)\cos\omega_o t\sin\phi(t)\big] \quad \ldots\ldots \text{(17-5)}$$

Simplifying:

$$\therefore e_m(t) = a(t)\,\beta\big[\cos\omega_o t\cos\psi(t)\sin\omega_o t\cos\phi(t) + \cos^2\omega_o t\cos\psi(t)\sin\phi(t) - \sin^2\omega_o t\sin\psi(t)\cos\phi(t) - \sin\omega_o t\sin\psi(t)\cos\omega_o t\sin\phi(t)\big] \quad \ldots\ldots \text{(17-6)}$$

Hence:

$$\therefore e_m(t) = a(t)\,\beta\big[\sin\omega_o t\cos\omega_o t\left(\cos\psi(t)\cos\phi(t) - \sin\psi(t)\sin\phi(t)\right) + \cos^2\omega_o t\cos\psi(t)\sin\phi(t) - \sin^2\omega_o t\sin\psi(t)\cos\phi(t)\big] \quad \ldots\ldots \text{(17-7)}$$

Using half angle trignometrical expansions gives:

$$\therefore e_m(t) = a(t)\,\beta\left[\frac{1}{2}\sin 2\omega_o t\left(\cos(\psi(t)+\phi(t))\right) + \left(\frac{1}{2}+\frac{1}{2}\cos 2\omega_o t\right)\left(\cos\psi(t)\sin\phi(t)\right) - \left(\frac{1}{2}-\frac{1}{2}\cos 2\omega_o t\right)\left(\sin\psi(t)\cos\phi(t)\right)\right] \quad \ldots\ldots \text{(17-8)}$$

$$e_m(t) = a(t)\beta\left[\frac{1}{2}\sin 2\omega_o t\cos\left(\psi(t)+\phi(t)\right)\right.$$
$$+\frac{1}{2}\cos\psi(t)\sin\phi(t)+\frac{1}{2}\cos 2\omega_o t\cos\psi(t)\sin\phi(t)$$
$$\left.-\frac{1}{2}\sin\psi(t)\cos\phi(t)+\frac{1}{2}\cos 2\omega_o t\sin\psi(t)\cos\phi(t)\right]$$

..... (17-9)

Collecting the second and fourth terms and the third and fifth terms:

$$\therefore e_m(t) = \frac{a(t)\beta}{2}\left[\sin 2\omega_o t\cos\left(\psi(t)+\phi(t)\right)+\left(\cos\psi(t)\sin\phi(t)-\sin\psi(t)\cos\phi(t)\right)\right.$$
$$\left.+\cos 2\omega_o t\left(\cos\psi(t)\sin\phi(t)+\sin\psi(t)\cos\phi(t)\right)\right]$$

..... (17-10)

Using standard trignometrical identities:

$$e_m(t) = \frac{a(t)\beta}{2}\left[\sin 2\omega_o t\cos\left(\psi(t)+\phi(t)\right)+\sin\left(\psi(t)-\phi(t)\right)+\cos 2\omega_o t\sin\left(\psi(t)-\phi(t)\right)\right]$$

..... (17-11)

Which may be written as:

$$e_m(t) = \frac{a(t)\beta}{2}\sin\left(\psi(t)-\phi(t)\right)+\text{second harmonic terms} \quad \text{.....} \quad (17\text{-}12)$$

This is the output of the multiplier. The characteristics of the loop filter are chosen to reject the second harmonic terms in the vicinity of $2\omega_o$. The output of the phase lock loop may thus be written as:

$$\dot{\phi}(t) = \left[\frac{a(t)\beta}{2}\sin\left(\psi(t)-\phi(t)\right)\right] * h_o(t) \quad \text{.....} \quad (17\text{-}13)$$

The impulse response of the loop filter is $h_o(t)$ and where * denotes convolution.

17.2.4 FMFB demodulator defining equation

(a) General

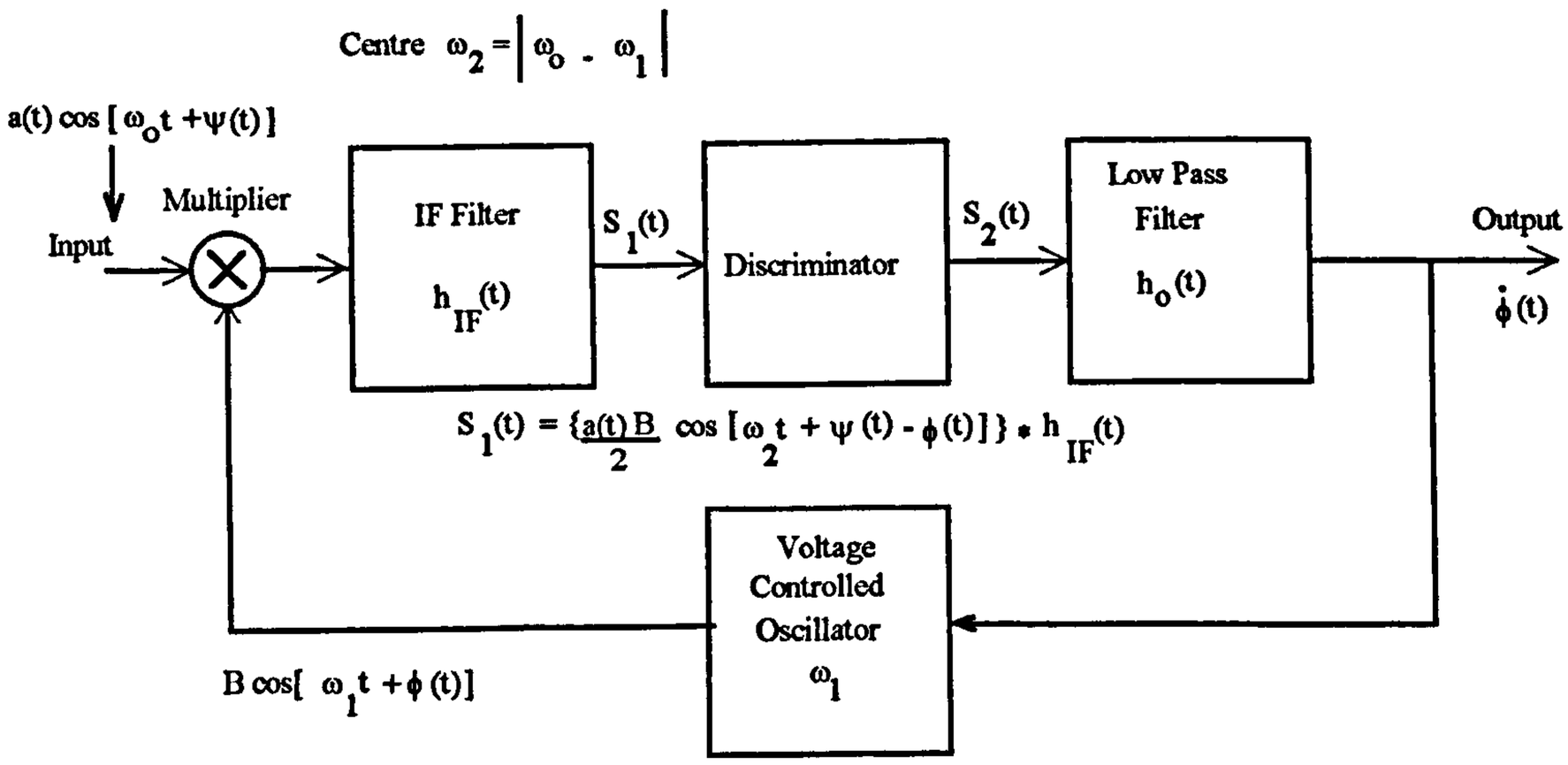

Figure 17/3 Block Diagram Frequency Demodulator with Feedback

Figure 17/3 illustrates the block diagram of the FMFB Demodulator. The same input signal is applied as that for the FLL and PLL above, viz. $e_1(t) = a(t)\cos[\omega_o t + \psi(t)]$. The output signal is again defined as $\phi(t)$. The constants of the VCO and the discriminator are chosen as unity. For stability the I.F. filter is chosen to have a transfer function as follows:

$$H_{IF}(s) = L[h_{IF}(t)] = \frac{2s}{s^2 + 2\alpha s + \omega_2^2} \qquad \text{..... (17-14)}$$

Now the low pass equivalent filter of the narrow band I.F. filter given in equation (17-14) is:

$$H_L(s) = L[\,h_L(t)\,] = \frac{1}{s+\alpha} \qquad \text{..... (17-15)}$$

Where:

$h_L(t)$ = impulse response of low pass equivalent filter of the narrow band I.F. filter.

$\omega_2 = |\omega_o - \omega_1|$, i.e. difference between VCO output frequency ω_1 and input frequency ω_o,

$\alpha =$ distance of the poles of $H_{IF}(s)$ from the imaginary axis in the complex s plane.

$L =$ Laplace transform operator

The discriminator in the loop has no limiter and has the property (see chapter 6 above) that if its input is given by:

$$S_1(t) = A(t)\cos\left[\omega_2 t + \theta(t)\right] \qquad \ldots\ldots\ (17\text{-}16)$$

Then its output (from chapter 6) above is given by:

$$S_2(t) = A(t)\,\dot{\theta}(t) \qquad \ldots\ldots\ (17\text{-}17)$$

Consider in the following the two limiting forms of the FMFB defining equation, namely if the bandwidth of $H_{IF}(s)$ is permitted to become large, and then if it is permitted to approach zero.

(b) <u>Large bandwidth loop I.F. filter</u>

As the bandwidth of the loop I.F. filter becomes large compared with the band of frequencies in the wanted signal at the output of the multiplier, the I.F. filter gives an attenuated but distorted version of its input at the output. The transfer function of the I.F. filter in the passband is $\left(\frac{1}{\alpha}\right)$.

From figure 17/3 the multiplier action can be written as:

$$e_m(t) = a(t)\cos\left[\omega_o t + \psi(t)\right] B\cos\left[\omega_1 t + \phi(t)\right] \qquad \ldots\ldots\ (17\text{-}18)$$

Expanding using standard trignometrical expansions gives:

$$e_m(t) = a(t)\,B\left[\cos\omega t\cos\psi(t) - \sin\omega_0 t\sin\psi(t)\right]\left[\cos\omega_1 t\cos\phi(t) + \sin\omega_1 t\sin\phi(t)\right]$$

$$\ldots\ldots\ (17\text{-}19)$$

Multiplying out the contents of the brackets and rearranging gives:

$$e_m(t) = a(t)\,B[\,\cos\omega_0 t\cos\omega_1 t\cos\psi(t)\cos\phi(t) - \cos\omega_0 t\sin\omega_1 t\cos\psi(t)\sin\phi(t) - \sin\omega_0 t\cos\omega_1 t\sin\psi(t)\cos\phi(t) + \sin\omega_0 t\sin\omega_1 t\sin\psi(t)\sin\phi(t)\,] \quad \text{..... (17-20)}$$

Expanding using half angle trignometrical expansions gives:

$$\begin{aligned} e_m(t) = a(t)\,B[\,&\left(\tfrac{1}{2}\cos(\omega_0 t+\omega_1 t)+\tfrac{1}{2}\cos(\omega_0 t-\omega_1 t)\right)\left(\tfrac{1}{2}\cos(\psi(t)+\phi(t))+\tfrac{1}{2}\cos(\psi(t)-\phi(t))\right)\\ &-\left(\tfrac{1}{2}\sin(\omega_0 t+\omega_1 t)-\tfrac{1}{2}\sin(\omega_0 t-\omega_1 t)\right)\left(\tfrac{1}{2}\sin(\psi(t)+\phi(t))-\tfrac{1}{2}\sin(\psi(t)-\phi(t))\right)\\ &-\left(\tfrac{1}{2}\sin(\omega_0 t+\omega_1 t)+\tfrac{1}{2}\sin(\omega_0 t-\omega_1 t)\right)\left(\tfrac{1}{2}\sin(\psi(t)+\phi(t))+\tfrac{1}{2}\sin(\psi(t)-\phi(t))\right)\\ &+\left(\tfrac{1}{2}\cos(\omega_0 t-\omega_1 t)-\tfrac{1}{2}\cos(\omega_0 t+\omega_1 t)\right)\left(\tfrac{1}{2}\cos(\psi(t)-\phi(t))-\tfrac{1}{2}\cos(\psi(t)+\phi(t))\right)\,] \end{aligned} \quad \text{..... (17-21)}$$

Multiplying the contents of the brackets out gives:

$$\begin{aligned} e_m(t) = \tfrac{a(t)\,B}{4}[\,&(\cos(\omega_0 t+\omega_1 t)\cos(\psi(t)+\phi(t))+\cos(\omega_0 t+\omega_1 t)\cos(\psi(t)-\phi(t))+\cos(\omega_0 t-\omega_1 t)\cos(\psi(t)+\phi(t))+\cos(\omega_0 t-\omega_1 t)\cos(\psi(t)-\phi(t)))\\ &-(\sin(\omega_0 t+\omega_1 t)\sin(\psi(t)+\phi(t))-\sin(\omega_0 t+\omega_1 t)\sin(\psi(t)-\phi(t))-\sin(\omega_0 t-\omega_1 t)\sin(\psi(t)+\phi(t))+\sin(\omega_0 t-\omega_1 t)\sin(\psi(t)-\phi(t)))\\ &-(\sin(\omega_0 t+\omega_1 t)\sin(\psi(t)+\phi(t))+\sin(\omega_0 t+\omega_1 t)\sin(\psi(t)-\phi(t))+\sin(\omega_0 t-\omega_1 t)\sin(\psi(t)+\phi(t))+\sin(\omega_0 t-\omega_1 t)\sin(\psi(t)-\phi(t)))\\ &+(\cos(\omega_0 t-\omega_1 t)\cos(\psi(t)-\phi(t))-\cos(\omega_0 t-\omega_1 t)\cos(\psi(t)+\phi(t))-\cos(\omega_0 t+\omega_1 t)\cos(\psi(t)-\phi(t))+\cos(\omega_0 t+\omega_1 t)\cos(\psi(t)+\phi(t)))\,] \end{aligned} \quad \text{..... (17-22)}$$

Cancelling out and simplifying gives:

$$e_m(t) = \frac{a(t)\,B}{4}[(\,2\cos(\omega_0 t+\omega_1 t)\cos(\psi(t)+\phi(t))+2\cos(\omega_0 t-\omega_1 t)\cos(\psi(t)-\phi(t))\,) - 2\sin(\omega_0 t+\omega_1 t)\sin(\psi(t)+\phi(t)) - 2\sin(\omega_0 t-\omega_1 t)\sin(\psi(t)-\phi(t))] \quad \text{..... (17-23)}$$

Using standard trignometrical identities gives the following expression that contains the wanted term:

$$e_m(t) = \frac{a(t)\,B}{2}\Big[\cos\big[(\omega_0 t + \omega_1 t) + (\psi(t) + \phi(t))\big] + \cos\big[(\omega_0 t - \omega_1 t) + (\psi(t) - \phi(t))\big]\Big]$$

..... (17-24)

Now as shown in equation (17-15) above, ω_2 = difference between the VCO output frequency ω_1 and the input frequency ω_o, hence $\omega_2 = |\omega_o - \omega_1|$. Therefore equation (17-24) may be written as follows:

$$e_m(t) = \frac{a(t)\,B}{2}\Big[\cos\big[(\omega_0 t + \omega_1 t) + (\psi(t) + \phi(t))\big] + \cos\big[\omega_2 t + (\psi(t) - \phi(t))\big]\Big]$$

..... (17-25)

The wanted output of the multiplier is given by the term:

$$\frac{a(t)\,B}{2}\cos\big[\omega_2 t + (\psi(t) - \phi(t))\big] \qquad \text{..... (17-26)}$$

The I.F. filter output is therefore given by:

$$S_1(t) = \left(\frac{1}{\alpha}\right)\left(\frac{a(t)\,B}{2}\cos\big[\omega_2 t + \psi(t) - \phi(t)\big]\right) \qquad \text{..... (17-27)}$$

Now as the I.F. bandwidth is increased it is assumed that the out-of-band signals at the multiplier output, centred at $\omega_o + \omega_1$ are still rejected. Consequently the output of the discriminator is given by:

$$S_2(t) = \frac{a(t)\,B}{2\alpha}\Big[\dot{\psi}(t) - \dot{\phi}(t)\Big] \qquad \text{..... (17-28)}$$

From figure 17/3 the low pass filter output and hence the defining equation for the FMFB is given by:

$$\dot{\phi} = S_2(t) * h_o(t) \qquad \text{..... (17-29)}$$

Hence $$\dot{\phi} = \frac{a(t)\,B}{2\,\alpha}\left\{\left[\dot{\psi}(t) - \dot{\phi}(t)\right]\right\} * h_o(t) \qquad \text{..... (17-30)}$$

Equation (17-30) is identical to that given for the Frequency Lock Loop above in equation (17-2), and thus demonstrates the equivalence between the defining equations for the FMFB and FLL when the FMFB I.F. bandwidth is large.

(c) <u>Small bandwidth loop I.F. filter</u>

Consider the wanted component of the I.F. output derived in equation (17-25) above, if the bandwidth of the I.F. filter becomes small compared with the band of frequencies occupied by:

$$\frac{a(t)\,B}{2}\cos\left[\omega_2 t + \left(\psi(t) - \phi(t)\right)\right] \qquad \text{..... (17-31)}$$

Then the filter output becomes a strongly distorted version of its input. Expanding the output of the I.F. filter as follows by using standard trignometrical cos (A+B) identities:

$$S_1(t) = \frac{a(t)\,B}{2}\left[\cos\left(\psi(t) - \phi(t)\right)\cos\omega_2 t - \sin\left(\psi(t) - \phi(t)\right)\sin\omega_2 t\right] * h_{IF}(t)$$

..... (17-32)

$$S_1(t) = \left[\left\{\frac{a(t)\,B}{2}\cos\left[\psi(t) - \phi(t)\right]\right\} * h_L(t)\right]\cos\omega_2 t - \left[\left\{\frac{a(t)\,\beta}{2}\sin\left[\psi(t) - \phi(t)\right]\right\} * h_L(t)\right]\sin\omega_2 t$$

..... (17-33)

Where $h_L(t)$ = impulse response of low pass equivalent filter of the narrow band I.F. filter given in equation (17-15) above, viz:

$$H_L(s) = L\left[\,h_L(t)\,\right] = \frac{1}{s+\alpha} \qquad \text{..... (17-34)}$$

Equation (17-33) may be rearranged as follows:

$$S_1(t) = [C + c(t)]\cos\omega_2 t - [D + d(t)]\sin\omega_2 t \qquad \text{.....} \quad (17\text{-}35)$$

Where C and D are average (d.c.) values of the respective coefficients of the $\cos\omega_2 t$ and $\sin\omega_2 t$ terms. The respective values of the coefficients, less their average values, are given by $c(t)$ and $d(t)$. If the RF filter preceding the loop is symmetric about ω_o and if the average VCO phase $\overline{\phi(t)} = 0$, then from symmetry considerations the average modulation phase $\overline{\psi(t)} = 0$ and the average multiplier output $\overline{a(t)\sin[\psi(t) - \phi(t)]} = 0$, hence the average d.c. value $D = 0$.

However C is not zero, thus equation (17-35) may be further rearranged to yield the I.F. filter output that is given by:

$$S_1(t) = \sqrt{[C + c(t)]^2 + [d(t)]^2}\cos\left[\omega_2 t + \tan^{-1}\frac{d(t)}{C + c(t)}\right] \qquad \text{.....} \quad (17\text{-}36)$$

The output of the discriminator is given by differentiating the tangent term, viz:

$$S_2(t) = \frac{[C + c(t)]\dot{d}(t) - d(t)\,\dot{c}(t)}{\sqrt{[C + c(t)]^2 + [d(t)]^2}} \qquad \text{.....} \quad (17\text{-}37)$$

Thus as the bandwidth of the I.F. filter approaches zero, $c(t)$ and $d(t)$ become very small compared to C, that is more and more of the a.c. component gets smaller whilst the d.c. component remains unchanged. Equation (17-37) reduces to the limiting form:

$$S_2(t) = \dot{d}(t) = \frac{d}{dt}\left[\left\{\frac{a(t)\,B}{2}\sin[\psi(t) - \phi(t)]\right\} * h_L(t)\right] \qquad \text{.....} \quad (17\text{-}38)$$

In addition as $\alpha \to 0$, $H_L(s) \to \frac{1}{s}$ which is a pure integrator. Hence convolution with $h_L(t)$ in equation (17-38) corresponds to integration that cancels with the differentiation

operation to yield:

$$S_2(t) = \frac{a(t)\,B}{2} \sin\left[\psi(t) - \phi(t)\right] \qquad \text{.....} \quad (17\text{-}39)$$

Thus $$\dot{\phi}(t) = S_2(t) * h_o(t)$$

$$\dot{\phi}(t) = \left\{\frac{a(t)\,B}{2} \sin\left[\psi(t) - \phi(t)\right]\right\} * h_o(t) \qquad \text{.....} \quad (17\text{-}40)$$

Equation (17-13) and (17-40) can be seen to be identical thus demonstrating the equivalence between the FMFB and PLL defining equations when the FMFB I.F. bandwidth approaches zero.

17.3 Discussion

17.3.1 The simplified analysis carried out produces some interesting conclusions and shows the PLL and the FLL are, in terms of their defining equations, limiting forms of the FMFB demodulator. If the loop I.F. bandwidth of the FMFB demodulator tends to zero, then the FMFB functions as a PLL with respect to a noise corrupted input carrier. If the loop I.F. bandwidth is infinite then the FMFB functions as a FLL demodulator.

Hess [1] has reported some interesting observations. Firstly the FMFB may have an arbitrarily narrow loop I.F. bandwidth and still successfully demodulate an input FM signal. Secondly, with a sufficiently narrow loop I.F. bandwidth, the FMFB has many of the loss of lock problems possessed by the PLL. Large deviations of the input carrier in the presence of noise are capable of throwing the FMFB out of lock with the result of a large number of signal induced clicks. However for wide I.F. bandwidths the FMFB can never lose lock. Hess suggests that some intermediate value of loop I.F. bandwidth may combine the best features of the PLL and the FLL.

17.3.2 Note however that the analysis does not consider the effects of distortion upon the signal. It is also a linear analysis that does not consider the effects of threshold. The highly non-linear operation of the FM demodulator in the threshold region for noisy signals will probably modify the above results considerably. Hess suggestion [1] of an intermediate I.F. bandwidth FMFB demodulator that may give improved performance is an interesting one. Resulting from the work done elsewhere (chapter 18) in this thesis, this suggestion can be extended further by making the I.F. bandwidth dependent upon a metric that measures the clicks that occur at threshold and that seeks to set a value of bandwidth that minimises them. By this approach not only could the characteristics be made to vary from those of a PLL through a FMFB to a FLL demodulator, but by including Cassera's approach [2] and limiting the I.F. signal, the characteristics could be made to include those of a conventional demodulator. This aspect is considered in chapter 18 of this report, where an error controlled adaptive threshold extension demodulator, based upon the FMFB demodulator, is proposed. This optimises its parameters to the signal structure by adjusting the I.F. bandwidth of the FMFB to obtain the minimum error rate of the signal, i.e. the I.F. bandwidth is made a function of the quality of the signal.

17.4 References

[1] Hess, D. T. "Equivalence of FM threshold extension receivers." IEEE Trans. Comms. Tech., October 1968, pp. 746 - 748.

[2] Cassara, F., Hess, D. T. "FM Threshold performance of the frequency demodulator with feedback", IEEE Trans. on Aerospace and Electronic Systems, Vol. AES-8, No. 5, September 1972.

Blank Page

18. AN ADAPTIVE THRESHOLD EXTENSION DEMODULATOR

18.1 Introduction

18.1.1 In attempting to identify the most suitable approach for threshold extension demodulation when applied to satellite DBS television systems, this thesis has considered all the known approaches to threshold extension demodulators and the factors that have restricted their performance. This study has shown that few, if any, of the known approaches can offer a satisfactory solution to the problem of DBS reception as they stand. This is due to several factors; firstly because of the complex nature of the television signal, the demodulator has difficulty in identifying the frequency component in the signal that should be tracked. This leads to different types of threshold, i.e. static and dynamic, depending on the nature of the picture. Secondly, establishing a suitable metric, or a reliable threshold criterion measurement, that detects when clicks or spikes occur at the onset of threshold. Finally, the inherent circuit (frequency) instabilities make it difficult to produce an economic design that offers a consistent performance in production. If a suitable metric can be established that overcomes these difficulties, then some alternative approaches to threshold extension demodulation become feasible that would offer a significant improvement in performance. These alternative solutions are discussed in this section, and have formed the basis of a U.K. patent application [3].

18.1.2 Although a number of threshold extension techniques have been identified and examined, all have been found to be lacking in attaining the successful objective of a device that provides a consistent performance for all conditions of input (picture) content. This lack of universal performance has been identified as being due to the dependence of the demodulator upon the nature of the carrier modulation, or picture content, and the difficulty in detecting when threshold has occurred.

The problem of detecting clicks at the output of the demodulator is not in itself a difficult

problem. What is difficult is discriminating between clicks that cause problems (those that have a low frequency component in the wanted passband) and those false clicks and doublets that do not, together with any transient data excursion. With the clicks being a Poisson process, the rate of occurrence of these clicks is required in order to determine their statistical properties. False clicks are rarer than real clicks and the net gain in phase for false clicks is zero, and so if only the mean value is considered the false clicks blend into the nearly Gaussian noise component of the Rice model. The characteristics of the noise threshold are discussed in more depth in chapter 4.

To a first approximation the false click and doublet can be classified as events that are smoothed out by a post-discriminator filter at high carrier-to-noise ratios, giving a negligible effect on the signal-to-noise output. Only the clicks that have an area of $\pm 2\pi$ strongly excite the low pass post discriminator filter and are therefore responsible for the noise threshold. This occurrence is more frequent than false clicks. Note that simply clipping doublets can cause increased interference due to their asymmetrical nature. Doublets also contain more high frequency components than the clicks.

One difficulty in any click elimination scheme is those large clicks appearing at the demodulator output can also be caused by the carrier modulation making discrimination between these various causes difficult. One of the characteristics of clicks is that they occur when the amplitude of the instantaneous envelope is likely to be small. This information helps to discriminate between clicks and modulating signals, but not between clicks and doublets. However this amplitude characteristic does not always occur and thus does not provide a reliable indicator to the occurrence of a click. A future method of click detection may be software based, namely that provided by signal processing. Current trends indicate that this technique may be approaching the speed required to process the signal in real time and discriminate against clicks. It may well be the technique used when all-digital television systems are adopted. The method of identifying clicks, whose energy is contained within the information band, described below, offers an approach that overcomes the deficiencies described previously.

The research carried in this thesis has shown that the basic mechanism for achieving threshold extension exists in terms of a number of circuit approaches that can, and do, for fixed signal structures, exhibit a threshold extension of several dB. The fundamental problem that prevents exploitation of these circuits is the actual measurement of when threshold occurs and the dependence of the threshold characteristic upon the signal information content, or modulation index. It is concluded that, because of the inherently non-linear nature of angle modulation, it is impractical to design a threshold extension demodulator that will function for all input carrier-to-noise ratios and for all values of modulation index by just using the characteristics of envelope amplitude $R(t)$ and the demodulated signal $\dot{\theta}(t)$. To overcome these limitations it is proposed to make use of the information content of the signal. This allows various solutions to become feasible, and some of the threshold demodulator designs considered in this thesis can be modified to operate over a wide range of input carrier-to-noise ratios and modulation indexes.

The information characteristic it is proposed to use as a metric of the quality of the demodulated signal, is the error rate that occurs at threshold with those digital signal structures contained in part or all, of the signal structure. This concept would be difficult to introduce with purely analogue systems as there is no easy reference to use for determining an error, such as clicks, in the demodulated signal. But with the introduction of digital structures (such as teletext) in conventional television systems, there is a measure available that allows the effects of threshold clicks, or other types of interference, to be determined. For the new proposed all-digital HDTV system, with its complex error coding structure, there is a ready measure of error rate in the system.

18.1.3 The various approaches to threshold extension demodulation considered in this report can be grouped into three categories. These are:

(i) Those threshold extension demodulators that rely for their action on reducing the effective bandwidth of the receiving system, e.g. tracking filter, phase lock loop, etc., thus enhancing the signal-to-noise performance of the

system.

(ii) Those threshold extension demodulators that operate on the received signal by effectively reducing its deviation and hence the bandwidth required to demodulate it, e.g. FMFB, switched capacitor demodulator, etc. This also permits the use of narrower bandwidth filters, thus enhancing the signal-to-noise performance of the system.

(iii) Those demodulators that process the demodulator output by eliminating the clicks or spikes that occur in the threshold region.

The first two factors result in a decrease in system bandwidth, with too great a decrease resulting in distortion of the signal. For the purpose of this section the tracking filter demodulator will be used as an example of the proposed error control technique, as its functions can be clearly be identified.

18.1.4 To summarise, the various demodulator approaches discussed in the previous sections has shown that the method of implementing, or controlling, threshold extension is well established. What has not been solved is the means of detecting when the threshold point is reached, particularly as this is a function of the input signal structure. Indeed one could suggest that many of these threshold extension demodulator designs have been originated in attempting to overcome these difficulties without realising what the basic problem actually is. If a successful design is to be achieved, then the following objectives should be satisfied.

(a) In any design of threshold extension demodulator, a means must be provided for reducing the bandwidth of the system to within acceptable distortion criteria. This has been done in one way or another with a number of the designs discussed in this thesis.

(b) A successful threshold extension demodulator must be capable of eliminating drifts or instability in the system. This means it must be capable of tracking any transmitter carrier frequency drift, or eliminating the effects of any receiver local oscillator instabilities, or any other instabilities that occur in the receiver. Many of the designs discussed previously do this and indeed some are mistakenly called threshold extension devices because by eliminating instabilities in the system, the receiver bandwidth can be optimised. This achievement should not be underrated, as this approach provides a significant performance improvement.

(c) The third objective in a successful threshold extension demodulator design is to detect the onset of clicks, or spikes, that indicate that the threshold point has been reached. This would allow the parameters of the demodulator to be optimised, delaying the onset of these effects. It is this detection problem or metric that has not previously been solved. To do so would allow various demodulators approaches to be improved, such as the tracking filter demodulator. Here the click metric would allow the bandwidth of the filter to be optimised as the spikes were detected. Secondly, the FMFB and PLL demodulators where similar bandwidth control would give advantages. The ability to differentiate between clicks, false clicks, doublets and transient modulation excursions would allow the performance of these demodulators to be significantly enhanced.

It is this third objective that the following techniques may offer a solution to, and which in conjunction with the first two objectives, will allow a successful demodulator design to be achieved.

18.2 Adaptive threshold extension demodulator concepts

18.2.1 General

Using the signal structure content itself to detect clicks that do harm, is an approach that does not appear to have been used previously. Although it has been used for eliminating the sources of frequency instability in the system by, for example, locking on to the chrominance frequency, it has not been used as a means of detecting the click rate and adjusting system parameters to reduce it. The method proposed of detecting clicks that do harm is to measure the error rate that occurs with certain coded parts of the signal structure. That is, the occurrence of clicks that have energy in the baseband will cause errors in any coded data that is contained within the video signal, or in any coded digital video signal, and is a measure of the quality of the signal. Thus by using this error rate a means exists to detect (measure) when the demodulator threshold point has been reached. This error rate signal can then be used either to reduce the system bandwidth, or to adjust some other system parameter, until the error rate has been reduced to an acceptable limit.

The basic scheme proposed is shown in figure 18/1 and assumes that the TV signal either is, or contains within it, a digital structure from which an error measurement can be derived that is a measure of the quality of the signal. The demodulator, which is termed the Error Controlled Adaptive Threshold Extension Demodulator, functions as follows. The input angle modulated (e.g. FM) signal is obtained from the preceding I.F. amplifier where it has been amplified and filtered. The signal is then applied to a discriminator, that may or may not contain a limiting stage, and whose characteristics can be modified by a measure of the error rate occurring in the digital structure contained within the signal. This error rate measure that controls the characteristics of the discriminator, is obtained from an error processing stage that derives its input from an error decoder stage that operates on the demodulated output of the discriminator. Note that the discriminator in this arrangement can be many of the threshold extension types discussed in this thesis and the characteristics controlled can be any of their parameters that affect the threshold extension characteristic.

The error decoder stage function is to detect the errors that have occurred, and to extract the error rate, from the demodulated coded signal structures, as well as processing the video signal. The error processing stage takes the digital error rate input and produces a function that controls the discriminator parameter that produces threshold extension. Implementations of the concept are shown below for various threshold extension demodulators together with an analytical treatment of key parameters.

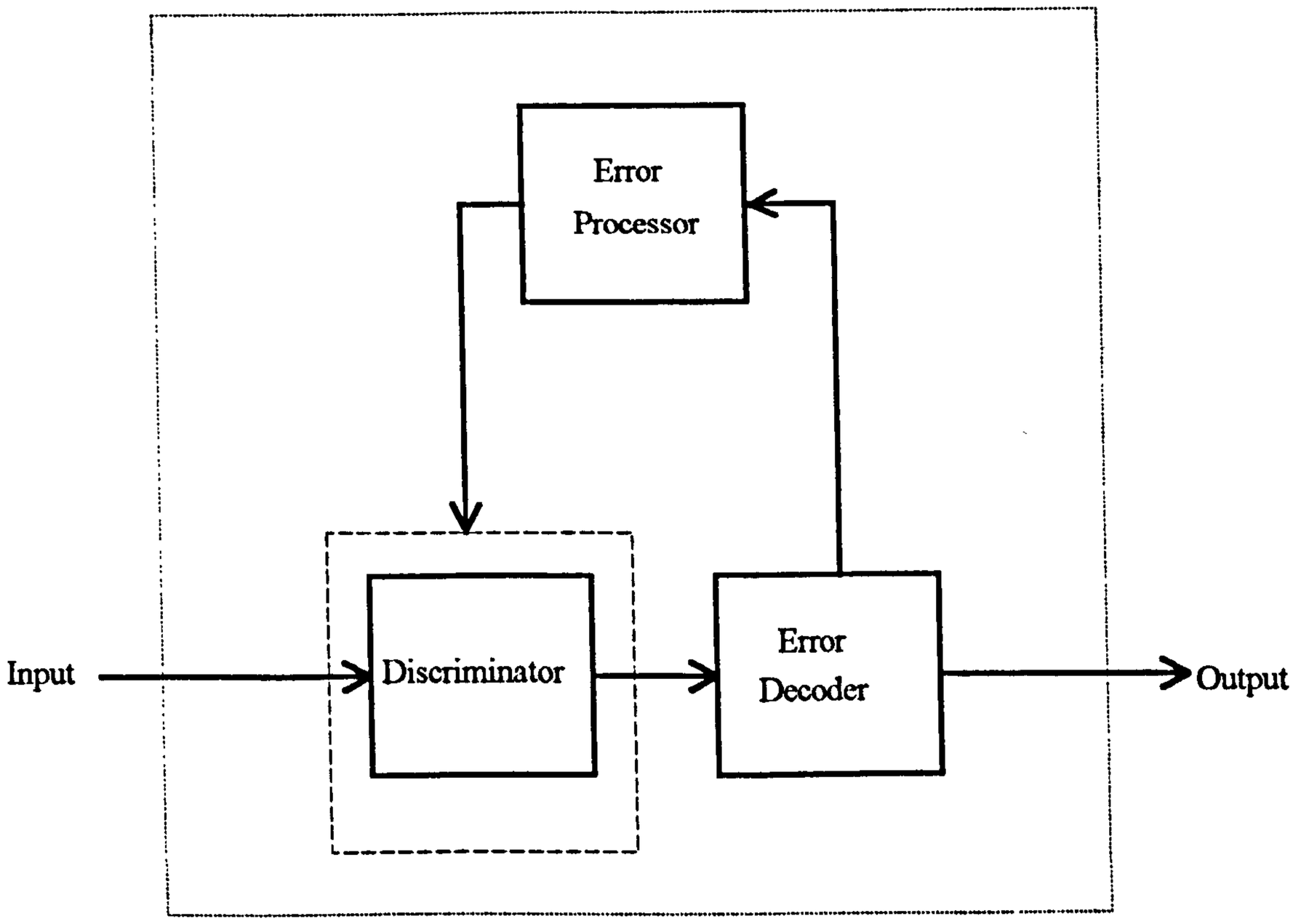

Figure 18/1 Error controlled adaptive threshold extension demodulator concept

As indicated previously the bit error rate (BER) measurement can be derived from a digital signal, or from an analogue signal that contains within it a digital structure from which the BER can be derived. One of the difficulties of using the BER (or one of its other functions such as the word error rate) is that it is a function of several separate system parameters, such as:

(i) Threshold level (i.e. carrier-to-noise ratio).

(ii) Receiver mistuning or offset frequency effects.

(iii) Carrier deviation (i.e. modulation index).

(iv) Receiver bandwidth (e.g. leading to intersymbol interference).

(v) Interference within the passband.

Several of these parameters have been discussed previously in this thesis in terms of their effect on the demodulator threshold. They will briefly be discussed below in term of their effect on the bit error rate. Multipath generated intersymbol interference, a propagation effect, will not be considered in detail as it is assumed not to be a serious effect with DBS transmission from a satellite. However the adaptive error controlled demodulator concept shown in figure 18/1 could be extended either to include error controlled antenna switching or antenna directional control, or possibly to control a transversal equaliser, to minimise the effects of multipath generated intersymbol interference. A version of the error controlled adaptive threshold extension demodulator incorporating a PLL, that minimises intersymbol interference, is given below in figure 18/17.

If the scheme proposed in figure 18/1 is used to detect the clicks that result in picture corruption, then ideally it should be capable of being used with any of the colour TV systems, past, present and future, viz:

(a) Conventional (i.e. PAL, NTSC, SECAM) systems

(b) MAC/Packet systems

(c) All-digital television systems

Examples will be given below of the application of the error controlled adaptive threshold extension demodulator concept to these systems. Future television systems tend to lend themselves more readily to advanced demodulation techniques since they have spare capacity in the signal structure, in the form of data channels, that may be used for threshold extension purposes.

18.2.2 Error rate as a function of carrier-to-noise ratio

There are many references that deal with the variation of error rate for a digital signal, as a

function of carrier-to-noise ratio, for a variety of conditions, among them [4], [5] and [6] are good examples. In determining this error rate relationship it is essential that the baseband signalling code is known, viz. NRZ, Manchester II, etc., as this influences the characteristic and performance of the discriminator. As the purpose of this section is to illustrate the concept of the error controlled adaptive threshold extension demodulator, a signal will be assumed that uses NRZ coded frequency shift keying (FSK). The advantage of this type of baseband signalling code is that the bit error rate is more tolerant of system degradation such as frequency drift, whereas Manchester II would be greatly affected by such effects. The major disadvantage of NRZ is its requirement for a d.c. response.

Figure 18/2 Prob. of Bit Error vs. Carrier-to-Noise Ratio for a NRZ baseband modulation waveform.

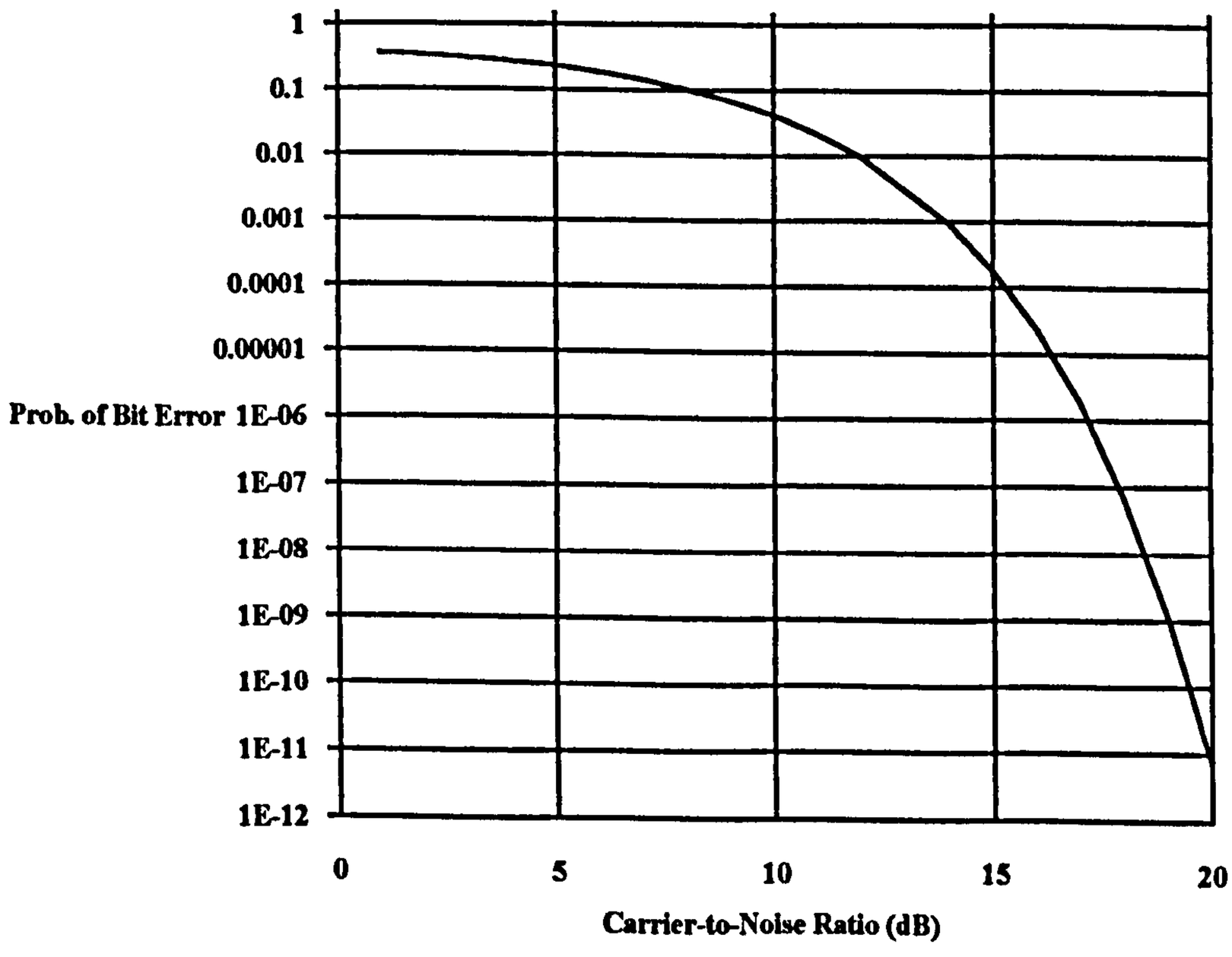

However it should be noted that the baseband signalling code will probably vary for most of the applications discussed in this chapter. For NRZ, a simple relationship [4] relating bit error rate and carrier-to-noise ratio is given by:

$$P_e = \frac{1}{2}\exp\left(-\frac{CNR}{4}\right) \qquad \text{..... (18-1)}$$

where: P_e = Probability of error

CNR = Carrier-to-noise ratio

This relationship is plotted in figure 18/2 and clearly shows the variation of Probability of Error against Carrier-to-Noise Ratio over the range 1 to 20 dB covering the threshold region. Although the characteristic is unreliable below threshold, because it does not take into account the effect of clicks, it does show how the error rate rapidly increases below some 15 dB. At 15 dB, the error rate is of the order of 2 parts in 10^4, and at an 8 dB carrier-to-noise ratio, it is of the order of 1 in 10. Thus it can be seen if these errors are occurring in a known received digital structure and if they can be measured, then the scheme proposed in figure 18/1 has a sensitive metric that is a function of the carrier-to-noise ratio, and that measures the quality of the signal that can be used to control the parameters of the threshold extension demodulator.

18.2.3 Estimation of probability of bit error rate from sync word error rate

The system parameters given in Appendix B specify that only part of the MAC signal structure is digital. For the threshold extension concept proposed in figure 18/1 the question arises how does the word error rate of the various sync words used in the signal structure relate to the bit error rate. Rohde [7] proposed a method that allows the bit error rate, P_e to be determined from the sync word error rate. The basic relationship he gives between these two parameters is:

$$P_\chi = \binom{W_L}{\chi} P_E^{\chi} (1 - P_E)^{W_L - \chi} \qquad \text{..... (18-2)}$$

where P_E = Probability of error

P_χ = Probability of observing χ errors in a (sync) word

W_L = Number of bits in word

χ = Number of errors in (sync) word

and where $\binom{W_L}{\chi} = \frac{W_L!}{\chi!(W_L - \chi)!}$

Inserting equation (18-1) into (18-2) allows a relationship between word (sync) error rate and the bit error rate to be formed:

$$P_x = \binom{W_L}{x}\left[\frac{1}{2}\exp\left(-\frac{CNR}{4}\right)\right]^x\left(1-\left[\frac{1}{2}\exp\left(-\frac{CNR}{4}\right)\right]\right)^{W_L-x} \quad \text{..... (18-3)}$$

Assume that the known sync structures in D2/MAC (see section 18.3.3 below) were being used to provide the error function in the demodulator concept shown in figure 18/1. Within each 625 line frame, every line commences with a 6-bit word to provide for line and frame synchronisation. Frame synchronisation can also be obtained from a further sequence of 64 bits transmitted within the data of line 625. Consider the example plotted in figure 18/3 where the sync word is 6 bits long and the specified sync word error rate is one bit per word (as is mentioned elsewhere in this thesis, 6 bits is considered to be too short a length for a sync word). The characteristics tend to follow that shown in figure 18/2 for the bit error rate, indicating that just measuring the word (sync) error rate in a signal structure offers a metric that is the measure of the quality of the signal.

Figure 18/3 Prob. of Word (6 Bit) Error vs. Carrier-to-Noise Ratio for 1 Bit word error and NRZ baseband modulation waveform.

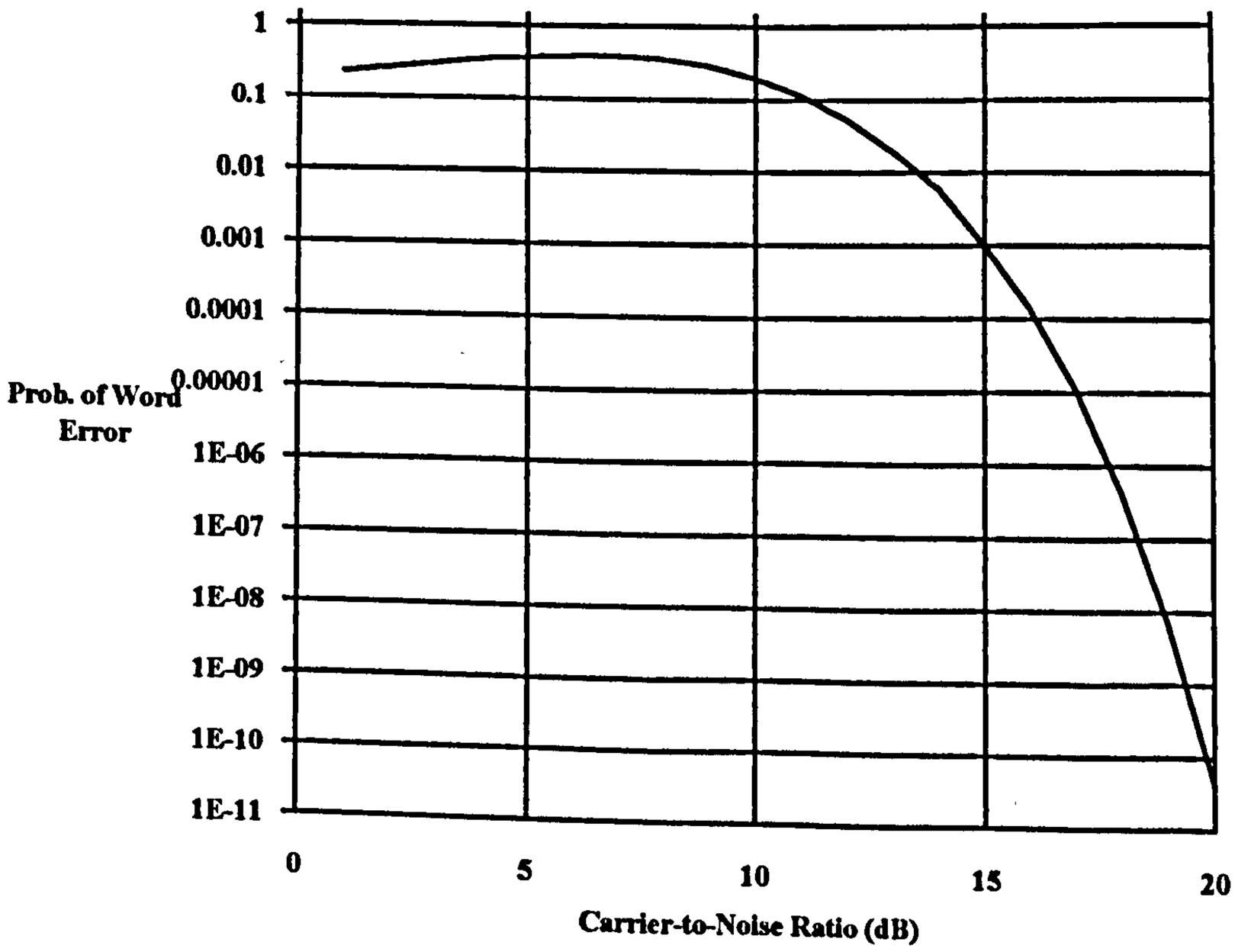

18.2.4 Error rate as a function of modulation index

Reference [7] is a far more complex treatment of the error rate for a digital signal at threshold and includes the effects of clicks as well as Gaussian noise. In this reference it is shown how the error rate is a function of modulation index, for which there appears to be optimum values at low values of carrier-to-noise ratios. This shows that the concept of figure 18/1 can also be used to optimise the demodulator performance if the modulation index varies as it does with changing picture content for some television modulation structures. For carrier-to-noise ratios above threshold, c.15 dB, the characteristics given in [7] shows that for low values of modulation index (c.0.7), the probability of error rate increases very rapidly over several orders of magnitude if the modulation index drops to c.0.4. This effect probably being due to an increase in distortion (or intersymbol interference) of the signal. In conditions such as these the error controlled demodulator concept of figure 18/1 may offer significant advantages. Reference [5] also contains modulation index (called deviation ratio in the reference) characteristics for both NRZ and Manchester baseband signalling codes that confirm the results given in [7].

18.2.5 Error rate as a function of receiver bandwidth

Reference [5] gives some excellent characteristics showing the effect of I.F. bandwidth on the probability of error rate for NRZ and Manchester baseband signalling codes. This shows how too great a reduction in bandwidth leads to an increase in distortion (or intersymbol interference) of the signal. This is produced by the high frequency cut-off of the channel.

18.2.6 Error rate as a function of offset frequency effects

Reference [8] is a useful reference that gives a brief treatment of the effects of frequency uncertainty on the demodulation of FSK and DPSK and in so doing shows how robust FSK is. Curves are given that show the increase in probability of error with increasing frequency offset for various carrier-to-noise ratios. For carrier-to-noise ratios below 11 dB, the

variation in probability of error is relatively flat. For high carrier-to-noise ratios the variation in probability of error with frequency offset is quite significant, albeit at low probability of error values.

To cope with variations in the receiver local oscillator frequency and other instabilities in the design of TV receiving systems, allowance is either made in the I.F. bandwidth for the expected maximum frequency offset or an automatic frequency control loop is incorporated. An alternative approach would be to use the adaptive error control demodulator concept of figure 18/1 to adjust the local oscillator to minimise the error rate. The characteristics shown in reference [8] show that this to be a particularly effective solution. Illustrations of this concept is shown below.

18.2.7 Error rate as a function of interference

Received interference within the receiver passband is a further source of degradation in the probability of error. It has the effect of degrading or reducing the carrier-to-noise ratio and the resulting demodulator performance is dependent upon the type and magnitude of the interference. For the purpose of this thesis the effects of interference will be treated as if the demodulator was dealing with a reduced carrier-to-noise ratio in Gaussian noise.

18.2.8 Summary of parameter variation on bit error rate

The characteristics discussed above, in terms of their effect on the probability of error characteristic of the demodulated signal, can be grouped into two main categories. Firstly those that can be minimised by controlling the receiver (I.F.) bandwidth and, secondly, those that can be minimised by controlling the receiver local oscillator frequency. In the first category can be grouped threshold level, modulation index variation and interference. In the second category falls the effects of offset frequency. Thus all these effects may be catered for by an adaptive error controlled demodulator with two feedback loops being derived from the measure of error rate. One loop controlling the bandwidth of the I.F. filter and the

other controlling the frequency of the receiver local oscillator. An example of this concept is given below in figure 18/9. For the special case of intersymbol interference there is a third category where a error control loop could be introduced to control the decision timing at the output of the demodulator. This is discussed below and illustrated in figure 18/17.

18.3 Error controlled adaptive threshold extension demodulator concepts

18.3.1 Error Controlled adaptive threshold extension demodulator utilising a tracking filter

The basic scheme shown in figure 18/1 is implemented using a tracking filter demodulator and is shown in figure 18/4 below. It assumes that the TV analogue signal contains within it a digital structure from which an error measurement can be derived that is a measure of the signal quality. This error controlled tracking filter demodulator functions as follows. The FM signal enters the I.F. amplifier where it is amplified and filtered. The signal is then applied to an adaptive filter whose bandwidth is controlled by a measure of the error rate in the signal. Initially the bandwidth of this adaptive filter is sufficiently wide enough for the signal spectrum to be predominately determined by the I.F. filter. The signal at the output of the adaptive filter is applied to a limiter that may or may not be included in the circuit. Assuming that it is, the limited signal is then applied to a conventional discriminator. Typically the latter would be followed by a video processing circuit whose function is to filter as well as processing the video signal. At the sync extraction stage, the extraction of frame and line sync structures in the demodulated signal occurs. For the purpose of this example these are assumed to consist of predetermined digital sync patterns. In addition to the demodulated video signal, a further signal is derived in this stage that is fed to a circuit where the digital content of the signal is extracted. This circuit contains an error decoder whose function is to detect the errors that have occurred in the coded digital signal structure.

In a typical communications system that contains an error coded digital signal structure, the

error decoder would detect and correct errors up to a limit determined by the code structure. For the proposed demodulator, all that is required is the error rate. An increase in error rate indicates the demodulator is, say, entering the threshold region. A measure of this is fed back to the error processing circuit; the output of which can be used in a variety of ways to control the bandwidth of the adaptive filter.

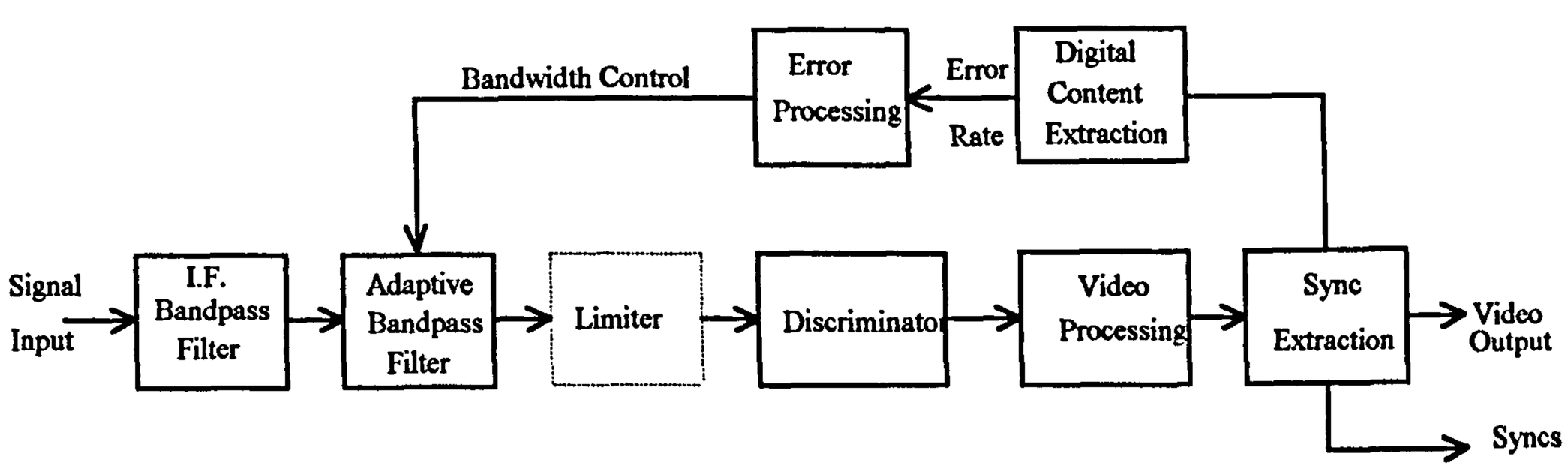

Figure 18/4 Error controlled demodulator concept

Firstly as the error rate increases the error processing circuit can reduce the adaptive filter bandwidth to some limit or to the point where the error rate starts to increase. Secondly an alternative approach can be used where an increase in error rate above a certain level causes the adaptive filter to switch to a lower predetermined bandwidth. The error controlled threshold extension demodulator operates on the basis that, due to the non-linearity of the demodulator action, an increase in (digital) error rate due to the reduction in filter bandwidth, is less than the improvement in error rate that occurs as a result of the enhanced carrier-to-noise ratio, particularly for those analogue signals that contains digital sync structures.

The action of the error controlled adaptive demodulator is illustrated in figure 18/5. This shows a graph of the probability of bit error in the demodulator digital content output versus the carrier-to-noise ratio at the demodulator input for a NRZ baseband modulation waveform.

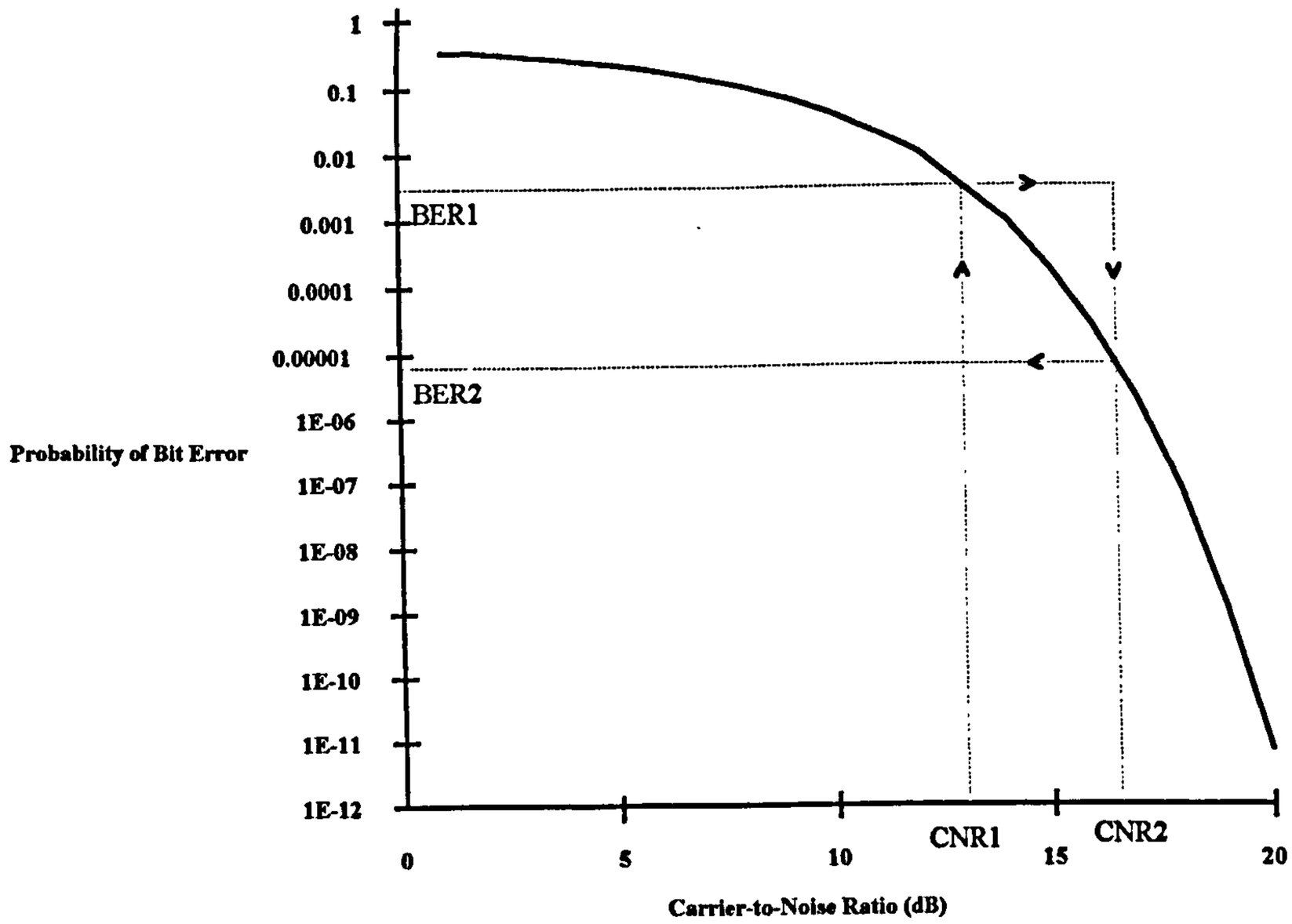

Figure 18/5 Probability of Bit Error vs. Carrier-to-Noise Ratio (NRZ) showing action of error adaptive demodulator

Assume that the initial condition is that the tracking filter error controlled adaptive demodulator is receiving a signal with a high carrier-to-noise ratio (denoted CNR2 in figure 18/5) that results in a low bit error rate, BER2, in the digital content of the demodulated output signal. Assume that due to a change in propagation (e.g. fading) conditions the carrier-to-noise ratio reduces to CNR1, causing a high bit error rate BER1 in the demodulated output. This high bit error rate results in the error processing circuit of figure 18/4 reducing the adaptive filter bandwidth to a level that increases the carrier-to-noise ratio at the input of the discriminator back to CNR2, that in turn reduces the bit error rate in the digital content of the demodulated output signal to BER2. The error processing circuit would hold it there, whilst periodically testing if the carrier-to-noise ratio in the initial bandwidth condition had improved. If it had it would revert back to its initial settings. Note that this is a simplistic description of the operation of the action since in practice the scheme would be arranged to reduce the bandwidth, so that the error rate reduced to below some threshold value and not to the original value.

Although this action has been described in terms of the tracking filter implementation of the

error controlled adaptive demodulator, figure 18/5 can be used to explain the action of other demodulator implementations of the circuit.

18.3.2 Error controlled adaptive threshold extension demodulator concepts applied to conventional TV systems

The signal structure of conventional TV systems (PAL, SECAM, NTSC) poses a particular problem when trying to introduce an information related metric for determining the occurrence of threshold related clicks. This is because of the analogue nature of the system. The use of Teletext [1] in the signal structure does however provide a method of obtaining a click occurrence measurement. In a teletext system, simple Hamming error coding is used in the address words for detecting double and correcting single errors; address words having two wrong bits are rejected. Thus the means exist in a conventional TV system with teletext, to detect the occurrence of threshold clicks, or interference, noise by measuring this teletext error rate. Whether the actual bit error rate, or the address word error rate, is used requires further study.

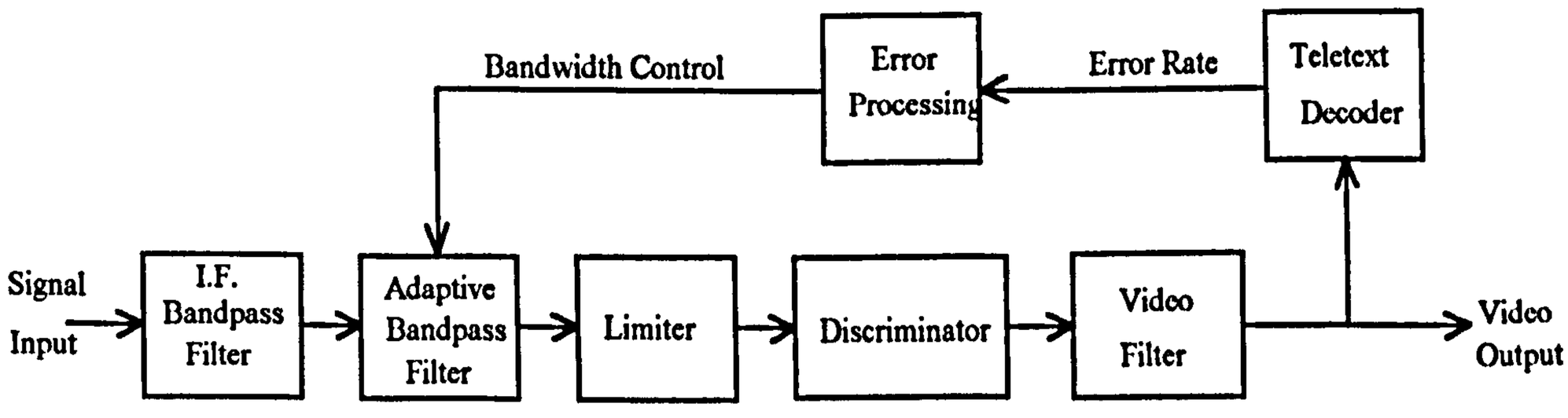

Figure 18/6 Teletext error controlled demodulator concept

An illustration of the teletext error controlled demodulator is given in figure 18/6. Its function is as described previously, where an increase in teletext bit rate error is applied to the error processing circuit, whose output provides a control signal to reduce the bandwidth of the adaptive bandpass filter, thus improving the threshold; albeit at the expense of resolution.

There is a facility [1] in teletext video input processing circuits termed a signal quality detector, whose function in the presence of high signal noise is to cut off the teletext data and allow the display to run. At first glance it would appear that this function could be used to reduce the bandwidth of the demodulator in high noise conditions. However a closer examination shows that this function is a simple one that basically just measures a level that exceeds a video output amplitude threshold. It is unlikely to have the characteristic required for click elimination.

18.3.3 Error controlled adaptive threshold extension demodulator concepts applied to MAC/Packet TV systems

A similar approach to that given above can be used with the signal structure of MAC/Packet TV systems, the detailed characteristics of which are given in Appendix B to this thesis. Here it is shown in table B.4 that teletext is also a feature of the MAC/Packet systems, and thus the same teletext approach can be used as that for conventional systems. However there are other features available in the MAC signal structure that allow an alternative, and possibly superior, approach to be adopted. Table B.4 in Appendix B, shows that digital synchronisation is also used for the MAC/Packet systems. All the frames in the D2/MAC system contain 625 lines at all times. Within each frame, every line commences with a 6-bit word to provide for line and frame synchronisation. Frame synchronisation can also be obtained from a further sequence of 64 bits transmitted within the data of line 625. Although the detailed sync patterns are not given in the MAC/Packet standards shown in Appendix B, a limited amount of information on the sync timing is given in [2]. The frame and line sync digital patterns do not include error coding and thus the approach used for teletext in counting the number of detected error bits in the coded structure cannot be used. However an alternative approach is available as the digital sync patterns are known and predefined. The number of bit positions in error, in both the line and frame syncs, can thus readily be identified in the receiver. An illustration of the sync pattern error controlled demodulator is given in figure 18/7. Its function is as described previously where an increase in the line and frame bit rate error is applied to the error processing circuit, whose

output provides a control signal to reduce the bandwidth of the adaptive bandpass filter, thus improving the threshold and reducing the resolution. Several points should be made about this proposed technique. Regardless of whether frame, line or both syncs are being used, the error rate is in effect being measured on a sampled basis. Although this modifies the actual value of bit error rate to carrier-to-noise relationship as is shown in section 18.2.3 above, it still provides an accurate indication of the occurrence of noise or interference spikes in the demodulated signal, and so can be used either to control the bandwidth of the adaptive filter or some other system parameter.

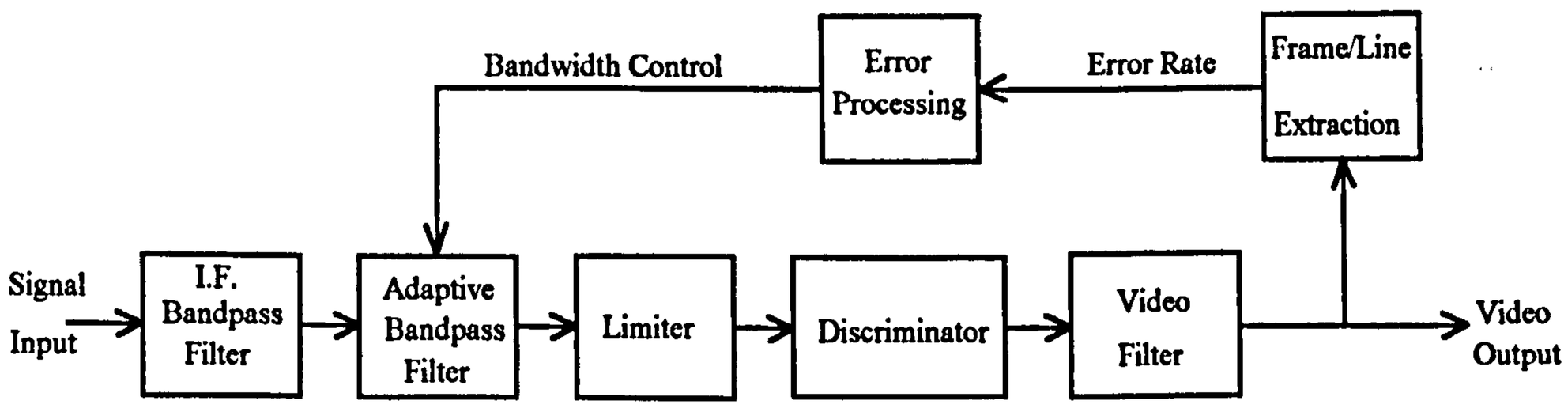

Figure 18/7 Sync pattern error controlled demodulator concept (D2/MAC)

It practice, it is considered better to use line sync for the error rate measurement because of the linear sampling characteristic that is obtained. If the frame sync in line 625 is used, then a variety of approaches are possible. Although frame sync consists of a 64 bit pattern with good correlation features, line 625 contains other structures such as static and dynamic data that could also be used. The static data is constant from frame to frame and could be utilised for error rate measurement. In addition each of the static and dynamic data frames contains a 14 bit error control structure that is used to detect most error patterns, and to correct one or two errors in the various groups. The error detected outputs of these two 14 bit error patterns could be used to provide an error rate measurement for the control signal to operate the error controlled adaptive threshold extension demodulator. There is considerable potential within the MAC/Packet system, and in particular D2/MAC, for obtaining an accurate measure of the onset of threshold clicks, and for it to be used in a variety of ways to control a threshold extension demodulator.

18.2.4 Error controlled adaptive threshold extension demodulator concepts applied to Digital TV Systems

The proposed all-digital HDTV systems signal structure is discussed in chapter 19 below. This system lends itself ideally to the concepts discussed above because of the sources of bit error measurement available. The received signal structure has Reed Solomon error control parity bits added to each data segment with additional protection being provided by a data interleaver. Long burst errors in the transmission path are spread out by this complementary de-leaver in the receiver preventing Reed-Solomon overload. The Reed-Solomon encoder is concatenated with a $\frac{2}{3}$ Rate Trellis encoder, with neither field sync and segment sync being encoded or interleaved. The data field sync provides the means to determine the data field onset. It is also compared to an internal reference in the receiver, the difference being used to adjust an equaliser that removes echoes and intersymbol interference. The concept of an error controlled adaptive threshold extension demodulator for digital signals is shown in figure 18/8. It is as for the other examples shown above based upon the tracking filter demodulator.

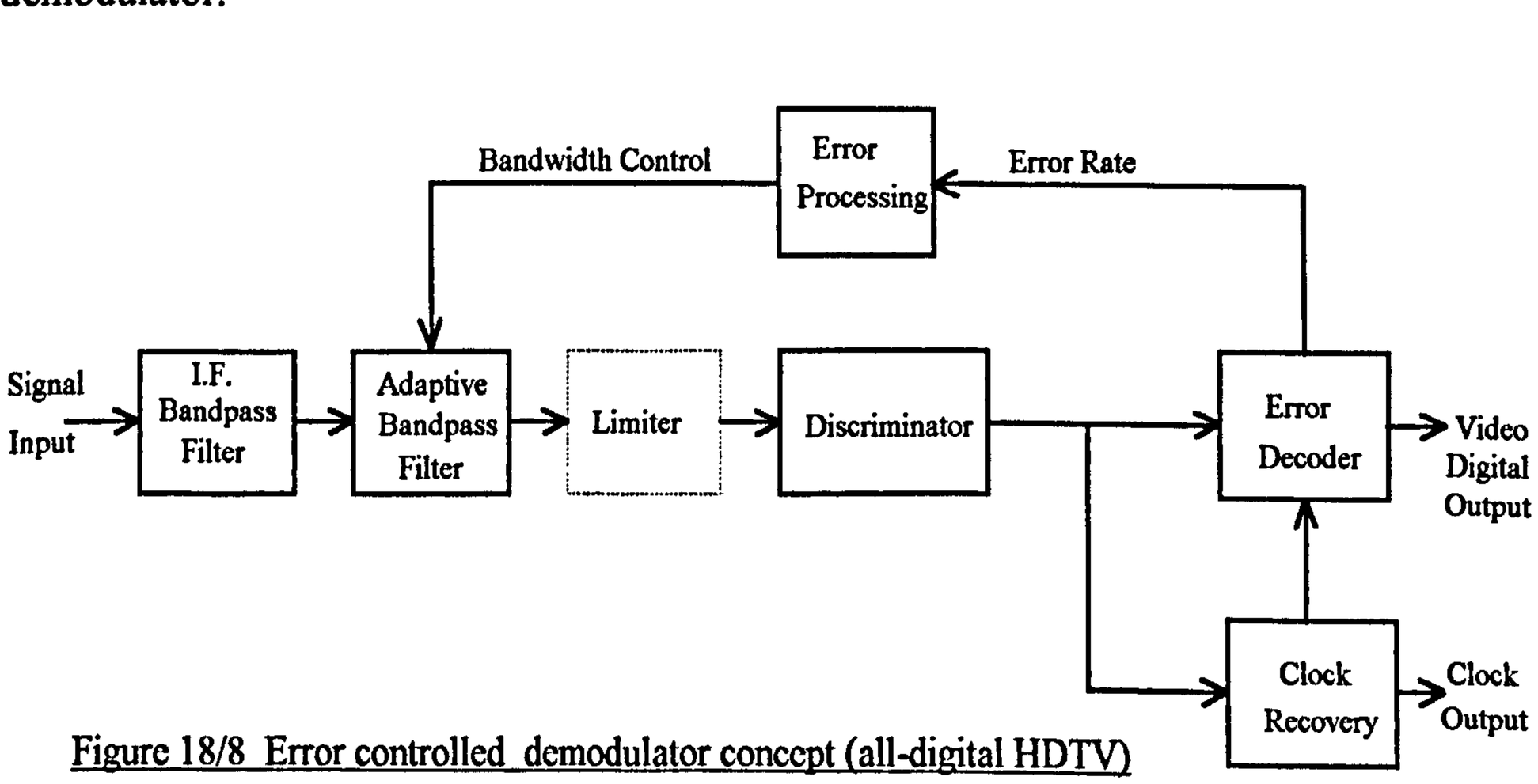

Figure 18/8 Error controlled demodulator concept (all-digital HDTV)

The FM signal enters the I.F. amplifier where it is amplified and filtered. The signal is then applied to an adaptive filter whose bandwidth is controlled by a measure of the error rate in the signal. Initially and at high carrier-to-noise ratios the bandwidth of this adaptive filter is sufficiently wide enough for the signal spectrum to be determined by the I.F. filter. The

signal at the output of the adaptive filter is applied to a limiter, that may or may not be included in the circuit. Assuming it is the limited signal is then applied to a conventional discriminator. In a digital system the latter would be followed by a clock recovery, or bit synchroniser, circuit whose function is to extract a clock timing signal for operating the timing of the subsequent circuits. The signal output of the clock recovery is applied to an error decoder whose function is to detect the errors that have occurred in the coded signal structure. In a typical digital communications system using an error coded signal structure, the error decoder would detect and correct the errors up to a certain limit determined by the code structure. For the proposed error controlled adaptive threshold extension demodulator all that is required is the error rate. A measure of this is fed back to the error processing circuit; the output of which can be used in a variety of ways either to control the bandwidth of the adaptive filter or some other system parameters. Here it is assumed as the error rate increases the error processing circuit can reduce the adaptive filter bandwidth to a lower value.

Care may need to be taken in an error controlled adaptive threshold extension demodulator application to an all-digital system, because of the effect on error rate of reducing the pre-demodulation bandwidth. If the system is optimised for say an NRZ baseband signalling code, then a reduction in effective I.F. bandwidth may increase the error rate significantly, due to intersymbol interference being generated. This problem should not be a severe problem in the error controlled adaptive threshold extension demodulator because it always seeks to minimise the error rate. For satellite all-digital TV systems the baseband signalling format has not yet been reported, but will probably be an M-ary type. If so, the problem may potentially be as severe as that for NRZ. This area is potentially a fruitful one for future study.

18.4 Error controlled adaptive threshold extension demodulator design aspects

18.4.1 Centre frequency and bandwidth control

Each of the three groups of TV systems discussed above (conventional, MAC/Packet and digital) contain an error coding facility that is capable of showing when the demodulator enters the threshold region. However differing design considerations apply to each approach. For the purpose of this thesis, the following discussion will apply to the D2/MAC system only. As was mentioned previously there are several sources of coding used within the D2/MAC system, where some or all the resulting error rates can be used as a quality indicator that shows when the carrier-to-noise ratio is falling to values that result in the demodulator operating in the threshold region. As these digital structures are at a low data rate compared to the vision bandwidth, it is considered that the digital subsystem characteristics are similar to a wide band system. Hence in a conventional digital system where the I.F. bandwidth is optimised for the digital signal, a reduction in bandwidth results in an increase in error rate, due to the (intersymbol) distortion of the signal; this can occur when the signal is well above threshold. However in a D2/MAC system, it is assumed that a reduction in I.F. bandwidth should not contribute to an increase in error rate due to the signal distortion, because the digital structure bandwidth is low compared to vision signal. The resolution of the latter would however be affected. There is another source of bit error rate increase that is not directly due to the threshold effect and which could be a significant factor in any design. If the receiver does not have a separate automatic frequency (A.F.C) system controlling the receiver local oscillator, then frequency drifts due to the satellite transmitter, terrestrial receiver local oscillator, or I.F. filter detuning, can in themselves increase the error rate. This is because the signal would begin to fall in the upper or lower cut-off region of the I.F. bandwidth resulting in an attenuation and distortion of the signal.

If a separate A.F.C. system does not exist then the error control adaptive demodulator concept shown in figure 18/7 could be modified to take this effect into account. The proposed error controlled adaptive threshold extension demodulator with an A.F.C. facility

is shown in figure 18/9.

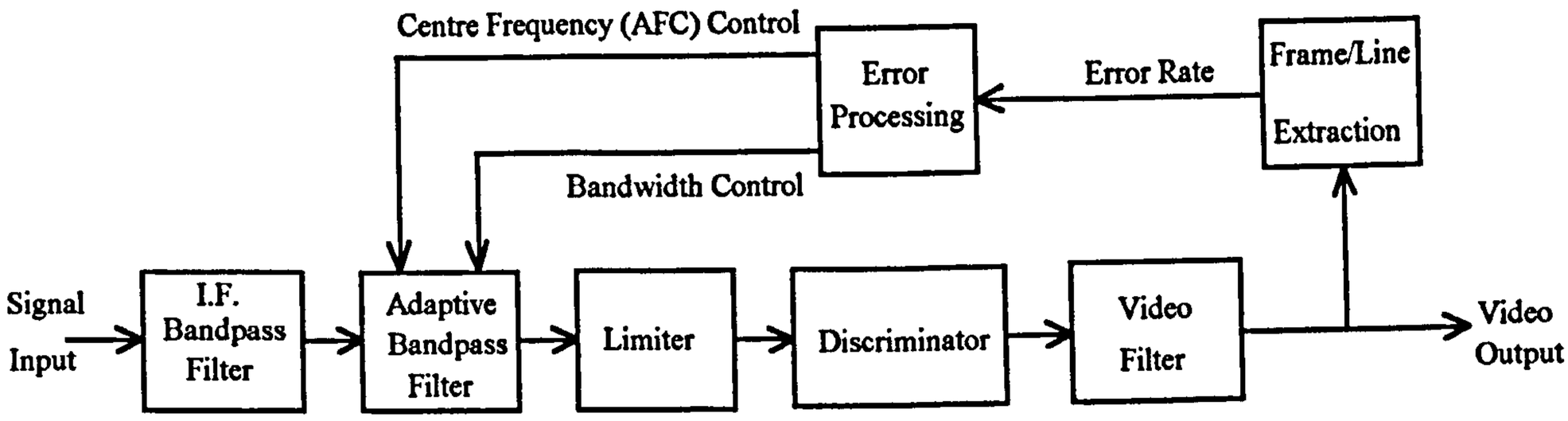

Figure 18/9 Sync pattern error controlled demodulator concept (D2/MAC) with A.F.C. capability

In figure 18/9 the error control function is shown producing a centre frequency control function as well as the bandwidth control. In this scheme it is assumed that the I.F. filter's bandwidth is sufficiently wide enough to accommodate all drifts and instability and that the overall bandwidth characteristic is determined by the adaptive filter. In addition note that instead of controlling the adaptive filter centre frequency, this error derived centre frequency control function could be used to control (or fine tune) the receiver local oscillator. Indeed this may be a simpler design approach to implement. A possible mode of operation is when the error rate increases above some predetermined level, the error control function would initially cause the centre frequency output to vary, seeking to minimise the error rate. When this had been achieved, and if the error rate was still above the set level, then the error control function would operate the bandwidth control until the error rate was again minimised, i.e. the threshold clicks had disappeared. In a modified form this technique could be applied to conventional as well as digital TV systems. In practice a modification to this algorithm would be required to be incorporated, to periodically open the adaptive filter bandwidth to its original value to see if the effect initially causing the error rate to reduce had disappeared. Alternative examples of error controlled frequency control are given below in the FMFB and PLL implementation of the error controlled threshold extension demodulator.

18.5 Alternative error controlled adaptive threshold extension demodulator concepts

18.5.1 General

Although the concept of measuring the increase in video signal digital structure error rate, to signify the occurrence of threshold clicks, has been applied in the above to the tracking filter demodulator, it can be applied to many of the threshold demodulators discussed in this thesis. In some of these demodulators the error rate control signal either adjusts a filter characteristic or, as is illustrated in one application, controls a switching function. In other approaches it can be used to control the loop gain, the voltage controlled oscillator frequency or the decision timing at the output of the demodulator. Some of these various concepts are briefly discussed in the following.

18.5.2 FMFB error controlled adaptive threshold extension demodulator

The FMFB error controlled threshold extension demodulator is one of the interesting applications of the error control principle enunciated. A version is shown in figure 18/10. Here the error control derived from the error processor is used to alter the bandwidth of the I.F. amplifier, in response to the measured error rate in the demodulated output. This technique is made to embody the equivalence of demodulator discussed in chapter 17, where by varying the bandwidth of the I.F. the characteristics of the FMFB can be made to vary from a PLL through an FMFB to a FLL, as the bandwidth of the I.F. varies from being very narrow to being very wide. In this particular approach the error control function would adjust the I.F. bandwidth to minimise the error rate. If the carrier-to-noise ratio was such that the FMFB, in its PLL mode loses lock with a resulting increase in click rate, then the error control could be arranged to adjust the demodulator towards the FLL mode until the error rate drops to an acceptable value. Indeed the approach could also be made to switch a limiter in and out of the loop thus making the wideband I.F. version to be equivalent to a

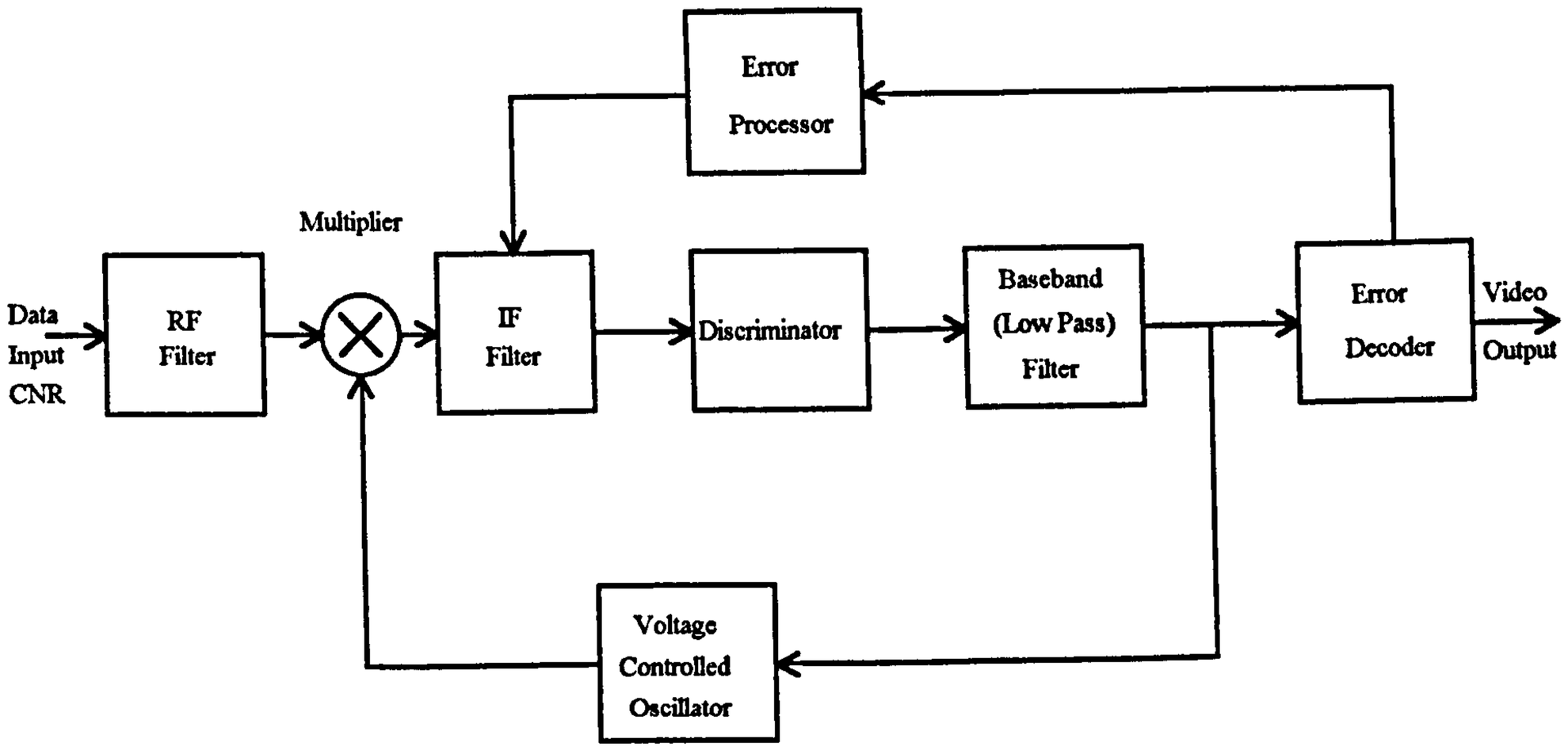

Figure 18/10 Frequency modulation with feedback error controlled adaptive demodulator with I.F. bandwidth control

conventional demodulator. In a FMFB demodulator system, it has in the past, been necessary to use very stable circuits, so as to ensure that the I.F. signal passing through the narrow pass-band I.F. filter, is not distorted by being very close to or in the edge of the pass band. If the signal is too close to the edge of the pass band, additional noise in the form of distortion products is created within the filter. Such additional noise defeats, in part the attempted extension of the threshold of the demodulator to the region of lower input signal power. The following implementation of the FMFB in an error controlled adaptive threshold extension demodulator offers some advantages in overcoming these limitations. Figure 18/11 shows a version of the error controlled adaptive threshold extension demodulator incorporating an FMFB that uses both I.F. bandwidth and VCO frequency control derived from the bit error rate feedback. Figure 18/11 is identical to figure 18/10 except that a sum network at the input of the VCO has been incorporated together with a frequency control from the error processor. The main purpose of this frequency control loop is to overcome the instability limitations described previously. In this design the error processor, that includes a control algorithm, produces two control function outputs. One, the bandwidth output control is applied to the I.F. filter where it controls the bandwidth. The second output (B) is applied to the summing network, where it is summed with the frequency compression feedback (A) from the FMFB low pass filter output. The output of

the summing network controls the frequency of the VCO.

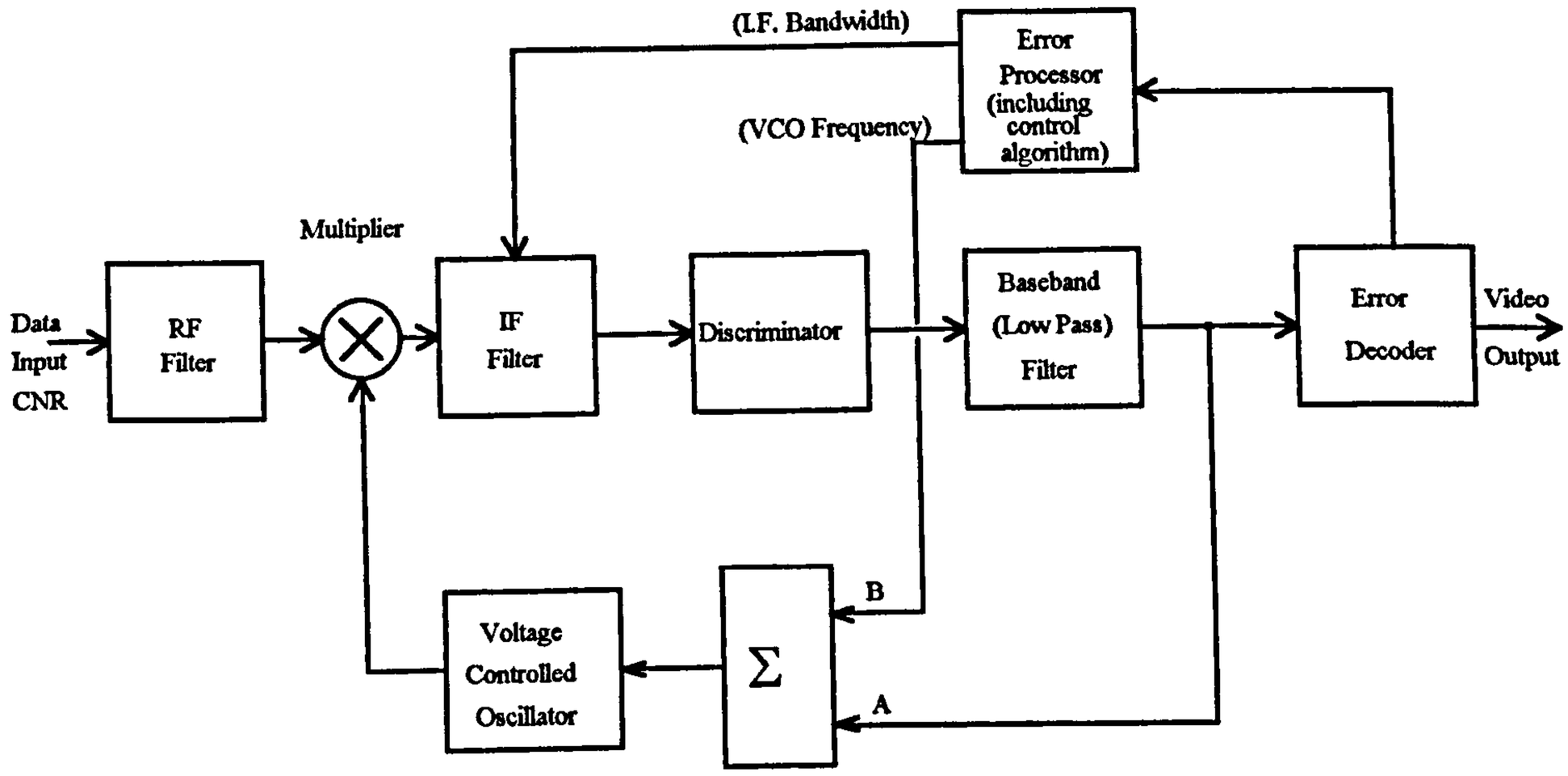

Figure 18/11 Frequency modulation with feedback error controlled adaptive demodulator with VCO frequency and I.F. bandwidth control

Assume the initial condition where the signal is applied to the receiver and the FMFB I.F filter is slightly off-tune, (say) due to temperature effects, and distortion occurs. In this condition the error processor algorithm (say) measures a high error rate and causes the bandwidth output control to set the FMFB I.F. filter to its wide bandwidth setting. In this wide bandwidth condition the signal falls within the I.F. pass band and the error decoder will measure an error rate that has fallen but is still high. This error rate is applied to the error processor where the algorithm will generate a VCO control output of one polarity that will either increase or decrease the error rate. Depending on the error rate measurement result the algorithm will either reverse the polarity of the control voltage or retain it. It will then find the control value, and hence the VCO frequency, that minimises the error rate. When this minimisation is achieved, the algorithm will then cause a bandwidth control output to be applied to the I.F. filter, reducing its bandwidth. This (say) results in the measured error rate being reduced. This VCO frequency/bandwidth reduction sequence is repeated until the error rate is at its minimum value, or at some predetermined acceptable limit. As well as improving the threshold, this technique offers a useful approach to overcoming the (environmental/ageing) stability problems encountered with the FMFB, that

normally results in increased cost and restricted application of the circuit.

18.5.3 Frequency lock loop error controlled adaptive threshold extension demodulator

The error controlled technique applied to a frequency lock loop demodulator is shown in figure 18/12. Here it is used to control the loop low pass filter. Due to its inherent wide band nature it is unlikely that, compared to the previous FMFB technique, much of an improvement in threshold extension will be obtained with this approach. The error control function could also be used to vary or pre-distort the positive envelope detector output in other versions of the technique.

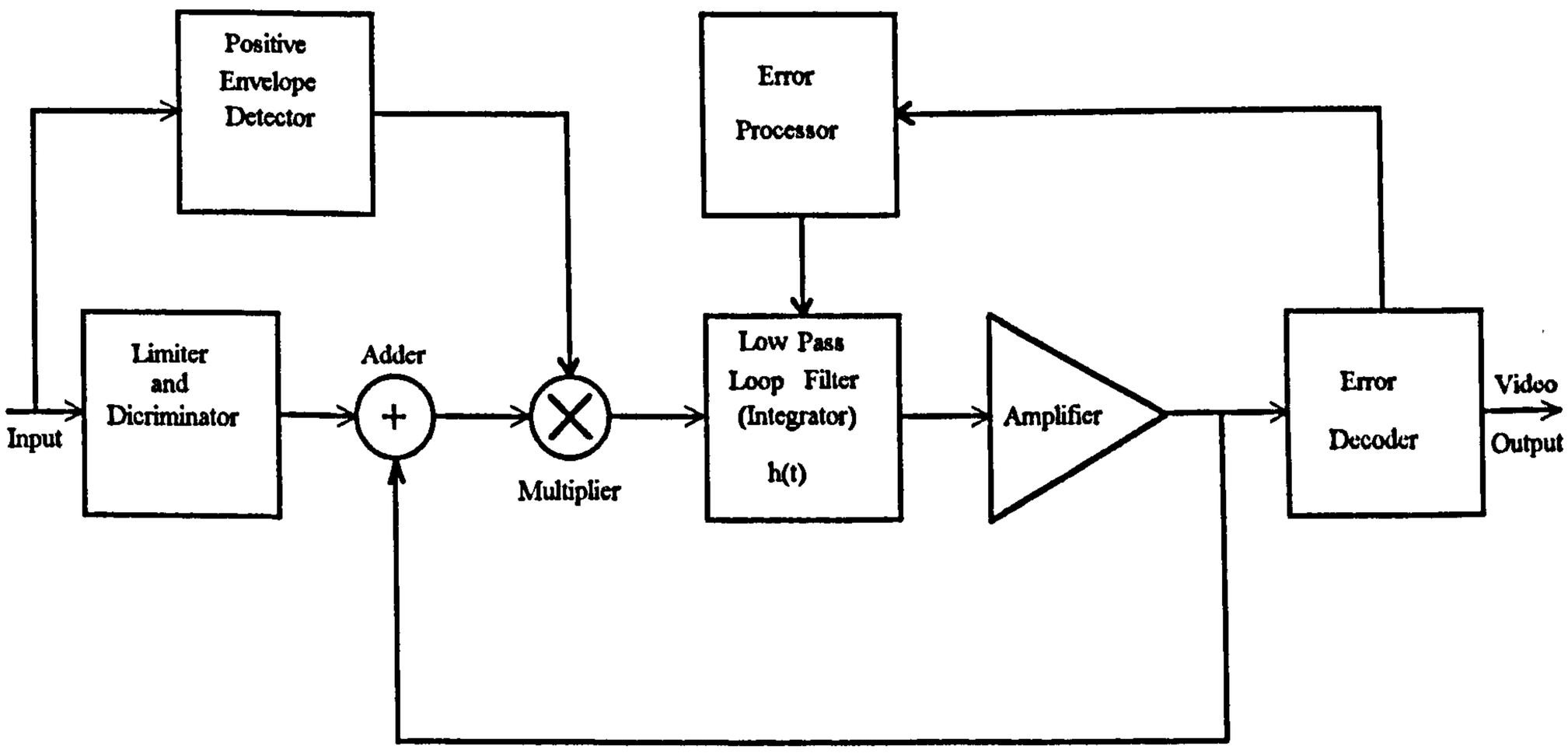

Figure 18/12 Frequency Lock Loop error controlled adaptive demodulator

18.5.4 Phase lock loop error controlled adaptive threshold extension demodulator

Figure 18/13 shows the error control concept applied to a phase lock loop demodulator. In this example the bandwidth of the loop low pass filter is controlled.

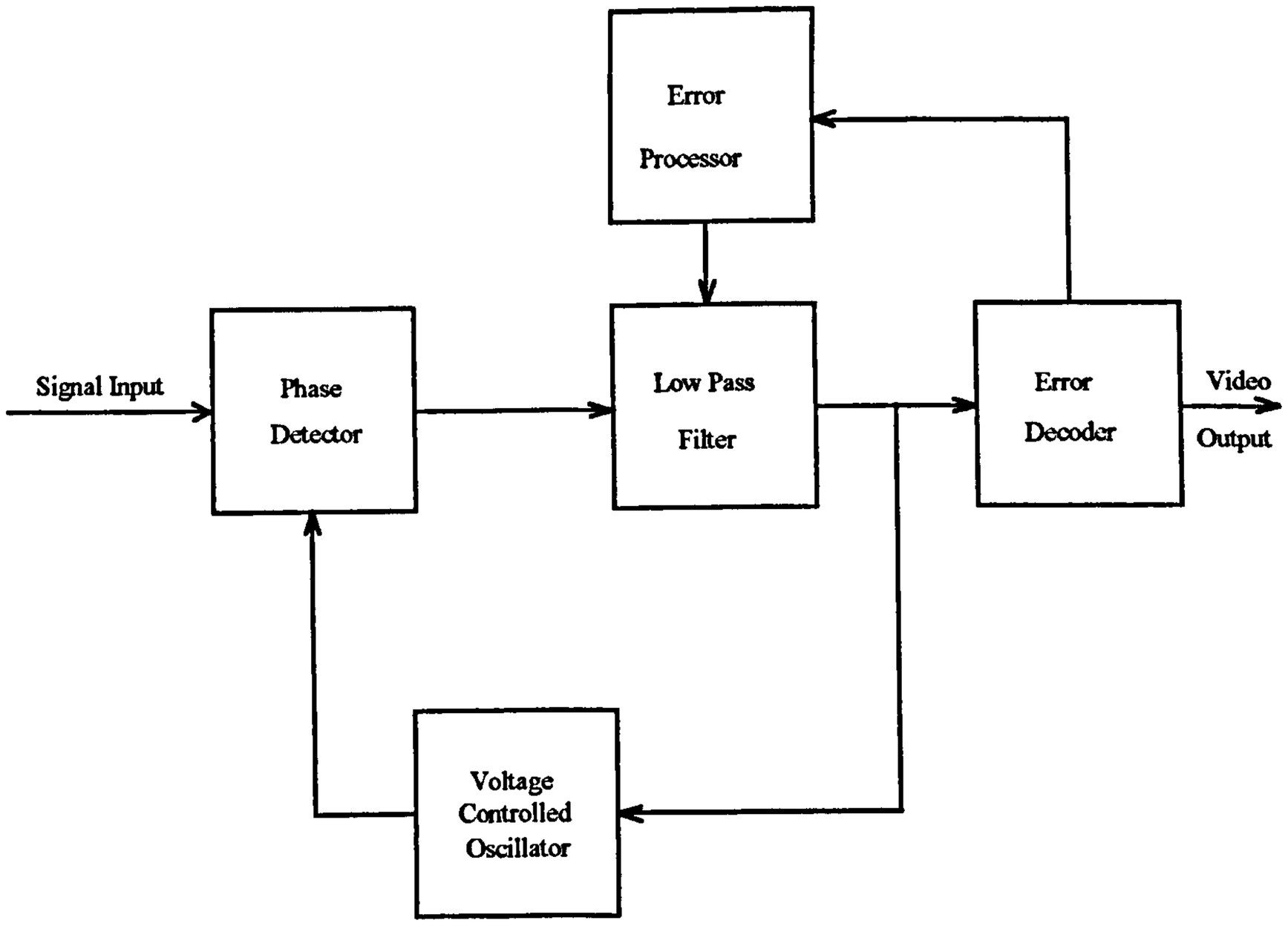

Figure 18/13 Phase lock loop error controlled adaptive demodulator

The error function could possibly also be used to control other functions in the PLL demodulator, such as the system order of the loop and the VCO frequency. As mentioned in chapter 10, there has long been interest [9] in increasing the system order of the phase lock loop demodulator. The operating characteristics that have prompted this consideration of increase in system order may be described in terms of various effects on the performance. Basically, with each increase in system order, the systems tend to oppose an instantaneous change in the next higher order derivative of the response function. The attraction of increasing the system order is the possibility of obtaining operation with a reduced noise bandwidth. But whether the advantage gained in increasing the system order above a third is worthwhile is questionable. Applying the error control concept to a phase lock loop demodulator allows the system order to be readily controlled by either switching or cascading the loop filter network. The design of the latter can be either active or passive.

A conceptual illustration showing the error control concept the system order of a phase lock loop demodulator is shown in figure 18/14. In this example different orders of loop filter are controlled by the measured error rate. In the initial state the switch would be arranged to select the loop filter with a transfer characteristic $H(s) = 1$. This results in a first order phase

lock loop. If the demodulated signal's error rate is still high, then the error control circuit would select the next higher order filter, $H(s) = 1 + \frac{K}{s}$, resulting in a second order phase lock loop. If the quality of the signal was still poor, whilst still remaining in lock, the error control would switch to the next higher order filter that results in a third order phase lock loop, namely $H(s) = K_f \frac{1 + 2\zeta_z \frac{s}{\omega_z} + \frac{s^2}{\omega_z^2}}{1 + 2\zeta_p \frac{s}{\omega_p} + \frac{s^2}{\omega_p^2}}$. These loop filter transfer characteristics are discussed in chapter 10. In a physical implementation of this circuit care would have to be taken in the means of switching between the loop filters to avoid switching transients and potential loss of lock. In practice it is likely that switching cascaded filters would be the optimum approach.

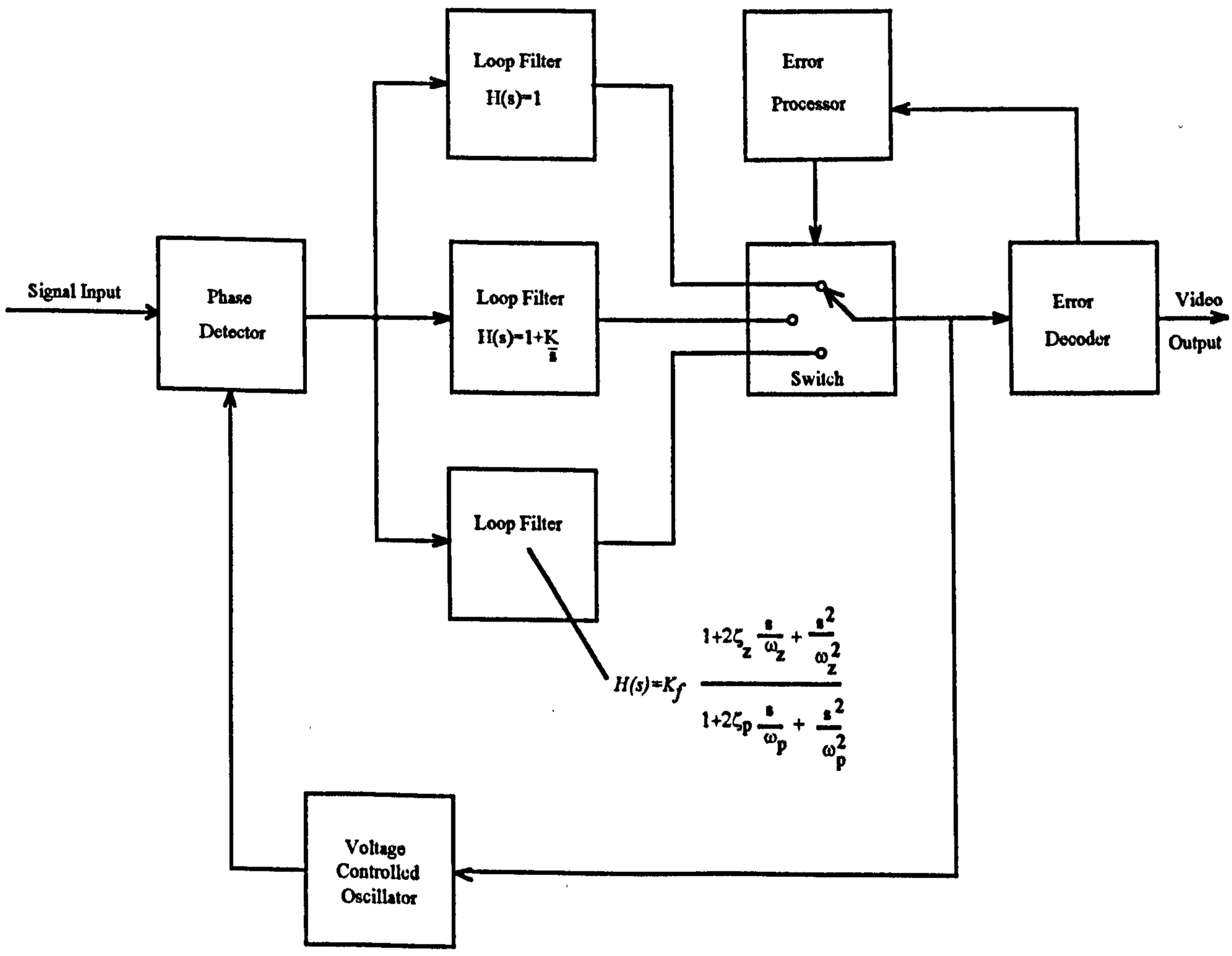

Figure 18/14 Phase lock loop error controlled adaptive demodulator utilizing error switched system order

One of the problems encountered with the use of the phase lock loop demodulator, is

knowing when the demodulator is in-lock, or out-of-lock, with the input signal. The error control concept readily allows the lock status of the demodulator to be determined. Thus in principle, it is possible to obtain fast acquisition and maintain lock in conditions of low carrier-to-noise ratio by controlling the loop bandwidth and VCO frequency.

An illustration of how the VCO frequency could be controlled is given in figure 18/15. In this circuit a summing network is introduced at the input of the VCO that sums the output feedback of the PLL, and the error control signal that is a function of the quality of the signal. Here if the error rate in the digital content of the demodulated signal increases, say, due to a loss-of-lock, the error detection signal would cause the error control circuit to provide a control voltage that would minimise the error. Variations of this circuit could be implemented where switching could be introduced into either of the two feedback loops, instead of the summing network, to disable them whilst the various corrective functions were being carried out.

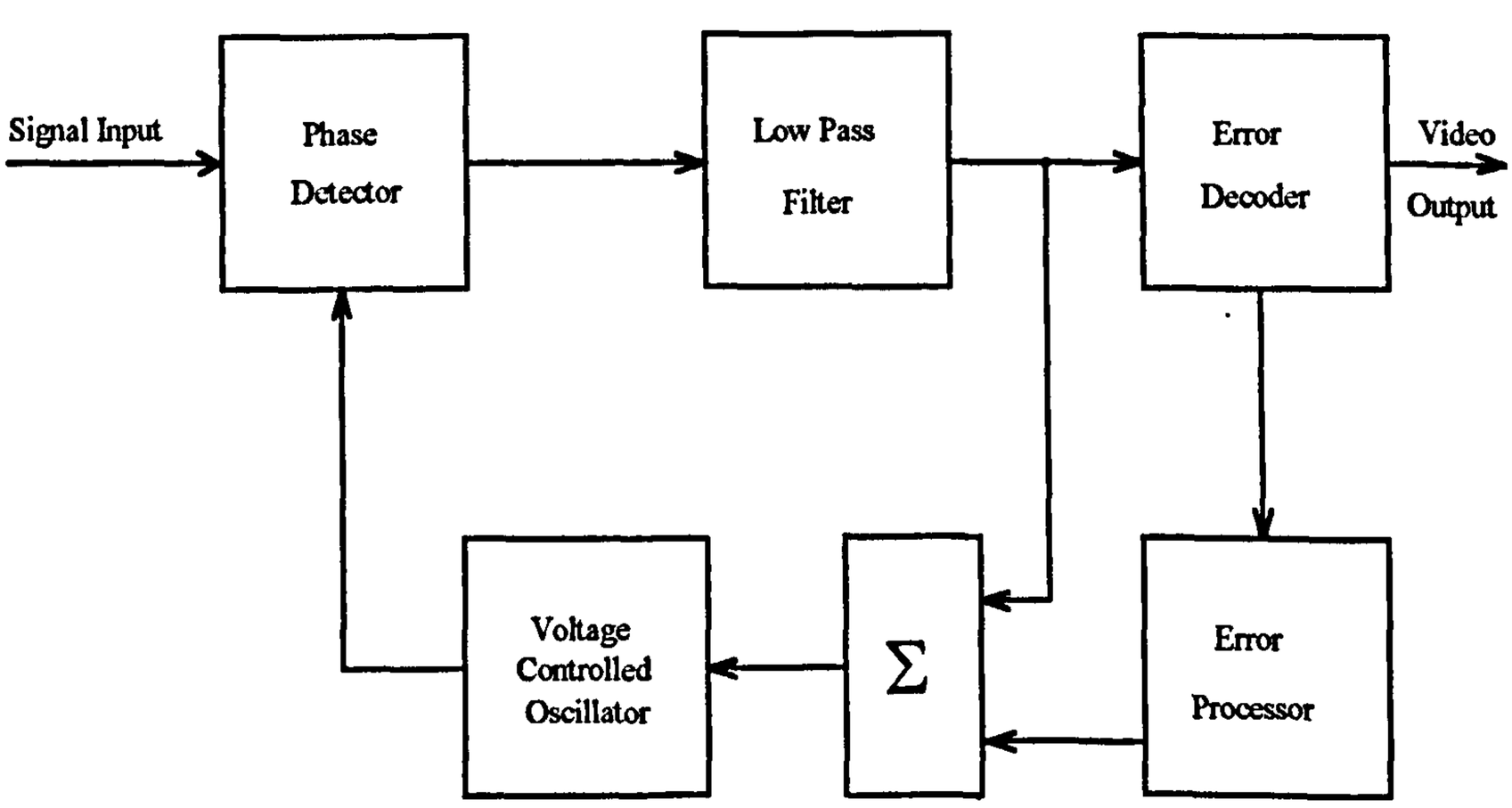

Figure 18/15 Phase lock loop error controlled adaptive demodulator showing VCO frequency control

A combination of both figure 18/13 (or 18/14) and 18/15 could be implemented to provide a means of obtaining fast synchronisation and of maintaining lock in the presence of burst noise or poor (i.e. threshold) signal strength. This implementation is shown in figure 18/16.

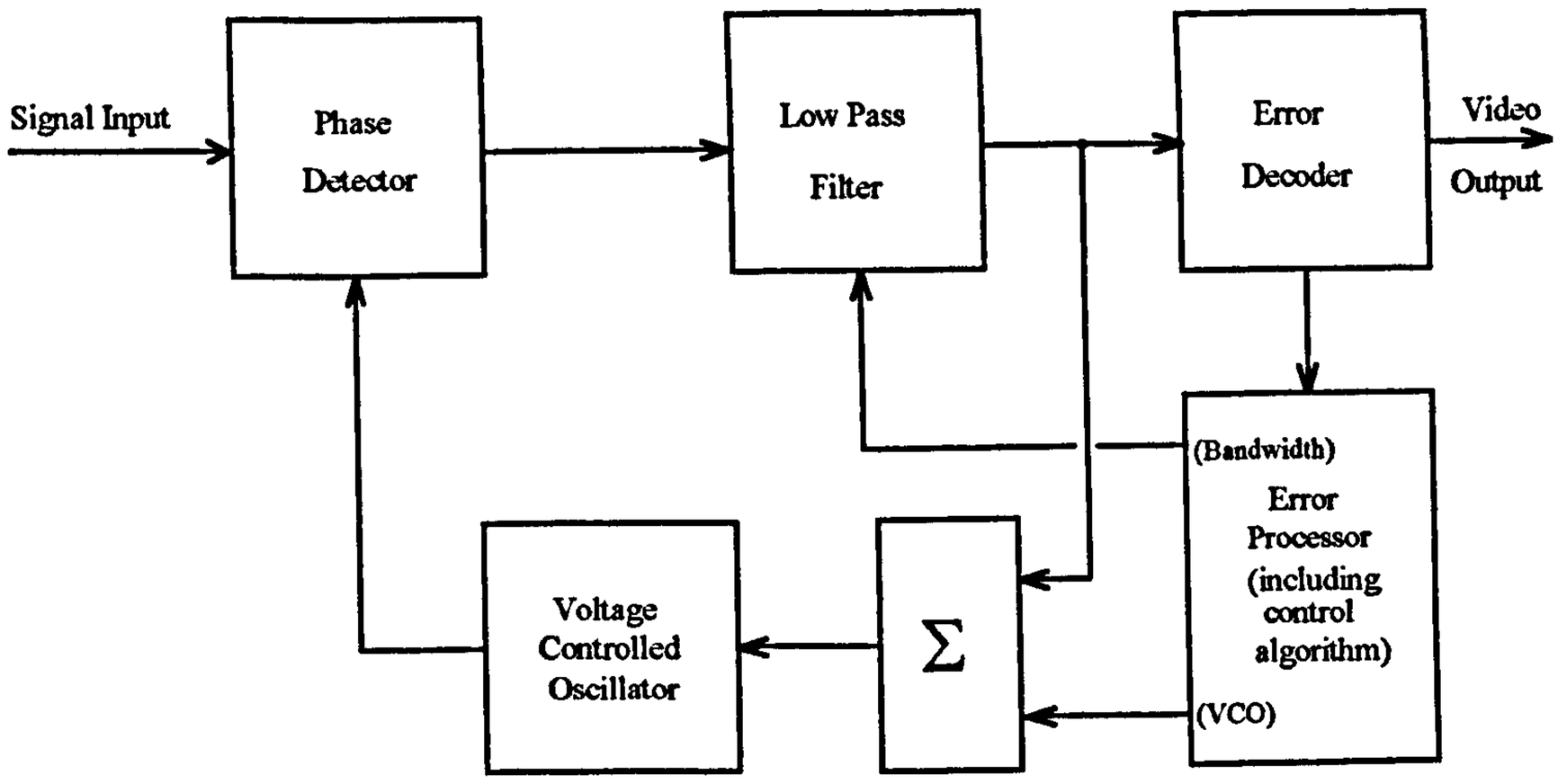

Figure 18/16 Phase lock loop error controlled adaptive demodulator showing VCO frequency and bandwidth control

In this design the error processor produces two outputs. One, the bandwidth output control is applied to the loop filter where it controls the bandwidth and/or order of the low pass filter. The second output is applied to the summing network, where it is summed with the loop feedback from the PLL output, and controls the frequency of the VCO. Assume the initial condition where the signal is applied to the receiver and PLL lock has not been achieved. In this condition the error processor control algorithm causes the bandwidth output control to set the PLL loop filter to its wide bandwidth setting. In this wide bandwidth condition, partial lock is achieved and the error decoder will measure a high error rate. This is applied to the error processor where the algorithm will generate a VCO control output that will assist the VCO to achieve fast lock. When complete lock is achieved then the algorithm will cause a bandwidth control output to be applied to the loop filter, that results in the measured error rate being reduced to its minimum value or to some predetermined acceptable limit.

For the intersymbol interference case, similar to those encountered in all-digital TV systems, an alternative approach based upon controlling the decision timing at the output of the demodulator can be implemented. This approach is illustrated in figure 18/17 that shows an error control adaptive demodulator with intersymbol correction.

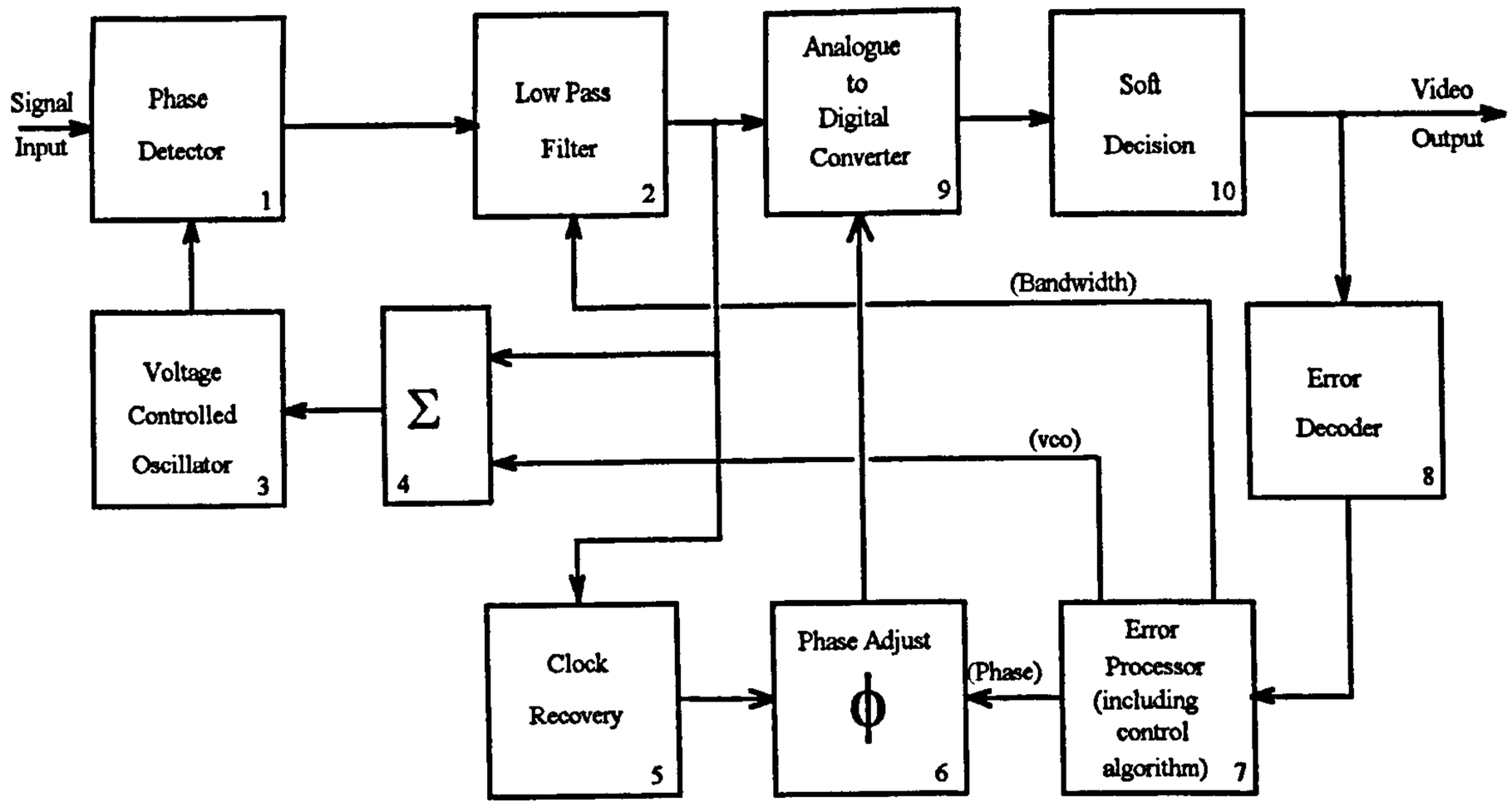

Figure 18/17 Phase lock loop error controlled demodulator with intersymbol correction

Figure 18/17 also includes bandwidth and VCO frequency control loops that are directly not part of the intersymbol interference correction function. Identifying the functional parts of the circuit, the basic phase lock loop circuit consists of the phase detector (block 1), low pass filter (block 2) and voltage controlled oscillator (block 3). The bandwidth control loop is provided by the connection between the error processor (block 7) and the low pass filter (block 2). The VCO frequency control loop is provided by the connection between the summing network (block 4) and the error processor (block 7). The intersymbol interference corrective function is provided by the analogue-to-digital converter (block 9), soft decision circuit (block 10), error processor (block 7), error decoder (block 8), phase adjust (block 6) and clock recovery circuit (block 5). The error decoder (block 8) and the error processor (block 7) are common to all three corrective functions (bandwidth, frequency and intersymbol interference).

The intersymbol interference correction circuit controls the timing of a decision circuit used for determining the logical value of the digital data at the output of the demodulator. The output of the phase lock loop is connected to three functions, one of which is the clock recovery (block 5) circuit that generates a clock waveform at the bit rate that is used in

subsequent stages for the reconstituting and recovery of the digital data. The bit rate clock output is applied to the phase adjust or shifting network (block 6) that controls the phase relationship between the demodulated output data and the clock waveform that is applied to the analogue-to-digital converter (block 9). The latter samples and converts the distorted data, at the output of the PLL, at a high rate. For every demodulated digital bit at the output of the PLL the analogue-to-digital converter produces several N bit words that are applied to the soft decision circuit (block 10). The latter examines each block of N bit words and decides whether the distorted PLL output bit is more likely to be a logical zero or one. The output of the soft decision circuit forms the video output of the error controlled adaptive demodulator. Connected to this output is the error decoder (block 8) that measures the quality of the demodulated output data in terms of the bit or word error rate. This measure is applied to the error processor stage (block 7) where it is processed into three control outputs, i.e. bandwidth control, VCO frequency control and phase control. The control algorithm contained within the error processor, apart from determining which of these three outputs is activated, would also determine initial acquisition (lock) of the signal by the PLL but monitor and control the lock conditions.

To examine the operation of the intersymbol error (or distortion) correction, assume that the error decoder (block 8) is measuring an error rate that the error processor stage (block 7) determines is too high. As part of its control algorithm, it produced a phase control output that causes the phase shift being applied in the phase adjust (block 6) to depart from its nominal vale, say, in an increased sense. This causes the phase relationship between the demodulated output data of the PLL and the clock waveform that is applied to the analogue-to-digital converter (block 9) to change, so affecting the decision timing of the point where the analogue-to-digital converter (block 9) samples the PLL output. If the resultant error rate measured by the error circuits (blocks 7 & 8) does not reduce but increases, then the error processor instead of increasing the phase shift from its nominal value, would reduce it to establish if the error rate was reduced. It would continue this procedure until the phase shift that provided the minimum error rate at the output had been established.

The VCO frequency control function operates in figure 18/17 as has been described previously for figure 18/17. To examine the operation of the VCO control function, assume that the error decoder (block 8) is measuring an error rate that the error processor stage (block 7) determines is too high. This may be due, say, to a loss-of-lock by the PLL. Again the error detection signal would cause the error processor circuit (block 7) to provide a VCO control voltage that would seek minimise the error. As part of its control algorithm, say, it produces a VCO frequency control output that is applied to the sum network (block 4). This causes the VCO frequency being generated (block 3) to depart from its previous value (either an increase or decrease) that was determined by the other input to the sum network, from the output of the loop filter (block 2) and the previous nominal value of the control input. If the resultant error rate measured by the error circuits (blocks 7 & 8) does not reduce but increases, then the error processor instead of increasing (say) the VCO frequency from its nominal value, would reduce it to establish if the error rate was reduced. It would continue this procedure until the VCO frequency that provided the minimum error rate at the output had been established, i.e. until the VCO frequency being generated was the best estimation of the signal frequency.

The bandwidth control function would operate as has been described previously for figures 18/13 and 18/14. To examine the operation of the bandwidth control function, assume that the error decoder (block 8) is measuring an error rate that the error processor stage (block 7) determines is too high. This may be due, say, to severe signal fading causing threshold conditions. Again the error detection signal would cause the error processor circuit (block 7) to provide a bandwidth control voltage that would seek minimise the error. As part of its control algorithm, say, it produces a bandwidth control output that is applied to the loop, or low pass, filter (block 2). This causes the bandwidth and/or order of the loop filter to depart from its previous value. If the resultant error rate measured by the error circuits (blocks 7 & 8) does not reduce but increases, then the error processor instead of increasing, say, the bandwidth its previous value, would reduce it to establish if the error rate was reduced. It would continue this procedure until the bandwidth that provided the minimum error rate at the output had been established.

A brief description has been provided above of the action of the error processor (block 7) in providing the three outputs viz. bandwidth control, VCO frequency control and phase control. Each of these functions is controlled by the error processor control algorithm. In practice this algorithm would have a number of functions to perform. Briefly these are:

(i) Initial acquisition of switch-on, or on initially receiving the signal. Although the bandwidth and VCO frequency controls would mainly be used for this condition, the phase control function would probably have to be optimised.

(ii) Minimising the reduction in the quality of the signal by threshold level, modulation index variation and interference. This would mainly be achieved by the bandwidth control function.

(iii) Minimising the reduction in the quality of the signal by the effects of offset frequency. This would mainly be achieved by the VCO frequency control function.

(iv) Minimising the reduction in the quality of the signal by the occurrence of intersymbol interference. This would mainly be achieved by the phase control (decision timing) function.

(v) Minimising the reduction in the quality of the signal by the effects of phase lock loop loss-of-lock. Again although the bandwidth and VCO frequency controls would be used for this condition, the phase control function would probably have to be optimised.

There are several approaches in implementing these functions into the control algorithm. The major factor that will influence the approach is that the measure of the quality of the signal is common to all the above variables and it will be difficult to distinguish the cause

without addition information available, such as signal level detectors or out-of-lock detectors, etc. being available. Thus it is likely that in practice the algorithm will have to sequence all three control functions from the error processor (block 7) regardless of the condition that causes a loss of data quality. Based on this approach a possible algorithm would be:

Prior to any signal being received, or on switch-on, the error processor (block 7) would set the bandwidth control function to provide the widest bandwidth, and/or the lowest system order, in the loop filter. Nominal, or default, values would be used for the VCO frequency and phase (decision timing) control functions. Upon receipt of a signal, the error rate would be measured at the output and the VCO frequency control function altered to find the optimum value that gave minimum error rate at the output. The phase control function would then be varied to obtain the optimum decision timing. The bandwidth control would then be reduced to establish if the error rate reduced, and the previous sequence repeated to find the optimum VCO frequency and decision timing. This procedure would be repeat until the optimum combination of the three control functions was found that gave the lowest error rate at the output. The procedure would be automatically repeated if any of system parameters changed that gave an increase in error at the demodulator output, viz. threshold level, modulation index variation, interference, offset frequency, intersymbol interference and loss-of-lock. In practice an error threshold would be contained in the error processor that would activate the corrective sequence if it was passed.

This algorithm indicates how potent the corrective features of this error controlled adaptive threshold extension demodulator can be made to be. The features indicated in this phase lock loop implementation of the error controlled adaptive demodulator can also be applied to other discriminators such as the FMFB demodulator, etc.

18.5.5 Envelope multiplication error controlled adaptive threshold extension demodulator

One technique that differs in approach from those discussed previously is an error controlled adaptive threshold extension demodulator based upon the Roberts envelope multiplication technique described in chapter 16. The approach is illustrated in figure 18/18. This circuit operates on the principle that at or below threshold an envelope multiplication demodulator provides a superior performance to a conventional limiter demodulator. The actual part of the envelope multiplication demodulator threshold characteristic where this occurs depends upon the deviation of the signal, a low value giving a greater improvement. The scheme would operate as follows. The normal signal path would be through the conventional demodulator with the error decoder monitoring the bit error rate. When the signal level is low and the demodulator enters the threshold region and clicks occur, the error decoder would measure a high bit error rate causing the error control function to switch the signal input and demodulated output of the conventional demodulator over to the envelope multiplication demodulator and, if the error rate reduces, remain in that position. It would be arranged that periodically the scheme would revert back to the conventional demodulator position to determine if the carrier-to-noise level had improved. The circuit of figure 18/18 basically seeks the demodulation path with the least bit error rate.

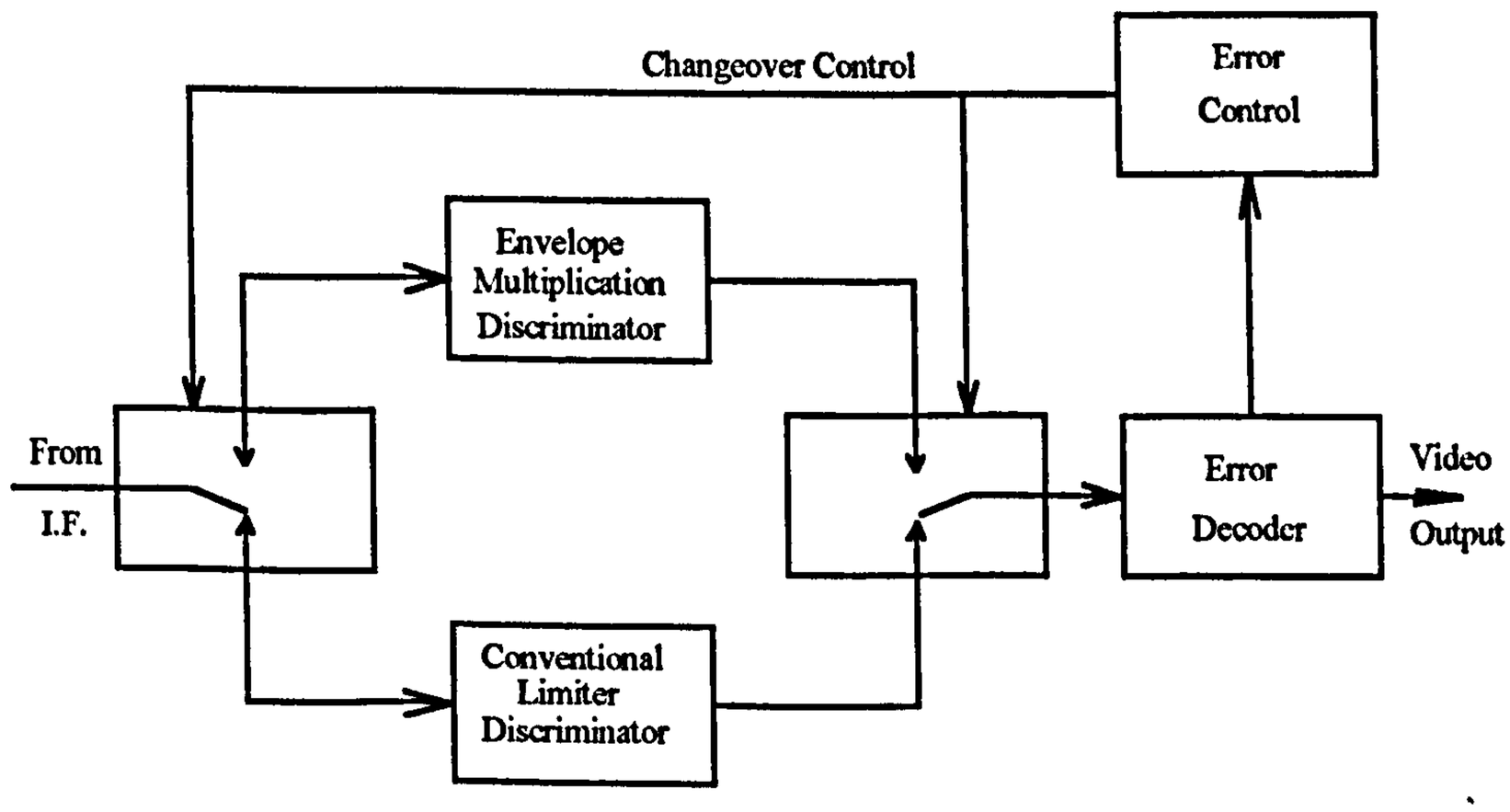

Figure 18/18 Adaptive error controlled demodulator using envelope multiplication

In practice two discriminators would not be needed as is shown in figure 18/18; the Roberts scheme shown in figure 16/1 could be modified to provide the same function by using the changeover control to switch the square law detector and multiplier in and out of circuit by monitoring the error rate. This implementation is shown in figure 18/19.

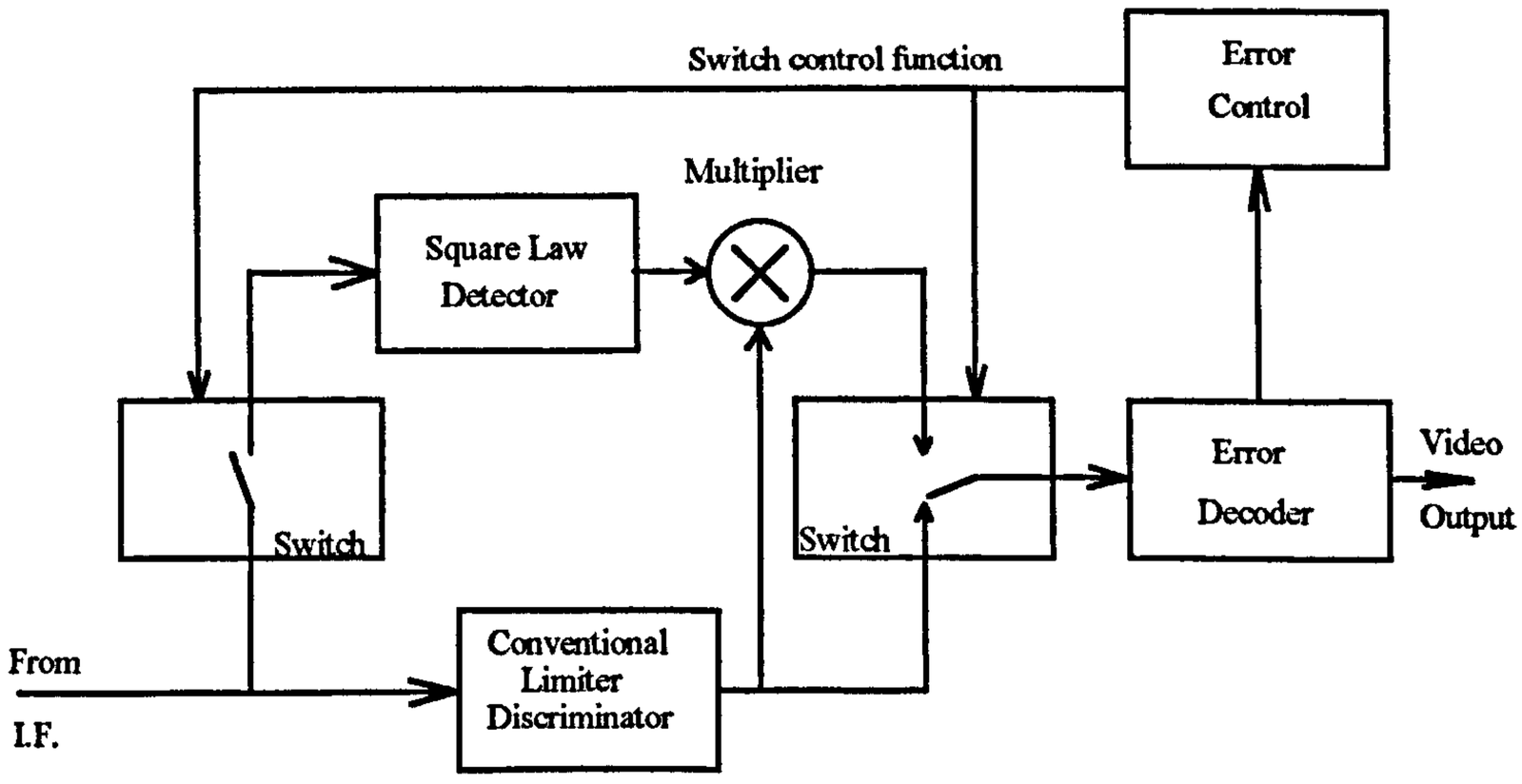

Figure 18/19 Roberts envelope multiplication discriminator implimented as an adaptive error controlled demodulator

In this concept the switch settings are shown for the high carrier-to-noise condition. The normal signal path would be through the conventional demodulator with the error decoder monitoring the bit error rate. When the signal level is low and the demodulator enters the threshold region and clicks occur, the error control function closes the switch at the signal input and changes over the switch at the demodulated output of the conventional demodulator. Thus connecting the input of the square law detector to the input of the conventional limiter/discriminator. The input to the error decoder is switched from the output of the conventional limiter/discriminator to the output of the multiplier. If the error rate reduces, the switches would remain in their new positions. It would be arranged that periodically the scheme would revert back to the conventional demodulator position to determine if the carrier-to-noise level had improved and the error rate reduced to a lower level. Note that figure 18/19 is a conceptual circuit. In practice the switching arrangements for the multiplier may have to be modified to minimise interference.

18.5.6 Other threshold extension demodulators

Although the bit error control concept could be applied to the click elimination demodulator of chapter 15, it could not be readily implemented and at an initial examination does not offer many advantages. In this application its operation would be similar to the error correcting function introduced by the error code pattern in error code correcting systems.

The switched capacitor demodulator approach with its disadvantages described in chapter 14, does not lend itself to the error controlled adaptive threshold extension demodulator approach and will not be considered further here.

18.6 Discussion

A conclusion of the previous work carried out is because of the inherent non-linear nature of angle modulation, it is impractical to design a threshold extension demodulator that will function for all values of input carrier-to-noise ratios and for all values of modulation index. Thus use of an additional parameter namely the digital (sub) structure information content of the signal is proposed that provides a quality measure of the latter. This allows an adaptive demodulator to be devised that uses the information error rate characteristic that occurs at threshold with those digital structures contained in part or all the signal structures used in conventional, MAC/Packet and all-digital systems. At threshold the click phenomena generate errors in the digital pattern that can be used to alter the configuration of the error controlled adaptive threshold extension demodulator.

The information characteristic proposed for use in conventional TV systems (PAL, SECAM and NTSC) is Teletext. For MAC/Packet type systems several digital sub structures exist, namely frame and line sync patterns, as well as other error control patterns in line 625. All-digital TV systems with their use of sophisticated error coding techniques (e.g. Reed-Solomon codes) have a ready source of error rate indication. Several types of threshold extension demodulator techniques are shown to lend themselves to being incorporated

within the error controlled adaptive threshold extension demodulator concept. Here the error rate derived from those digital (sub) structures at threshold is used either to reduce the bandwidth of the I.F. filter, to modify the characteristics of the loop filter or to control the decision timing used to reconstitute the demodulator output. An example is given of an adaptive demodulator, using a PLL, where by controlling the three latter functions, the circuit can respond to any change of system parameters that give rise to an increase in error at the demodulator output, e.g. threshold level, modulation index variation, interference, offset frequency, intersymbol interference and loss-of-lock. The error rate function can also be used either to alter other parameters of the adaptive demodulator (such as the system order of a PLL) or to switch to a different demodulator technique entirely, such as an envelope multiplication scheme, that provides a superior demodulation characteristic at or below threshold. The uses of the increased bit error rates at threshold, in addition to the other signal characteristics, allow a wide variety of techniques to be adopted that should make the demodulator relatively independent of the input carrier-to-noise ratio and allow for a wide range of modulation index value variation.

The whole purpose in designing a successful threshold demodulator for TV signals can be simply summarised as producing a design that prevents the onset of click or spike phenomena at threshold; an effect that is so objectionable to the viewer. The gentle degradation in picture quality that occurs with the reduction in the (Gaussian) carrier-to-noise ratio is generally acceptable. The error controlled adaptive threshold extension demodulator design approaches discussed above go some way to achieving this objective.

18.7 References

[1] Independent Broadcasting Authority, "Developments in Teletext", IBA Technical Review, 20, May 1983.

[2] Independent Broadcasting Authority "The D-MAC/packet system for satellite and cable", IBA Technical Review, 24 November 1988.

[3] Marzolini, R. G. A. "Improvements to Demodulation Systems", U.K. Patent Application GB 9514126.3, July 11th, 1995.

[4] Gonsalves, R. A. "Performance of Manchester Coded FSK", IEEE Trans. Aero. and Elect. Syst., Vol. AES-6, No. 4, July 1970, pp. 598 - 599.

[5] Cartier, D. E. "Limiter-Discriminator Detection Performance of Manchester and NRZ Coded FSK", IEEE Trans. Aero. and Elect. Syst., Vol. AES-13, No. 1, Jan. 1977, pp. 62 - 70.

[6] Schilling, D. L., Hoffman, E., Nelson, E. A., "Error Rates for Digital Signals Demodulated by an FM Discriminator", IEEE Trans. Comm. Tech., Vol. COM-15, No. 4, August 1967, pp. 507 - 517.

[7] Rohde, C. A., "Estimation of Bit Probability of Error Using Sync Word Error Rate Data", IEEE Trans. Comm. Tech., Vol. COM-18, No. 6, December 1970, pp. 811 - 814.

[8] Henry, J. C., "DPSK versus FSK with frequency uncertainty", IEEE Trans. Comm. Tech., Vol. COM-18, No. 6, December 1970, pp. 814 - 817.

[9] Lewis, P. H. and Weingarten, W. E. "A comparison of second, third, and fourth order phase-locked loops", IEEE Trans. Aero. and Elect. Syst., Vol. AES-3, No. 4, July 1967, pp. 720 - 727.

Blank Page

19. DIGITAL TELEVISION SYSTEMS

19.1 Introduction

As discussed in Appendix B to this thesis, the proposed standard for future satellite television transmission to Europe was to be based upon an analogue MAC system with future high definition television capabilities. However as a result of the successful demonstration [1] of a digital high definition television system by General Instruments in the U.S.A. in 1990, the majority of the world's authorities abandoned the MAC system and decided to base all future TV systems on digital techniques. A restricted form of satellite digital television became operational [5] in the U.S.A. in 1994 with a limited service being provided by two GM Hughes satellites. It uses the MPEG-1 standard for video compression. Problems are currently being experienced with colour smearing in fast action scenes and loss of picture during rain and other types of bad weather. Although this system has limitations it has been well received by consumers, however it is unlikely to find wide application. The future U.S. national standard is likely to be the proposed all-digital HDTV system; this section will therefore briefly consider the effect of this all-digital system upon the demodulator process and how the performance at threshold is expected to differ.

19.2 Digital TV Systems

19.2.1 Digital television systems have several advantages over analogue systems. They can be implemented at lower power levels, they interfere less with existing systems and their quality is generally constant throughout a given service area. There has been interest in the approach for several years and an early reference is [3].

Although at the time of writing this thesis, an agreed system specification for a proposed (satellite or terrestrial) digital HDTV system has not yet been published, either in Europe, the U.S.A. or Japan, limited information has become available for the U.S. system. For the

latter, certain subsystem features have been defined in [1]. Developments subsequent to this reference are given in [2] which contains a tentative specification for a terrestrial HDTV digital system. This specification is given in Appendix A. In this specification it should be noted that the U.S. approach is determined by the basic requirement that the transmission spectrum should be contained within a single 6 MHz (U.S.) channel allocation and that a future HDTV system should have a resolution 6 times that of the current NTSC system. To achieve this requirement, an all digital system is proposed with video compression and 8 level vestigial sideband suppressed amplitude modulated carrier (entitled 8-VSB). One objective is to provide a high picture quality within the bit-rate constraints of terrestrial broadcasting, i.e. approximately 18 Mb/s. The major objective of the video compression system is to represent a video source with as few bits as possible while preserving the level of quality required for the given application.

19.2.2 To achieve a suitable compression technique, the video technology uses source adaptive processing, motion estimation/compensation, transform domain data representation and statistical coding. The salient subsystem characteristics of the digital HDTV system are:

(i) A packet system for data transmission will be used.

(ii) The sound system will be based upon the Dolby AC-3 technology.

(iii) Video compression will be based upon the MPEG-2 standards to provided a coded representation of the video and audio signals. This standard outlines a structure for data blocks as well as the allocation of bits within those blocks, like chrominance and luminance. The compression scheme proposed relies on the analysis of images, compressing them by eliminating redundancies and coding only the changes between frames rather entire new pictures for every frame.

(iv) A set of scanning formats has been proposed. These include 24, 30 or 60 frames/second progressively scanned at 720 lines of active resolution, 24 or 30 frames progressively scanned and 60 interlaced fields, both at 1080 lines of resolution. These formats are intended to encourage an evolution towards progressive scan rate of 60 frames of 1080 active lines.

19.2.3 In the digital HDTV system the video source is encoded by the vision encoder, whose output is a string of bits that represent the video source. This is followed by a channel encoder that transforms the bits into a modulation format suitable for transmission over the communications channel. Error correction is introduced to compensate for noise added to the signal over the communication channel. The inverse process occurs at the receiver. The audio and video compression used consists of three stages. Firstly the critical information required to be encoded is identified. The second stage is the quantisation of the information to be transmitted and thirdly, the assignment of codewords to represent the quantisation levels. Each of the three stages seeks to exploit the redundancy present in the video source and the limitations of the human visual system.

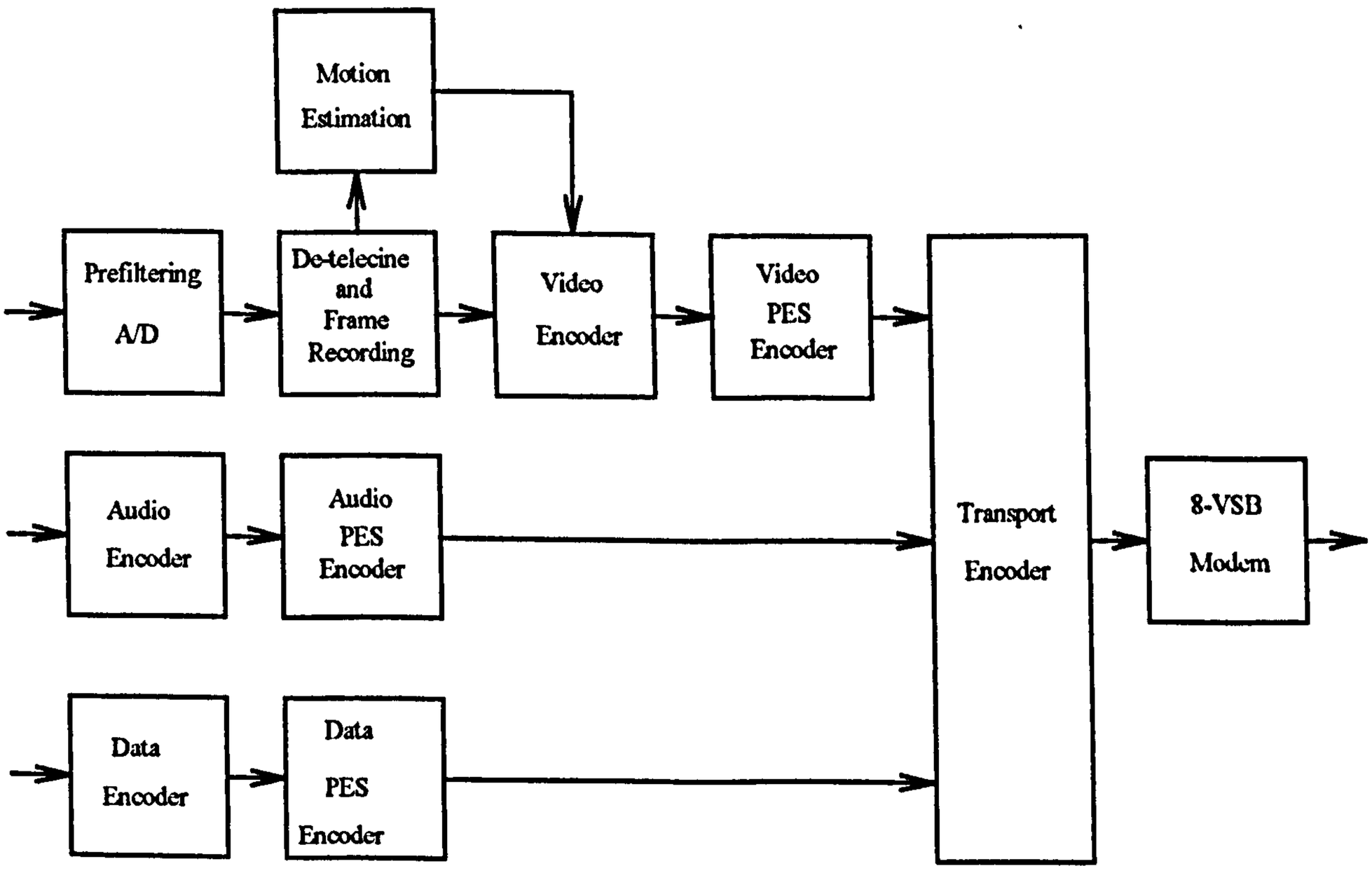

Figure 19/1 Digital encoder system block diagram

A block diagram of the proposed encoder system is shown in figure 19/1. The functions contained within this system are video encoding, audio encoding, a transport layer to perform multiplexing, an 8-VSB (vestigial sideband) transmission layer for terrestrial transmission. The MEPG-2 standard is used for the compressed digital video data. It uses the discrete cosine transform (DCT) to reduce spatial redundancy, and motion compensated temporal prediction to alleviate temporal redundancy. A further objective of the design is to meet the requirements of adaptive multiple formats, i.e. sources consisting of video cameras, film standards, magnetic and optical media, and synthetic imagery. In the proposed system one interlaced format is supported because of HDTV camera requirements, but the ultimate system objective is to eliminate interlace in the transmission path. Progressive formats will be used in the system that will allow a trade-off between spatial and temporal resolution, and between resolution and coding artefacts. The display format will be independent of the transmission format.

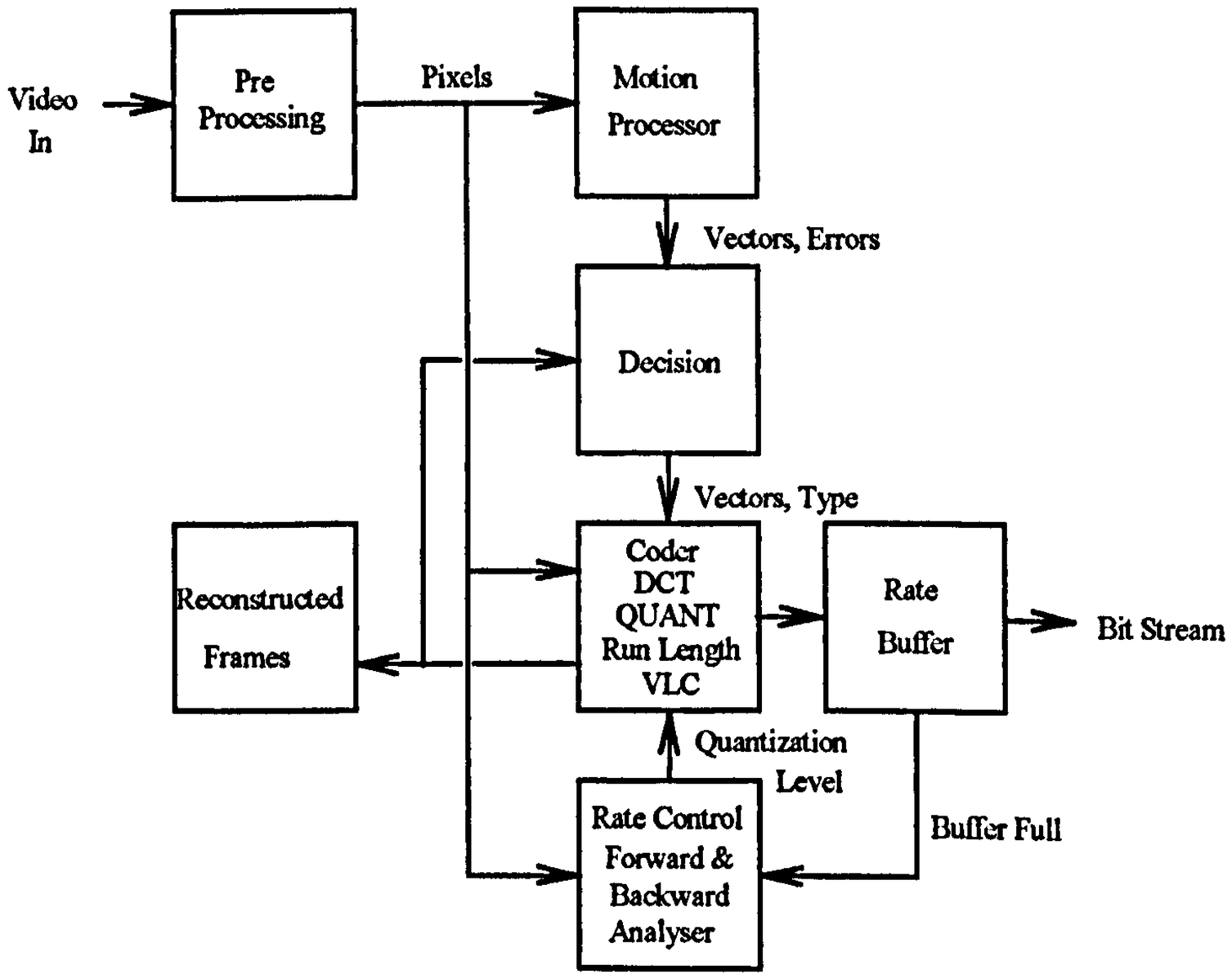

Figure 19/2 Digital video encoder

The video encoder block contained within figure 19/1, is shown in amplified form in figure 19/2. It consists of a pre-processor, a motion estimation subsystem, a discrete cosine transform and quantisation subsystem, and a variable word-length encoder subsystem. A rate buffer is also included to smooth the data for a constant bit rate transmission. This functional block diagram's input consists of the three primary (RGB) colour inputs which are highly correlated with each other. Advantage is taken of the differing human responses to the luminance and chrominance components. The compensation algorithm utilises multiple predication methods to effectively provide motion compensation for progressive and interlaced pictures. The prediction methods include frame prediction, adaptive field prediction, dual prime for forward prediction and bi-directional prediction.

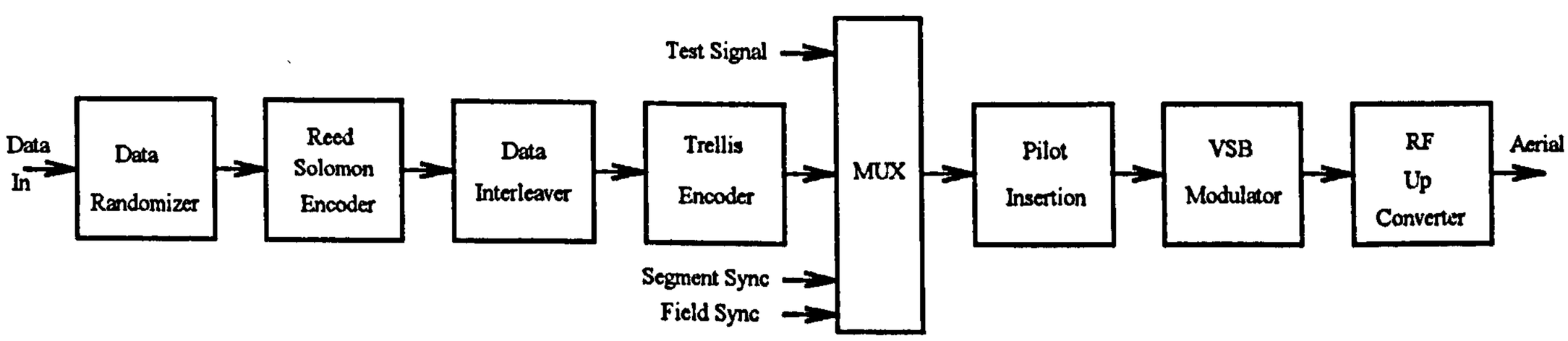

Figure 19/3 8-VSB Transmitter Scheme

The 8-VSB transmitter block diagram is shown in figure 19/3. The digital data generated by the video and audio encoders are digital-to-analogue converted (A/D) into 8-level symbols (3 bits/symbol) which are then modulated into a vestigial sideband (VSB) suppressed AM carrier. The system is claimed to be a robust transmission system. The 8-VSB RF signal includes a pilot signal at the carrier location. This enables receiver tuning to be carried out under severe noise conditions.

Referring to figure 19/3 data enters at the Data Randomiser, whose function is to prevent a constant output for a constant input. The Reed Solomon error control parity bits are added to each segment; additional protection is also provided by the Data Interleaver. Long burst

errors in the transmission path are spread out by the complementary de-leaver in the receiver preventing Reed-Solomon overload. The Reed-Solomon encoder is concatenated with a $\frac{2}{3}$ Rate Trellis encoder. Synchronisation data is added in the subsequent multiplexer (MUX) bloc. Field sync and segment sync are at a constant binary level. Neither sync is encoded or interleaved. The data field sync provides the means to determine the data field onset; in addition it is compared to an internal reference in the receiver, the difference being used to adjust the Equaliser that removes echoes and intersymbol interference; in addition two other facilities are provided namely whether the receiver interference rejection filter is used or not, as well as controlling the receiver phase tracker.

The VSB modulator operates at a RF carrier frequency of 46.69 MHz. The lower sideband is upconverted to the wanted carrier frequency. The receiver features the transmitter complementary block diagram scheme in reverse order but with three additions that precede the Trellis Decoder, these are the NTSC rejection filter, Equaliser and the Phase Tracker.

19.3 Digital Demodulation

19.3.1 The provisional information published on the proposals for the US HDTV system [2], does not give any information on the satellite DBS version, although it does contain some results for cable applications. It is assumed that the same constraints that apply to current DBS systems regarding transmitter restrictions will apply to this digital HDTV system. Thus it is likely that the modulation technique that will be used in a future digital HDTV satellite DBS system will be FM. Little information has been published in the technical literature on the threshold demodulation characteristics of high data rate digital television systems. One reference that gives a guide to what may be expected is [4], which although considering a digital phase lock loop demodulator does give some indication of the threshold characteristic that is obtained.

19.3.2 Reference [1] gives the threshold characteristics for an offset modulation condition for a first, second and third order all digital phase lock loop and two conditions of

modulation index. The interesting threshold characteristics shown in this reference is the sharpness of the characteristic below threshold, where a change of some 2 dB in the input carrier-to-noise ratio gives a drop of some 15 - 20 dB change in the output signal-to-noise ratio. Although the threshold point is the same for a digital and analogue PLL demodulator, under some conditions some threshold extension for the digital high order PLL is obtained compared to the analogue PLL. This sharpness in below threshold characteristic could cause some difficult system problems as is discussed in 19.4.1 below.

19.4 Discussion

19.4.1 Although to date there has been little comment on the satellite version of HDTV, there are indications of the problems that may be encountered. For example, will the system be adequate for satellite transmission with its complex video compression scheme, when satellite systems operate so close to threshold and suffer fades and multipathing for a percentage of the transmission time. Unless error coding is used then video compression makes the system very vulnerable to interference. The use of Reed Solomon coding is an effective solution that gives the system good protection against burst errors. The indication that digital demodulation will have a more rapid fall-off below threshold makes it likely that the degradation in quality will be very abrupt, unlike an analogue system that has a gradual degradation in picture quality. With a digital system the picture will probably maintain its quality until threshold is reached, and then there will be a sudden loss of picture as the reduction in input carrier-to-noise ratio gives a large change in the output signal-to-noise ratio. As with all systems of this nature the synchronisation technique does not have error coding protection, relying on the receiver internal reference to overcome the effects of noise of a burst nature. If the signal is at, or below, threshold for any length of time, this internal reference may not provide adequate synchronisation. Where digital systems have error protected data, and synchronisation without error protection, it may be considered that two thresholds exist. These are the data threshold and the sync threshold. Ideally both should be equal, or as occurs in practice the sync threshold is lower (better) than the data threshold. Thus ensuring that when the input carrier-to-noise level enters the threshold region, the data

is lost before there is a loss of sync. Little information has been published on the sync strategy that will be used in the proposed all digital HDTV system, but it is assumed that the Field Sync will use a digital pattern (word) which, to give good sync and anti-noise characteristics, will have a length of the order 28 to 33 bits.

19.4.2 Although insufficient information currently exists on the all digital HDTV system, indications are that because of the conventional demodulator characteristic at threshold, it may be those threshold extension demodulators with modest improvement figures may offer significant performance gain. Particularly if use is made of the error correction facility to control the threshold extension demodulator. This aspect is discussed in chapter 18. Future studies in this area may be beneficial.

19.5 References

[1] Anastassiou, D. "Digital television", Proc. IEEE, April 1994, pp. 510 - 519.

[2] Challapli, K., Lebegue, X., Lim, J., Paik, W., Girons, R., Petajan, E., Sathe, K., Snopko, P., Zdepski, J., "The grand alliance system for US HDTV", Proc. IEEE, Vol. No. 2, February 1995, pp. 158 - 173.

[3] Independent Broadcasting Authority, "Techniques for digital television", IBA Review, No. 12, January 1979.

[4] Garodnick, J., Greco, J., Schilling, D. "Response of an all digital phase locked-loop", IEEE Trans. Comms. Vol. COM - 22, No. 6, June 1974.

[5] Perry, T. S. "Consumer electronics", IEEE Spectrum, January 1995, Vol. 32, No. 1, pp. 40-43.

20. SUMMARY AND CONCLUSIONS

20.1 Summary

The studies carried out and given in this thesis, into demodulator techniques in satellite communication systems for direct broadcast systems, are summarised below together with the conclusions derived. An examination has been carried out into FM demodulation threshold phenomena, and in particular those demodulators that exhibit the effect termed threshold extension, with particular application to satellite direct broadcast systems. This threshold effect is defined as the point on the input carrier-to-noise/output signal-to-noise relationship of the FM demodulator, where the essentially Gaussian nature of the noise changes to a Poisson characteristic; namely the point where the onset of spikes, or clicks, in the demodulated output occur.

A description of the MAC format satellite TV systems are given with emphasis on the D2-MAC version. Relevant extracts of the international CCIR standards applying to these systems are given in appendix C. From these standards, key parameters pertinent to threshold extension demodulators have been derived for the D2-MAC system. The maximum bitrate for a future typical digital system within a standard satellite channel allocation is derived and descriptions of typical MAC format satellite transmitters and terrestrial receivers are given; figures of merit for the latter are specified. The effects of threshold extension on a typical satellite to ground DBS TV link has been assessed for a typical system. It is shown that for the system considered the clear air transmission exceeds the threshold figure and provides continuous reception. The 3 dB rain condition, with an outage of 0.1%, just satisfies the threshold point. Any rain attenuation more than 3 dB increases the outage figure. If a threshold extension demodulator is introduced with a threshold improvement factor of some 4 dB, then the performance of the whole system is improved. In this case the 3 dB rain condition has a margin above the new threshold figure, thus reducing the 0.1 % outage.

FM threshold noise characteristics are discussed and briefly analysed and Rice's noise model is described. The effects of clicks on TV pictures are discussed, together with the nature of clicks, noise clicks, doublets and modulation transients.

The quality criterion chosen for use with TV pictures is considered and the bandwidth criteria used, in terms of Carson's rule, is described. A limited discussion of the pre-emphasis and de-emphasis characteristics used is also given.

The relationship between the input signal's carrier-to-noise ratio and the demodulated output signal-to-noise ratio has been given for a conventional demodulator, for the conditions of unmodulated carrier, sinusoidal modulation and Gaussian modulation. These show a non-linear dependence of the demodulation process upon the nature of the frequency content of the carrier modulation in the threshold region. A change in picture content from a predominately single frequency component to a Gaussian type frequency component alters the point at which threshold clicks occurs to a higher input signal level. This non-linear operation is one the major source of difficulties preventing the successful operation of a threshold extension demodulator. The expressions for an unmodulated carrier, for sinusoidal modulation and for Gaussian modulation, clearly show the effect of the nature of the modulation upon the threshold of the demodulator. The sinusoidal and Gaussian characteristics have been plotted. These show how the characteristic, and the threshold break point, of the demodulator changes as the modulation becomes more complex. In addition these characteristics are also a function of the modulation index changing, which in turn as the result of the maximum modulation frequency content of the signal. Thus, when a complex signal is in the threshold region, the spike or click phenomena that occur will be influenced by the increase in complexity of the modulation. For a TV signal in the vicinity of the threshold region, and for a constant input carrier-to-noise level, the noise that appears in the picture will depend upon the picture content.

The tracking filter threshold extension demodulator has been examined and analysed. It has been widely used as a threshold extension device. The reason may be that it

is the only demodulator where all the circuit functions are clearly separate, i.e. adaptive filter, demodulator, control function, etc. The simplified analysis of the tracking filter carried out shows clearly how an improvement in threshold extension is achieved by reducing the bandwidth of the system. However the disadvantages incurred include a lack of picture resolution, and increased distortion resulting from reducing the higher order sidebands in the signal. This distortion occurs with other demodulators such as the FMFB, but is not so clearly identified. The survey of various tracking filter design approaches published illustrate the basic problem. Namely the two control functions required for adjusting the centre frequency of the filter and its bandwidth respectively. The adjustment of the centre frequency does not pose a major problem as there are several characteristics in the signal structure that can be used as the control functions, e.g. the chrominance frequency in conventional TV systems. However the metric for detecting the occurrence of threshold has not really been solved. How the metric detects the click, rather than the doublet, false click or modulation transient and controls the filter, is a problem that the references cited had not solved. A proposed solution resulting from this study is given in this thesis.

The analysis of the FMFB demodulator has followed two approaches. Firstly a simplified global FMFB analysis has been given, and secondly a brief summary of the analysis proposed by Iwanami. The simplified global analysis has shown how the noise characteristic is modified by the FMFB action. The summary of the Iwanami approach followed gives a deeper insight into the operation of the FMFB demodulator and of the close control it gives to the various circuit parameters. However like all other threshold extension demodulators it can only be designed for a specific set of signal conditions and hence threshold level. Since the signal structure is dependent upon the picture content, the threshold point of the demodulator will vary, thus altering the performance of the demodulator. For the successful application of the FMFB demodulator to DBS reception, an adaptive design is required which optimises its parameters to the signal structure. This is discussed in the adaptive demodulator section.

This examination of the phase lock loop demodulator and its traditional analysis has shown that there are many unsolved problems remaining, when it is operating in the threshold region and when the input signal is complex. When the input signal structure is fixed, such as in deep space satellite transmission, successful operation of the PLL demodulator is possible and a 2 to 3 dB improvement in performance is obtained. In general it may be concluded that any improvement in the phase lock loop demodulator that is obtained is due to its unusual threshold characteristic. That is when the input amplitude is reduced, the PLL bandwidth reduces. This characteristic bears some similarity to that of the oscillating limiter discussed in tracking filter demodulator section. When the input signal contains no modulation, and when operating in the threshold region, the numbers of spikes in the output of the PLL demodulator reduce as the gain of the PLL is reduced. When modulation is present, there is a minimum loop bandwidth below which distortion results. In this region the spikes present are large. Increasing the PLL bandwidth results in a decrease in the number of spikes. If the bandwidth is made very large then the operation tends to approach that of a conventional discriminator. Thus when modulation is present there is an optimum PLL bandwidth, which in turn depends upon the nature of the modulation. The proposed adaptive threshold extension demodulator approach when applied to the PLL may overcome this limitation.

At an initial glance the frequency lock loop demodulator looks an attractive threshold extension demodulator concept, with its lack of VCO. It is one of those rare concepts that makes use of the additional (amplitude) information in the carrier signal that is normally discarded when a limiter is used. However the analysis carried out reveals that the assumption made that the value of the envelope goes low when a click occurs is not a reliable metric for signifying the occurrence of a click; frequently this change in amplitude does not occur. When it does, it can occur for both clicks and doublets, thus preventing essential discrimination taking place between them. The reduction in FLL loop bandwidth that occurs as a result of the envelope going low and minimises the effects of clicks, is very similar to the effects described previously in other demodulators such as the PLL and oscillating limiter. The difficulty in determining the bandwidth of the demodulator, as a

compromise between a low bandwidth for click elimination and a wide bandwidth for minimises distortion of the signal, is a severe limitation. The design of the loop filter in this demodulator is rather critical, and for a DBS system probably impractical, given the changing picture content. It may be for this reason that the approach does not appear to have found wide application. However the adaptive demodulator technique described in this thesis may overcome this restriction.

Hamer's autocorrelation demodulator is an interesting approach. It appears to obtain any threshold improvement that it has, by changing the carrier modulation from FM to PM, taking advantage of the inherent 3 dB advantage that coherent (PM) demodulation offers. The problem with the autocorrelation demodulator is that it is drastically affected by the signal modulation and that the FM improvement factor at high modulation indices is lost. Although equivalent to the Park and Murakami demodulator approaches, its characteristics are very similar to the Roberts envelope multiplication approach discussed elsewhere in this thesis. Because these approaches give an improvement below threshold and not above, they may offer some advantages in DBS applications.

The analysis for the phase filter demodulator has followed that given by Hummels. The approach is interesting as a theoretical concept but the approach would not be suitable for DBS applications because of its very wide band requirements. The approach illustrates several interesting features. Firstly the mathematical representation of the concept shows the approach consists of a linear phase filter followed by a conventional phase lock loop demodulator. This is again an illustration of how many of the threshold extension demodulator approaches are basically similar. Secondly the potential to reduce the effective deviation of the message (modulation). This characteristic is similar to the concept discussed in other sections of this thesis. Thirdly the impulse cancellation technique inherent in the concept is similar to the spike cancellation technique that is also discussed. The practical limitations that prevent this concept being put into practice are several. Among these are that an ideal demodulator cannot be realised, and a VCO that has its output phase the exact integral of the input is not feasible. Inherently a wide band discriminator is

required and the time delay of the discriminator and of the linear filter must be compensated for. This is a problem that is not uncommon in other threshold extension demodulators. A limitation of the above analysis is that it treats threshold effects as appearing outside the wanted modulation bandwidth. The fundamental problem is that threshold effect contain clicks, false clicks, doublets and modulation amplitude transients. The basic click that does all the harm, contains low frequency energy in the modulation passband. This remains a problem common to all threshold extension demodulator approaches.

The switched capacitor demodulator concept initially appears attractive as it is an open loop system without many of the stability problems associated with the more common FMFB and PLL demodulators. It achieves its threshold extension effect by frequency compression of the signal. Any threshold improvement that occurs is not due to the frequency compression action itself, but to the reduction in bandwidth of the pre-detection filter that result. An illustration of the technique has been given for a D2-MAC system with a switched capacitor oscillator inserted between the I.F. and the pre-detection filter. For the parameters assumed there is a reduction in occupied bandwidth that gives a threshold improvement of some 1.6 dB. On the surface, using typical system characteristics, this is an improvement in performance. However what is not revealed is the effect on the modulation index and consequently on system performance. At the output of the I.F. amplifier the modulation index is unity, but at the input to the demodulator for the parameters chosen, it has been reduced to one third. This value of modulation index results in the transmission system being classed as narrow-band FM, which results in the modulation characteristics being very similar to AM; hence the FM improvement factor is lost. In an FM system it is in the demodulator where the FM improvement occurs. As the demodulator does not known that the switched capacitor oscillator has been introduced, it considers that the characteristic of the modulation appearing at it's input to have originated at the transmitter. This raises the question, what is the point of this approach? The modulation originating at the transmitter may as well have had these narrow-band FM characteristics to start with. It is this limitation - the effect on the modulation index - which may be why this approach does not appear to have found application. This concept is mentioned in this thesis for its originality and for

completeness. The approach is unlikely to be suitable for DBS television applications, because of the effect on the modulation index, and because of the difficulty of making a switched capacitor oscillator at the I.F. frequencies involved.

The limited reviews of spike cancellation, or click elimination, techniques have shown that many attempts have been made to use this approach to achieve threshold extension, but with limited success. Using the click elimination technique in tandem with a threshold extension demodulator does not offer much advantage as the performance figures quoted are of the same order as the basic threshold extension demodulator. Where in carefully controlled conditions the click technique has been made to work, the results achieved are good. As has been shown with previous demodulators, the basic problem is in discriminating between clicks, false clicks, doublets and modulation amplitude spikes, and in correctly activating the click elimination circuitry. Current trends are to use an appropriately designed filter to do this discrimination, but with complex signal (picture) structures this is unlikely to prove satisfactory. Brief mention has been made of those click elimination techniques, which do not form part of the demodulator but operate directly upon the video signal. These are strictly signal processing approaches, and is mentioned here to shown the number of approaches that have been made to try to solve the threshold or interference problem.

Roberts's envelope multiplication concept for multiplying the demodulated signal by the square of the envelope, although a sound theoretical concept does not appear to have been exploited. Roberts points out that using this approach a conventional demodulator cannot be improved upon at high carrier-to-noise ratios, but when the carrier-to-noise ratio is low and at or below threshold, then signal suppression occurs. By multiplying by the square of the envelope the effect of signal suppression is reduced. This means that with this technique a (low) carrier-to-noise ratio exists below which the performance is superior to a conventional demodulator. A version of the adaptive threshold extension demodulator concept has been proposed in this thesis using Roberts technique.

The simplified analysis carried out on the equivalence of certain threshold extension demodulators produces some interesting conclusions, and shows the PLL and the FLL are, in terms of their defining equations, limiting forms of the FMFB demodulator. If the loop I.F. bandwidth of the FMFB demodulator tends to zero, then the FMFB functions as a PLL with respect to a noise corrupted input carrier. If the loop I.F. bandwidth is infinite then the FMFB functions as a FLL demodulator. Hess in his source reference has reported some interesting observations. Firstly the FMFB may have an arbitrarily narrow loop I.F. bandwidth and still successfully demodulate an input FM signal. Secondly, with a sufficiently narrow loop I.F. bandwidth, the FMFB has many of the loss of lock problems possessed by the PLL. Large deviations of the input carrier in the presence of noise are capable of throwing the FMFB out of lock with the result of a large number of signal induced clicks. However for wide I.F. bandwidths, the FMFB can never lose lock. Hess suggests that some intermediate value of loop I.F. bandwidth may combine the best features of the PLL and the FLL. However that this analysis does not consider the effects of distortion upon the signal. It is a linear analysis that does not consider the effects of threshold. The highly non-linear operation of the FM demodulator in the threshold region for noisy signals will modify the above results considerably. Hess suggestion of an intermediate I.F. bandwidth FMFB demodulator that may give improved performance is an interesting one. In the adaptive demodulator design proposed elsewhere in this thesis, this suggestion can be extended further by making the I.F. bandwidth dependent upon a metric that measures the clicks that occur at threshold and seeking to set a value of bandwidth that minimises them. By this approach not only could the characteristics could be made to vary from those of a PLL through a FMFB to a FLL demodulator, but by using Cassera's approach and limiting the I.F. signal, the characteristics could be made to include those of a conventional demodulator.

On the basis of the studies carried for this thesis, an adaptive threshold extension demodulator concept is proposed that may overcome some of the limitations of existing designs. A conclusion of the previous work carried out is that because of the inherent non-linear nature of angle modulation, it is impractical to design a threshold extension

demodulator that will function for all values of input carrier-to-noise ratios and for all values of modulation index. Thus use of an additional parameter namely the digital (sub) structure information content of the signal is proposed. This allows an adaptive demodulator to be devised, that uses the information error rate characteristic that occurs at threshold with those digital structures contained in part, or all, the signal structures used in conventional, MAC and all-digital systems. At threshold the click phenomena generate errors in the digital pattern that can be used to alter the configuration of the adaptive demodulator. For conventional TV systems (PAL, SECAM and NTSC), the information characteristic proposed for use in the adaptive demodulator is Teletext. For MAC format systems several digital sub structures exist, namely frame and line sync patterns, as well as other error control patterns in line 625. All-digital TV systems with their use of sophisticated error coding techniques (e.g. Reed-Solomon codes), have a ready source of error rate indication. Several types of threshold extension demodulator techniques are shown to lend themselves to being incorporated within an adaptive demodulator. Here the error rate derived from those digital (sub) structures at threshold is used either to reduce the bandwidth of the I.F. filter, to modify the characteristics of the loop filter or to control the decision timing used to reconstitute the demodulator output. An example is given of an adaptive demodulator, using a PLL, where by controlling the three latter functions, the circuit can respond to any change of system parameters that give rise to an increase in error at the demodulator output, e.g. threshold level, modulation index variation, interference, offset frequency, intersymbol interference and loss-of-lock. The error rate function can also be used to alter the parameters of the adaptive demodulator (such as the system order of a PLL) or to switch to a different demodulator technique entirely, such as an envelope multiplication scheme, that provides a superior demodulation characteristic at or below threshold. The use of the increased bit error rates at threshold, in addition to the other signal characteristics, allows a wide variety of techniques to be adopted which should make the demodulator relatively independent of the input carrier-to-noise ratio and for a wide range of modulation index values.

A limited review has been carried out of the proposed (U.S.) all-digital HDTV

terrestrial system. Although to date there has been little comment on the satellite version of HDTV, there are indications of the problems that may be encountered. For example, will the system be adequate for satellite transmission with its complex video compression scheme, when satellite systems operate so close to threshold and suffer fades and multipathing for a percentage of the transmission time. Unless error coding is used then video compression makes the system very vulnerable to interference. The use of Reed Solomon coding is an effective solution that gives the system good protection against burst noise but nor necessarily Gaussian noise. The indication that digital threshold extension (PLL) demodulation will have a more rapid fall-off below threshold makes it likely that the degradation in quality will be very abrupt, unlike an analogue system that has a gradual degradation in picture quality. With a digital system, the picture will probably maintain its quality until threshold is reached, and then there will be a sudden loss of picture as the reduction in input carrier-to-noise ratio gives a large change in the output signal-to-noise ratio. As with all systems of this nature, the synchronisation technique does not have error coding protection, but relies on a receiver internal reference to overcome the effects of noise of a burst nature. If the signal is at, or below, threshold for any length of time, this internal reference may not provide adequate synchronisation. Where digital systems have error protected data, and the synchronisation is without error protection, it may be considered that two thresholds exist; these are the data threshold and the sync threshold. Ideally both should be equal, or as occur in practice the sync threshold is lower (better) than the data threshold. Thus ensuring that when the input carrier-to-noise level enters the threshold region, the data is lost before there is a loss of sync. Little information has been published on the sync strategy that will be used in the proposed all-digital HDTV system, but it is assumed that the Field Sync will use a digital pattern (word) which, to give good sync and anti-noise characteristics, will have a minimum length of the order 28 to 33 bits. Indications are that for the all-digital HDTV system, because of the conventional demodulator characteristic at threshold, it may be those threshold extension demodulators with modest improvement figures may offer significant performance gain. Particularly if use is made of the error correction facility to control the adaptive threshold extension

demodulator.

20.2 Conclusions

Although a number of threshold extension techniques have been identified and examined, all have been found to be lacking in attaining the successful objective of a demodulator that provides a consistent performance for all conditions of input (picture) content. This lack of universal performance has been identified as being due to the dependence of the demodulator upon the nature of the carrier modulation and the difficulty in detecting when threshold has occurred. This non-linear dependence of the demodulation process upon the signal structure is one of the major difficulties that occurs in designing a threshold extension demodulator with a satisfactory performance. It is this non linearity that may be considered to be the source of variable performance of threshold extension demodulators reported in the literature. Because angle modulation is an inherently non-linear process, it is difficult to obtain analytical expressions for the performance of these systems that are valid for all input carrier-to-noise ratios and for all values of modulation index.

The research carried in this thesis has shown that the basic mechanisms for achieving threshold extension exist in terms of a number of demodulator circuit approaches which can, and do, exhibit threshold extension of several dB. The fundamental problem that prevents exploitation of these circuits is the actual measurement of when threshold occurs and the dependence of the threshold characteristic on the signal information content, or modulation index. This non-linear operation is one the major source of difficulties preventing the successful operation of a threshold extension demodulator. It is concluded that because of the inherently non-linear nature of angle modulation it is a formidable, if not impractical task, to design a threshold extension demodulator that will function for all input carrier-to-noise ratios and for all values of modulation index by just using the characteristics of carrier amplitude $R(t)$ and the demodulated signal $\dot{\theta}(t)$. A further conclusion is that a satisfactory metric for detecting the occurrence of threshold has not really been devised.

How the metric detects the click, rather than the doublet, false click or modulation transient and controls the filter, is a problem that the references cited had not solved. A proposed solution, an adaptive error controlled threshold extension demodulator, resulting from this study is given in this thesis. By making use of the information content of the signal, various approaches become feasible for most of the threshold extension demodulators designs considered.

The whole point in designing a successful threshold demodulator can be simply summarised as producing a design that prevent the onset of click or spike phenomena at threshold; an effect that is so objectionable to the viewer. The gentle degradation in picture quality that occurs with the reduction in the (Gaussian) signal-to-noise ratio is generally acceptable. The importance of implementing a successful threshold extension demodulator is that it offers a relatively economic improvement to performance. To achieve a similar improvement elsewhere in the system would require an increase either in satellite transmitter power or antenna gain, or terrestrial receiving antenna gain; solutions that are relatively costly, particularly those involving the satellite. The adaptive error controlled threshold extension demodulator design concepts proposed in this thesis go some way to achieving this economic objective.

20.3 Suggestions for future research studies.

Introducing an information metric in terms of the error rate occurring, allows several lines of future investigation to be carried out into an adaptive controlled threshold extension demodulator to establish if the apparent potential system gain can be realised. Notable areas of investigation are application of the technique to the tracking filter demodulator and to the FMFB demodulators with a metric controlled I.F. filter bandwidth. This latter approach, especially with a signal dependent switchable limiter included, may give all the advantages of the conventional, FFB, PLL, and FMFB demodulators.

Other possible areas of investigation concerning the proposed adaptive

demodulator, are to establish how well the error rate for Teletext gives an accurate indication of the occurrences of system threshold in conventional TV systems, namely PAL, SECAM and NTSC. For MAC format television systems, and in particular D2-MAC, a suitable area of investigation is to establish the optimum method of obtaining an error rate measurement from digital sub structures. Whether some or all the various sources of error measurement should be used merits study. For the proposed all-digital system investigating the sources of error rates from the complex error coding structures used, and the effect of varying the I.F. bandwidth upon these error rates, would be a fruitful field of investigation.

At the time of writing this thesis it became apparent that several crucial parameters for the MAC format system could benefit from further study. The optimisation of the pre/de-emphasis characteristic at threshold, particularly using linear and non-linear networks would also benefit from further research studies. These could be made adaptive and a function of the input carrier-to-noise ratio. These studies should also include establishing the optimum deviation and noise weighting factors for the particular MAC system being proposed.

The oscillating limiter discussed in chapter 8, is a fascinating circuit whose bandwidth is a function of the input signal level. There has only been as far as can be ascertained, only three source papers on this approach. It merits further study to take advantage of its unique characteristics and to establish if with current analytical techniques a stable design with predictable characteristics can be obtained. If successful, such a solution may find wide application. A characteristic that bears some similarity to that of the oscillating limiter is the input amplitude/bandwidth of the PLL. That is when the input signal amplitude is reduced, the PLL bandwidth reduces. The investigation of this similarity may be a possible area of future investigation.

The proposed all-digital television system will be a fruitful area for future research studies, particularly in its satellite DBS version. Its carrier modulation structure and its performance at threshold for Gaussian and Poisson noise conditions and for the proposed

error coding and video compression schemes, provides a number of areas that merit further investigation.

APPENDIX A PROPOSED US DIGITAL TELEVISION STANDARD

A.1 Introduction

This appendix gives the limited information available on the proposed US all-digital high definition television (HDTV) standard for terrestrial applications which is contained in reference [1]. The system is known as the 8-VSB system and, although it is designed to satisfy US terrestrial channel bandwidth allocations, it is intended with a probable change of carrier modulation to satisfy future satellite DBS and cable applications.

A.2 Proposed standard

Table A/1 shows the basic parameters of the 8-VSB system. Further refinement of these is anticipated.

Table A/1 8-VSB System

Parameter	Value
Channel Bandwidth	6 MHz
Excess Bandwidth	11.5%
Symbol Rate	10.762 Msymbols/s
Bits per Symbol	3
Bit Rate	32.287 Mbps
Trellis FEC	2/3 Rate
RS - FEC	t = 10, (207, 187) Bytes
RS Bit Rate	2.063 Mbps
Segment Length	832 Symbol
Segment Sync	4 Symbols/Segment
Segment Rate	12.935 Kilosegment/s
Segment/Frame	313
Frame Rate	41.327 frames/s
Payload Data Rate	19.290 Mbps
Pilot Power Contribution	0.3 dB
Receiver C/N Threshold	14.9 dB
Co - channel Rejection	NTSC Rejection Filter

A.3 References

[1] Challapli, K., Lebegue, X., Lim, J., Paik, W., Girons, R., Petajan, E., Sathe, K., Snopko, P., Zdepski, J., "The grand alliance system for US HDTV", Proc. IEEE, Vol. No. 2, February 1995, pp. 158 - 173.

APPENDIX B TELEVISION STANDARDS FOR THE BROADCASTING SATELLITE SERVICE

B.1 Introduction

The following television standards for the broadcasting-satellite service are defined by the CCIR and are given in [1]. The standards given in this appendix are those extracts that are relevant to the studies carried out for this thesis. Those standards appertaining to the NTSC system are not included. In addition footnotes to the tables that are shown in reference [1] are not included here. All systems given herein utilise digital techniques for the sound, and for the data, in order to utilise to the greatest possible extent the capacity available in the channel. The systems identified in the tables have been optimised under different constraints and meet the various broadcasting - satellite service requirements in the 12 GHz band when the 625 line standard is used with a satellite channel of 27 MHz bandwidth.

The essential elements of broadcasting - satellite system design, and their relationship, is given in reference [2], together with the various technical, political and economic constraints that affect the choice of system parameters. This report is an excellent concise summary of broadcasting - satellite system design.

The general characteristics of MAC systems are discussed in reference [3]. Reasons are given for the choice of parameters for the 625 and 525 line MAC vision systems and it discusses future enhancement of the systems.

Reference [4] discusses the various methods of modulation that are suitable for broadcasting - satellite systems. Experimental results for the MAC systems are given including the experimental performance of certain threshold extension demodulator techniques.

B.2 Vision Data/Multiplex Structure

Reference	Parameter/System	MAC Packet Systems			B - MAC (625 lines)
		C	D	D2	
	General Parameters				
1.1	Modulation Frame Frequency (Hz)	25	25	25	25
1.2	No. of Lines per Picture (Frame)	625	625	625	625
1.3	Line Frequency (Hz)	15625	15625	15625	15625
1.4	No. of Time Increments/Line	1296	1296	1296	1296
1.5	Nominal Ref. Clock Freq. (MHz)	20.25	20.25	20.25	20.25
	Multiplex Structure				
1.6	Multiplexing Principle	Radio Freq.	Baseband	Baseband	Baseband
1.7	Vision Coding	Time Multiplexed Analogue Components			
1.8	Nominal Transmitted Vision Bandwidth	8.4 MHz	7.5 MHz	6.3 MHz	4.5 MHz
1.9	Nominal Vision Amplitude (V p-p)	1	1	1	1
1.10	Data Coding	2-4-PSK	Duobinary	Duobinary	Quaternary / Binary
1.11	Symbol Rate (MBaud)	20.25	20.25	10.125	7.11
1.12	Occupied Data Spectrum (MHz)	N/A	10	5	7.11
1.13	Nominal Data Amplitude (V p-p)	N/A	0.8	0.8	0.77
1.14	No. of Bits/Symbol	1	1	1	(2/1)
1.15	Instantaneous Bit Rate (Mbits/s)	20.25	20.25	10.125	14.22/7.11
1.16	Multiplex Description	Flexible	Flexible	Flexible	Rigid
1.17	Basic Frame Multiplex Configuration	Fig. B.1	Fig. B.1	Fig. B.1	Fig. B.1
1.18	Baseline Multiplex Configuration	Fig. B.2(a)	Fig. B.2(b)	Fig. B.3	Fig. B.4
	Reference Signals				
1.19	Synchronization Principle	Digital Code Word			
1.20	Clock Recovery	Recovered from data			
1.21	Line Synchronisation	6 Bit Word	6 Bit Word	6 Bit Word	N/A
1.22	Frame Synchronisation	64 bit word in line 625			1131 symbols in line 2
1.23	Reference Level for Video and Data Clamping	Constant level			Average level of 20 symbols (binary). Ref. burst in HB1
1.24	Clamp Period (Microsecs.)	0.75	0.75	0.75	2.81
	No. of Clock Periods	15	15	15	60
1.25	AGC Reference Level (V)	(+/-) 0.500 relative to clamp level on one line per field in the VB1			(-) 0.500 rel.to clamp level on 1 line per field in the VB1

B.3 Vision Coding

Reference	Parameter/System	MAC Packet Systems			B - MAC (625 Lines)
		C	D	D2	
	General Video Parameters				
2.1	Scanning Method	Left to Right, Top to Bottem			
2.2	Active Lines per Frame	574	574	574	574
2.3	Spare Lines per Frame (Available for additional services and test signals)	47	47	47	21/38
2.4	Interlace Ratio	(2:1)	(2:1)	(2:1)	(2:1)
2.5	Aspect Ratio	(4:3)	(4:3)	(4:3)	(4:3)
2.6	(a) Assumed Gamma of Display	2.8	2.8	2.8	2.8
	(b) Overall Gamma	1.2	1.2	1.2	1.2
2.7	Primary Colour Chromaticities				
	Red	x = 0.67, y = 0.33			
	Green	x = 0.21, y = 0.71			
	Blue	x = 0.14, y = 0.08			
2.8	Chromaticity Coordinates for Equal Primary Signals. Er' = Eg' = Eb'	Illuminant D65 x=0.313 y=0.329			
2.9	Luminance Signal Equation	Ey' = 0.299Er' + 0.567Eg' + 0.114Eb'			
2.10	Colour Difference Signal Equations	(Er'-Ey') = (0.701Er' - 0.587Eg' - 0.114Eb') (Eb'-Ey') = (- 0.299Er' - 0.587Eg' + 0.886Eb')			
	Luminance				
2.11	Number of Clock Periods	696	696	696	750
2.12	Compression Ratio	(3:2)	(3:2)	(3:2)	(3:2)
2.13	Nominal Sampling Frequency (MHz)	13.5	13.5	13.5	14.219
2.14	Nominal Uncompressed Bandwidth (MHz)	5.6	5.6	5.6	5
2.15	Reference Black Level (v)	(- 0.500) relative to clamping level			
2.16	Transmitted Luminance Signal Equation (v)	(- 0.500) + Ey'			
2.17	Amplitude Range (V p-p)	(-0.500) to (+0.500)			
	Chrominance				
2.18	Number of Clock Periods	348	348	348	375
2.19	Compression Ratio	(3:1)	(3:1)	(3:1)	(3:1)
2.20	Sampling Frequency (MHz)	6.75	6.75	6.75	7.109
2.21	Nominal Uncompressed Bandwidth	2.4	2.4	2.4	2.1
2.22	Zero Chrominance Reference Level (v)	Zero Relative to Clamping Level			
2.23	Transmitted Chrominance Signal Equations (v)	Edb' = 0.733 (Eb'-Ey'). Edr' = 0.927 (Er'-Ey')			Edb' = 0.694(Eb'-Ey') Edr' = 0.926(Er'-Ey')
2.24	Amplitude Range (V p-p)	From (-0.500) to (+0.500)			
2.25	Sequential Transmission	Edb' transmitted on odd active lines of each field. Edr' transmitted on even active lines of each field.			
2.26	Vertical Pre-filtering	Filter parameter's left to choice of Broadcaster			0.25, 0.5, 0.25
2.27	Coincidence between Luminance and Chrominance	Chrominance is transmitted one line before associated Luminance			
	Scrambling Process				
2.28	Scrambling Process for Conditional Access	Double cut component rotation or single cut line rotation			Line Translation

B.4 Data Multiplex Structure

Reference	Parameter/System	MAC Packet Systems			B-MAC (625 Lines)
		C	D	D2	
	General Data Requirements				
3.1	Useful Data Burst (bits/Line)	2x99	2x99	99	102/51
3.2	Type of Multiplex	Packet	Packet	Packet	Continuous
3.3	Organisation	2x82 packets of 751 bits/frame	2x82 packets of 751 bits/frame	82 packets of 751 bits/frame	6 channels of 203 kBits/s plus one channel of 62.5 kBits
3.4	Mean Data Rate	3.08 (2x2050 packet/s)	3.08 (2x2050 packet/s)	1.54 (2050 packet/s)	1.59
3.5	Scrambling (for conditional access)	By addition of Mod.2 of pseudo random binary sequence of data channel level synchronised on modulation frame			Not Disclosed
	Sound Coding				
3.6	Audio Sampling Frequency	32 kHz for high quality (HQ). 16 kHz for medium quality (MQ)			Basic audio rate for HQ 203 kB/s. Step size control 7.8 kHz. Emphasis control 7.8 kB/s.
3.7	Audio Pre-Emphasis	CCIT Recommendation J17			Adaptive
3.8	Audio Coding Metho	Linear 14 bit/sample (L) or Near Instantaneous 10 bit/sample (I). Coding Range : 5 Levels			Adaptive Delta Modulation
3.9	Protection	Protection Range: 2 levels. (I) First level by one parity bit/sample, or, (ii) Second level by 5 bit Hamming code per sample.			2.33 bits per 13 bit block
3.10	Packet Rate per Monophonic or Sterophonic channel (packets/s)	MQ Mono: I1=253, L1=336.3, I2=336.3, L2=447.4: HQ Mono: I1=503, L1=669.7, I2=669.7, L2=891.9; HQ Stero: I1=1003, L1=1336.3, I2=1336.3, L2=1780.8			Not Applicable
3.11	Identification of Coding Method	Explicit by Interpretation Blocks			Not Applicable
3.12	Maximum Number of High Quality Monophonic Audio Channels	8	8	8	(6/3)
	Service Identification				
3.13	Service Identification	One line per frame in VB1 and data channel D of packet multiplex			Two lines per frame in VB1
3.14	Service Description Data Organisation	Data groups,commands and parameters carried by packets.			Not Applicable
	Conditional Access				
3.15	Control of Descrambling	Control word for initialisation of pseudo random binary sequence.			Not Disclosed
3.16	Secret Information	Authorisation keys per service. Distribution key per subscriber.			Not Disclosed
3.17	Entitlement Checking and Management	Encrypted control words and authorisation keys per subscriber.			Not Disclosed
3.18	Addressing Rate (Addresses/H)	150,000 per kilobit	150,000 per kilobit	150,000 per kilobit	1000000
3.19	Maximum Number of Addresses	64,000 million			256 million

	Data Broadcasting				
3.20	Teletext Coding	CCIR Recommendation 1986-90d			
3.21	Protection	Protection range - 2 levels: (i) CRC within teletext data block (two teletext data blocks/packet), (ii) CRC within teletext data block plus (24,12) Golay code FEC overall (one protected teletext data block/packet).			
3.22	Identification of Coding Method	Set by paramater (DCINF) in the service identification channel.			

B.5 Modulation Parameters

Reference	Parameter/System	MAC Packet Systems			B - MAC (625 lines)
	Modulation Parameters				
4.1	Nominal Channel Bandwidth (MHz)	27	27	27	24
4.2	Data Signal Modulation	2-4-PSK	FM	FM	FM
4.3	Vision Signal Modulation	FM			
4.4	Polarity of Frequency Modulation	Positive			
4.5	Reference Level Frequency Position	Exactly centred in channel.			
4.6	DC Component	Preserved			
4.7	Frequency Deviation (MHz/volt)	13.5	13.5	13.5	16.5
4.8	Pre-Emphasis Characteristic	E1 = H(f) = A(1+jf/f1)/(1+jf/f2)			
4.9	Pre-Emphasis Parameters				
	A:	0.7071			
	f1 (MHz)	0.84	0.84	0.84	1.87
	f2 (MHz)	1.5	1.5	1.5	3.74
4.10	Energy Dispersal (kHz)	600 (Triangular frame synchronous waveform)			

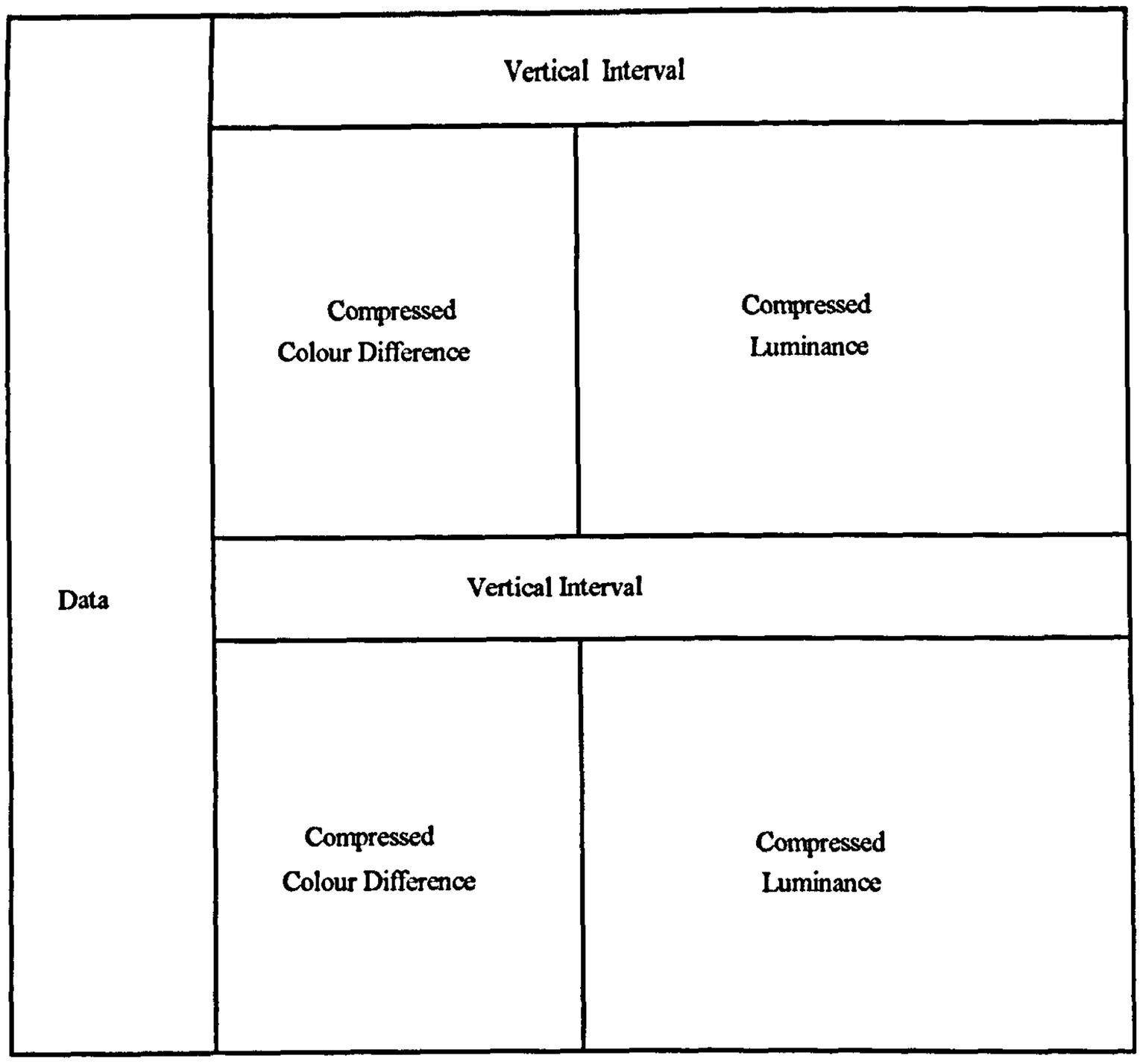

Figure B.1 - Basic TDM Frame Configuration

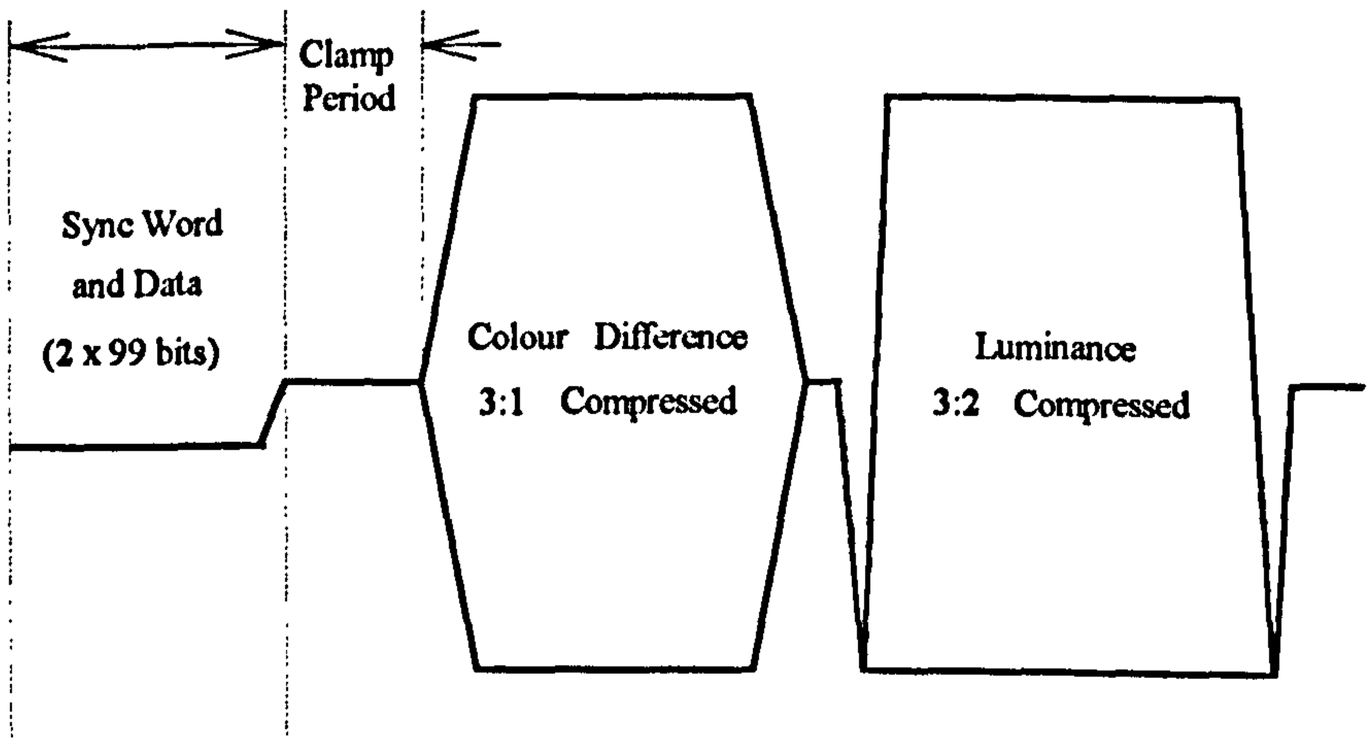

Figure B.2(a) - C-MAC/Packet Signal Waveform (Unscrambled)

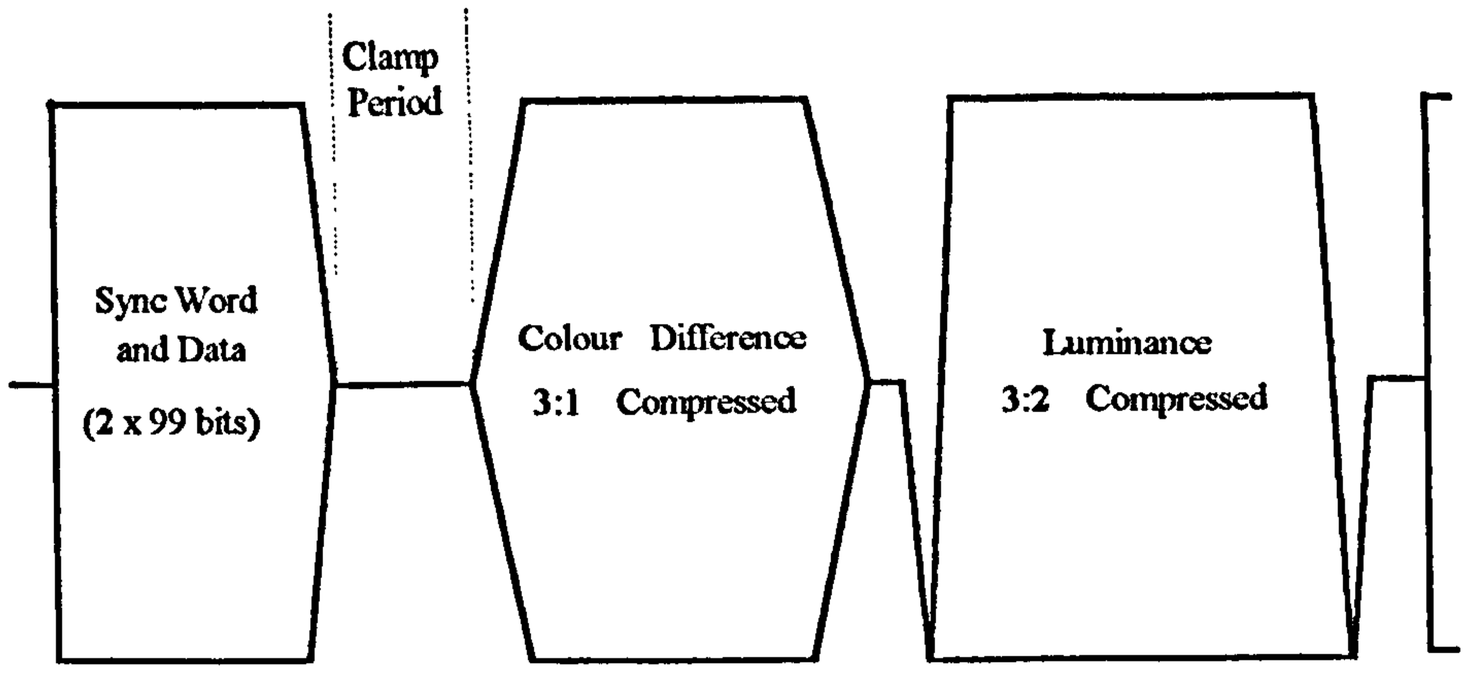

Figure B.2(b) - D-MAC/Packet Signal Waveform (Unscrambled)

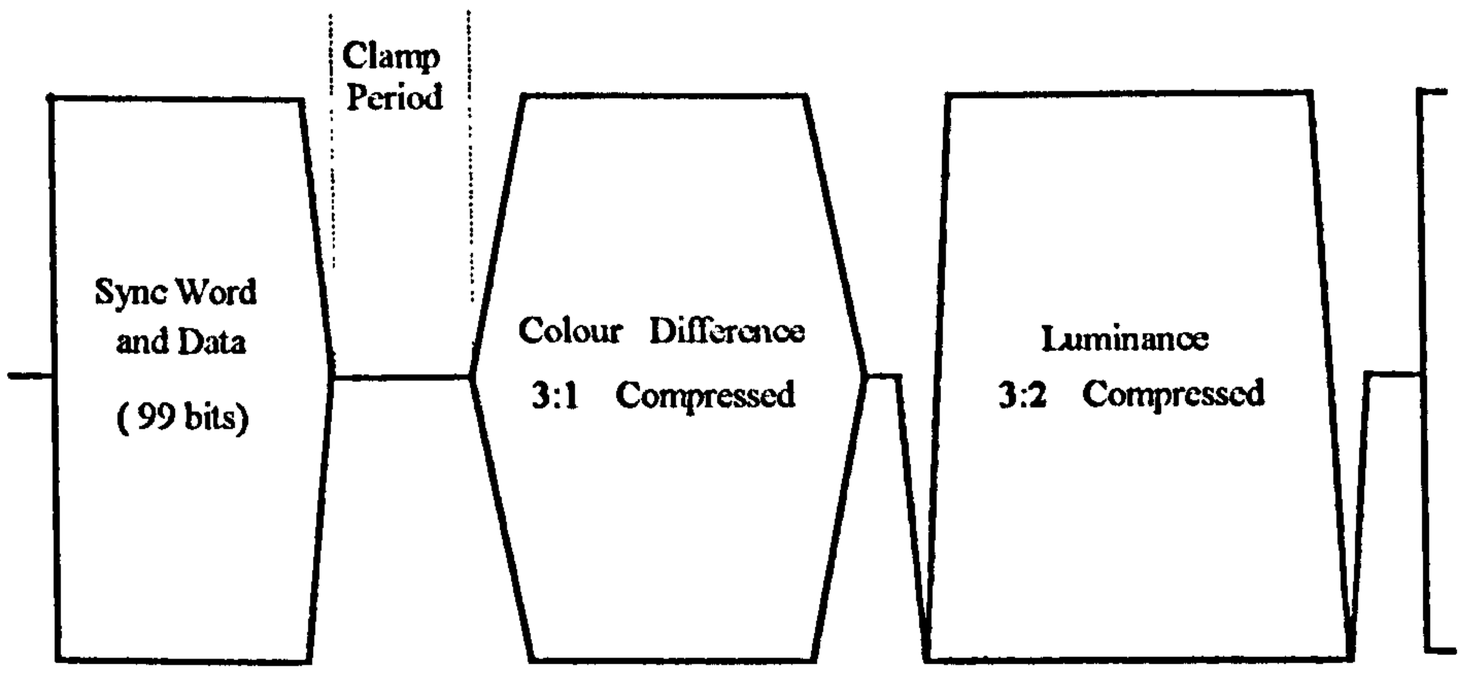

Figure B.3 - D2-MAC/Packet Baseband Signal Waveform (Unscrambled)

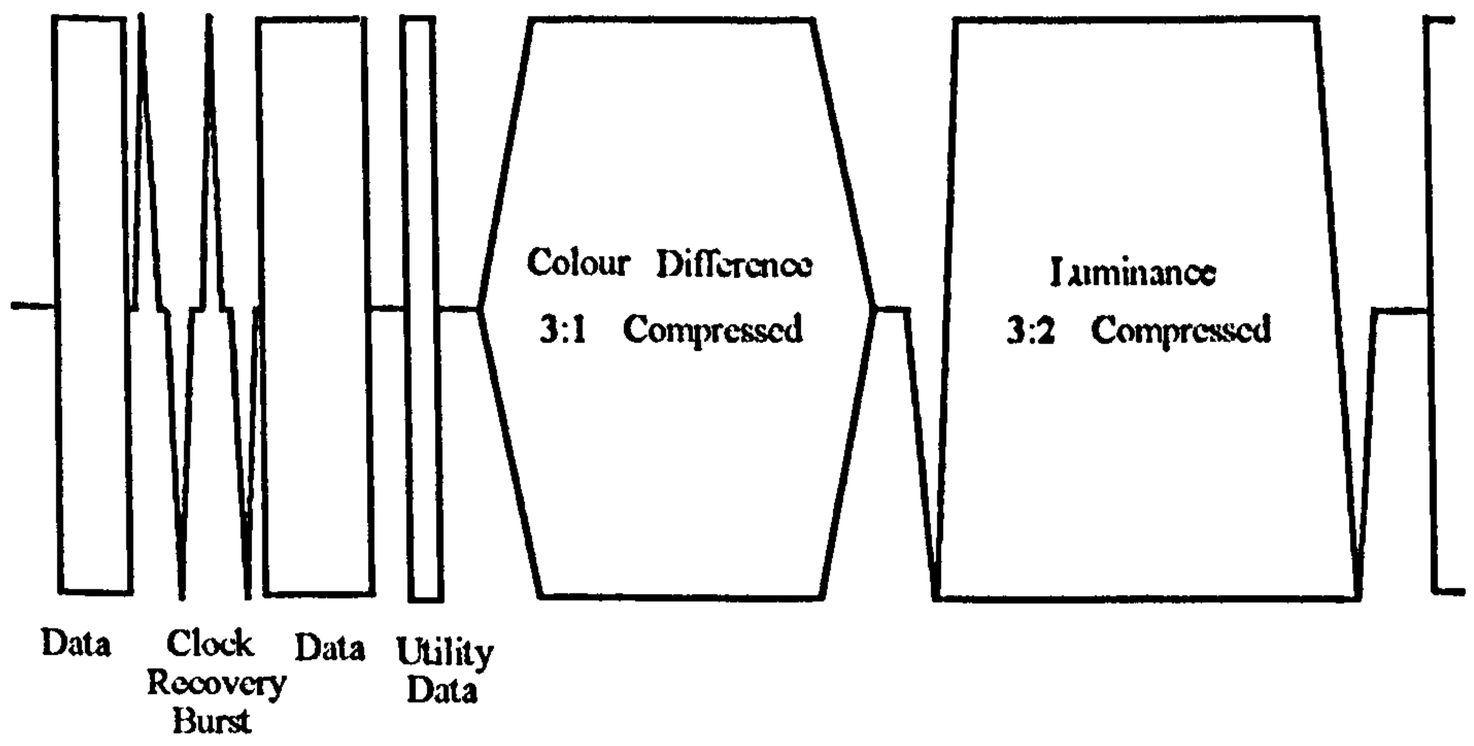

Figure B.4 - B-MAC Signal Waveform (Unscrambled)

B.6 References

[1] CCIR "Television standards for the broadcasting satellite service". Report No. 1073-1.

[2] CCIR "Systems for the broadcasting satellite service (sound and television)". Report No. 215-7.

[3] CCIR "Satellite Transmission of Multiplexed Analogue Component (MAC) Vision Signals". Report No. 1074-1.

[4] CCIR "Broadcasting - Satellite Service (Sound and Television)". Report No. 623-4.

APPENDIX C DBS LINK PERFORMANCE

C.1 Introduction

This appendix considers the basic performance of a DBS downlink between the satellite transmitter and the terrestrial television receiver, including the propagation path and end terminal characteristics. Assume that the basic DBS satellite down link and certain of its characteristics are as shown in section 3, figures 3/7, 3/8 and 3/10. Other characteristics have been derived from references [1-3]. For such a system the salient data parameters are defined below:

P_{RX} = Signal power at terrestrial TV receiver input (watts).

C/N = Carrier-to-Noise Ratio

C/N_0 = Carrier-to-Noise spectral power density ratio (dB/Hz)

P_R = Signal power at receiving aerial terminal (watts).

P_T = Isotropic radiated power of satellite transmitter (watts)

P_{TX} = Satellite transmitter power output, 110 watts.

G_T = Satellite transmitter aerial gain with respect to isotropic

G_R = Terrestrial receiver aerial gain with respect to isotropic.

$G_{R_{MAX}} = G_R$ Modified by losses.

A_{eff} = Terrestrial TV receiver aerial effective aperture (square meters)

D_R = Terrestrial TV aerial diameter, 0.9 meters.

D_T = Satellite transmitting aerial effective diameter, 70 meters.

θ = Satellite transmitting aerial beamwidth, 2^0.

η_1 = Satellite transmitting aerial efficiency, 0.55.

η_2 = Terrestrial TV receiving aerial efficiency, 0.6.

α_R = Maximum misalignment, 0.45^0 .

λ = Wavelength (metres)

f_o = Carrier frequency, 12 GHz.

N = System thermal noise (watts)

k = Boltzmann's constant (1.38×10^{-23} J/K)

B_M = Baseband bandwidth (Hz)

c = Velocity of light in a vacuum, (2.998×10^8 m/s).

F_{NF} = Terrestrial TV receiver noise figure, 2.2 dB

L_P = Total path loss, $(L_{FS} + L_A)$.

L_1 = Loss between satellite transmitter and satellite aerial, 1 dB.

L_2 = Loss between terrestrial TV aerial and receiver, 0.5 dB.

L_A = Atmospheric attenuation, 0.3 dB. The value assumed is the typical attenuation by atmospheric gases at 12 GHz for a receiving antenna elevation of 10^0.

L_α = Receiving aerial pointing loss.

L_T = Edge of coverage footprint, -n dB contour, 3 dB, (at edge of -3 dB contour, $\alpha_T = \frac{\theta}{2} = 1^0$)

L_{FS} = Free space path loss.

L_0 = Polarisation loss (0 dB).

T_S = System temperature (K)

T_F = Thermodynamic temperature of terrestrial connection, 290 K.

T_G = Ground noise temperature, 45 K.

T_A = Aerial noise temperature

T_R = Noise temperature of receiver

T_0 = Reference temperature, 290 K

T_{Sky} = Noise contribution of clear sky (20K for $F_D = 12$ GHz and 10^0 receiving aerial elevation).

T_M = Mean thermodynamic temperature of rain and cloud formations (This value lies between 260K to 280K. Here 275 K will be assumed).

R = Range of terrestrial receiver from satellite, 40×10^6 metres.

A_R = Attenuation due to rain and cloud formations (7 dB).

C.2 Analysis

Now the signal power at the receiver input is given by:

$$P_{RX} = \frac{P_T}{4\,\pi R^2}\;\; G_T\, A_{eff} \qquad \text{..... (C-1)}$$

Where
$$A_{eff} = \frac{G_R\,\lambda^2}{4\,\pi} \qquad \text{..... (C-2)}$$

Thus
$$P_{RX} = \frac{P_T}{4\,\pi R^2}\, G_T \left(G_R \frac{\lambda^2}{4\,\pi} \right) \qquad \text{..... (C-3)}$$

Now noise power
$$N = k\, T_S\, B_M \qquad \text{..... (C-4)}$$

Dividing equations (C-4) into (C-3)

$$\therefore \text{ Carrier-to-Noise Ratio } \; C/N = \frac{P_{RX}}{N} = \frac{P_T\, G_T}{\left(\frac{4\,\pi R}{\lambda}\right)^2}\;\; \frac{G_R}{T_S}\;\; \frac{1}{k\, B_M} \qquad \text{..... (C-5)}$$

Where: $P_T\, G_T$ = Equivalent isotropic radiated power (EIRP)

$\left(\frac{4\,\pi R}{\lambda}\right)^2$ = Free space loss

$\left(\frac{G_R}{T_s}\right)$ = Is the normal G/T factor used to judge the quality of the receiving system.

Now if in equation (C-4), N_0 is defined as kT_S, (viz. $N_O = k\, T_S$) then equation (C-5) can be written in a form independent of the bandwidth, where C/N_0 is the system carrier power to noise spectral power density ratio (dB/Hz). Thus:

$$\frac{C}{N_0} = \frac{P_T G_T}{\left(\frac{4\pi R}{\lambda}\right)^2} \quad \frac{1}{k} \quad \left(\frac{G_R}{T_S}\right) \qquad \text{..... (C-6)}$$

Converting equation (C-6) to the equivalent decibel value:

$$10\log\left(\frac{C}{N_0}\right) = 10\log\left(P_T G_T\right) - 10\log\left(\frac{4\pi R}{\lambda}\right)^2 + 10\log\left(\frac{G_R}{T_S}\right) - 10\log k$$

$$\therefore \quad \left[\frac{C}{N_0}\right]_{dB} = \left[P_T G_T\right]_{dB} - \left[\left(\frac{4\pi R}{\lambda}\right)^2\right]_{dB} + \left[\frac{G_R}{T_S}\right]_{dB} - \left[k\right]_{dB} \qquad \text{..... (C-7)}$$

Four factors are contained within equation (C-7). These are:

(i) $\left[P_T G_T\right]$ is the equivalent isotropic radiated power (EIRP) of the satellite transmitting equipment.

(ii) $\left(\frac{4\pi R}{\lambda}\right)^2$ characterises the transmission medium, i.e. the path losses.

(iii) $\left(\frac{G_R}{T_S}\right)$ characterise the receiver gain/noise temperature of the receiving system. This is the figure of merit or G/T.

(iv) $\left(\frac{1}{k}\right)$ is Boltzmann's constant. This can be written as $10\log\left(1.38 \times 10^{-23}\right)$ and is equal to 228.6 dBW $Hz^{-1}K^{-1}$

The numerical value for defined conditions of the first three factors is defined below in the next section where calculations for a typical DBS system are given.

C.3 Typical characteristics (clear sky)

(a) The geometry of a typical DBS downlink transmission is shown in figure C/1. In this example it is assumed that the domestic (terrestrial) TV receiver is located at the edge of the 3 dB coverage area of the satellite transmitting aerial. The following calculations are for a clear sky. The effects of rain are considered in section C-4 below.

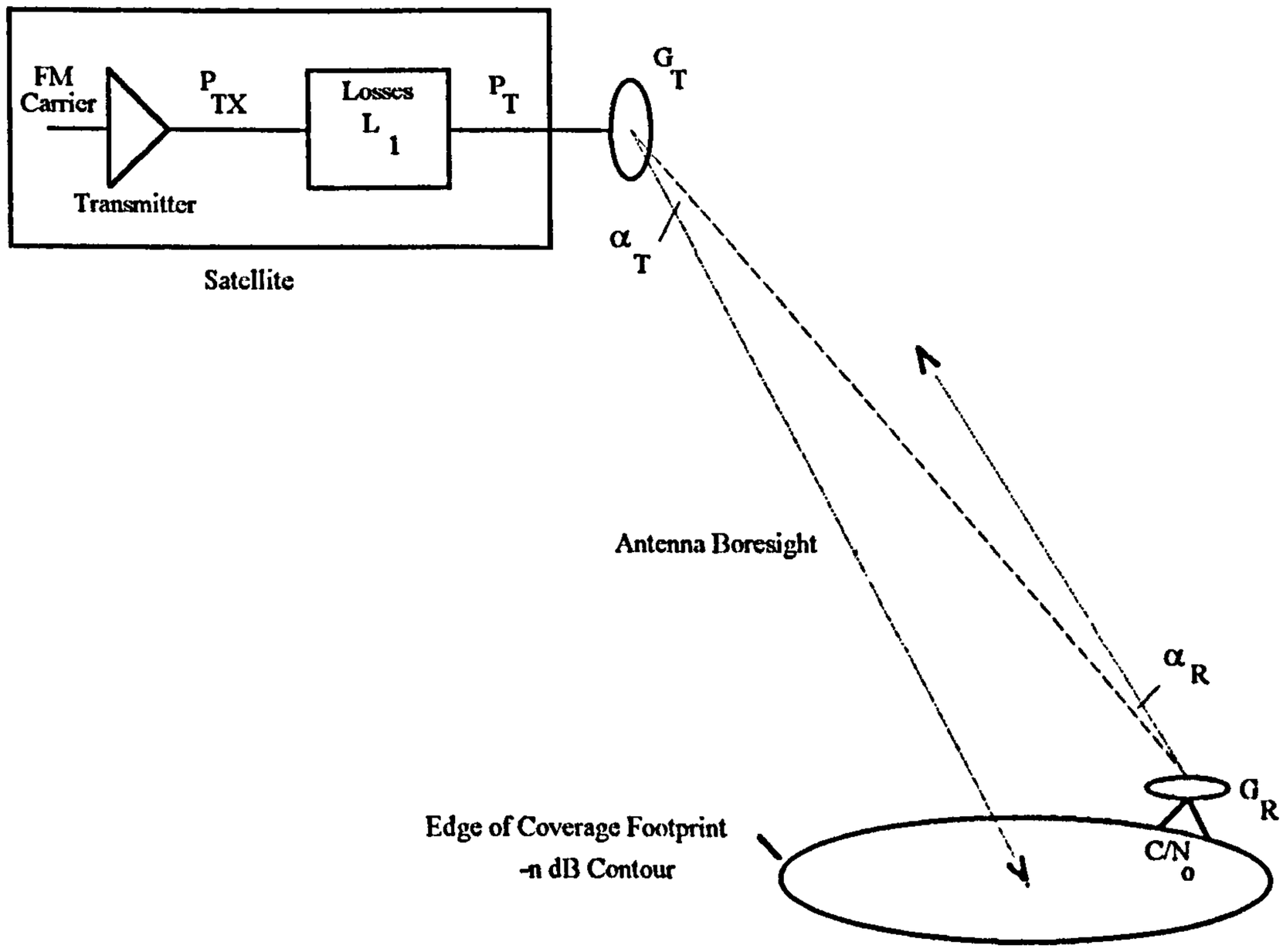

Figure C/1 The Geometry of a Downlink

(b) Referring to equation C-7 above, the first factor, EIRP, will be calculated, as modified by the various loss components.

$$EIRP = P_T G_T \text{ with zero losses.}$$

When modified by L_T (edge of coverage contour) and L_1 (losses between satellite transmitter and aerial) the relationship is modified to:

$$EIRP = \frac{P_{TX} G_T}{L_T L_1}$$

where $P_{TX} = 110 \text{ watts} = +20.41 \text{ dBw.}$

and $G_T = \eta_1 \left(\frac{\pi D_T}{\theta}\right)^2$ for a parabolic antenna

$$\therefore \quad G_T = 0.55\left(\frac{\pi 70}{2}\right)^2 = 6649.6 = +38.22\,\text{dB}$$

and let $L_T = 3$ dB and $L_1 = 1$ dB

Now $$EIRP_{dB} = (P_T)_{dB} + (G_T)_{dB} - (L_T)_{dB} - (L_1)_{dB}$$

$$\therefore \quad EIRP = 20.41\,\text{dBw} + 38.22\,\text{dBw} - 3\,\text{dBw} - 1\,\text{dBw}$$

$$EIRP = \underline{+54.61\,\text{dBw}}$$

(c) Considering the second factor in equation C-7 above, that of the path loss and the atmospheric loss.

Free space path loss, $L_{FS} = \left(\frac{4\pi R}{\lambda}\right)^2 = \left(\frac{4\pi R F_D}{c}\right)^2$

$$= \left(\frac{4 \times \pi \times 40.10^6 \times 12.10^9}{3.10^8}\right)^2$$

$$= 4.043 \times 10^{20}$$

Free space path loss, $L_{FS} = 4.043 \times 10^{20} = 206.07$ dB

This value is modified by the atmospheric attenuation L_A, (0.3 dB).

$\therefore$ Total Path Loss $L_P = L_{FS} + L_A$

$$\therefore \quad L_P = 206.07 + 0.3 \quad = \underline{206.37\ \text{dB}}$$

(d) The third factor in equation C-7 is the figure of merit G/T of the receiving station. The following calculation includes the relevant losses and temperature components.

G_R , when modified by losses, becomes $G_{R_{MAX}} = \dfrac{G_R}{L_\alpha\, L_2}$

now let $G_R = \eta_2 \left(\dfrac{\pi D F_D}{c}\right)^2$ the receiving antenna gain

$$= \quad 0.6\left(\frac{\pi \times 0.9 \times 12 \times 10^9}{2.998 \times 10^8}\right)^2 \quad = \quad 7674 = \quad 38.85\ \text{dB}$$

Now the pointing loss $L_{\alpha_{dB}} \quad = 12\left[\dfrac{\alpha_R}{\theta_{3_{dB}}}\right] = 12\left[\dfrac{\alpha_R\, D_R\, F_D}{70\, c}\right]^2$

$$\therefore \quad L_{\alpha_{dB}} \quad = 12\left[\frac{0.45 \times 0.9 \times 12.10^9}{70 \times 2.998 \times 10^8}\right]^2$$

$$\therefore \quad L_\alpha = 0.6\ \text{dB} \quad \text{pointing loss}$$

and $L_2 = 0.5\ \text{dB}$

$$\therefore \qquad G_{R_{max}} = 38.85 - 0.6 - 0.5 = \quad \underline{37.75\ \text{dB}}$$

The effects of sky temperature on the receiving system are shown in figure C/2. Now in terms of all the temperature components:

$$T_S \quad = \quad \frac{T_A}{L_2} + T_F\left(1 - \frac{1}{L_2}\right) + \ T_R \qquad \ldots\ldots\ldots \text{(C-8)}$$

Calculating the individual temperature components as follows:

Now $T_R = T_0 (F_{NF} - 1)$ where $T_0 = 290\text{K}$, and $F_{NF} = 2.2$ dB

Thus $T_R = 290\left(10^{0.22} - 1\right) = 191.3\text{ K}$

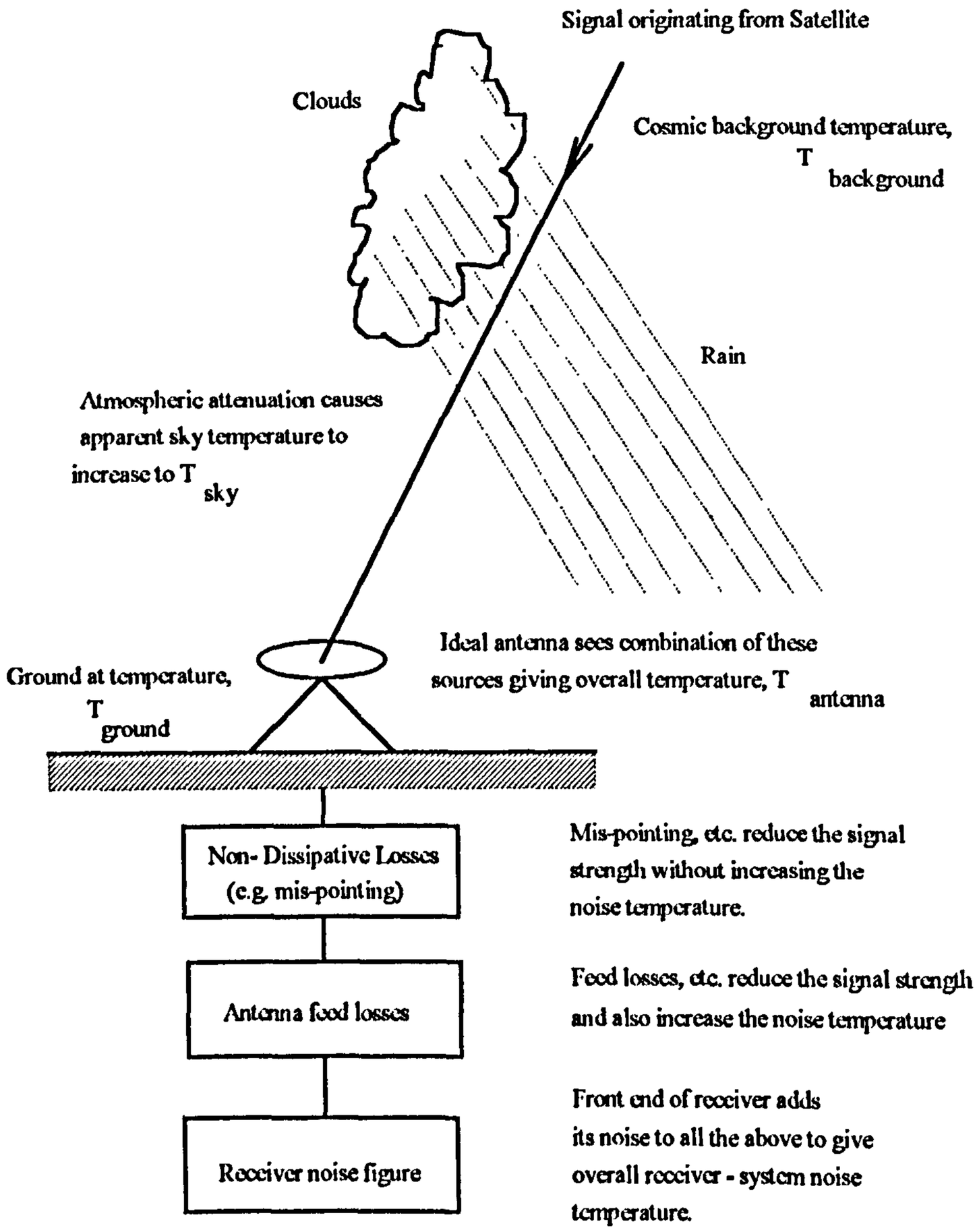

Figure C/2 Showing the effects of sky temperature upon the receiving system

Now $T_A = T_{SKY} + T_G$

Where $T_{SKY} = 20\,K$ for $F_D = 12\text{GHz}$ and 10^0 receiving aerial elevation.

and $T_G = 45\,K$,

$$\therefore \quad T_A = 20 + 45 = 65\,K$$

Now from equation C-8 above, where $T_F = 290$and $L_2 = 0.5\,\text{dB}$, then:

$$T_S = \frac{65}{10^{0.05}} + 290\left(1 - \frac{1}{10^{0.05}}\right) + 191.3$$

$$T_S = 57.93 + 31.54 + 191.3$$

$$\therefore \quad T_S = 280.77\,K$$

$$\therefore \quad T_{S\,dB} = \underline{24.48\,\text{dB}}$$

To calculate the figure of merit G/T_S:

$$\frac{G}{T_S} = \left(\frac{G_{R_{max}}}{L_0}\right) \Big/ T_S$$

Where $L_0 =$ polarisation loss $= 0$ dB.

$$\therefore \quad G/T_S = G_{R_{max}} - T_{S_{dB}} = 37.75 - 24.48 = \underline{13.27\,\text{dB}\,(\text{K}^{-1})}$$

(d) To calculate the down link C/N_0 :

$$\frac{C}{N_0} = EIRP \times \frac{1}{L_P} \times \frac{G}{T_S} \times \frac{1}{k}$$

$$\left(\frac{C}{N_0}\right)_{dB} = (EIRP)_{dB} - \left(\frac{1}{L_P}\right)_{dB} + \left(\frac{G}{T_S}\right)_{dB} - \left(\frac{1}{k}\right)_{dB}$$

Inserting the values obtained from sections (a), (b) and (c) above:

$$\left(\frac{C}{N_0}\right) = +54.61 - 206.37 + 13.27 + 228.6$$

$$\left(\frac{C}{N_0}\right) = \underline{90.11\,\text{dB(Hz)}}$$

A power level diagram showing the above power levels and losses for a clear sky are given in figure C/3.

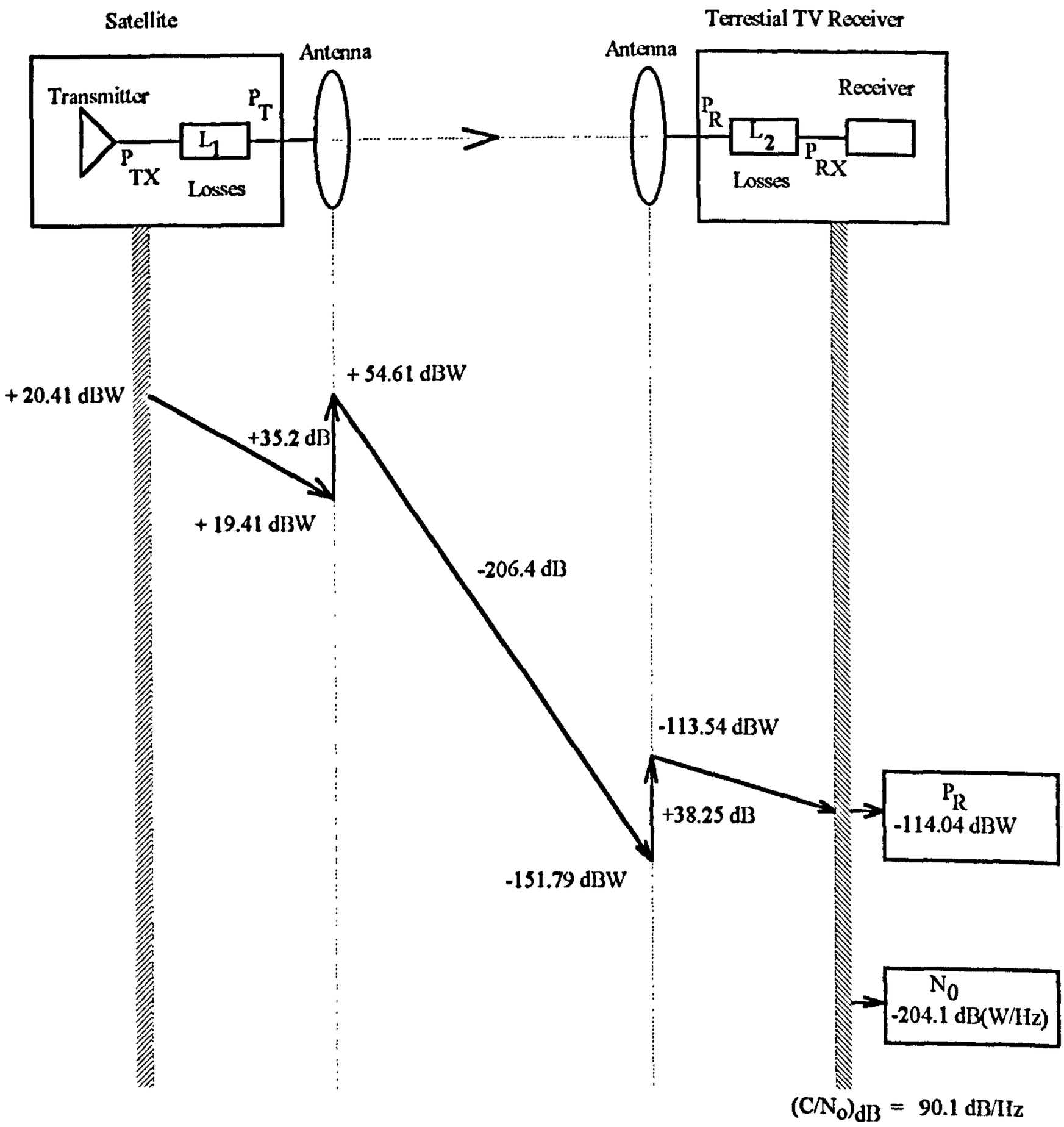

Figure C/3 Downlink Power Level Diagram (Clear Sky)

C.4 Typical characteristics (rain)

(a) The calculations given in section C-3 above are for a clear sky. This section will consider the effects of rain upon the characteristics of the downlink. Illustrations will be given for two values of rain attenuation (3 dB and 7 dB) so that their differing effects upon the system may be seen.

(b) For a rain attenuation that will be exceeded for 0.1 % of the time during an average year, at the down link frequencies used (12 GHz), a typical value of the additional attenuation (A_R) incurred due to rain would be 2.5 dB for a domestic receiver situated in a temperate climate zone such as Europe.

This gives: $L_A = 0.3\,\text{dB} + 2.5\,\text{dB} = 2.8\,\text{dB}$

Which gives a total path loss of $L_P = 206.07 + 2.8 = 208.87\,\text{dB}$

The aerial noise temperature is given by:

$$T_A = \frac{T_{SKY}}{A_R} + T_M \left(1 + \frac{1}{A_R}\right) + T_G$$

Where $T_M = 275\,K$

$$\therefore \quad T_A = \frac{20}{10^{0.25}} + 275\left(1 - \frac{1}{10^{0.25}}\right) + 45 = 177.25\,K$$

Now from equation C-8 above:

$$T_S = \frac{T_A}{L_2} + T_F\left(1 - \frac{1}{L_2}\right) + T_R$$

Using the value of T_A for rain derived above and the values for T_F and T_R either previously given or derived, then:

$$T_S = \frac{177.25}{10^{0.05}} + 290\left(1 - \frac{1}{10^{0.05}}\right) + 191.3 = 380.8\ \text{K}$$

$$\therefore \quad T_{S_{dB}} = 25.8\ \text{dB}$$

$$\therefore \quad \frac{G}{T_S} = G_{R_{max}} - T_{S\,dB} = 37.75 - 25.8 = 11.95\ \text{dB}\left(\text{K}^{-1}\right)$$

From which using equation (C-9) above but with the value of $\frac{G}{T_S}$ derived here, gives:

$$\left(\frac{C}{N_0}\right)_{dB} = 54.61 - 208.87 + 11.95 + 228.6 = \underline{86.28\ \text{dB(Hz)}}$$

This ratio of $\left(\frac{C}{N_0}\right)$ for the downlink will be greater than the value calculated in this way for 99.9 % of the time during an average year.

(c) For a rain attenuation that will be exceeded for 0.01 % of the time during an average year, at the down link frequencies used (12 GHz), a typical value of the additional attenuation (A_R) incurred due to rain would be 7 dB for a domestic receiver situated in a temperate climate zone such as Europe.

This gives: $L_A = 0.3\ \text{dB} + 7\ \text{dB} = 7.3\ \text{dB}$

Which gives a total path loss of $L_P = 206.07 + 7.3 = 213.37\ \text{dB}$

The aerial noise temperature is given by:

$$T_A = \frac{T_{SKY}}{A_R} + T_M \left(1 + \frac{1}{A_R}\right) + T_G$$

Where $T_M = 275\,\text{K}$

$$\therefore \quad T_A = \frac{20}{10^{0.73}} + 275\left(1 - \frac{1}{10^{0.73}}\right) + 45 \quad = \quad 265\,\text{K}$$

Now from equation C-8 above:

$$T_S = \frac{T_A}{L_2} + T_F\left(1 - \frac{1}{L_2}\right) + T_R$$

Using the value of T_A for rain derived above and the values for T_F and T_R either previously given or derived, then:

$$T_S = \frac{265}{10^{0.05}} + 290\left(1 - \frac{1}{10^{0.05}}\right) + 191.3 \quad = 459\,\text{K}$$

$$\therefore \quad T_{S_{dB}} = 26.62\,\text{dB}$$

$$\therefore \quad \frac{G}{T_S} \quad = \quad G_{R_{max}} - \quad T_{S\,dB} = \quad 37.75 - 26.62 \quad = \quad 11.13\ \text{dB}\left(\text{K}^{-1}\right)$$

From which using equation (C-9) above but with the value of $\frac{G}{T_S}$ derived here, gives:

$$\left(\frac{C}{N_0}\right)_{dB} \quad = \quad 54.61 - 213.37 + 11.13 + 228.6 \; = \; \underline{80.97\ \text{dB(Hz)}}$$

This ratio of $\left(\frac{C}{N_0}\right)$ for the downlink will be greater than the value calculated in this way for 99.99 % of the time during an average year. A power level diagram showing the above power levels and losses for a (7 dB) rain environment is given in figure C-4.

C.5 Summary

A discussion of the above results are given in section 3.7. The margins above or below a conventional demodulator threshold of the derived carrier-to-noise ratio $\left(\frac{C}{N}\right)$ are determined and the improvement in system performance obtained with a threshold extension demodulator considered.

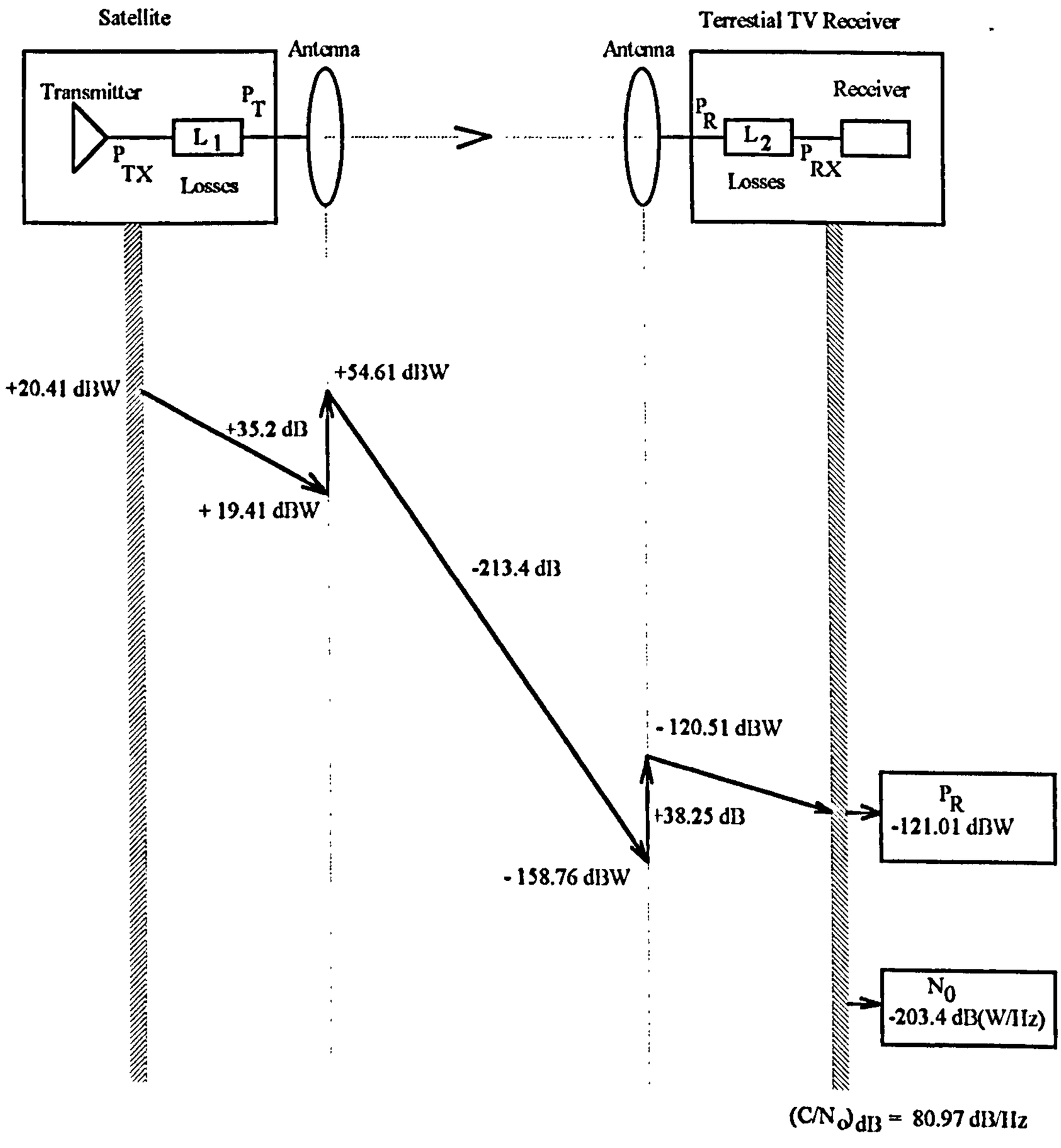

Figure C-4 Downlink Power Level Diagram (Rain 7 dB attenuation)

C.6 References

[1] Stott, J. H. "Satellite Broadcasting: Requirements for the Receiving Antenna", BBC Research Report BBC RD1989/5.

[2] Gandy, C. "Satellite Links for Television Contribution", BBC Research Report BBC RD 1991/5

[3] CCIR "*Broadcasting Satellite Systems*", Geneva, 1983, (ISBN 92.61.01751.7)

Blank Page

APPENDIX D GAUSSIAN ANGLE MODULATED SIGNAL BANDWIDTH RELATIONSHIPS

D.1 Introduction

In various sections of this thesis the requirement arises to establish the channel bandwidth for a Gaussian angle modulated wideband signal. This appendix provides such a relationship. The method follows that described by Taub, et. al. [1].

D.2 Analysis

To establish the channel bandwidth for a Gaussian angle modulated wideband signal consider the power spectral density of a wideband waveform, that is determined by, and has the same form as, the power spectral density function of the modulating waveform:

$$S(f) = \frac{A^2}{4\sqrt{2\pi}\Delta f_{rms}} \left(\exp\left[-\left(\frac{[f - f_C]^2}{2[\Delta f_{rms}]^2} \right) \right] + \exp\left[-\left(\frac{[f + f_C]^2}{2[\Delta f_{rms}]^2} \right) \right] \right) \quad \text{..... (D-1)}$$

Were: $S(f)$ = Double-sided spectral power density

A = Amplitude of FM waveform

Δf_{rms} = Variance of Gaussian spectral density

Now the power P_{TW} in an FM waveform of amplitude A is given by:

$$P_{TW} = \int_{-\infty}^{\infty} S(f)\, df \quad \text{..... (D-2)}$$

$$P_{TW} = \int_{-\infty}^{\infty} \frac{A^2}{4\sqrt{2\pi}\Delta f_{rms}} \left(\exp\left[-\left(\frac{[f - f_C]^2}{2[\Delta f_{rms}]^2} \right) \right] + \exp\left[-\left(\frac{[f + f_C]^2}{2[\Delta f_{rms}]^2} \right) \right] \right) df \quad \text{..... (D-3)}$$

$$\therefore \qquad P_{TW} = \frac{A^2}{2} \qquad \text{..... (D-4)}$$

To establish the bandwidth B_C of a rectangular bandpass filter centred on f_C, that will pass 98 % of the FM waveform's power similar to that determined by Carson's rule for sinusoidal modulation make the substitution $v = f \pm f_C$ in equation (D-1) which gives:

$$\frac{1}{\sqrt{2\pi}\Delta f_{rms}} \int_{-\frac{B_C}{2}}^{\frac{B_C}{2}} e^{-\frac{v^2}{2(\Delta f_{rms})^2}} dv = 0.98 \qquad \text{..... (D-5)}$$

Letting $x = \frac{v}{\sqrt{2}\Delta f_{rms}}$ and inserting in equation (D-5):

$$0.98 = \frac{2}{\sqrt{\pi}} \int_{-\frac{B_C}{2\sqrt{2}\Delta f_{rms}}}^{\frac{B_C}{2\sqrt{2}\Delta f_{rms}}} e^{-x^2} dx \qquad \text{..... (D-6)}$$

$$0.98 = erf \frac{B_C}{2\sqrt{2}\Delta f_{rms}} \qquad \text{..... (D-7)}$$

Thus $$B_C = 2\sqrt{2}\,(1.645)\,\Delta f_{rms} \qquad \text{..... (D-8)}$$

Hence $$B_C = 4.6\ \Delta f_{rms} \qquad \text{..... (D-9)}$$

D.3 References

[1] Taub, H., Schilling, D. "*Principles of Communication Systems*" McGraw-Hill, 1986, New York, ISBN 0-07-062955-2

END OF THESIS